Dissertation zur Erlangung des Doktorgrades
der Fakultät für Chemie und Pharmazie
der Ludwig-Maximilians-Universität München

Marine Natural Products from *Aplysia dactylomela* and *Streptomyces spectabilis*

Biomimetic and Non-Biomimetic Total Synthesis of Aplydactone

and

Biomimetic Total Synthesis of Merochlorin B

von

Robin Michael Meier

aus

Eggenfelden, Deutschland

2016

Erklärung

Diese Dissertation wurde im Sinne von § 7 der Promotionsordnung vom 28. November 2011 von Herrn Prof. Dr. Dirk Trauner betreut.

Eidesstattliche Versicherung

Diese Dissertation wurde eigenständig und ohne unerlaubte Hilfsmittel erarbeitet.

München, den 20. Dezember 2016

……..

Robin Meier

Dissertation eingereicht am:	29. Dezember 2016
1. Gutachter:	Prof. Dr. Dirk Trauner
2. Gutachter:	Prof. Dr. Oliver Trapp
Mündliche Prüfung am:	21. Februar 2017

To my significant other,
the love of my life.

A man is a success if he gets up in the morning and goes to bed at night, and in between does what he wants to do.

(Bob Dylan, Musician and Nobel Prize winner)

Parts of this thesis have been published in peer-reviewed journals:

"Unravelling Photochemical Relationships Among Natural Products from *Aplysia dactylomela"* Bryan S. Matsuura,[†] Patrick Kölle,[†] Dirk Trauner, Regina de Vivie-Riedle and Robin Meier, *ACS Cent. Sci.* **2017**, *3*, 39–46.

"A Synthesis of (±)-Aplydactone"
Robin Meier, Dirk Trauner, *Angew. Chem. Int. Ed.* **2016**, *55*, 11251–11255.
This work was highlighted in: E. M. Carreira, M. Brandstätter, *Synfacts* **2016**, *12*, 893.

"Biomimetic Total Synthesis of (±)-Merochlorin B"
Robin Meier, Dirk Trauner, *Org. Lett.* **2014**, *16*, 2634–2637.
This work was highlighted in: E. M. Carreira, M. J. Jacobsen, *Synfacts* **2014**, *10*, 785.

[†] These authors contributed equally to this work.

Parts of this thesis have been presented at scientific conferences:

Syngenta workshop for talented chemistry PhD students
Biomimetic and Non-Biomimetic Synthesis of the Ladderane Natural Product (±)-Aplydactone (poster). *Stein, Switzerland, September 2016.*

XXVII European Colloquium on Heterocyclic Chemistry 2016
Total Synthesis of the Ladderane Natural Product Aplydactone (poster). *Amsterdam, Netherlands, July 2016.*

ABSTRACT

PART I: Marine organisms have been a rich source of fascinating halogenated natural products. Several brominated sesquiterpenoids have been isolated from the sea hare *Aplysia dactylomela*, which is frequently found in the shallow seawater of tropical and subtropical coasts. Interestingly, these compounds appear to originate from the seaweed diet of the opistobranch mollusks. A remarkable representative is aplydactone, an unprecedented [2]-ladderane natural product, whose isolation reflects the diversity and beauty of naturally-occurring frameworks. Moreover, the high density of stereogenic and non-stereogenic quaternary centers as well as the low decoration with functional groups in combination with the intrinsic ring strain of the system renders its total synthesis highly challenging and therefore attractive for the synthetic community.

In a first approach, the non-biomimetic total synthesis of aplydactone was investigated relying onto a key photochemical [2+2] cycloaddition for the formation of tricycle **II** in high diastereoselectivity (Scheme A). The required photoprecursor **I** was synthesized in a multi-step sequence from simple starting materials on gram scale which was essential for further developments. A photo-induced Wolff ring contraction of an α-diazo ketone, accessed *via* a modified Regitz diazo transfer, allowed for the synthesis of the pivotal bicyclo[2.2.0]hexane containing intermediate **III**. Functional group interconversions led to the desired primary iodide **IV** which cyclized in a Barbier-type ring closure following a substantial conformational change of the intermediate lithium organyl species. For the completion of the first total synthesis of aplydactone, new radical conditions for the conversion of a thiocarbonyl imidazole to the corresponding neopentylic bromide had to be developed.

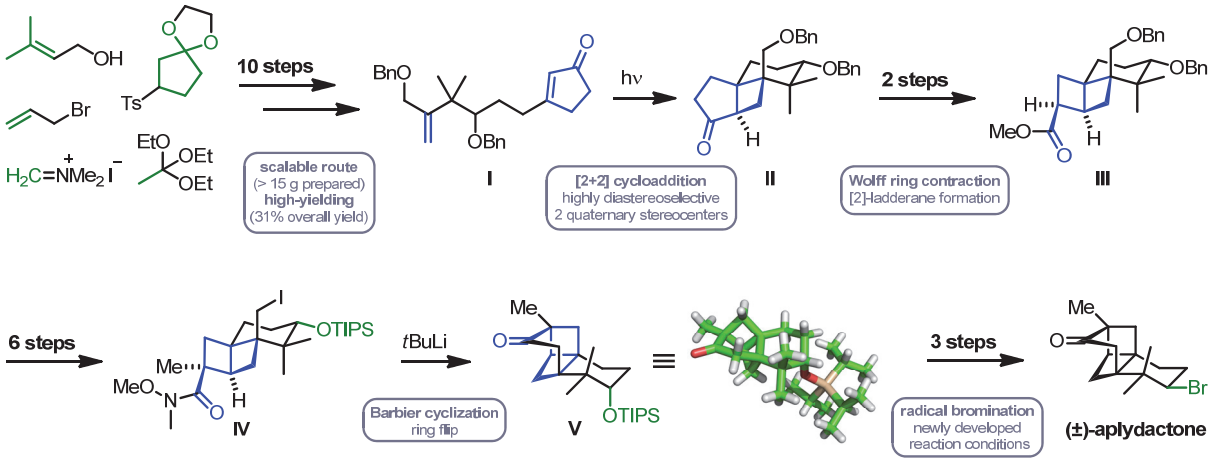

Scheme A. Non-biomimetic total synthesis of aplydactone.

In a combined synthetic and computational approach, studies on the biosynthetic connection of aplydactone led to the synthesis of three additional chamigrane natural products from *Aplysia dactylomela* (Scheme B). Furthermore, 8-*epi*-isoaplydactone was

identified as an anticipated natural product resulting from a photocycloaddition under biomimetic conditions.

Our synthesis commenced with the preparation of the spiro[5.5]undecane core structure of the chamigrane carbon skeleton by a Diels–Alder reaction of enone **VI** and isoprene under high pressure conditions. The introduction of a trimethylsilyl group as traceless directing element is unprecedented and solved diastereoselectivity issues recently reported in the literature. Global deprotection involving a rare Brook rearrangement in combination with the developed radical bromination conditions gave access to 10-bromo-β-chamigrene which was transformed to dactylone and 10-*epi*-dactylone in bioinspired diastereodivergent oxidation sequences. Investigations guided by excited-state theory allowed for the biomimetic synthesis of aplydactone *via* a photochemical [2+2] cycloaddition of dactylone that violates the photochemical "rule of five", first mentioned by Srinivasan and Hammond. In contrast, photochemical conversion of 10-*epi*-dactylone forms the less strained bicyclo[2.1.1]hexane structure due to the conformational anchoring by the secondary bromide.

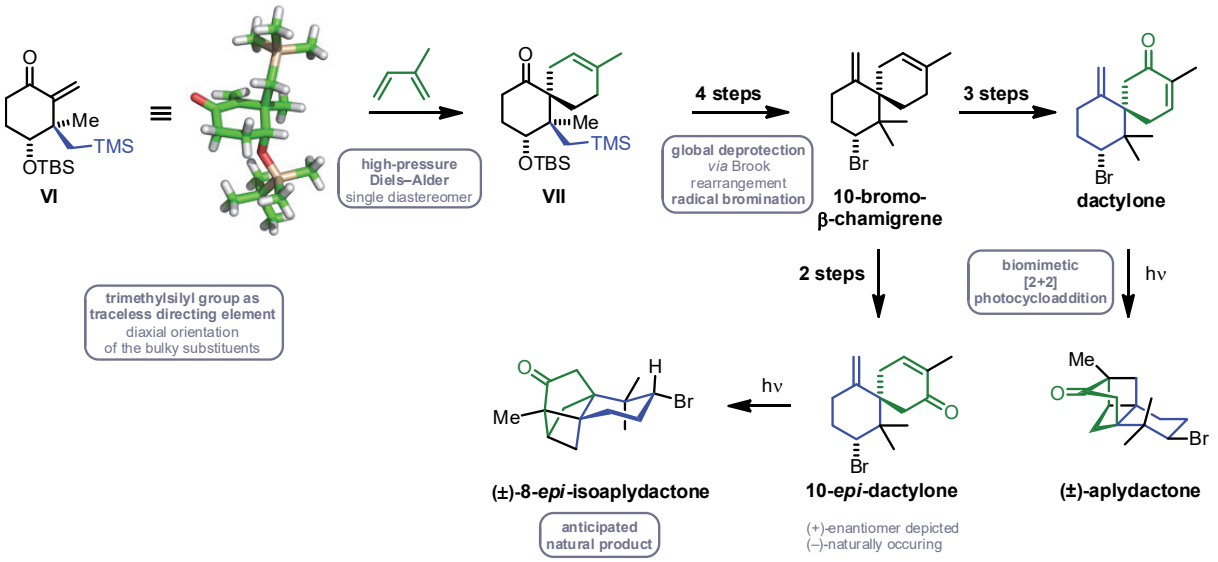

Scheme B. Biomimetic total synthesis of aplydactone.

PART II: The second part of this thesis describes the investigations on the biomimetic total synthesis of merochlorin A and B, two members of a small family of chlorinated meroterpenoids isolated from the marine bacterium *Streptomyces spectabilis* strain CNH-189. These efforts, which also aimed for uncovering a possible biosynthetic pathway, culminated in the first total synthesis of merochlorin B.

The synthetic investigations were initiated by a biosynthetic proposal for the isomeric members merochlorin A and B based on an oxidative (5+2) or (3+2) cycloaddition, respectively, of an intermediate phenoxonium cation. A convergent and scalable synthesis of the biomimetic cyclization precursor **X** involving the tetrahydroxynaphthalene fragment **VIII**

and the isosesquilavandulyl side chain **IX** allowed for an in-depth investigation of the proposed cyclization step. To this end, the use of an *in situ* generated derivative of Koser's reagent led to the selective formation of merochlorin B. This approach complements a recently reported selective biomimetic synthesis of merochlorin A by the George group which described the use of a related precursor. These results demonstrate the significant influence of subtle structural changes on the outcome of biomimetic key steps in natural product total synthesis.

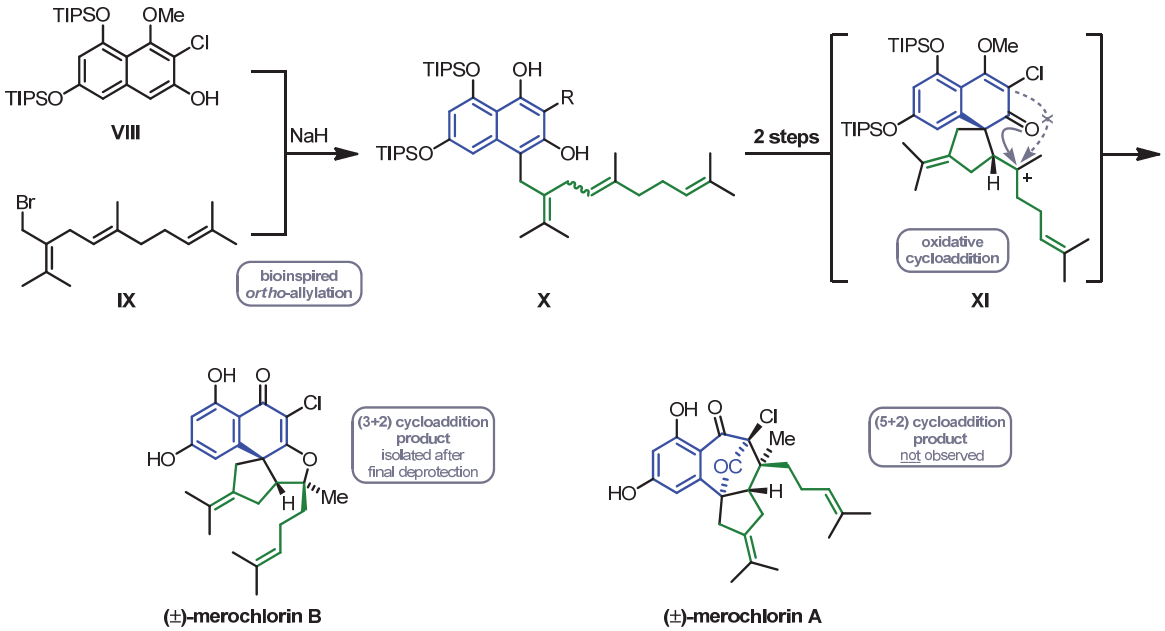

Scheme C. Biomimetic total synthesis of merochlorin B.

ACKNOWLEDGEMENTS

During my time as a Ph.D. student in the group of Professor Dr. Dirk Trauner, I was always motivated to start my work in the morning. However, this is just possible if the working environment and atmosphere is as excellent as I have been privileged to experience over the last years. Therefore, I acknowledge all people, which rendered the last years interesting and enjoyable.

At first, I would like to thank Prof. Dr. Dirk Trauner for giving me the opportunity to conduct my Ph.D. studies in his research group. As I accomplished my Bachelor's, Master's and finally my Ph.D. thesis within the Trauner research group, it might be justified to call myself a "real" Trauner student. His guidance, inspiration and patience for science and above all for total synthesis have never subsided in all these years. His advice to believe in and to follow unconventional ways is supposedly the most important lesson that I have learned. I wish him all the best for his future at the New York University.

Furthermore, I am very thankful to Prof. Dr. Oliver Trapp for agreeing to be the second reviewer of this thesis. I would also like to thank Prof. Dr. Franz Bracher, Prof. Dr. Konstantin Karaghiosoff, Prof. Dr. Klaus T. Wanner and Dr. Henry Dube for being on my defense committee.

In addition, Bryan Matsuura has a large share in the completion of the biomimetic total synthesis of aplydactone and it was a great pleasure and lesson to work with such an inspiring and enthusiastic chemist.

I want to thank all current and former members of the Orange Lab who contributed with theoretical and psychological support on very hard and long days in the lab. Therefore, Antonio Rizzo, Matthias Schmid, Ivica Zamarija, Julie Trads, Desiree Stichnoth, Florian Huber, Takayuki Furukawa, Cenbin "Fritz" Lu, Susanne Gerndt, Laura Salonen and Bichu Cheng are acknowledged.

In addition, I want to thank Felix Hartrampf, Daniel Terwilliger, Katharina Hüll, Benjamin Williams, Nina Vrielink, Bryan Matsuura, Nicolas Armanino and Pascal Ellerbrook not only for their proofreading of this thesis and other manuscripts during my Ph.D., but also for their continuous support, ideas and discussions through all these years, which made me a better chemist for sure.

My interns Jordan Donat, Moritz Claßen and Nicolas Müller deserve special thanks for their hard and enthusiastic work and I am dead certain that they will have a successful future in science.

I am also very grateful for the backing by all other group members of the Trauner research group and the academic staff in the person of Heike Traub, Alexandra Grilic, Dr. Martin Sumser, Carrie Louis, Luis de la Osa de la Rosa and Mariia Palchyk.

Thanks go to Dr. Thomas Magauer, Cedric Hugelsdorfer, Klaus Speck and all other members of the Magauer group for bringing new inspiration and enthusiasm to the whole research group.

Finally, I would like to give special thanks to my family and above all to my girlfriend Susanne who had to get along with my long working hours through all these years.

LIST OF ABBREVIATIONS

Å	angstrom
A	single electron acceptor
Ac	acetyl
acac	acetylacetone
AIBN	azobisisobutyronitrile
Ar	undefined aryl substituent
ATR	attenuated total reflection
Bn	benzyl
bpy	2,2′-bipyridine
br	broad (NMR spectroscopy, IR spectroscopy)
Bu	butyl
°C	degree Celsius
CAN	ceric ammonium nitrate
cap	ε-caprolactamate
CASSCF	complete active space self-consistent field
CASPT2	complete active space perturbation theory second order
Cbz	carboxybenzyl
CCDC	Cambridge Crystallographic Data Centre
CCSD	coupled cluster single double excitation
CFL	compact fluorescent lamp
CoA	coenzyme A
COSY	homonuclear correlation spectroscopy
CoIn	conical intersection
Δ	heating (under reflux)
D	single electron donor
d	doublet (NMR spectroscopy)
deg	degree
d.r.	diastereomeric ratio
DBU	1,8-diazabicyclo[5.4.0]undec-7-ene
DCE	1,2-dichloroethane
DDQ	2,3-dichloro-4,5-dicyano-1,3-benzoquinone
DFT	density functional theory
$(DHQ)_2PHAL$	hydroquinine 1,4-phthalazinediyl diether
$(DHQ)_2PYR$	hydroquinine 2,5-diphenyl-4,6-pyrimidinediyl diether
DIBAL-H	diisobutylaluminium hydride
DIPA	diisopropylamine
DIPEA	diisopropylethylamine
DMA	dimethylacetamide
DMAP	4-(dimethylamino)pyridine
DMAPP	dimethylallyl pyrophosphate
DME	1,2-dimethyoxyethane
DMF	dimethylformamide
DMSO	dimethylsulfoxide
DoM	directed *ortho*-metalation
dppf	1,1´-bis(diphenylphosphino) ferrocene
EDC·HCl	*N*-(3-dimethylaminopropyl)-*N´*-ethylcarbodiimide hydrochloride
ee	enantiomeric excess
EI	electron impact ionization (mass spectrometry)
ent	enantiomer
Enz	enzyme
esp	α,α,α′,α′-tetramethyl-1,3-benzenedipropionate
epi	epimer
eq	equivalent(s)
ESI	electron spray ionization (mass spectrometry)
ESIPT	excited state intramolecular proton transfer
Et	ethyl
fac	*facies* (complex)
FAD	flavin adenine dinucleotide
FPP	farnesyl diphosphate
ΔG	difference in Gibbs free energy
g	gram(s)
G-I	Grubbs catalyst I
G-II	Grubbs catalyst II
gem	geminal
GH-II	Grubbs-Hoveyda II catalyst
GPP	geranyl diphosphate
h	hour(s)
hfacac	hexafluoroacetylacetonato
Hg-lamp	mercury-vapor lamp
HMPA	hexamethylphosphoramide
HPLC	high-performance liquid chromatography
hν	irradiation
HSQC	heteronuclear single quantum coherence
Hz	Hertz (frequency)
i	*iso* (isomer)
IC	internal conversion
*i*Pr	isopropyl
imid	imidazole

IR	infrared
ISC	intersystem crossing
kb	kilobase(s)
kbar	kilobar(s)
KHMDS	potassium hexamethyldisilazide
kJ	kilojoule(s)
LDA	lithium diisopropylamide
LED	light-emitting diode
LHMDS	lithium hexamethyldisilazide
LLS	longest linear sequence
LTA	lead(IV) tetraacetate
LUMO	lowest unoccupied molecular orbital
M	molar
m	meter(s)
m	medium (IR spectroscopy)
m	multiplet (NMR spectroscopy)
mcl	gene in the merochlorin biosynthesis gene cluster
*m*CPBA	*meta*-chloroperbenzoic acid
Me	methyl
Mes-Acr	9-mesityl-10-methylacridinium
min	minute(s)
Min	minimum
mL	milliliter
mmol	millimole
M^n	transition metal with oxidation state n
MOM	methoxymethyl
MS	mass spectrometry
MVK	methylvinylketone
NBS	*N*-bromosuccinimide
NPhth	phthalimide
NIS	*N*-iodosuccinimide
nm	nanometer(s)
NMO	*N*-morpholine *N*-oxide
NMR	nuclear magnetic resonance
NOESY	nuclear Overhauser effect correlation spectroscopy
Ns	4-nitrobenzene-1-sulfonyl
OPP	pyrophosphate, diphosphate
p	*para* (isomer)
*p*ABSA	4-acetamidobenzenesulfonyl azide
pfb	perfluorobutyrate
Ph	phenyl
PIDA	phenyliodonium diacetate
ppm	parts per million
PPTS	pyridinium *para*-toluenesulfonate
ppy	2-phenylpyridine
p-TsOH	*para*-toluenesulfonic acid
q	quartet (NMR spectroscopy)
R	undefined substituent
rac	racemic
R_f	retardation factor
r.t.	room temperature
S_0	singlet ground state
S_1	first excited singlet state
s	strong (IR spectroscopy)
s	singlet (NMR spectroscopy)
SEM	2-(trimethylsilyl)ethoxymethyl
sens.	triplet sensitizer
SET	single electron transfer
SI	supporting information
T_1	first excited triplet state
t	triplet (NMR spectroscopy)
t	(*tert*-) tertiary (isomer)
TBAF	tetrabutylammonium fluoride
TBAI	tetrabutylammonium iodide
TBAS	tetrabutylammonium hydrogensulfate
TBDPS	*tert*-butyldiphenylsilyl
TBS	*tert*-butyldimethylsilyl
TBS	*N*-*tert*-butylsalicylaldiminato (ligand)
*t*Bu	*tert*-butyl
TCDI	1,1'-thiocarbonyldiimidazole
TDDFT	time-dependent density functional theory
TEMPO	2,2,6,6-tetramethylpiperidinyl-1-oxyl
Tf	trifluoromethanesulfonyl
TFA	trifluoroacetic acid
TFE	trifluoroethanol
THF	tetrahydrofuran
THN	tetrahydroxynaphthalene
TIPS	triisopropyl
TLC	thin layer chromatography
TMAO	trimethylamine *N*-oxide
TMEDA	tetramethylethylenediamine
TMS	trimethylsilyl
TS	transition state
Ts	*para*-toluenesulfonyl
UV	ultraviolet (irradiation)
W	watt(s) (unit of power)
w	weak (IR spectroscopy)
wt%	weight percent

TABLE OF CONTENTS

PART I

TOTAL SYNTHESIS OF APLYDACTONE

1 PHOTOCHEMICAL SYNTHESIS

1.1 A brief historical perspective

The conversion of an organic compound under irradiation of light represents an economical and "green" procedure[1] for the formation of organic materials, especially in a world of limited resources. The long history of photochemical conversions dates back to 1834, when Hermann Trommsdorff observed a color change of santonin (**1.1**) crystals upon exposure to sunlight (Scheme 1.1a).[2,3] Although a structural identification of the product, lumisantonin (**1.2**), was not feasible in those days, Trommsdorff could demonstrate a wavelength dependence for this transformation by selective irradiation with the spectral colors of visible light, which he generated with a prism.[3] The structural elucidation of lumisantonin **1.2** was eventually accomplished by Barton in 1958.[4] The mechanism follows a di-π-methane-type rearrangement starting from a triplet biradical intermediate of the corresponding dienone structure.[5]

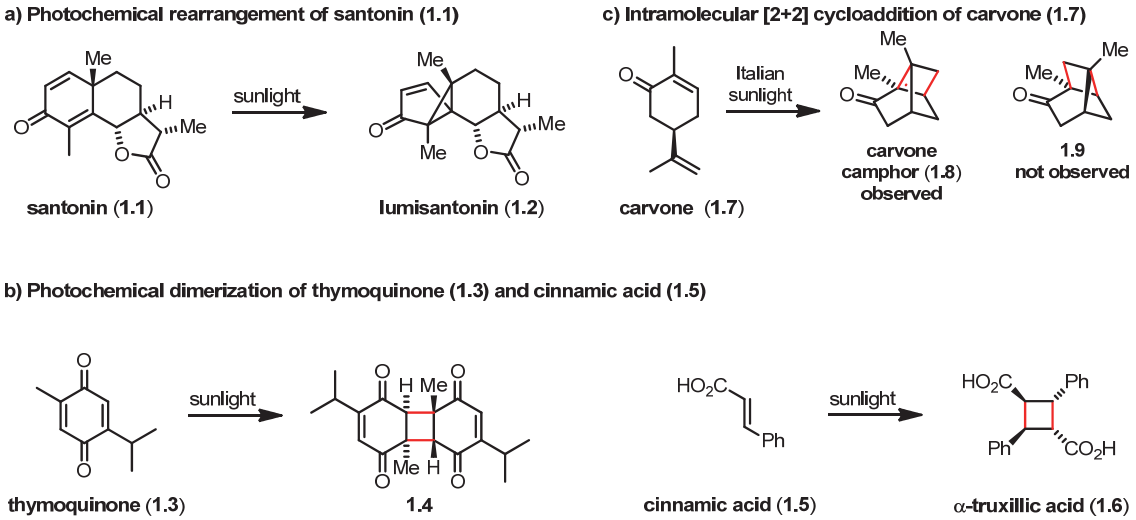

Scheme 1.1 Early photochemical transformations of a) santonin (**1.1**); b) thymoquinone (**1.3**) and cinnamic acid (**1.5**) and c) carvone (**1.7**).

In 1877, Carl Liebermann dimerized thymoquinone (**1.3**) in the solid state under sunlight irradiation in a photochemical [2+2] cycloaddition (Scheme 1.1b).[6] Although Liebermann suggested an incorrect dimeric structure, this experiment represents a starting point for the development of modern organic photochemistry. An analogous dimerization of cinnamic acid (**1.5**) into α-truxillic acid (**1.6**) was reported by Riiber in 1902.[7] Photoinduced halogenations and photoreductions of carbonyl compounds were investigated at the same time by Schramm[8] and Klinger.[9] The first intramolecular [2+2] photocycloaddition was observed by Ciamician in 1908, when he exposed carvone (**1.7**) in ethanolic solution to Italian sunlight for several months (Scheme 1.1c).[10] The obtained photoadduct was identified

by Ciamician as carvone camphor (**1.8**) containing a bicyclo[2.1.1]hexane. Interestingly, the corresponding isomeric bicyclo[2.2.0]hexane **1.9** was not obtained in this experiment. The favored formation of the regioisomer which contains a five-membered ring in intramolecular photochemical [2+2] cycloadditions arising from a triplet biradical pathway was formulated by Srinivasan and Hammond in 1967 and is known today as the “rule of five”.[11]

In the middle of the 20th century, the chemical community realized the advantages of photochemical excitation of organic compounds during the formation of complex structures which would be otherwise difficult or impossible to synthesize. The first use of a photochemical enone [2+2] cycloaddition in natural product total synthesis in 1963 is depicted in Scheme 1.2a.[12]

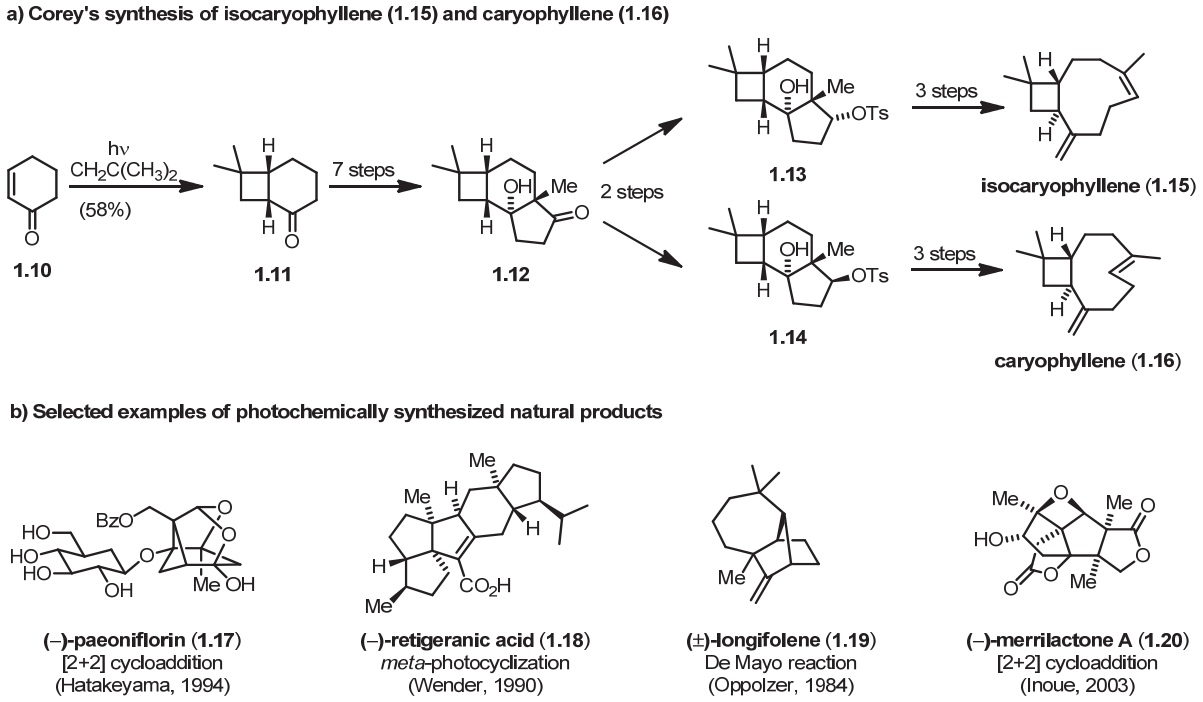

Scheme 1.2 a) The first photochemical enone [2+2] cycloaddition in natural product total synthesis; b) Structures of paeoniflorin (**1.17**), retigeranic acid (**1.18**), longifolene (**1.19**) and merrilactone A (**1.20**).

Corey and coworkers reported the stereodivergent synthesis of racemic isocaryophyllene (**1.15**) and caryophyllene (**1.16**) starting from cyclohexenone (**1.10**), which was transformed into cyclobutane **1.11** upon irradiation with isobutylene at −40 °C. Initially, a 4:1 mixture of *trans*- and *cis*-product was formed. However, basic treatment quantitatively converted the mixture into the thermodynamically favored *cis*-product. It was possible to reach intermediate **1.12** within seven steps, which could be selectively transformed to isocaryophyllene (**1.15**) and caryophyllene (**1.16**) by a Grob fragmentation of tosylates **1.13** and **1.14** followed by epimerization to the *trans*-products. The use of photochemical key steps in the field of natural product synthesis has culminated in elegant total syntheses, exemplified by paeoniflorin (**1.17**) using a photochemical [2+2] cycloaddition,[13] retigeranic

acid A (**1.18**) by applying a *meta*-photocyclization,[14] and longifolene (**1.19**) using a sequence of photocycloaddition/*retro*-aldol reaction (De Mayo reaction, Scheme 1.2b).[15] Furthermore, Inoue and coworkers synthesized merrilactone A (**1.20**) relying on a photochemical [2+2] cycloaddition to form a key cyclobutane intermediate which was opened later in the synthesis to provide the core structure of **1.20**.[16]

In the last two decades, the control of stereoselectivity in photochemical reactions by catalysis has attracted significant attention from the synthetic community.[17] The challenge in the realization of such a process is the suppression of racemic background reactions. Bach and coworkers reported the enantioselective conversion of prochiral lactam **1.21** into cyclobutane **1.23** by irradiation with 300 nm light in the presence of the chiral host **1.24** (Scheme 1.3).[18] Through hydrogen bonding, **1.24** controls the orientation of the allylic side chain during the cyclization event, thus providing **1.23** in 93% *ee*. However, superstoichiometric quantities of the chiral host **1.24** were necessary to suppress racemic background reactions.

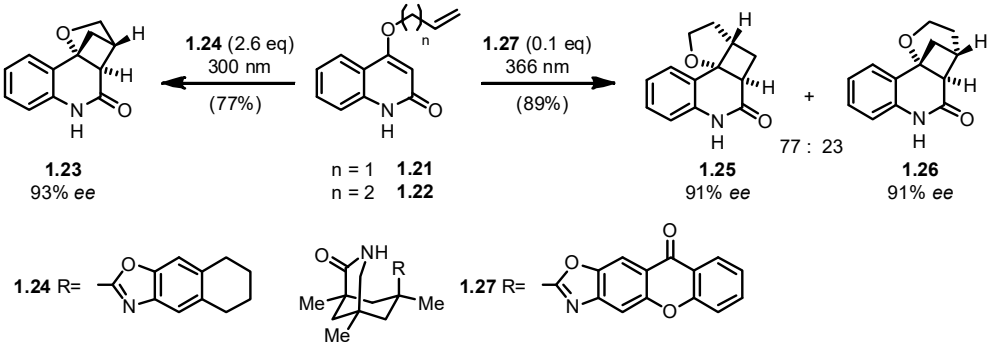

Scheme 1.3 Asymmetric [2+2] photocycloaddition of lactams **1.21** and **1.22**.

To overcome this problem, a triplet sensitizer was incorporated into the host structure, resulting in xanthone **1.27**, which can be excited in the presence of lactam **1.22** and results in selective sensitization of host-bound alkene **1.22**.[19] In this case, a regioisomeric mixture of photoadducts **1.25** and **1.26** in 91% *ee* was obtained in the presence of just 10 mol% of xanthone **1.27**. In addition, chiral organocatalysts have been used to control the stereoselectivity in photochemical [2+2] cycloadditions.[20] However, these methods suffer from structural restrictions of the starting material and are not broadly applicable.

The use of visible light in combination with photoredox catalysts has recently gained the attention from the synthetic community,[21] despite the first use of $[Ru(bpy)_3]Cl_2$ (**1.220**, Scheme 1.24b) as a photoredox catalyst in organic synthesis already being reported by Kellogg in 1978. Sulfonium ions were reduced to the corresponding alkanes and thioethers using *N*-substituted 1,4-dihydropyridines as the terminal reductant under photomediated conditions.[22] Interestingly, the full impact of this new type of reactivity was only recognized over two decades after the first report by Kellogg, leading to the vibrant field of visible light

photoredox catalysis observed in recent years. The general idea behind visible light photoredox catalysis is the use of metal complexes or organic dyes which are poor oxidants and reductants in their ground state, but possess excited states which show a strong ability to start single-electron transfer (SET) events. This opens up the possibility of chemoselective transformation without the use of high-energy UV irradiation.

An exciting example, which combines photoredox and enamine organocatalysis, was reported by the MacMillan group for the synthesis of α-trifluoromethylated aldehydes **1.31** (Scheme 1.4a).[23] In the presence of imidazolidinone organocatalyst **1.32**, iridium photocatalyst **1.33** and trifluoroiodomethane, several aldehydes **1.28** could be converted into the corresponding enantioenriched trifluoromethylated aldehydes by attack of a nucleophilic enamine intermediate **1.29** onto an electrophilic trifluoromethyl radical **1.30**.

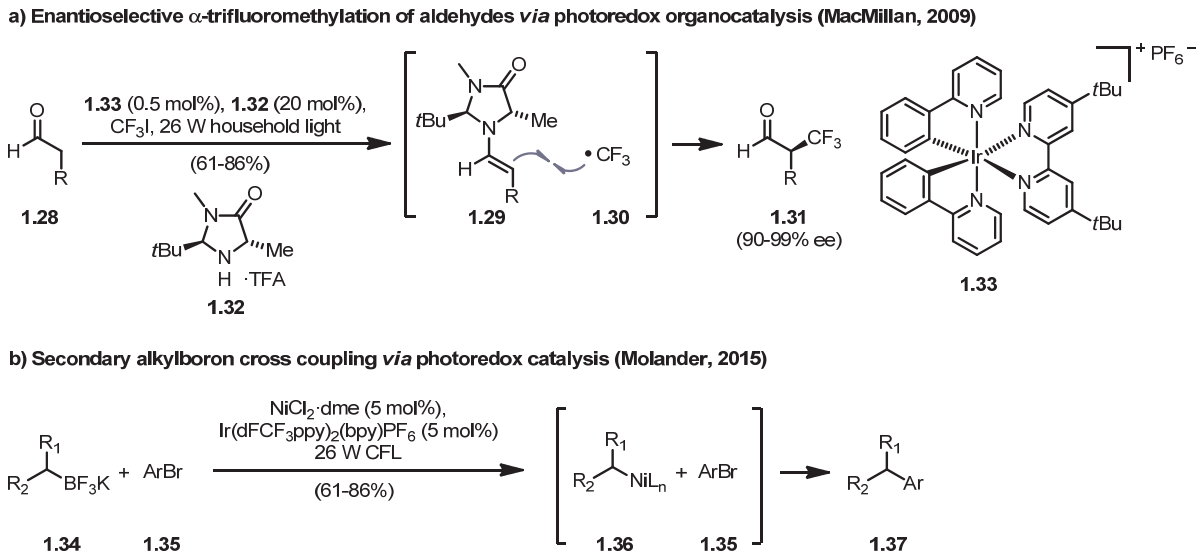

Scheme 1.4 Recent examples of photoredox catalytic transformations.

Furthermore, the merger of photoredox and transition metal catalysis allows difficult Csp^3–Csp^2 couplings as exemplified by the work of Molander (Scheme 1.4b).[24] The secondary alkyl radicals formed from the trifluoroborates **1.34** under photoredox catalytic conditions are proposed to form an alkyl-Ni(I) complex **1.36** followed by oxidative addition to the aryl halide **1.35**. Reductive elimination provides the desired cross-coupled products **1.37**.

In addition to these two selected recent examples, the fascinating field of photochemistry and photoredox catalysis seems to undergo a renaissance and the continuously growing scope of the reported methods generates high expectations for future developments.

1.2 Photochemical key steps in the total synthesis of natural products

1.2.1 Biomimetic transformations

Photochemical key reactions which occur late in the biosynthesis of natural products are relatively rare. However, existing examples display the power of these transformations in the efficient synthesis of complex structures of high biological activity. The biosynthetic formation of the secosteroids vitamin D_2 (ergocalciferol) and vitamin D_3 (cholecalciferol **1.41**, Scheme 1.5) might be the most prominent examples in this class. In the human body, vitamin D_3 (**1.41**) upregulates the intestinal absorption of calcium and other ions. This is essential for the prevention of rickets, which causes deformation of the bones due to calcium deficiency during childhood, among other diseases.[25]

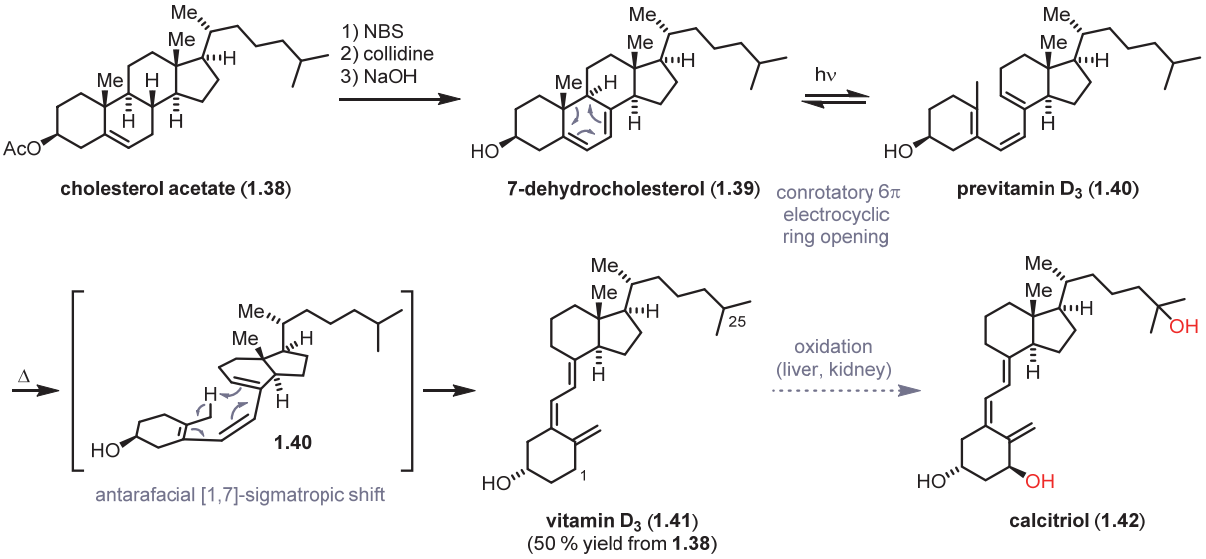

Scheme 1.5 Industrial synthesis of vitamin D_3 (**1.41**) and conversion to calcitriol (**1.42**) in vertebrates.

Interestingly, 37.5 tons of vitamin D_3 (**1.41**) are produced annually worldwide, particularly for the production of fodder and food additives.[26] An industrial synthesis of **1.41** was reported by Hoffmann–La Roche which applies a semisynthetic route mimicking the biosynthesis performed in the skin by irradiation under UV-B light (Scheme 1.5). The synthesis starts from cholesterol acetate (**1.38**), which is brominated in the allylic position followed by elimination to give 7-dehydrocholesterol (**1.39**). Irradiation of this compound with UV light yields previtamin D_3 (**1.40**) *via* a photochemical conrotatory 6π electrocyclic ring opening. This intermediate undergoes a thermal antarafacial [1,7]-sigmatropic hydride shift to vitamin D_3 (**1.41**). However, the active compound in vertebrates is actually calcitriol (**1.42**), which is formed by hydroxylases in the liver and kidneys by oxidation at C1 and C25.[26,27]

1.2.1.1 Photochemical [2+2] cycloadditions

Cyclobutanes are fascinating structural motifs that are frequently found in nearly all natural product classes. They are either formed by cationic cyclization or by photochemical [2+2] cycloaddition.[28] Figure 1.1 shows a selection of natural products which are supposedly made by inter- or intramolecular [2+2] photocycloaddition, typically by excitation of an enone-type structure within the biosynthetic precursor due to the ease by which this motif is excited by sunlight.[29]

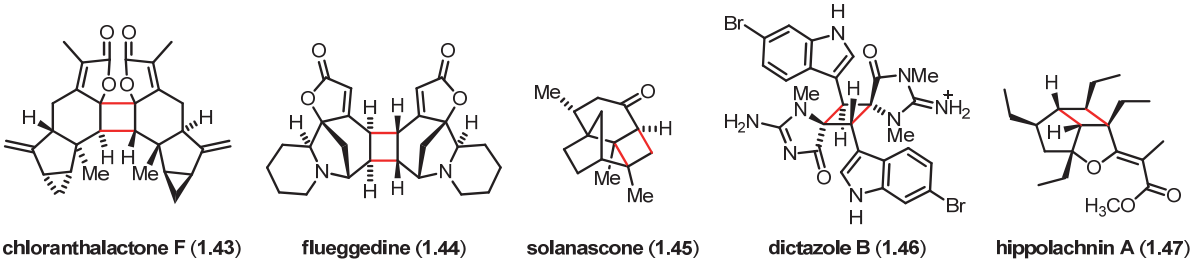

Figure 1.1 Natural products biosynthetically formed by photochemical [2+2] cycloaddition.

Mechanistically, upon irradiation of an enone structure **1.48**, a short-lived singlet state (S_1), formed by nπ* excitation, decays by intersystem crossing (ISC) to a lower-lying, biradical triplet state (**1.48** T_1, Scheme 1.6).[30] In acyclic systems, *cis-trans* isomerization by rotation of the biradical structure can be a competing event leading to reduced intersystem crossing and cycloaddition. Therefore, cyclic enone structures are favorable substrates since bond rotation cannot occur. The triplet biradical state forms a triplet exciplex **1.50** with a ground state alkene **1.49**, which is part of the same molecule in the case of intramolecular reactions. From this exciplex, a triplet 1,4-biradical **1.51** is generated by the first bond formation. Before the formation of the second σ-bond and the closure to cyclobutane **1.52**, an additional ISC to a singlet 1,4-biradical **1.51** has to occur.

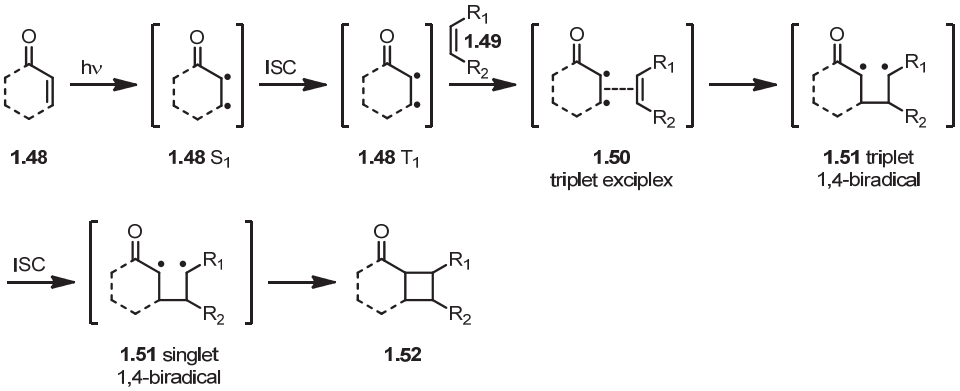

Scheme 1.6 General mechanism of enone-alkene [2+2] photocycloadditions.

Several total syntheses of naturally occurring cyclobutanes were inspired by their proposed biosynthetic formation.[30c,31] A fascinating example of an intramolecular [2+2]

photocycloaddition as a key step in the biosynthesis of a natural product was demonstrated by the MacMillan group in their work on the total synthesis of the constituents of *Verbena littoralis*, a perennial herb used in traditional folk medicine (Scheme 1.7a).[32] The heptacyclic iridoid constituent littoralisone (**1.57**) was proposed to be biosynthetically derived from brasoside (**1.58**), isolated from the same plant, and coumaric acid (**1.59**).

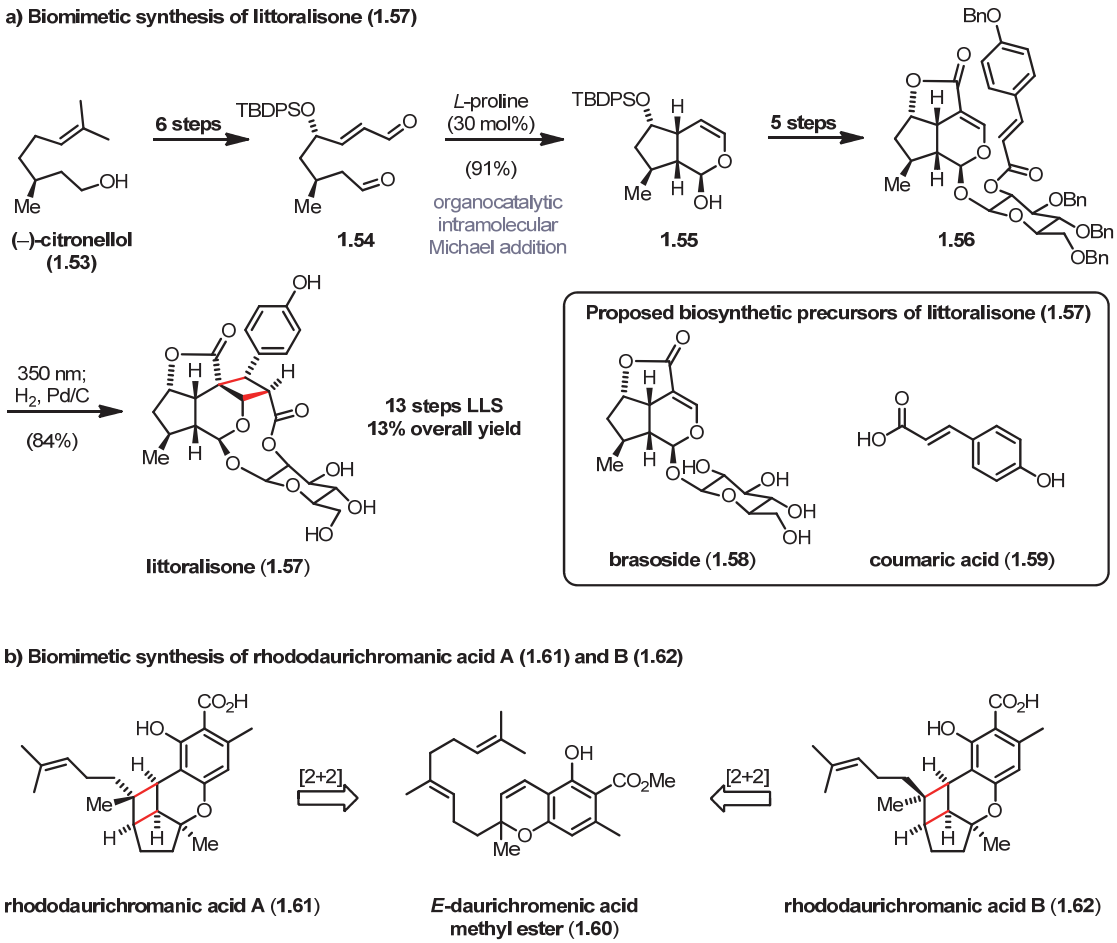

Scheme 1.7 Biomimetic intramolecular [2+2] photocycloaddition in the total synthesis of a) littoralisone (**1.57**) and b) rhododaurichromanic acid A (**1.61**) and B (**1.62**).

In their synthesis, MacMillan and coworkers were able to synthesize the iridoid core structure **1.55** in only seven steps by use of an organocatalyzed intramolecular Michael addition. The use of *L*-proline as catalyst was necessary to overcome the undesired substrate-directed *trans*-selectivity in the cyclization step to give bicycle **1.55**. The proposed glucose-tethered photoprecursor **1.56** was reached in a five step sequence. Irradiation of **1.56** with UV-A light provided littoralisone (**1.57**) selectively in excellent yield after global deprotection, thus validating the proposed biosynthesis. An analogous intramolecular photocyclization was reported in the total synthesis of rhododaurichromanic acid A (**1.61**) and B (**1.62**), which could be formed as a separable mixture by the irradiation of *E*-daurichromenic acid methyl ester (**1.60**), as depicted in Scheme 1.7b. The formation of

both epimers in a single step was rationalized by the *E*/*Z*-isomerization of the starting material **1.60** under irradiation with UV-A light.[33]

However, [2+2]-cycloadditions in the biosynthesis of cyclobutane-containing natural products are not limited to intramolecular reactions. Biyouyanagin A (**1.72**), isolated from the leaves of *Hypericum chinense* L. var. *salicifolium*, represents an exciting example of how substrate control can provide regio- and stereoselectivity in intramolecular photochemical [2+2] cycloadditions.[34]

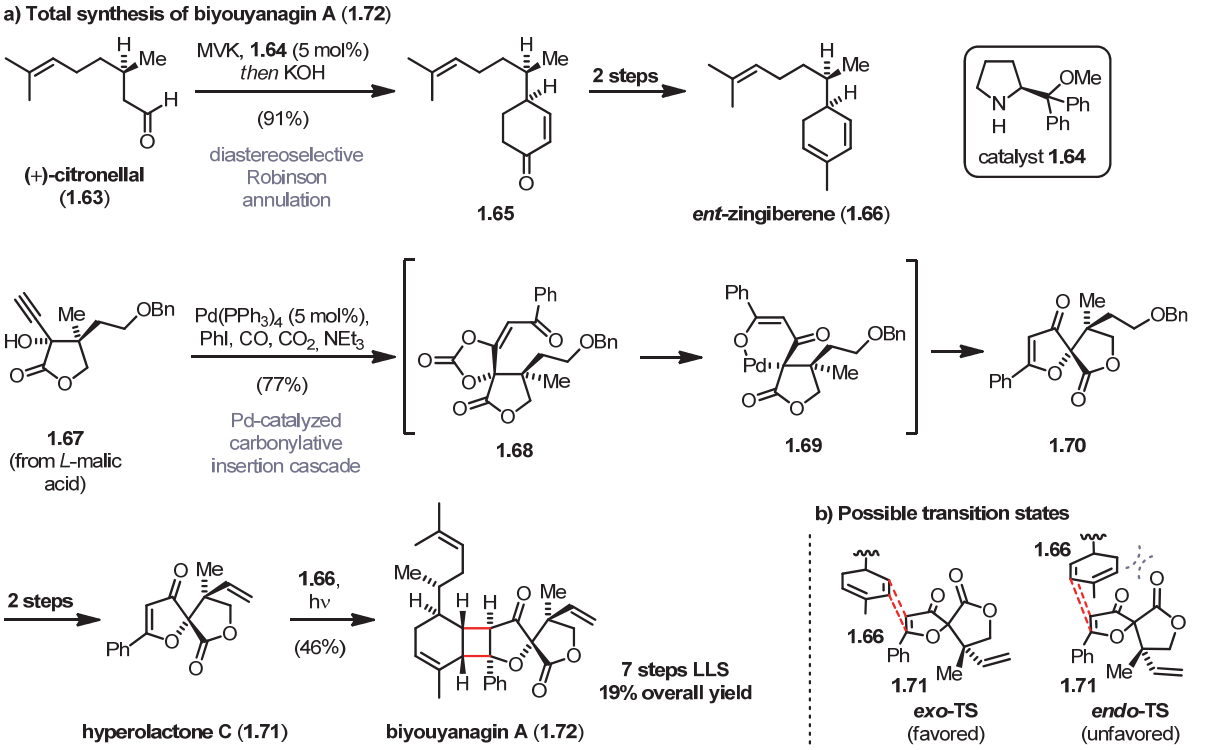

Scheme 1.8 a) Total synthesis of biyouyanagin A (**1.72**) by Nicolaou et al.; b) Transition state structures in the biomimetic [2+2] cycloaddition.

As outlined in Scheme 1.8a, Nicolaou and coworkers were able to synthesize the two biosynthetic photoprecursors *ent*-zingiberene (**1.66**) and hyperolactone C (**1.71**) in a concise and elegant fashion.[35] Asymmetric access to cyclohexadiene **1.66** was made possible by an organocatalytic, diastereoselective Robinson annulation starting from citronellal (**1.63**), whereas the spirocyclic core structure of hyperolactone C (**1.71**) was formed in a carbonylative insertion cascade. Treatment of alkyne **1.67**, derived from *L*-malic acid, in the presence of phenyl iodide with $Pd(PPh_3)_4$ under a CO/CO_2 atmosphere resulted in a sequence of carbonylative cross coupling, carbonate formation and 1,4-addition to intermediate **1.68**. Formation of palladium allyl species **1.69** by extrusion of CO_2 followed by reductive elimination provided spirocyclic intermediate **1.70** as a single stereoisomer, which could be converted to **1.71**. Irradiation of hyperolactone C (**1.71**) and *ent*-zingiberene (**1.66**) with UV-A light in the presence of a triplet sensitizer provided regio- and stereoselectively

biyouyanagin A (**1.72**) *via* a favored *exo*-transition state (Scheme 1.8b). Nicolaou's biomimetic approach allowed for an efficient synthesis of **1.72** in a longest linear sequence of 7 steps from a literature known compound in 19% overall yield. Furthermore, it was possible to revise the originally proposed all-*cis* cyclobutane structure which would be formed by a sterically unfavored *endo*-transition state.

The cyclobutane ring formed in a [2+2] cycloaddition does not have to be preserved during further biosynthetic transformations to the natural product, especially as the ring strain in a four-membered system makes them prone to opening. The biosynthesis of the racemic natural products linderaspirone A (**1.78**) and bi-linderone (**1.80**) represents one example where an initially formed four-membered ring has enough intrinsic reactivity to fragment (Scheme 1.9).[36] The Wang group synthesized methyl linderone (**1.76**), the biomimetic precursor, *via* a semipinacol rearrangement of dithiane **1.73** upon heating. Irradiation of **1.76** as a thin film in the solid state with UV-A light or simply sunlight provided mixtures of cyclobutane **1.77**, linderaspirone A (**1.78**) and bi-linderone (**1.80**) accompanied by its 3-epimer.[36a] The high regioselectivity can be explained by π-stacking effects in the crystal packing of **1.76**, which has been recently reported.[37] Irradiation in solution provided only trace amounts of the desired natural products.[36a,38]

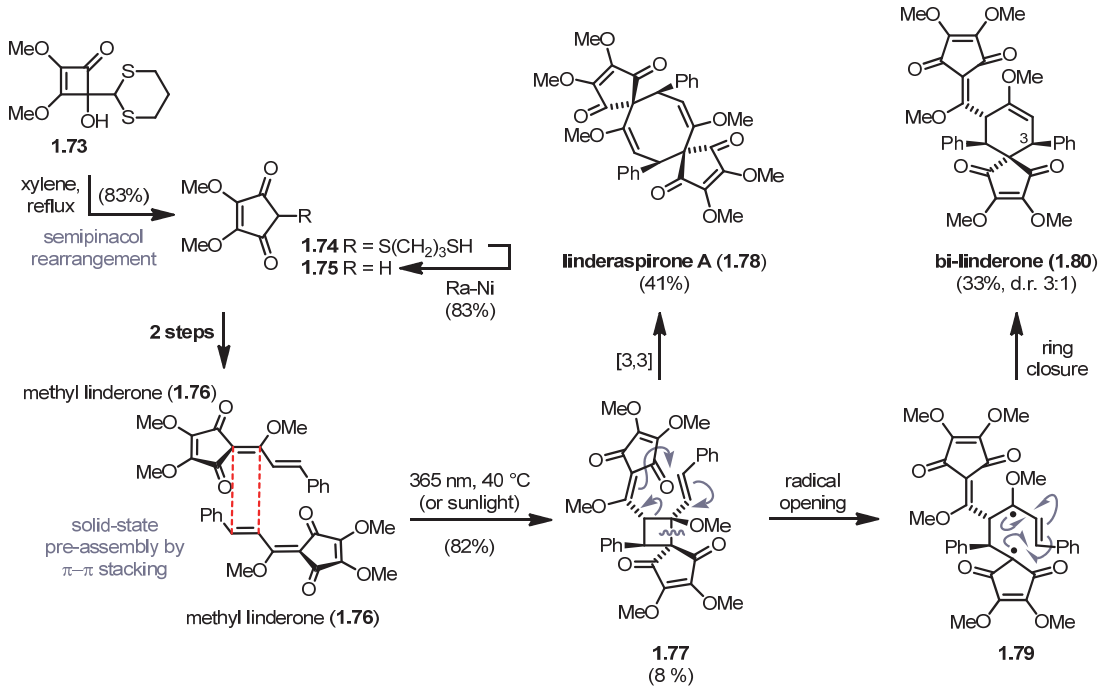

Scheme 1.9 Solid state photochemical formation of linderaspirone A (**1.78**) and bi-linderone (**1.80**).

Presumably, **1.78** is formed by a strain-releasing Cope rearrangement from cyclobutane **1.77**, whereas **1.80** could be formed by a radical opening of the cyclobutane ring to the allylic radical **1.79** followed by radical recombination to the six-membered ring system

of bi-linderone (**1.80**). This proposal is supported by the fact that cyclobutane **1.77** quantitatively forms the two natural products **1.78** and **1.80** upon heating in the dark.

In conclusion, four-membered rings are present in the structure of natural products and their formation is often mediated under solar irradiation. This has been utilized to synthesize these compounds in a step-economic way. Furthermore, the strain-releasing opening of the cyclobutane structures allows nature to broaden the structural complexity of its products.

1.2.1.2 Other photochemical cycloadditions, rearrangements and electrocyclizations

The repertoire of photochemical reactions found in the biosynthesis of natural products exceeds the simple [2+2] photocycloadditions mentioned in the previous chapter by far. Not only have other modes of cycloaddition been reported for the biosynthesis of natural metabolites, but also different types of rearrangements, isomerizations and electrocyclizations.

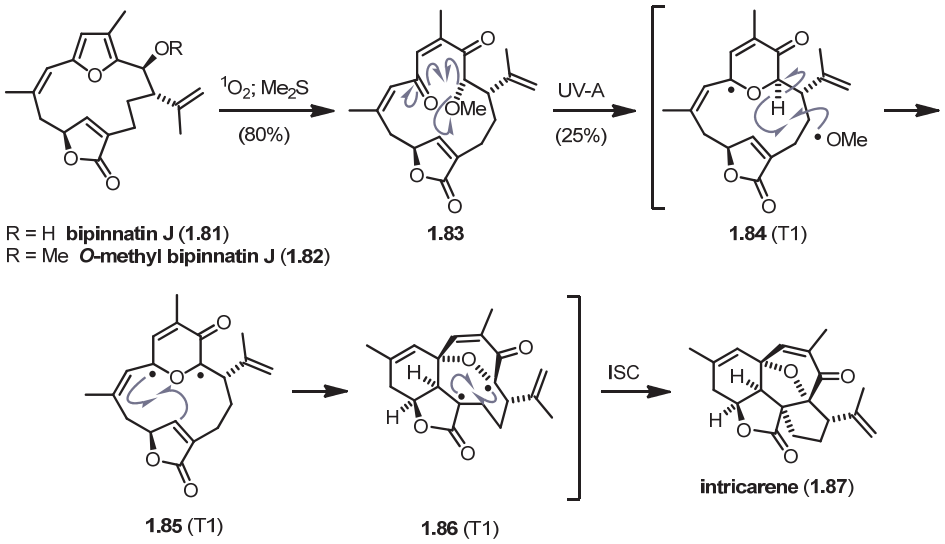

Scheme 1.10 Photochemical formation of intricarene (**1.87**) from *O*-methyl bipinnatin J (**1.82**).

Intricarene (**1.87**) represents a polycyclic furanocembranoid isolated from the octocoral *Pseudopterogorgia* kallos (Scheme 1.10).[39] Trauner[40] and Pattenden[41] reported bioinspired syntheses of **1.87**, relying on a thermal, ionic oxidopyrilium-alkene (5+2) cycloaddition under refluxing conditions in DMSO or MeCN, starting from the natural precursor bipinnatin J (**1.81**), in three steps. Nevertheless, these conditions clearly do not represent the biosynthetic pathway chosen by nature. One possibility is the participation of an enzyme to lower the activation barrier for the cyclization. However, the biological specimens, from which the natural product was isolated, were collected near the Columbian Caribbean Isla de Providencia (water depth 1−45 m), an intensely irradiated region. This prompted Trauner and coworkers to investigate a photochemical pathway to intricarene

(**1.87**).[42] In a combined synthetic and computational approach, it was possible to show that irradiation of diene dione **1.83**, obtained by photochemical singlet oxygen cycloaddition of *O*-methyl bipinnatin J (**1.82**), with a UV-A rich reptile lamp yielded the natural product intricarene (**1.87**) at ambient temperature. The formal (5+2) mechanism can be described by an initial excitation of **1.83** to its first excited singlet state (S1) followed by ISC to the triplet radical intermediate **1.84** (T_1) which is further transformed to triplet oxidopyrilium **1.85** (T_1). A two-step cyclization pathway involving a final ISC to a singlet state yields **1.87**. These findings raise doubts if intricarene (**1.87**) is a real natural product synthesized in corals, especially as **1.82** has been reported to be an isolation artefact from the methanolysis of bipinnatin J (**1.81**).[43]

Another mechanism for the photochemical formation of an oxidopyrilium species was reported by Porco and coworkers in their synthesis of methyl rocaglate (**1.93**), a member of the polycyclic rocaglamide natural product family isolated from the tropical plant genus *Aglaia* (Scheme 1.11).[44] Upon irradiation, an excited-state intramolecular proton transfer (ESIPT) forms an oxidiopyrilium species **1.90** from 3-hydroxyflavone **1.88** which reacts with cinnamate **1.89** in an *endo*-transition state to form the tricyclic intermediate **1.91**. The proposed biomimetic ketal rearrangement could be induced under basic conditions to yield methyl rocaglate (**1.93**) after subsequent reduction. The use of a TADDOL ligand in the cycloaddition step enabled the asymmetric synthesis of several rocaglamide natural products and derivatives based on this biomimetic consideration.[44b,45]

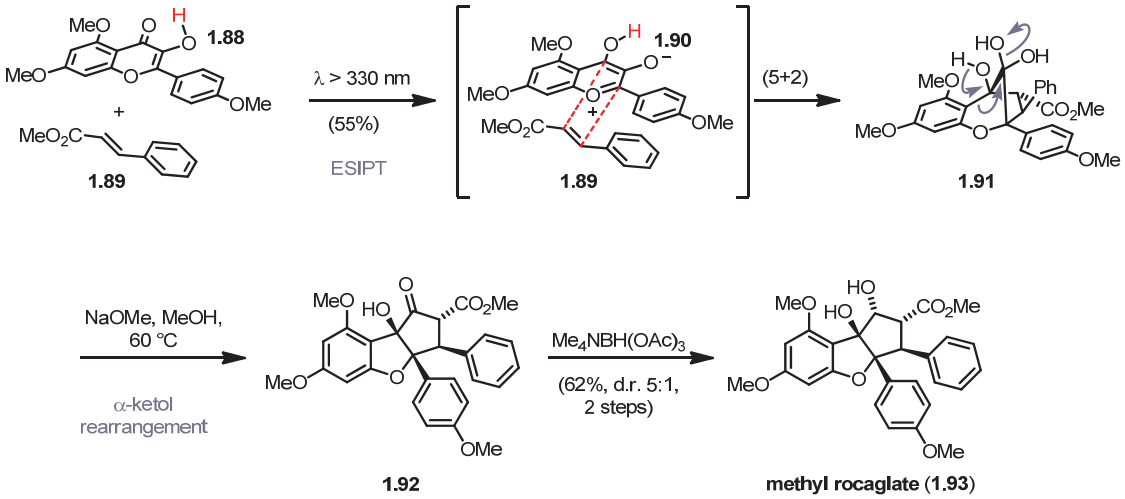

Scheme 1.11 Biomimetic synthesis of the *Aglaia* natural product methyl rocaglate (**1.93**) *via* ESIPT induced (5+2) cycloaddition.

The occurrence of a di-π-methane rearrangement[46] in the biosynthesis of erythrolide A (**1.97**), a chlorinated diterpenoid from a Caribbean octocoral, could be demonstrated by irradiation of a methanolic seawater solution of erthyrolide B (**1.94**) with sunlight (Scheme 1.12a).[47] By excitation of the enone structure, biradical **1.95** should be

formed after initial cyclopropyl ring closure, followed by a subsequent cyclopropyl opening. Erythrolide A (**1.97**) is obtained by final ring closure of singlet biradical **1.96**.

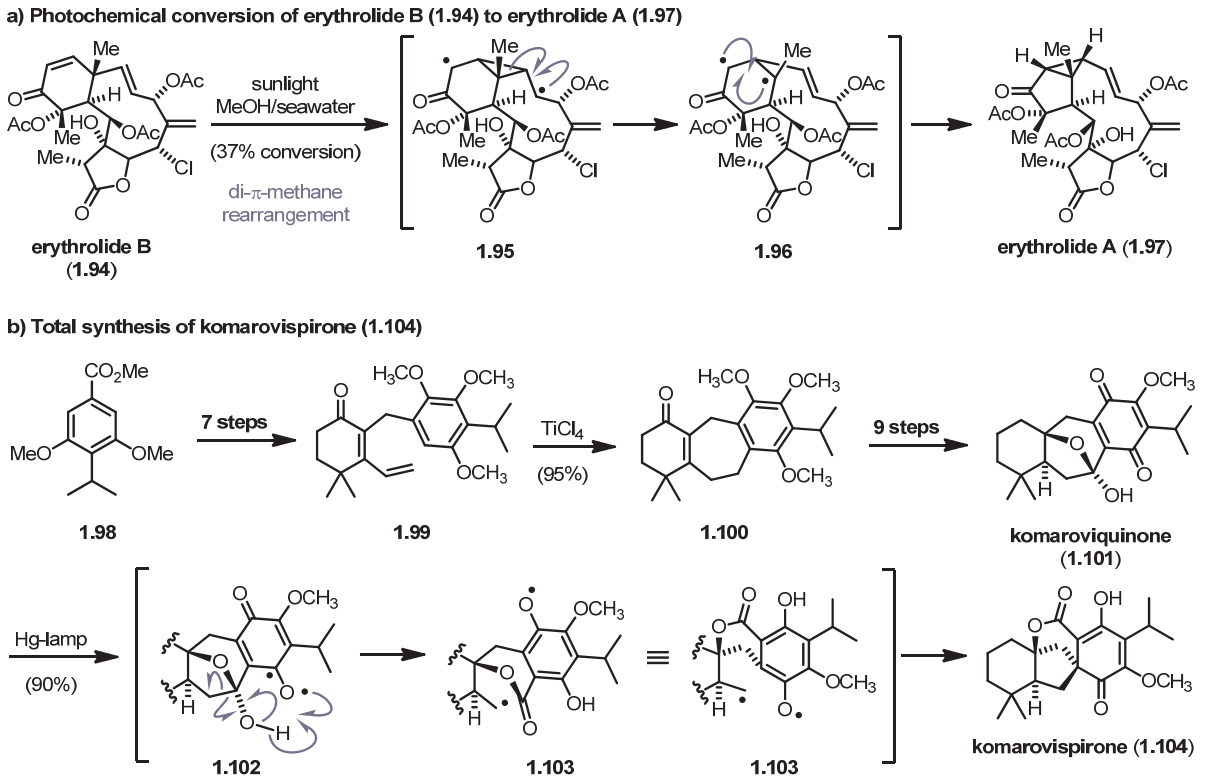

Scheme 1.12 Rearrangement reactions in the biomimetic formation of a) erythrolide A (**1.97**) and b) komarovispirone (**1.104**).

Majetich and Yu described a photochemically-induced radical cascade for the formation of a spirocyclic center in their biomimetic synthesis of komarovispirone (**1.104**) (Scheme 1.12b).[48] The precursor, komaroviquinone (**1.101**), was synthesized *via* a multistep sequence containing a key Friedel–Crafts cyclization of enone **1.99** to the tricyclic core structure **1.100**.[49] Irradiation of **1.101**, which was accessible in nine steps from **1.100**, led to a nπ* excitation of the quinone moiety forming **1.102** followed by a [1,5]-hydrogen atom transfer and opening of the seven-membered ring to give biradical **1.103**. Generation of the spirocyclic center yielded komarovispirone (**1.104**) diastereoselectively. The same non-enzymatic rearrangement was selectively observed under normal daylight within two days, demonstrating the efficiency of photochemical conversions in the preparation of quaternary stereocenters.

Interestingly, Gademann and coworkers[50] recently elucidated the biogenetic connection between komarivispirone (**1.104**) and cyclocoulterone (**1.108**) isolated from the same plant *Dracocephalum komarovi* (Scheme 1.13).[51] Under their conditions using sunlight irradiation of komaroviquinone (**1.101**) an equimolar ratio of **1.108** and **1.104** was obtained in 63% overall yield. A possible mechanism for the formation of cyclocoulterone (**1.108**) is depicted in Scheme 1.13, which contains a similar reaction cascade involving **1.102** as

described for the formation of **1.104**. A fascinating consecutive [1,5]- and [1,6]-hydrogen atom transfer forms the benzo[1,3]dioxole structure of **1.108** via the intermediates **1.105**–**1.107**. A similar cascade was reported in the biosynthesis of taiwaniaquinol A from taiwaniaquinol F under sunlight irradiation.[52]

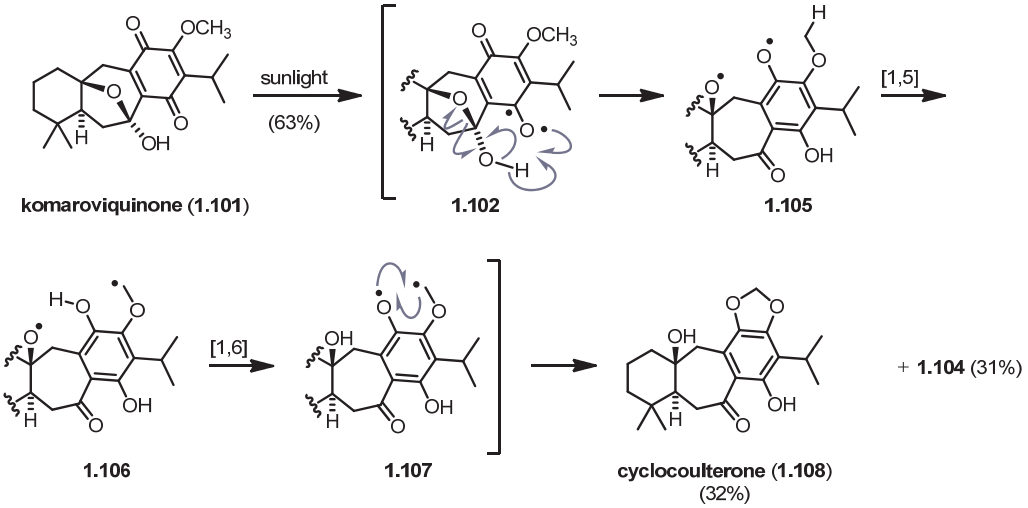

Scheme 1.13 Photochemical formation of cyclocoulterone (**1.108**) and kamorovispirone (**1.104**) under sunlight irradiation.

Photochemical irradiation is also capable of generating intermediates which can undergo subsequent reactions under thermal conditions in complex cascade processes. As outlined in Scheme 1.14, Hu and Tang described the biomimetic synthesis of several xanthanolide dimers by photochemically triggered reaction cascades.[53] Irradiation of xanthatin (**1.109**) with a high-pressure mercury lamp led to the isomerization of the C1–C5 double bond within the seven-membered ring, leading to *trans*-cycloheptene (*Z*,*E*)-**1.109**. One possible reaction pathway is the dimerization of this reactive intermediate in a [4+2] cycloaddition to cyclohexene intermediate **1.110** which could be identified as a minor reaction product under certain reaction conditions. However, **1.110** is prone to undergo an additional intramolecular photochemical [2+2] cycloaddition to mogolide A (**1.112**) and its epimer 3-*epi*-mogolide A (**1.111**). Interestingly, **1.112** was only identified as a natural product in the *Xanthium mogolium Kitag* plant after its biomimetic total synthesis.

Additionally, in the presence of DBU, the dimerization is prevented and an epimeric mixture of **1.114** was observed as the sole reaction product, presumably arising from isomerization of the C2–C3 double bond followed by 6π electrocyclic ring closure. For the success of the isomerization step, UV irradiation and the addition of DBU was absolutely critical, which led to the prediction of enolate **1.113**, formed by 1,6-addition of DBU to the vinylogous Michael system, as a possible key intermediate in the isomerization. A subsequent [4+2] cycloaddition with photochemically generated singlet oxygen provided

access to endoperoxide **1.116**, which was isolated from the aerial parts of *Xanthium strumarium*, and its epimer **1.115**.[54]

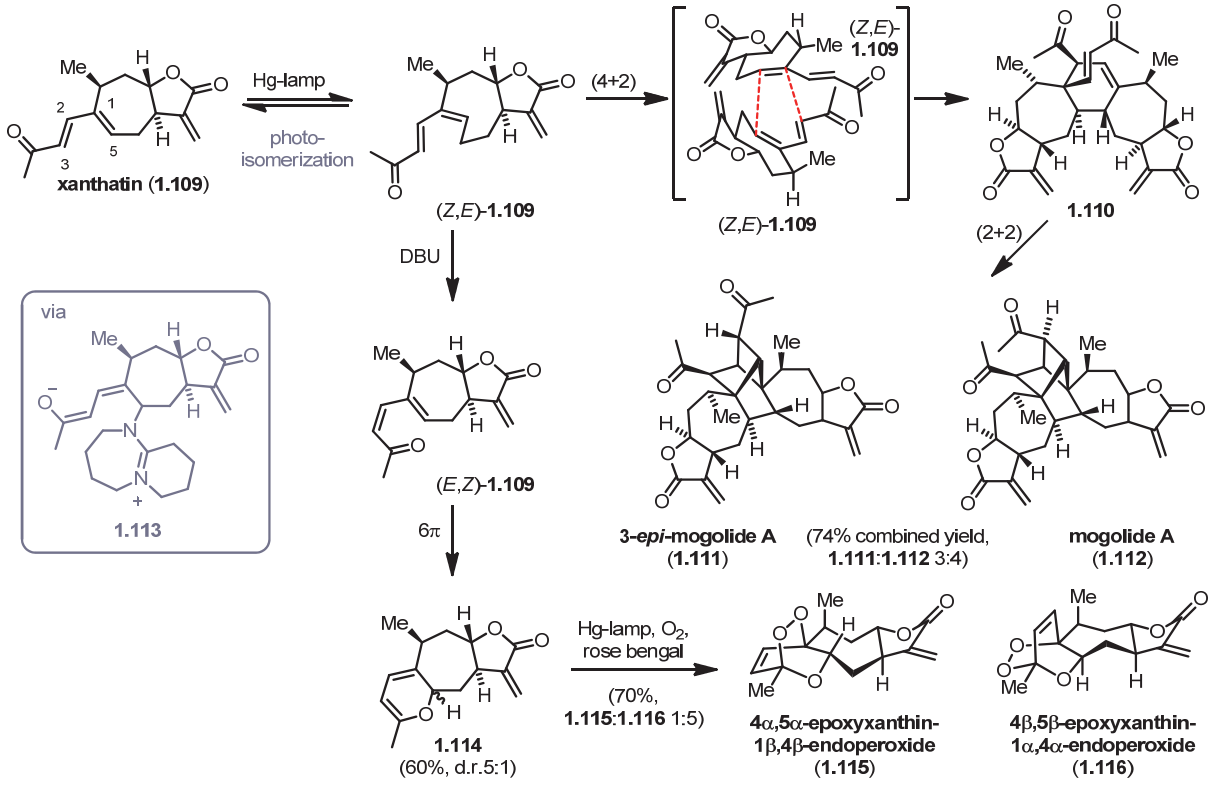

Scheme 1.14 Photoisomerization triggered reaction cascades towards xanthatin dimers.

The use of a photochemical 6π electrocyclization in a biomimetic fashion enabled the formation of granulatimide (**1.117**), a G2 cell cycle checkpoint inhibitor from the Brazilian ascidian *Didemnum granulatum*, after oxidative rearomatization (Scheme 1.15).[55] Furthermore, the γ-pyrone-containing sacoglossan mollusk natural products tridachiahydropyrone (**1.118**) and photodeoxytridachione (**1.120**) were prepared by relying on photomediated electrocyclizations.[56] In the case of **1.120**, it was demonstrated by *in vitro*[57] as well as *in vivo*[58] experiments that this compound is made from 9,10-deoxytridachione (**1.119**) in a photochemical transformation which can be either described as a $[_{\sigma}2_a+_{\pi}2_a]$ elctrocyclization or *via* a triplet biradical mechanism.[59]

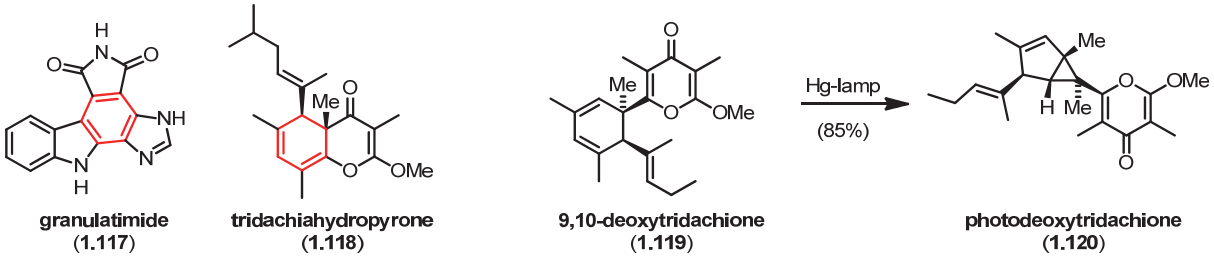

Scheme 1.15 Natural products **1.117**–**1.120** synthesized by biomimetic photochemical electrocyclizations.

1.2.2 Non-biomimetic transformations

Photochemical reactions have been extensively used as non-biomimetic key steps in the synthesis of natural products.[30c,31] In the following chapter, a short selection of total syntheses involving such key steps are described. Firstly, [2+2] cycloadditions and different photochemical cyclizations and rearrangements are presented. The last part of this chapter concerns the use of modern visible light photoredox catalysis in natural product total synthesis.

1.2.2.1 Photochemical [2+2] cycloadditions

One of the most unusual and extraordinary class of cyclobutane-containing natural products is represented by the so called ladderane lipids, which contain up to five condensed cyclobutane rings ([5]-ladderanes) within their backbone (**1.121**, **1.122**, Scheme 1.16a).[60] These compounds were isolated from ammonium-oxidizing bacteria found in the Black Sea, at a water depth of 90 m. The oxidation process of ammonia occurs in a specialized cell compartment (anammoxosome), where toxic intermediates in the form of NH_2NH_2 and NH_2OH are formed. The ladderane lipids constitute a significant fraction of the anammoxosome membrane and are thought to prevent the diffusion of these toxic intermediates into the cytosol by forming densely packed membranes.

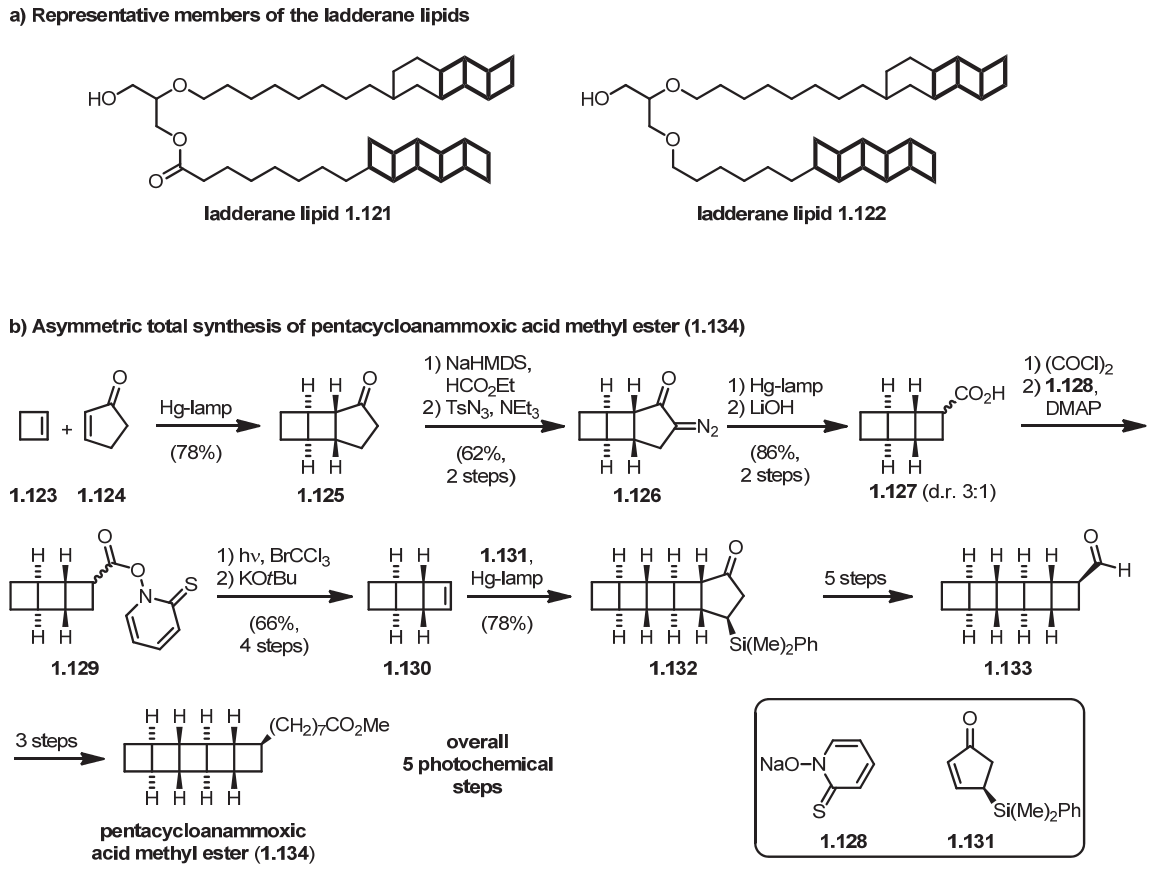

Scheme 1.16 Structure and total synthesis of ladderane lipids by the Corey group.

The Corey group described an efficient asymmetric synthesis of pentacycloanammoxic acid methyl ester (**1.134**, Scheme 1.16b), which was also found in anammox bacteria, starting with a photochemical [2+2] cycloaddition of cyclopentenone (**1.124**) and cyclobutene (**1.123**).[61] The resulting cyclopentanone **1.125** was ring-contracted *via* a sequence of formylation and deformylative Regitz diazo transfer followed by a photochemical Wolff ring contraction of the corresponding α-diazo ketone **1.126** to obtain an epimeric mixture of the [3]-ladderane carboxylic acid **1.127** after saponification. Formation of the acid chloride upon heating with oxalyl chloride and subsequent addition of sodium salt **1.128** led to the formation of Barton ester **1.129**. This labile intermediate was transformed into a secondary bromide under irradiation with a sunlamp *via* a radical decarboxylation to a secondary alkyl radical which was trapped with $BrCCl_3$. Elimination afforded the reactive cyclobutene **1.130**, which was diastereoselectively converted to silane **1.132** by an additional photochemical [2+2] cycloaddition. This adduct **1.132** could be converted into pentacycloanammoxic acid methyl ester (**1.134**) in eight steps including a second Wolff ring contraction to **1.133**. The use of no less than five photochemical key reactions in the whole synthesis demonstrates thereby the synthetic power of photo-induced transformations. Interestingly, the biosynthesis of the ladderane lipids is unknown to date. It seems unlikely that photochemical transformations are involved due to the dark habitat of the bacteria.[62]

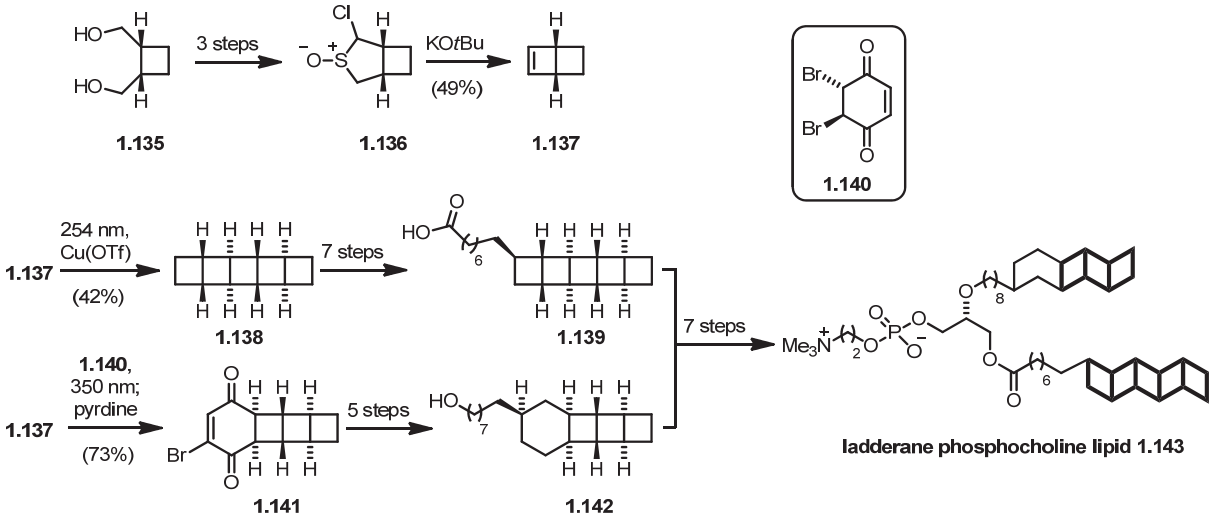

Scheme 1.17 Total synthesis of a ladderane lipid by the Burns group.

In 2016, the Burns group reported on the synthesis of a full phosphatidylcholine ladderane lipid **1.143** containing [3]- and [5]-ladderane moieties (Scheme 1.17).[63] Key to their successful synthesis was the multigram preparation of bicyclo[2.2.0]hexene (**1.137**) using a Ramberg–Bäcklund olefination strategy starting from the maleic anhydride-derived cyclobutandiol **1.135**. Dimerization of **1.137** was performed by irradiation with UV-C light in presence of a copper catalyst, as reported by Kochi and Salomon,[64] to obtain intermediate **1.138**. This intermediate was converted into [5]-ladderanoic acid (**1.139**) relying on an

asymmetric hydroboration and Zweifel olefination. The photochemical dimerization had to be carried out in a benzene matrix at temperatures below 0 °C to suppress the electrocyclic ring opening of **1.137** mediated by the copper catalyst which also occurred in absence of light. Moreover, photochemical [2+2] cycloaddition of bicyclohexene (**1.137**) with dibromide **1.140** provided the [3]-ladderane structure **1.141** after stereoselective deprotonation from the convex face. Within additional five steps, [3]-ladderanol **1.142** could be synthesized which was transformed in a short sequence to ladderane phosphocholine lipid **1.143**. Initial investigations of the biophysical behavior showed facile self-assembly of this lipid to unilamellar vesicles.

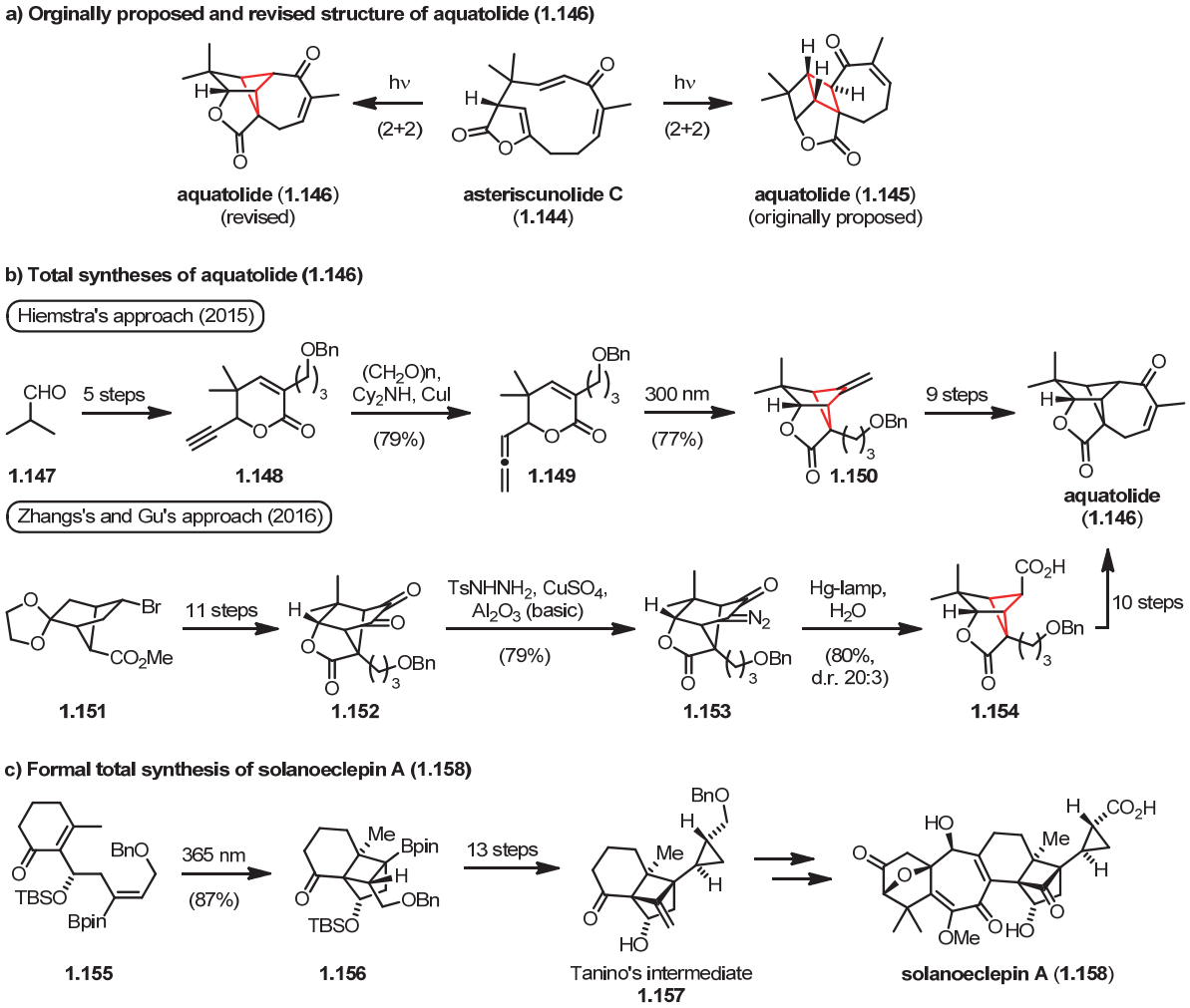

Scheme 1.18 a) Structure and b) total syntheses of aquatolide (**1.146**); c) Formal total synthesis of solanoeclepin A (**1.158**).

Another ladderane-containing structure was originally proposed for aquatolide (**1.145**) in 1989 by San Feliciano and coworkers (Scheme 1.18a).[65] This structure was later revised to bicyclo[2.1.1]hexane **1.146** based on computational calculations and, eventually, confirmed by single-crystal X-ray analysis.[66] The [2]-ladderane structure **1.145** and the

revised structure **1.146** represent regioisomers of the proposed [2+2] cycloaddition of the presumptive biogenetic precursor asteriscunolide C (**1.144**).[67]

The group of Hiemstra reported the first total synthesis of **1.146** by an allene-enone [2+2] cycloaddition of **1.149** to yield intermediate **1.150**, which they converted to the natural product in nine steps using a key Mukaiyama aldol reaction for the closure of the seven-membered ring (Scheme 1.18b).[68] Just recently, Zhang and Gu reported a completely different approach to **1.146** by a late-stage photo-Wolff ring contraction of α-diazo ketone **1.153**, which was derived from diketone **1.152** *via* tosyl hydrazone formation followed by α-elimination.[69] The resulting ring-contracted carboxylic acid **1.154** was transformed to **1.146** by a key epimerization of the stereocenter next to the carbonyl atom and subsequent ring closure by a Nozaki–Hiyama–Kishi reaction.

Hiemstra again reported a formal total synthesis of the intriguing structure of solanoeclepin (**1.158**), a terpenoid hatching agent of the potato cyst nemato, by making use of Tanino's intermediate **1.157** (Scheme 1.18c).[70] In their approach, Hiemstra and coworkers cyclized cyclohexanone **1.155** regio- and diastereoselectively to key intermediate **1.156** under photochemical flow conditions.

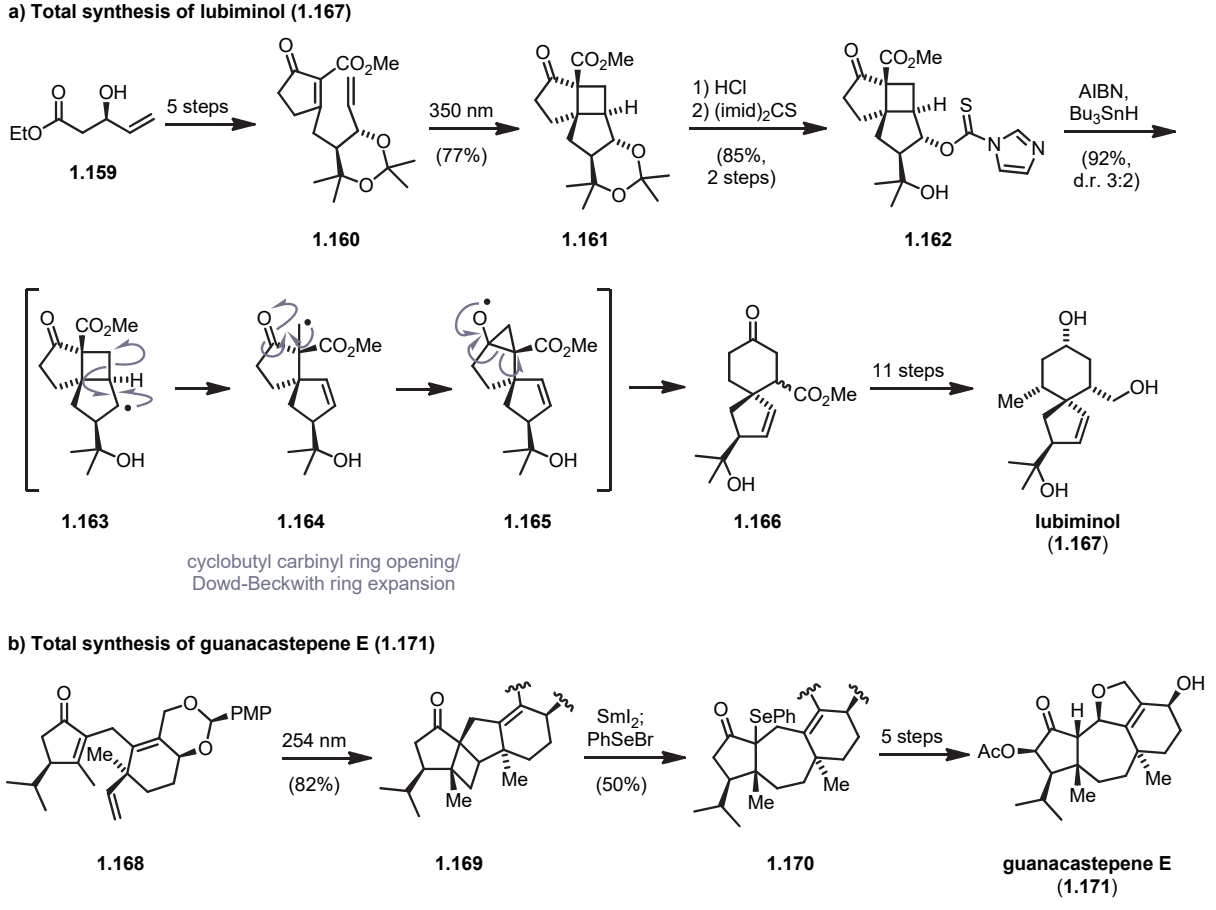

Scheme 1.19 Radical cyclobutane fragmentation in the total synthesis of a) lubiminol (**1.167**) and b) guanacastepene E (**1.171**).

A cyclobutane-containing ring system that is formed *via* intra- or intermolecular cycloaddition can be used to access other complex polycyclic structures by opening of the four-membered ring. As depicted in Scheme 1.19a, Crimmins and coworkers reported a total synthesis of the spirovetivane natural product lubiminol (**1.167**) by a radical cyclobutane opening/rearrangement reaction cascade.[71]

The key enone precursor was synthesized from β-hydroxy ester **1.159** diastereoselectively *via* a zinc homoenolate addition. Irradiation of **1.160** yielded a single diastereomer **1.161** which was converted to thiocarbonyl imidazole **1.162** as a precursor for the radical ring opening. Slow addition of Bu_3SnH to the reaction mixture led to the formation of a secondary cyclobutylcarbinyl radical **1.163** which opened up to primary radical **1.164**. At this stage of the mechanism, a radical ring expansion, originally described by Dowd and Beckwith,[72] took place with an initial attack of the primary radical onto the carbonyl group. The resulting bicyclo[3.1.0]hexane-1-oxyl radical **1.165** is immediately fragmented to obtain the desired spirocyclic compound **1.166** after hydrogen atom transfer from Bu_3SnH. No diastereoselectivity in the hydrogen transfer was observed, delivering **1.166** in a 3:2 diastereomeric mixture. With key intermediate **1.166** in hand, it was possible to finish the synthesis of lubiminol (**1.167**) in eleven steps.

Another reductive radical fragmentation was used as a key reaction for the synthesis of guanacastepene E (**1.171**) by Sorensen and coworkers (Scheme 1.19b).[73] The corresponding radical fragmentation precursor **1.169** was obtained by intramolecular [2+2] cycloaddition of enone **1.168**. Treatment of the obtained cyclobutane **1.169** with SmI_2 generated a ketyl radical anion and a subsequent opening of the cyclobutylcarbinyl radical to the required seven-membered ring. The intermediate samarium enolate that is formed by a second reduction was quenched with PhSeBr. The selective fragmentation of the exocyclic cyclobutane bond can be explained by its almost parallel orientation towards the π-system of the carbonyl group. The introduction of the selenyl ether into **1.170** provided a regioselective handle for the further functionalization to guanacastepene E (**1.171**) in five steps.

1.2.2.2 Other photochemical cycloadditions, rearrangements and electrocyclizations

The excitation of a carbonyl group **1.172** can lead to several reaction pathways involving cleavage of C–C and C–H bonds which are referred as the Norrish fragmentations (Scheme 1.20). Norrish type I reactions involve the cleavage of the bond between the carbonyl C-atom and one of the α-C-atoms, whereas the reaction outcome after the first bond cleavage depends on the exact nature of the starting material.[30c,74]

Decarbonylative recombination to **1.175**, C–H abstraction/alkene **1.177** formation and ketene **1.178** or carbene **1.176** formation are possible. A Norrish type II reaction is characterized by an intramolecular γ-hydrogen abstraction forming a 1,4-biradical **1.180**

which can fragment either to a carbonyl **1.183** and an alkene compound **1.182**, or in the case of a Norrish–Yang cyclization, close up to a cyclobutanol **1.181**.[30c,75]

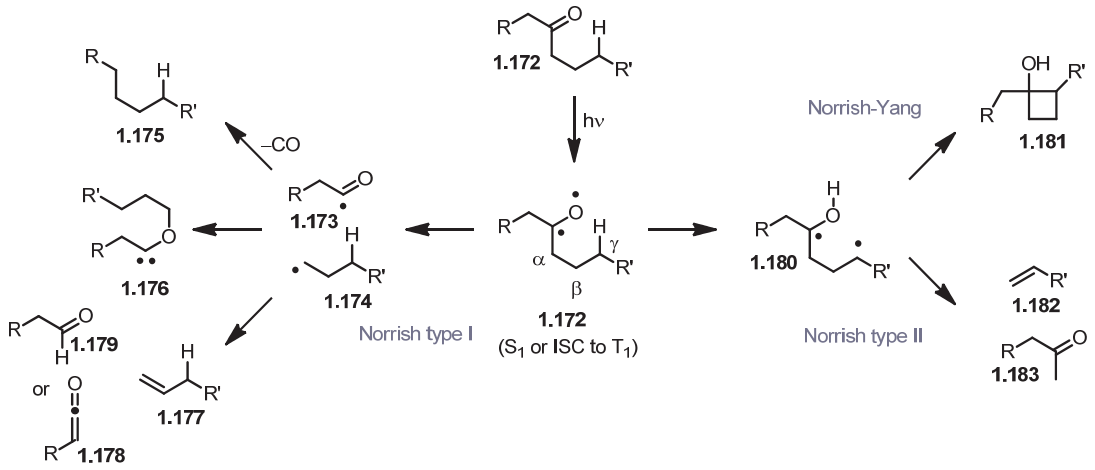

Scheme 1.20 Norrish fragmentations of carbonyl compounds.

A Norrish type I reaction was used by Iwabuchi and coworkers in their synthesis of the sesquiterpenoid juvabione (**1.186**, Scheme 1.21a).[76] When ketone **1.184**, synthesized by an asymmetric intramolecular aldol reaction, was irradiated, the desired C–C bond cleavage occurred followed by C–H abstraction and formation of the unsaturated aldehyde **1.185**.

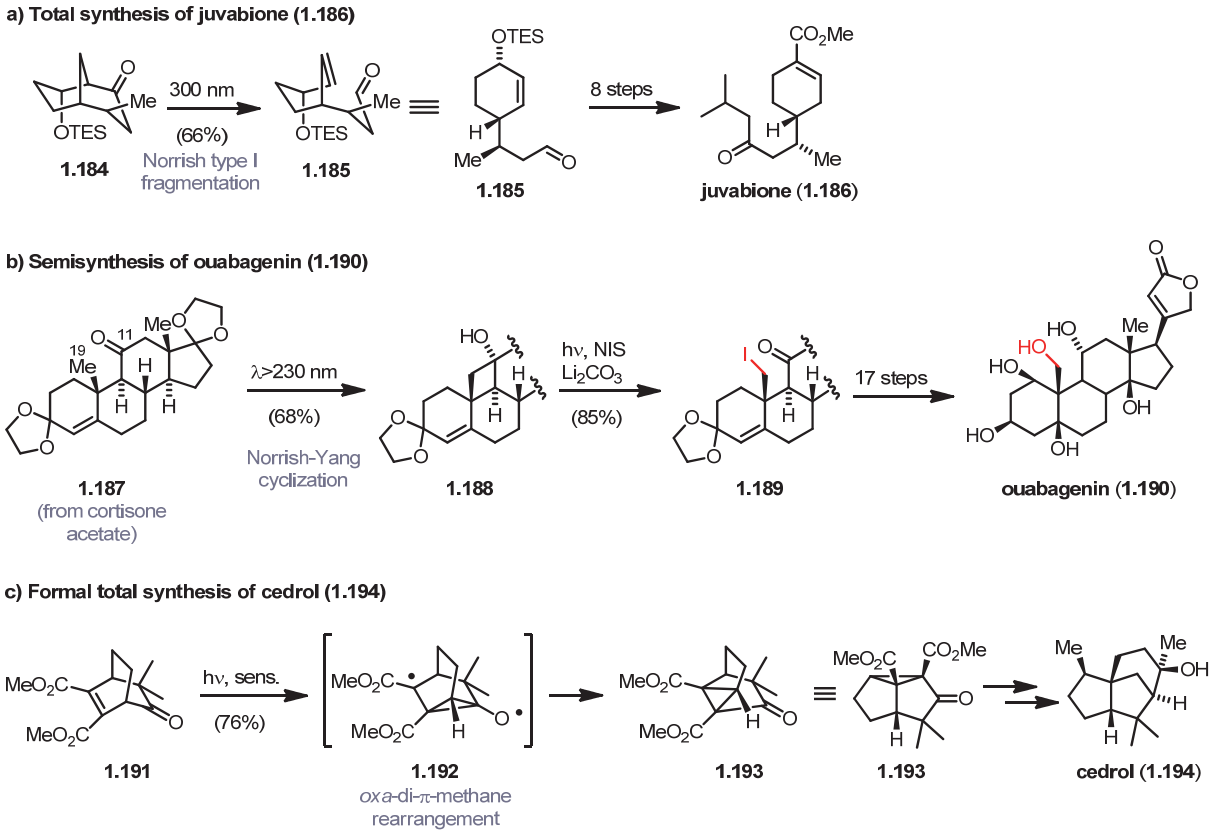

Scheme 1.21 Use of photochemical fragmentations in the total synthesis of natural products.

In addition, Norrish–Yang cyclizations have been used in the synthesis of natural products, exemplified by Baran's work on the semisynthesis of the aglyconic cardiotonic steroid ouabagenin (**1.190**, Scheme 1.21b).[77] Starting from ketal **1.187**, the C19 oxidation could be achieved by Norrish–Yang cyclization to cyclobutanol **1.188**. Interestingly, in order to suppress competitive Norrish type I side reactions, the irradiation of **1.187** had to be carried out in the solid state as an aqueous suspension. Cyclobutanol **1.188** could be opened *via* an unstable hypoiodite species under photochemical conditions. Selective homolysis of the C11–C19 bond and radical recombination afforded the desired iodide **1.189** which was converted to ouabagenin (**1.190**).

Yates and Stevens applied an *oxa*-di-π-methane rearrangement (Scheme 1.21c), which generally occurs upon triplet sensitization of a β,γ-unsaturated ketone,[46] in the formal synthesis of the cedranoid sesquiterpene cedrol (**1.194**).[78] Using acetophenone as a solvent and triplet sensitizer, irradiation of **1.191** led to cyclopropane **1.193** *via* sensitization of the carbonyl group followed by generation of biradical intermediate **1.192**. Six additional steps converted this key compound to an intermediate of the cedrol synthesis of Stork and Clark.[79]

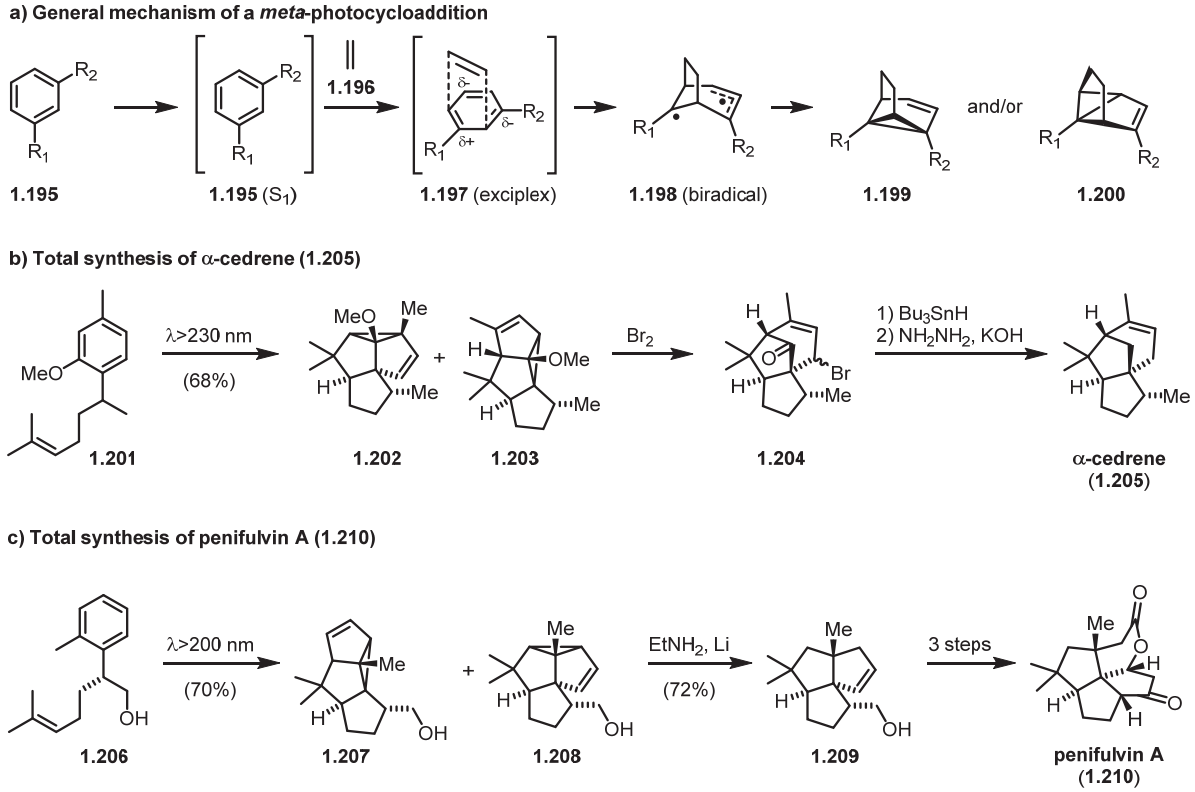

Scheme 1.22 Use of *meta*-photocycloadditions in the total synthesis of natural products.

Another cedranoid sesquiterpene, α-cedrene (**1.205**), was synthesized by Wender using arene photocycloaddition (Scheme 1.22b).[80] In general, upon excitation of an arene in the presence of an alkene or an alkyne, three different cyclization modes, *ortho*, *meta* and *para*, are possible.[81] However, only the *meta*-photocycloaddition is of synthetic use, forming

three new rings and up to six stereocenters in a single step. It has been extensively applied in the field of natural product synthesis.[82] From a mechanistic point of view, irradiation with UV light leads to an excitation of the aromatic system **1.195** to the excited singlet state **1.195** (S_1) which forms a polarized exciplex adduct **1.197** with an inter- or intramolecular alkene **1.196** controlling the regioselectivity by the optimal stabilization of the partial charges (Scheme 1.22a). From **1.197**, a biradical **1.198** is formed which can in general recombine to the cyclopropyl-containing allylic regioisomers **1.199** and **1.200**.

In his synthesis of **1.205**, Wender irradiated arene **1.201** to obtain the two isomeric photocycloadducts **1.202** and **1.203**. Both compounds could be converted to bromide **1.204** by cyclopropane cleavage induced by a nucleophilic attack of the alkene onto bromine. Reduction of the C–Br bond and removal of the carbonyl group under Wolff-Kishner conditions afforded α-cedrene (**1.205**).

The *oxa*-fenestrane insecticide penifulvin A (**1.210**), isolated from the fungus *Penicillium griseofulvum*,[83] was synthesized by Mulzer and Gaich through application of a *meta*-photocycloaddition of arene **1.206** (Scheme 1.22c).[84] Asymmetric formation of **1.206** was possible by Myers alkylation. The resulting regioisomers **1.207** and **1.208** could be separated and **1.208** was ring opened under Birch conditions to deliver key intermediate **1.209** which was transformed to the natural product **1.210** within three steps. This strategy allowed for the generation of the triquinane structure of **1.210** in just eight steps in an asymmetric fashion.

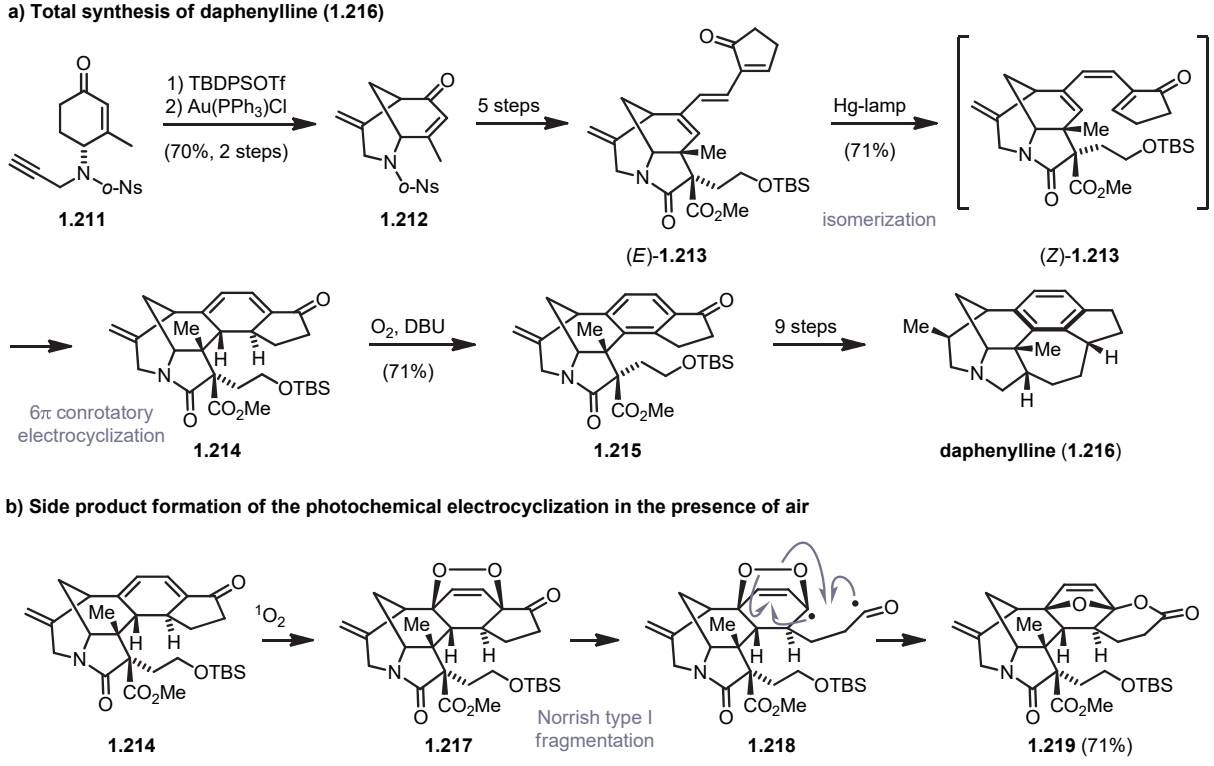

Scheme 1.23 Photochemical transformations in the total synthesis of daphenylline (**1.216**).

The *daphniphyllum* alkaloid daphenylline (**1.216**), isolated from the fruit bodies of *D. longeracemosum*,[85] contains an intriguing tetrasubstituted arene core unique among this class of natural products (Scheme 1.23a). Li and coworkers synthesized this structural element using a photochemical isomerization/6π-electrocyclization/aromatization sequence.[86] Starting from sulfonamide **1.211**, the central bicyclic core of **1.216** was generated *via* a gold catalyzed 6-*exo*-dig Conia-ene reaction. The resulting ketone **1.212** was put forward to triene (*E*)-**1.213** which underwent *E*/*Z*-isomerization to (*Z*)-**1.213** followed by a conrotatory electrocyclization under photochemical conditions. Thermal conditions for the electrocyclization failed, presumably due to steric hindrance in the disrotatory cyclization by forming a *cis*-substituted cyclohexadiene. Aromatization was observed by treatment with DBU under an oxygen atmosphere. The first total synthesis of **1.216** could be finished in just nine additional steps. Interestingly, attempts for direct oxidative aromatization in the electrocyclization step under air failed, delivering a single side product **1.219** (Scheme 1.23b). The formation of this compound was rationalized by an initial singlet oxygen [4+2] cycloaddition of **1.214** followed by a Norrish type I fragmentation of **1.217**. The resulting biradical **1.218** is able to form lactone **1.219** through the homolytic cleavage of the O–O bond.

1.2.2.3 Visible light photoredox catalysis

As mentioned in chapter 1.1, redox catalysis under the irradiation of visible light using organic dyes and transition metal complexes is a modern and growing field in photochemistry.

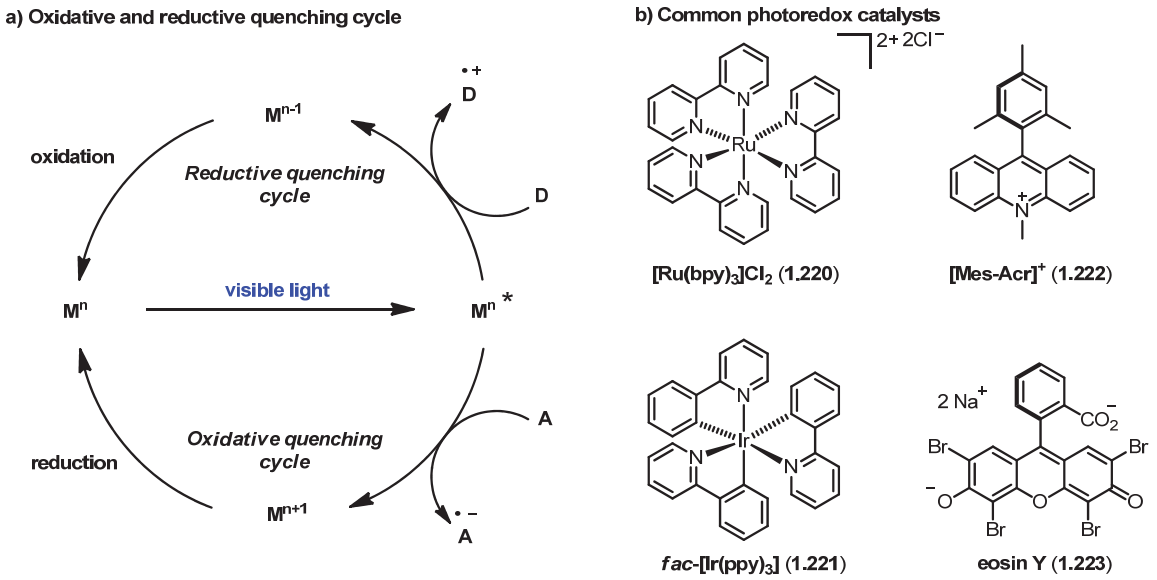

Scheme 1.24 a) General photocatalytic cycles; b) Common photoredox catalysts **1.220**–**1.223**.

Consequently, several total syntheses were reported within the last years relying on the radical pathways initiated under mild conditions.[21b,30c] Generally, the reaction pathway can be described either by an oxidative quenching cycle generated by single electron transfer from an excited, long-lived triplet state of the catalyst to an acceptor molecule forming a radical anion or by a reductive quenching cycle forming a radical cation of a donor compound by single electron transfer (Scheme 1.24a). In each case, the catalytic cycle has to be closed by reduction or oxidation of the catalyst. Common organic and transition metal complex photocatalysts **1.220**–**1.223** are depicted in Scheme 1.24b.

A powerful tertiary radical formation enabled Overman to make the difficult C8–C14 bond in the synthesis of the spongian diterpenoid aplyviolene (**1.231**, Scheme 1.25a).[87] In an earlier approach, an enolate Michael addition was used for this crucial bond formation whereas the carbonyl group, essential for the enolate formation, had to be removed afterwards.[88] This could be circumvented by the synthesis of *N*-acyloxyphthalimide **1.225** from fenchnone (**1.224**). Conversion of this compound in the presence of a photocatalyst **1.220** and Hantzsch ester **1.226** led to radical anion **1.227**, which generated the tertiary radical **1.228** under the extrusion of CO_2. A 1,4-addition with enone **1.229** afforded the coupling product **1.230**, which was converted by analogy with the earlier synthesis into aplyviolene (**1.231**). A similar generation of tertiary radicals from the corresponding alcohol

via the *N*-phthalimidoyl oxalates or the cesium oxalates was recently described by the same group.[89]

Another intermolecular coupling reaction mediated by visible light photoredox catalysis, reported by the Stephenson group, is highlighted in Scheme 1.25b. In their synthesis of the hexahydropyrroloindole alkaloid gliocladin C (**1.236**), the authors used a photoredox catalytic reductive dehalogenation of bromopyrrolindoline **1.232** to generate the benzylic radical **1.233**.[90] In the presence of indole **1.234**, the desired coupling product **1.235** was observed. The introduction of the aldehyde group, which was removed by Tsuji–Wilkinson decarbonylation, was necessary to block the C2 position.[91] In just five additional steps, the total synthesis of gliocladin C (**1.236**) could be completed.

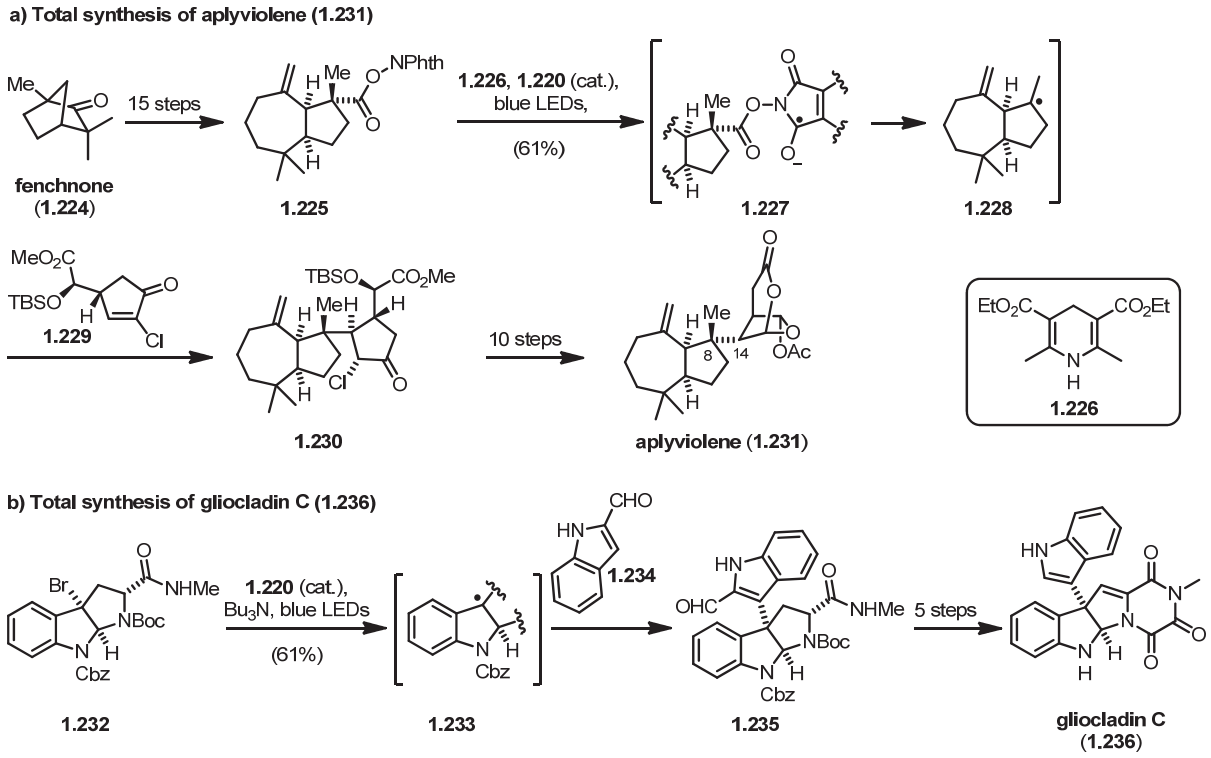

Scheme 1.25 Photoredox catalysis in natural product total synthesis.

To conclude, photochemical transformations have been extensively used by synthetic chemists to generate complex structures, particularly in the field of natural product total synthesis. Furthermore, biomimetic syntheses have exploited photochemical conversions observed in nature to access secondary metabolites in an efficient way. More recently, the field of photoredox catalysis has led to a new era of synthetic photochemistry independent of high energy UV irradiation and expensive lamps or reaction setups.

2 NON-BIOMIMETIC AND BIOMIMETIC TOTAL SYNTHESIS OF APLYDACTONE

2.1 Introduction

2.1.1 Isolation and structure

The opistobranch mollusks of the genus *Aplysia* have been a rich source of bioactive natural products including a considerable proportion of organohalogens (Figure 2.1a).[92] The content of halogenated natural products found in all sea slugs mainly depends on their diet which largely consists of the red algae *Laurencia* and cyanobacteria on the seaweed.[92a,93] Furthermore, this quite abundant genus of algae is a known source of halogenated natural products including a class of spiro[5.5]undecane sesquiterpenoids, called chamigranes (Figure 2.1b).[94] It is proposed that the mollusks which live in the shallow seawater of tropical regions use this natural source of bioactive and cytotoxic compounds, which they chemically modify and store in their digestive gland, as a defensive strategy against various predators.

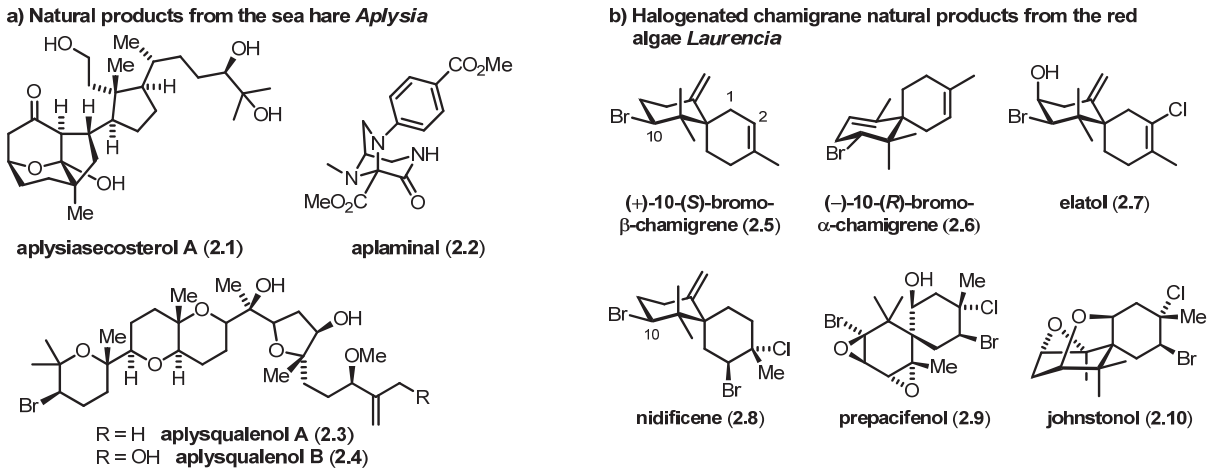

Figure 2.1 a) Natural products **2.1**–**2.4** from the sea hare *Aplysia*; b) Chamigranes **2.5**–**2.10** from the red algae *Laurencia*.

In 2001, Stonik and coworkers reported the isolation of aplydactone (**2.11**, Figure 2.2a), a complex brominated sesquiterpeniod with a low molecular weight, from the sea hare *Aplysia dactylomela*.[95] The biological specimens had been already collected in 1986 at the northern coast of Madagascar in a water depth of 3−5 m. Nevertheless, it took more than a decade to elucidate the structure of **2.11** which was finally confirmed by single-crystal X-ray analysis (Figure 2.2a). In addition, the Stonik group isolated several brominated chamigrane natural products from the same source including the anticancer compound dactylone (**2.12**) and its epimer 10-*epi*-dactylone (**2.13**, Figure 2.2b).[96] Furthermore, debromochamigrene **2.14**

is proposed to be biosynthetically derived from dactylone (**2.12**) as the result of a bromide elimination, [1,2]-methyl shift and subsequent *exo*-methylene formation.[96d]

The structure of aplydactone (**2.11**) contains a unique tetracyclo-[4.4.2.$0^{1,6}$.$0^{3,11}$]dodecane skeleton which possesses an unprecedented [2]-ladderane moiety. As previously mentioned, condensed cyclobutane structures are scarce in nature's repertoire of structural elements, and the [3]- and [5]-ladderane containing lipids described in chapter 1.2.2.1 represent, to the best of our knowledge, the only other natural product class with this feature. Furthermore, **2.11** is a halogenated natural product with a sterically encumbered secondary neopentylic bromide and contains five stereocenters, three of which are quaternary. A *gem*-dimethyl moiety, contiguous to two of the quaternary stereocenters, increases the steric hindrance within the structure.

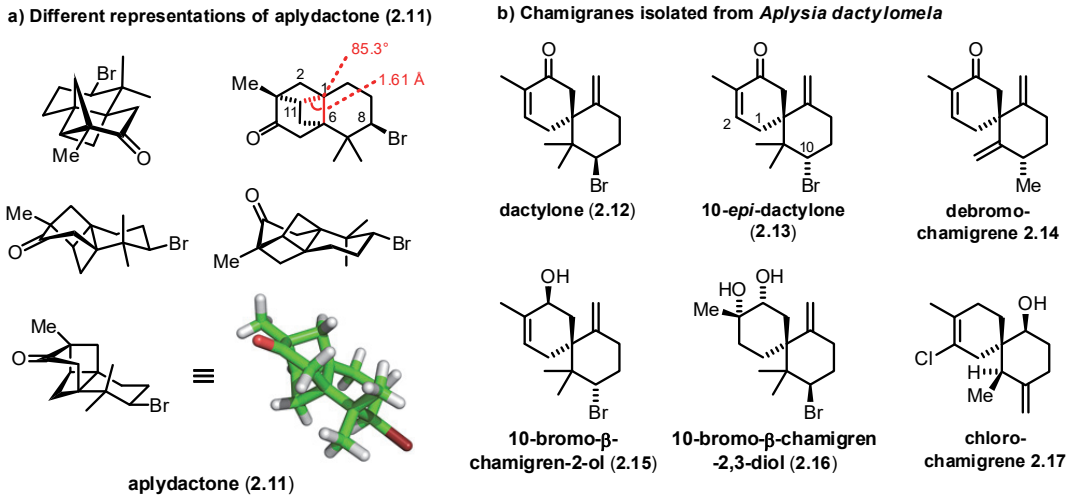

Figure 2.2 a) Structure of aplydactone (**2.11**); b) Chamigranes **2.12**–**2.17** isolated from *Aplysia dactylomela*.

Careful inspection of the bond angles and bond lengths within the compressed core structure of **2.11** reveals a large aberrance from the usual values of puckered cyclobutanes. The longest bond is the C1–C6 connection with a value of 1.61 Å, which is significantly longer than 1.55 Å found in an isolated cyclobutane (Figure 2.2a). Furthermore, a bond angle of just 85.3° is found for the C11–C1–C6 bond angle, reflecting the highly compressed and sterically hindered core structure.

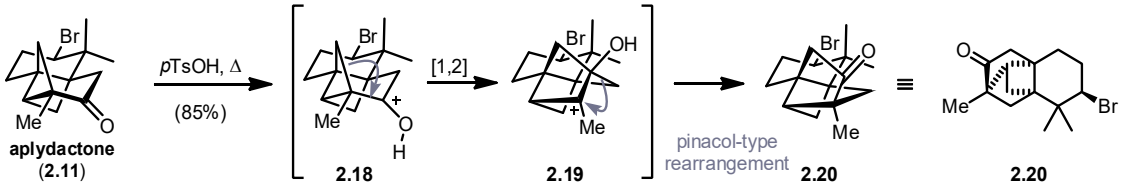

Scheme 2.1. Strain-releasing rearrangement of aplydactone (**2.11**) to isomer **2.20**.

Consequently, aplydactone (**2.11**) readily rearranges to the less strained polycycle **2.20** upon treatment with *p*TsOH (Scheme 2.1).[95] The mechanism was described as a rearrangement cascade and involves an initial protonation of the carbonyl oxygen followed by a Wagner–Meerwein shift to obtain carbocation **2.19** as an intermediate. A pinacol-type [1,2]-shift delivers isomer **2.20** as a single compound.

2.1.2 Biosynthesis

The spirocyclic core structure of chamigrane natural products isolated from the mollusk genus *Aplysia* is presumably synthesized by the red algae *Laurencia* that constitutes the main diet for these sea hares. For the biosynthesis of spirocyclic [5.5]undecane sesquiterpenoids, a bromonium cation-induced cyclization of a farnesyl precursor has been proposed. Biomimetic approaches towards α- and β-chamigranes supporting this hypothesis have been reported (Scheme 2.2). Faulkner and coworkers could diastereoselectively cyclize geranylacetone (**2.21**) to the bicyclic ether **2.23** *via* the intermediate bromonium cation **2.22** (Scheme 2.2a).[97] Tertiary alcohol **2.24**, derived from the cyclization product **2.23**, formed 10-bromo-α-chamigrene (**2.6**) under acidic conditions. However, an alternative cyclization mode was reported by Martin and coworkers in their bioinspired synthesis of 10-bromo-β-chamigrene (**2.5**) based on a bromonium-induced spirocyclization of intermediate **2.26** (Scheme 2.2b).[98]

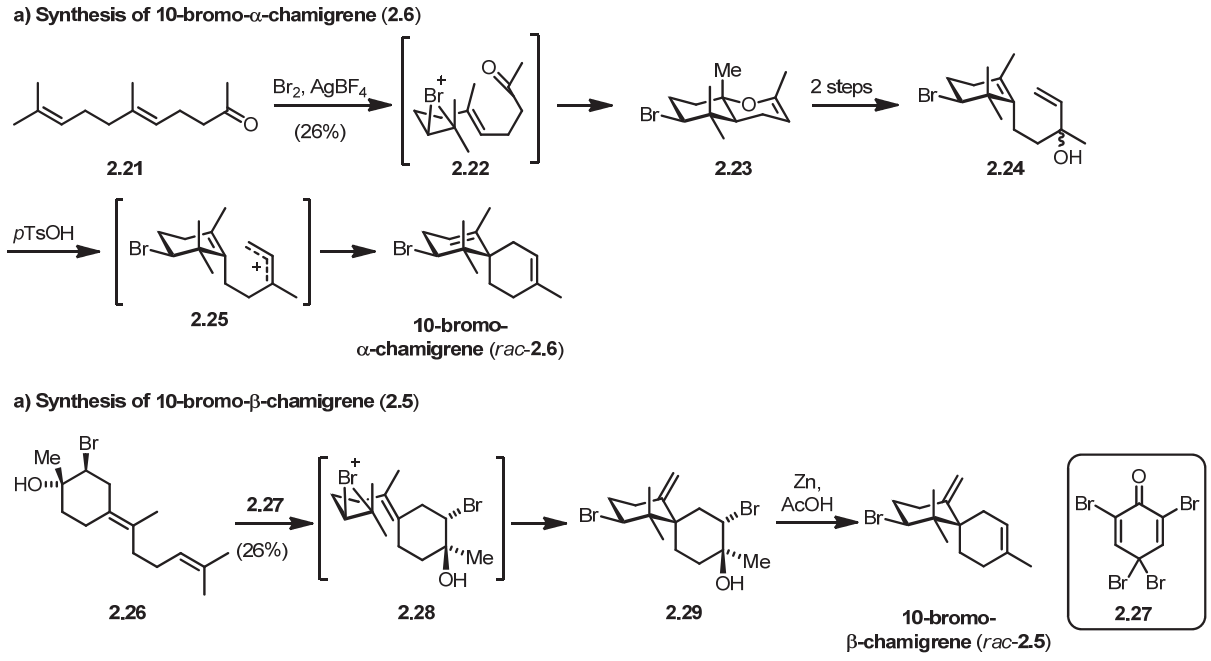

Scheme 2.2. Biomimetic approaches towards chamigranes **2.6** and **2.5**.

As a result of these observations, two possible biosynthetic pathways for the formation of C10-brominated chamigranes can be formulated depending on the order of ring formation, as depicted in Scheme 2.3.[97b,99] Nucleophilic attack of the trisubstituted double

bond of farnesyl pyrophosphate (**2.30**, FPP) onto a formal Br^+-species and subsequent cyclization delivers bromomonocyclofarnesyl pyrophosphate (**2.32**) *via* the formation of bromonium cation **2.31**. Upon expulsion of pyrophosphate, allylic cation **2.25** is formed which is prone to formation of spirocycle **2.5**. However, it is also feasible that FPP (**2.30**) first cyclizes to γ-bisabolene (**2.34**) followed by a subsequent bromonium-induced spirocyclization to 10-(*S*)-bromo-β-chamigrene (**2.5**). In general, the bromonium cation or a synthetic equivalent (HOBr, Br_3^-, Enz-Br^+) is most likely provided by a haloperoxidase, or more specifically by a vanadium-dependent haloperoxidase (chapter 3).[100] To date, just the 10-(*S*)-enantiomer of **2.5** has been isolated from several *Laurencia* species. However, different chamigranes with *R*-configuration at this stereocenter have been reported.[94a]

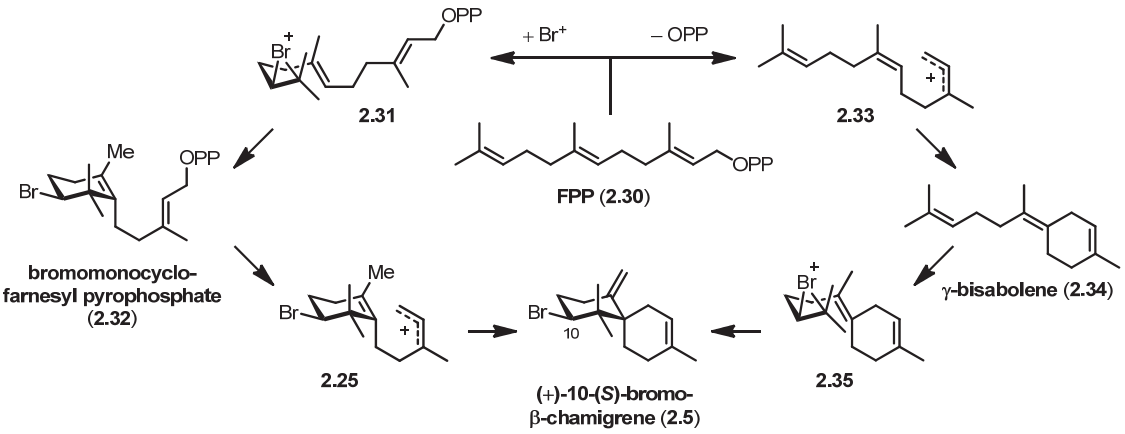

Scheme 2.3. Proposed biosynthesis of 10-(*S*)-bromo-β-chamigrene (**2.5**).

The concomitant isolation of dactylone (**2.12**) and 10-*epi*-dactylone (**2.13**) from *Aplysia dactylomela* suggests a biosynthetic hypothesis where both metabolites are formed by modification of a chamigrane precursor ingested as part of the diet. Allylic oxidation of naturally occurring **2.5**, followed by subsequent oxidation to the enone system would generate 10-*epi*-dactylone (**2.13**, Scheme 2.4a). Starting from the enantiomeric 10-(*R*)-bromo-β-chamigrene (*ent*-**2.5**), which has yet to be isolated, allows for the biosynthesis of dactylone (**2.12**). At first, diol **2.16**, isolated from the same mollusk, could be formed by a diastereoselective dihydroxylation. From this intermediate, a two-step procedure including oxidation of the secondary alcohol and elimination of the tertiary alcohol to the α,β-unsaturated ketone would afford the natural product **2.12**. In general, the existence of the enantiomeric 10-bromo-β-chamigrenes **2.5** and *ent*-**2.5** can be either explained *via* a nonselective bromonium-induced cyclization *via* a formal Br^+-species outside the active site of the haloperoxidase or by the existence of two haloperoxidases which deliver enantioselectively one of the cyclized brominated chamigrane intermediates **2.5** and *ent*-**2.5**. Face-selective and racemic bromination–cyclization modes of vanadium dependent

haloperoxidases in the biosynthesis of terpenoids were recently reported by Butler and coworkers.[101]

Due to the shallow seawater habitat of *Aplysia dactylomela* in tropical and subtropical regions with high intensity of solar irradiation, it is reasonable to consider a photochemical [2+2] cycloaddition for the formation of the ladderane structure within aplydactone (**2.11**). Therefore, irradiation exciting the enone moiety of dactylone (**2.12**) could deliver the ladderane structure of **2.11** (Scheme 2.4b). However, the less strained "rule of five" product (Chapter 1.1), called isoaplydactone (**2.36**) would be feasible by regioisomeric photocycloaddition. Nonetheless, this compound has not been isolated yet from any natural source. By analogy, 10-*epi*-dactylone (**2.13**) could cyclize under solar irradiation to provide the ladderane containing 8-*epi*-aplydactone (**2.38**) or the "rule of five" product 8-*epi*-isoaplydactone (**2.37**).

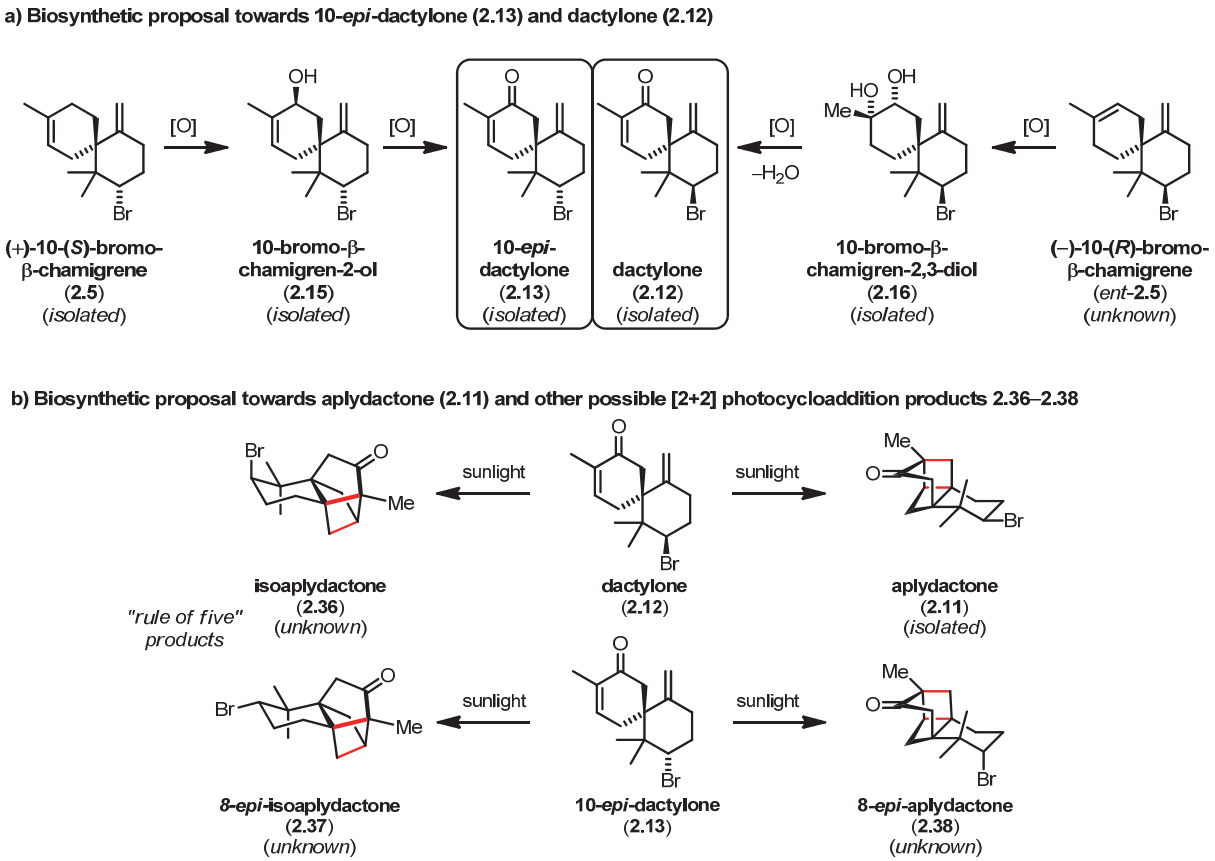

Scheme 2.4 a) Proposed biosynthesis of dactylone (**2.12**) and 10-*epi*-dactylone (**2.13**); b) Possible photocycloaddition products of dactylone (**2.12**) and 10-*epi*-dactylone (**2.13**).

Stonik and coworkers attempted to cyclize dactylone (**2.12**) under UV irradiation, which did not yield any desired product.[95] However, no detailed reaction conditions including wavelengths, solvent, temperature or reaction time were reported.

2.1.3 Project outline

Aplydactone (**2.11**) and the epimeric chamigranes dactylone (**2.12**) and 10-*epi*-dactylone (**2.13**) represent a unique and challenging target for total synthesis and, at the beginning of this project, no completed synthesis for any of these products had been reported.[102] Above all, the unprecedented [2]-ladderane scaffold condensed onto a decalin system within the carbon framework of **2.11** was expected to cause several difficulties in its preparation. Furthermore, the low degree of functionalization present in **2.11** severely limited the possible retrosynthetic disconnections.

Therefore, we planned to access aplydactone (**2.11**) by two approaches. At first, we aimed to synthesize the complex core structure of **2.11** in a non-biomimetic approach by disconnection of either bond a and b (chapter 2.2.1.1–2.2.1.2) or c and d (chapter 2.2.1.3–2.2.1.6) relying on established methodology for the synthesis of cyclobutanes and ladderanes (Figure 2.3 left).

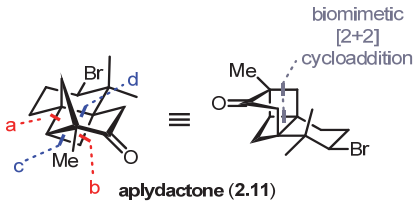

Figure 2.3 Planned non-biomimetic (left) and biomimetic (right) retrosynthetic bond disconnections.

In addition, we wanted to synthesize the biomimetic precursor dactylone (**2.12**), and its epimer **2.13**, to prove if irradiation of **2.12**, as reported by Stonik, is not able to deliver **2.11** (Scheme 2.3 right). However, we were concerned about the reported investigations, since the presence of a secondary alkyl bromide within the photoprecursor **2.12** could enable possible degradation pathways under irradiation with UV-light, especially if non-biomimetic wavelengths were chosen. Furthermore, we were interested if the other possible cyclization products **2.36**–**2.38** might be observable under carefully designed reaction conditions. This purpose rendered a synthesis of both compounds, **2.12** and **2.13**, essential and was intended to be achieved in a diastereodivergent manner.

To support our experimental work with theoretical investigations, computational calculations on the excited states of dactylone (**2.12**) and 10-*epi*-dactylone (**2.13**) were absolutely crucial and performed by our collaborators Dr. Patrick Kölle and Prof. Dr. Regina de Vivie-Riedle at the Ludwig-Maximilians Universität, Munich.

2.2 Results and discussion

2.2.1 Non-biomimetic total synthesis of aplydactone

2.2.1.1 First generation approach – Retrosynthetic analysis

The initial approach for the synthesis of aplydactone (**2.11**) is depicted in Scheme 2.5. It was envisioned to access **2.11** *via* a final intramolecular alkylation of intermediate cyclobutyl cation **2.39**, which should undergo a ring closure with the methyl vinyl ether moiety. Two ideas for the generation of the cyclobutyl cation **2.39** were elaborated. On the one hand, **2.39** could be generated by a cyclopropylcarbinyl-cyclobutyl rearrangement starting from the corresponding cyclopropylcarbinol intermediate **2.40**.[103] For the diastereoselective formation of **2.40** the best solution would be an intramolecular cyclopropanation of diazo compound **2.41** accessed from **2.42**.[104] On the other hand, cationic intermediate **2.39** can be traced back to cyclobutanone **2.43**, which should be accessible *via* intramolecular ketene [2+2] cycloaddition of **2.44**.[105]

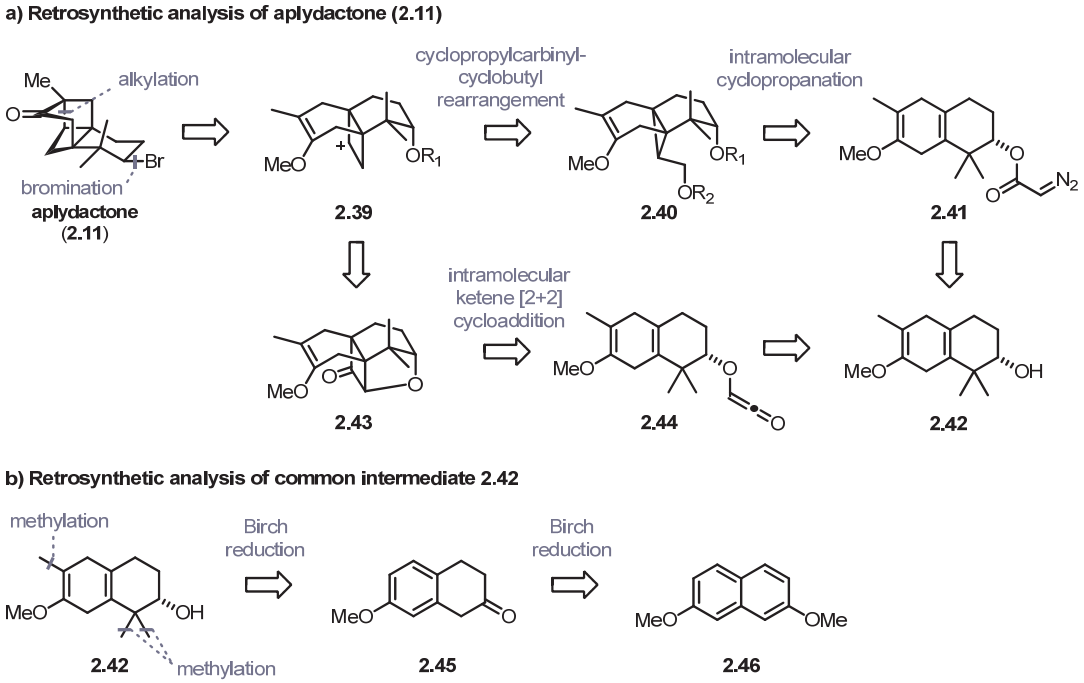

Scheme 2.5. Retrosynthetic analysis of a) aplydactone (**2.11**) and b) common intermediate **2.42**.

The advantage of this retrosynthetic analysis is that intermediate **2.42**, used for both synthetic pathways, could be synthesized *via* Birch reduction of tetralone **2.45** derived from naphthalene **2.46**.

2.2.1.2 Cyclopropanation and ketene cycloaddition towards aplydactone

The synthesis commenced with the preparation of methyl vinyl ether **2.42** (Scheme 2.6) starting from 2,7-dimethoxynaphthalene (**2.46**). Hydrolysis of the intermediate methyl

vinyl ether obtained from the Birch reduction of **2.46** afforded 2-tetralone **2.45**, which could be dimethylated in the α-position of the ketone upon treatment with methyl iodide and potassium hydroxide in a biphasic system.[106] Initial attempts to introduce the methyl group on the aromatic ring by formylation and subsequent reduction failed. Therefore, **2.47** was selectively brominated with NBS followed by Negishi cross coupling with dimethylzinc to obtain trimethylated tetralone **2.48** in gram quantities.[107]

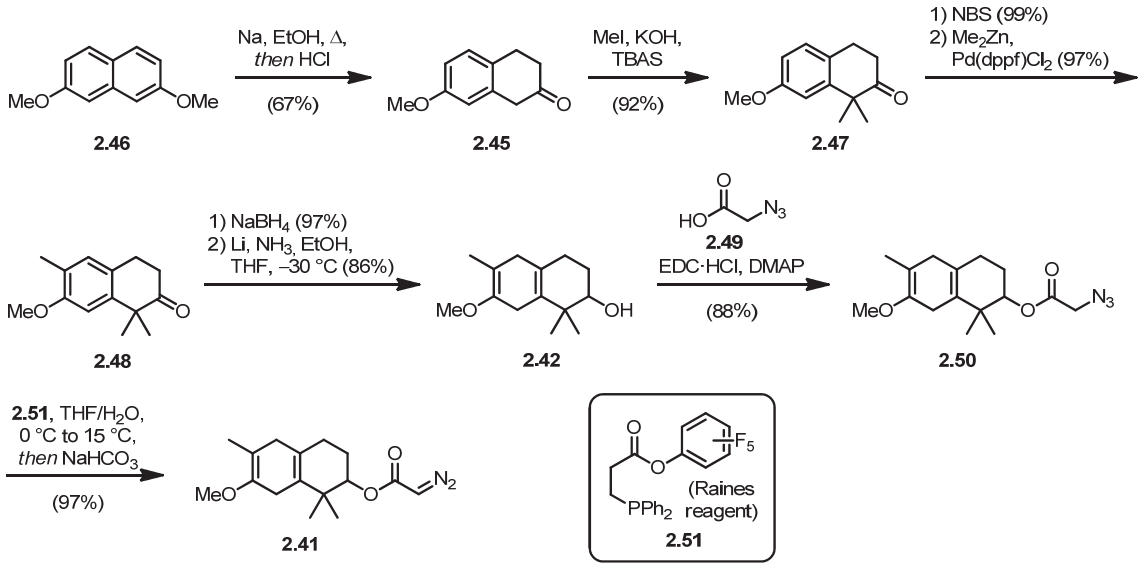

Scheme 2.6. Synthesis of key diazo compound **2.41**.

The asymmetric reduction of tetralone systems like intermediate **2.47** were reported,[108] however we decided to use racemic material in preliminary investigations of this synthetic route. Therefore, ketone **2.48** was reduced with $NaBH_4$ and a subsequent second Birch reduction provided the desired cyclohexadiene **2.42** in good yield.[109]

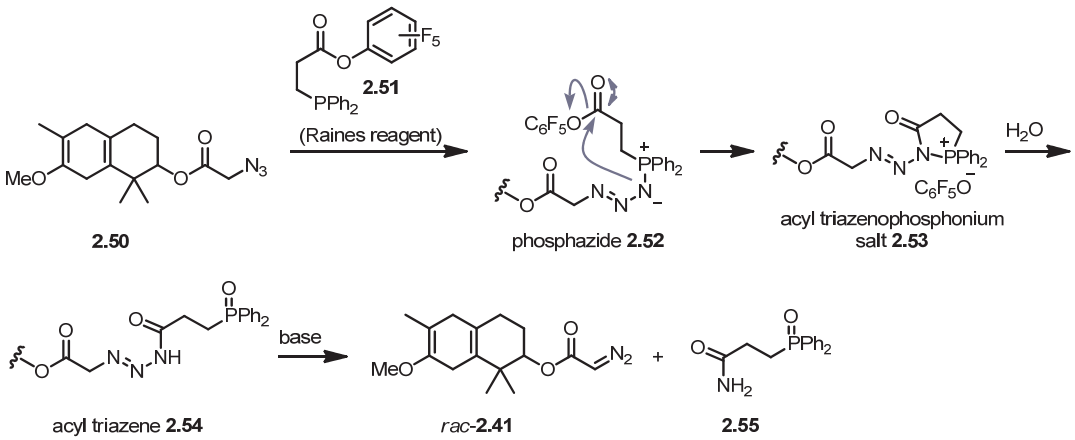

Scheme 2.7. Mechanism of the formation of diazo compound **2.41** under Raines conditions.

With compound **2.42** in hand, several literature known procedures for the formation of α-diazo esters and acetates were tested.[110] To this end, a methodology, introduced by

Raines and coworkers for the conversion of azides to diazo compounds, provided the desired compound **2.41** in excellent yield.[111] Alcohol **2.42** was esterified in the presence of α-azido acid **2.49** and EDC·HCl followed by treatment of the azide **2.50** with Raines reagent **2.51**. In order to obtain high yields, the initial temperature of the reaction had to be kept below 15 °C. From a mechanistic point of view, this reaction is proposed to start with the formation of phosphazide **2.52** which is trapped due to the reactive ester functionality as acyl triazenophosphonium salt **2.53** (Scheme 2.7).[111a] Hydrolysis of **2.53** generates acyl triazene **2.54** which upon basic treatment fragments to diazo compound **2.41** and amide **2.55**.

With key diazo compound **2.41** in hand, several transition metal-catalyzed cyclopropanation conditions were screened, which are presented in Table 2.1.

Table 2.1. Screening of the intramolecular cyclopropanation of **2.41**.

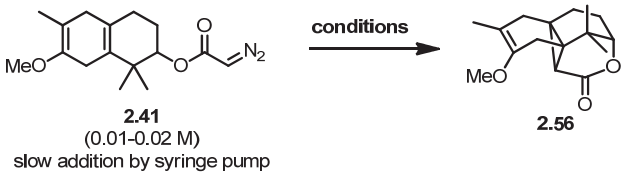

2.41
(0.01-0.02 M)
slow addition by syringe pump

2.56

No.	solvent	temperature	catalyst (mol%)	observation
1	CH_2Cl_2	r.t.	$Rh_2(OAc)_4$ (2.0)	complex mixture
2	CH_2Cl_2	−30 °C to 0 °C	$Rh_2(OAc)_4$ (2.0)	complex mixture
3	CH_2Cl_2	−30 °C to 40 °C	$Rh_2(TFA)_4$ (2.0)	decomposition
4	CH_2Cl_2	−10 °C to r.t.	$Rh_2(esp)_2$ (2.0)	complex mixture
5	CH_2Cl_2	−10 °C to r.t.	$Rh_2(pfb)_4$ (2.0)	complex mixture
6	CH_2Cl_2	0 °C to r.t.	$Rh_2(cap)_4$·2 MeCN (2.0)	no reaction
7	DCE	50 °C	$Rh_2(cap)_4$·2 MeCN (2.0)	decomposition
8	toluene	45 °C	$Cu(TBS)_2$ (2.0)	complex mixture
9	$MeNO_2$	r.t.	$Cu(OTf)_2$ (2.0)	decomposition
10	CH_2Cl_2	0 °C to 40 °C	$Cu(OTf)_2$ (2.0)	decomposition
11	CH_2Cl_2	0 °C to r.t.	$Cu(acac)_2$ (2.0)	dimerization
12	CH_2Cl_2	40 °C to r.t.	CuI·$P(OEt)_3$ (2.0)	dimerization
13	DCE	40 °C	$Cu(hfacac)_2$ (2.0)	dimerization

All screening conditions were performed under high dilution conditions with a starting material concentration of 0.01−0.02 M. Furthermore, a solution of diazo compound **2.41** was slowly added to the catalyst solution by syringe pump to prevent intermolecular dimerization reactions. Unfortunately, all conditions using dimeric rhodium(II) catalysts[104,112] only provided complex mixtures (entry 1,2,4,5) or resulted in decomposition (entry 3). In the case of $Rh_2(cap)_4$, which was reported to be highly selective for cyclopropanation whilst avoiding competitive C–H insertion,[113] no conversion of the diazo compound **2.41** was observed at r.t. (entry 6), whereas elevated temperatures led to decomposition (entry 7). Due to the

unsuccessful conversion to the desired cyclopropane **2.56**, several copper (II) and copper (I) catalysts were screened.[114] However, most reactions again afforded complex mixtures of several unidentified products (entry 8–10). In the case of $Cu(acac)_2$, CuI and $Cu(hfacac)_2$, the undesired dimerized alkene product was identified as major product despite the high dilution and the slow addition of the starting material **2.41** (entry 11–13). Possibly, the ester functionality adopts a *s-cis* conformation where the diazo group or the resulting metal carbenoid is pointing away from the alkene as described for α-diazo amides.[115] This conformation could be even more pronounced by the steric bulk of the *gem*-dimethyl moiety.

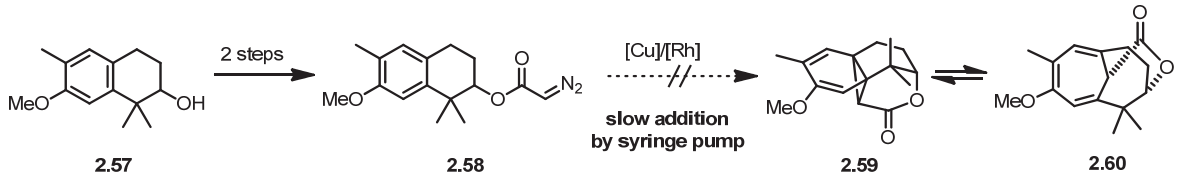

Scheme 2.8 Arene cyclopropanation of diazo compound **2.58**.

Inspired by the recent work of the Reisman group on arene cyclopropanation,[116] we examined the cyclopropanation of the corresponding aromatic diazo compound **2.58** (Scheme 2.8), which was prepared by a similar sequence (see supporting information). It was proposed that the desired norcaradiene **2.59** would be favored over cycloheptatriene **2.60**, formed by 6π electrocyclic ring opening, due to geometric constraints.[117] However, complex mixtures or dimerization were observed even under high dilution and slow addition using rhodium or copper catalysis. Neither the norcaradiene **2.59** nor cycloheptatriene **2.60** could be identified in the reaction mixtures which supports the proposal of strong steric hindrance due to the neighboring quaternary carbon.

Consequently, attention was turned towards an intramolecular [2+2] cycloaddition. Moreover, it was realized that the use of keteniminium salts in the [2+2] cycloaddition would have several advantages.[105,118] First, these reactive species are known to be much more electrophilic and reactive than their oxygen equivalents. Second, keteniminium salts are much less prone to dimerization. Therefore, cyclohexadiene **2.42** was converted to amide **2.62** under basic treatment with α-chloro amide **2.61** (Scheme 2.9a). Treatment of amide **2.62** with triflic anhydride under different conditions, originally reported by Ghosez and coworkers, did not provide the desired cyclobutanone **2.43**.[119] The majority of conditions yielded a complex mixture of several products or, in the case of elevated temperatures, one major reaction product. After full NMR analysis of this unstable compound, enamine **2.63** represents a plausible structure which can be formed by the mechanism in Scheme 2.9b.

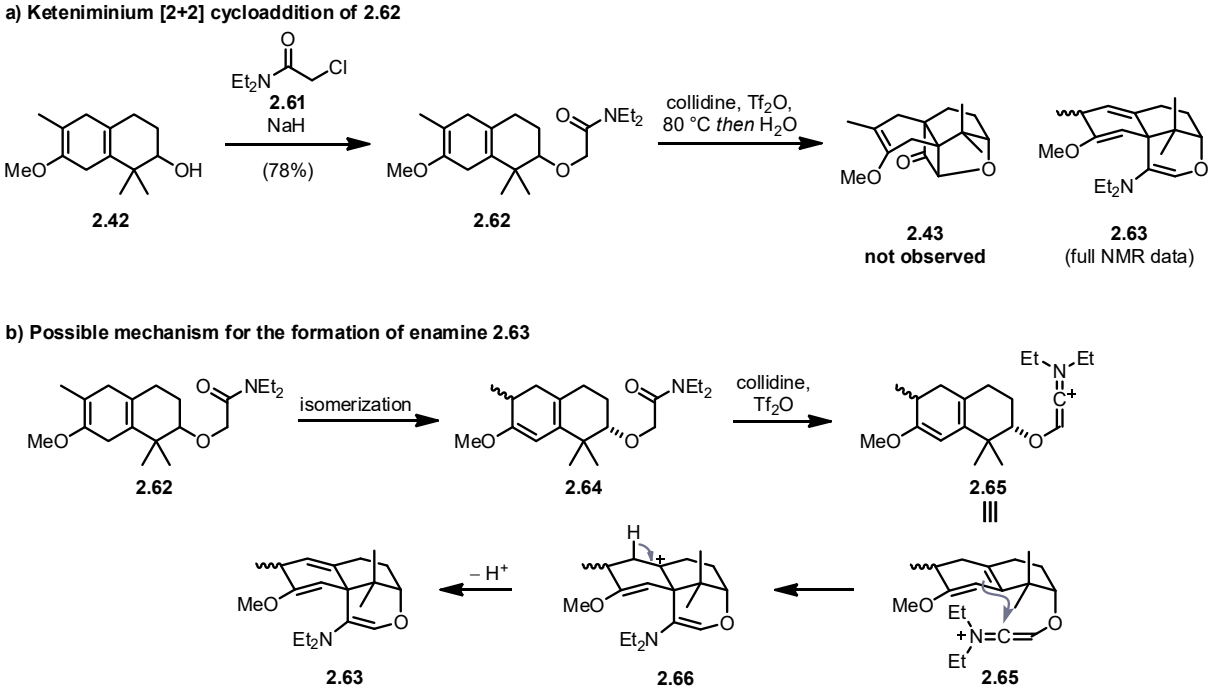

Scheme 2.9 a) Keteniminium [2+2] cycloaddition of amide **2.62**; b) Possible mechanism for the formation of enamine **2.63**.

After an initial isomerization of the 1,4- to the 1,3-cyclohexadiene **2.64**, which was observed in other transformations at elevated temperature, the desired keteniminium ion **2.65** is formed. Attack by the nucleophilic tetrasubstituted double bond forms a quaternary stereocenter. Instead of nucleophilic attack by the enamine onto the tertiary cation, elimination takes place to deliver alkene **2.63**.

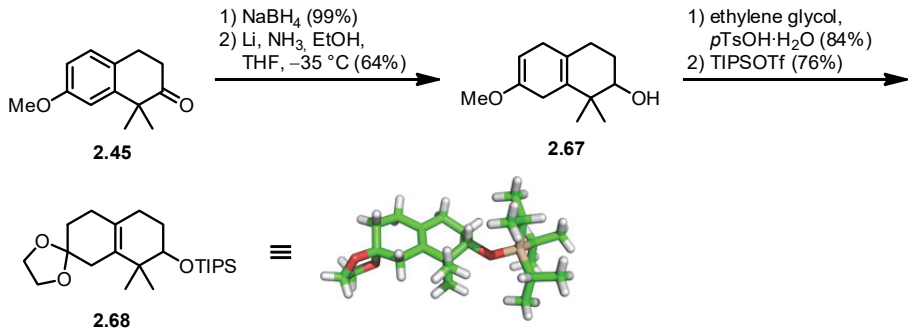

Scheme 2.10 Synthesis of ketal **2.68**.

In addition, intermolecular ketene and keteniminium [2+2] cycloadditions were investigated.[120] Therefore precursor **2.68**, which lacks the methyl vinyl ether to avoid chemoselectivity problems, was synthesized by a straightforward sequence (Scheme 2.10). Formation of dichloroketene or keteniminium triflate in the presence of **2.68** did not result in the formation cyclobutanone **2.69** and mainly unreacted starting material was recovered, demonstrating the steric hindrance of the tetrasubstituted alkene (Table 2.2). At elevated temperature, the ketal moiety was opened followed by oxidative aromatization (entry 4).

Table 2.2 Screening of the intermolecular ketene or keteniminium [2+2] cycloaddition of **2.68**.

2.68 **2.69**

No.	solvent	reagents (eq)	temperature/time	observation
1	C_6H_{12}	NEt_3 (2.5), Cl_2HCOCl (2.5)	r.t./overnight	no reaction
2	C_6H_{12}	NEt_3 (2.5), Cl_2HCOCl (2.5)	55 °C/overnight	no reaction
3	DCE	Tf_2O (3.5), DMA (3.0), collidine (3.5)	−30 °C to r.t./15 h	no reaction
4	DCE	Tf_2O (3.5), DMA (3.0), collidine (3.5)	−30 °C to 80 °C/15 h	ketal opening
5	C_6H_6	Tf_2O (3.5), DMA (3.0), collidine (3.5)	80 °C/9 h	no reaction
6	DCE	Tf_2O (3.5), DMA (3.0), collidine (7.0)	−15 °C to 80 °C/9 h	no reaction

As a result of the unsuccessful formation of the quaternary stereocenters from an unsaturated decalin system, it was decided to change the strategy focusing on the formation of the ladderane substructure, as described in the next chapter.

2.2.1.3 Second generation approach – Retrosynthetic analysis

For the second generation strategy, it was envisioned to trace aplydactone (**2.11**) back to an intermediate which contains a [2]-ladderane substructure to build upon reported strategies towards ladderane systems (Scheme 2.11).[60b,121]

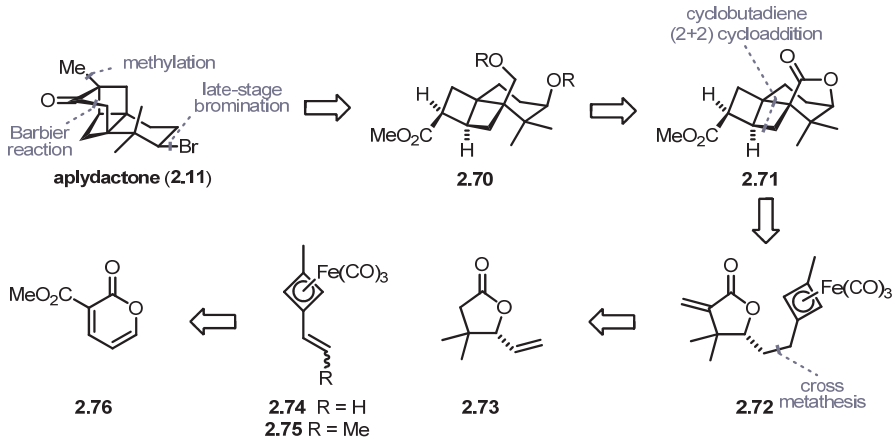

Scheme 2.11 Retrosynthetic analysis of aplydactone (**2.11**) *via* cyclobutadiene (2+2) cycloaddition.

Therefore, we aimed to generate the decalin substructure in **2.11** by a late stage Barbier-type ring closure. Furthermore, the secondary bromide as well as the α-methyl group could be introduced at a later stage of the synthesis. Taking all of these ideas into consideration, one arrives at diol intermediate **2.70**, which is accessible from the ladderane-containing lactone **2.71**. For the generation of the bicyclo[2.2.0]hexane system, the intramolecular oxidative (2+2) cycloaddition of cyclobutadiene iron tricarbonyl complexes, reported by the Snapper group, represented a promising approach. The desired precursor **2.72** also fulfills the requirement of reduced degrees of conformational freedom due the lactone moiety.[122] This is important because intermolecular dimerization of free cyclobutadiene is the main side reaction observed during cyclobutadiene cycloadditions, which necessitates substrate preorganization. Key intermediate **2.72** was planned to be derived by cross metathesis of γ-butyrolactone **2.73** and iron complex **2.74** or **2.75**,[123] which in turn was intended to be generated from the commercially available pyrone **2.76**.

2.2.1.4 A cross metathesis approach towards the cycloaddition precursor

For the preparation of the key iron tricarbonyl complexes **2.74** and **2.75**, pyrone **2.76** was irradiated with a Rayonet lamp (350 nm, 250 W) in degassed benzene to accomplish a 4π disrotatory electrocyclization to β-lactone **2.77**, which was not isolated (Scheme 2.12). Treatment of **2.77** with $Fe_2(CO)_9$ at 50 °C led to iron tricarbonyl complex **2.78** *via* extrusion of CO_2. This procedure was originally described by Roberts[124] and further optimized by Snapper and coworkers.[122b] In general, cyclobutadiene iron tricarbonyl complexes are considered to be ”metalloaromatic”[125] exemplified by their aromatic reactivity.[126] The ester moiety could be

completely reduced to the methyl group in presence of $LiAlH_4$ and boron trifluoride diethyl etherate to obtain **2.79**.[122b] Subsequent formylation under Vilsmeier–Haack conditions delivered a separable 4:1 mixture of *ortho*- and *para*-substitution products **2.80** and **2.81**.[126d,127] The necessary alkene moiety for the desired cross metathesis was installed after some optimization by Kauffmann olefination[128] of aldehyde **2.81** for the formation of the terminal alkene **2.74** or by Takai olefination[129] *via* a *gem*-dichromium species to generate disubstituted alkene **2.75**.

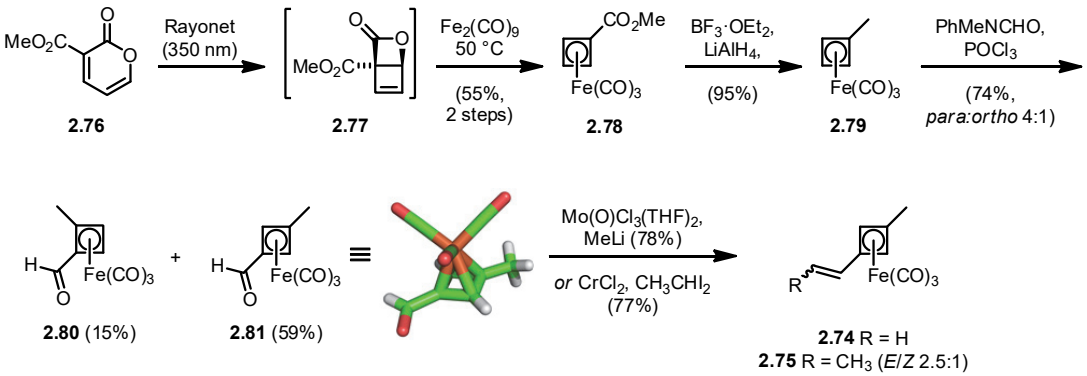

Scheme 2.12 Synthesis of iron tricarbonyl complexes **2.74** and **2.75**.

The synthesis of the other cross metathesis coupling partner **2.73** commenced with a literature known Johnson–Claisen rearrangement of prenol **2.82** and triethyl orthoactete (Scheme 2.13).[130] Subsequent Sharpless asymmetric dihydroxylation afforded the desired γ-lactone **2.84** after spontaneous cyclization of the intermediate diol **2.86** in varying yields and moderate enantioselectivity. The use of $(DHQ)_2PYR$ as catalyst, which is known to provide generally better enantioselectivity for terminal alkenes, did not lead to improved selectivity.[131]

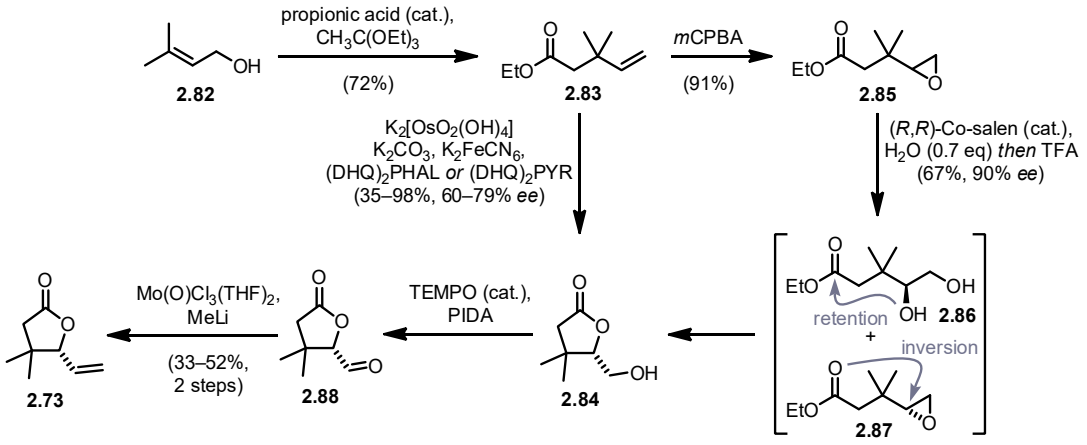

Scheme 2.13 Synthesis of γ-butyrolactone **2.73**.

Alternatively, alkene **2.83** was treated with *m*CPBA to obtain epoxide **2.85**. A kinetic resolution of **2.85** provided a mixture of diol **2.86** and epoxide **2.87** which, inspired by the work of Liu,[132] was upon addition of trifluoroacetic acid converted to a single enantiomer **2.84** in 67% yield by lactonization under inversion or retention. The enantiomeric excess of 90% was determined from the diastereomeric ratio of the corresponding Mosher ester (see supporting information).

The transformation of the primary alcohol **2.84** to the corresponding terminal alkene **2.73** turned out to be challenging due to the instability of the intermediate aldehyde **2.88** and the volatility of the target alkene **2.73**. After extensive optimization, **2.73** could be obtained in varying yields by use of an oxoammonium oxidation under Piancatelli's conditions[133] followed by immediate Kauffmann olefination of the crude material.

With both coupling partners in hand, the cross metathesis reaction was investigated (Table 2.3).[123] The use of Grubbs-II catalyst in combination with the terminal alkene **2.74** in benzene led to isolation of the desired cross metathesis product (*E*)-**2.89** with dimerization of the iron tricarbonyl complex **2.74** as major side product (entry 1). In addition, a further consumption of the isolated dimer in the reaction was not observed whereas dimerization of alkene **2.73** could not be detected. Changing the solvent to DCE or switching to the Grubbs I catalyst resulted in isolation of starting material (entry 2 and 3). The more reactive Grubbs-Hoveyda II catalyst in CH_2Cl_2 provided only dimer formation (entry 4), whereas in benzene the cross metathesis product could be isolated in 26% yield (entry 6). Slow addition of **2.74** over 2 h by syringe pump did not improve the yield (entry 5). Several other metathesis catalysts were tested and nitro-Grela catalyst **2.93**[134] provided a slightly improved yield and a clean reaction (entry 7–11). However, the main problem in all cases was dimerization of **2.74** as major competing side reaction.

These observations imply that based on the classification of alkenes and their reactivity reported by Grubbs and coworkers,[135] alkene **2.73** represents a Type III olefin whereas iron tricarbonyl complex **2.74** can be categorized as Type II olefin due to the fast generation of dimerized product which is not further consumed. In general, those systems can be successfully coupled if the reaction rate of the cross metathesis event is not too slow compared to the dimerization process. To overcome the dimerization problem, a large excess of lactone **2.73** was added leading to an improvement of the yield to 47% with 40% of competing dimer formation. It was reported that 1,2-disubstituted alkenes tend to give better yields in the case of dimerization side products.[135] However, when alkene **2.75** was reacted in presence of excess lactone **2.73** and different catalysts, dimerization could not be suppressed (entry 12–16).

The modest yield obtained in the cross metathesis also in presence of a large excess of lactone **2.73** limited the scalability and the practicability of this synthetic route. Therefore, it

was decided to change the initially envisioned synthesis which is presented in the next chapter.

Table 2.3 Cross metathesis of cyclobutadiene iron tricarbonyl complex **2.74** or **2.75** and lactone **2.73**.

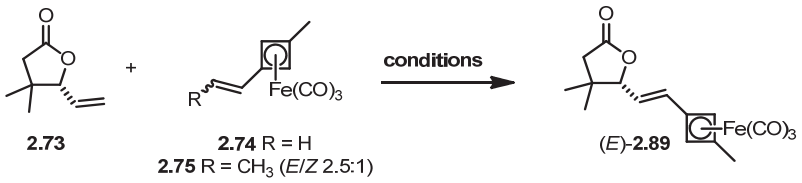

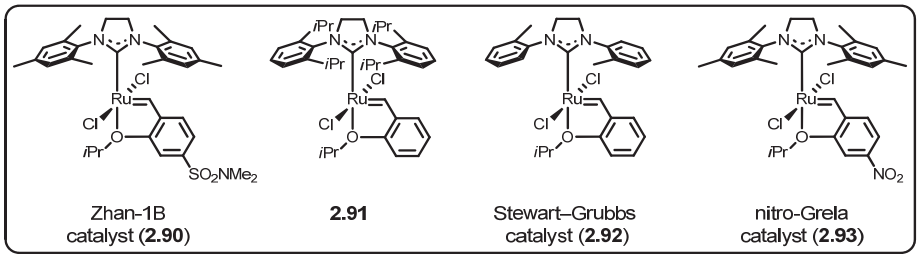

No.	solvent	catalyst	temperature	**2.74**/**2.75** (eq **2.73**)	observation
1	C_6H_6	G-II (20 mol%)	40 °C	**2.74** (2.0)	26%
2	DCE	G-II (10 mol%)	35 °C	**2.74** (2.7)	no reaction
3	C_6H_6	G-I (10 mol%)	40 °C	**2.74** (2.0)	no reaction
4	CH_2Cl_2	GH-II (10 mol%)	40 °C	**2.74** (2.0)	dimerization
5[a]	C_6H_6	G-II (15 mol%)	40 °C	**2.74** (2.0)	26%
6	C_6H_6	GH-II (10 mol%)	40 °C	**2.74** (2.0)	26%
7	C_6H_6	**2.90** (10 mol%)	40 °C	**2.74** (2.0)	~25%
8	C_6H_6	**2.91** (10 mol%)	40 °C	**2.74** (2.0)	traces
9	C_6H_6	**2.92** (10 mol%)	40 °C	**2.74** (2.0)	no reaction
10	C_6H_6	**2.93** (10 mol%)	40 °C	**2.74** (2.0)	30%
11	C_6H_6	**2.93** (10 mol%)	40 °C	**2.74** (8.0)	47%, 40% dimer
12	C_6H_6	**2.93** (15 mol%)	40 °C	**2.75** (4.0)	30%, 35% dimer
13	C_6H_6	**2.93** (20 mol%)	40 °C	**2.75** (4.0)	27%
14	C_6F_6	**2.93** (20 mol%)	40 °C	**2.75** (4.0)	50% conversion
15	C_6H_6	Schrock (20 mol%)	40 °C	**2.75** (4.0)	no reaction
16	C_6H_6	**2.92** (15 mol%)	40 °C	**2.75** (4.0)	no reaction

[a] slow addition of **2.74** *via* syringe pump.

2.2.1.5 Revised second generation strategy – An alkyne addition approach

An alkyne addition strategy was assumed to be a more scalable and practical approach towards the synthesis of the desired cyclization precursor **2.72**. Asymmetric additions of aryl substituted alkynes were reported which were assumed to be adaptable for the "metalloaromatic" system.[136] Nevertheless, we decided to test the synthetic route with racemic material initially. The synthesis of the desired iron tricarbonyl complex **2.72** is depicted in Scheme 2.14. Under Bestmann–Ohira conditions, aldehyde **2.81** could be converted to the corresponding terminal alkyne **2.95** in good yield.[137] Furthermore, the Johnson–Claisen product **2.83** was ozonolyzed to aldehyde **2.96**, which was found to be very unstable upon concentration and had to be stored at low temperature in solution.

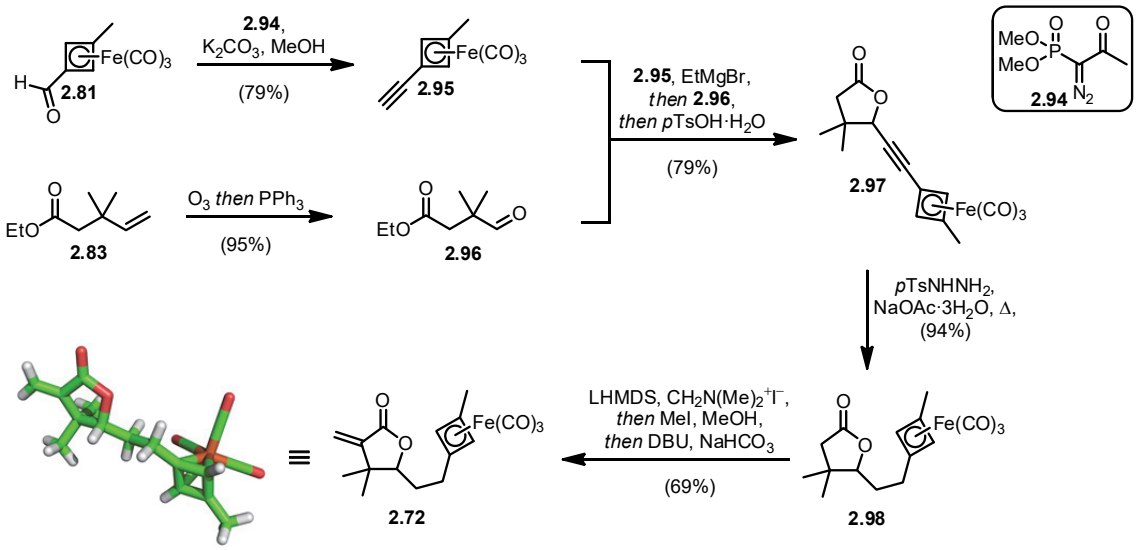

Scheme 2.14 Synthesis of enone **2.72**.

With both fragments **2.95** and **2.96** in hand, the crucial alkyne addition was investigated. Deprotonation of the terminal alkyne **2.95** at low temperature followed by addition of aldehyde **2.96** resulted in a mixture of the corresponding secondary alcohol and lactone **2.97**. However, the crude reaction mixture could be completely converted to the closed lactone **2.97** in good yield under acidic conditions. In the next step, the triple bond had to be completely reduced to the alkyl side chain. Initial results using heterogeneous catalysis were promising. Unfortunately, upon scale up, the reactions did not go to completion even when high pressure conditions (up to 11 bar H_2) were applied. After some optimization, diimide reduction conditions using tosyl hydrazide and sodium acetate in large excess at elevated temperatures proved to be ideal, delivering the fully reduced compound **2.98** in very good yield.[138] The installation of the alkene, necessary for the intramolecular cycloaddition, was performed by Eschenmoser methenylation[139] and *exo*-methylene lactone **2.72** could be unambiguously identified by single crystal X-ray analysis.

Table 2.4 Intramolecular cyclobutadiene (2+2) cycloaddition of **2.72**.

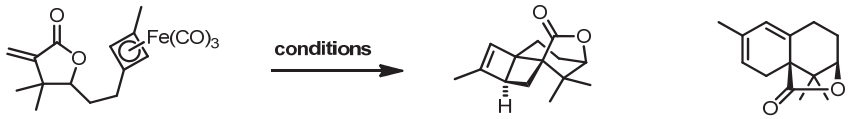

2.72 **2.99** **2.100**

No.	oxidant (eq)	temperature	solvent	time	observation
1	CAN (5.0)	r.t.	acetone	10 min	degradation
2[a]	CAN (5.0)	r.t. to 40 °C	C_6H_6	20 h	degradation
3	CAN (5.0)	75 °C	DMF	10 min	degradation
4	DDQ (4.0)	r.t.	C_6H_6	3.5 h	no conversion
5	DDQ (4.0)	65 °C	C_6H_6	3.5 h	no conversion
6	$Pb(OAc)_4$ (2×5.0)	r.t.	pyridine	15 min	no conversion
7	$Pb(OAc)_4$ (15.0)	75 °C	C_6H_6	5 min	degradation
8	O_2 (1 atm)	45 °C	$C_6H_5CF_3$	12 h	no conversion
9	pyridine-*N*-oxide (15)	55 °C	$C_6H_5CF_3$	20 h	no conversion
10	$CuCl_2 \cdot H_2O$ (15)	40 °C	$C_6H_5CF_3$	1 h	degradation
11	$FeCl_3 \cdot 6H_2O$ (10)	r.t.	THF/EtOH	13 h	no conversion
12	TMAO (2×10)	50 °C	acetone	12.5 h	complex mixture
13	TMAO (2×4.0)	60 °C	acetone	7.5 h	complex mixture
14	TMAO (2×4.0)	85 °C	C_6H_6	21 h	39% diene **2.100**
15	TMAO (15)	75 °C	C_6H_6	12 h	**2.72**:**2.99**:**2.100** 0.7:1.0:1.5
16	TMAO (15)	65 °C	$C_6H_5CH_3$	12 h	**2.72**:**2.99**:**2.100** 1.0:1.0:0.8
17	TMAO (15)	65 °C	xylene	12 h	no conversion
18	TMAO (15)	55 °C	$C_6H_5CH_3$	12 h	no conversion
19	TMAO (15)	55 °C	$C_6H_5CF_3$	12 h	traces of **2.99**
20	TMAO (15)	55 °C	THF	13 h	complex mixture
21	TMAO (15)	55 °C	1,4-dioxane	13 h	complex mixture
22	TMAO (15)	55 °C	MeCN	13 h	no conversion
23	TMAO (15)	55 °C	EtOH	16 h	no conversion
24	TMAO (15)	55 °C	TFE	16 h	no conversion
25	TMAO (15)	55 °C	EtOAc	13 h	complex mixture
26	TMAO (15)	55 °C	DMA	13 h	degradation
27	TMAO (15)	40 °C	DMA	13 h	3% **2.99** (NMR), degradation

[a] slow addition of the starting material **2.72**.

For the intramolecular [2+2] cycloaddition, iron tricarbonyl complex **2.72** was treated with several oxidants known to promote oxidative decomplexation, releasing the reactive cyclobutadiene (Table 2.4).[122a] However, initial experiments using several single- and two-electron oxidants (CAN,[140] DDQ,[141] $Pb(OAc)_4$,[142] O_2, pyridine-*N*-oxide, $CuCl_2$,[143] $FeCl_3$[141])

were not successful (entry 1–11). When trimethylamine N-oxide[144] was added as oxidant at 85 °C, the undesired cyclohexadiene **2.100** was observed as major reaction product (entry 14). Presumably, this compound is formed by ring opening of the desired cyclobutene **2.99** *via* a diradical mechanism (Scheme 2.15a). This reactivity was used by Snapper for the synthesis of cyclohexadienes. However, the reported standard procedure was conducted at temperatures above 200 °C,[145] reflecting the labile C–C bond in ladderane intermediate **2.99**.

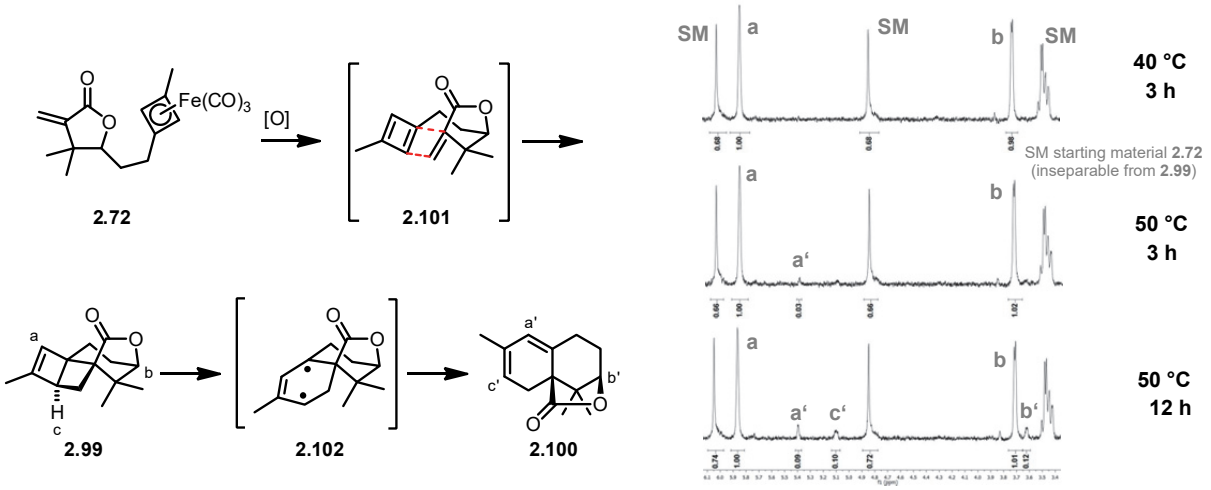

Scheme 2.15 Thermal opening of the cycloaddition product **2.99**.

At lower reaction temperature, the desired cycloaddition product **2.99** could be isolated as an inseparable mixture with residual starting material **2.72** and identified by full NMR analysis and high resolution mass spectroscopy (entry 15 and 16). Subjecting this material to a temperature gradient experiment (Scheme 2.15b), a slow opening of the unsaturated ladderane system to cyclohexadiene **2.100** was observed at 50 °C.

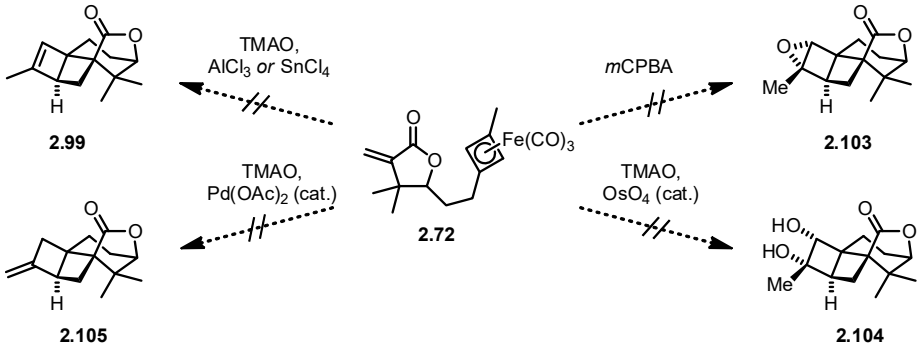

Scheme 2.16 Attempts to prevent ring opening during the (2+2) cycloaddition.

Attempts to lower the reaction temperature in different solvents led to either no reaction or complete decomposition (entry 12, 13, 17–27). Furthermore, the feasibility of an *in situ* trapping of the reactive cyclobutene double bond by dihydroxylation or epoxidation *via* the addition of OsO_4 or *m*CPBA was investigated (Scheme 2.16). These experiments were

just as unsuccessful as the attempt to isomerize the double bond *in situ* to the exocyclic position in the presence of $Pd(OAc)_2$.[146] The use of substoichiometric quantities of Lewis acid to decrease the reaction temperature by LUMO-lowering activation of the enone system led to either degradation or no conversion.

In addition, a possible reason for the inefficient cyclization of the system could be the difficulty of the formation of six-membered rings by cyclobutadiene cycloadditions, as described by Snapper.[122a] Consequently, (*Z*)-alkene **2.106** was synthesized in two steps from the known intermediate **2.97** to obtain an even more organized transition state in the oxidative cyclization step (Scheme 2.17). Interestingly, hydrogenation of the triple bond in EtOH stopped chemoselectively at (*Z*)-**2.89**. Unfortunately, upon oxidative decomplexation with CAN or trimethylamine *N*-oxide, no desired cyclization product **2.107** could be identified in the reaction mixture.

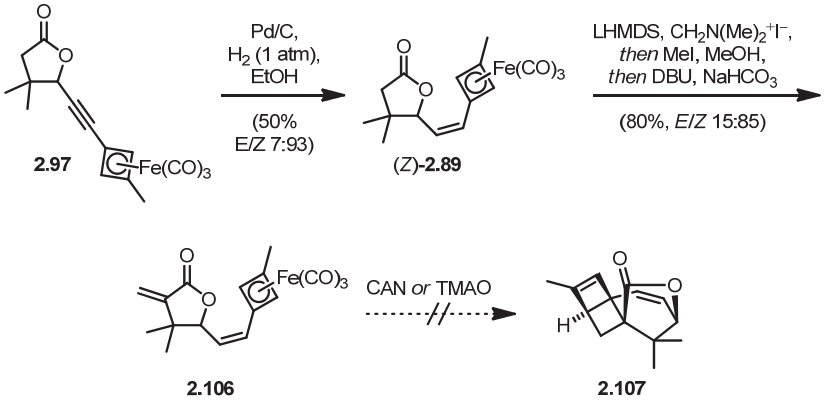

Scheme 2.17 Synthesis of (*Z*)-alkene **2.107**.

Moreover, the unexpected instability of the desired cyclobutene **2.99** was justified by the additional strain introduced by the polycyclic lactone structure within the desired product **2.99**. Hence, derivatization of **2.72** or **2.98** to several linear cyclization precursors was investigated (Scheme 2.18). The opening of the exocyclic unsaturated lactone moiety was difficult and resulted in 1,4-addition products or complex mixtures (MeMgBr; KOH/BnBr; $HC(OMe)_3/H_2SO_4$).

Treatment of lactone **2.98** with pyrrolidine under Lewis acidic conditions afforded the desired amide **2.115** after protection of the neopentylic alcohol. However, formation of the unsaturated linear precursor **2.116** under Eschenmoser methenylation conditions failed, presumably due to the steric hindrance of the neighboring *gem*-dimethyl moiety.

Diol formation by reduction of **2.72** with DIBAL-H occurred cleanly and protection of the allylic alcohol **2.109** afforded TBS-protected alcohol **2.110**. Compounds **2.109** and **2.110**, however, provided complex mixtures upon oxidative decomplexation using CAN or trimethylamine *N*-oxide. This might be explained by the higher degrees of freedom in the case of linear precursors leading to a slower cyclization rate. As the intermolecular dimerization of

cyclobutadienes is known to proceed in a diffusion controlled manner, it is likely that the cyclization of the linear precursors **2.109** and **2.110** is too slow to compete with the dimerization.[122a]

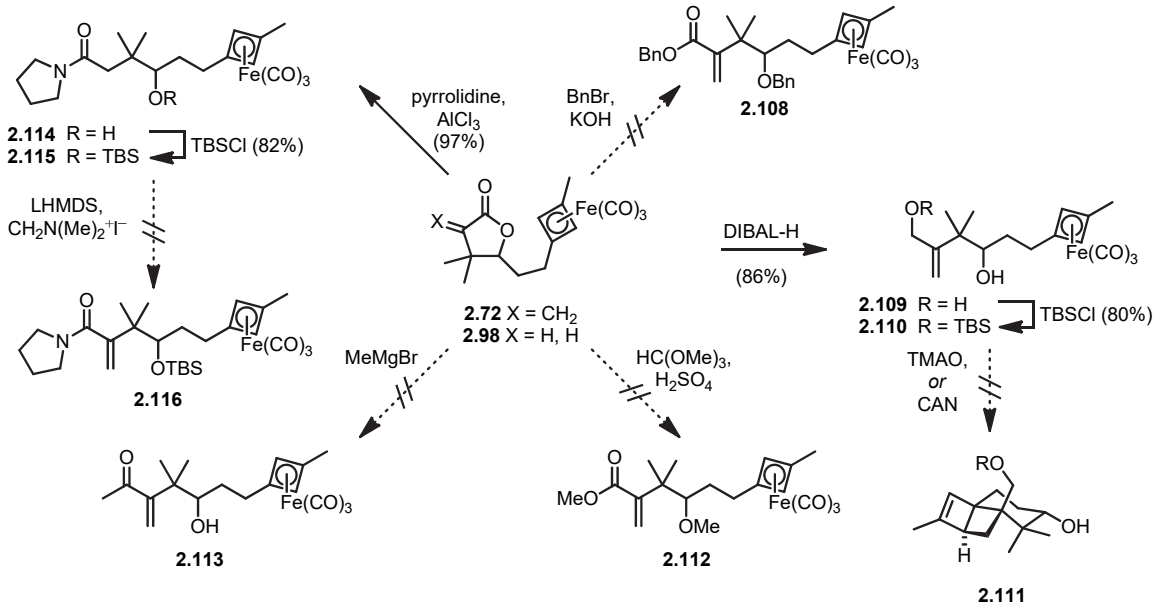

Scheme 2.18 Derivatization of iron tricarbonyl complexes **2.72** and **2.98**.

In conclusion, the oxidative (2+2) cycloaddition of iron tricarbonyl complex **2.72** provided the desired ladderane moiety present in aplydactone (**2.11**). Nonetheless, the instability of the desired intermediate **2.99** rendered its synthetic use impossible. Thus, it was envisioned to use another type of (2+2) cycloaddition for the formation of the desired ladderane structure which would result in a more stable intermediate (Scheme 2.19). This seemed especially attractive due to the formation of three adjacent quaternary carbons in a single operation which was shown to be feasible by the observation of intermediate **2.99**.

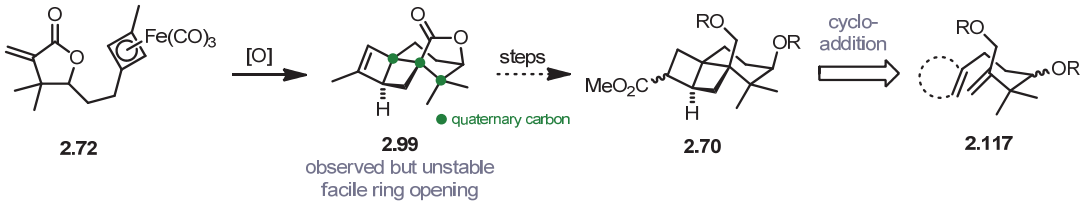

Scheme 2.19 General idea for a revised cycloaddition approach towards the ladderane scaffold.

2.2.1.6 Third generation approach – A non-biomimetic photochemical total synthesis of aplydactone

GDCh Communications Angewandte International Edition Chemie

Natural Product Synthesis

International Edition: DOI: 10.1002/anie.201604102
German Edition: DOI: 10.1002/ange.201604102

A Synthesis of (±)-Aplydactone

*Robin Meier and Dirk Trauner**

Dedicated to Professor Samuel J. Danishefsky on the occasion of his 80th birthday

Abstract: *Aplydactone is an unusual brominated sesquiterpenoid isolated from the sea hare Aplysia dactylomela. Its highly strained skeleton contains two four- and three six-membered rings and features three adjacent quaternary carbon atoms. Although it is most likely of photochemical origin, attempts to generate it from a chamigrane precursor have failed thus far. In this work, we present a total synthesis of aplydactone that relies on two photochemical key steps that are not biomimetic but highly effective in establishing the two cyclobutane rings. Our synthesis also features an unusual Barbier-type cyclization and culminates in new radical conditions to install the sterically hindered secondary bromide of the natural product.*

Photochemical steps are rare in biosynthesis but can give rise to natural products with unusual architectures.[1] They seem to be especially relevant in organisms that live in shallow seawater and at latitudes where solar irradiation is comparatively intense.[2]

In 2001, Stonik and co-workers reported the isolation of aplydactone (**1**), an intriguing cyclobutane-containing natural product, from *Aplysia dactylomela* (Figure 1).[3] This sea hare also produces dactylone (**2**) and the brominated chamigranes **3** and **4**.[4] The biological specimens were collected at a water depth of 3–5 m at the northern coast of Madagascar. Therefore, it is reasonable to assume that the cyclobutane rings in **1** are formed from **2** by intramolecular photochemical [2+2] cycloaddition.[5] Nevertheless, Stonik et al. reported that **2** could not be converted into **1** under "long-term UV irradiation".[3] Although this result is worthy of revisiting using modern theoretical and photochemical methods, we decided to explore alternative approaches to synthesize **1**.

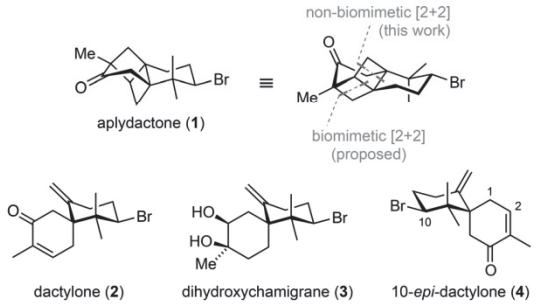

Figure 1. Aplydactone (**1**) and the brominated chamigranes **2**–**4**, isolated from the sea hare *Aplysia dactylomela*.

From a synthetic point of view, the polycyclic structure of **1** provides a considerable challenge owing to the high ring strain and steric congestion of the unique tetracyclo[4.4.2.$0^{1,6}$.$0^{3,11}$]dodecane skeleton. This framework features an unprecedented [2]-ladderane moiety,[6] which is connected to a *cis*-decalin system comprising four quaternary centers and a secondary neopentyl bromide. As a result of this bridged core structure, the bond lengths and angles within the four-membered rings are highly distorted from the usual values of puckered cyclobutanes. Indeed, aplydactone (**1**) readily undergoes a Wagner–Meerwein rearrangement under acidic conditions to relieve ring strain.[3]

To the best of our knowledge, just one synthetic study towards **1** has been reported despite its intriguing structure.[7] Herein, we disclose the first total synthesis of aplydactone (**1**), which hinges on photochemical transformations.

A survey of the literature suggested that either a [2+2] cycloaddition of a transient cyclobutadiene[6,8] or a contraction of a bicyclo[3.2.0]heptane ring system[6,8d,9] would be most suitable for the establishment of the central bicyclo[2.2.0]hexane moiety of aplydactone (**1**). As cyclobutadiene cycloaddition proved to be non-viable, we based our retrosynthetic analysis on a photochemical [2+2] cycloaddition and a ring contraction (Scheme 1). Late-stage bromination and disconnection of one of the six-membered rings would suggest **5** as a suitable intermediate, which could be traced back to **6** by a Wolff ring contraction and methylation. Furthermore, we rationalized that intermediate **6** could be prepared in one step through an intramolecular [2+2] photocycloaddition from cyclopentenone **7**, which can be derived from known ester **8**.

Our actual synthesis began with the preparation of alkyl bromide **10** starting from known ester **8**, which was prepared on decagram scale by a Johnson–Claisen rearrangement (Scheme 2).[10] A reaction sequence involving ozonolysis,[10b] allylation[11] with subsequent lactonization, a second ozonolysis with full reduction, and protection afforded lactone **9**. Methenylation,[12] reduction, and double benzylation of lactone **9** were followed by selective deprotection of the SEM group[13] and bromination to obtain **10**. This opening sequence was scalable and provided bromide **10** from ester **8** in 43% overall yield on multigram scale. For the installation

[*] R. Meier, Prof. Dr. D. Trauner
Department of Chemistry
Ludwig-Maximilians-Universität München
81377 Munich (Germany)
E-mail: dirk.trauner@lmu.de

Supporting information and the ORCID identification numbers for the authors of this article can be found under http://dx.doi.org/10.1002/anie.201604102.

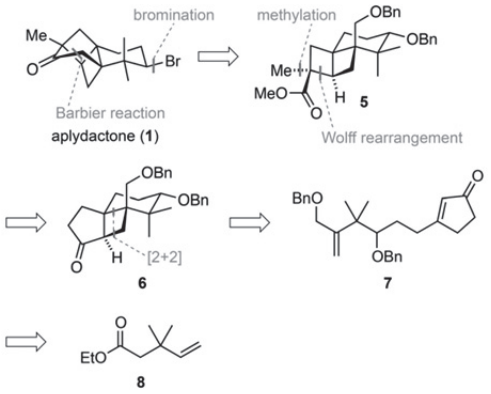

Scheme 1. Retrosynthetic analysis of aplydactone (**1**).

of the cyclopentenone moiety, we used a method introduced by Yoshida and Saito.[14] Coupling of sulfone **11** with bromide **10** followed by acid-induced deprotection and elimination gave precursor **7** in excellent yield. With gram quantities of **7** in hand, we turned our attention to the photochemical [2+2] cycloaddition, which needed to build up two quaternary stereocenters next to a sterically hindered *gem*-dimethyl moiety.[5b,15] After some optimization, key intermediate **6** could be obtained in decent yield and very good diastereoselectivity upon irradiation of **7** with UV light. The relative configuration of the complex ring system was established by NOESY experiments.

To establish the ladderane motif of aplydactone (**1**), the cyclopentanone ring of **6** had to be contracted. To our surprise, the formation of α-diazo ketone **13** turned out to be more challenging than expected. Activation of **6** through formylation[16] or trifluoroacetoxylation[17] followed by diazo transfer as well as direct-transfer conditions[18] suffered from low yield. However, **13** could be prepared by treatment of enaminone **12** with *p*ABSA.[9a,19] The subsequent photochemical Wolff rearrangement[20] proceeded smoothly and provided ladderane **14** in good yield as a 3:1 diastereomeric mixture (major diastereomer shown). Following deprotonation, methylation occurred from the less hindered face of the bicyclo[2.2.0]hexane scaffold generating ester **5**, which features all requisite quaternary stereocenters, in very good yield. The structure of **5** was established by NOESY experiments and was ultimately confirmed by X-ray structure analysis of diol **15**, which was obtained by double debenzylation.

The next phase of our synthesis required the closure of the six-membered ring to obtain the full carbon skeleton of **1**. Whereas selective functionalization of the primary neopentyl alcohol was not feasible, we were able to selectively deprotect the secondary alcohol of **5** under reductive conditions (Scheme 3). Reprotection as a silyl ether and deprotection of the primary alcohol followed by conversion of the ester into the Weinreb amide gave **16**. Iodination of **16** under Garegg–Samuelsson conditions[21] produced the highly sensitive iodide **17**, which readily rearranged to cyclopentene **18**.[22] Conducting the reaction and the quenching at low temperature suppressed the ring expansion and provided the desired iodide **17** as the major reaction product. Treatment of iodide

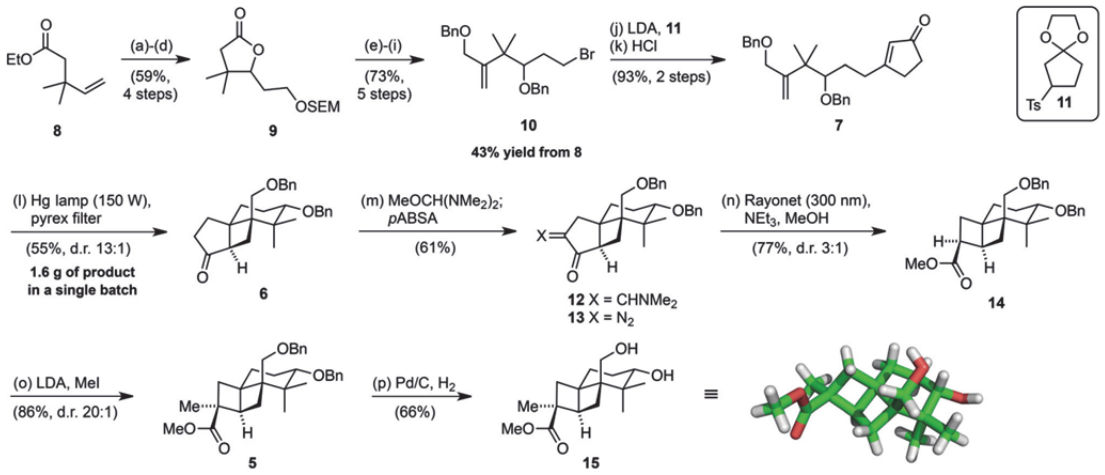

Scheme 2. Synthesis of key intermediate **5**. a) O_3, CH_2Cl_2/MeOH, −78 °C; then PPh_3, −78 °C→RT, 95 %; b) Zn, allyl bromide, THF, 0 °C→RT, 78 %; c) O_3, CH_2Cl_2/MeOH, −78 °C; then PPh_3, −78 °C→RT; then $NaBH_4$, 0 °C→RT; d) SEMCl, DIPEA, CH_2Cl_2, 0 °C→RT, 80 % over 2 steps; e) LHMDS, $CH_2NMe_2^+I^-$, THF, −78 °C→RT; then MeI, MeOH, 0 °C→RT; then DBU, $NaHCO_3$, CH_2Cl_2/H_2O, 0 °C→RT, 92 %; f) DIBAL-H, THF, 0 °C→RT, 94 %; g) NaH, BnBr, TBAI, THF, 0 °C→50 °C, 90 %; h) *n*BuSH, $MgBr_2{\cdot}OEt_2$, K_2CO_3, Et_2O, RT, quant.; i) PPh_3, NBS, CH_2Cl_2, 0 °C→RT, 94 %; j) **11**, LDA, THF, −78 °C; then **10**, −78 °C→RT; k) HCl, THF, 60 °C, 93 % over 2 steps; l) medium-pressure Hg lamp (150 W), pyrex filter, EtOAc, −78 °C, 55 % (13:1 d.r.); m) $MeOCH(NMe_2)_2$, THF, N_2 stream (open flask), 60 °C; then *p*ABSA, dioxane, 70 °C, 61 %; n) NEt_3, Rayonet lamp (300 nm), MeOH, RT, 77 % (3:1 d.r.); o) LDA, THF, −78 °C; then MeI, −78 °C→−50 °C, 86 % (20:1 d.r.); p) Pd/C, H_2 (1 atm), MeOH, RT, 66 %. Bn = benzyl, DIBAL-H = diisobutylaluminum hydride, DIPEA = diisopropylethylamine, LDA = lithium diisopropylamide, LHMDS = lithium hexamethyldisilazide, NBS = *N*-bromosuccinimide, *p*ABSA = 4-acetamidobenzenesulfonyl azide, SEMCl = [2-(trimethylsilyl)ethoxy]methyl chloride, TBAI = tetra-*n*-butylammonium iodide, Ts = *para*-toluenesulfonyl.[30]

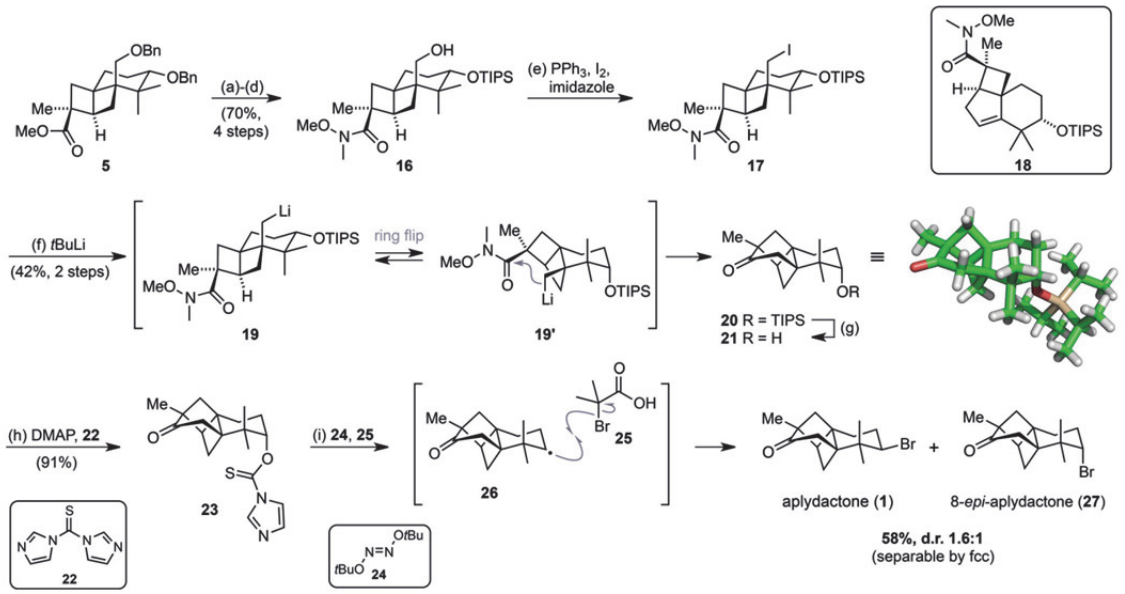

Scheme 3. Completion of the synthesis of aplydactone (**1**). a) Pd/C, H_2 (1 atm), EtOH, RT; b) TIPSOTf, 2,6-lutidine, CH_2Cl_2, 0 °C→RT, 83 % over 2 steps; c) $Pd(OH)_2$, H_2 (1 atm), MeOH, RT, 97 %; d) LHMDS, $Me(OMe)NH_2Cl$, THF, −78 °C→0 °C, 87 %; e) PPh_3, I_2, imidazole, CH_2Cl_2, −20 °C→−15 °C; f) *t*BuLi (reverse addition), pentane/Et_2O, −115 °C→−60 °C, 42 % over 2 steps; g) TBAF, THF, 0 °C→RT, 91 %; h) **22**, DMAP, THF, 60 °C, 91 %; i) **24** (4 equiv, syringe pump), **25** (5 equiv), benzene, 60 °C, 58 % (1.6:1 d.r.). DMAP = 4-(dimethylamino)pyridine, TBAF = tetra-*n*-butylammonium fluoride, TIPSOTf = triisopropylsilyl trifluoromethanesulfonate.[30]

17 with 2.2 equiv *t*BuLi at −115 °C in an ether/pentane solvent mixture afforded the desired ketone **20** in 42 % overall yield from **16**.[23] This unusual ring closure warrants further analysis. Under the chosen conditions, first organolithium species **19** should form via an ionic ate complex,[24] thus preventing a radical ring opening or expansion.[25] Subsequently, **19** must undergo a substantial conformational rearrangement (**19**→**19′**) to bring the nucleophilic site into close proximity to the electrophilic Weinreb amide. This rearrangement entails an inversion of the cyclohexane ring that brings the silyl-protected alcohol into an axial position. The resulting conformation is clearly visible in the crystal structure of product **20**, which already possesses the full carbon skeleton of aplydactone (**1**). Subsequent silyl deprotection with TBAF afforded alcohol **21**.

Unsurprisingly, attempts to convert activated derivatives of the secondary neopentyl alcohol into the desired bromide by nucleophilic displacement were unsuccessful owing to steric hindrance.[26] This prompted us to seek radical bromination conditions as an alternative method for the final C−Br bond formation. The conversion of alcohols and their derivatives into alkyl halides under radical conditions has been rarely explored, and the known methods failed in our hands.[27] Therefore, we decided to develop new conditions for this transformation based on the work of Zard et al. on the conversion of *S*-alkyl-*O*-ethyl xanthates into alkyl bromides.[28] To this end, alcohol **21** was converted into the corresponding imidazole **23**. Slow addition of di-*tert*-butyl hyponitrite (**24**)[29] to a solution of **23** and α-bromo acid **25** led to the formation of radical **26**, which abstracted a bromine atom from **25** to afford aplydactone (**1**) and its C8 epimer **27** in 36 % and 22 % yield, respectively. The applied combination of radical initiator and bromine source was essential for the success of this transformation. Di-*tert*-butyl hyponitrite (**24**) enabled low-temperature initiation, thereby preventing competitive thermal elimination of the thiocarbonylimidazole. Furthermore, α-bromo acid **25** showed better reactivity than bromotrichloromethane and was more easily removed from the reaction mixture than α-bromo esters and malonates. The two epimers **1** and **27** were separable by standard flash column chromatography, and the analytical data of synthetic **1** were in full accordance with those reported for the isolated natural product. Incidentally, 8-*epi*-aplydactone (**27**) may emerge as a natural product arising from the photocycloaddition of 10-*epi*-dactylone (**4**), which was isolated together with dactylone (**2**) and aplydactone (**1**) from *Aplysia dactylomela*.

In summary, we have achieved the first total synthesis of the unusual brominated sesquiterpenoid aplydactone (**1**) in racemic form. Our approach relies on two non-biomimetic photoreactions to construct the [2]-ladderane scaffold. An initial diastereoselective [2+2] cycloaddition generated the three adjacent quaternary centers present in the natural product. A photochemical Wolff rearrangement followed by late-stage Barbier-type ring closure provided the core structure of **1**. New reaction conditions were developed for the radical conversion of a sterically hindered thiocarbonylimidazole into an alkyl bromide to complete the synthesis. Further investigations on the substrate scope of this reaction and the biosynthesis of **1** are underway.

Acknowledgements

We thank the Center for Integrated Protein Science Munich (CIPSM) for financial support. We would like to acknowledge Prof. Dr. Thorsten Bach and his co-workers Dr. Andreas Bauer and Christoph Brenninger for technical support and helpful discussions regarding the photochemistry. Furthermore, Dr. Nicolas Armanino and Dr. Bryan Matsuura are acknowledged for helpful discussions and excellent support with the preparation of this manuscript.

Keywords: cycloaddition · halogenation · natural products · photochemistry · radical reactions

How to cite: *Angew. Chem. Int. Ed.* **2016**, *55*, 11251–11255
Angew. Chem. **2016**, *128*, 11418–11422

[1] For selected examples, see: a) S. A. Look, W. Fenical, D. Van Engen, J. Clardy, *J. Am. Chem. Soc.* **1984**, *106*, 5026–5027; b) R. G. S. Berlinck, R. Britton, E. Piers, L. Lim, M. Roberge, R. Moreira da Rocha, R. J. Andersen, *J. Org. Chem.* **1998**, *63*, 9850–9856; c) I. K. Mangion, D. W. C. MacMillan, *J. Am. Chem. Soc.* **2005**, *127*, 3696–3697; d) K. C. Nicolaou, T. R. Wu, D. Sarlah, D. M. Shaw, E. Rowcliffe, D. R. Burton, *J. Am. Chem. Soc.* **2008**, *130*, 11114–11121; e) G. Majetich, J. Yu, *Org. Lett.* **2008**, *10*, 89–91; f) B.-X. Zhao, Y. Wang, C. Li, G.-C. Wang, X.-J. Huang, C.-L. Fan, Q.-M. Li, H.-J. Zhu, W.-M. Chen, W.-C. Ye, *Tetrahedron Lett.* **2013**, *54*, 4708–4711.

[2] For selected examples, see: a) C. Ireland, J. Faulkner, *Tetrahedron* **1981**, *37*, 233–240; b) S. J. Eade, M. W. Walter, C. Byrne, B. Odell, R. Rodriguez, J. E. Baldwin, R. M. Adlington, J. E. Moses, *J. Org. Chem.* **2008**, *73*, 4830–4839; c) S.-J. Piao, Y.-L. Song, W.-H. Jiao, F. Yang, X.-F. Liu, W.-S. Chen, B.-N. Han, H.-W. Lin, *Org. Lett.* **2013**, *15*, 3526–3529; d) D. Stichnoth, P. Kölle, T. J. Kimbrough, E. Riedle, R. de Vivie-Riedle, D. Trauner, *Nat. Commun.* **2014**, *5*, 5597.

[3] S. N. Fedorov, O. S. Radchenko, L. K. Shubina, A. I. Kalinovsky, A. V. Gerasimenko, D. Y. Popov, V. A. Stonik, *J. Am. Chem. Soc.* **2001**, *123*, 504–505.

[4] a) S. N. Fedorov, M. V. Reshetnyak, A. P. Schedrin, S. G. Ilyin, J. T. Struchkov, V. A. Stonik, G. B. Elyakov, *Dokl. Akad. Nauk SSSR* **1990**, *307*, 877–879; b) L. K. Shubina, S. N. Fedorov, A. I. Kalinovskiy, A. S. Dmitrenok, J. O. Jin, M. G. Song, J. Y. Kwak, V. A. Stonik, *Russ. Chem. Bull.* **2007**, *56*, 2109–2114.

[5] a) J. Iriondo-Alberdi, M. F. Greaney, *Eur. J. Org. Chem.* **2007**, 4801–4815; b) T. Bach, J. P. Hehn, *Angew. Chem. Int. Ed.* **2011**, *50*, 1000–1045; *Angew. Chem.* **2011**, *123*, 1032–1077; c) Y. J. Hong, D. J. Tantillo, *Chem. Soc. Rev.* **2014**, *43*, 5042–5050; for a related [2+2] photocycloadduct, see: d) J. Bordner, L. R. Morrow, *Cryst. Struct. Commun.* **1976**, *5*, 523–526.

[6] D. H. Nouri, D. J. Tantillo, *Curr. Org. Chem.* **2006**, *10*, 2055–2074.

[7] J. M. Rohde, Ph.D. Thesis, The Scripps Research Institute, La Jolla, California, **2005**.

[8] a) J. C. Barborak, L. Watts, R. Pettit, *J. Am. Chem. Soc.* **1966**, *88*, 1328–1329; b) J. A. Tallarico, M. L. Randall, M. L. Snapper, *J. Am. Chem. Soc.* **1996**, *118*, 9196–9197; c) J. Limanto, J. A. Tallarico, J. R. Porter, K. S. Khuong, K. N. Houk, M. L. Snapper, *J. Am. Chem. Soc.* **2002**, *124*, 14748–14758; for a review on this topic, see: d) H. Hopf, *Angew. Chem. Int. Ed.* **2003**, *42*, 2822–2825; *Angew. Chem.* **2003**, *115*, 2928–2931.

[9] a) K. B. Wiberg, B. L. Furtek, L. K. Olli, *J. Am. Chem. Soc.* **1979**, *101*, 7675–7679; b) W. G. Dauben, D. M. Walker, *Tetrahedron Lett.* **1982**, *23*, 711–714; c) V. B. Rao, S. Wolff, W. C. Agosta, *J. Chem. Soc. Chem. Commun.* **1984**, 293–294; d) V. Mascitti, E. J. Corey, *J. Am. Chem. Soc.* **2004**, *126*, 15664–15665; e) V. Mascitti, E. J. Corey, *J. Am. Chem. Soc.* **2006**, *128*, 3118–3119.

[10] a) W. A. Kleschick, *J. Org. Chem.* **1986**, *51*, 5429–5433; b) L. Carman, L. D. Kwart, T. Hudlicky, *Synth. Commun.* **1986**, *16*, 169–182.

[11] a) Y. Yamamoto, N. Asao, *Chem. Rev.* **1993**, *93*, 2207–2293; b) B. C. Ranu, A. Majee, A. R. Das, *Tetrahedron Lett.* **1995**, *36*, 4885–4888.

[12] J. L. Roberts, P. S. Borromeo, C. D. Poulter, *Tetrahedron Lett.* **1977**, *18*, 1621–1623.

[13] S. Kim, I. S. Kee, Y. H. Park, J. H. Park, *Synlett* **1991**, 183–184.

[14] a) T. Yoshida, S. Saito, *Chem. Lett.* **1982**, *11*, 165–168; b) T. Yoshida, S. Saito, *Bull. Chem. Soc. Jpn.* **1982**, *55*, 3931–3932.

[15] a) M. T. Crimmins, *Chem. Rev.* **1988**, *88*, 1453–1473; b) M. T. Crimmins, P. S. Watson, *Tetrahedron Lett.* **1993**, *34*, 199–202; c) M. T. Crimmins, S. Huang, L. E. Guise-Zawacki, *Tetrahedron Lett.* **1996**, *37*, 6519–6522; d) N. Hoffmann, *Chem. Rev.* **2008**, *108*, 1052–1103; e) J. P. Hehn, C. Müller, T. Bach in *Handbook of Synthetic Photochemistry* (Eds.: A. Albini, M. Fagnoni), Wiley-VCH, **2010**, pp. 171–215; f) S. Poplata, A. Tröster, Y.-Q. Zou, T. Bach, *Chem. Rev.* **2016**, DOI: 10.1021/acs.chemrev.5b00723.

[16] M. Regitz, J. Rüter, *Chem. Ber.* **1968**, *101*, 1263–1270.

[17] R. L. Danheiser, R. F. Miller, R. G. Brisbois, S. Z. Park, *J. Org. Chem.* **1990**, *55*, 1959–1964.

[18] a) L. Lombardo, L. N. Mander, *Synthesis* **1980**, 368–369; b) T. Uyehara, N. Takehara, M. Ueno, T. Sato, *Bull. Chem. Soc. Jpn.* **1995**, *68*, 2687–2694.

[19] a) M. Regitz, G. Himbert, *Justus Liebigs Ann. Chem.* **1970**, *734*, 70–85; b) T. Ye, M. A. McKervey, *Chem. Rev.* **1994**, *94*, 1091–1160; c) G. Maas, *Angew. Chem. Int. Ed.* **2009**, *48*, 8186–8195; *Angew. Chem.* **2009**, *121*, 8332–8341; d) A. Ford, H. Miel, A. Ring, C. N. Slattery, A. R. Maguire, M. A. McKervey, *Chem. Rev.* **2015**, *115*, 9981–10080.

[20] W. Kirmse, *Eur. J. Org. Chem.* **2002**, 2193–2256.

[21] a) P. J. Garegg, B. Samuelsson, *J. Chem. Soc. Perkin Trans. 1* **1980**, 2866–2869; b) P. J. Garegg, R. Johansson, C. Ortega, B. Samuelsson, *J. Chem. Soc. Perkin Trans. 1* **1982**, 681–683.

[22] For the use of cyclobutane fragmentation in organic synthesis, see: a) J. D. Winkler, C. M. Bowen, F. Liotta, *Chem. Rev.* **1995**, *95*, 2003–2020; b) J. C. Namyslo, D. E. Kaufmann, *Chem. Rev.* **2003**, *103*, 1485–1538.

[23] For selected examples, see: a) T. van der Does, G. H. Klumpp, M. Schakel, *Tetrahedron Lett.* **1986**, *27*, 519–520; b) D. Kim, Y. K. Lee, *Tetrahedron Lett.* **1991**, *32*, 6885–6886; c) I. S. Aidhen, J. R. Ahuja, *Tetrahedron Lett.* **1992**, *33*, 5431–5432; d) A. M. Baylis, M. P. H. Davies, E. J. Thomas, *Org. Biomol. Chem.* **2007**, *5*, 3139–3155; e) T. Burns, M. Helliwell, E. J. Thomas, *Tetrahedron Lett.* **2013**, *54*, 2120–2123.

[24] a) K. B. Wiberg, S. Sklenak, W. F. Bailey, *J. Org. Chem.* **2000**, *65*, 2014–2021; b) W. F. Bailey, J. D. Brubaker, K. P. Jordan, *J. Organomet. Chem.* **2003**, *681*, 210–214.

[25] For selected examples of cyclobutylcarbinyl radical fragmentation, see: a) F. E. Ziegler, R. X. Kover, N. N. K. Yee, *Tetrahedron Lett.* **2000**, *41*, 5155–5159; b) W. D. Shipe, E. J. Sorensen, *J. Am. Chem. Soc.* **2006**, *128*, 7025–7035; c) J. P. Hehn, M. Kemmler, T. Bach, *Synlett* **2009**, 1281–1284; d) J. P. Hehn, E. Herdtweck, T. Bach, *Org. Lett.* **2011**, *13*, 1892–1895; e) J. Shi, S.-S. Chong, Y. Fu, Q.-X. Guo, L. Liu, *J. Org. Chem.* **2008**, *73*, 974–982.

[26] a) A. Fukuzawa, H. Sato, T. Masamune, *Tetrahedron Lett.* **1987**, *28*, 4303–4306; b) V. Bhat, J. A. MacKay, V. H. Rawal, *Tetrahedron* **2011**, *67*, 10097–10104; c) V. Bhat, V. H. Rawal, *Chem. Commun.* **2011**, *47*, 9705–9707; d) W.-J. Chung, C. D. Vanderwal, *Angew. Chem. Int. Ed.* **2016**, *55*, 4396–4434; *Angew. Chem.* **2016**, *128*, 4470–4510.

[27] a) F. R. Jensen, T. I. Moder, *J. Am. Chem. Soc.* **1975**, *97*, 2281–2283; b) S. J. Cristol, D. G. Seapy, *J. Org. Chem.* **1982**, *47*, 132–

136; c) D. Crich, S. M. Fortt, *Synthesis* **1987**, 35–37; d) W. Damm, B. Giese, J. Hartung, T. Hasskerl, K. N. Houk, O. Hueter, H. Zipse, *J. Am. Chem. Soc.* **1992**, *114*, 4067–4079; e) B. Giese, J. Hartung, *Chem. Ber.* **1992**, *125*, 1777–1779; for the hydrobromination of alkenes by hydrogen-atom transfer, see: f) X. Ma, S. B. Herzon, *Chem. Sci.* **2015**, *6*, 6250–6255.

[28] F. Barbier, F. Pautrat, B. Quiclet-Sire, S. Z. Zard, *Synlett* **2002**, 811–813.

[29] For the preparation of **24**, see: a) G. D. Mendenhall, *Tetrahedron Lett.* **1983**, *24*, 451–452; b) J. T. Banks, J. C. Scaiano, W. Adam, R. S. Oestrich, *J. Am. Chem. Soc.* **1993**, *115*, 2473–2477.

[30] CCDC 1475334 (**15**) and 1475333 (**20**) contain the supplementary crystallographic data for this paper. These data are provided free of charge by The Cambridge Crystallographic Data Centre.

Received: April 27, 2016
Published online: June 30, 2016

2.2.2 Investigations on the biosynthesis of chamigrane natural products from *Aplysia dactylomela* – Total synthesis of dactylone, 10-*epi*-dactylone, aplydactone and 8-*epi*-isoaplydactone

† These authors contributed equally to this work.

ACS central science

Research Article

http://pubs.acs.org/journal/acscii

Unravelling Photochemical Relationships Among Natural Products from *Aplysia dactylomela*

Bryan S. Matsuura,[†] Patrick Kölle,[†] Dirk Trauner,* Regina de Vivie-Riedle,* and Robin Meier*

Department of Chemistry, Ludwig-Maximilians-Universität, 81377 Munich, Germany

Supporting Information

ABSTRACT: Aplydactone (**1**) is a brominated ladderane sesquiterpenoid that was isolated from the sea hare *Aplysia dactylomela* together with the chamigranes dactylone (**2**) and 10-*epi*-dactylone (**3**). Given the habitat of *A. dactylomela*, it seems likely that **1** is formed from **2** through a photochemical [2 + 2] cycloaddition. Here, we disclose a concise synthesis of **1**, **2**, and **3** that was guided by excited state theory and relied on several highly stereoselective transformations. Our experiments and calculations confirm the photochemical origin of **1** and explain why it is formed as the sole isomer. Irradiation of **3** with long wavelength UV light resulted in a [2 + 2] cycloaddition that proceeded with opposite regioselectivity. On the basis of this finding, it seems likely that the resulting regioisomer, termed "8-*epi*-isoaplydactone", could also be found in *A. dactylomela*.

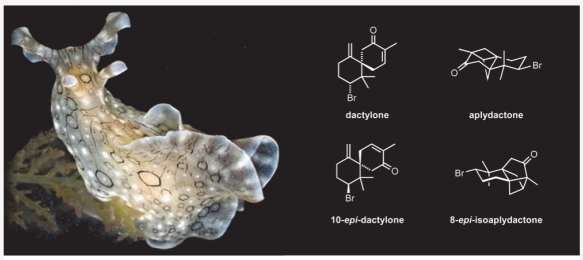

Photo credit: David Mullins - nudibranch.com.au

The "spotted sea hare" *Aplysia dactylomela* is a marine mollusk that likes to dwell in tropical seas and feast on algae that produce halogenated terpenoids.[1−3] Several brominated natural products have been isolated from *A. dactylomela* itself (Figure 1). They include dactylone (**2**)[4] and its epimer 10-*epi*-dactylone (**3**), as well as the chamigranes **4** and **5**.[5] Their most remarkable representative to date, however, is aplydactone (**1**).[6] It was isolated by Stonik et al. in 2001 from specimens collected in the shallow waters surrounding Nosy Hara, an island off the coast of Madagascar. Aplydactone possesses an unprecedented tetracyclic skeleton that is highly strained and contains three quaternary stereocenters, which are all embedded in the ladderane substructure.[7,8]

Given the sea hare's tropical habitat and the relatively intense solar irradiation it is exposed to, it is reasonable to assume that **2** is converted into aplydactone (**1**) via a photochemical [2 + 2] cycloaddition. This cycloaddition is noteworthy in several respects. First, Stonik reported that **2** failed to yield **1** under "long-term UV irradiation" and suggested that the formation of **1** may be due to a non-photochemical enzymatic reaction.[6] Given our experience with natural products whose biosynthesis includes a photochemical step, we suspected that this failure might be due to the experimental conditions chosen.[9,10] We reasoned that high energy UV light might affect the carbon−bromine bond or lead to other unwanted reactions and that the use of a "biomimetic" light source would be critical. While our studies were ongoing, this was independently verified by Burns and co-workers in their elegant synthesis of **1** and **2**.[11] Second, the photocycloaddition reaction appears to produce the highly strained [2]-ladderane skeleton in an apparent violation of the "rule of five".[12,13] This rule refers to the observation that intramolecular [2 + 2] reactions (for molecules in the triplet excited state) tend to form regioisomers that contain five-membered rings (Figure 2). In Ciamician's classic photochemical synthesis of "carvone camphor" from carvone, this was indeed the case.[14] We therefore wondered whether irradiation of **2** at appropriate wavelengths could also yield the less strained "isoaplydactone" (**6**) and, if not, what the reasons for this might be. Finally, no mention was made whether 10-*epi*-dactylone (**3**) was subjected to irradiation as well. We wondered whether **3** would also yield a photocycloaddition product and, if so, whether this product would be 8-*epi*-aplydactone (**7**) or its isomer 8-*epi*-isoapydactone (**8**), which abides by the rule of five.

To address these questions, we decided to take a two-pronged approach that involved both theory and experiment. We would synthesize both natural products **2** and **3** and then study their photochemical conversions guided by high-level quantum chemical calculations carried out in parallel. These calculations served two purposes: (a) to predict the optimal wavelength with which to irradiate the chamigranes and (b) to rationalize the outcomes of the cycloadditions.

■ QUANTUM CHEMICAL ANALYSIS

The quantum chemical calculations were performed at the CASSCF/CASPT2,[15] CCSD,[16] and DFT/TDDFT[17,18] level of theory. Since intersystem crossing (ISC) plays a key role in photochemical [2 + 2] cycloadditions,[19] we investigated the singlet as well as the triplet states of dactylone (**2**). First, the ground state geometry of **2** was optimized and was found to be

Received: September 29, 2016
Published: December 19, 2016

DOI: 10.1021/acscentsci.6b00293
ACS Cent. Sci. 2017, 3, 39−46

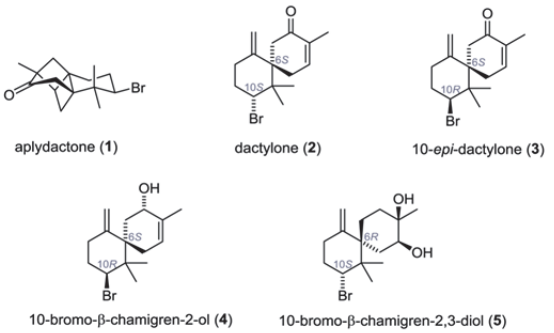

Figure 1. Brominated sesquiterpenoids from *Aplysia dactylomela*.

in good agreement with the crystal structure of the isolated natural product[1] represented by the conformer **2a** (see Figure 2 and Figure B1, Supporting Information). The other possible chair conformer **2b** exhibits the bromine in the axial position and is 0.12 eV (11.6 kJ/mol) higher in Gibbs free energy (ΔG), and a barrier of 0.48 eV (46.3 kJ/mol) has to be overcome for the ring-flip to occur (see Figure B2, Supporting Information). Therefore, the conformer **2a** is the one most populated and will be considered in the following analysis.

The calculated absorption spectrum of **2a** reveals two strong absorption bands in the UVC region, which cannot be reached by solar irradiation (Figure 3a). Only the weak absorption band of **2a** in the UVA region, predicted to occur around λ_{max} = 323 nm, can be accessed by the solar light.

The calculated absorption band in the UVA region (red bar in Figure 3b) is in good agreement with the experimentally determined spectrum. This absorption band is attributed to the transition from the S_0 to S_1 state and is characterized by an excitation from the lone pair of the oxygen atom to the π-system of the enone moiety ($n_O\pi^*$) of **2a** (see Figure 3b) and is therefore completely localized on the enone moiety of **2a**. The excitation into this band will initiate the photochemical reaction under biomimetic conditions.

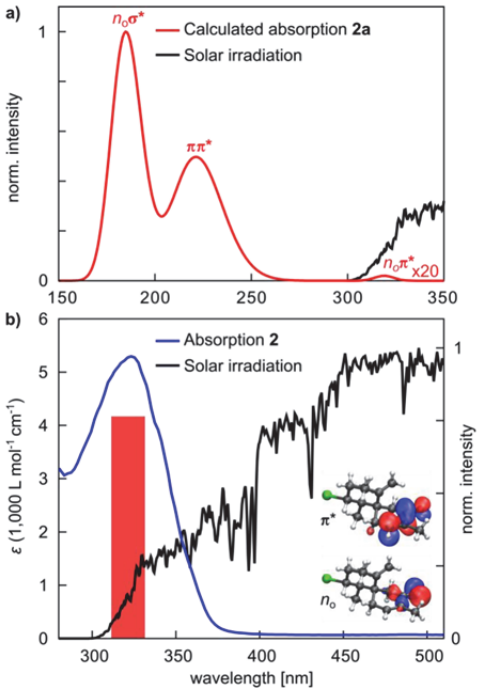

Figure 3. (a) Comparison of the calculated absorption spectrum of **2a** with the solar spectral irradiance AM 1.5.[20] The spectrum was obtained by plotting Gaussian functions around the calculated electronic transitions (see Table B1, Supporting Information). The corresponding characters of the excited states are given, and the interval from 300 to 340 nm is enhanced by a factor of 20. (b) Experimental absorption spectrum of **2**. The calculated transition from the S_0 to S_1 state of **2a** is shown as a red bar as well as the orbitals describing the excitation.

The main relaxation pathway from the excited precursor **2a** to the starting point of the cycloaddition is shown in Figure 4. The calculated spin−orbit coupling and S_1-triplet energy gaps

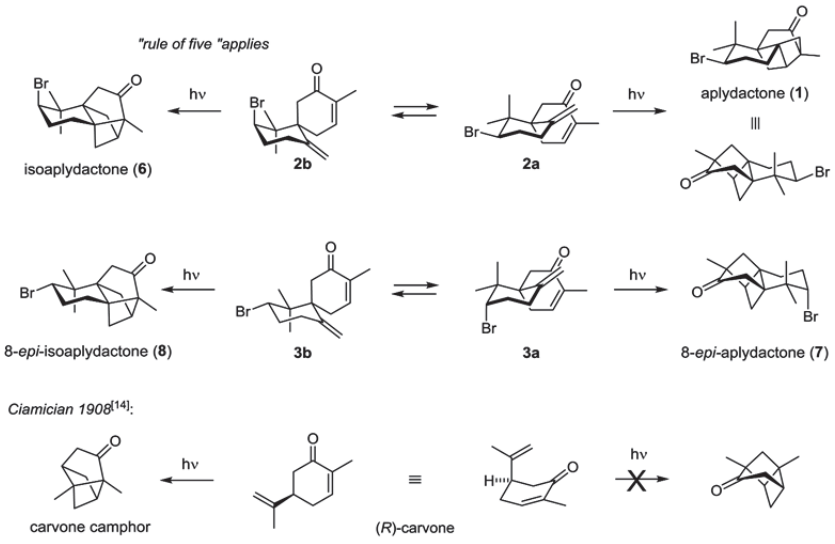

Figure 2. "Rule of five" in photochemical [2 + 2] cycloadditions and its application to the *Aplysia* terpenoids.

DOI: 10.1021/acscentsci.6b00293
ACS Cent. Sci. 2017, 3, 39−46

reveal that after excitation to the S_1 ($n_O\pi^*$) state, a large ISC probability exists for the S_1 with the T_2 ($\pi\pi^*$) state. Both states run parallel along the initial relaxation coordinate until they reach a low lying S_1/T_2 intersection (IS) located in the vicinity of the S_1-Min (S_1/T_2 IS in Figure 4, see section B.2.3, Supporting Information for details).

Once the T_2 ($\pi\pi^*$) state is populated, an energetically close lying conical intersection with the T_1 state can be reached (T_2/T_1 CoIn in Figure 4). Here, the relaxation path splits into three branches leading to different minima on the T_1 potential energy surface. The two minima of $\pi\pi^*$ character (T_1-Min2 and T_1-Min3 (not shown)) are slightly lower in energy than T_1-Min1 with $n\pi^*$ character (see Table B2, Supporting Information). This should lead to their preferred population, which is supported by dynamic simulations of small α,β-unsaturated enones.[21] At T_1-Min2 the hydrogen atom is positioned under the ring plane, which allows the direct attack onto the *exo*-double bond. Therefore, T_1-Min2 represents the starting point of the cycloaddition (see Figure B5, Supporting Information for details).

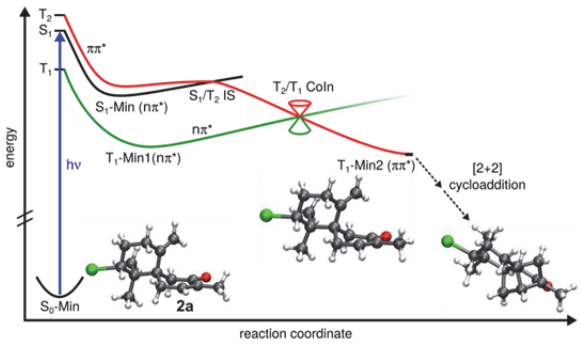

Figure 4. Schematic illustration of the proposed relaxation pathway from the excited S_1 state of precursor **2a** to the starting point of the [2 + 2] cycloaddition (T_1-Min2). The electronic characters and relevant optimized geometries are given.

In principle, there is the possibility of a relaxation from the excited state back to the ground state of **2a** via internal conversion (IC) or ISC. However, these processes are very unlikely due to the high barriers present for these deactivation pathways for precursor **2a** (see section B.2.4 and B.2.5, Supporting Information for details).

The first step of the cycloaddition is the formation of a triplet 1,4-diradical (^{3}DR) intermediate.[19] From the triplet minimum T_1-Min2, four different 1,4-diradicals (DR1-DR4) are possible (Figure 5). Once formed, the triplet diradicals (^{3}DR) lead to the singlet diradicals (^{1}DR), from which either the cycloadduct can be formed or a relaxation back to the diene can occur. Both diradicals DR1 and DR2 can lead to aplydactone (**1**) (Figure 5b). In contrast, isoaplydactone (**6**) can only be formed from the diradical DR3 because for diradical DR4 the second bond formation is prohibited for geometrical reasons.

The quantum chemical calculations reveal that both diradical pathways leading to aplydactone (**1**)—DR2 and especially DR1—are associated with smaller barriers than the DR3 pathway leading to isoaplydactone (**6**) (see section B.2.6, SI). Thus, the formation of **1** should be strongly favored over the formation of the "rule of five" product **6**.

Overall, the theoretical results predict that an optical excitation to the singlet S_1 ($n_O\pi^*$) state of dactylone (**2**) should allow for the photochemical and biomimetic synthesis of aplydactone (**1**).

SYNTHESIS OF DACTYLONE AND 10-*EPI*-DACTYLONE

With these results in hand, we endeavored to validate the photochemical cycloaddition hypothesis and sought a stereoselective synthesis of dactylone (**2**). We reasoned that both dactylone (**2**) and 10-*epi*-dactylone (**3**) could be synthesized from the natural product 10-bromo-β-chamigrene (**9**)[1] via an allylic oxidation (Figure 6). Remarkably, the Burns and Snyder

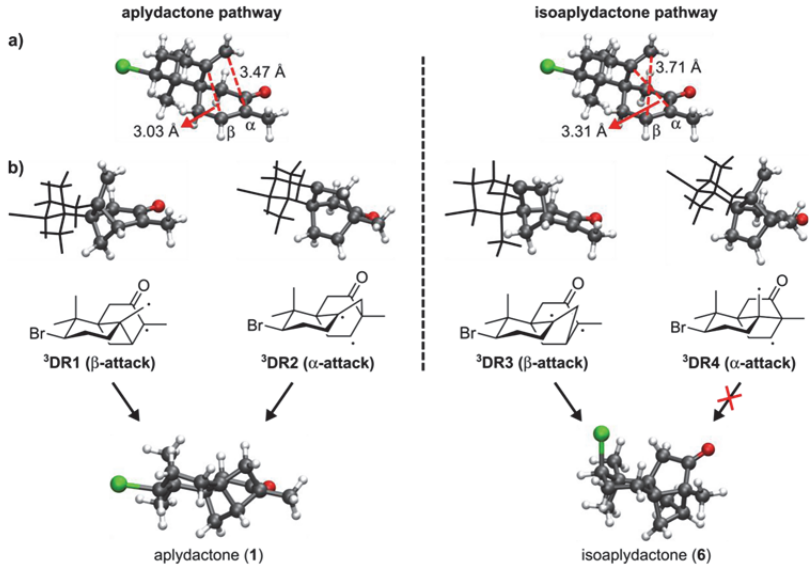

Figure 5. (a) Intercarbon distances for the reaction pathways leading to aplydactone (**1**) and isoaplydactone (**6**) at the triplet minimum T_1-Min2 of **2a**. (b) Optimized geometries of the four triplet diradicals (^{3}DR) possible from T_1-Min2.

DOI: 10.1021/acscentsci.6b00293
ACS Cent. Sci. 2017, 3, 39−46

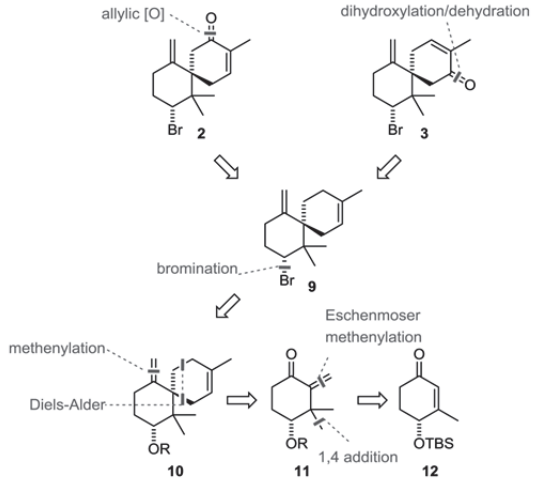

Figure 6. Retrosynthetic analysis of dactylone (**2**) and 10-*epi*-dactylone (**3**).

group disclosed their total syntheses **9** using the same strategy almost simultaneously.[11,22] The synthesis of halogenated chamigranes remains a significant challenge due to the difficulty in forging sterically encumbered spirocyclic quaternary centers and 2° neopentyl bromides.[23−26] We envisioned that the synthesis of the spiroundecane **10** could be achieved through a Diels−Alder reaction between exocyclic enone **11** and isoprene, followed by a late stage bromination (Figure 6). The first key intermediate **11** would be derived from hydroxy cyclohexenone **12** via a conjugate addition reaction followed by an Eschenmoser methenylation. Although cyclohexenone **12** is available in enantiopure form, we elected to synthesize **9** in racemic fashion for economic reasons.[27]

Our synthesis began with a copper mediated conjugate addition of trimethylsilylmethyl magnesium chloride, which served as a masked methyl group, followed by trapping with trimethylsilyl chloride. This afforded silyl enol ether **13** in excellent yield and as the only stereoisomer (Figure 7). Exposure of **13** to Li_2CO_3 and Eschenmoser's salt,[28] followed by treatment with *m*-CPBA, then afforded exocyclic enone **14** in good yield.

With a reliable route to **14** in hand, we turned our attention to the key Diels−Alder reaction to introduce the spiroundecane scaffold.[29] Unfortunately, **14** was found to be either unreactive toward isoprene or unstable in the presence of several Lewis acids. Reacting **14** with 4 equiv of isoprene and 1.5 equiv of BCl_3 converted **14** into the desired spirocyclic ketone **15** in moderate yield but as a single diastereoisomer.

However, this reaction was not scalable and difficult to reproduce. We therefore turned to high pressure chemistry, which had previously served us well in cycloadditions. After extensive optimization, we found that reacting **14** in the presence of 6 equiv of isoprene and 0.2 equiv of $ZnBr_2$ under 6 kbar of pressure afforded the silylated spiroundecane **15** in good yield and on a gram scale.[30] The structure of **15** was confirmed by crystallography of the deprotected adduct **16** (see Supporting Information). The presence of the trimethylsilyl group was critical for the high level of diastereoselectivity in the Diels−Alder reaction. The steric bulk of the silane forces both large substituents of **14** to reside in an axial position, blocking the top face of the dienophile (see X-ray in Figure 7).

At this stage, we needed to introduce the exocyclic methylene on the C7 position, remove the silyl groups, and convert the C10 hydroxyl into an alkyl bromide to arrive at **9**. The sterically hindered C7 carbonyl of **15** was found to be unreactive toward several standard methenylation conditions, including Tebbe, Petasis, Lombardo, Peterson, Wittig, and Kauffmann olefinations.[31] However, we were finally able to overcome this obstacle by heating spirocycle **15** with the

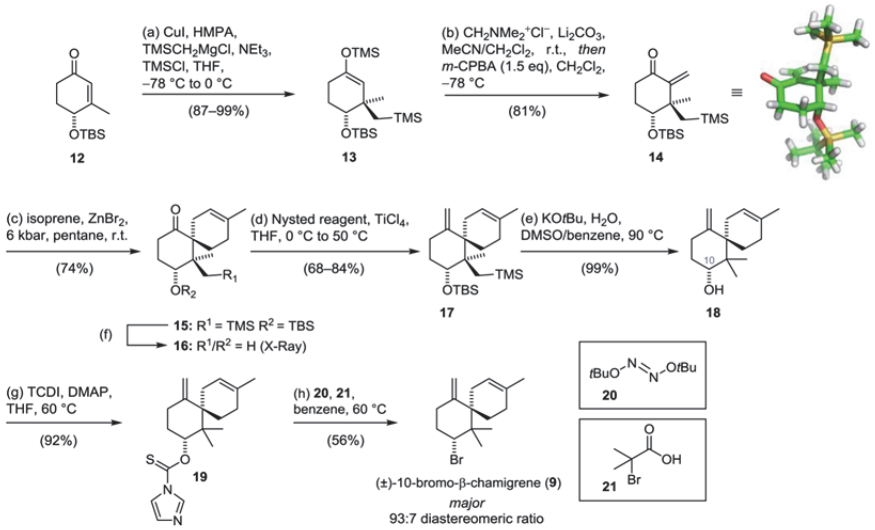

Figure 7. Synthesis of (±)-10-bromo-β-chamigrene (**9**). (a) CuI (0.14 equiv), HMPA (1.1 equiv), $TMSCH_2MgCl$ (1.5 equiv), NEt_3 (3.0 equiv), TMSCl (2.0 equiv) THF, −78 to 0 °C, 40 min, 87−99%; (b) $CH_2NMe_2^+Cl^-$ (2.0 equiv), Li_2CO_3 (1.1 equiv), $MeCN/CH_2Cl_2$, r.t., 6 h *then* *m*-CPBA (1.5 equiv), CH_2Cl_2, −78 °C, 90 min, 81%; (c) isoprene (6.0 equiv), $ZnBr_2$ (0.2 equiv), 6 kbar, pentane, r.t., 24 h, 74%; (d) Nysted reagent (10.8 equiv), $TiCl_4$ (10.0 equiv), THF, 0 to 50 °C, 18 h, 68−84%; (e) KO*t*Bu (1.15 equiv), H_2O (1.0 equiv), DMSO/benzene, 90 °C, 17 h, 99%; (f) KO*t*Bu (1.15 equiv), H_2O (1.0 equiv), DMSO, 90 °C, 45 min, 37−46%; (g) TCDI (5.0 equiv), DMAP (3.0 equiv), THF, 60 °C, 16 h, 92%; (h) **20** (4.0 equiv) **21** (5.0 equiv) benzene, 60 °C, 2.5 h, 56%.

DOI: 10.1021/acscentsci.6b00293
ACS Cent. Sci. 2017, 3, 39−46

Nysted/Utimoto reagent[32] in the presence of $TiCl_4$, which cleanly provided the desired exocyclic alkene **17** in good yield. Both the Diels−Alder reaction and the olefination could be performed in a one-pot procedure (see Supporting Information for details). Compound **17** could then be desilylated to afford **18** in nearly quantitative yield. Presumably, the removal of the TMS group involved a rare 1,4-Brook-rearrangement.[33] Interestingly, the implementation of the TMS-methylene as a "traceless" directing group to improve diastereoselectivity appears to have little precedence in the literature.[34]

Next, we turned to the introduction of the requisite C10 bromide from the corresponding hydroxy group. The steric hindrance of neopentyl alcohols makes them unsuitable toward C−O bond activation/nucleophilic displacement and is a notoriously difficult challenge in halogenation chemistry.[35] In our previous non-biomimetic synthesis of aplydactone, we faced a similar challenge which we overcame with a late stage radical bromination protocol specifically developed to address this issue.[36] Using those conditions, we found that the bromination of **19** was unexpectedly diastereoselective, providing **9** as a 93:7 mixture of diastereoisomers.[37]

The explanation for this favorable outcome is shown in Figure 8. Attack of the methyl radical generated by thermal decomposition of hyponitrite **20** onto thiocarbamate **19** gives intermediary radical **22**, which undergoes fragmentation to afford the secondary radical **23a**. A fast bimolecular reaction with the bromine source **21** via an equatorial attack then gives the observed major product **9**. This equatorial attack has a very low calculated activation barrier of 19.1 kJ/mol (see Figure B16, Supporting Information). The minor product **24** could arise via axial attack onto **23a**, which we calculated to have an activation barrier of 25.6 kJ/mol. This is consistent with selectivities for equatorial vs axial attack reported in the literature[28] and matches the observed diastereomeric ratio of 93:7. Alternatively, the minor isomer **24** could arise from equatorial attack onto the radical conformer **23b**. However, we calculated that the activation barrier for the necessary ring inversion is 43.4 kJ/mol. This means that the unimolecular ring-flip is considerably slower than the bimolecular bromine transfer at the given concentrations and temperature and that the observed diastereoselectivity is solely due to the preferences of conformer **23a** (see Figure B15, Supporting Information for details).

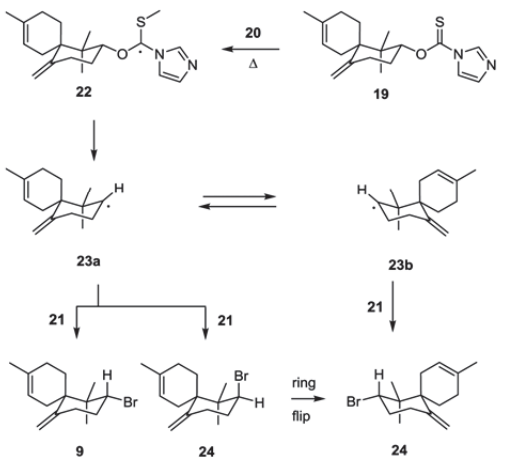

Figure 8. Stereoselectivity of the radical bromination of **19**.

For the final stage of the synthesis, we sought to access dactylone (**2**) and 10-*epi*-dactlyone (**3**) by exploiting the inherent *pseudo*-symmetry of **9**. By implementing divergent oxidation strategies, it was possible to either "retain" or "invert" the stereocenter at C6 relative to the C10 bromide (Figure 9).[38,39] Starting with **9**, a catalytic Upjohn dihydroxylation proceeded with exclusive regio- and diastereoselectivity, providing **25** in nearly quantitative yield. Diol **25** could then be oxidized with IBX followed by dehydration with $SOCl_2$ and pyridine, affording dactylone (**2**) in 66% yield over two steps. Very recently, this natural product was also reached by Snyder using a similar oxidative end game.[22] Conversely, 10-*epi*-dactylone (**3**) could be obtained from **9** by an allylic oxidation using SeO_2, which provided allylic alcohol **22** in moderate yield, followed by further oxidation with an excess of MnO_2, consistent with the reaction sequence reported by Burns and co-workers.[11] Using this strategy, were able to reach both **2** and **3** in the racemic series from a single precursor, viz. chamigrane **9**.

PHOTOCHEMICAL [2 + 2] CYCLOADDITION OF DACTYLONE AND 10-*EPI*-DACTYLONE

With ample quantities of dactylone (**2**) and 10-*epi*-dactylone (**3**) in hand, we then proceeded to investigate their photochemistry.

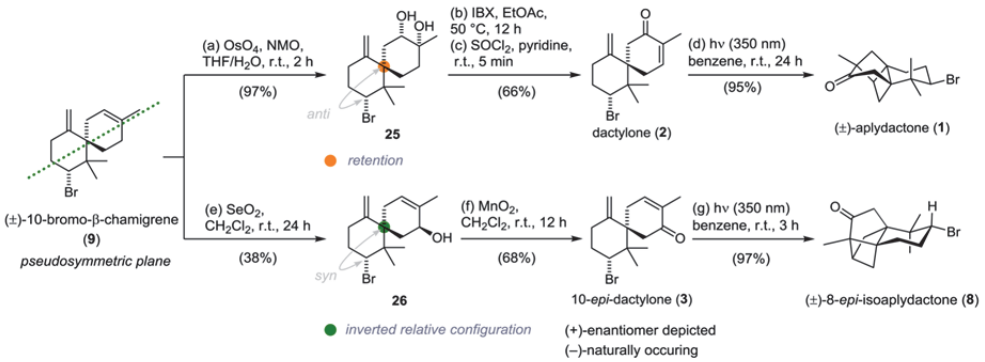

Figure 9. Synthesis of aplydactone and 8-*epi*-isoaplydactone by stereodivergent synthesis and selective irradiation. (a) OsO_4 (5 mol %), NMO (1.5 equiv), THF/H_2O, r.t., 2 h, 97%; (b) IBX (2.5 equiv), EtOAc, 50 °C, 12 h; (c) $SOCl_2$ (6.7 equiv), pyridine, r.t., 5 min, 66% over two steps; (d) *hν* (350 nm), benzene, r.t., 24 h, 95%; (e) SeO_2, (2.0 equiv), CH_2Cl_2, r.t., 24 h, 38%; (f) MnO_2 (20.0 equiv), CH_2Cl_2, r.t., 12 h, 50%; (g) *hν* (350 nm), benzene, r.t., 24 h, 97%.

DOI: 10.1021/acscentsci.6b00293
ACS Cent. Sci. 2017, 3, 39−46

Using a Rayonet photoreactor, we irradiated dactylone at different wavelengths. When **2** was exposed to 300 nm UVB light, we observed rapid degradation and found only minor quantities of aplydactone in the crude product mixture. However, irradiation with 350 nm light (UVA) over a period of 24 h led to the complete conversion of dactylone (**2**) into aplydactone (**1**). The wavelength dependence and quantitative conversion of **2** to **1** corroborate results recently disclosed by the Burns lab.[11] Finally, we found that exposure of **2** to Munich sunlight converted it to aplydactone over a period of 6 days in good agreement with Burns and co-workers.[11]

Our calculations show why the choice of a light source was so critical (Figure 10). Upon irradiation with 350 nm light (blue arrow, Figure 10), the majority of the S_1 population undergoes energetically favorable ISC leading to the formation of aplydactone. However, 300 nm irradiation (purple arrow, Figure 10) deposits more energy (0.6 eV) into the system. Now a larger fraction of the excited molecules can reach the conical intersection of the S_1 with the S_2 state (S_2/S_1 CoIn, Figure 10). The S_2 state is characterized by an excitation from the lone pair of the bromine to the antibonding σ^*-orbital of the carbon−bromine bond ($n_{Br}\sigma^*$). At the Franck−Condon (FC) region, the S_2 state is too high in energy to be reached by direct excitation under our reaction conditions (see Figure 10 and Table B1, Supporting Information). However, an elongation of the carbon−bromine bond stabilizes this state and leads to the conical intersection with the S_1 state which is located 0.23 eV above the resonant S_0−S_1 transition and can therefore be accessed through the 300 nm excitation (see Table B3, Supporting Information). The population of the $n_{Br}\sigma^*$ state leads to a minimum on the S_1 potential energy surface (S_1-Min ($n_{Br}\sigma^*$)) and to the homolytic cleavage of the carbon−bromine bond. The separated radical pair can then cause unwanted side reactions, resulting in the observed substrate degradation.

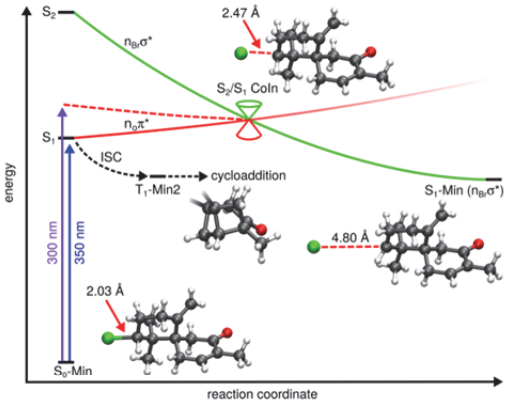

Figure 10. Schematic illustration of the homolytic cleavage of the carbon−bromine bond via the S_2/S_1 conical intersection after excitation to the S_1 state of **2a**. The bromine−carbon distances at the relevant optimized geometries are shown.

When 10-*epi*-dactylone (**3**) was irradiated with 350 nm light, **3** was converted to the [2 + 2] product **8**, termed "8-*epi*-isoaplydactone", as the sole product in 97% yield. The conversion of **3** to **8** was complete in 3 h and is significantly faster than the conversion of **2** to **1**. We were unable to detect the presence of 8-*epi*-aplydactone (**7**), which we had obtained in our previous nonbiomimetic synthesis.[36]

Again, our experimental results could be rationalized with excited state computations. Analogous to dactylone (**2**), for 10-*epi*-dactylone (**3**) the excitation to the S_1 state of the preferred conformer **3b** leads to a triplet minimum T_1-min2 (see section B.3, Supporting Information for details). From here, four different 1,4-diradicals (DR1-DR4) are possible as well (Figure 11). In the case of **3**, the calculations reveal that the formation of 8-*epi*-isoaplydactone (**8**) via the two diradical pathways DR3 and DR4 is preferred over the formation of 8-*epi*-aplydactone (**7**) through the diradical pathway DR2 (see section B.3.4, Supporting Information).

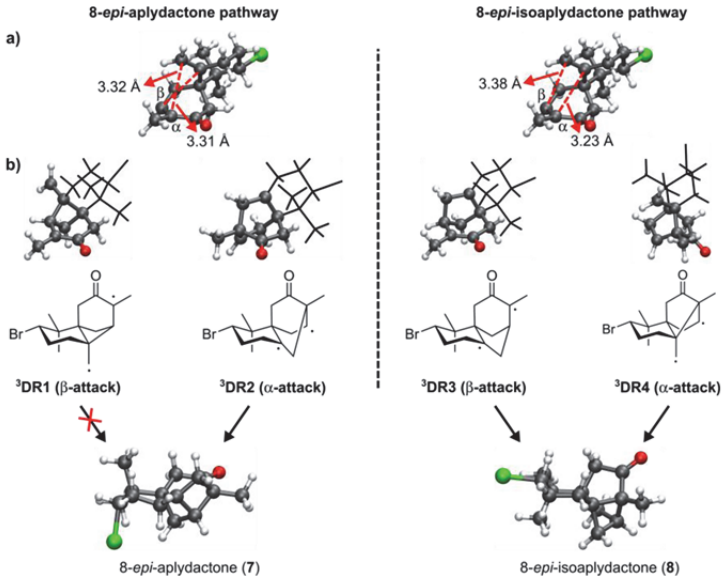

Figure 11. (a) Intercarbon distances for the reaction pathways leading to 8-*epi*-aplydactone (**7**) and 8-*epi*-isoaplydactone (**8**) at the triplet minimum T_1-Min2 of **3b**. (b) Optimized geometries of the four triplet diradicals (^{3}DR) possible from T_1-Min2.

DOI: 10.1021/acscentsci.6b00293
ACS Cent. Sci. 2017, 3, 39−46

Taken together, our results demonstrate the powerful influence of the C10 bromide on the reaction outcome for **2** and **3**. In both cases, the C10 bromide prefers the equatorial position and controls the conformation of the molecule in the ground state (**2a** and **3b** in Figure 2). For dactylone, the conformer **2a** leads to the preferred formation of aplydactone (**1**). In contrast, for 10-*epi*-dactylone (**3**) the conformer **3b** favors the formation of "8-*epi*-isoaplydactone".

The configuration at C10 thus determines the conformation and controls the regioselectivity of the photochemical reaction. The facility with which **3** is converted into **8** and the biomimetic irradiation used suggests that "8-*epi*-isoaplydactone" may also occur naturally in *A. dactylomela*. If this can be confirmed, it would be another case of natural product prediction through synthesis.[9,23,40−44]

■ ASSOCIATED CONTENT

Supporting Information

The Supporting Information is available free of charge on the ACS Publications website at DOI: 10.1021/acscentsci.6b00293.

Procedures for the synthesis of all compounds and characterization data, and computational details (PDF)

■ AUTHOR INFORMATION

Corresponding Authors

*(D.T.) E-mail: dirk.trauner@cup.uni-muenchen.de.
*(R.d.V.R.) E-mail: regina.de_vivie@cup.uni-muenchen.de.
*(R.M.) E-mail: romech@cup.uni-muenchen.de.

ORCID

Dirk Trauner: 0000-0002-6782-6056

Author Contributions

†B.S.M. and P.K. contributed equally to this work.

Notes

The authors declare no competing financial interest.

■ ACKNOWLEDGMENTS

We thank the Deutsche Forschungsgemeinschaft (SFB749) for financial support. B.S.M. gratefully acknowledges the support of the Alexander von Humboldt Foundation for postdoctoral funding. The authors thank Dr. Peter Mayer for X-ray crystallographic assistance and Prof. Hendrik Zipse for informative discussions on the stereoselectivity of radical bromination reaction. The authors would also like to acknowledge Mr. Moritz Claßen, Mr. Nicolas Müller, Mr. Jordan Donat, and Mr. Jerome Ring for their preliminary contributions towards this project.

■ REFERENCES

(1) König, G. M.; Wright, A. D. Laurencia Rigida: Chemical Investigations of Its Antifouling Dichloromethane Extract. *J. Nat. Prod.* **1997**, *60*, 967−970.

(2) Pennings, S. C.; Paul, V. J. Sequestration of Dietary Secondary Metabolites by Three Species of Sea Hares: Location, Specificity and Dynamics. *Mar. Biol.* **1993**, *117*, 535−546.

(3) Benkendorff, K. Molluscan Biological and Chemical Diversity: Secondary Metabolites and Medicinal Resources Produced by Marine Molluscs. *Biol. Rev.* **2010**, *85*, 757−775.

(4) Fedorov, S. N.; Reshetnyak, M. V.; Schedrin, A. P.; Ilyin, S. G.; Struchkov, J. T.; Stonik, V. A.; Elyakov, G. B. Isolation of Dactylone. *Dokl. Akad. Nauk SSSR* **1990**, *307*, 877−879.

(5) Shubina, L. K.; Fedorov, S. N.; Kalinovskiy, A. I.; Dmitrenok, A. S.; Jin, J. O.; Song, M. G.; Kwak, J. Y.; Stonika, V. A. Four New Chamigrane Sesquiterpenoids from the Opistobranch Mollusk Aplysia Dactylomela. *Russ. Chem. Bull.* **2007**, *56*, 2109−2114.

(6) Fedorov, S. N.; Radchenko, O. S.; Shubina, L. K.; Kalinovsky, A. I.; Gerasimenko, A. V.; Popov, D. Y.; Stonik, V. A. Aplydactone, a New Sesquiterpenoid with an Unprecedented Carbon Skeleton from the Sea Hare Aplysia Dactylomela, and Its Cargill-Like Rearrangement. *J. Am. Chem. Soc.* **2001**, *123*, 504−505.

(7) Nouri, D.; Tantillo, D. They Came From the Deep: Syntheses, Applications, and Biology of Ladderanes. *Curr. Org. Chem.* **2006**, *10*, 2055−2074.

(8) Novak, I. Ring Strain in [N]ladderanes. *J. Phys. Chem. A* **2008**, *112*, 10059−10063.

(9) Volgraf, M.; Lumb, J.-P.; Brastianos, H. C.; Carr, G.; Chung, M. K. W.; Münzel, M.; Mauk, A. G.; Andersen, R. J.; Trauner, D. Biomimetic Synthesis of the IDO Inhibitors Exiguamine A and B. *Nat. Chem. Biol.* **2008**, *4*, 535−537.

(10) Stichnoth, D.; Kölle, P.; Kimbrough, T. J.; Riedle, E.; de Vivie-Riedle, R.; Trauner, D. Photochemical Formation of Intricarene. *Nat. Commun.* **2014**, *5*, 5597.

(11) Burckle, A. J.; Vasilev, V. H.; Burns, N. Z. A Unified Approach for the Enantioselective Synthesis of the Brominated Chamigrene Sesquiterpenes. *Angew. Chem., Int. Ed.* **2016**, *55*, 11476−11479.

(12) Srinivasan, R.; Carlough, K. H. Mercury(3P1) Photosensitized Internal Cycloaddition Reactions in 1,4-, 1,5-, and 1,6-Dienes. *J. Am. Chem. Soc.* **1967**, *89*, 4932−4936.

(13) Liu, R. S. H.; Hammond, G. S. Photosensitized Internal Addition of Dienes to Olefins. *J. Am. Chem. Soc.* **1967**, *89*, 4936−4944.

(14) Ciamician, G.; Silber, P. Chemische Lichtwirkungen. *Ber. Dtsch. Chem. Ges.* **1908**, *41*, 1928−1935.

(15) Celani, P.; Werner, H.-J. Multireference Perturbation Theory for Large Restricted and Selected Active Space Reference Wave Functions. *J. Chem. Phys.* **2000**, *112*, 5546−5557.

(16) Stanton, J. F.; Bartlett, R. J. The Equation of Motion Coupled-cluster Method. A Systematic Biorthogonal Approach to Molecular Excitation Energies, Transition Probabilities, and Excited State Properties. *J. Chem. Phys.* **1993**, *98*, 7029−7039.

(17) Becke, A. D. Density-functional Thermochemistry. III. The Role of Exact Exchange. *J. Chem. Phys.* **1993**, *98*, 5648−5652.

(18) Yanai, T.; Tew, D. P.; Handy, N. C. A New Hybrid Exchange−correlation Functional Using the Coulomb-Attenuating Method (CAM-B3LYP). *Chem. Phys. Lett.* **2004**, *393*, 51−57.

(19) Poplata, S.; Tröster, A.; Zou, Y.-Q.; Bach, T. Recent Advances in the Synthesis of Cyclobutanes by Olefin [2 + 2] Photocycloaddition Reactions. *Chem. Rev.* **2016**, *116*, 9748−9815.

(20) Solar Spectral Irradiance: Air Mass 1.5 http://rredc.nrel.gov/solar/spectra/am1.5/ (accessed August 21, 2016).

(21) Cao, J.; Xie, Z.-Z. Internal Conversion and Intersystem Crossing in α,β-Enones: A Combination of Electronic Structure Calculations and Dynamics Simulations. *Phys. Chem. Chem. Phys.* **2016**, *18*, 6931−6945.

(22) Shen, M.; Kretschmer, M.; Brill, Z. G.; Snyder, S. A. Strategies for the Total Synthesis of Diverse Bromo-Chamigrenes. *Org. Lett.* **2016**, *18*, 5018−5021.

(23) Wolinsky, L. E.; Faulkner, D. J. Biomimetic Approach to the Synthesis of Laurencia Metabolites. Synthesis of 10-Bromo-.alpha.-Chamigrene. *J. Org. Chem.* **1976**, *41*, 597−600.

(24) Ichinose, I.; Kato, T. Biogenetic Type Synthesis of 10-Bromo-α-Chamigrene. *Chem. Lett.* **1979**, *8*, 61−62.

(25) Martin, J. D.; Perez, C.; Ravelo, J. L. Enantioselective Ring Construction: Synthesis of Halogenated Marine Natural spiro[5.5]-undecane Sesquiterpenes. *J. Am. Chem. Soc.* **1986**, *108*, 7801−7811.

(26) White, D. E.; Stewart, I. C.; Grubbs, R. H.; Stoltz, B. M. The Catalytic Asymmetric Total Synthesis of Elatol. *J. Am. Chem. Soc.* **2008**, *130*, 810−811.

(27) Nicolaou, K. C.; Li, H.; Nold, A. L.; Pappo, D.; Lenzen, A. Total Synthesis of Kinamycins C, F, and J. *J. Am. Chem. Soc.* **2007**, *129*, 10356−10357.

(28) Dao, H. T.; Baran, P. S. Quinone Diazides for Olefin Functionalization. *Angew. Chem., Int. Ed.* **2014**, *53*, 14382−14386.

DOI: 10.1021/acscentsci.6b00293
ACS Cent. Sci. 2017, 3, 39−46

(29) Antonsen, S.; Skattebøl, L.; Stenstrøm, Y. Synthesis of Racemic β-Chamigrene, a Spiro[5.5]undecane Sequiterpene. *Molecules* **2014**, *19*, 20664−20670.
(30) Hugelshofer, C. L.; Magauer, T. High-Pressure Transformations in Natural Product Synthesis. *Synthesis* **2014**, *46*, 1279−1296.
(31) Edmonds, M.; Abell, A. The Wittig Reaction. In *Modern Carbonyl Olefination*; Takeda, T., Ed.; Wiley-VCH Verlag GmbH & Co. KGaA: Weinheim, 2003; pp 1−17.
(32) Wang, Z. Nysted Reagent. In *Comprehensive Organic Name Reactions and Reagents*; John Wiley & Sons, Inc.: Hoboken, 2010.
(33) Hudrlik, P. F.; Holmes, P. E.; Hudrlik, A. M. Protiodesilylation Reactions of β- and γ-Hydroxysilanes: Deuterium Labeling and Silicon-Directed Epoxide Openings. *Tetrahedron Lett.* **1988**, *29*, 6395−6398.
(34) Rousseau, G.; Breit, B. Removable Directing Groups in Organic Synthesis and Catalysis. *Angew. Chem., Int. Ed.* **2011**, *50*, 2450−2494.
(35) Chung, W.; Vanderwal, C. D. Stereoselective Halogenation in Natural Product Synthesis. *Angew. Chem., Int. Ed.* **2016**, *55*, 4396−4434.
(36) Meier, R.; Trauner, D. A Synthesis of (±)-Aplydactone. *Angew. Chem., Int. Ed.* **2016**, *55*, 11251−11255.
(37) Damm, W.; Giese, B.; Hartung, J.; Hasskerl, T.; Houk, K. N.; Hueter, O.; Zipse, H. Diastereofacial Selectivity in Reactions of Substituted Cyclohexyl Radicals. An Experimental and Theoretical Study. *J. Am. Chem. Soc.* **1992**, *114*, 4067−4079.
(38) Fukuzawa, A.; Sato, H.; Masamune, T. Synthesis of (±)-Prepinnaterpene, a Bromoditerpene from the Red Alga Laurencia Pinnata Yamada. *Tetrahedron Lett.* **1987**, *28*, 4303−4306.
(39) Kim, D.; Kim, I. H. A Stereoselective Total Synthesis of (±)-Oppositol by a Doubly Diastereoselective Intramolecular Ester Enolate Alkylation. *Tetrahedron Lett.* **1997**, *38*, 415−416.
(40) Gravel, E.; Poupon, E. Biogenesis and Biomimetic Chemistry: Can Complex Natural Products Be Assembled Spontaneously? *Eur. J. Org. Chem.* **2008**, *2008*, 27−42.
(41) Zhao, K.; Cheng, G.-J.; Yang, H.; Shang, H.; Zhang, X.; Wu, Y.-D.; Tang, Y. Total Synthesis of Incarvilleatone and Incarviditone: Insight into Their Biosynthetic Pathways and Structure Determination. *Org. Lett.* **2012**, *14*, 4878−4881.
(42) Strych, S.; Journot, G.; Pemberton, R. P.; Wang, S. C.; Tantillo, D. J.; Trauner, D. Biomimetic Total Synthesis of Santalin Y. *Angew. Chem., Int. Ed.* **2015**, *54*, 5079−5083.
(43) Ellerbrock, P.; Armanino, N.; Ilg, M. K.; Webster, R.; Trauner, D. An Eight-Step Synthesis of Epicolactone Reveals Its Biosynthetic Origin. *Nat. Chem.* **2015**, *7*, 879−882.
(44) Lam, H. C.; Spence, J. T. J.; George, J. H. Biomimetic Total Synthesis of Hyperjapones A−E and Hyperjaponols A and C. *Angew. Chem., Int. Ed.* **2016**, *55*, 10368−10371.

DOI: 10.1021/acscentsci.6b00293
ACS Cent. Sci. 2017, 3, 39−46

2.3 Conclusion

In conclusion, the first total synthesis of the complex ladderane natural product aplydactone was achieved and biosynthetic relationships between the isolated chamigrane natural products from *Aplysia dactylomela* were uncovered.

Initial attempts to access the complex core structure of aplydactone *via* a cyclopropanation or ketene cycloaddition strategy failed due to the high steric congestion of the unsaturated decalin system. An approach using intramolecular cyclobutadiene (2+2) cycloaddition for the formation of the essential [2]-ladderane system provided promising results. During these investigations the two crucial neighboring quaternary stereocenters next to a *gem*-dimethyl moiety could be formed in a single step. Although this cycloaddition could not be optimized to exclusively yield the desired cyclization product due to a competing radical ring opening of a highly strained cyclobutene subunit, this approach was crucial for the subsequent successful planning of a non-biomimetic photochemical strategy.

A high yielding and scalable route towards the [2+2] photoprecursor was achieved from cheap starting materials and the key [2+2] cycloaddition provided the necessary tricyclic 6-4-5 system in good yield and high diastereoselectivity. A photochemical Wolff ring contraction provided not only the desired [2]-ladderane structure of aplydactone, but also an ester functionality which served as a handle to diastereoselectively install the last quaternary stereocenter. For the completion of the first total synthesis of aplydactone, the decalin system had to be closed. This was achieved by an intramolecular Barbier reaction which involved a fascinating conformational ring flip of a highly strained intermediate. For the final introduction of the secondary bromide, new radical conditions had to be developed in order to finish the synthesis.

In a second approach, aplydactone was synthesized from its proposed biomimetic precursor dactylone *via* an intramolecular [2+2] photocycloaddition. Although this transformation was reported to be nonviable, computational investigations by Dr. Patrick Kölle and Prof. Dr. Regina de Vivie-Riedle demonstrated that the choice of wavelength in this photochemical transformation is essential to prevent degradation pathways originating from C–Br bond cleavage. A Diels–Alder approach using a highly optimized enone intermediate containing a traceless directing group allowed us, in combination with our radical bromination conditions, to synthesize the natural product 10-bromo-β-chamigrene. This key intermediate could be converted in a diastereodivergent manner to either dactylone or its naturally occurring epimer 10-*epi*-dactylone using bioinspired oxidation strategies. Irradiation of dactylone with UV-A light provided aplydactone as a single reaction product, thereby violating the “rule of five”. Moreover, irradiation under the same biomimetic conditions, converted 10-*epi*-dactylone to a so far unknown “rule of five” product, which was named 8-*epi*-isoaplydactone. Based on these results, it was proposed that this compound is a natural

product produced non-enzymatically in *Aplysia dactylomela*. Further computational investigations unveiled that the secondary bromide, in the structure of dactylone and its epimer, is the decisive controlling element for the outcome of the photochemical [2+2] cycloaddition.

To conclude, these two strategically different approaches towards aplydactone highlight the outstanding synthetic possibilities offered by photochemistry to access connectivities which are otherwise impossible to generate.

PART II

TOTAL SYNTHESIS OF MEROCHLORIN B

Synthetic studies towards merochlorin A and B were previously covered in the Master's thesis of Robin Meier, LMU Munich, 2013. Results on the synthesis of the two fragments were already described there.

3 HALOGENATED NATURAL PRODUCTS

The incorporation of halogens into natural products has been observed frequently and more than 5000 organohalogens have been isolated and structurally identified to date with new compounds being reported at a rate of about 200 members annually.[147] The vast majority has been isolated from marine sources like sponges, corals, seaweed and sea slugs, presumably due to the high content of the corresponding salts in seawater. Furthermore, chloride and bromide substituents are most abundant compared to the relatively small number of iodide and especially fluoride containing natural products.[148] Halogenation is not limited to a special natural product class as halogens have been found in the structures of alkaloids, terpenoids, polyketides, fatty acids, steroids and simple alkanes (**3.1**–**3.13** Figure 3.1).[147a,149] In humans, relatively few organohalogens are synthesized. The most prominent members of human halogenated natural products are the iodinated thyroid hormones represented by the structure of thyroxine (**3.2**).[147c,d] Interestingly, bromoacetoacetate **3.13** was isolated from human cerebrospinal fluid and was identified to be an inducer of rapid-eye-movement (REM) sleep.[150]

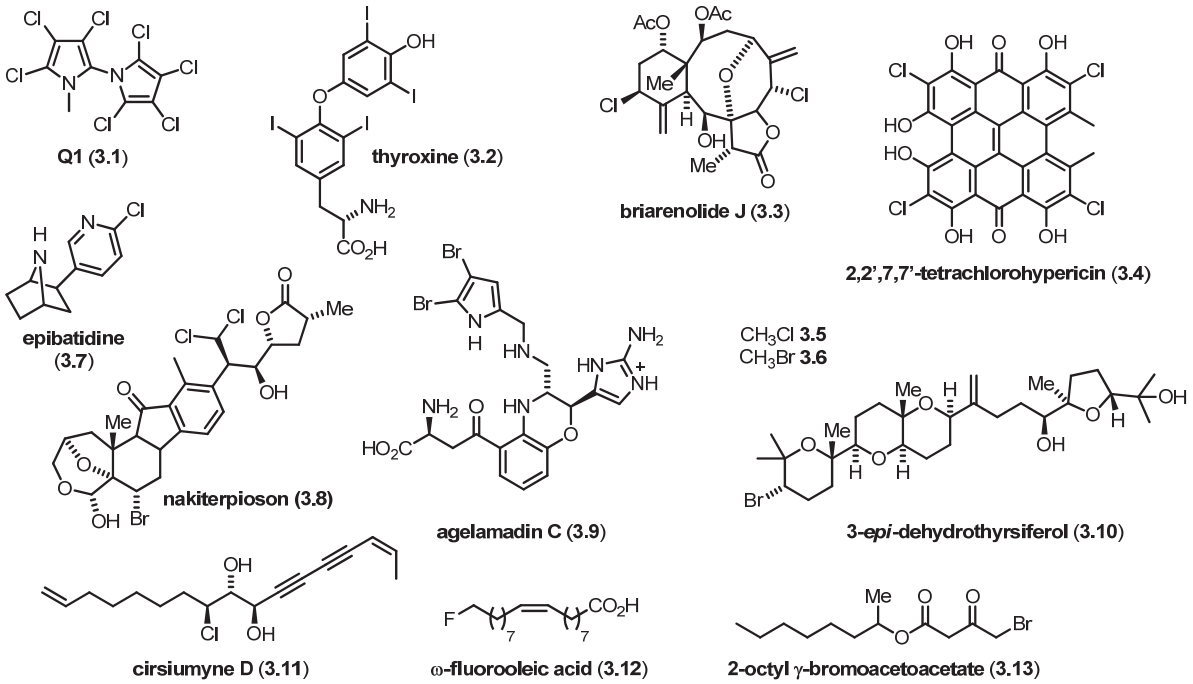

Figure 3.1 Structures of representative naturally occurring organohalogens **3.1**–**3.13**.

Halogen-containing natural products in general show high bioactivity and different members have been described to show antimicrobial, antifungal, antibiotic, antiviral and anticancer activity.[147a] The role of the halogen-containing natural products for the producing organism is not always known, however antifeedant and chemical defense function have been reported as well as their function as regulatory hormones and signaling molecules.

Solvated halide anions serve as the major halogen source and are introduced by nature using three general reaction pathways which are summarized in Scheme 3.1a.[151] Oxidation of a halide anion forms an electrophilic halonium species ("X^+") which is transferred to a nucleophilic aromatic system or an alkene. Three mechanistically and structurally different enzymes were reported to follow this electrophilic halogenation pathway. While haem- and vanadium-dependent haloperoxidases generate hypohalous acid from hydrogen peroxide and a halide by making use of their metal center, a FAD (flavin-adenine dinucleotide) cofactor is used by flavin-dependent haloperoxidases.

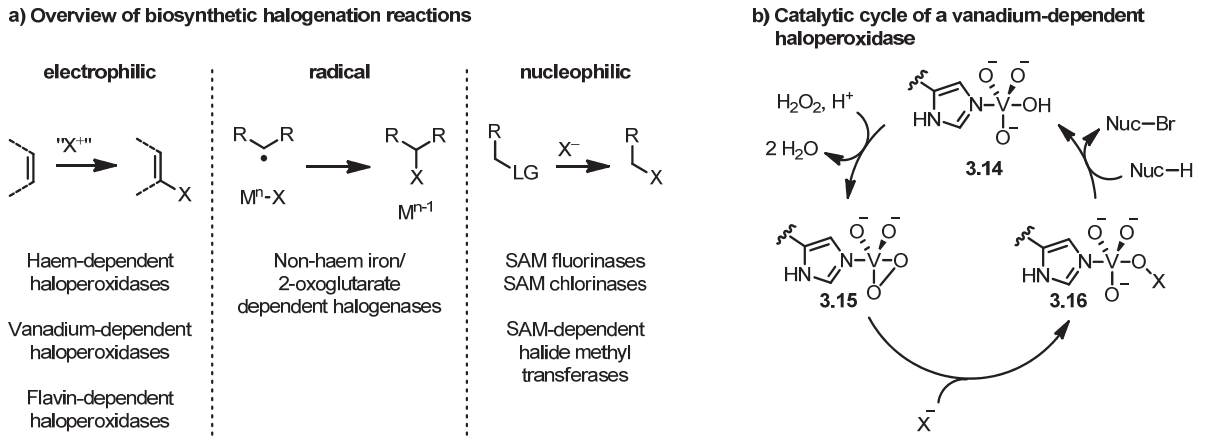

Scheme 3.1 a) Overview of the halogenation mechanisms in biosynthesis; b) Catalytic cycle of a vanadium-dependent haloperoxidase.

A radical rebound mechanism, similar to the one used by FeNH-αKG-oxygenases, allows for the halogenation of unactivated C_{sp3}-H bonds by the activity of a non-haem iron halogenase. The mechanism involves the oxidative decarboxylation of α-ketoglutarate to succinate for the generation of an active Fe(IV)-oxo intermediate.

In the biosynthesis of organofluorides, it is not possible to generate a formal "F^+" or "F·" under physiological conditions as consequence of the positive reduction potential of fluorine, which would be necessary to synthesize fluorinated natural products by an electrophilic or radical enzyme mechanism. Therefore, nature uses the nucleophilicity of fluoride to incorporate fluorine into secondary metabolites. Mechanistically, the fluorinases have to dissolvate the fluoride anion in their active site by specific interactions with the protein scaffold to generate a strong nucleophile for the substitution reaction.[147f] Similar transformations were reported for *S*-adenosyl methionine chlorinases and halide methyl transferases.

In the biosynthesis of halogenated marine natural products, which represent the majority of natural organohalogens, vanadium-dependent haloperoxidases are proposed to play a prevalent role, e.g. in the formation of halogenated cyclic terpenes or the formation of halogenated cyclic ethers.[100] From a mechanistic point of view, these enzymes coordinate hydrogen peroxide in the active site forming a side-on bound η^2-peroxo complex **3.15**, which

can oxidize a halide to the corresponding hypohalous acid bound to the vanadate center **3.16** (Scheme 3.1b). At this point, it is not known if this reactive bromination reagent is attacked by the nucleophilic substrate within the active site or if hypohalite is released from the metal center. Compared to the haem-dependent haloperoxidases, the metal center does not change its oxidation state during the catalytic cycle in the case of vanadium-dependent haloperoxidases.

4 BIOMIMETIC TOTAL SYNTHESIS OF THE MARINE NATURAL PRODUCT MEROCHLORIN B

4.1 Introduction

4.1.1 Isolation and structure

In 2012, the isolation of merochlorin A (**4.1**, Figure 4.1), a chlorine containing mixed polyketide-terpenoid natural product from the marine sediment bacterium *Streptomyces spectabilis* strain CNH-189 collected at the Californian coast, was reported.[152] In the same year, Moore and Fenical isolated three other members of this marine meroterpenoid family, named merochlorin B–D (**4.2**–**4.4**).[153] The antibiotic activity of merochlorin A (**4.1**) and B (**4.2**) against *Clostridium difficile* and various multi-drug resistant *Staphylococcus aureus* strains was of major interest along with the unprecedented carbon frameworks of **4.1** and **4.2**.

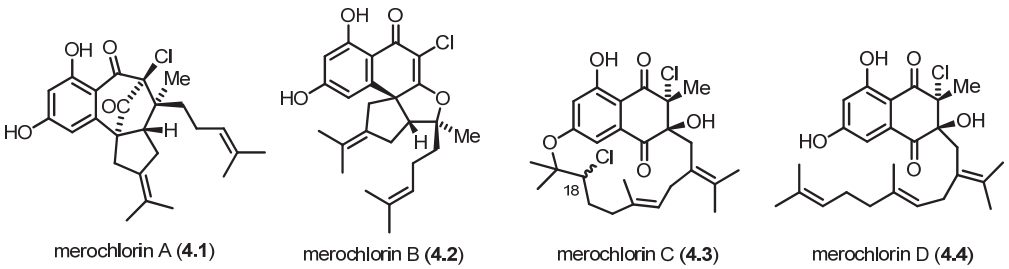

Figure 4.1 Members of the merochlorin family.

In addition to their isomeric chemical formula, merochlorin A (**4.1**) and B (**4.2**) represent several common structural motifs including a resorcinol unit, a propan-2-ylidenecyclopentane substructure and a terpene side chain. Moreover, **4.1** contains a unique chlorinated bicyclo[3.2.1]octadiene, whereas **4.2** possesses a chlorinated 6-5-5-fused tricycle with three stereogenic centers. The carbon skeleton of merochlorin A (**4.1**) could be unambiguously determined by single crystal X-ray analysis of a methylated and acetylated derivative.[153]

The macrocyclic merochlorin C (**4.3**), most likely derived from merochlorin D (**4.4**) *via* chloroetherification, contains two chloride substituents and a 1,4-cyclohexanedione structure. The absolute configuration of the secondary C18-chloride substituent has not yet been assigned. An additional methyl and hydroxyl substituent on the framework of merochlorin C (**4.3**) and D (**4.4**) indicate contribution of an oxygenase and a methyltransferase to modify the common biosynthetic precursor of the merochlorin family.

4.1.2 Biosynthesis

The isolation chemists could identify a 57.6 kb merochlorin gene cluster containing 41 open reading frames (*mcl 1–41*).[153] By making use of sequence homology, enzymatic synthesis and gene knock out experiments, a polyketide type III synthase (*mcl 17*) was reported to catalyse the formation of 1,3,6,8-tetrahydroxynaphthalene (**4.6**) from five malonyl-CoA subunits (**4.5**, Scheme 4.1).[154]

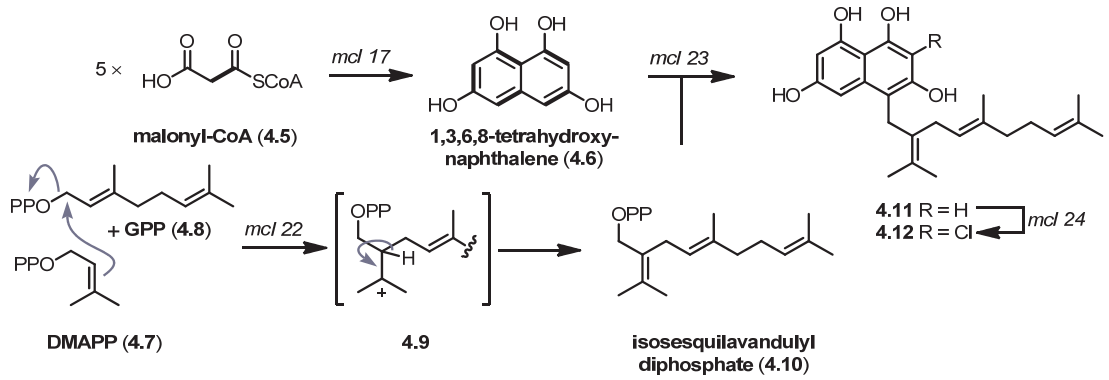

Scheme 4.1 Biosynthesis of the key cyclization precursor **4.12**.

The synthesis of the unusual sesquiterpene isosesquilavandulyl diphosphate (**4.10**) was rationalized by a “head-to-torso” coupling of geranyl pyrophosphate (GPP, **4.8**) and dimethyl allyl diphosphate (DMAPP, **4.7**). A Mg^{2+}-dependent polyprenyl synthase (*mcl 22*) was detected within the gene cluster catalyzing this transformation. A possible mechanism for the formation of **4.10** involves an initial attack of the nucleophilic double bond of DMAPP (**4.7**) onto the allylic position of GPP (**4.8**) followed by an elimination of the tertiary cation to the tetrasubstituted double bond.

For the formation of merochlorin A (**4.1**) and B (**4.2**), the electron-rich polyketide fragment **4.6** is coupled by a prenyltransferase (*mcl 23*) to the sesquiterpenoid side chain **4.10** to deliver the intermediate **4.11**, which can be chlorinated at the aromatic core to **4.12** by the activity of a vanadium-dependent chloroperoxidase (*mcl 24*).

For the formation of **4.1** and **4.2** from intermediate **4.12**, Moore and coworkers initially proposed a cascade involving epoxidation or chlorination of the central trisubstituted double bond.[153] However, an oxidative dearomatization of the electron-rich naphthalene core to phenoxonium ion **4.13** and subsequent stepwise (5+2) cyclization to merochlorin A (**4.1**) is another possibility (Scheme 4.2a). For the formation of the complex structure of merochlorin B (**4.2**), a (3+2) cyclization of the intermediate phenoxonium cation **4.13** was proposed by us and others.[155] This oxidative process was recently shown to be catalyzed by the same chloroperoxidase (*mcl 24*) which is responsible for the chlorination of the naphthalene core.[156]

While our investigations were ongoing, George and coworkers synthesized merochlorin A (**4.1**) from cyclization precursor **4.15** by oxidation with $Pb(OAc)_4$ (Scheme 4.2b). Interestingly, they could not identify merochlorin B (**4.2**) under the applied conditions.

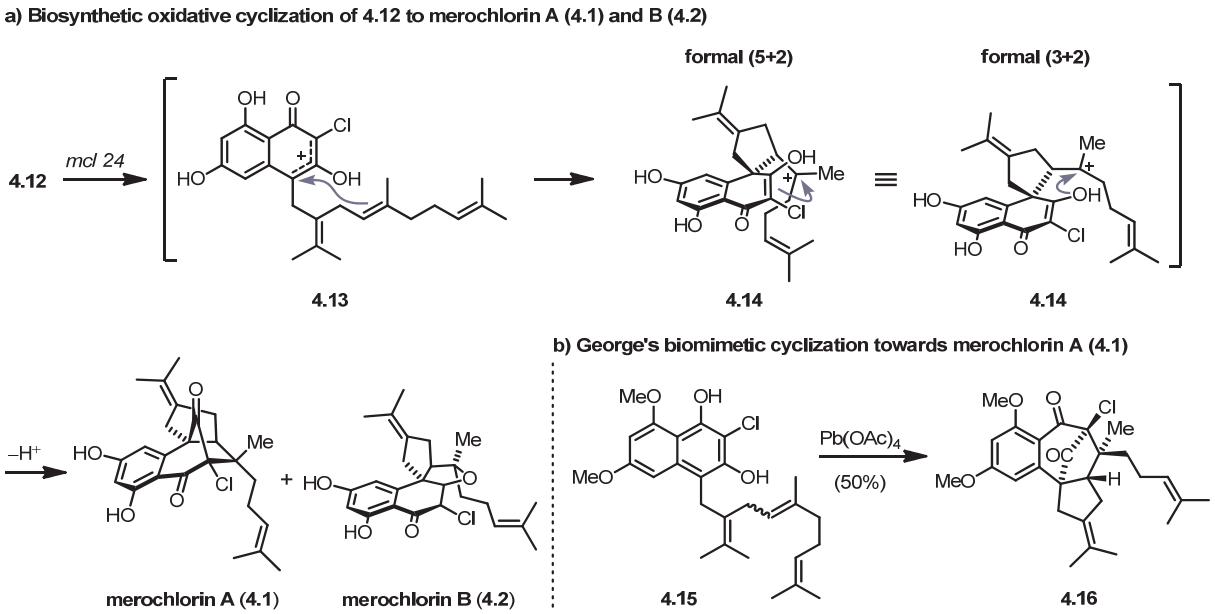

Scheme 4.2 a) Oxidative (5+2) and (3+2) cyclization to merochlorin A (**4.1**) and B (**4.2**); b) Biomimetic cyclization of **4.15** by George and coworkers.

Further oxidation of **4.6** leads to flaviolin hydroquinone (**4.17**) which is proposed to be coupled to **4.10** to obtain merochlorin D (**4.4**) after chlorination (*mcl 24*) and methylation (*mcl 21*, Scheme 4.3). A second vanadium-dependent chloroperoxidase (*mcl 40*) within the gene cluster can mediate the chloroetherification of **4.4** to merochlorin C (**4.3**) *via* an intermediate tertiary cation **4.19**.

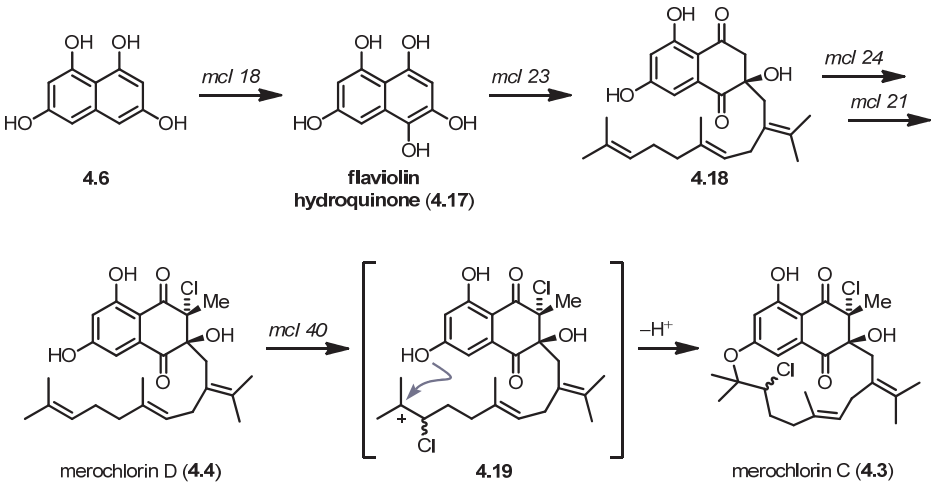

Scheme 4.3 Biosynthesis of merochlorin C (**4.3**) and D (**4.4**).

In conclusion, all members of the merochlorin family are derived from a polyketide and sesquiterpenoid fragment which are modified by oxidation, chlorination, cyclization

towards the different family members. Interestingly, the natural products **4.1** and **4.2** were obtained as single enantiomers implying formation within the chiral environment of the vanadium-dependent chloroperoxidase (*mcl 24*) to induce asymmetric cyclization of the prochiral phenoxonium cation **4.13**.

4.2 Results and discussion

Organic LETTERS
Letter
pubs.acs.org/OrgLett

Biomimetic Synthesis of (±)-Merochlorin B

Robin Meier, Sebastian Strych, and Dirk Trauner*

Department of Chemistry and Center for Integrated Protein Science, University of Munich (LMU), Butenandtstraße 5-13, 81377 München, Germany

Supporting Information

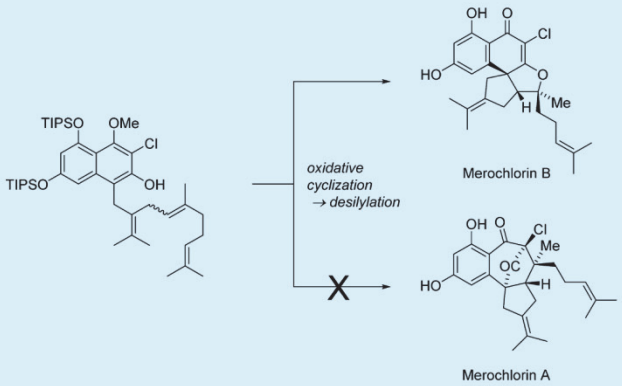

ABSTRACT: A short total synthesis, guided by biosynthetic considerations, of racemic merochlorin B is presented. The formation of its isomer, merochlorin A, was not observed under the conditions. Key steps include a directed *ortho*-metalation (DoM), a selective demethylation, an *ortho*-allylation, and an oxidative [3 + 2]-cycloaddition mediated by an iodine(III) reagent.

The merochlorins, **1**–**4**, are a small family of meroterpenoids recently isolated from the sediment bacterium *Streptomyces spectrabilis* strain CNH 189 (Figure 1).[1] Merochlorins A, **1**, and B, **2**, have attracted considerable attention due to their unusual structures and their high activity against methicillin-resistant strains of *Staphylococcus aureus*.[1]

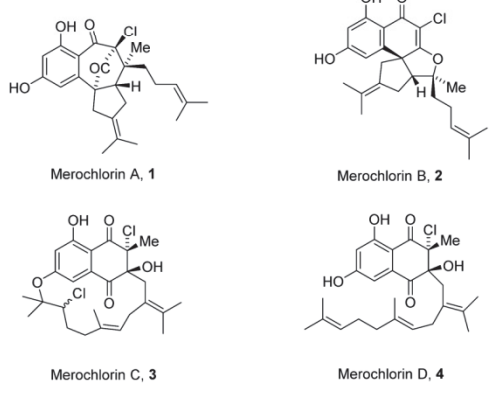

Figure 1. Merochlorins A–D, **1**–**4**, isolated from *Streptomyces spectrabilis* strain CNH-189.

Merochlorin A, **1**, features a tetracarbocyclic ring system with four contiguous stereocenters, two of which are quaternary. Its isomer, merochlorin B, **2**, possesses a ring system that incorporates a heterocycle, a chlorinated vinylogous ester, and, like merochlorin A, **1**, a propan-2-ylidenecyclopentane. Furthermore, **2** features three contiguous stereocenters, one of which is quaternary.

Biosynthetically, all members of the merochlorin family have been proposed to derive from a common chlorinated tetrahydroxynaphthalene (THN) derivative **5** (Scheme 1).[1,2] Moore and co-workers identified the biosynthetic gene cluster associated with **5** and proposed that a THN synthase, a polyprenyl synthase, a prenyltransferase, and a vanadium-dependent haloperoxidase are involved in its formation.[1b] Its subsequent cyclization to merochlorin A, **1**, and B, **2**, would proceed via epoxidation or chlorination of the central double bond.

This proposal was modified by George and co-workers who recently disclosed a biomimetic synthesis of merochlorin A, **1**.[2] They assumed that oxidation of the electron-rich aromatic core of **5**, possibly by an enzyme that contains an iron–sulfur cluster, would give rise to phenoxonium ion **6**. This reactive intermediate would then cyclize to merochlorin A, **1**, or B, **2**, via a [5 + 2]- or [3 + 2]-cycloaddition depending on the orientation of the terpenoid side chain (Scheme 1).

We now report the total synthesis of (±)-merochlorin B, **2**, that was guided by similar biosynthetic considerations. Interestingly, the formation of merochlorin A, **1**, was not observed under our conditions, whereas George and co-workers did not observe the

Received: March 17, 2014
Published: May 7, 2014

   dx.doi.org/10.1021/ol500800z | *Org. Lett.* 2014, 16, 2634–2637

Scheme 1. Presumed Biosynthetic Origin of Merochlorin A, 1, and B, 2[2]

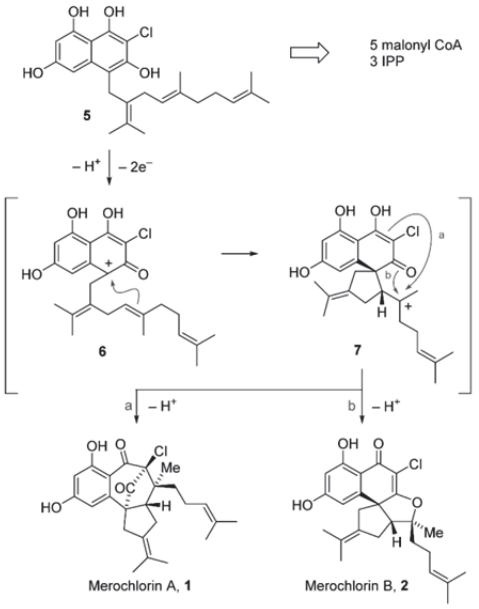

formation of merochlorin B, **2**, under theirs. As such, our work provides another example for a subtle variation of a substrate that results in a markedly different outcome of a cascade reaction.

Retrosynthetically, we envisioned that **1** and **2** could be obtained from naphthalene **8**, which is a protected version of **5** (Scheme 2).[3] Compound **8** could be accessed by a late stage

Scheme 2. Retrosynthetic Analysis of Merochlorins A, 1, and B, 2

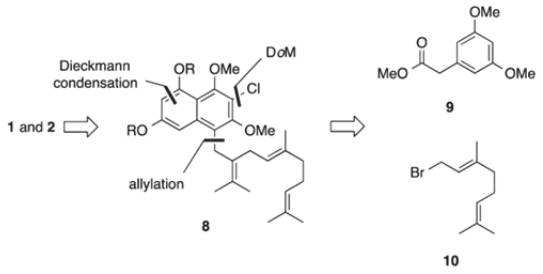

allylation with a terpenoid side chain ultimately derived from commercially available geranyl bromide, **10**. Furthermore, the incorporation of the chlorine atom could be achieved by a directed *ortho*-metalation (D*o*M) of a protected dimethoxynaphthalene derivative which in turn could be accessed via Dieckmann condensation starting from phenylacetic acid methyl ester **9**.

Accordingly, our synthesis commenced with the preparation of 6,8-dihydroxy-1,3-dimethoxynaphthalene, **12**, from phenylacetic acid **9** using a modification of a known procedure (Scheme 3).[4] Friedel–Crafts acylation of **9** then afforded acetophenone **11** which underwent Dieckmann cyclization in excellent yield upon treatment with sodium hydride.[5,6] Protection of both phenolic hydroxyl groups with TBS or TIPS triflate afforded naphthalenes **13** and **14**. The use of the more reactive triflate reagents was

Scheme 3. Synthesis of the Naphthalene Building Blocks 15 and 16 and of Allylic Bromide 19

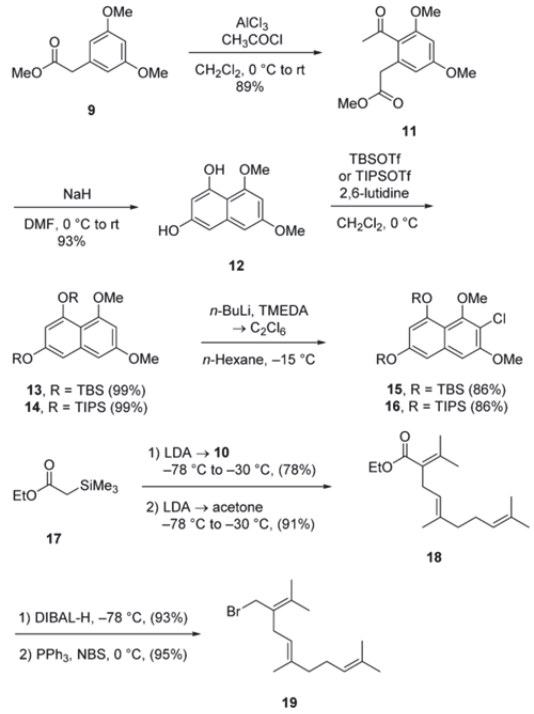

necessary at this point to achieve the protection of the sterically more hindered hydroxyl group in the *peri*-position of the naphthalene core **12**.

The ability of methoxy groups to direct the metalation of aromatic systems is well described in the literature.[7] In our case, the cooperative interaction of the two methoxy groups led to a completely regioselective metalation. Treatment of naphthalene **13** or **14** with *n*-BuLi and TMEDA formed the corresponding lithiated species, which was quenched with hexachloroethane (C_2Cl_6) to form the chlorinated naphthalene cores **15** and **16**, respectively, in high yield. The advantages of C_2Cl_6 over other Cl^+-sources have been documented in the literature.[8]

Initial experiments to access the terpenoid side chain using a Horner–Wadsworth–Emmons strategy[9] did not lead to acceptable results in our case. We therefore took recourse to a Peterson olefination[10] starting from commercially available silyl acetate **17** which was alkylated with geranyl bromide, **10**, in good yield (Scheme 3).[11] Subsequent treatment with LDA followed by the addition of acetone gave α,β-unsaturated ester **18**.[12] Reduction followed by Appel reaction then provided the sensitive bromide **19** in good yield.

With compounds **15**, **16**, and **19** in hand we investigated the formation of cyclization precursor **21** (Scheme 4). Our initial plan was to incorporate the side chain by a second directed *ortho*-metalation of the aromatic core **15** followed by reaction of the resulting organolithium compound **20** with the bromide **19**.[13] Although the regioselective formation of **20** could be proven by D_2O quench, it was impossible to connect side chain **19** in that manner. The transmetalation of **20** with various metals (Cu, Mg, Zn, $SnMe_3$) and addition of **19** with and without palladium catalysis did not lead to the desired coupling product **21** either. As a consequence, we changed the order of events and

dx.doi.org/10.1021/ol500800z | Org. Lett. 2014, 16, 2634–2637

Scheme 4. Synthesis of Cyclization Precursor 23

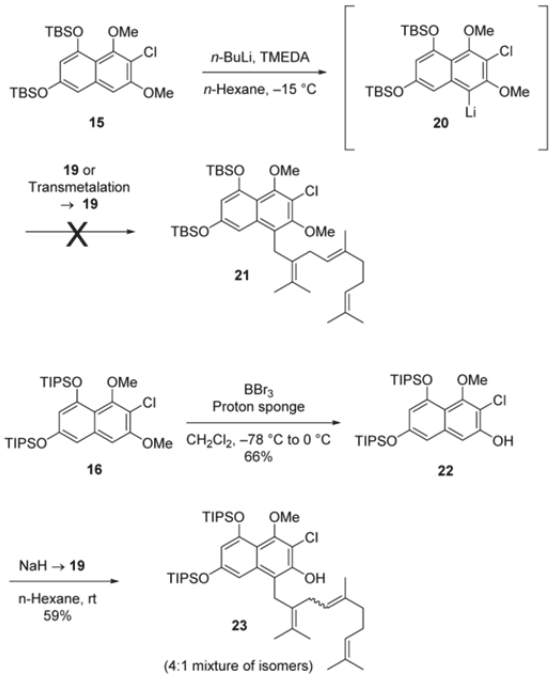

Scheme 5. Synthesis of Merochlorin B, 2

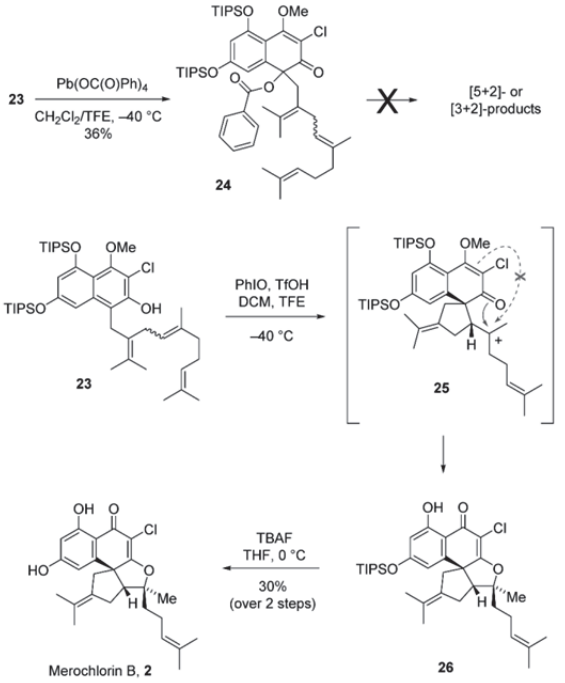

investigated demethylation of the chlorinated naphthalenes **15** and **16**. After extensive optimization, compound **16** could be selectively deprotected by boron tribromide in good yield. The addition of proton sponge and use of the TIPS protected core **16** was found to be essential for a fast and clean conversion to naphthol **22** in the presence of silyl protecting groups.[14] Importantly, double demethylation was not observed under these conditions.

Gratifyingly, naphthol **22** underwent clean *ortho*-allylation by treatment with sodium hydride and subsequent trapping with allylic bromide **19**.[15] The resulting prenylated naphthol **23** was obtained in good yield as an inseparable 4:1 mixture of isomers, presumably due to an isomerization at the double bond indicated in Scheme 4. An analogous isomerization was observed by George and co-workers in their synthesis of merochlorin A, **1**.[2]

In an attempt to synthesize both merochlorin A, **1**, and B, **2**, we treated **23** with lead(IV) tetraacetate (LTA). These conditions, also used by George and co-workers,[2] resulted in a complex mixture of products. Based on ^{1}H NMR and mass spectroscopy data, we determined that the major component of this mixture resulted from Wessely oxidation (not shown).[16] A much cleaner reaction was observed by changing the oxidant to lead(IV) tetrabenzoate, which can be prepared from LTA via ligand exchange,[17] and use of a mixture of dichloromethane and trifluoroethanol (TFE) as a solvent (Scheme 5). Under these conditions, the Wessely oxidation product **24** could be isolated in moderate yield. Inspired by the work of Horne et al.,[3d] we tried to use **24** as a precursor of the requisite phenoxonium ion. However, when **24** was treated with a variety of Brønsted and Lewis acids, no [5 + 2]- or [3 + 2]-cycloaddition products could be observed.

We next turned to iodine(III) reagents[18] as oxidants. After extensive screening, we found that a variant of Koser's reagent [PhI(OH)OTs],[19] generated *in situ*, gave a desired product. Mixing iodosobenzene (PhIO) with trifluoromethanesulfonic acid,[20] followed by addition to naphthol **23**, afforded merochlorin B derivative **26**, which still contained one of the two silyl ethers of the starting material (Scheme 5). Subsequent deprotection afforded merochlorin B, **2**, as a single diastereomer and in 30% overall yield from **23**. The spectral data of our synthetic compound are in accordance with those reported by Moore et al.,[1b] and Prof. Moore agrees with this analysis (see Supporting Information).[21]

Interestingly, we did not observe the formation of merochlorin A, **1**, under our oxidative conditions. We believe that this is not due to a variation in the oxidant but rather due to the presence of a methyl ether in intermediate **25**. In the case of George's merochlorin A, **1**, synthesis,[2] the corresponding cyclization precursor bears a free hydroxyl group at the C-1 position, which can be deprotonated, rendering the resultant enolate highly nucleophilic. Presumably, the methyl substituent in intermediate **25** increases the relative nucleophilicity of the carbonyl, thus favoring the [3 + 2]-pathway. The resulting oxocarbenium ion is either directly demethylated by nucleophilic attack or forms a labile acetal that is lost upon aqueous workup.

In conclusion, we have achieved the first total synthesis of (±)-merochlorin B, **2**, a biologically active chlorinated meroterpenoid, by a longest linear sequence of eight steps starting from commercially available phenylacetic acid methyl ester **9**. Key steps include a directed *ortho*-metalation (DoM), a chemoselective demethylation of a naphthalene, and a biosynthetically inspired oxidative [3 + 2]-cycloaddition using an iodine(III) reagent generated *in situ*. Attempts to achieve asymmetric syntheses of the merochlorins are currently underway in our laboratories and will be reported in due course.

■ ASSOCIATED CONTENT

Supporting Information

Experimental details as well as spectroscopic and analytical data for all compounds. This material is available free of charge via the Internet at http://pubs.acs.org.

dx.doi.org/10.1021/ol500800z | Org. Lett. 2014, 16, 2634–2637

AUTHOR INFORMATION

Corresponding Author

*E-mail: dirk.trauner@lmu.de.

Notes

The authors declare no competing financial interest.

ACKNOWLEDGMENTS

Financial support by the Deutsche Forschungsgemeinschaft (SFB 749) is acknowledged. Additionally, the authors would like to acknowledge Dr. Tatsuya Urushima (LMU, München) for helpful discussions and experimental assistance.

REFERENCES

(1) (a) Sakoulas, G.; Nam, S.-J.; Loesgen, S.; Fenical, W.; Jensen, P. R.; Nizet, V.; Hensler, M. *PLoS One* **2012**, *7*, e29439. (b) Kaysser, L.; Bernhardt, P.; Nam, S.-J.; Loesgen, S.; Ruby, J. G.; Skewes-Cox, P.; Jensen, P. R.; Fenical, W.; Moore, B. S. *J. Am. Chem. Soc.* **2012**, *134*, 11988.

(2) Pepper, H. P.; George, J. H. *Angew. Chem.* **2013**, *125*, 12392; *Angew. Chem., Int. Ed.* **2013**, *52*, 12170.

(3) For literature precedents of oxidative [3 + 2]- and [5 + 2]-cycloadditions, see the following and references therein: By preformed quinone derivatives: (a) Büchi, G.; Chu, P.-S. *Tetrahedron* **1981**, *37*, 4509. (b) Grieco, P. A.; Walker, J. K. *Tetrahedron* **1997**, *53*, 8975. (c) Engler, T. A.; Scheibe, C. M. *J. Org. Chem.* **1998**, *63*, 6247. (d) Horne, D. A.; Yakushijin, K.; Büchi, G. *Tetrahedron Lett.* **1999**, *40*, 5443. By electrochemical approaches: (f) Quideau, S.; Pouységu, L.; Deffieux, D. *Curr. Org. Chem.* **2004**, *8*, 113. (g) Yamamura, S.; Nishiyama, S. *Synlett* **2002**, *4*, 533. By one- or two-electron oxidants: (h) Gates, B. D.; Dalidowicz, P.; Tebben, A.; Wang, S.; Swenton, J. S. *J. Org. Chem.* **1992**, *57*, 2135. (i) Wu, K.-L.; Wilkinson, S.; Reich, N. O.; Pettus, T. R. R. *Org. Lett.* **2007**, *9*, 5537. (j) Zhao, J.-C.; Yu, S.-M.; Liu, Y.; Yao, Z.-J. *Org. Lett.* **2013**, *15*, 4300. (k) Green, J. C.; Pettus, T. R. R. *J. Am. Chem. Soc.* **2011**, *133*, 1603. (l) Wu, K.-L.; Mercado, E. V.; Pettus, T. R. R. *J. Am. Chem. Soc.* **2011**, *133*, 6114.

(4) (a) Bycroft, B. W.; Roberts, J. C. *J. Chem. Soc.* **1962**, 2063. (b) Beekman, A. M.; Martinez, E. C.; Barrow, R. A. *Org. Biomol. Chem.* **2013**, *11*, 1109. (c) Bycroft, B. W.; Roberts, J. C. *J. Chem. Soc.* **1963**, 4868.

(5) Gonzalez-Bello, C.; Abell, C.; Leeper, F. J. *J. Chem. Soc., Perkin Trans. 1* **1997**, 1017.

(6) McCulloch, M. W. B.; Barrow, R. A. *Tetrahedron Lett.* **2005**, *46*, 7619.

(7) (a) Gschwend, M. W.; Rodriguez, H. R. *Org. React.* **1979**, *26*, 1. (b) Slocum, D. W.; Jennings, C. A. *J. Org. Chem.* **1976**, *41*, 3653. (c) Slocum, D. W.; Dumbris, S.; Brown, S.; Jackson, G.; LaMastus, R.; Mullins, E.; Ray, J.; Shelton, P.; Walstrom, A.; Wilcox, J. M.; Holman, R. W. *Tetrahedron* **2003**, *59*, 8275. For a review on directed *ortho*-metalation, see: (d) Snieckus, V. *Chem. Rev.* **1990**, *90*, 879.

(8) Mani, N. S.; Jablonowski, J. A.; Jones, T. K. *J. Org. Chem.* **2004**, *69*, 8115.

(9) Mitasev, B.; Porco, J. A., Jr. *Org. Lett.* **2009**, *11*, 2285.

(10) For a review on Peterson olefination, see: (a) Ager, D. J. *Org. React.* **1990**, *38*, 1. (b) Van Staden, L. F.; Gravestock, D.; Ager, D. J. *Chem. Soc. Rev.* **2002**, *31*, 195.

(11) Gembus, V.; Poisson, T.; Oudeyer, S.; Marsais, F.; Levacher, V. *Synlett* **2009**, *15*, 2437. (b) Andrey, O.; Glanzmann, C.; Landais, Y.; Parra-Papado, L. *Tetrahedron* **1997**, *53*, 2835.

(12) (a) Greene, A. E.; Le Drian, C.; Crabbe, P. *J. Org. Chem.* **1980**, *45*, 2713. (b) Tiseni, P. S.; Peters, R. *Angew. Chem.* **2007**, *119*, 5419; *Angew. Chem., Int. Ed.* **2007**, *46*, 5325.

(13) Raikar, S. B.; Nuhant, P.; Delpech, B.; Marazano, C. *Eur. J. Org. Chem.* **2008**, 1358.

(14) Only a few examples of a Lewis acidic demethylation in the presence of phenolic silyl protecting groups have been described so far: (a) Clive, D. L. J.; Daigneault, S. *J. Org. Chem.* **1991**, *56*, 5285. (b) Tanaka, T.; Kumamoto, T.; Ishikawa, T. *Tetrahedron Lett.* **2000**, *41*, 10229. (c) Yamaguchi, S.; Kobayashi, M.; Harada, S.; Miyazawa, M.; Hirai, Y. *Bull. Chem. Soc. Jpn.* **2008**, *81*, 863.

(15) (a) Yamada, S.; Takeshita, T.; Tanaka, J. *Bull. Chem. Soc. Jpn.* **1986**, *59*, 2901. (b) Hoarau, C.; Pettus, T. R. R. *Synlett* **2003**, *1*, 127. (c) Le Noble, W. J. *Synthesis* **1970**, *1*, 1. (d) Kornblum, N.; Lurie, A. P. *J. Am. Chem. Soc.* **1959**, *81*, 2705. (e) Bates, R. W.; Gabel, C. J. *Tetrahedron Lett.* **1993**, *34*, 3547.

(16) (a) Wessely, F.; Lauterbach-Keil, G.; Sinwel, F. *Monatsh. Chem.* **1950**, *81*, 811. (b) Wessely, F.; Sinwel, F. *Monatsh. Chem.* **1950**, *81*, 1055.

(17) (a) Bachman, G. B.; Wittmann, J. W. *J. Org. Chem.* **1963**, *28*, 65. (b) Buston, J. E. H.; Howell, H. J.; Moloney, M. G.; Manson, V. C.; Thompson, R. M. *Main Group Met. Chem.* **1998**, *21*, 51.

(18) For the use of hypervalent iodine(III) reagents in oxidative dearomatization reactions, see the following and references therein: (a) Pouységu, L.; Deffieux, D.; Quideau, S. *Tetrahedron* **2010**, *66*, 2235. (b) Quideau, S.; Pouységu, L.; Deffieux, D. *Synlett* **2008**, *4*, 467. (c) Silva, L. F., Jr.; Olofsson, B. *Nat. Prod. Rep.* **2011**, *28*, 1722.

(19) (a) Koser, G. F.; Wettach, R. H.; Troup, J. M.; Frenz, B. A. *J. Org. Chem.* **1976**, *41*, 3609. (b) Moriarty, R. M.; Vaid, R. K.; Koser, G. F. *Synlett* **1990**, 365.

(20) (a) Kitamura, T.; Furuki, R.; Taniguchi, H.; Stang, P. J. *Tetrahedron Lett.* **1990**, *31*, 703. (b) Kitamura, T.; Furuki, R.; Taniguchi, H.; Stang, P. J. *Tetrahedron* **1992**, *48*, 7149.

(21) Moore, B. S. Personal communication.

dx.doi.org/10.1021/ol500800z | *Org. Lett.* 2014, 16, 2634−2637

4.3 Conclusion

In this chapter, the first total synthesis of merochlorin B, a chlorinated meroterpenoid isolated from the marine sediment bacterium *Streptomyces spectabilis* strain CNH-189 in a biomimetic fashion was described. Crucial for the completion of the synthesis of this complex natural product was the development of a reliable route towards the chlorinated naphthalene core. This could be achieved by a directed-*ortho* metalation (D*o*M) relying on the cooperative effect of two methoxy groups in *meta*-position. The desired isosesquilavandulyl side chain was accessible *via* a Peterson olefination-based strategy. Both fragments could be accessed on multigram scale allowing for the screening of the crucial coupling reaction and the proposed biomimetic oxidative dearomization cascade.

Ortho-allylation of a 2-naphthol intermediate with the isosesquilavandulyl bromide afforded the desired biomimetic cyclization precursor. Initial investigations using lead(IV) oxidants, as described in the synthesis of merochlorin A by George and coworkers, just provided the corresponding Wessely oxidation products, which could not be converted to any desired cyclization product. However, after intense screening of oxidative conditions, a rarely applied *in situ* generated version of Koser's reagent provided merochlorin B in a formal (3+2) cycloaddition of an intermediate phenoxonium cation after final deprotection. This result confirmed the initial biomimetic proposal for the formation of merochlorin A and B.

This is even more fascinating due to the fact that merochlorin A which was the only product in George's biomimetic synthesis formed by a (5+2) cycloaddition, could not be identified in the reaction mixture. A comparison of the two similar biomimetic cyclization precursors gave rise to the assumption that a methyl protecting group in the merochlorin B precursor alters the nucleophilicity within the system to such an extent that the (3+2) cyclization mode is favored. This reflects that a subtle change in the reactant structure can drastically alter the outcome of a biomimetic transformation.

EXPERIMENTAL PART

5 GENERAL EXPERIMENTAL DETAILS

All reactions were carried out with magnetic stirring, and if moisture or air sensitive, under nitrogen or argon atmosphere using standard Schlenk techniques in oven-dried glassware (140 °C oven temperature), further dried under vacuum with a heat-gun at 650 °C. External bath temperatures were used to record all reaction temperatures. If catalytic amounts of transitions metals were used and in the case of photochemical reactions, the solvents were degassed by freeze-pump-thaw method (3 × 10 min) or by sparging with argon (20–30 min). Low temperature reactions were carried out in a Dewar vessel filled with Et_2O/liq. N_2 (–115 °C), acetone/dry ice (–78 °C) or distilled water/ice (0 °C). High temperature reactions were conducted using a heated silicon oil bath in reaction vessels equipped with a reflux condenser or in a pressure tube. Tetrahydrofuran (THF) and diethyl ether (Et_2O) were distilled over sodium and benzophenone prior to use. Dichloromethane (CH_2Cl_2), triethylamine (Et_3N), diisopropylethylamine (DIPEA) and diisopropylamine (DIPA) were distilled over calcium hydride under a nitrogen atmosphere. All other solvents were purchased from Acros Organics as 'extra dry' reagents. All other reagents with a purity > 95% were obtained from commercial sources (Sigma Aldrich, Acros, Alfa Aesar and others) and used without further purification.

Photochemical reactions were performed in a Rayonet RPR-200 photochemical reactor using 300 nm or 350 nm lamps (16 × RPR-3000Å, 250W) at room temperature or in a vacuum isolated Pyrex® immersion well equipped with a medium pressure mercury lamp (150 W) using a Heraeus power supply at –78 °C.

Flash column chromatography was carried out with Merck silica gel 60 (0.040–0.063 mm). In a few cases, flash column chromatography was carried out with Grace Davison silica (Davisil® LC60A 40–63 Micron).

Analytical thin layer chromatography (TLC) was carried out using Merck silica gel 60 F254 glass-backed plates and visualized under UV light at 254 nm. Staining was performed with ceric ammonium molybdate (CAM) or by oxidative staining with an aqueous basic potassium permanganate ($KMnO_4$) solution and subsequent heating.

NMR spectra (^{1}H NMR and ^{13}C NMR) were recorded in deuterated chloroform ($CDCl_3$), benzene (C_6D_6), dichloromethane (CD_2Cl_2), acetonitrile (CD_3CN) or dimethylsulfoxide (d_6-DMSO) on a Bruker Avance III HD 400 MHz spectrometer equipped with a CryoProbe™, a Varian VXR400 S spectrometer, a Bruker AMX600 spectrometer or a Bruker Avance III HD

800 MHz spectrometer equipped with a CryoProbe™ and are reported as follows: chemical shift δ in ppm (multiplicity, coupling constant J in Hz, number of protons) for ^{1}H NMR spectra and chemical shift δ in ppm for ^{13}C NMR spectra. Multiplicities are abbreviated as follows: s = singlet, d = doublet, t = triplet, q = quartet, quint = quintet, br = broad, m = multiplet, or combinations thereof. Residual solvent peaks of $CDCl_3$ (δ_H = 7.26 ppm, δ_C = 77.16 ppm), C_6D_6 (δ_H = 7.16 ppm, δ_C = 128.06 ppm), CD_2Cl_2 (δ_H = 5.32 ppm, δ_C = 54.00 ppm), CD_3CN (δ_H = 1.94 ppm, δ_C = 118.26 ppm) or d_6-DMSO (δ_H = 2.50 ppm, δ_C = 39.52 ppm) were used as an internal reference. NMR spectra were assigned using information ascertained from COSY, HMBC, HSQC and NOESY experiments.

High resolution mass spectra (HRMS) were recorded on a Varian MAT CH7A or a Varian MAT 711 MS instrument by electron impact (EI) or electrospray ionization (ESI) techniques at the Department of Chemistry, Ludwig-Maximilians-University Munich.

Infrared spectra (IR) were recorded from 4000 cm^{-1} to 600 cm^{-1} on a PERKIN ELMER Spectrum BX II, FT-IR instrument. For detection a SMITHS DETECTION DuraSampl*IR* II Diamond ATR sensor was used. Samples were prepared as a neat film or a thin powder layer. IR data in frequeny of absorption (cm^{-1}) is reported as follows: w = weak, m = medium, s = strong, br = broad or combinations thereof.

Melting Points were measured with a BÜCHI Melting Point B-450 instrument in open glascapillaries and are uncorrected.

Optical rotation values were recorded on a polarimeter P8000-T from A. Krüss Optronic GmbH or on a PERKIN ELMER 241 polarimeter. The specific rotation is calculated as follows:

$$[\alpha]_{\lambda}^{\vartheta} = \frac{\alpha \cdot 100}{c \cdot d}$$

The wavelength λ is reported in nm and the measuring temperature ϑ in °C. The recorded optical rotation is α, the concentration of the analyte is used in 10 mg/mL and the length of the cuvette is in dm. Thus, the specific rotation is given in 10^{-1} deg cm^2 g^{-1}. Usage of the sodium D line (λ = 589 nm) is indicated by D. The concentration as well as the solvent is reported at the relevant section of the experimental part.

UV-visible spectra were recorded on a Varian Cary 50 Bio UV-Visible Spectrophotometer using Starna 29/B/12 quartz cuvettes with 10 mm section thickness.

All yields are isolated, unless otherwise specified.

6 EXPERIMENTAL PROCEDURES, SPECTROSCOPIC AND X-RAY CRYSTALLOGRAPHIC DATA

6.1 Supporting information for Chapter 2.2.1.1–2.2.1.5

6.1.1 Experimental procedures

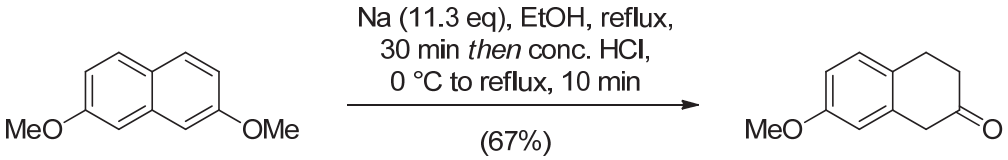

2.46 **2.45**

7-Methoxy-3,4-dihydronaphthalen-2-one (2.45) To a stirred solution of naphthalene **2.46** (15.0 g, 79.7 mmol, 1.0 eq) in EtOH (315 mL) was carefully added sodium metal (20.7 g, 901 mmol, 11.3 eq) at reflux and the resulting reaction mixture was stirred for 30 min. The reaction mixture was cooled to 0 °C followed by addition of H_2O (100 mL) and conc. HCl (300 mL). The resulting mixture was refluxed for 10 min. The layers were separated and the aqueous layer was extracted with CH_2Cl_2 (3 × 150 mL). The combined organic layers were washed with brine (150 mL) and dried over Na_2SO_4. After filtration and concentration *in vacuo*, the crude product was purified by flash column chromatography (hexanes:EtOAc 9:1) on silica to afford ketone **2.45** (9.40 g, 53.3 mmol, 67%) as a white solid. Compound **2.45** has been reported in the literature.[106b]

Data for 2.45: R_f: 0.24 (hexanes:EtOAc 9:1); **^{1}H NMR (400 MHz, $CDCl_3$):** δ = 7.14 (d, J = 8.3 Hz, 1H), 6.76 (dd, J = 8.3, 2.6 Hz, 1H), 6.67 (d, J = 2.5 Hz, 1H), 3.79 (s, 3H), 3.56 (s, 2H), 3.00 (t, J = 6.7 Hz, 2H), 2.56 – 2.52 (m, 2H) ppm; **^{13}C NMR (100 MHz, $CDCl_3$):** δ = 210.8, 158.7, 134.6, 128.9, 128.7, 113.6, 112.5, 55.5, 45.4, 38.7, 27.6 ppm; **IR (ATR):** ν_{max} = 2968 (w), 2958 (w), 2903 (w), 2840 (w), 1712 (s), 1607 (m), 1585 (m), 1501 (s), 1464 (m), 1455 (m), 1442 (m), 1393 (m), 1342 (m), 1315 (m), 1253 (s), 1234 (m), 1207 (m), 1186 (m), 1155 (s), 1118 (m), 1103 (m), 1032 (s), 976 (m), 942 (m), 896 (m), 870 (m), 833 (s), 821 (s), 771 (m), 737 (m), 692 (m) cm^{-1}; **melting point:** 24.5 °C (semisolid at r.t.; lit.: 23.0 – 24.0 °C)[157]; **HRMS (EI):** calc. for $C_{11}H_{12}O_2$ $[M]^+$: 204.1145, found:204.1152.

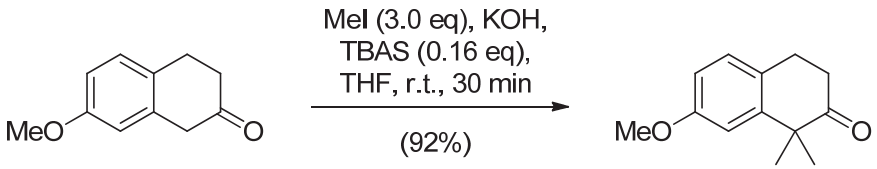

2.45 **2.47**

7-Methoxy-1,1-dimethyl-3,4-dihydronaphthalen-2-one (2.47) To a stirred solution of ketone **2.45** (6.58 g, 37.3 mmol, 1.0 eq), tetrabutylammonium hydrogensulfate (2.03 g, 5.97 mmol, 0.16 eq) and MeI (7.00 mL, 112 mmol, 3.0 eq) in THF (30 mL) was carefully added aq. KOH solution (50 wt%, 44 mL) at r.t. and the resulting reaction mixture was stirred for 30 min. The reaction was quenched by addition of H_2O (100 mL). The layers were separated and the aqueous layer was extracted with Et_2O (3 × 150 mL). The combined organic layers were washed with sat. aq. NH_4Cl solution (150 mL) and dried over Na_2SO_4. After filtration and concentration *in vacuo*, the crude product was purified by flash column chromatography (hexanes:EtOAc 14:1) on silica to afford dimethylated ketone **2.47** (7.02 g, 34.4 mmol, 92%) as a white solid. Compound **2.47** has been reported in the literature.[106c]

Data for 2.47: R_f: 0.43 (hexanes:EtOAc 9:1); **^{1}H NMR (400 MHz, $CDCl_3$):** δ = 7.10 (d, J = 8.3 Hz, 1H), 6.88 (d, J = 2.6 Hz, 1H), 6.75 (dd, J = 8.3, 2.6 Hz, 1H), 3.81 (s, 3H), 3.10 – 2.97 (m, 2H), 2.71 – 2.59 (m, 2H), 1.42 (s, 6H) ppm; **^{13}C NMR (100 MHz, $CDCl_3$):** δ = 214.8, 158.8, 145.0, 129.2, 127.5, 112.3, 111.4, 55.5, 48.0, 37.6, 27.8, 26.9 ppm; **IR (ATR):** ν_{max} = 2997 (w), 2933 (w), 2835 (w), 1708 (s), 1609 (m), 1577 (m), 1503 (m), 1494 (m), 1462 (m), 1422 (w), 1380 (m), 1359 (w), 1343 (w), 1315 (m), 1285 (m), 1264 (s), 1217 (s), 1201 (m), 1178 (m), 1096 (m), 1075 (s), 1041 (s), 881 (m), 847 (m), 808 (s), 718 (m) cm^{-1}; **melting point:** 58.7 – 59.5 °C; **HRMS (EI):** calc. for $C_{13}H_{16}O_2$ $[M]^+$: 176.0832, found: 176.0826.

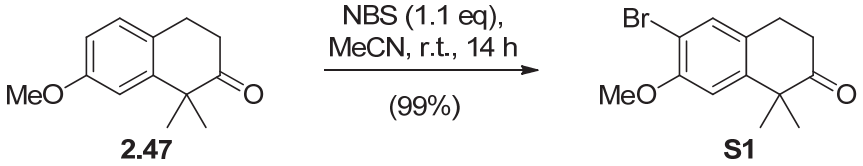

2.47 **S1**

6-Bromo-7-methoxy-1,1-dimethyl-3,4-dihydronaphthalen-2-one (S1) To a stirred solution of ketone **2.47** (3.00 g, 14.7 mmol, 1.0 eq) in MeCN (60 mL) was added NBS (2.88 g, 16.2 mmol, 1.1 eq) at r.t. and the resulting reaction mixture was stirred for 14 h. The reaction was quenched by addition of H_2O (100 mL). The layers were separated and the aqueous layer was extracted with Et_2O (3 × 100 mL). The combined organic layers were washed with brine (100 mL) and dried over Na_2SO_4. After filtration and concentration *in vacuo*, the crude product was purified by flash column chromatography (hexanes:EtOAc 10:1) on silica to

afford bromide **S1** (4.14 g, 14.6 mmol, 99%) as a white solid. Compound **S1** has been reported in the literature.[107a]

Data for S1: R_f: 0.33 (hexanes:EtOAc 9:1); **^{1}H NMR (400 MHz, $CDCl_3$):** δ = 7.35 (s, 1H), 6.83 (s, 1H), 3.90 (s, 3H), 3.10 – 2.95 (m, 2H), 2.71 – 2.60 (m, 2H), 1.43 (s, 6H) ppm; **^{13}C NMR (100 MHz, $CDCl_3$):** δ = 213.9, 155.1, 144.2, 132.8, 129.0, 109.9, 109.7, 56.5, 48.0, 37.2, 27.5, 26.9 ppm; **IR (ATR):** ν_{max} = 2969 (w), 2933 (w), 2837 (w), 1710 (s), 1594 (m), 1510 (w), 1490 (m), 1459 (m), 14651 (m), 1418 (m), 1389 (m), 1383 (w), 1330 (s), 1304 (m), 1274 (m), 1264 (m), 1240 (m), 1220 (m), 1194 (m), 1093 (s), 1045 (s), 865 (s), 843 (m), 795 (m), 751 (m), 724 (m) cm^{-1}; **melting point:** 99.1 – 99.8 °C **HRMS (EI):** calc. for $C_{13}H_{15}O_2Br^{79}$ $[M]^+$: 282.0250, found: 282.0245.

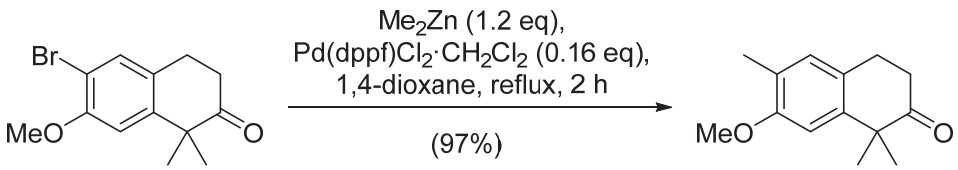

S1 **2.48**

7-Methoxy-1,1,6-trimethyl-3,4-dihydronaphthalen-2-one (2.48) To a stirred solution of bromide **S1** (1.70 g, 6.00 mmol, 1.0 eq) and $Pd(dppf)Cl_2{\cdot}CH_2Cl_2$ (131 mg, 180 µmol, 0.16 eq) in 1,4-dioxane (24 mL) was added Me_2Zn (0.8 M, 9.00 mL, 7.20 mmol, 1.2 eq) at r.t. and the resulting reaction mixture was refluxed for 2 h. The reaction was quenched by addition of H_2O (100 mL) and aq. HCl solution (1.0 M, 50 mL). The layers were separated and the aqueous layer was extracted with Et_2O (3 × 100 mL) and EtOAc (3 × 100 mL). The combined organic layers were washed with brine (150 mL) and dried over Na_2SO_4. After filtration and concentration *in vacuo*, the crude product was purified by flash column chromatography (hexanes:EtOAc 15:1) on silica to afford ketone **2.48** (1.27 g, 5.82 mmol, 97%) as a white solid.

Data for 2.48: R_f: 0.50 (hexanes:EtOAc 9:1); **^{1}H NMR (400 MHz, $CDCl_3$):** δ = 6.94 (s, 1H), 6.76 (s, 1H), 3.84 (s, 3H), 3.10 – 2.93 (m, 2H), 2.73 – 2.60 (m, 2H), 2.20 (s, 3H), 1.43 (s, 6H) ppm; **^{13}C NMR (100 MHz, $CDCl_3$):** δ = 215.0, 156.9, 141.8, 130.4, 126.7, 124.9, 107.6, 55.5, 47.7, 37.5, 27.8, 27.0, 15.7 ppm; **IR (ATR):** ν_{max} = 2967 (w), 2930 (w), 2852 (w), 2833 (w), 1709 (s), 1615 (m), 1579 (w), 1501 (s), 1461 (m), 1406 (m), 1379 (m), 1328 (m), 1317 (m), 1271 (m), 1247 (s), 1228 (m), 1220 (m), 1153 (m), 1132 (m), 1100 (m), 1059 (s), 1017 (m), 1001 (m), 959 (w), 880 (m), 848 (m), 819 (m), 758 (w), 716 (w), 666 (w) cm^{-1}; **melting point:** 45.6 – 46.1 °C; **HRMS (EI):** calc. for $C_{14}H_{18}O_2$ $[M]^+$: 218.1301, found: 218.1300.

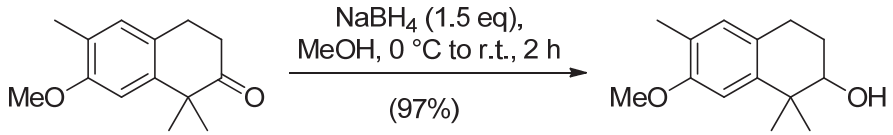

2.47 **2.57**

7-Methoxy-1,1,6-trimethyl-1,2,3,4-tetrahydronaphthalen-2-ol (2.57) To a stirred solution of ketone **2.47** (1.27 g, 5.82 mmol, 1.0 eq) in MeOH (35 mL) was added $NaBH_4$ (330 mg, 8.73 mmol, 1.5 eq) at 0 °C and the resulting reaction mixture was allowed to warm to r.t. over 2 h. After concentration *in vacuo*, the crude product was purified by flash column chromatography (hexanes:EtOAc 5:1→3:1) on silica to afford alcohol **2.57** (1.24 g, 5.63 mmol, 97%) as a white solid.

Data for 2.57: R_f: 0.40 (hexanes:EtOAc 3:1); **^{1}H NMR (400 MHz, C_6D_6):** δ = 6.73 (s, 1H), 6.70 (s, 1H), 3.49 (dd, *J* = 9.1, 3.0 Hz, 1H), 3.41 (s, 3H), 2.69 (dt, *J* = 16.5, 5.8 Hz, 1H), 2.57 (ddd, *J* = 16.1, 8.7, 6.5 Hz, 1H), 2.30 (s, 3H), 1.82 – 1.62 (m, 2H), 1.32 (s, 3H), 1.28 (s, 3H), 0.94 (s, 1H) ppm; **^{13}C NMR (100 MHz, C_6D_6):** δ = 156.9, 143.2, 131.2, 126.2, 124.4, 108.0, 75.6, 54.8, 39.5, 29.0, 27.9, 27.0, 25.3, 16.1 ppm; **IR (ATR):** ν_{max} = 3408 (br w), 2957 (w), 2929 (m), 2863 (w), 2357 (w), 1720 (br w), 1614 (w), 1497 (s), 1461 (m), 1451 (m), 1400 (w), 1375 (m), 1312 (m), 1247 (s), 1237 (m), 1208 (m), 1184 (m), 1141 (m), 1046 (s), 1009 (m), 997 (m), 956 (m), 849 (m), 780 (m), 634 (m) cm^{-1}; **melting point:** 72.3 – 73.3 °C; **HRMS (EI):** calc. for $C_{14}H_{20}O_2$ $[M]^+$: 220.1458, found: 220.1463.

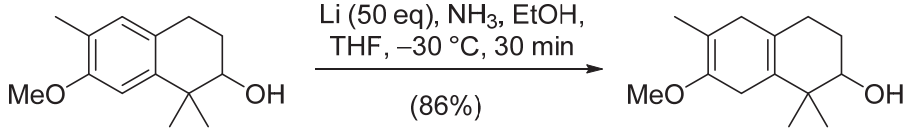

2.57 **2.42**

1,4-Cyclohexadiene 2.42 To a stirred solution of alcohol **2.57** (700 mg, 3.18 mmol, 1.0 eq) in a mixture of liquid ammonia (~40 mL, condensed at −78 °C), EtOH (12 mL) and THF (12 mL) in a three-necked 500 mL-flask equipped with a dry-ice condenser at −30 °C was added granulated lithium (1.10 g, 159 mmol, 50 eq) portionwise and the resulting dark blue reaction mixture was stirred for 30 min. The reaction was quenched by careful addition of NH_4Cl (4 g) and the reaction flask was left open while stirring at r.t. for 1.5 h followed by the addition of H_2O (150 mL) and sat. aq. NH_4Cl solution (150 mL). The layers were separated and the aqueous layer was extracted with Et_2O (3 × 100 mL) and the combined organic layers were washed with brine (100 mL) and dried over Na_2SO_4. After filtration and concentration *in vacuo*, the crude product was purified by flash column chromatography

(hexanes:EtOAc 9:1) on silica to afford cyclohexadiene **2.42** (605 mg, 2.72 mmol, 86%) as a colorless oil.

Data for 2.42: R_f: 0.40 (hexanes:EtOAc 3:1); **^{1}H NMR (400 MHz, C_6D_6):** δ = 3.37 (dd, J = 7.1, 5.6 Hz, 1H), 3.32 (s, 3H), 2.82 – 2.70 (m, 2H), 2.49 – 2.26 (m, 2H), 1.84 – 1.74 (m, 2H), 1.73 (s, 3H), 1.66 – 1.58 (m, 2H), 1.16 (s, 1H), 1.00 (s, 6H) ppm; **^{13}C NMR (100 MHz, C_6D_6):** δ = 146.3, 130.8, 124.8, 110.2, 75.5, 56.0, 39.1, 39.0, 28.1, 27.1, 25.9, 25.5, 21.2, 14.7 ppm; **IR (ATR):** ν_{max} = 3422 (br w), 2966 (m), 2934 (m), 2906 (m), 2871 (m), 2829 (m), 1718 (m), 1461 (m), 1438 (m), 1201 (s), 1142 (s), 1108 (m), 1023 (w), 1001 (m) cm^{-1}; **HRMS (EI):** calc. for $C_{14}H_{22}O_2$ $[M]^+$: 222.1614, found: 222.1609.

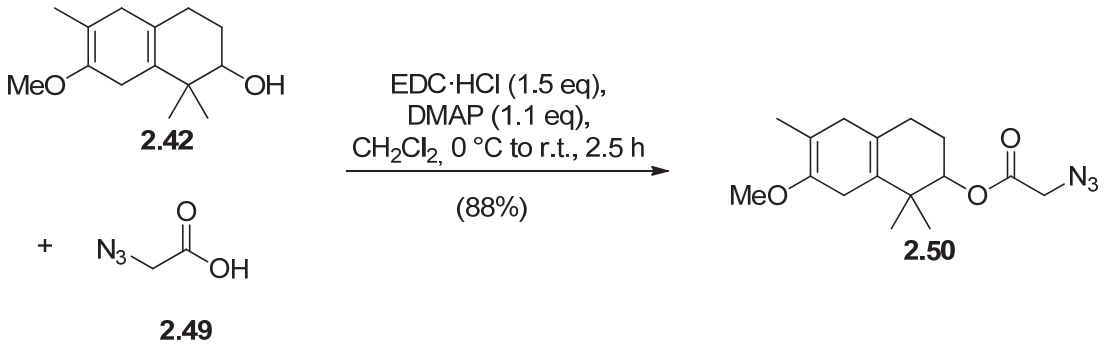

Azide 2.50 To a stirred solution of alcohol **2.42** (240 mg, 1.08 mmol, 1.0 eq), EDC·HCl (311 mg, 1.62 mmol, 1.5 eq) and DMAP (145 mg, 1.19 mmol, 1.1 eq) in CH_2Cl_2 (3.0 mL) at 0 °C was added a solution of azide **2.49** (153 mg, 1.51 mmol, 1.4 eq) in CH_2Cl_2 (1.0 mL) and the resulting reaction mixture was stirred at r.t. for 2.5 h. The reaction was quenched by addition of H_2O (10 mL). The layers were separated and the aqueous layer was extracted with CH_2Cl_2 (3 × 25 mL). The combined organic layers were dried over Na_2SO_4. After filtration and concentration *in vacuo*, the crude product was purified by flash column chromatography (hexanes:EtOAc 8:1) on silica to afford ester **2.50** (291 mg, 953 µmol, 88%) as a colorless oil.

Data for 2.50: R_f: 0.73 (hexanes:EtOAc 3:1); **^{1}H NMR (400 MHz, C_6D_6):** δ = 4.94 (dd, J = 8.0, 3.8 Hz, 1H), 3.30 (s, 3H), 3.13 (s, 2H), 2.68 (t, J = 7.2 Hz, 2H), 2.35 (t, J = 7.2 Hz, 2H), 1.77 – 1.65 (m, 7H), 0.95 (s, 3H), 0.84 (s, 3H) ppm; **^{13}C NMR (100 MHz, C_6D_6):** δ = 168.0, 146.0, 130.0, 125.2, 110.4, 80.0, 56.0, 50.12, 38.9, 37.7, 27.5, 25.7, 25.2, 23.6, 21.9, 14.7 ppm; **IR (ATR):** ν_{max} = 2970 (w), 2932 (w), 2904 (w), 2876 (w), 2827 (w), 2102 (s), 1738 (s), 1716 (m), 1461 (w), 1358 (m), 1287 (m), 1196 (s), 1173 (m), 1142 (s), 1101 (m), 1089 (m), 1022 (m), 994 (m), 972 (m), 933 (w), 733 (w) cm^{-1}; **HRMS (EI):** calc. for $C_{16}H_{23}O_3N_3$ $[M]^+$: 305.1734, found: 305.1737.

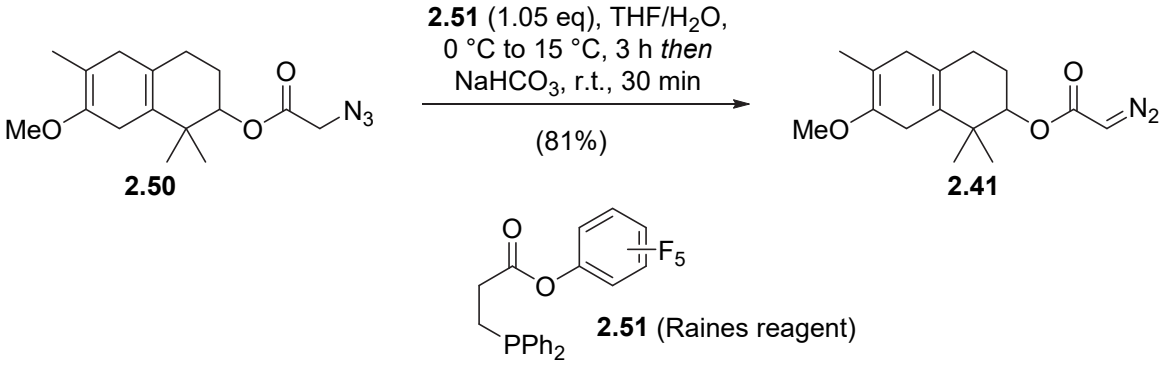

Diazoester 2.41 To a stirred solution of azide **2.50** (290 mg, 950 µmol, 1.0 eq) in THF/H_2O (20:3, 3.45 mL) at 0 °C was added phosphine **2.51**[111b] (424 mg, 998 µmol, 1.05 eq) and the resulting reaction mixture was allowed to warm up to 15 °C over 3 h. Sat. aq. $NaHCO_3$ solution (3 mL) was added and the resulting reaction mixture was stirred at r.t. for 30 min. The reaction was quenched by addition of H_2O (40 mL). The layers were separated and the aqueous layer was extracted with CH_2Cl_2 (3 × 30 mL). The combined organic layers were dried over Na_2SO_4. After filtration and concentration *in vacuo*, the crude product was purified by flash column chromatography (hexanes:EtOAc 15:1) on silica to afford diazo compound **2.41** (224 mg, 771 µmol, 81%) as a yellow oil.

The ^{13}C-shift of the carbonyl atom is not visible in the ^{13}C-data or the HMBC-data.

Data for 2.41: R_f: 0.70 (hexanes:EtOAc 3:1); **^{1}H NMR (400 MHz, C_6D_6):** δ = 5.09 (d, J = 8.5 Hz, 1H), 4.04 (s, 1H), 3.29 (s, 3H), 2.69 (t, J = 6.5 Hz, 2H), 2.34 (q, J = 6.8 Hz, 2H), 1.91 – 1.64 (m, 7H), 1.01 (s, 3H), 0.92 (s, 3H) ppm; **^{13}C NMR (100 MHz, C_6D_6):** δ = 146.0, 130.2, 125.2, 110.3, 78.3, 55.9, 45.8, 38.9, 37.9, 27.8, 25.7, 25.3, 24.1, 21.8, 14.7 ppm; **IR (ATR):** ν_{max} = 3097 (w), 2970 (w), 2935 (w), 2910 (w), 2876 (w), 2830 (w), 2105 (s), 1685 (s), 1462 (w), 1378 (s), 1361 (m), 1335 (m), 1243 (m), 1186 (s), 1144 (s), 1102 (m), 1090 (m), 1021 (m), 997 (m), 960 (m), 847 (w), 810 (w), 738 (m) cm^{-1}; **HRMS (EI):** calc. for $C_{16}H_{22}O_3N_2$ $[M]^+$: 290.1625, found: 290.1618.

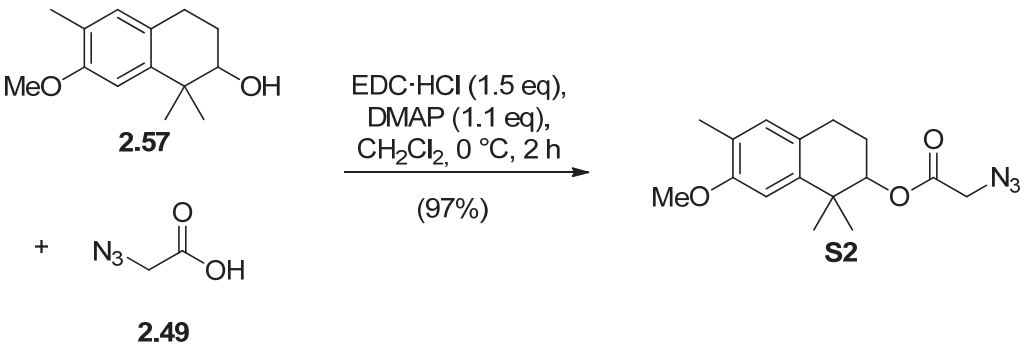

Azide S2 To a stirred solution of alcohol **2.57** (350 mg, 1.59 mmol, 1.0 eq), EDC·HCl (458 mg, 2.39 mmol, 1.5 eq) and DMAP (214 mg, 1.75 mmol, 1.1 eq) in CH_2Cl_2 (3.0 mL) at

0 °C was added a solution of azide **2.49** (225 mg, 2.23 mmol, 1.4 eq) in CH_2Cl_2 (2.5 mL) and the resulting reaction mixture was stirred for 2 h. The reaction was quenched by addition of H_2O (10 mL). The layers were separated and the aqueous layer was extracted with CH_2Cl_2 (3 × 15 mL). The combined organic layers were dried over Na_2SO_4. After filtration and concentration *in vacuo*, the crude product was purified by flash column chromatography (hexanes:EtOAc 20:1→15:1) on silica to afford ester **S2** (470 mg, 1.55 mmol, 97%) as a colorless oil.

Data for S2: R_f: 0.75 (hexanes:EtOAc 3:1); **^{1}H NMR (400 MHz, C_6D_6):** δ = 6.69 (s, 1H), 6.61 (s, 1H), 5.10 (t, *J* = 6.0 Hz, 1H), 3.40 (s, 3H), 3.11 (s, 2H), 2.62 (dt, *J* = 16.5, 6.7 Hz, 1H), 2.53 (dt, *J* = 16.6, 6.8 Hz, 1H), 2.26 (s, 3H), 1.84 (q, *J* = 6.3 Hz, 2H), 1.25 (s, 3H), 1.16 (s, 3H) ppm; **^{13}C NMR (100 MHz, C_6D_6):** δ = 168.0, 157.0, 141.7, 131.3, 125.8, 124.9, 107.5, 79.6, 54.8, 50.1, 38.2, 29.4, 26.1, 26.0, 24.3, 16.0 ppm; **IR (ATR):** ν_{max} = 2947 (w), 2104 (s), 1739 (s), 1618 (w), 1501 (m), 1464 (m), 1404 (w),1366 (m), 1289 (m), 1248 (m), 1205 (s), 1188 (s), 1147 (m), 1059 (m), 1038 (m), 1004 (m), 887 (m), 848 (m), 776 (w), 661 (w) cm^{-1}; **HRMS (EI):** calc. for $C_{16}H_{21}O_3N_3$ $[M]^+$: 303.1577, found: 303.1573.

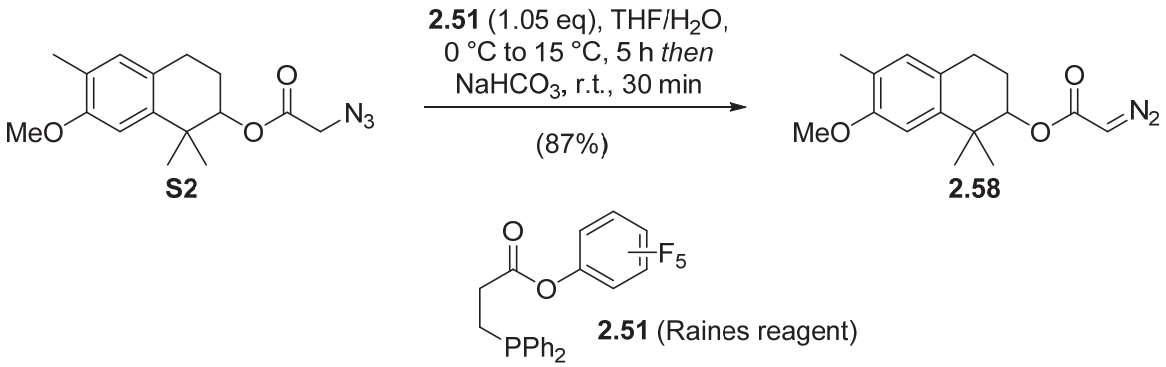

Diazoester 2.58 To a stirred solution of azide **S2** (208 mg, 686 µmol, 1.0 eq) in THF/H_2O (20:3, 2.99 mL) at 0 °C was added phosphine **2.51**[111b] (306 mg, 720 µmol, 1.05 eq) and the resulting reaction mixture was allowed to warm up to 15 °C over 5 h. Sat. aq. $NaHCO_3$ solution (2.6 mL) was added and the resulting reaction mixture was stirred at r.t. for 30 min. The reaction was quenched by addition of H_2O (15 mL). The layers were separated and the aqueous layer was extracted with CH_2Cl_2 (3 × 25 mL). The combined organic layers were dried over Na_2SO_4. After filtration and concentration *in vacuo*, the crude product was purified by flash column chromatography (hexanes:EtOAc 15:1) on silica to afford diazo compound **2.58** (172 mg, 597 µmol, 87%) as a yellow oil.

The ^{13}C-shift of the carbonyl atom is not visible in the ^{13}C-data or the HMBC-data.

Data for 2.58: R_f: 0.70 (hexanes:EtOAc 3:1); **^{1}H NMR (400 MHz, C_6D_6):** δ = 6.68 (s, 1H), 6.62 (s, 1H), 5.26 (t, J = 5.6 Hz, 1H), 4.00 (s, 1H), 3.38 (s, 3H), 2.68 (dt, J = 16.5, 6.6 Hz, 1H), 2.57 (dt, J = 16.5, 6.8 Hz, 1H), 2.26 (s, 3H), 1.94 (q, J = 6.6 Hz, 2H), 1.32 (s, 3H), 1.23 (s, 3H) ppm; **^{13}C NMR (100 MHz, C_6D_6):** δ = 156.9, 142.1, 131.3, 126.0, 124.7, 107.6, 78.2, 54.8, 45.8, 38.5, 29.5, 26.2, 26.0, 24.7, 16.0 ppm; **IR (ATR):** ν_{max} = 3100 (w), 2967 (w), 2945 (w), 2851 (w), 2105 (s), 1684 (s), 1618 (w), 1501 (s), 1464 (m), 1378 (s), 1362 (s), 1338 (s), 1243 (s), 1174 (s), 1147 (s), 1059 (s), 1038 (s), 1004 (s), 918 (m), 888 (m), 848 (m), 838 (m), 737 (s) cm^{-1}; **HRMS (EI):** calc. for $C_{16}H_{20}O_3N_2$ $[M]^+$: 288.1468, found: 288.1470.

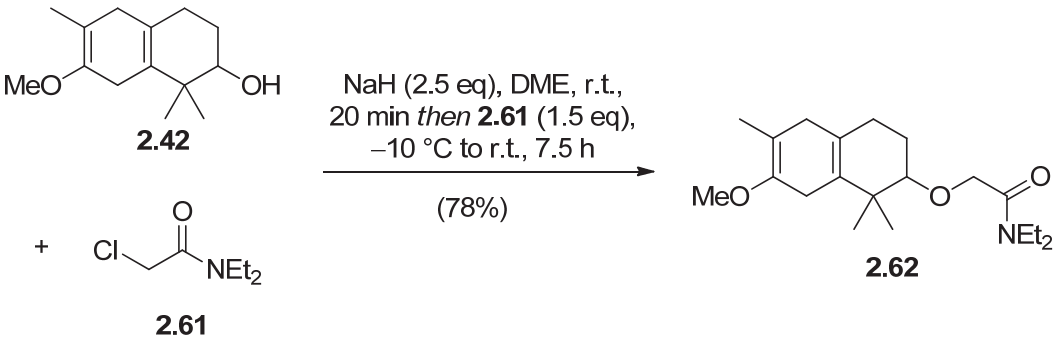

Amide 2.62 To a stirred solution of alcohol **2.42** (230 mg, 1.03 mmol, 1.0 eq) in DME (5.0 mL) at −10 °C was added NaH (60% dispersion in mineral oil, 103 mg, 2.58 mmol, 2.5 eq) and the resulting reaction mixture was stirred for 20 min. Chloride **2.61** (213 µL, 1.55 mmol, 1.5 eq) in DME (1.0 mL) was added dropwise and the resulting reaction mixture was allowed to warm up to r.t. over 7.5 h. The reaction was quenched by addition of sat. aq. NH_4Cl solution (5 mL) and H_2O (10 mL). The layers were separated and the aqueous layer was extracted with Et_2O (3 × 10 mL). The combined organic layers were dried over Na_2SO_4. After filtration and concentration *in vacuo*, the crude product was purified by flash column chromatography (hexanes:EtOAc 6:1→3:1) on silica to afford amide **2.62** (271 mg, 808 µmol, 78%) as a colorless oil.

Data for 2.62: R_f: 0.28 (hexanes:EtOAc 3:1); **^{1}H NMR (400 MHz, C_6D_6):** δ = 4.06 (d, J = 12.4 Hz, 1H), 4.00 (d, J = 12.4 Hz, 1H), 3.32 (s, 3H), 3.31 – 3.21 (m, 2H), 3.20 – 3.01 (m, 2H), 2.98 – 2.85 (m, 1H), 2.83 – 2.74 (m, 2H), 2.49 – 2.32 (m, 2H), 1.91 – 1.63 (m, 7H), 1.14 (s, 3H), 1.08 (s, 3H), 0.99 (t, J = 7.1 Hz, 3H), 0.77 (t, J = 7.1 Hz, 3H) ppm; **^{13}C NMR (100 MHz, C_6D_6):** δ = 168.3, 146.3, 130.9, 124.8, 110.2, 84.3, 69.9, 55.9, 41.2, 39.8, 39.1, 39.0, 28.4, 25.8, 25.6, 22.4, 21.8, 14.7, 14.4, 13.1 ppm; **IR (ATR):** ν_{max} = 2969 (m), 2934 (m), 2905 (w), 2831 (w), 1717 (w), 1641 (s), 1462 (m), 1434 (m), 1380 (m), 1358 (m), 1311 (w),

1265 (w), 1221 (m), 1202 (m), 1144 (m), 1083 (s), 1026 (m), 1002 (m), 793 (w), 736 (w) cm^{-1}; **HRMS (EI):** calc. for $C_{20}H_{33}O_3N$ $[M]^+$: 335.2455, found: 335.2449.

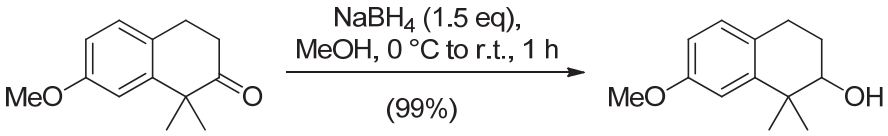

2.45 **S3**

7-Methoxy-1,1-dimethyl-1,2,3,4-tetrahydronaphthalen-2-ol (S3) To a stirred solution of ketone **2.45** (200 mg, 980 µmol, 1.0 eq) in MeOH (5 mL) was added $NaBH_4$ (55.6 mg, 1.47 mmol, 1.5 eq) at 0 °C and the resulting reaction mixture was allowed to warm to r.t. over 1 h. After concentration *in vacuo*, the crude product was purified by flash column chromatography (hexanes:EtOAc 8:1→5:1) on silica to afford alcohol **S3** (200 mg, 970 µmol, 99%) as a white solid. This compound has been reported in the literature.[158]

Data for S3: R_f: 0.10 (hexanes:EtOAc 3:1); **^{1}H NMR (400 MHz, $CDCl_3$):** δ = 6.99 (d, J = 8.4 Hz, 1H), 6.88 (d, J = 2.7 Hz, 1H), 6.70 (dd, J = 8.4, 2.7 Hz, 1H), 3.80 (s, 3H), 3.75 (dd, J = 8.7, 2.9 Hz, 1H), 2.90 (dt, J = 16.7, 6.3 Hz, 1H), 2.84 – 2.74 (m, 1H), 2.00 (dddd, J = 12.4, 9.3, 6.2, 3.0 Hz, 1H), 1.96 – 1.86 (m, 1H), 1.60 (s, 1H), 1.34 (s, 3H), 1.29 (s, 3H) ppm; **^{13}C NMR (100 MHz, $CDCl_3$):** δ = 158.0, 145.6, 129.6, 126.7, 112.4, 111.4, 75.6, 55.3, 39.3, 29.0, 27.0, 26.1, 25.0 ppm; **IR (ATR):** ν_{max} = 3367 (br w), 2962 (m), 2930 (m), 2859 (w), 2836 (w), 1610 (m), 1580 (w), 1570 (w), 1488 (m), 1457 (w), 1441 (w), 1434 (w), 1421 (w), 1382 (w), 1355 (w), 1314 (w), 1288 (m), 1281 (s), 1240 (s), 1229 (s), 1187 (m), 1169 (m), 1136 (w), 1079 (m), 1058 (s), 1043 (s), 967 (m), 949 (m), 867 (s), 809 (m), 711 (m), 695 (m), 662 (m) cm^{-1}; **melting point:** 82.5 – 83.7 °C (lit.: 85.0 – 88.0 °C)[159]; **HRMS (EI):** calc. for $C_{13}H_{18}O_2$ $[M]^+$: 206.1301, found: 206.1299.

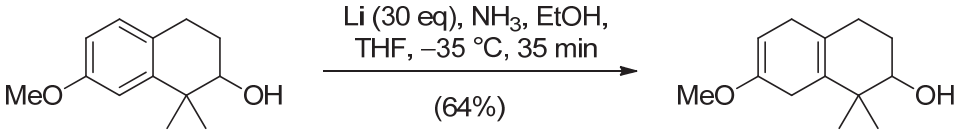

S3 **2.67**

1,4-Cyclohexadiene 2.67 To a stirred solution of alcohol **S3** (200 mg, 970 µmol, 1.0 eq) in a mixture of liquid ammonia (~10 mL, condensed at −78 °C), EtOH (3 mL) and THF (3 mL) in a three-necked 100 mL-flask equipped with a dry-ice condenser at −35 °C was added granulated lithium (202 mg, 29.1 mmol, 30 eq) portionwise and the resulting dark blue

reaction mixture was stirred for 35 min. The reaction was quenched by careful addition of NH_4Cl (2 g) and the reaction flask was left open while stirring at r.t. for 1.5 h followed by the addition of H_2O (50 mL) and sat. aq. NH_4Cl solution (50 mL). The layers were separated and the aqueous layer was extracted with Et_2O (3 × 50 mL) and the combined organic layers were dried over Na_2SO_4. After filtration and concentration *in vacuo*, the crude product was purified by flash column chromatography (hexanes:EtOAc 9:1) on silica to afford cyclohexadiene **2.67** (130 mg, 624 µmol, 64%) as a colorless oil.

Data for 2.67: R_f: 0.37 (hexanes:EtOAc 3:1); **^{1}H NMR (400 MHz, C_6D_6):** δ = 4.46 (t, J = 3.4 Hz, 1H), 3.35 – 3.30 (m, 4H), 2.90 – 2.81 (m, 2H), 2.68 – 2.54 (m, 2H), 1.92 – 1.76 (m, 2H), 1.66 – 1.52 (m, 2H), 0.94 (s, 6H) ppm; **^{13}C NMR (100 MHz, C_6D_6):** δ = 154.1, 130.7, 124.7, 89.6, 75.4, 53.6, 38.9, 32.8, 28.7, 28.2, 27.1, 25.3, 20.9 ppm; **IR (ATR):** ν_{max} = 3397 (br w), 2965 (w), 2936 (m), 2874 (m), 2830 (m), 1698 (m), 1665 (w), 1465 (m), 1440 (m), 1389 (m), 1361 (m), 1257 (w), 1231 (m), 1212 (s), 1168 (s), 1128 (m), 1112 (m), 1062 (m), 1032 (s), 1011 (s), 980 (m), 908 (m), 858 (w), 834 (m), 782 (m), 706 (m), 680 (m) cm^{-1}; **melting point:** 76.0 – 77.8 °C; **HRMS (EI):** calc. for $C_{13}H_{20}O_2$ $[M]^+$: 208.1458, found: 208.1460.

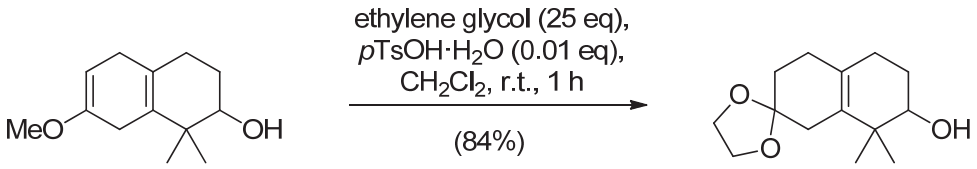

2.67 **S4**

Ketal S4 To a stirred solution of enol ether **2.67** (237.0 mg, 1.14 mmol, 1.0 eq) and ethylene glycol (1.59 mL, 28.5 mmol, 25 eq) in CH_2Cl_2 (8.0 mL) at r.t. was added pTsOH·H_2O (2.0 mg, 11.4 µmol, 0.01 eq) and the resulting reaction mixture was stirred for 1 h. The reaction was quenched by addition of half-sat. aq. $NaHCO_3$ solution (20 mL). The layers were separated and the aqueous layer was extracted with CH_2Cl_2 (3 × 20 mL). The combined organic layers were dried over Na_2SO_4. After filtration and concentration *in vacuo*, the crude product was purified by flash column chromatography (hexanes:EtOAc 3:1) on silica to afford ketal **S4** (227 mg, 952 µmol, 84%) as a white solid.

Data for S4: R_f: 0.15 (hexanes:EtOAc 3:1); **^{1}H NMR (400 MHz, C_6D_6):** δ = 3.67 – 3.49 (m, 4H), 3.35 (dd, J = 8.9, 3.6 Hz, 1H), 2.37 (d, J = 17.0 Hz, 1H), 2.31 (d, J = 17.4 Hz, 1H), 2.11 (dt, J = 15.1, 7.4 Hz, 1H), 2.00 (dt, J = 16.9, 5.9 Hz, 1H), 1.89 – 1.77 (m, 2H), 1.77 – 1.65 (m, 2H), 1.65 – 1.44 (m, 2H), 1.01 (s, 3H), 1.01 (s, 3H), 0.93 (s, 1H) ppm; **^{13}C NMR (100 MHz, C_6D_6):** δ = 131.7, 125.9, 109.1, 75.5, 64.3 (2C), 39.2, 35.3, 31.4, 30.2, 28.6, 27.2, 25.3,

20.8 ppm; **IR (ATR):** ν_{max} = 3319 (br w), 2970 (w), 2934 (m), 2876 (m), 2830 (w), 2361 (w), 2337 (w), 1734 (w), 1466 (w), 1438 (w), 1362 (m), 1217 (m), 1122 (m), 1105 (m), 1084 (m), 1058 (m), 1034 (s), 997 (m), 946 (m), 875 (w), 851 (m), 709 (m) cm^{-1}; **melting point:** 77.0 – 79.5 °C; **HRMS (EI):** calc. for $C_{14}H_{22}O_3$ $[M]^+$: 238.1563, found: 238.1564.

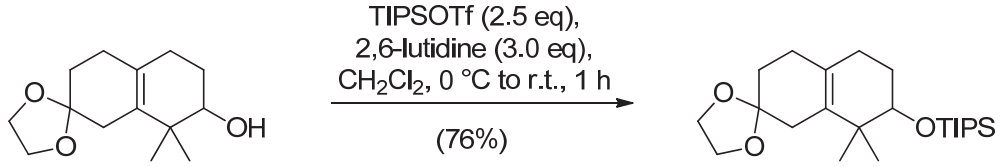

S4 **2.68**

Protected ketal 2.68 To a stirred solution of alcohol **S4** (175 mg, 734 µmol, 1.0 eq) in CH_2Cl_2 (5.0 mL) at 0 °C was added 2,6-lutidine (256 µL, 2.20 mmol, 3.0 eq) and TIPSOTf (507 µL, 1.88 mmol, 2.5 eq) and the resulting reaction mixture was stirred at r.t. for 1 h. The reaction was quenched by addition of H_2O (30 mL). The layers were separated and the aqueous layer was extracted with CH_2Cl_2 (3 × 30 mL). The combined organic layers were dried over Na_2SO_4. After filtration and concentration *in vacuo*, the crude product was purified by flash column chromatography (hexanes:EtOAc 25:1) on silica to afford ketal **2.68** (220 mg, 557 µmol, 76%) as a white solid. A crystal, suitable for single crystal X-ray diffraction analysis, was obtained by crystallization from acetone.

Data for 2.68: R_f: 0.70 (hexanes:EtOAc 3:1); **^{1}H NMR (400 MHz, C_6D_6):** δ = 3.77 (dd, J = 10.9, 3.6 Hz, 1H), 3.71 – 3.49 (m, 4H), 2.48 (d, J = 16.8 Hz, 1H), 2.37 (d, J = 16.7 Hz, 1H), 2.22 (dt, J = 16.3, 8.0 Hz, 1H), 1.99 (dt, J = 17.1, 5.0 Hz, 1H), 1.94 – 1.67 (m, 6H), 1.21 – 1.03 (m, 24H) ppm; **^{13}C NMR (100 MHz, C_6D_6):** δ = 132.6, 125.5, 109.1, 77.5, 64.4, 64.3, 40.4, 35.6, 31.5, 30.2, 29.9, 28.2, 25.1, 20.5, 18.6, 13.4 ppm; **IR (ATR):** ν_{max} = 2956 (w), 2938 (m), 2892 (w), 2864 (m), 1462 (w), 1454 (w), 1378 (w), 1363 (w), 1262 (w), 1231 (w), 1144 (m), 1116 (s), 1081 (m), 1069 (m), 1059 (m), 1043 (s), 1013 (s), 1006 (m), 945 (m), 918 (w), 883 (s), 862 (m), 827 (m), 778 (w), 706 (w), 682 (s) cm^{-1}; **melting point:** 63.9 – 65.5 °C; **HRMS (EI):** calc. for $C_{23}H_{42}O_3Si$ $[M]^+$: 394.2898, found: 394.2894.

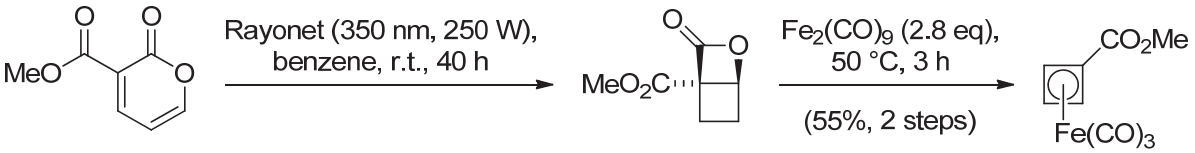

2.76 **2.77** **2.78**

Iron tricarbonyl complex 2.78 A stirred solution of pyrone **2.76** (2.00 g, 13.0 mmol, 1.0 eq) in benzene (130 mL, degassed by sparging with argon for 30 min) in a Duran® cylinder at r.t was irradiated for 43 h using a Rayonet lamp (350 nm, 250 W). The reaction was removed from the lamp and transferred into a round-bottom flask. $Fe_2(CO)_9$ (11.3 g, 31.2 mmol, 2.4 eq) was added and the resulting reaction mixture was heated to 50 °C for 2 h . Additional $Fe_2(CO)_9$ (1.88 g, 5.19 mmol, 0.4 eq) was added followed by heating for 1h. After evaporation of the solvent, the crude product was purified by flash column chromatography (1st column: pentane:Et_2O 9:1→2:3, 2nd column: pentane:Et_2O 20:1→4:1) on silica to afford iron tricarbonyl complex **2.78** (1.77 g, 7.08 mmol, 55%) as a yellow solid. Compound **2.78** has been reported in the literature.[122b]

Data for 2.78: R_f: 0.80 (hexanes:EtOAc 4:1); **^{1}H NMR (400 MHz, $CDCl_3$):** δ = 4.51 (s, 2H), 4.29 (s, 1H), 3.68 (s, 3H) ppm; **^{13}C NMR (100 MHz, $CDCl_3$):** δ = 212.2, 167.7,* 67.9, 65.1, 62.3, 51.9 ppm; **IR (ATR):** ν_{max} = 3117 (w), 2956 (w), 2361 (w), 2341 (w), 2052 (s), 1955 (s), 1707 (s), 1455 (s), 1416 (m), 1310 (m), 1198 (s), 1174 (s), 1117 (m), 1047 (m), 951 (m), 930 (m), 826 (m), 798 (w), 759 (m) cm^{-1}; **melting point:** 34.7 – 36.0 °C (lit.: 33.0 – 34.0 °C)[122b]; **HRMS (EI):** calc. for $C_9H_6Fe^{56}O_5$ [*M*]$^+$: 249.9559, found: 249.9565.

* The shift of the ester carbonyl was not visible in the ^{13}C spectra, but was extracted from the HMBC data showing corresponding correlations at 167.7 ppm.

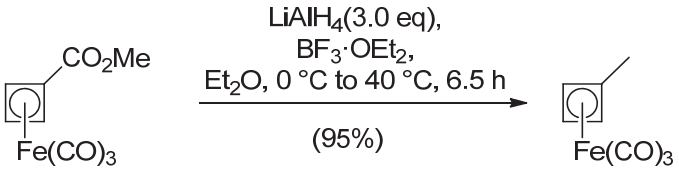

2.78 **2.79**

Iron tricarbonyl complex 2.79 To a stirred solution of ester **2.78** (500 mg, 2.00 mmol, 1.0 eq) and $BF_3{\cdot}OEt_2$ (7 mL) in Et_2O (5.4 mL) in a pressure tube at 0 °C was added $LiAlH_4$ (1.0 M in Et_2O, 6.00 mL, 6.0 mmol, 3.0 eq) and the resulting reaction mixture was stirred at 0 °C for 1.5 h followed by heating to 40 °C for 5 h. The reaction was quenched by addition of ice-water (150 mL). The layers were separated and the aqueous layer was extracted with Et_2O (4 × 40 mL). The organic layer was dried over Na_2SO_4. After filtration and concentration *in vacuo*, the crude product was purified by flash column chromatography (pentane) on silica

to afford iron tricarbonyl complex **2.79** (391 mg, 1.89 mmol, 95%) as a yellow oil. Compound **2.79** has been reported in the literature.[122b]

Data for 2.79: R_f: 0.66 (pentane); **^{1}H NMR (400 MHz, $CDCl_3$):** δ = 4.00 (s, 2H), 3.86 (s, 1H), 1.75 (s, 3H) ppm; **^{13}C NMR (100 MHz, $CDCl_3$):** δ = 215.2, 85.5, 65.0, 58.2, 13.7 ppm; **IR (ATR):** ν_{max} = 2980 (w), 2924 (w), 2861 (w), 2361 (w), 2333 (w), 2036 (s), 1935 (s), 1448 (s), 1375 (w), 1286 (w), 1147 (w), 1061 (w), 1028 (w), 947 (w), 933 (w), 831 (w), 775 (w), 668 (w) cm^{-1}; **HRMS (EI):** calc. for $C_8H_6Fe^{56}O_3$ $[M]^+$: 205.9661, found: 205.9661.

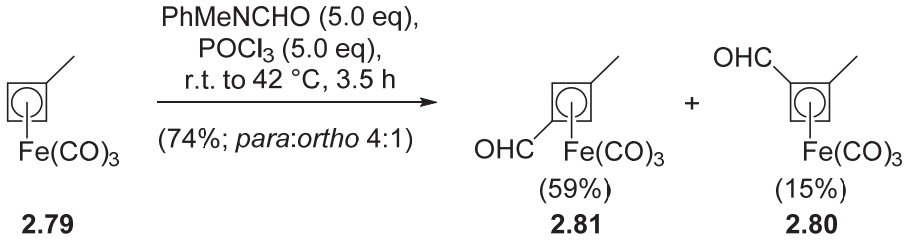

2.79 **2.81** **2.80**

Aldehyde 2.80 and 2.81 Under vigorous stirring of PhMeNCHO (1.11 mL, 9.00 mmol, 5.0 eq) was added $POCl_3$ (821 µL, 9.00 mmol, 5.0 eq) at r.t. and the resulting reaction mixture was stirred for 1 h. Iron tricarbonyl complex **2.79** (370 mg , 1.80 mmol, 1.0 eq) was added followed by heating to 42 °C for 3.5 h. The reaction was quenched by addition of ice-water (100 mL). The layers were separated and the aqueous layer was extracted with Et_2O (3 × 50 mL). The organic layer was dried over Na_2SO_4. After filtration and concentration *in vacuo*, the crude product was purified by flash column chromatography (pentane:Et_2O 6:1) on silica to afford aldehyde **2.81** (247 mg, 1.06 mmol, 59%) as yellow needles and regioisomeric aldehyde **2.80** (63.4 mg, 271 µmol, 15%) as a yellow solid. Compound **2.81** was suitable for single crystal X-ray diffraction analysis.

Data for 2.81 (major regioisomer): R_f: 0.39 (hexanes:EtOAc 4:1); **^{1}H NMR (400 MHz, C_6D_6):** δ = 8.87 (s, 1H), 3.77 (s, 2H), 1.00 (s, 3H) ppm; **^{13}C NMR (100 MHz, C_6D_6):** δ = 211.9, 186.5, 93.2, 65.4, 65.0, 12.0 ppm; **IR (ATR):** ν_{max} = 3085 (w), 2990 (w), 2965 (w), 2921 (w), 2044 (m), 1956 (s), 1638 (s), 1467 (m), 1427 (m), 1384 (m), 1190 (m), 1112 (m), 1085 (m), 1042 (m), 1027 (m), 994 (m), 854 (m), 794 (m), 781 (m), 677 (m), 656 (m) cm^{-1}; **melting point:** 76.5 – 77.3 °C; **HRMS (EI):** calc. for $C_9H_6Fe^{56}O_4$ $[M]^+$: 233.9610, found: 233.9614.

Data for 2.80 (minor regioisomer): R_f: 0.49 (hexanes:EtOAc 4:1); **^{1}H NMR (400 MHz, C_6D_6):** δ = 8.90 (s, 1H), 3.57 (s, 1H), 3.36 (s, 1H), 1.41 (s, 3H) ppm; **^{13}C NMR (100 MHz, C_6D_6):** δ = 212.6, 187.0, 87.7, 71.9, 71.0, 60.3, 11.8 ppm; **IR (ATR):** ν_{max} = 3115 (w), 3102 (w), 2980 (w), 2960 (w), 2926 (w), 2860 (w), 2048 (m), 1948 (s), 1658 (s), 1476 (m),

1461 (m), 1451 (m), 1433 (m), 1384 (m), 1410 (m), 1380 (m), 1354 (m), 1297 (m), 1192 (m), 1101 (m), 1030 (m), 989 (m), 946 (w), 860 (m), 821 (m), 776 (s), 690 (w) cm^{-1}; **melting point:** 35.1 – 35.8 °C; **HRMS (EI):** calc. for $C_9H_6Fe^{56}O_4$ $[M]^+$: 233.9610, found: 233.9613.

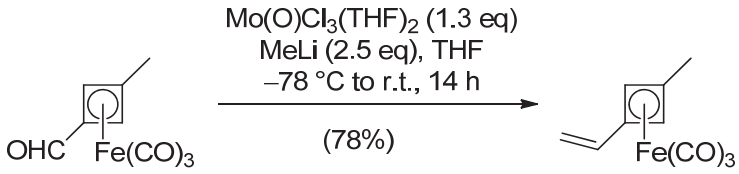

2.81 **2.74**

Alkene 2.74 To a stirred solution of $Mo(O)Cl_3(THF)_2$[128a] (246 mg, 683 µmol, 1.3 eq) in THF (5.0 mL) at −78 °C was added MeLi (1.6 M in Et_2O, 800 µL, 1.28 mmol, 2.5 eq) and the resulting reaction mixture was stirred for 1 h. Aldehyde **2.81** (120 mg, 513 mmol, 1.0 eq) in THF (2.0 mL) was added dropwise and the reaction mixture was allowed to warm up to r.t. overnight. The reaction was quenched by addition of H_2O (10 mL). The layers were separated and the aqueous layer was extracted with Et_2O (3 × 15 mL). The combined organic layers were dried over Na_2SO_4. After filtration and concentration *in vacuo*, the crude product was purified by flash column chromatography (pentane) on silica to afford alkene **2.74** (93.0 mg, 401 µmol, 78%) as a yellow liquid.

Data for 2.74: R_f: 0.55 (pentane); **^{1}H NMR (400 MHz, C_6D_6):** δ = 5.56 (dd, J = 17.3, 10.7 Hz, 1H), 4.92 (d, J = 17.3 Hz, 1H), 4.77 (d, J = 10.7 Hz, 1H), 3.66 (s, 2H), 1.23 (s, 3H) ppm; **^{13}C NMR (100 MHz, C_6D_6):** δ = 215.1, 129.8, 113.5, 84.6, 75.9, 64.2, 12.5 ppm; **IR (ATR):** ν_{max} = 3097 (w), 2973 (w), 2924 (w), 2032 (s), 1936 (s), 1620 (w), 1445 (w), 1373 (w), 1264 (w), 1046 (w), 1026 (w), 978 (m), 898 (m), 827 (w), 735 (w), 708 (m), 604 (m), 575 (s) cm^{-1}; **HRMS (EI):** calc. for $C_{10}H_9Fe^{56}O_3$ $[M+H]^+$: 232.9896, found: 232.9905.

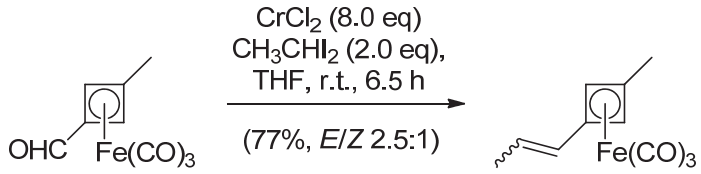

2.81 **2.75**

Alkene 2.75 To a stirred suspension of $CrCl_2$ (420 mg, 3.42 mmol, 8.0 eq) in THF (5.5 mL) at r.t. was added a mixture of aldehyde **2.81** (100 mg, 427 µmol, 1.0 eq) and 1,1-diiodoethane (240 mg, 854 µmol, 2.0 eq) in THF (2.0 mL) and the resulting reaction mixture was stirred for 6.5 h. The reaction was quenched by addition of H_2O (60 mL). The layers were separated

and the aqueous layer was extracted with Et_2O (3 × 30 mL). The combined organic layers were dried over Na_2SO_4. After filtration and concentration *in vacuo*, the crude product was purified by flash column chromatography (pentane) on silica to afford alkene **2.75** (80.6 mg, 328 µmol, 77%) as a yellow oil in an inseparable 2.5:1 mixture of the (*E*)- and (*Z*)-isomer.

NMR shifts which could be clearly assigned to the major diastereomer are marked with an asterisk * and shifts which could be clearly assigned to the minor diastereomer are marked with a hash #. Due to the ratio of the two diastereomer the integrals in the ^{1}H-NMR differ from the expected values.

Data for 2.75: R_f: 0.80 (pentane); **^{1}H NMR (400 MHz, C_6D_6):** δ = 5.45 – 5.19 (m, 2H),*# 3.71 (s, 2H),*# 1.37 (d, J = 6.4 Hz, 2H),* 1.33 (d, J = 5.8 Hz, 1H),# 1.29 (s, 2H),* 1.26 (s, 1H)# ppm; **^{13}C NMR (100 MHz, C_6D_6):** δ = 215.2,* 215.1,# 126.4,# 126.0,* 122.6,* 121.5,# 84.4,# 82.8,* 77.7,* 75.3,# 66.0,# 63.5,* 17.8,* 13.9,# 12.3,* 12.3# ppm; **IR (ATR):** ν_{max} = 3021 (w), 2972 (w), 2921 (w), 2853 (w), 2031 (s), 1944 (s), 1444 (m), 1435 (m), 1374 (w); 1045 (w), 1026 (w), 955 (m), 931 (w), 827 (w), 733 (w) cm^{-1}; **HRMS (EI):** calc. for $C_{11}H_{10}Fe^{56}O_3$ [M]$^+$: 245.9979, found: 245.9990.

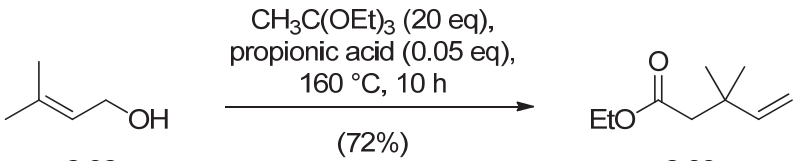

2.82 **2.83**

Ethyl 3,3-dimethylpent-4-enoate (2.83) A stirred solution of prenol (**2.82**, 19.5 mL, 191 mmol, 1.0 eq) and propionic acid (715 µL, 9.55 mmol, 0.05 eq) in triethylorthoacetate (700 mL, 3.82 mol, 20 eq) was refluxed for 10 h. The reaction mixture was poured into a solution of conc. H_2SO_4 (50 mL) in ice-water (800 mL) and the resulting mixture was stirred for 24 h at r.t. The layers were separated and the aqueous layer was extracted with Et_2O (3 × 500 mL). The combined organic layers were washed with sat. aq. Na_2CO_3 solution (5 × 400 mL), brine (500 mL) and dried over Na_2SO_4. After filtration and concentration *in vacuo*, the crude product was purified by distillation under reduced pressure (80 – 90 °C, 75 – 89 mbar) to afford ethyl ester **2.83** (21.5 g, 138 mmol, 72%) as a colorless liquid. Compound **2.83** has been reported in the literature.[130]

Data for 2.83: R_f: 0.71 (hexanes:EtOAc 7:1); **^{1}H NMR (400 MHz, $CDCl_3$):** δ = 5.89 (dd, J = 17.4, 10.7 Hz, 1H), 5.01 – 4.90 (m, 2H), 4.10 (q, J = 7.1 Hz, 2H), 2.28 (s, 2H), 1.24 (t, J = 7.1 Hz, 3H), 1.13 (s, 6H) ppm; **^{13}C NMR (100 MHz, $CDCl_3$):** δ = 171.9, 147.0, 110.9, 60.2, 47.0, 36.3, 27.1, 14.5 ppm; **IR (ATR):** ν_{max} = 3086 (w), 2966 (w), 2932 (w), 2873 (w),

1731 (s), 1641 (w), 1465 (w), 1447 (w), 1416 (w), 1367 (m), 1325 (w), 1236 (m), 1207 (m), 1126 (m), 1096 (w), 1033 (w), 999 (w), 913 (m), 845 (w), 792 (w), 715 (w), 678 (w) cm^{-1}; **HRMS (EI):** calc. for $C_9H_{16}O_2$ $[M]^+$: 156.1145, found: 156.1150.

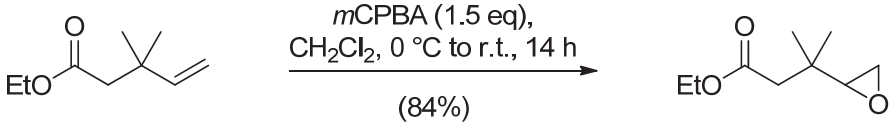

2.83 **2.85**

Epoxide 2.85 To a stirred solution of alkene **2.83** (12.5 g, 80.0 mmol, 1.0 eq) in CH_2Cl_2 (500 mL) at 0 °C was added carefully *m*CPBA (77% purity, 26.9 g, 120 mmol, 1.5 eq) and the resulting reaction mixture was stirred at r.t. for 14 h. The reaction was quenched by addition of sat. aq. $NaHCO_3$ solution (300 mL) and sat. aq. $Na_2S_2O_3$ solution (300 mL). The layers were separated and the aqueous layer was extracted with CH_2Cl_2 (3 × 300 mL). The combined organic layers were dried over Na_2SO_4. After filtration and concentration *in vacuo*, the crude product was purified by flash column chromatography (pentane:Et_2O 7:1) on silica to afford epoxide **2.85** (11.6 g, 67.4 mmol, 84%) as a colourless liquid.

Data for 2.85: R_f: 0.51 (hexanes:EtOAc 6:1); **^{1}H NMR (400 MHz, $CDCl_3$):** δ = 4.13 (q, J = 7.1 Hz, 2H), 2.94 – 2.89 (m, 1H), 2.68 (t, J = 4.3 Hz, 1H), 2.64 (dd, J = 4.4, 3.0 Hz, 1H), 2.30 (q, J = 13.7 Hz, 2H), 1.26 (t, J = 7.1 Hz, 3H), 1.02 (s, 3H), 0.99 (s, 3H) ppm; **^{13}C NMR (100 MHz, $CDCl_3$):** δ = 171.6, 60.3, 58.8, 44.4, 44.2, 33.5, 23.8, 22.2, 14.3 ppm; **IR (ATR):** ν_{max} = 2960 (w), 2935 (w), 2855 (w), 1730 (s), 1704 (m), 1681 (w), 1589 (w), 1474 (m), 1440 (w), 1407 (w), 1382 (w), 1367 (m), 1330 (w), 1258 (m), 1233 (m), 1174 (m), 1166 (m), 1114 (s), 1037 (s), 957 (m), 912 (m), 832 (s), 810 (m), 794 (m), 774 (m), 688 (w), 672 (w) cm^{-1}; **HRMS (EI):** calc. for $C_9H_{17}O_3$ $[M+H]^+$: 173.1172, found: 173.1165.

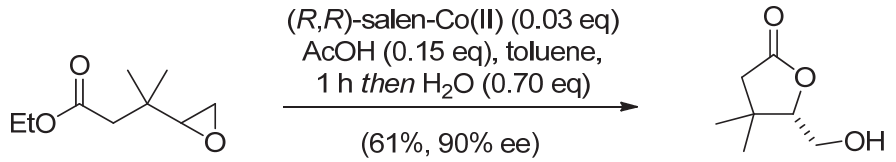

2.85 **2.84**

Lactone 2.84 To a stirred solution of (*R*,*R*)-salen-Co(II) (525 mg, 870 µmol, 0.03 eq) in toluene (20 mL) at r.t. was added AcOH (249 µL, 4.35 mmol, 0.15 eq) and the resulting reaction mixture was stirred open to air for 1 h. The solvent was evaporated and epoxide **2.85** (5.00 g, 29.0 mmol, 1.0 eq) was added to the reaction mixture followed by cooling to 0 °C. H_2O (365 µL, 20.3 mmol, 0.70 eq) was added and the reaction mixture was stirred at

r.t. for 10.5 h. After cooling to −20 °C, TFA (4 mL) was added and the resulting reaction mixture was allowed to warm up to −5 °C over 15 min. The reaction was quenched by addition of benzene (100 mL). After concentration *in vacuo*, the crude product was purified by flash column chromatography (hexanes:EtOAc 2:1) on silica. The obtained material was dissolved in CH_2Cl_2 (150 mL) and stirred with powdered activated charcoal (50 g) overnight to afford lactone **2.84** (2.54 g, 17.6 mmol, 61%) as a white solid. A crystal, suitable for single crystal X-ray diffraction analysis, was obtained by crystallization from Et_2O.

Data for 2.84: R_f: 0.25 (hexanes:EtOAc 1:1); **^{1}H NMR (400 MHz, $CDCl_3$):** δ = 4.18 (t, J = 4.6 Hz, 1H), 3.82 (d, J = 5.6 Hz, 2H), 2.48 (d, J = 17.0 Hz, 1H), 2.36 (d, J = 17.0 Hz, 1H), 1.76 (t, J = 6.2 Hz, 1H), 1.23 (s, 3H), 1.13 (s, 3H) ppm; **^{13}C NMR (100 MHz, $CDCl_3$):** δ = 176.3, 88.6, 61.9, 44.3, 38.3, 27.3, 21.9 ppm; **IR (ATR):** ν_{max} = 3433 (m), 2968 (w), 2933 (w), 2880(w), 1774 (m), 1730 (s); 1467 (w), 1416 (m), 1391 (w), 1368 (m), 1290 (m), 1263 (m), 1238 (m), 1200 (m), 1151 (m), 1130 (m), 1096 (m), 1041 (s), 1016 (s), 983 (s), 940 (s), 905 (m), 830 (m), 674 (m) cm^{-1}; **melting point:** 65.3 – 68.7 °C **HRMS (EI):** calc. for $C_7H_{12}O_3$ $[M]^+$: 144.0781, found: 144.0837; **optical rotation:** $[\alpha]_D^{21}$ = +49.4° (c = 1.00, MeOH).

The *ee* value of the reaction was determined by formation of the corresponding Mosher ester:

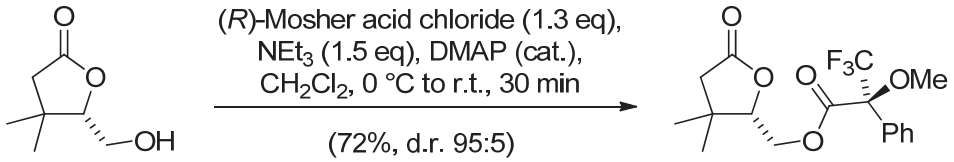

2.84 **S5**

Mosher ester S5 To a stirred solution of alcohol **2.84** (7.5 mg, 52.0 µmol, 1.0 eq), NEt_3 (10.9 µL, 78.0 µmol, 1.5 eq) and DMAP (cat.) in CH_2Cl_2 (1.0 mL) at 0 °C was added (*R*)-(−)-α-methoxy-α-(trifluoromethyl)phenylacetyl chloride (12.7 µL, 67.6 µmol, 1.3 eq) and the resulting reaction mixture was stirred at r.t. for 30 min. The reaction was quenched by addition of sat. aq. $NaHCO_3$ (5 mL). The layers were separated and the aqueous layer was extracted with Et_2O (5 mL). The organic layer was dried over Na_2SO_4. After filtration and concentration *in vacuo*, the crude product was purified by flash column chromatography (pentane:acetone 9:1) on silica to afford ester **S5** (13.4 mg, 37.2 µmol, 72%) as a colourless liquid in a 95:5 diastereomeric mixture.

For clarity just the ^{1}H-NMR and ^{13}C-shifts of the major diastereomer are reported.

Data for S5: R_f: 0.66 (hexanes:acetone 3:2); **^{1}H NMR (400 MHz, $CDCl_3$):** δ = 7.60 – 7.47 (m, 2H), 7.42 (d, *J* = 6.3 Hz, 3H), 4.58 – 4.39 (m, 2H), 4.36 – 4.25 (m, 1H), 3.53 (s, 3H), 2.34 (s, 2H), 1.20 (s, 3H), 1.07 (s, 3H) ppm; **^{13}C NMR (100 MHz, $CDCl_3$):** δ = 175.2, 166.5, 131.8, 123.0, 128.7, 127.4, 123.3 (q, *J* = 288 Hz), 84.8 (q, *J* = 27.9 Hz), 84.4, 64.4, 55.7, 43.8, 38.5, 26.7, 21.6 ppm; **^{19}F NMR (375 MHz, $CDCl_3$):** δ = −71.5 (s, major), −71.6 (s, minor) ppm; **IR (ATR):** ν_{max} = 2965 (w), 2885 (w), 2851 (w), 1786 (m), 1750 (m); 1452 (w), 1422 (m), 1271 (m), 1229 (m), 1158 (s), 1120 (m), 1082 (m), 1067 (m), 1021 (m), 1001 (m), 940 (m), 766 (m), 720 (m), 698 (m) cm^{-1}; **HRMS (ESI):** calc. for $C_{17}H_{23}O_5NF_3$ $[M+NH_4]^+$: 378.1523, found: 378.1520; **optical rotation:** $[\alpha]_D^{21}$ = +10.8° (c = 0.50, $CHCl_3$).

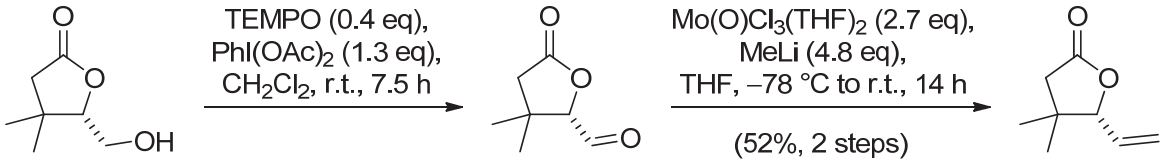

2.84 **2.88** **2.73**

Alkene 2.73 To a stirred solution of alcohol **2.84** (250 mg, 1.73 mmol, 1.0 eq) in CH_2Cl_2 (8.0 mL) at r.t. was added $PhI(OAc)_2$ (725 mg, 2.25 mmol, 1.3 eq) and TEMPO (108 mg, 692 µmol, 0.4 eq) and the resulting reaction mixture was stirred at r.t. for 7.5 h. The reaction was quenched by addition of sat. aq. $Na_2S_2O_3$ (30 mL). The layers were separated and the aqueous layer was extracted with CH_2Cl_2 (3 × 30 mL). The combined organic layers were dried over Na_2SO_4. After filtration and careful concentration *in vacuo* (30 °C, 650 mbar), crude aldehyde **2.88** was obtained and used in the next step without further purification.

To a stirred solution of $Mo(O)Cl_3(THF)_2$[128a] (1.68 g, 4.67 mmol, 2.7 eq) in THF (8.0 mL) at −78 °C was added MeLi (1.6 M in Et_2O, 5.19 mL, 8.30 mmol, 4.8 eq) and the resulting reaction mixture was stirred for 1 h. Crude aldehyde **2.88** in THF (8.0 mL) was added dropwise and the reaction mixture was allowed to warm up to r.t. overnight. The reaction was quenched by addition of H_2O (40 mL). The layers were separated and the aqueous layer was extracted with Et_2O (4 × 20 mL). The combined organic layers were washed with brine (40 mL) and dried over Na_2SO_4. After filtration and concentration *in vacuo*, the crude product was purified by flash column chromatography (pentane:Et_2O 6:1) on silica to afford alkene **2.73** (125 mg, 891 µmol, 52%) as a colourless liquid.

Data for 2.73: R_f: 0.47 (hexanes:EtOAc 4:1); **^{1}H NMR (400 MHz, $CDCl_3$):** δ = 5.81 (ddd, *J* = 17.3, 10.6, 6.7 Hz, 1H), 5.45 – 5.30 (m, 2H), 4.50 (d, *J* = 6.7 Hz, 1H), 2.42 (d, *J* = 16.9 Hz, 1H), 2.35 (d, *J* = 16.8 Hz, 1H), 1.18 (s, 3H), 1.01 (s, 3H) ppm; **^{13}C NMR (100 MHz, $CDCl_3$):** δ = 176.1, 131.6, 119.2, 89.1, 44.0, 40.2, 25.3, 22.2 ppm; **IR (ATR):**

ν_{max} = 2964 (w), 2933 (w), 2876 (w), 1776 (s), 1466 (w), 1420 (w), 1392 (w), 1374 (w), 1322 (w), 1287 (m), 1230 (m), 1198 (m), 1162 (m), 1112 (m), 1031 (m), 989 (s), 948 (m), 927 (s), 890 (m), 800 (w), 715 (w), 592 (w) cm^{-1}; **HRMS (EI):** calc. for $C_8H_{12}O_2$ $[M]^+$: 140.0832, found: 140.0837; **optical rotation:** $[\alpha]_D^{22}$ = +55.6° (c = 1.00, $CHCl_3$).

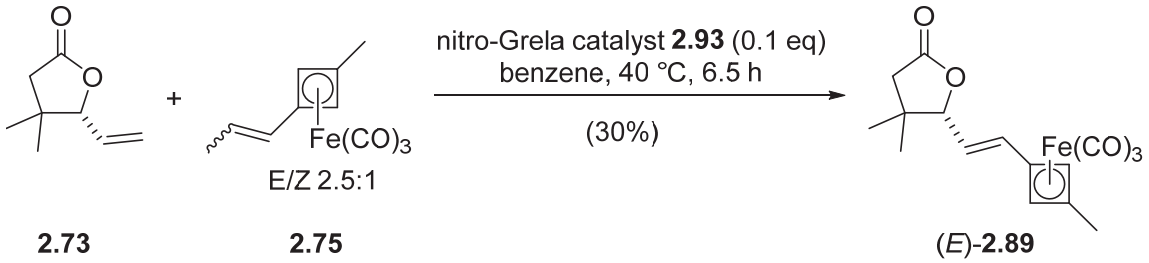

2.73 **2.75** (*E*)-**2.89**

Alkene (*E*)-2.89 To a stirred solution of lactone **2.73** (36.4 mg, 260 µmol, 4.0 eq) and iron tricarbonyl complex **2.75** (16.0 mg, 65.0 µmol, 1.0 eq) in benzene (0.5 mL, degassed by sparging with argon for 20 min) at r.t. was added nitro-Grela catalyst (**2.93**, 2.2 mg, 3.25 µmol, 0.05 eq) and the resulting reaction mixture was stirred for 1.5 h at 40 °C followed by addition of catalyst **2.93** (2.2 mg, 3.25 µmol, 0.05 eq). After 4 h the solvent was evaporated and the crude product was purified by flash column chromatography (pentane:Et_2O 4:1) on silica to afford alkene (*E*)-**2.89** (6.7 mg, 19.5 µmol, 30%) as a yellow oil.

Data for (*E*)-2.89: R_f: 0.23 (hexanes:EtOAc 4:1); **^{1}H NMR (400 MHz, C_6D_6):** δ = 5.49 (d, *J* = 15.7 Hz, 1H), 5.27 (dd, *J* = 15.7, 7.2 Hz, 1H), 3.82 (d, *J* = 7.2 Hz, 1H), 3.68 (d, *J* = 9.2 Hz, 1H), 3.63 (d, *J* = 9.2 Hz, 1H), 1.86 (d, *J* = 16.6 Hz, 1H), 1.74 (d, *J* = 16.6 Hz, 1H), 1.25 (s, 3H), 0.57 (s, 3H), 0.54 (s, 3H) ppm; **^{13}C NMR (100 MHz, C_6D_6):** δ = 214.9, 174.3, 126.5, 123.0, 87.7, 85.3, 73.9, 65.2, 63.7, 43.8, 40.0, 24.5, 21.6, 12.5 ppm; **IR (ATR):** ν_{max} = 3099 (w), 2964 (w), 2928 (w), 2875 (w), 2031 (s), 1941 (s), 1774 (s), 1646 (m), 1465 (m), 1451 (m), 1438 (m), 1373 (m); 1284 (m), 1228 (m), 1195 (m), 1158 (m), 1116 (m), 1022 (m), 993 (m), 961 (s), 928 (m), 837 (m) cm^{-1}; **HRMS (EI):** calc. for $C_{16}H_{16}Fe^{56}O_5$ $[M]^+$: 344.0342, found: 344.0342; **optical rotation:** $[\alpha]_D^{21}$ = −65.7° (c = 0.35, CH_2Cl_2).

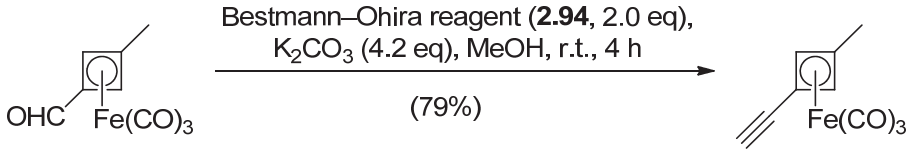

2.81 **2.95**

Alkyne 2.95 To a stirred solution of aldehyde **2.81** (340 mg, 1.45 mmol, 1.0 eq) in MeOH (11.0 mL) at 0 °C was added K_2CO_3 (422 mg, 3.05 mmol, 2.1 eq) and Bestmann-Ohira reagent (**2.94**, 279 mg, 1.45 µmol, 1.0 eq) in MeOH (2.0 mL) and the resulting reaction mixture was stirred at r.t. for 1 h. Additional K_2CO_3 (422 mg, 3.05 mmol, 2.1 eq) and Bestmann−Ohira reagent (**2.94**, 279 mg, 1.45 µmol,1.0 eq) was added and the reaction was stirred for 3 h. The reaction was quenched by addition of H_2O (30 mL) and sat. aq. $NaHCO_3$ solution (30 mL). The layers were separated and the aqueous layer was extracted with Et_2O (3 × 30 mL). The combined organic layers were dried over Na_2SO_4. After filtration and concentration *in vacuo*, the crude product was purified by flash column chromatography (pentane) on silica to afford alkyne **2.95** (265 mg, 1.15 µmol, 79%) as a yellow oil.

Data for 2.95: R_f: 0.71 (hexanes:EtOAc 4:1); **^{1}H NMR (400 MHz, C_6D_6):** δ = 3.66 (s, 2H), 2.42 (s, 1H), 1.00 (s, 3H) ppm; **^{13}C NMR (100 MHz, C_6D_6):** δ = 214.0, 87.3, 79.1, 77.0, 68.0, 54.0, 12.1 ppm; **IR (ATR):** ν_{max} = 3305 (m), 2041 (s), 1951 (s), 1447 (w), 1405 (w), 1376 (w), 1044 (w), 1027 (w), 826 (w), 724 (w), 659 (w) cm^{-1}; **HRMS (EI):** calc. for $C_{10}H_6Fe^{56}O_3$ $[M]^+$: 229.9661, found: 229.9653.

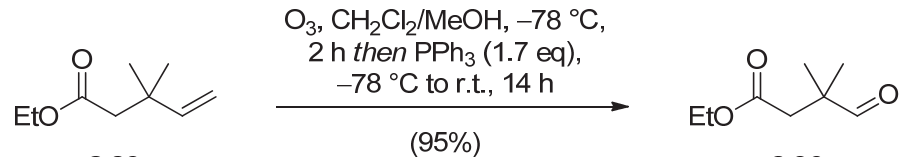

2.83 **2.96**

Ethyl 3,3-dimethyl-4-oxobutanoate (2.96) Ozone was bubbled through a stirred solution of ester **2.83** (21.5 g, 138 mmol, 1.0 eq) in CH_2Cl_2/MeOH (500 mL, 4:1) at –78 °C. After a slightly blue color persisted (2 h), N_2 was bubbled through the reaction mixture for 15 min followed by addition of PPh_3 (61.3 g, 234 mmol, 1.7 eq). The resulting mixture was stirred at r.t. for 14 h. After concentration *in vacuo*, the crude product was purified by flash column chromatography (pentane:Et_2O 9:1) on silica to afford aldehyde **2.96** (20.7 g, 131 mmol, 95%) as a colorless liquid. **2.96** was stored as solution in THF (72 mL) at –20 °C. Compound **2.96** has been reported in the literature.[130,160]

Data for 2.96: R_f: 0.77 (hexanes:EtOAc 4:1); **^{1}H NMR (400 MHz, C_6D_6):** δ = 9.33 (s, 1H), 3.84 (q, J = 7.1 Hz, 2H), 2.17 (s, 2H), 0.89 (t, J = 7.1 Hz, 3H), 0.82 (s, 6H) ppm; **^{13}C NMR (100 MHz, C_6D_6):** δ = 202.9, 170.7, 60.4, 44.0, 42.0, 21.7, 14.2 ppm; **IR (ATR):** ν_{max} = 2980 (w), 2938 (w), 2877 (w), 2815 (w), 2713 (w), 1727 (s), 1472 (w), 1448 (w), 1397 (w), 1370 (m), 1342 (m), 1207 (m), 1135 (m), 1097 (m), 1032 (m), 948 (w), 922 (w), 888 (m), 860 (w), 808 (w), 733 (w) cm^{-1}; **HRMS (EI):** calc. for $C_8H_{14}O_3$ [M]$^+$: 158.0937, found: 158.0940.

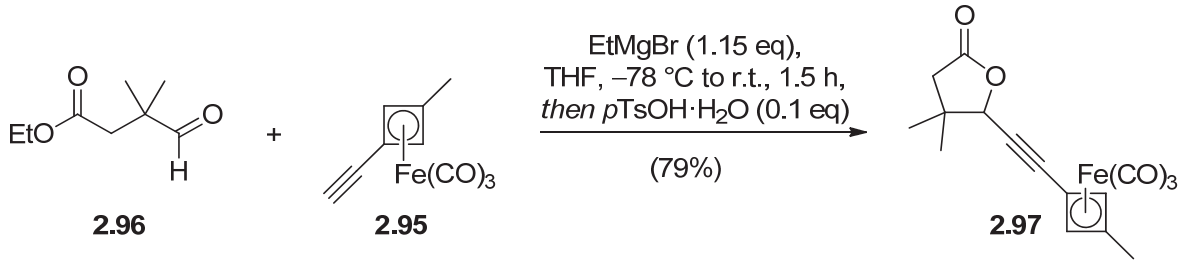

2.96 **2.95** **2.97**

Lactone 2.97 To a stirred solution of alkyne **2.95** (250 mg, 1.09 mmol, 1.0 eq) in THF (7 mL) at −78 °C was added EtMgBr (1.0 M in MTBE, 1.25 mL, 1.25 mmol, 1.15 eq) and the resulting reaction mixture was stirred for 2.5 h at 0 °C. The reaction was cooled to −78 °C and aldehyde **2.96** (0.43 M in THF, 4.57 mL, 1.96 mmol, 1.8 eq) was added dropwise. The reaction mixture was allowed to warm up to r.t. over 1.5 h. The reaction was quenched by addition of H_2O (40 mL) and sat. aq. NH_4Cl solution (20 mL). The layers were separated and the aqueous layer was extracted with Et_2O (3 × 30 mL). The combined organic layers were dried over Na_2SO_4. After filtration and concentration *in vacuo*, the crude product was dissolved in toluene (10 mL) and *p*TsOH·H_2O (20.7 mg, 109 µmol, 0.1 eq) was added and the resulting reaction mixture was stirred for 30 min at r.t. The reaction was quenched by addition of H_2O (30 mL) and sat. aq. $NaHCO_3$ solution (30 mL). The layers were separated and the aqueous layer was extracted with Et_2O (3 × 20 mL). The combined organic layers were dried over Na_2SO_4. After filtration and concentration *in vacuo*, the crude product was purified by flash column chromatography (pentane:Et_2O 5:1→2:1) on silica to afford lactone **2.97** (293 mg, 857 µmol, 79%) as a yellow solid.

Data for 2.97: R_f: 0.43 (hexanes:EtOAc 4:1); **^{1}H NMR (400 MHz, C_6D_6):** δ = 4.20 (s, 1H), 3.70 (s, 2H), 1.88 (d, J = 16.7 Hz, 1H), 1.58 (d, J = 16.7 Hz, 1H), 1.04 (s, 3H), 0.84 (s, 3H), 0.55 (s, 3H) ppm; **^{13}C NMR (100 MHz, C_6D_6):** δ = 213.9, 173.7, 88.1, 84.3, 83.0, 78.4, 68.2, 68.1, 53.1, 42.5, 40.2, 24.5, 22.9, 12.2 ppm; **IR (ATR):** ν_{max} = 2966 (w), 2931 (w), 2877 (w), 2224 (w), 2040 (s), 1952 (s), 1781 (s), (m), 1465 (m), 1434 (m), 1375 (m), 1340 (w); 1284 (m), 1230 (m), 1195 (m), 1146 (m), 1135 (m), 1112 (m), 1052 (m), 1025 (m), 988 (m),

966 (m), 952 (m), 925 (m), 888 (m), 857 (m), 844 (m), 727 (m), 658 (w) cm^{-1}; **melting point:** 82.0 – 83.8 °C; **HRMS (EI):** calc. for $C_{16}H_{14}Fe^{56}O_5$ $[M]^+$: 342.0185, found: 342.0179.

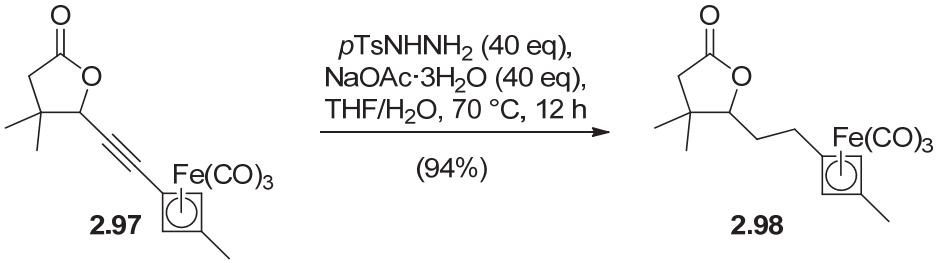

Iron tricarbonyl complex 2.98 To a stirred solution of alkyne **2.97** (250 mg, 731 µmol, 1.0 eq) in THF/H_2O (1:1, 15 mL) at r.t. was added *p*-toluenesulfonyl hydrazide (5.43 g, 29.2 mmol, 40 eq) and $NaOAc·3H_2O$ (3.97 g, 29.2 mmol, 40 eq) and the resulting reaction mixture was stirred for 12 h at 70 °C. The reaction was quenched by addition of H_2O (120 mL) and sat. aq. $NaHCO_3$ solution (120 mL). The layers were separated and the aqueous layer was extracted with Et_2O (3 × 50 mL) and EtOAc (50 mL). The combined organic layers were dried over Na_2SO_4. After filtration and concentration *in vacuo*, the crude product was purified by flash column chromatography (pentane:Et_2O 3:1) on silica to afford iron tricarbonyl complex **2.98** (238 mg, 688 µmol, 94%) as a yellow solid.

Data for 2.98: R_f: 0.43 (hexanes:EtOAc 3:1); **^{1}H NMR (400 MHz, C_6D_6):** δ = 3.56 (d, J = 9.3 Hz, 1H), 3.51 (d, J = 9.3 Hz, 1H), 3.37 (dd, J = 10.6, 1.6 Hz, 1H), 2.05 (ddd, J = 15.1, 10.1, 4.9 Hz, 1H), 1.82 (d, J = 16.7 Hz, 1H), 1.77 (d, J = 13.9 Hz, 1H), 1.71 (td, J = 9.7, 4.9 Hz, 1H), 1.32 (s, 3H), 1.31 – 1.18 (m, 1H), 1.16 – 1.05 (m, 1H), 0.51 (s, 3H), 0.49 (s, 3H) ppm; **^{13}C NMR (100 MHz, C_6D_6):** δ = 215.9, 174.3, 86.9, 82.3, 81.9, 65.9, 65.7, 44.2, 38.5, 29.7, 24.7, 24.6, 20.9, 12.6 ppm; **IR (ATR):** ν_{max} = 2969 (w), 2919 (w), 2874 (w), 2033 (s), 1947 (s), 1777 (m), 1462 (w), 1451 (m), 1420 (w), 1391 (w), 1372 (w), 1289 (w), 1227 (w), 1197 (w), 1145 (w), 947 (w), 928 (w), 614 (m), 589 (m) cm^{-1}; **melting point:** 59.7 – 61.2 °C; **HRMS (ESI):** calc. for $C_{16}H_{22}Fe^{56}NO_5$ $[M+NH_4]^+$: 364.0842, found: 364.0843.

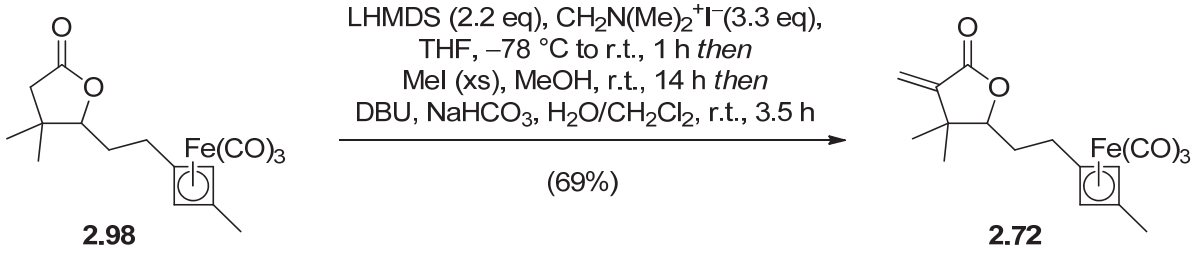

2.98 **2.72**

Enone 2.72 To a stirred solution of lactone **2.98** (140 mg, 404 µmol, 1.0 eq) in THF (5 mL) at –78 °C was added LHMDS (1.0 M in THF, 888 µL, 888 µmol, 2.2 eq) and the resulting mixture was allowed to warm up to –45 °C within 1 h. Eschenmoser's salt (247 mg, 1.33 mmol, 3.3 eq) was added to the reaction mixture in one portion at –78 °C and the resulting reaction mixture was allowed to warm up to r.t. over 1 h. The solvent was evaporated and the crude material was dissolved in MeOH (3 mL). Methyliodide (3 mL) was added and the reaction was stirred at r.t. overnight. The solvent was evaporated and the crude material was dissolved in CH_2Cl_2 (2 mL). Aq. $NaHCO_3$ solution (5 wt%, 1 mL) and DBU (0.5 mL, 3.35 mmol, 8.3 eq) were added and the resulting reaction mixture was stirred at r.t. for 3.5 h followed by addition of H_2O (5 mL) and sat. aq. NH_4Cl solution (5 mL). The layers were separated and the aqueous layer was extracted with CH_2Cl_2 (4 × 5 mL). The combined organic layers were dried over Na_2SO_4. After filtration and concentration *in vacuo*, the crude product was purified by flash column chromatography (pentane:Et_2O 4:1) on silica to afford enone **2.72** (99.9 mg, 279 µmol, 69%) as a slightly yellow solid. A crystal, suitable for single crystal X-ray diffraction analysis, was obtained by crystallization from acetone.

Data for 2.72: $\mathbf{R_f}$**:** 0.60 (hexanes:EtOAc 3:1); **^{1}H NMR (400 MHz, C_6D_6):** δ = 6.05 (s, 1H), 4.85 (s, 1H), 3.53 – 3.41 (m, 3H), 2.04 (ddd, *J* = 15.1, 9.7, 5.0 Hz, 1H), 1.70 (ddd, *J* = 15.6, 9.3, 6.6 Hz, 1H), 1.31 (s, 3H), 1.26 – 1.09 (m, 2H), 0.67 (s, 3H), 0.60 (s, 3H) ppm; **^{13}C NMR (100 MHz, C_6D_6):** δ = 215.8, 169.0, 146.4, 118.5, 85.5, 82.1, 82.0, 65.9, 65.7, 41.6, 30.6, 25.3, 24.1, 22.2, 12.6 ppm; **IR (ATR):** ν_{max} = 2967 (w), 2927 (w), 2869 (w), 2031 (s), 1943 (s), 1765 (m), 1465 (w), 1445 (m), 1410 (w), 1371 (w), 1348 (w), 1296 (m), 1194 (m), 1127 (w), 1106 (w), 1023 (w), 940 (w), 815 (w), 612 (m), 589 (m) cm^{-1}; **melting point:** 43.2 – 45.5 °C; **HRMS (ESI):** calc. for $C_{17}H_{22}Fe^{56}NO_5$ $[M+NH_4]^+$: 376.0842, found: 376.0844.

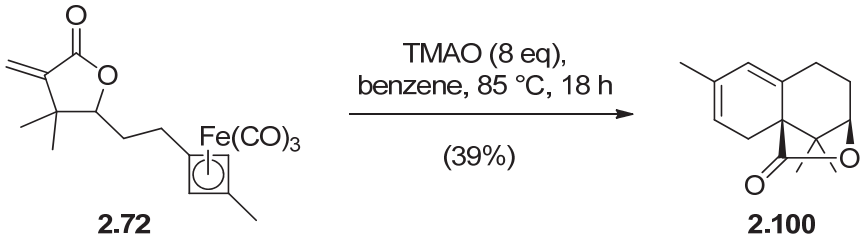

Cyclohexadiene 2.100 To a stirred solution of enone **2.72** (5.0 mg, 14.0 µmol, 1.0 eq) in benzene (14 mL) at r.t. was added trimethylamine *N*-oxide (4.2 mg, 55.9 µmol, 4.0 eq) and the resulting mixture was heated to 85 °C for 5.5 h. Additional trimethylamine *N*-oxide (4.2 mg, 55. mmol, 4.0 eq) was added and the resulting reaction mixture was heated over 12.5 h. The reaction was quenched by addition of sat. aq $NaHCO_3$ solution (14 mL) and sat. aq $Na_2S_2O_3$ solution (7 mL). The layers were separated and the aqueous layer was extracted with CH_2Cl_2 (3 × 30 mL). The combined organic layers were dried over Na_2SO_4. After filtration and concentration *in vacuo*, the crude product was purified by flash column chromatography (pentane:Et_2O 5:1) on silica to afford cyclohexadiene **2.100** (1.2 mg, 5.50 µmol, 39%) as a colourless oil.

Data for 2.100: R_f: 0.57 (hexanes:EtOAc 3:1); **^{1}H NMR (400 MHz, C_6D_6):** δ = 5.39 (s, 1H), 5.10 (s, 1H), 3.62 (d, *J* = 4.2 Hz, 1H), 3.20 (d, *J* = 19.5 Hz, 1H), 2.44 – 2.32 (m, 1H), 2.05 (dd, *J* = 19.2, 5.7 Hz, 1H), 1.76 (dd, *J* = 15.0, 6.9 Hz, 1H), 1.53 (s, 3H), 1.49 (dd, *J* = 8.0, 4.7 Hz, 1H), 1.28 (td, *J* = 13.4, 12.6, 7.0 Hz, 1H), 0.68 (s, 3H), 0.66 (s, 3H) ppm; **^{13}C NMR (100 MHz, C_6D_6):** δ = 178.3, 132.2, 128.0,* 124.0, 117.9, 83.9, 54.1, 46.3, 27.6, 25.9, 23.8, 22.6, 21.3, 18.0 ppm; **IR (ATR):** ν_{max} = 3030 (w), 2948 (w), 2876 (w), 2853 (w), 1776 (s), 1761 (s), 1672 (w), 1612 (w), 1467 (w), 1452 (w), 1492 (w), 1372 (w), 1339 (m), 1290 (w), 1264 (w), 1180 (w), 1167 (w), 1142 (m), 1100 (m), 1036 (m), 1011 (w), 981 (m), 964 (m), 941 (w), 922 (m), 773 (w) cm^{-1}; **HRMS (EI):** calc. for $C_{14}H_{18}O_2$ $[M]^+$: 218.1301, found:218.1306.

* One alkene ^{13}C-shift overlapped with the solvent peak, but could be extracted from the HMBC data showing corresponding correlations at 128.0 ppm.

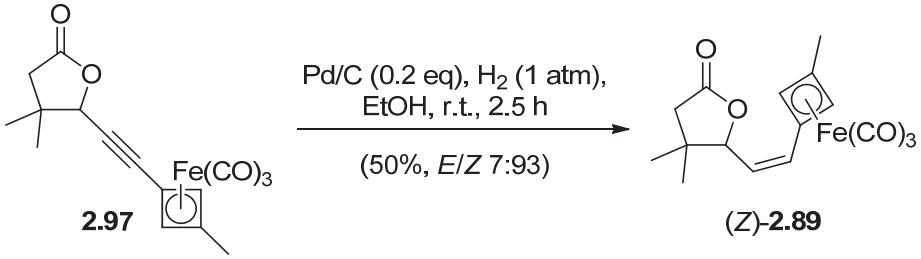

Alkene (*Z*)-2.89 To a stirred solution of alkyne **2.97** (43.3 mg, 127 µmol, 1.0 eq) in EtOH (4 mL) at r.t. was added Pd/C (10% Pd on activated charcoal, 21.7 mg, 20.5 µmol, 0.2 eq)

and the reaction vessel was backfilled three times with H_2 followed by sparging with H_2 for 1 min. After 2.5 h the reaction was filtered over Celite (EtOAc) and the crude product was purified by flash column chromatography (pentane:Et_2O 5:1) on silica to afford alkene (*Z*)-**2.89** (21.8 mg, 63.3 µmol, 50%) as a yellow oil.

For clarity just the ^{1}H-NMR and ^{13}C-shifts of the major diastereomer are reported.

Data for (*Z*)-2.89: R_f: 0.38 (hexanes:EtOAc 4:1); **^{1}H NMR (400 MHz, C_6D_6):** δ = 5.29 (d, *J* = 11.4 Hz, 1H), 5.00 (dd, *J* = 10.7, 9.7 Hz, 1H), 4.31 (d, *J* = 9.4 Hz, 1H), 3.79 (d, *J* = 9.2 Hz, 1H), 3.61 (d, *J* = 9.2 Hz, 1H), 1.87 (d, *J* = 16.9 Hz, 1H), 1.82 (d, *J* = 16.5 Hz, 1H), 1.24 (s, 3H), 0.64 (s, 3H), 0.55 (s, 3H) ppm; **^{13}C NMR (100 MHz, C_6D_6):** δ = 214.7, 174.5, 127.7, 123.7, 86.0, 83.1, 71.8, 66.8, 66.7, 43.9, 39.8, 25.4, 21.7, 12.6 ppm; **IR (ATR):** ν_{max} = 2965 (w), 2936 (w), 2877 (w), 2038 (s), 1956 (s), 1782 (s), 1468 (w), 1445 (w), 1374 (w), 1287 (w), 1232 (w), 1198 (w), 1151 (w), 1116 (w), 1024 (w), 995 (w), 969 (w), 928 (w) cm^{-1}; **HRMS (EI):** calc. for $C_{16}H_{16}Fe^{56}O_5$ [*M*]$^+$: 344.0342, found: 344.0339.

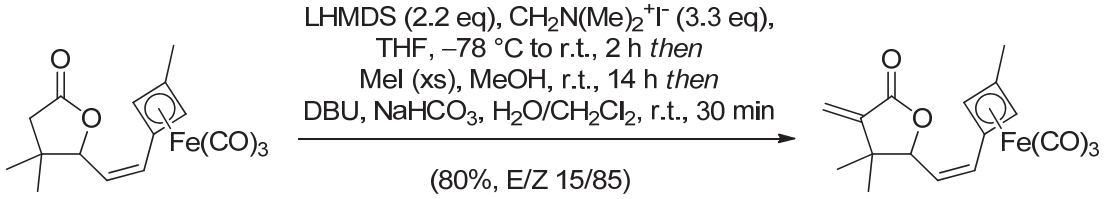

(*Z*)-**2.89** **2.106**

Enone 2.106 To a stirred solution of alkene (*Z*)-**2.89** (20.0 mg, 58.1 µmol, 1.0 eq) in THF (1 mL) at –78 °C was added LHMDS (1.0 M in THF, 128 µL, 128 µmol, 2.2 eq) and the resulting mixture was allowed to warm up to –45 °C within 1 h. Eschenmoser's salt (35.5 mg, 192 µmol, 3.3 eq) was added to the reaction mixture in one portion at –78 °C and the resulting reaction mixture was allowed to warm up to r.t. over 2 h. The solvent was evaporated and the crude material was dissolved in MeOH (1 mL). Methyliodide (0.5 mL) was added and the reaction was stirred at r.t. overnight. The solvent was evaporated and the crude material was dissolved in CH_2Cl_2 (1 mL). Aq. 5% $NaHCO_3$ solution (0.5 mL) and DBU (0.2 mL, 1.34 mmol, 23 eq) were added and the resulting reaction mixture was stirred at r.t. for 30 min followed by addition of aq. phosphate buffer (pH = 7.0, 15 ml). The layers were separated and the aqueous layer was extracted with CH_2Cl_2 (3 × 15 mL). The combined organic layers were dried over Na_2SO_4. After filtration and concentration *in vacuo*, the crude product was purified by flash column chromatography (pentane:Et_2O 3:1) on silica to afford enone **2.106** (16.6 mg, 46.6 µmol, 80%) as a slightly yellow oil.

For clarity just the ^{1}H-NMR shifts of the major diastereomer are reported. In the ^{13}C-data shifts of the minor isomer are marked by an asterisk *.

Data for 2.106: R_f: 0.53 (hexanes:EtOAc 4:1); **^{1}H NMR (400 MHz, C_6D_6):** δ = 6.09 (s, 1H), 5.28 (d, *J* = 11.3 Hz, 1H), 4.98 (t, *J* = 10.5 Hz, 1H), 4.88 (s, 1H), 4.39 (d, *J* = 9.7 Hz, 1H), 3.68 (d, *J* = 9.1 Hz, 1H), 3.55 (d, *J* = 9.1 Hz, 1H), 1.22 (s, 3H), 0.82 (s, 3H), 0.68 (s, 3H) ppm; **^{13}C NMR (100 MHz, C_6D_6):** δ = 214.9,* 214.7, 169.2, 169.1,* 146.1, 145.9,* 127.7,[#] 127.1,* 123.8, 123.2,* 118.8, 86.5,* 86.2, 85.4,* 81.7, 73.7,* 71.6, 66.8, 66.6, 65.4,* 63.6,* 42.9,* 42.6, 25.6, 24.8,* 23.3,* 23.1, 12.6, 12.5* ppm; **IR (ATR):** ν_{max} = 2968 (w), 2932 (w), 2869 (w), 2038 (s), 1957 (s), 1766 (s), 1465 (w), 1446 (w), 1407 (w), 1371 (w), 1295 (w), 1193 (w), 1169 (w), 1131 (w), 1111 (w), 985 (w), 814 (w) cm^{-1}; **HRMS (EI):** calc. for $C_{17}H_{16}Fe^{56}O_5$ [*M*]$^{+}$: 356.0342, found: 356.0344.

[#] One alkene ^{13}C-shift overlapped with the solvent peak, but could be extracted from the HMBC data showing corresponding correlations at 127.7 ppm.

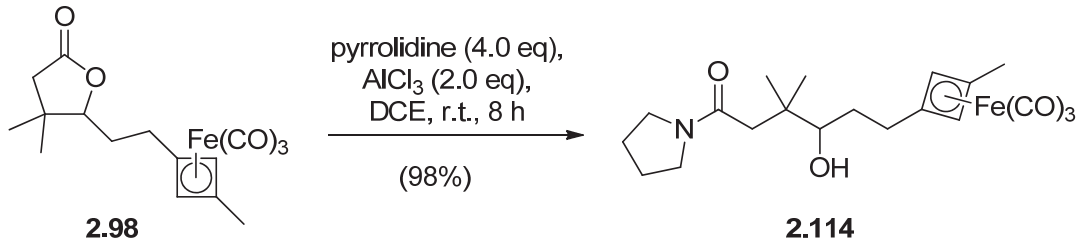

2.98 **2.114**

Amide 2.114 To a stirred suspension of $AlCl_3$ (26.9 mg, 202 µmol, 1.0 eq) in DCE (2 mL) at r.t. was added pyrrolidine (33.2 µL, 408 µmol, 4.0 eq) and the resulting mixture was stirred for 20 min. Lactone **2.98** (35.0 mg, 101 µmol, 1.0 eq) in DCE (2 mL) was added and the resulting reaction mixture was stirred for 8 h. The reaction was quenched by addition of H_2O (10 mL). The layers were separated and the aqueous layer was extracted with CH_2Cl_2 (3 × 30 mL). The combined organic layers were dried over Na_2SO_4. After filtration and concentration *in vacuo*, the crude product was purified by flash column chromatography (EtOAc) on silica to afford amide **2.114** (41.3 mg, 99.0 µmol, 98%) as a yellow oil.

Data for 2.114: R_f: 0.55 (EtOAc); **^{1}H NMR (400 MHz, C_6D_6):** δ = 5.84 (d, *J* = 6.5 Hz, 1H), 3.66 (d, *J* = 9.3 Hz, 1H), 3.63 (d, *J* = 9.3 Hz, 1H), 3.48 (ddd, *J* = 9.5, 6.7, 3.0 Hz, 1H), 3.24 (t, *J* = 6.4 Hz, 2H), 2.73 – 2.53 (m, 3H), 2.32 (d, *J* = 14.7 Hz, 1H), 2.15 – 2.02 (m, 1H), 1.89 (d, *J* = 14.7 Hz, 1H), 1.62 – 1.47 (m, 2H), 1.30 (s, 3H), 1.22 – 1.07 (m, 4H), 1.03 (s, 3H), 0.94 (s, 3H) ppm; **^{13}C NMR (100 MHz, C_6D_6):** δ = 216.4, 171.1, 85.5, 81.3, 77.0, 66.4, 66.3, 47.1, 46.0, 44.6, 38.9, 32.7, 26.0, 25.9, 25.3, 24.8, 24.2, 12.7 ppm; **IR (ATR):** ν_{max} = 3336 (br w), 2964 (w), 2928 (w), 2875 (w), 2031 (s), 1946 (s), 1612 (m), 1470 (w), 1447 (w), 1260 (w),

1076 (w), 1025 (w), 799 (w) cm^{-1}; **HRMS (EI):** calc. for $C_{19}H_{27}Fe^{56}NO_4$ $[M\text{-}CO]^+$: 389.1284, found: 389.1283.

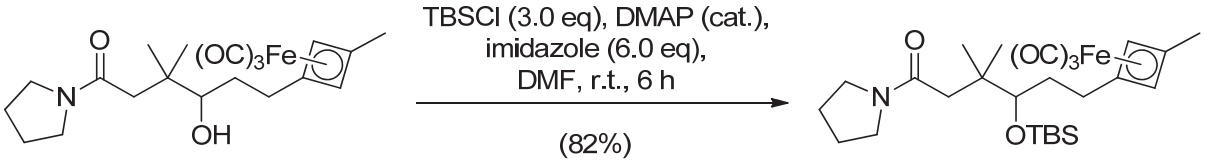

2.114 **2.115**

Protected amide 2.115 To a stirred solution of amide **2.114** (20.0 mg, 47.9 µmol, 1.0 eq) in DMF (1 mL) at r.t. was added TBSCl (21.7 mg, 144 µmol, 3.0 eq), imidazole (19.5 mg, 287 µmol, 6.0 eq) and DMAP (cat.) and the resulting mixture was stirred for 6 h. The reaction was quenched by addition of H_2O (10 mL). The layers were separated and the aqueous layer was extracted with Et_2O (3 × 10 mL). The combined organic layers were dried over Na_2SO_4. After filtration and concentration *in vacuo*, the crude product was purified by flash column chromatography (pentane:EtOAc 4:1) on silica to afford protected amide **2.115** (21.0 mg, 39.5 µmol, 82%) as a yellow oil.

Data for 2.115: R_f: 0.65 (hexanes:EtOAc 1:1); **^{1}H NMR (400 MHz, C_6D_6):** δ = 4.23 (dd, *J* = 7.0, 3.1 Hz, 1H), 3.78 (d, *J* = 9.3 Hz, 1H), 3.66 (d, *J* = 9.3 Hz, 1H), 3.38 (t, *J* = 6.7 Hz, 2H), 2.87 (t, *J* = 6.7 Hz, 2H), 2.30 (d, *J* = 15.5 Hz, 1H), 2.18 (ddd, *J* = 15.5, 10.7, 5.2 Hz, 1H), 2.05 (d, *J* = 15.7 Hz, 1H), 1.98 (td, *J* = 10.4, 5.3 Hz, 1H), 1.70 (tdd, *J* = 15.9, 7.6, 4.8 Hz, 1H), 1.50 (td, *J* = 15.6, 13.2, 5.9 Hz, 1H), 1.32 (s, 3H), 1.30 – 1.21 (m, 4H), 1.20 (s, 6H), 1.03 (s, 9H), 0.18 (s, 3H), 0.13 (s, 3H) ppm; **^{13}C NMR (100 MHz, C_6D_6):** δ = 216.1, 169.5, 84.0, 81.7, 77.5, 66.1, 65.9, 46.7, 45.7, 42.7, 39.2, 33.7, 26.5, 26.3, 25.3, 24.4, 24.4, 24.4, 18.7, 12.7, −3.4, −3.7 ppm; **IR (ATR):** ν_{max} = 2954 (w), 2929 (w), 2857 (w), 2031 (s), 1943 (s), 1638 (m), 1423 (m), 1383 (w), 1361 (w), 1341 (w), 1252 (w), 1192 (w), 1168 (w), 1081 (m), 1046 (w), 1005 (w), 834 (m), 773 (w), 719 (m), 664 (w) cm^{-1}; **HRMS (EI):** calc. for $C_{26}H_{41}Fe^{56}NSiO_5$ $[M]^+$: 531.2098, found:531.2095.

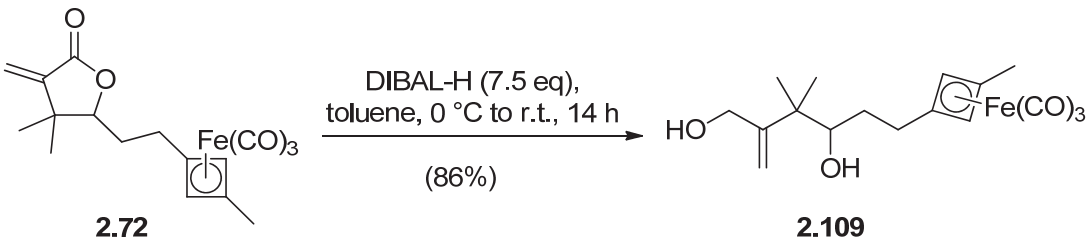

2.72 **2.109**

Diol 2.109 To a stirred solution of lactone **2.72** (30.0 mg, 83.8 µmol, 1.0 eq) in toluene (1 mL) at 0 °C was added DIBAL-H (1.0 M in toluene, 629 µL, 629 µmol, 7.5 eq) and the resulting

mixture was allowed to warm up to r.t. overnight. The reaction was quenched by addition of aq. sat. K^+-Na^+-tartrate solution (3 mL) and Et_2O (2 mL) and the biphasic mixture was vigorously stirred for 30 min. The layers were separated and the aqueous layer was extracted with Et_2O (2 × 20 mL) and EtOAc (20 mL). The combined organic layers were dried over Na_2SO_4. After filtration and concentration *in vacuo*, the crude product was purified by flash column chromatography (hexanes:EtOAc 2:1) on silica to afford diol **2.109** (26.1 mg, 72.1 µmol, 86%) as a yellow oil.

Data for 2.109: R_f: 0.50 (hexanes:EtOAc 1:1); **^{1}H NMR (400 MHz, C_6D_6):** δ = 5.10 (s, 1H), 4.95 (s, 1H), 3.93 (d, *J* = 11.2 Hz, 1H), 3.85 – 3.69 (m, 1H), 3.69 – 3.52 (m, 2H), 3.23 (d, *J* = 9.5 Hz, 1H), 2.30 (ddd, *J* = 14.8, 10.0, 4.8 Hz, 1H), 1.87 (ddd, *J* = 15.5, 9.8, 6.6 Hz, 1H), 1.51 – 1.34 (m, 2H), 1.32 (s, 3H), 0.99 (s, 3H), 0.96 (s, 3H) ppm; **^{13}C NMR (100 MHz, C_6D_6):** δ = 215.8, 153.1, 114.5, 84.0, 81.0, 76.6, 65.8, 65.6, 63.9, 43.1, 32.0, 24.6, 23.9, 22.5, 12.3 ppm; **IR (ATR):** ν_{max} = 3295 (br w), 2967 (w), 2925 (w), 2880 (w), 2029 (s), 1938 (s), 1634 (w), 1445 (w), 1384 (w), 1372 (w), 1331 (w), 1198 (w), 1107 (w), 1069 (w), 1046 (w), 1025 (w), 907 (w), 829 (w), 770 (w), 729 (w) cm^{-1}; **HRMS (EI):** calc. for $C_{17}H_{22}Fe^{56}O_5$ $[M]^+$: 362.0811, found:362.0786.

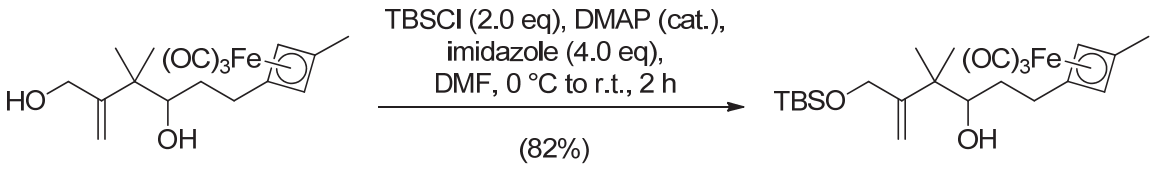

2.109 **2.110**

Monoprotected diol 2.110 To a stirred solution of diol **2.109** (19.0 mg, 52.5 µmol, 1.0 eq) in DMF (1 mL) at r.t. was added TBSCl (15.8 mg, 105 µmol, 2.0 eq), imidazole (14.3 mg, 210 µmol, 4.0 eq) and DMAP (cat.) and the resulting mixture was stirred for 2 h. The reaction was quenched by addition of H_2O (10 mL). The layers were separated and the aqueous layer was extracted with Et_2O (2 × 5 mL) and EtOAc (5 mL). The combined organic layers were dried over Na_2SO_4. After filtration and concentration *in vacuo*, the crude product was purified by flash column chromatography (hexanes:EtOAc 9:1) on silica to afford monoprotected diol **2.110** (20.0 mg, 42.0 µmol, 80%) as a yellow oil.

Data for 2.110: R_f: 0.53 (hexanes:EtOAc 9:1); **^{1}H NMR (400 MHz, C_6D_6):** δ = 5.25 (s, 1H), 5.02 (s, 1H), 4.14 (d, *J* = 12.3 Hz, 1H), 3.97 (d, *J* = 12.4 Hz, 1H), 3.63 (d, *J* = 9.3 Hz, 1H), 3.58 (d, *J* = 9.3 Hz, 1H), 3.36 (dd, *J* = 9.4, 4.0 Hz, 1H), 2.64 (d, *J* = 4.9 Hz, 1H), 2.39 (ddd, *J* = 15.1, 10.1, 4.9 Hz, 1H), 1.94 (ddd, *J* = 15.6, 10.1, 6.1 Hz, 1H), 1.54 – 1.35 (m, 2H), 1.32 (s, 3H), 1.05 (s, 3H), 1.01 (s, 3H), 0.95 (s, 9H), 0.04 (s, 6H) ppm; **^{13}C NMR (100 MHz, C_6D_6):**

δ = 216.1, 153.2, 114.7, 84.4, 81.3, 76.7, 66.1, 65.9, 64.9, 43.6, 32.3, 26.0, 25.1, 24.2, 22.4, 18.5, 12.7, −5.3, −5.4 ppm; **IR (ATR):** ν_{max} = 3417 (br w), 2956 (w), 2930 (w), 2884 (w), 2858 (w), 2033 (s), 1950 (s), 1636 (w), 1471 (w), 1445 (w), 1390 (w), 1362 (w), 1256 (w), 1083 (m), 1046 (w), 1005 (w), 837 (m), 777 (w), 679 (w) cm^{-1}; **HRMS (EI):** calc. for $C_{22}H_{36}Fe^{56}SiO_4$ $[M\text{-}CO]^+$: 448.1727, found: 448.1728.

6.1.2 ^{1}H and ^{13}C NMR spectra

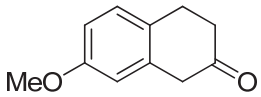

2.45

400 MHz, $CDCl_3$

100 MHz, $CDCl_3$

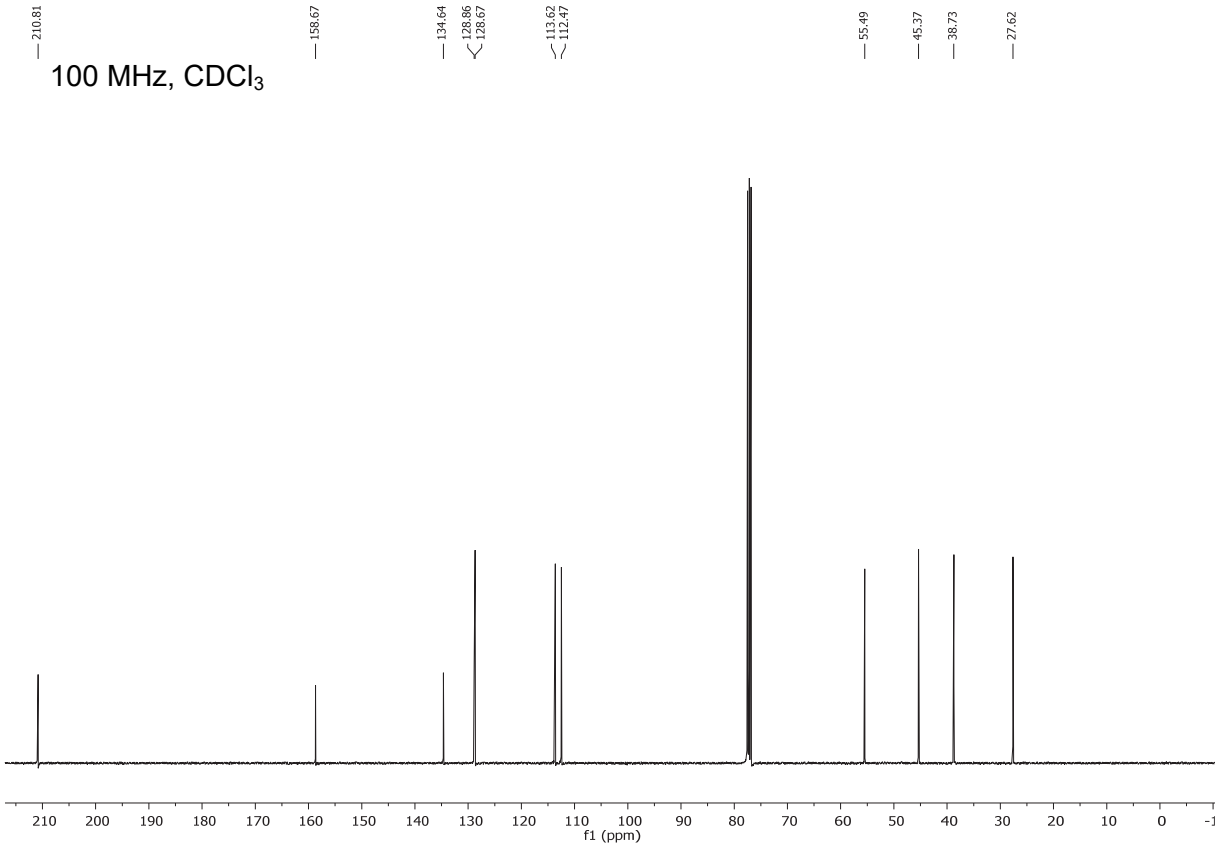

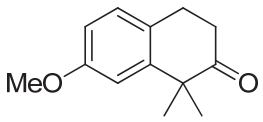

2.47

400 MHz, $CDCl_3$

100 MHz, $CDCl_3$

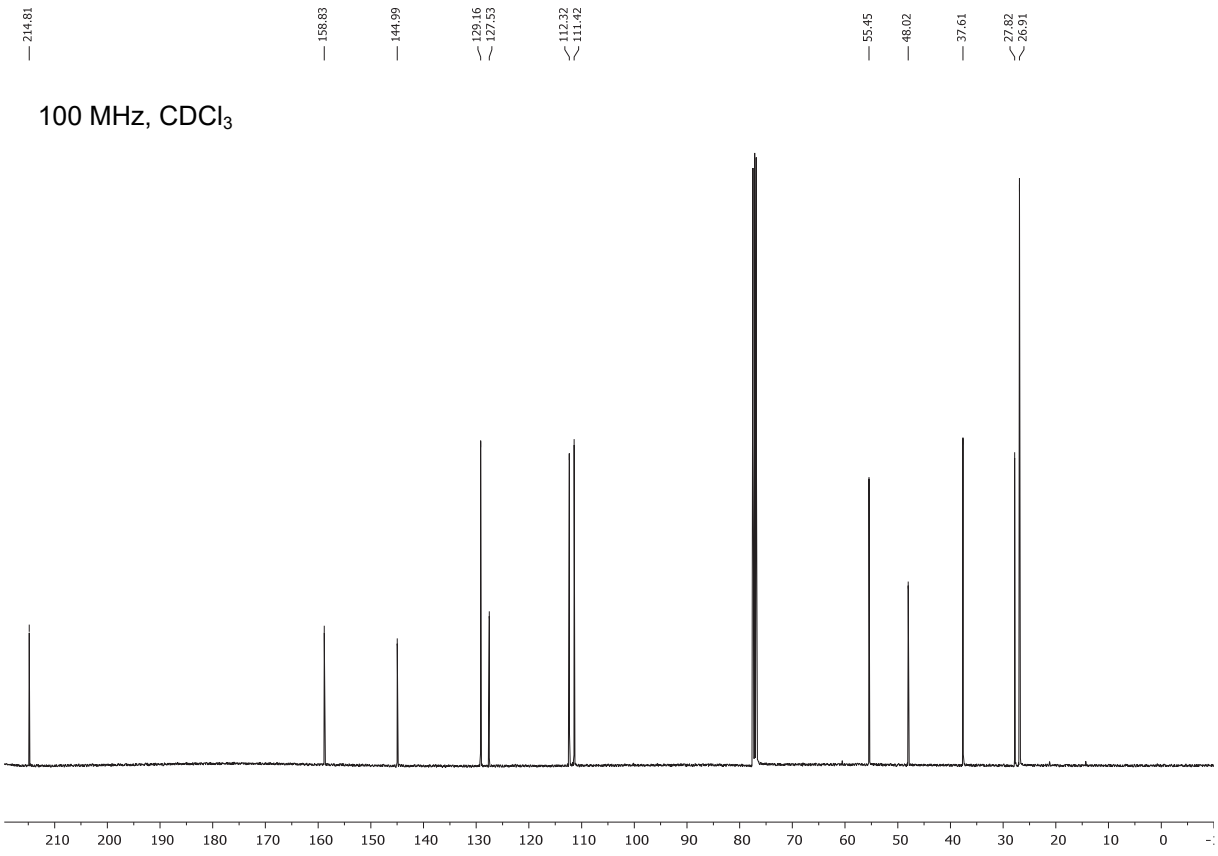

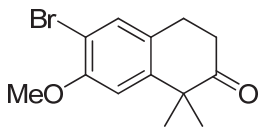

S1

400 MHz, $CDCl_3$

100 MHz, $CDCl_3$

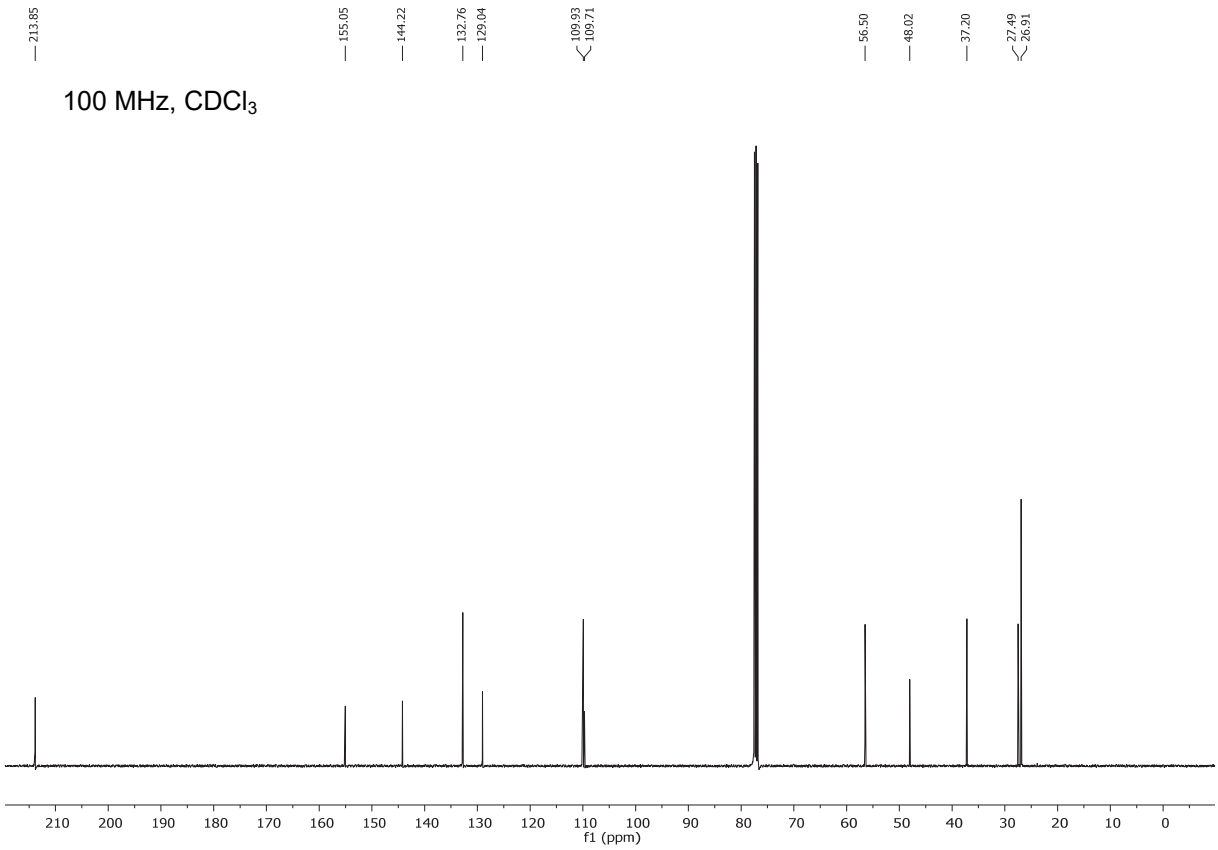

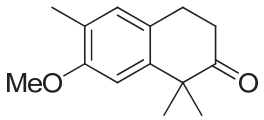

2.48

400 MHz, $CDCl_3$

100 MHz, $CDCl_3$

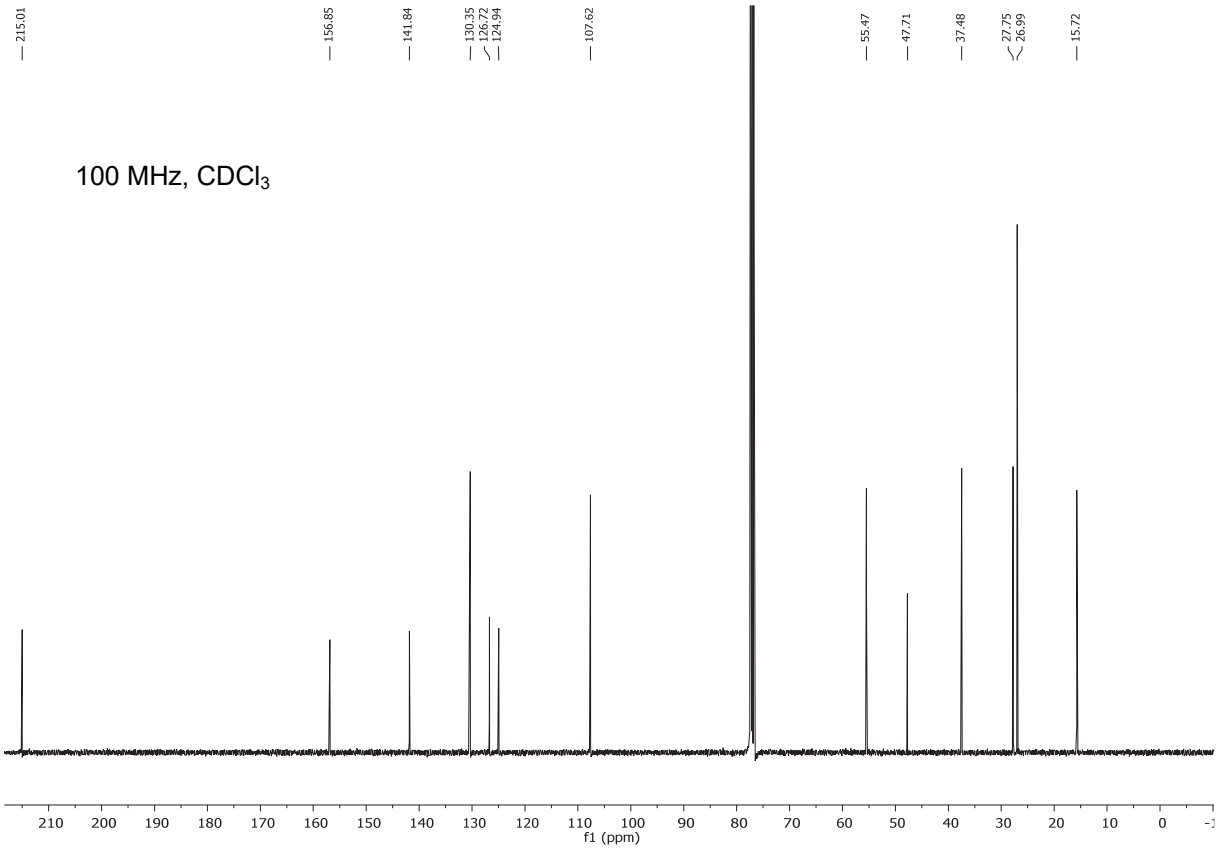

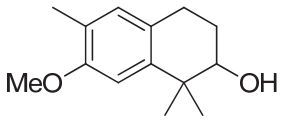

2.57

400 MHz, C_6D_6

100 MHz, C_6D_6

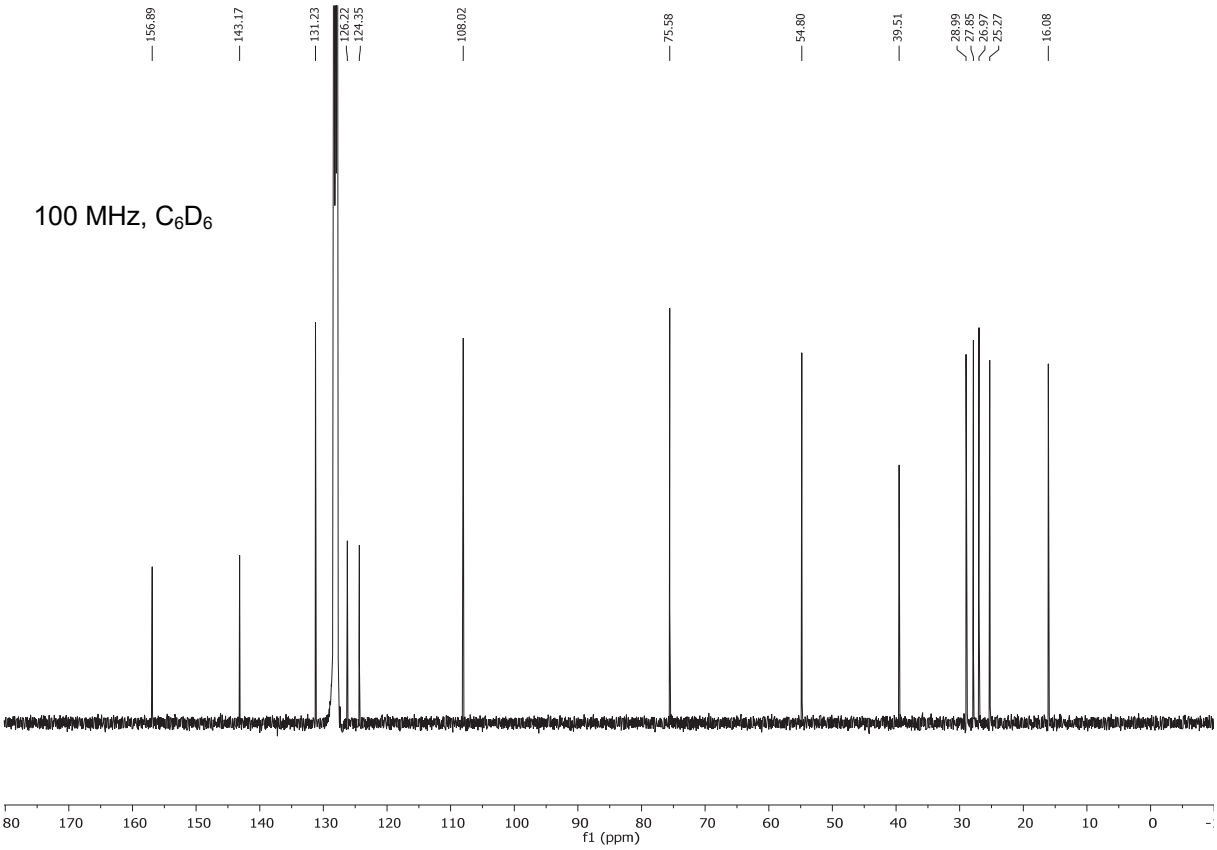

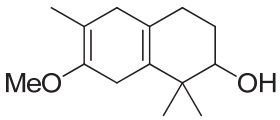

2.42

400 MHz, C_6D_6

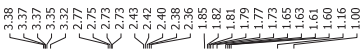

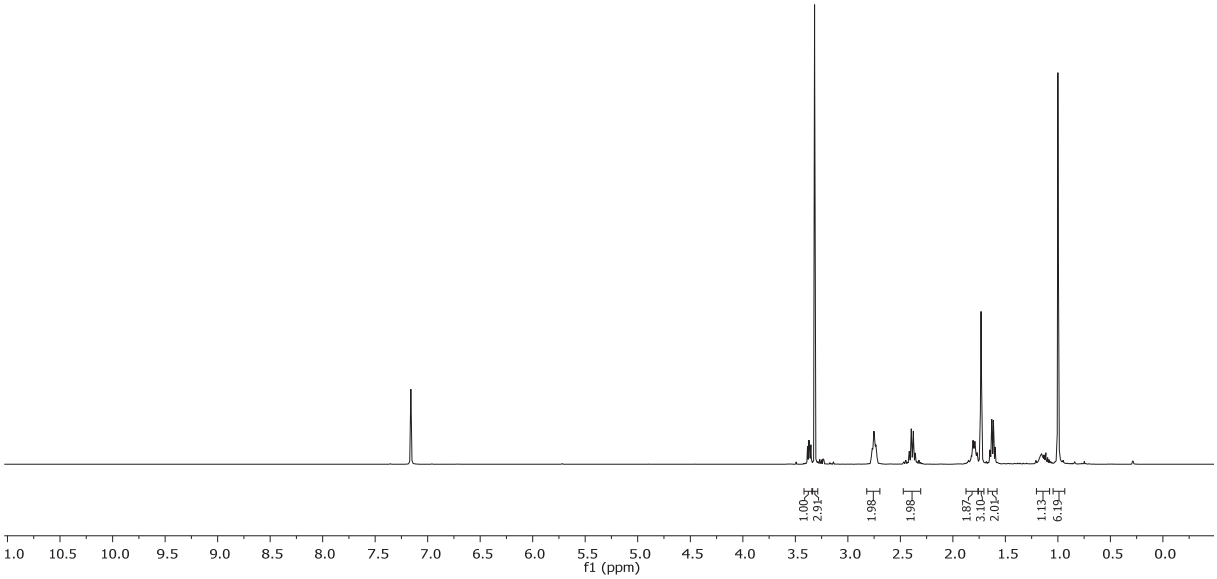

100 MHz, C_6D_6

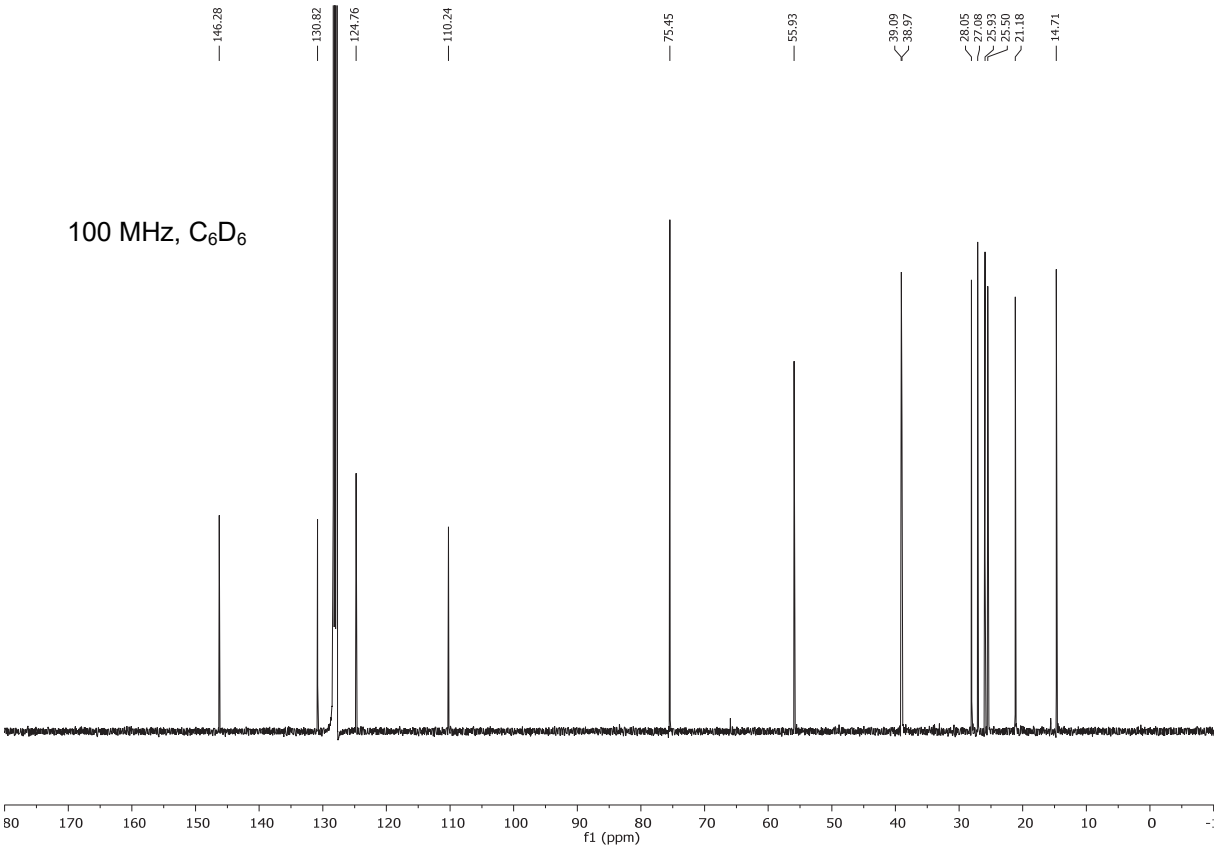

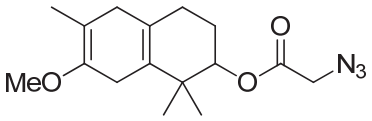

2.50

400 MHz, C_6D_6

100 MHz, C_6D_6

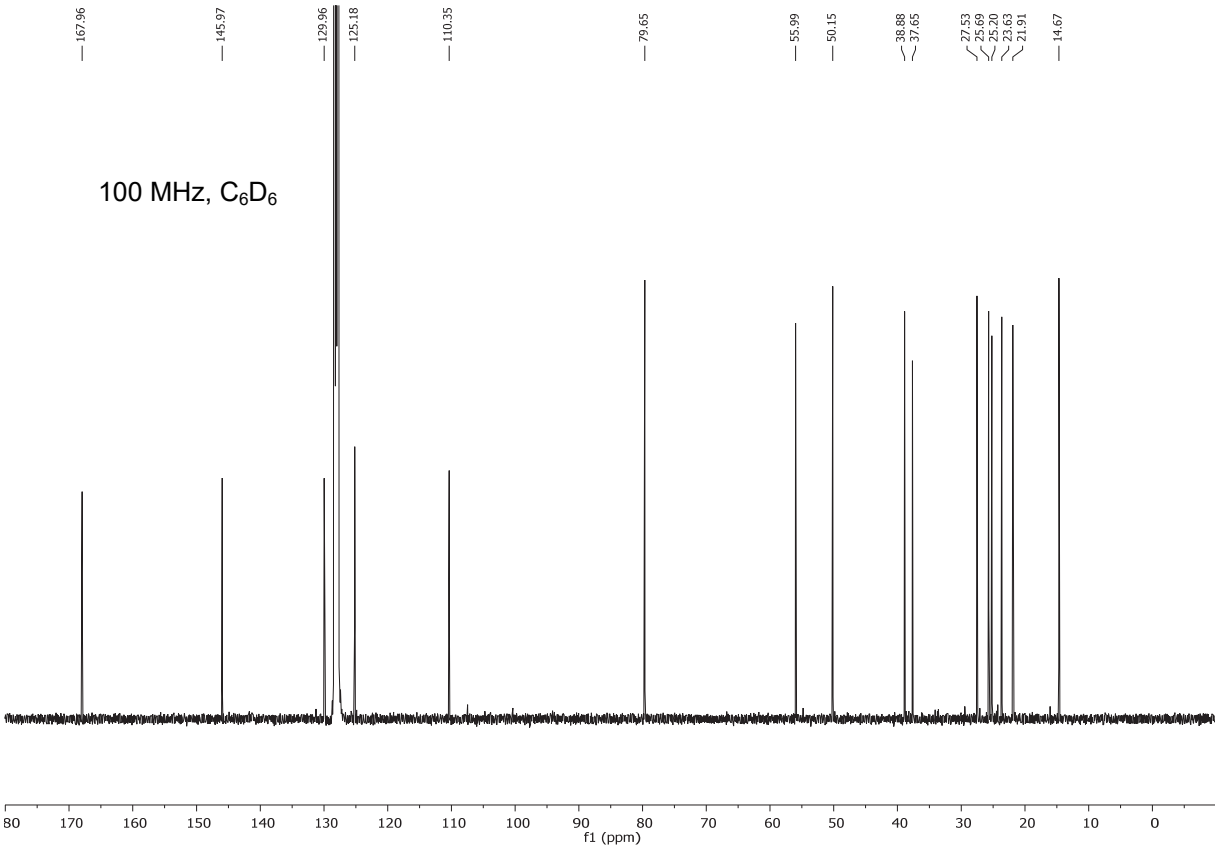

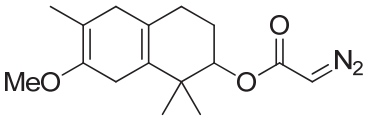

2.41

400 MHz, C_6D_6

100 MHz, C_6D_6

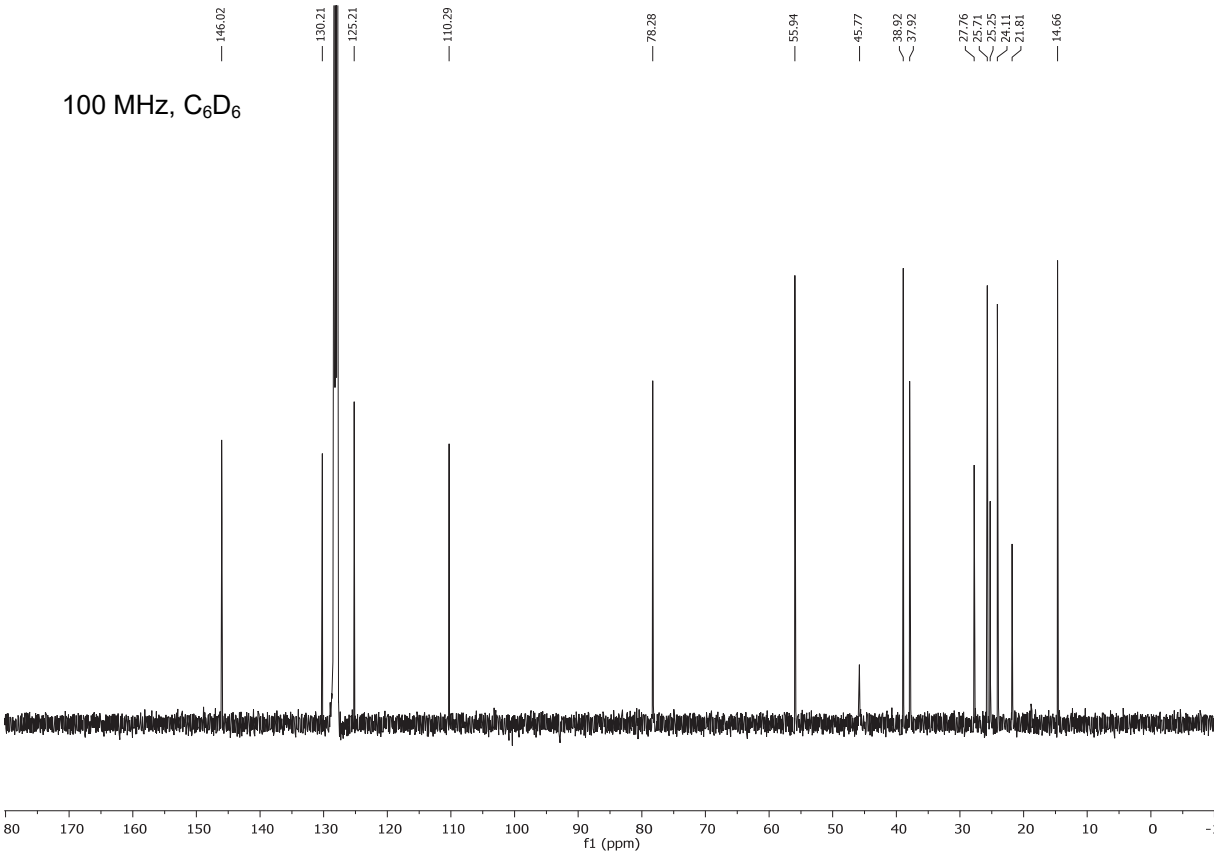

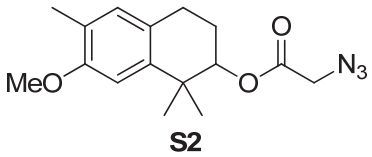

S2

400 MHz, C_6D_6

100 MHz, C_6D_6

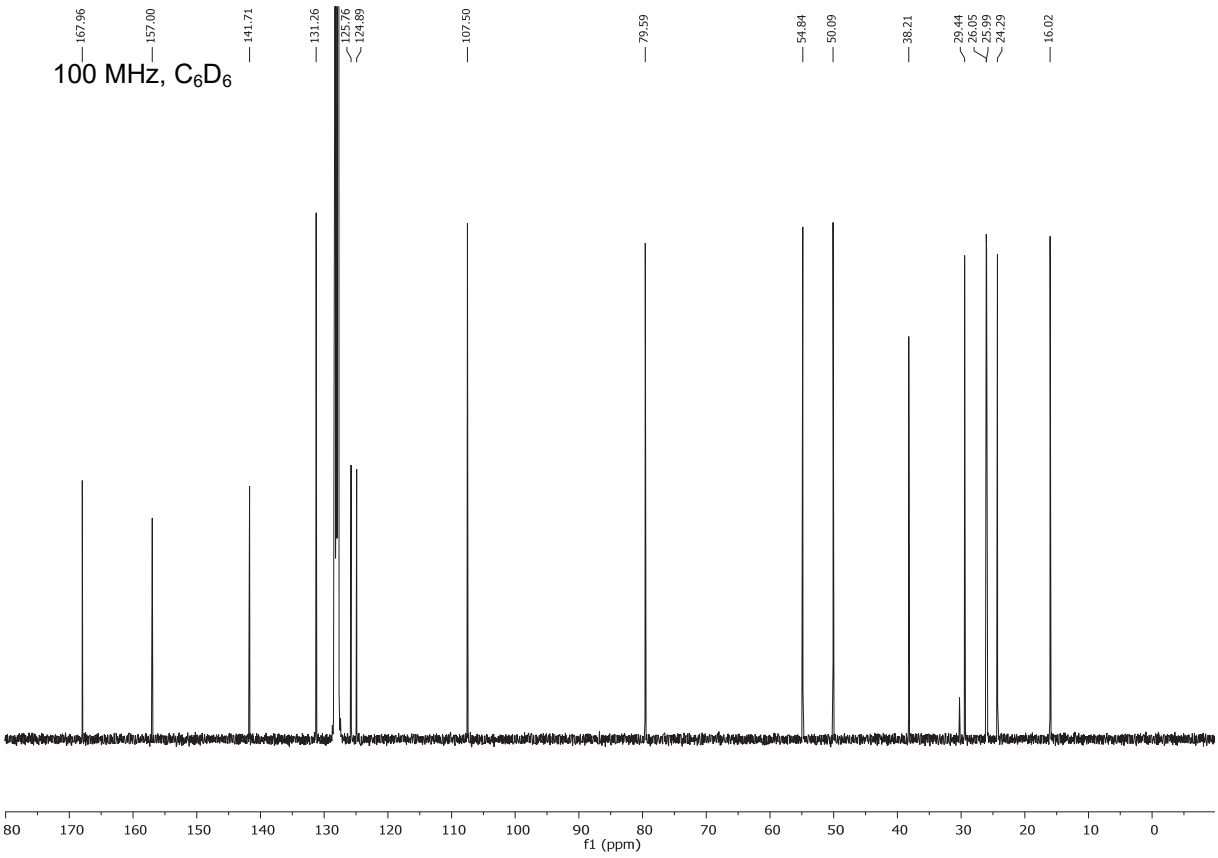

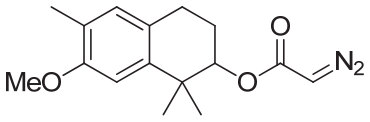

2.58

400 MHz, C_6D_6

100 MHz, C_6D_6

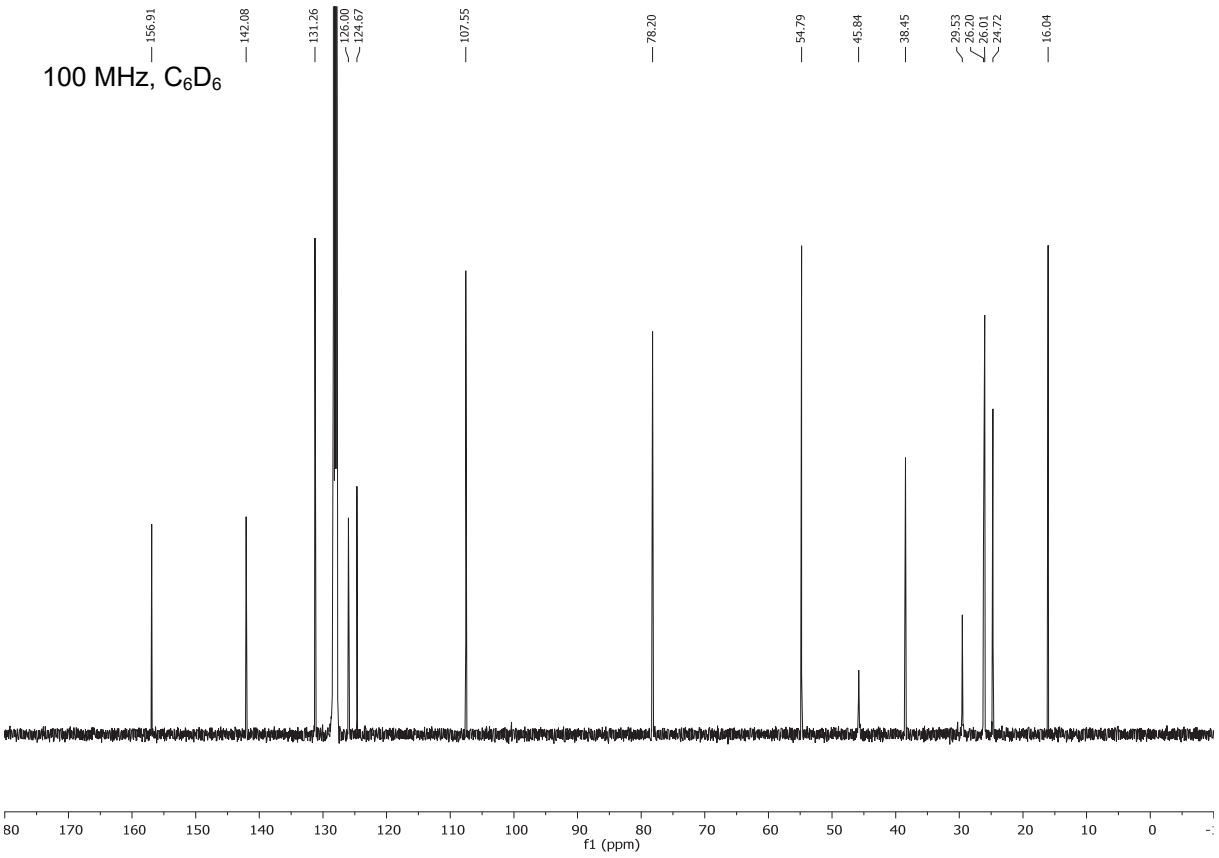

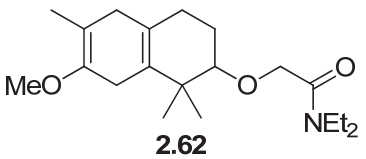

2.62

400 MHz, C_6D_6

100 MHz, C_6D_6

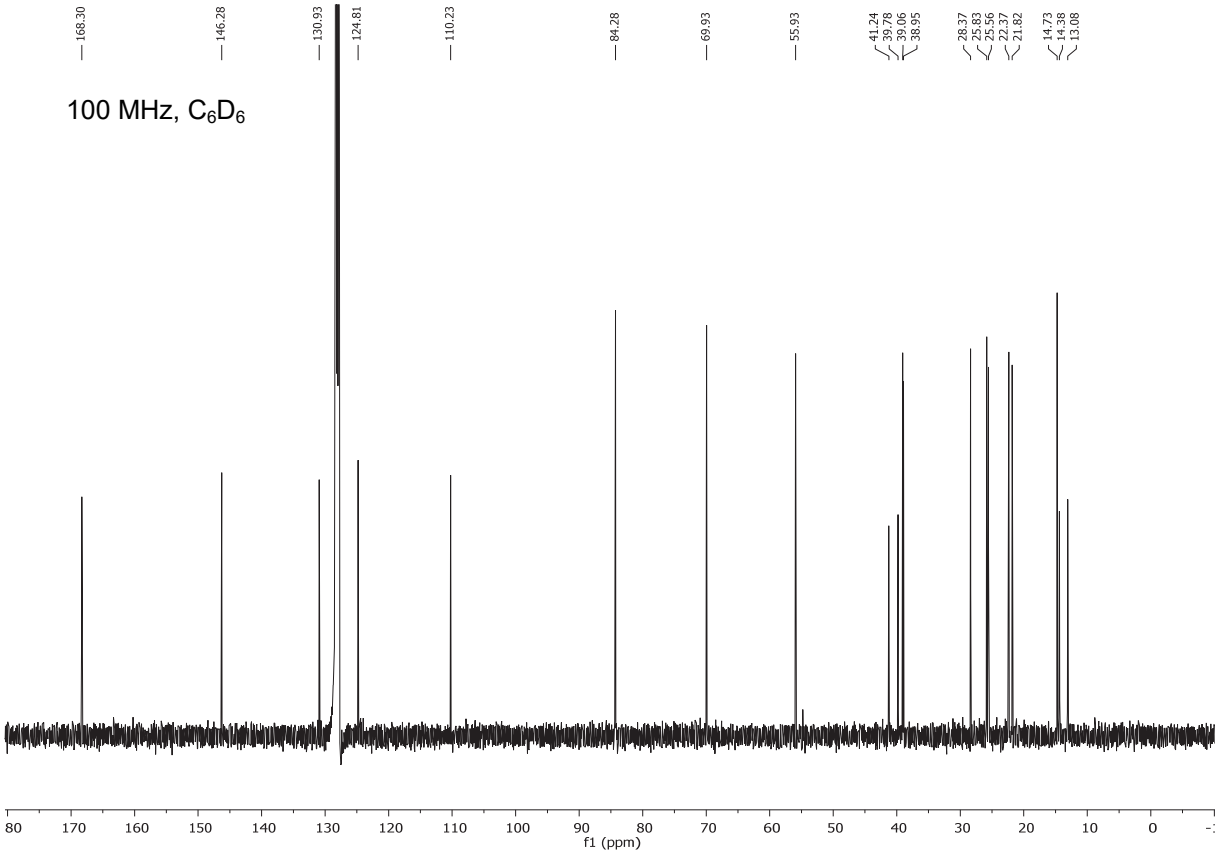

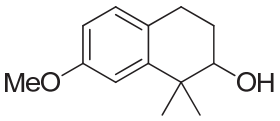

S3

400 MHz, $CDCl_3$

100 MHz, $CDCl_3$

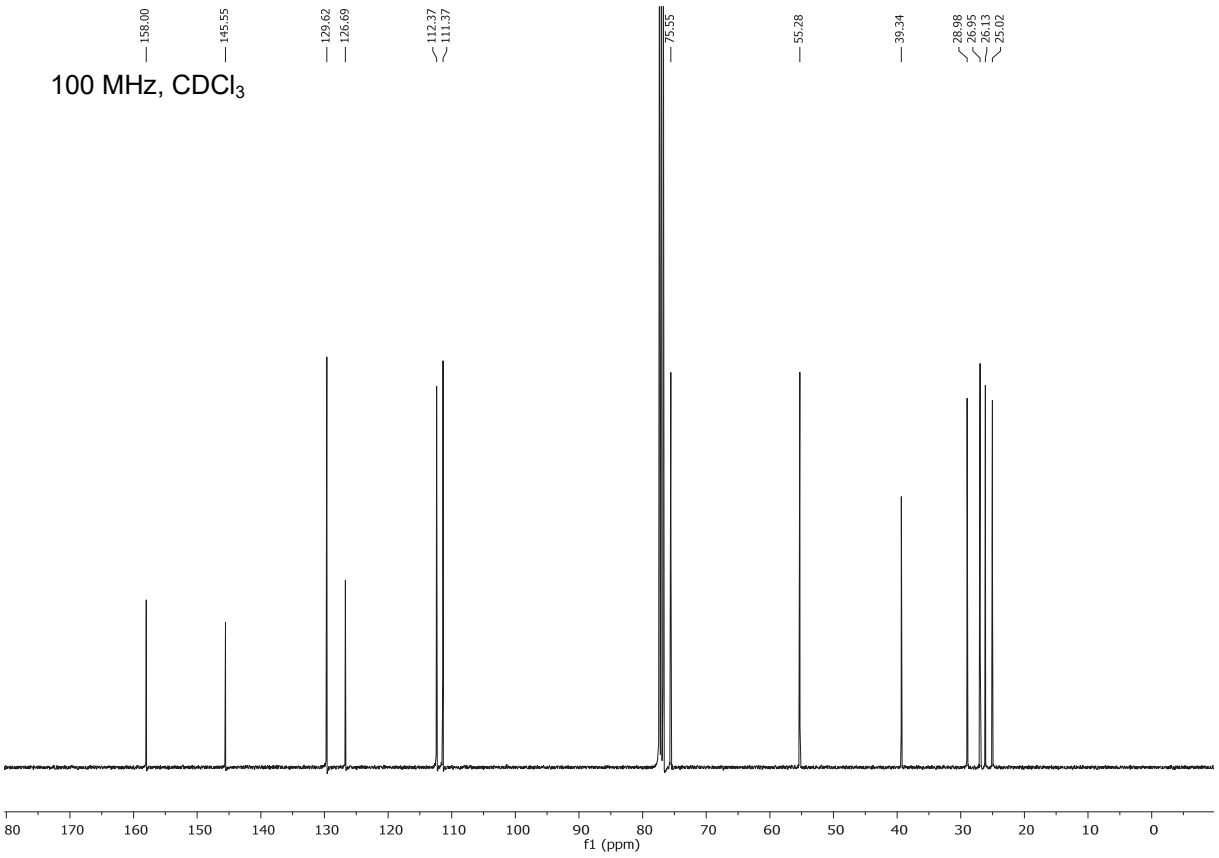

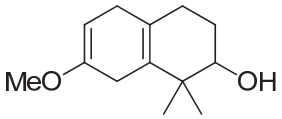

2.67

400 MHz, C_6D_6

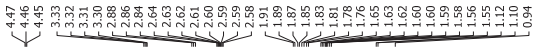

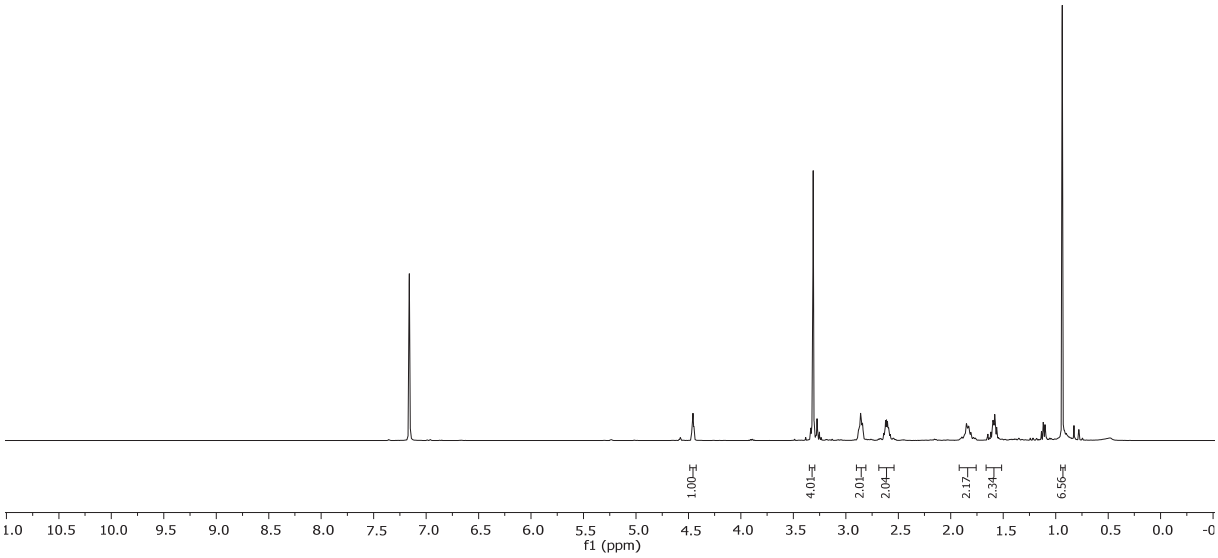

100 MHz, C_6D_6

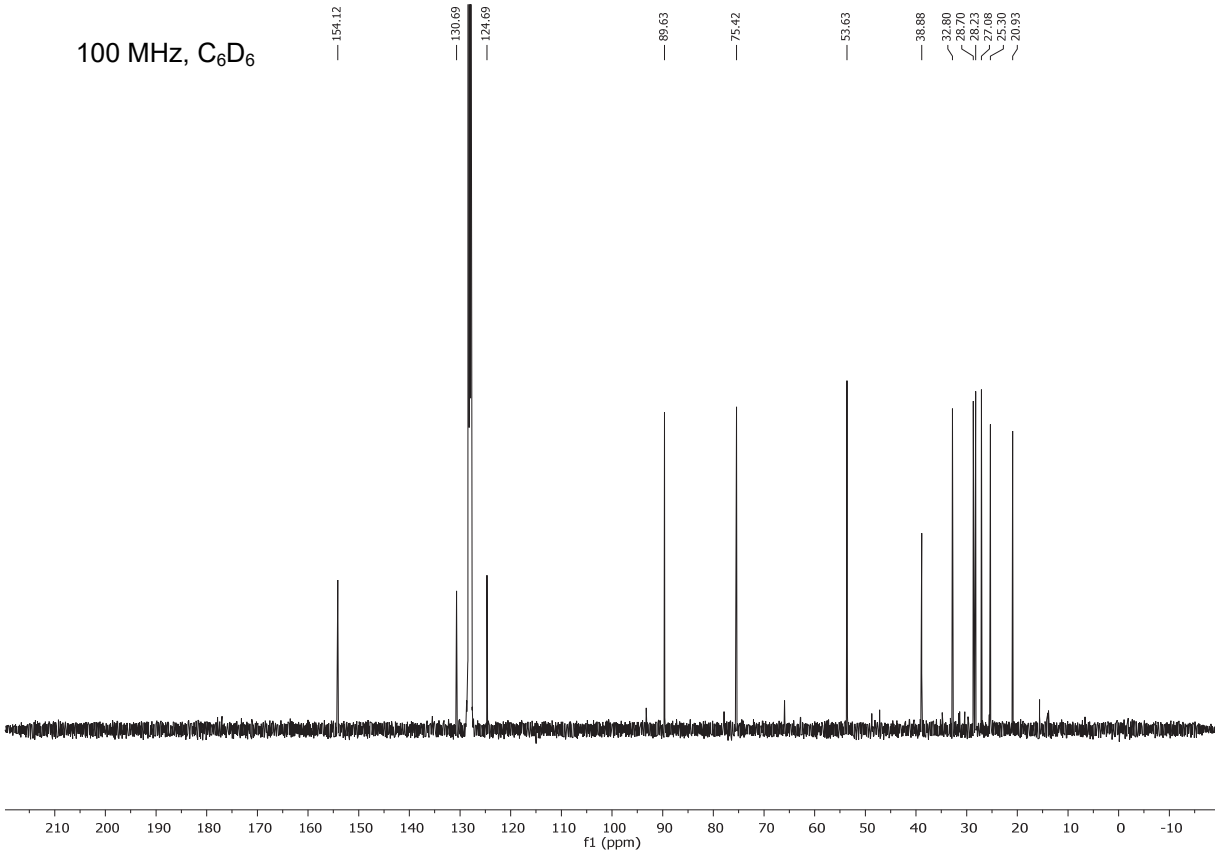

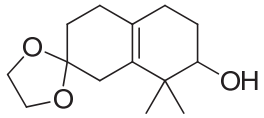

S4

400 MHz, C_6D_6

100 MHz, C_6D_6

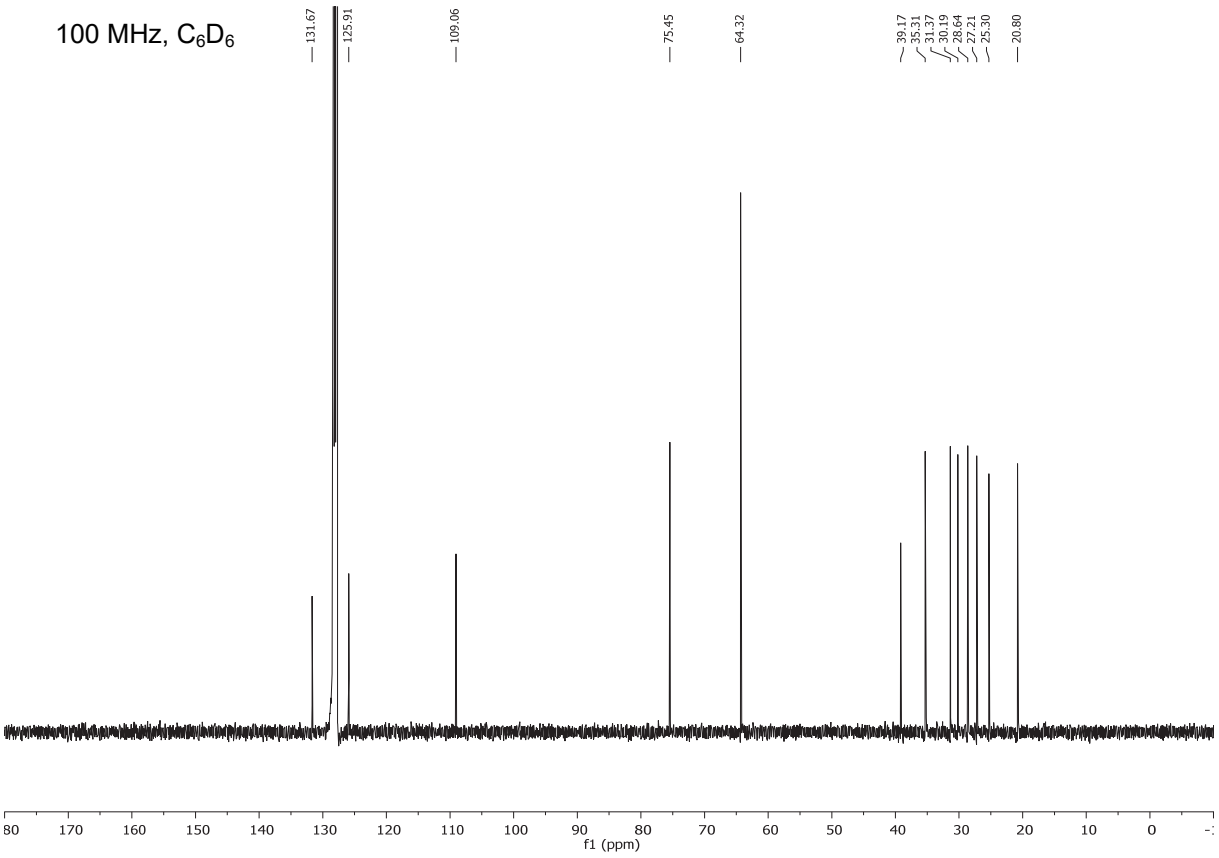

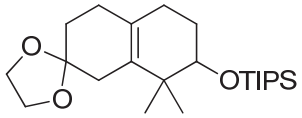

2.68

400 MHz, C_6D_6

100 MHz, C_6D_6

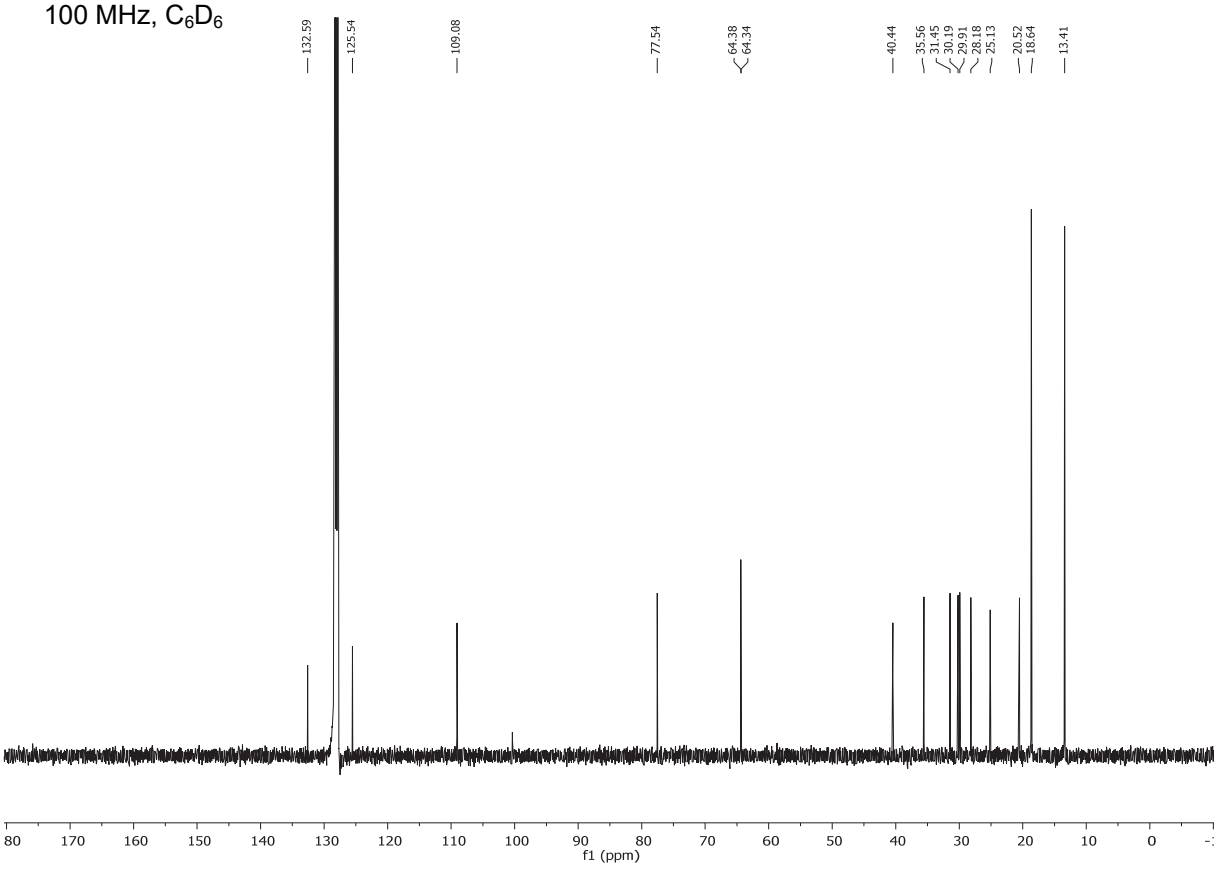

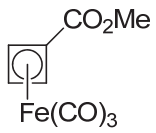

2.78

400 MHz, $CDCl_3$

100 MHz, $CDCl_3$

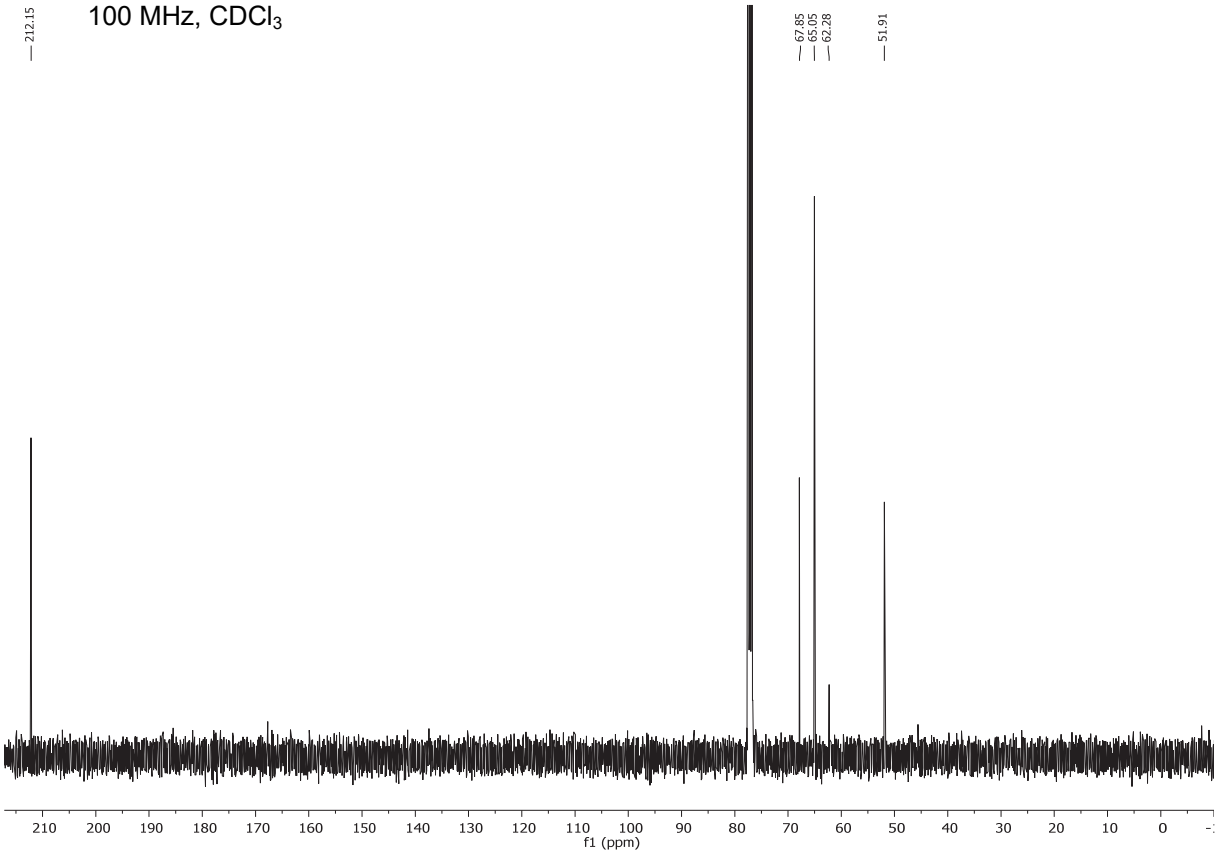

$Fe(CO)_3$

2.79

400 MHz, $CDCl_3$

100 MHz, $CDCl_3$

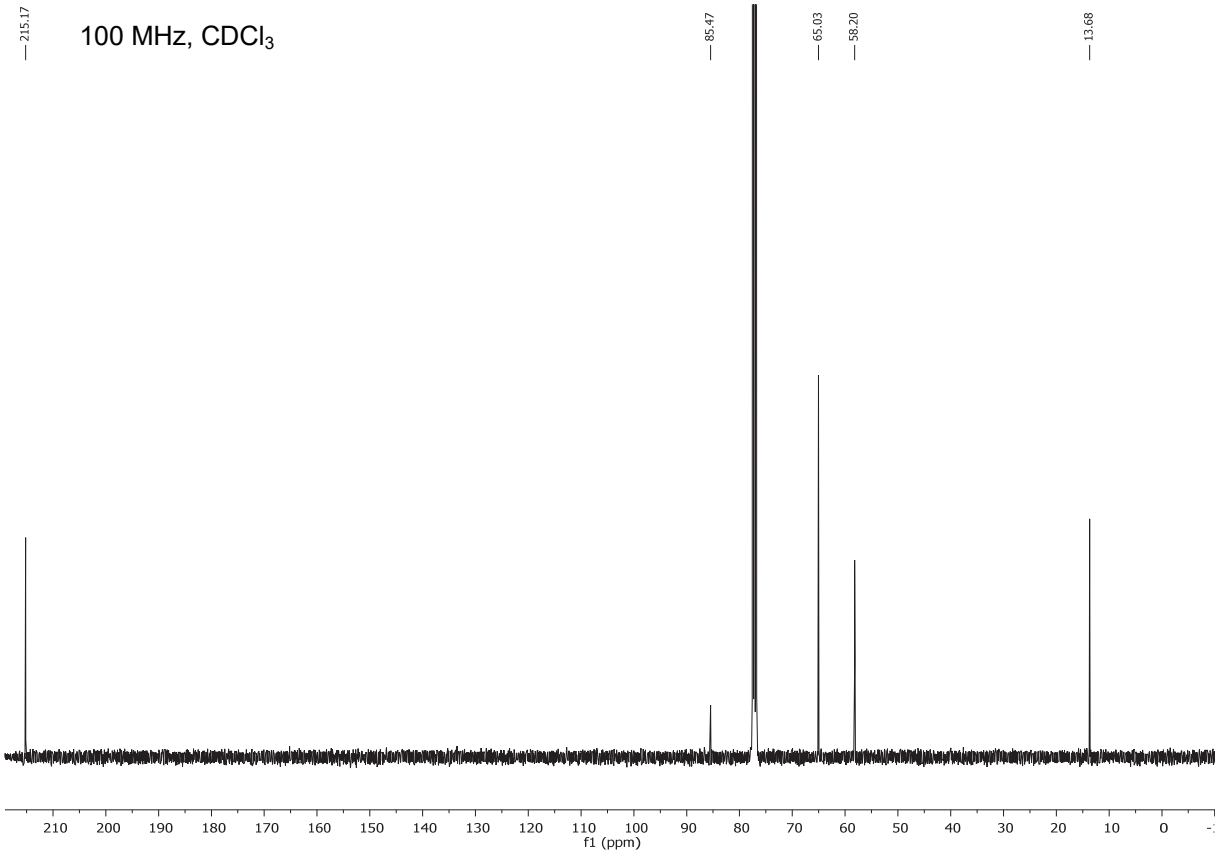

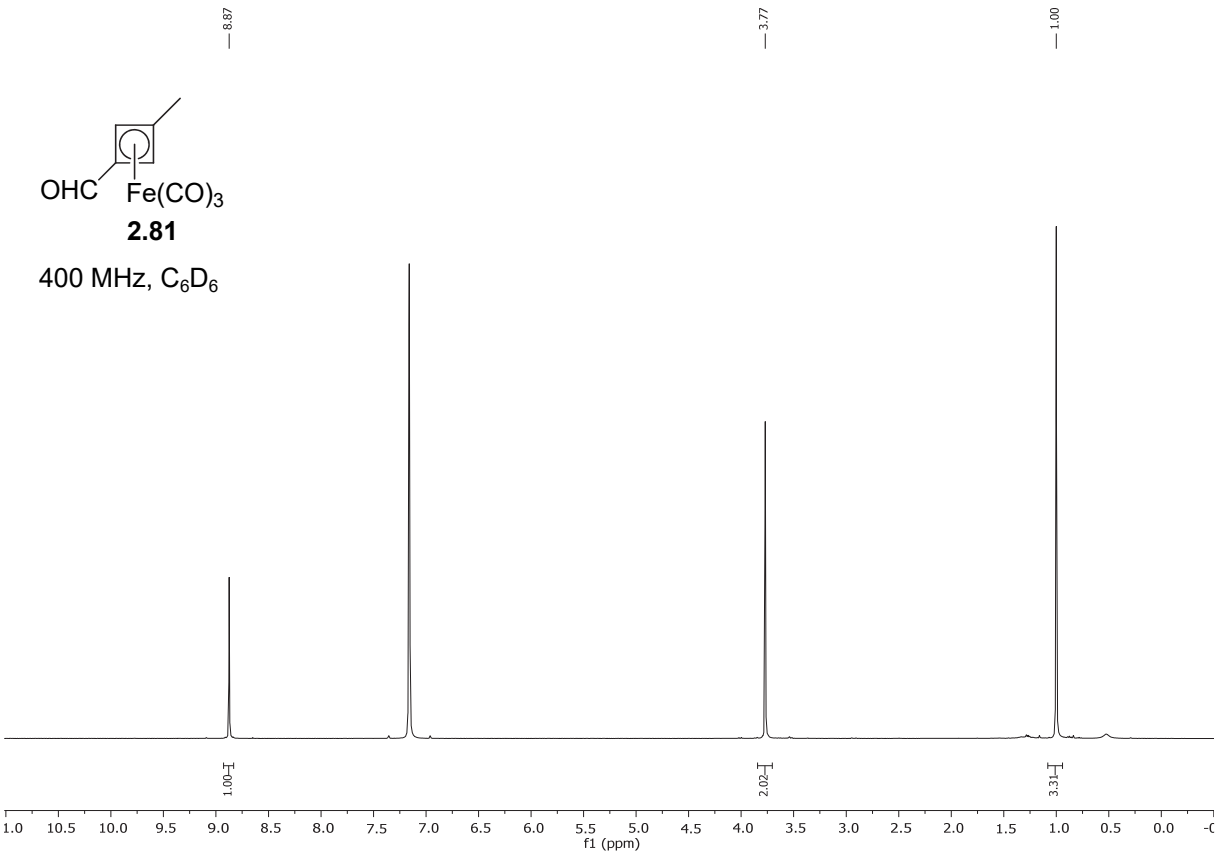
8.87
3.77
1.00
OHC
Fe(CO)3
2.81
400 MHz, C6D6
1.00
2.02
3.31
f1 (ppm)

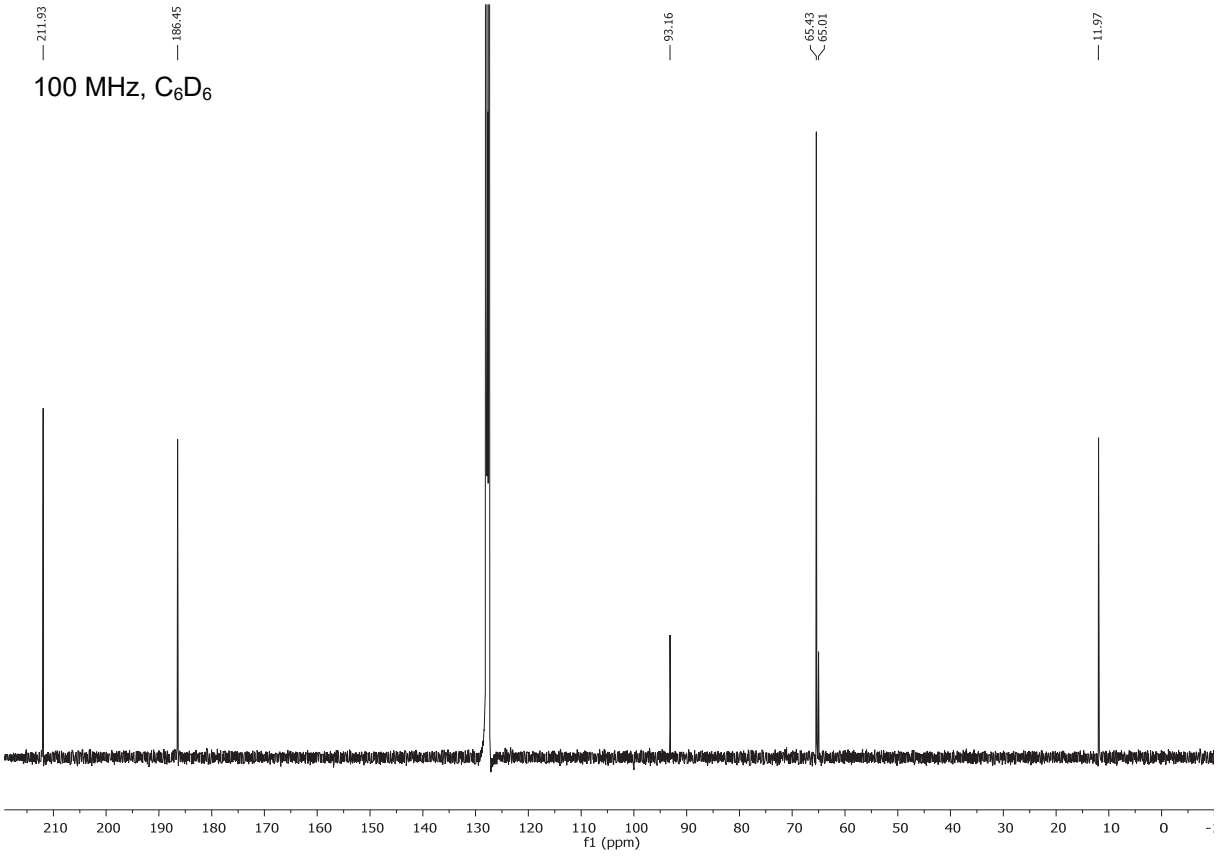
211.93
186.45
93.16
65.43
65.01
11.97
100 MHz, C6D6
f1 (ppm)

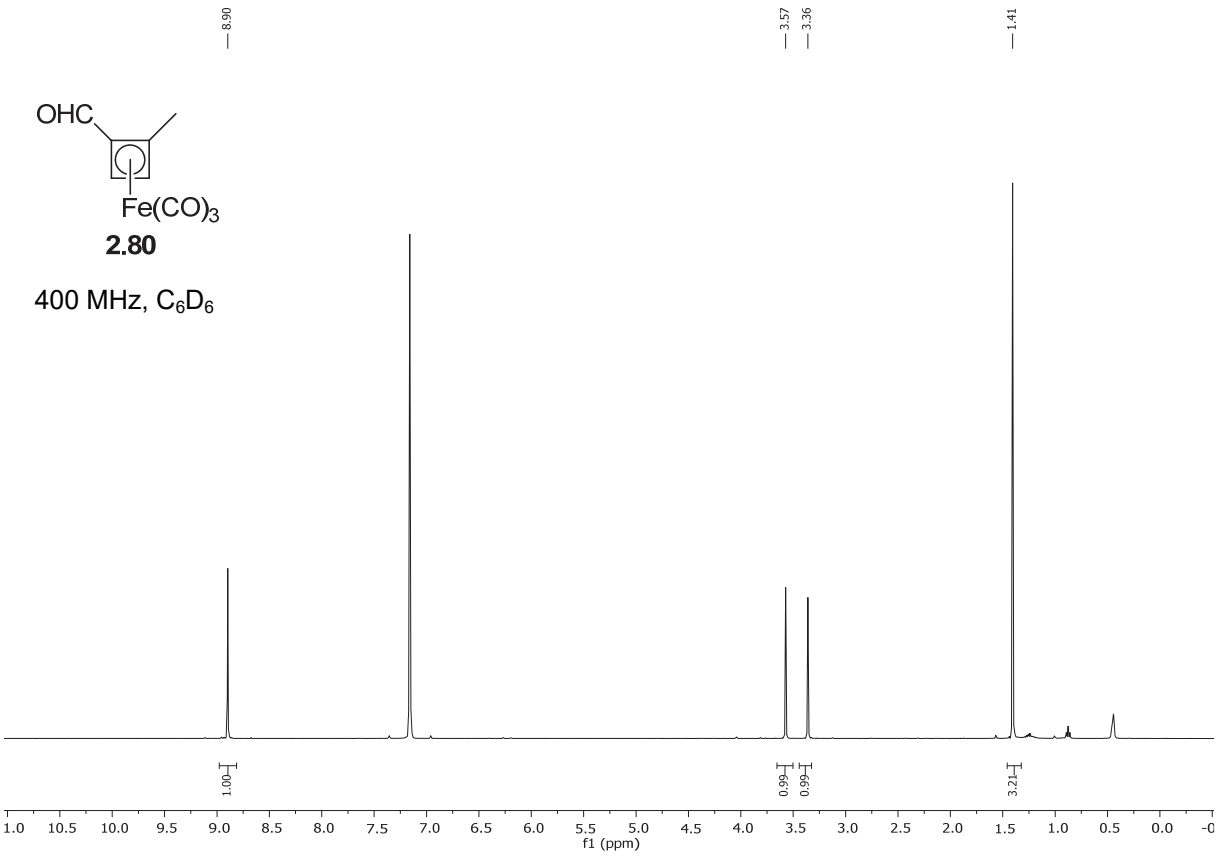

2.80

400 MHz, C_6D_6

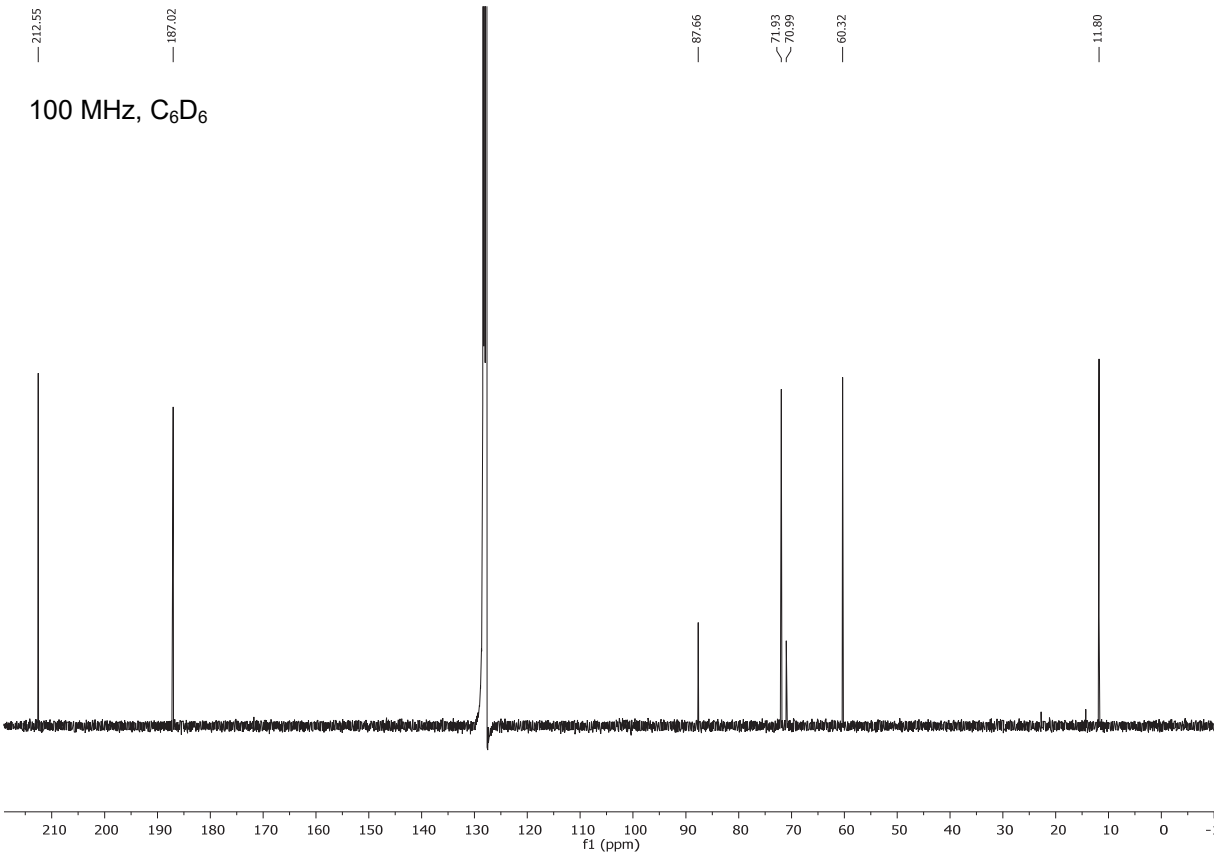

100 MHz, C_6D_6

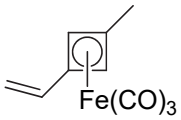

2.74

400 MHz, C_6D_6

100 MHz, C_6D_6

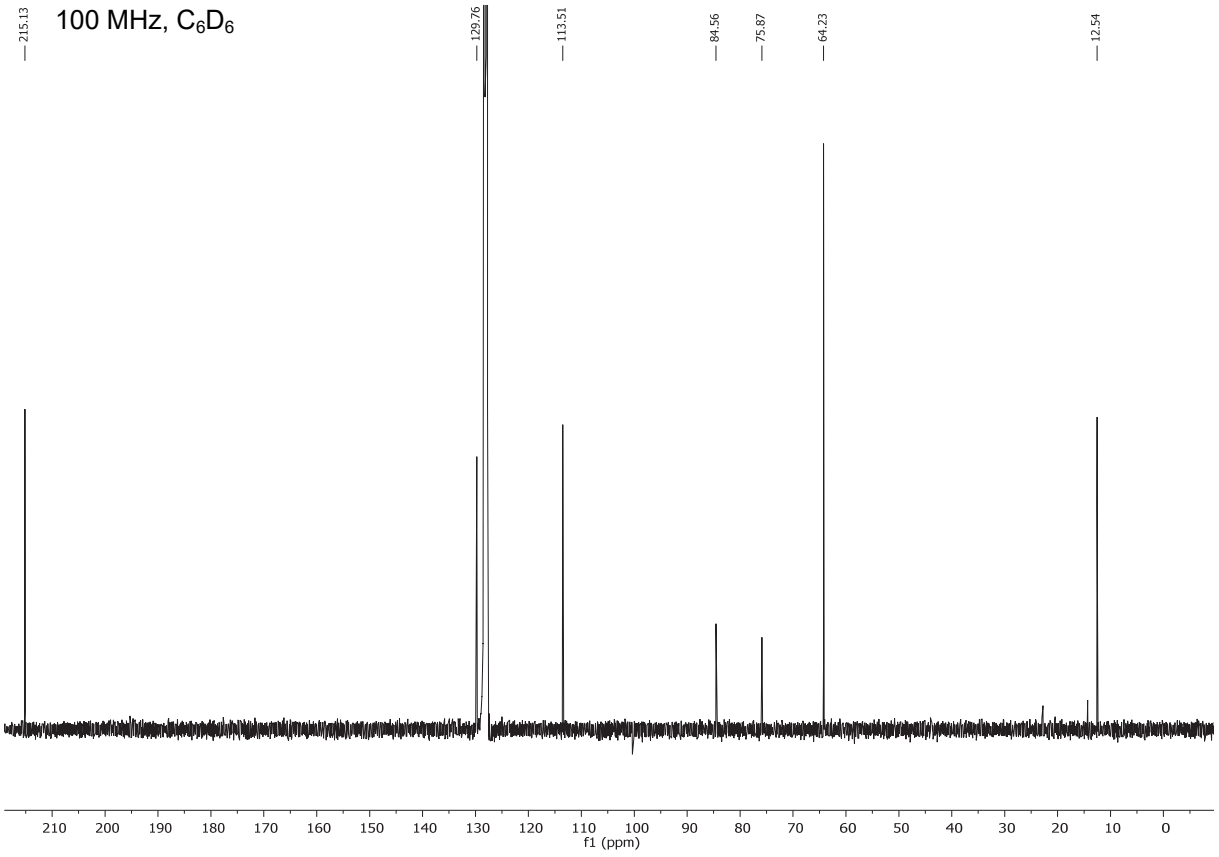

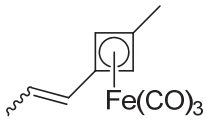

2.75

(*E*/*Z* 2.5:1)

400 MHz, C_6D_6

100 MHz, C_6D_6

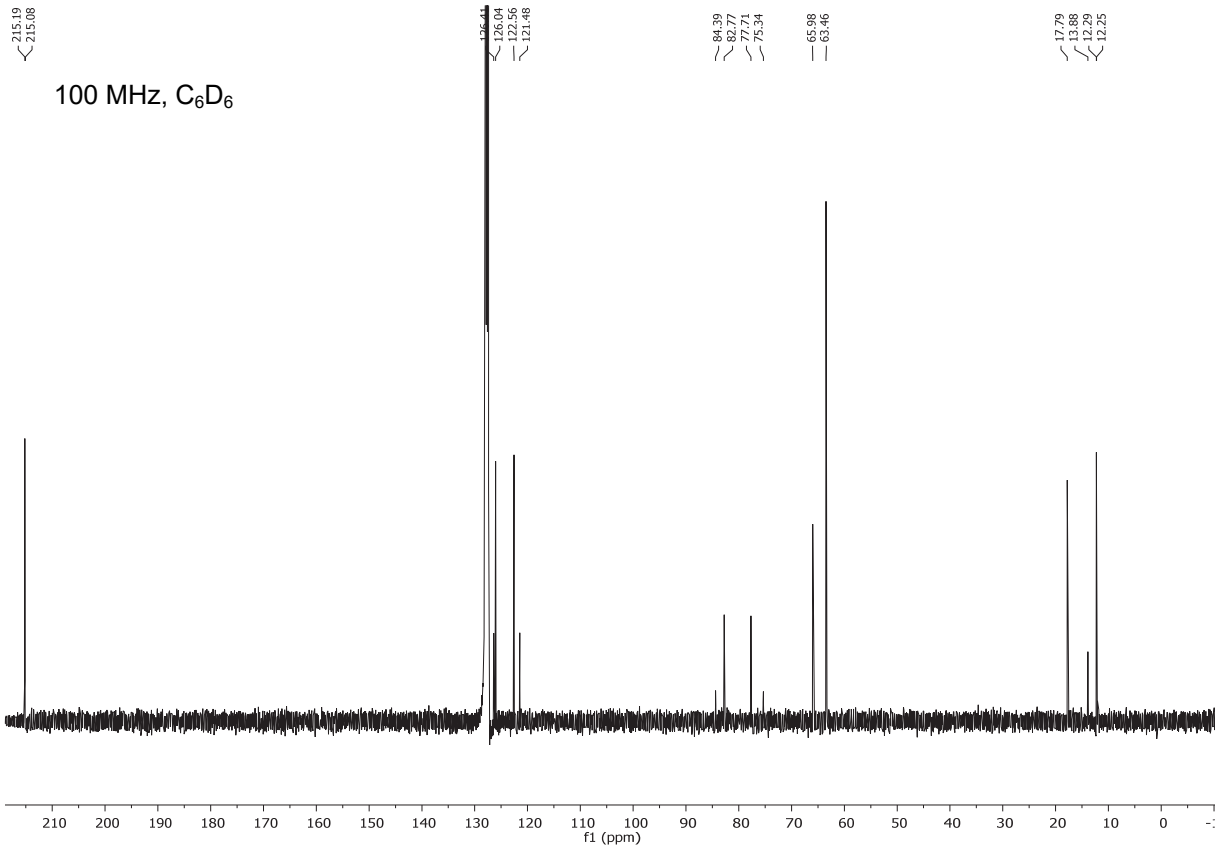

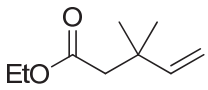

2.83

400 MHz, $CDCl_3$

100 MHz, $CDCl_3$

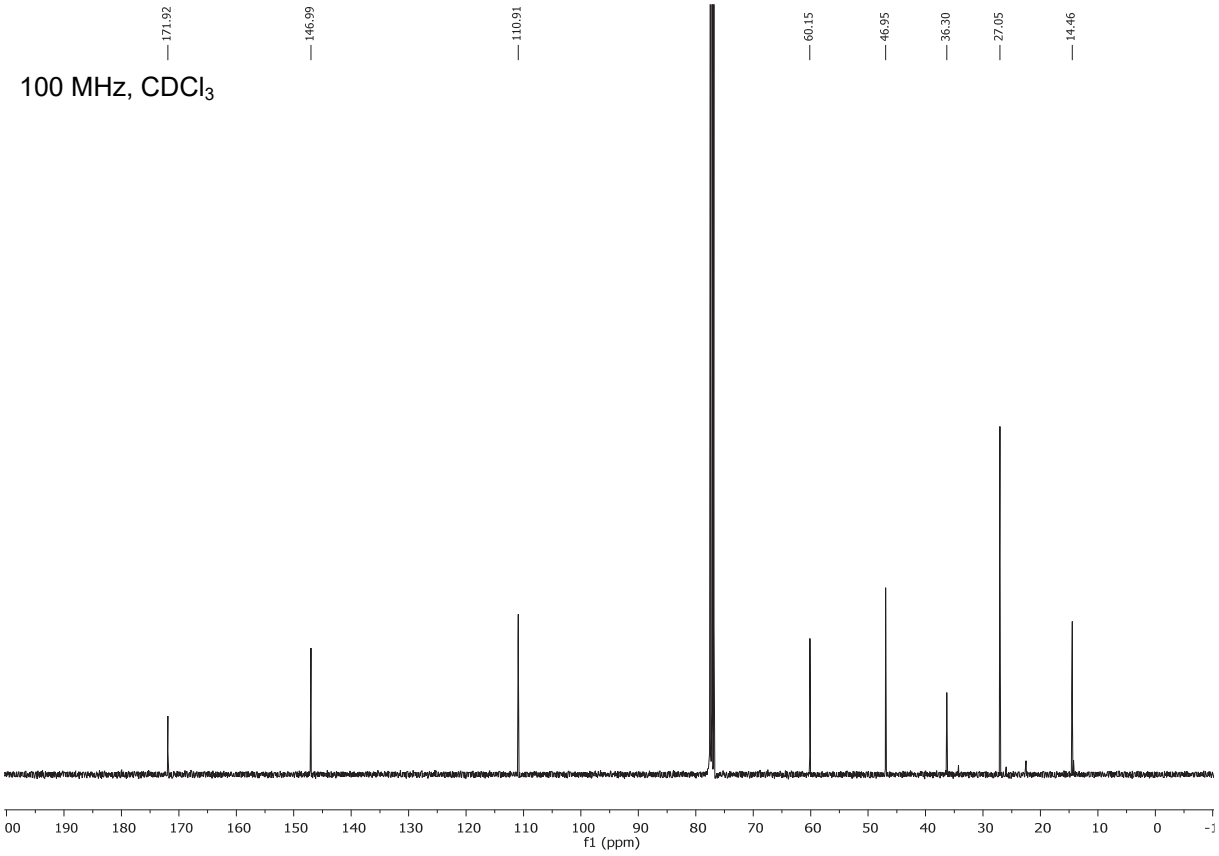

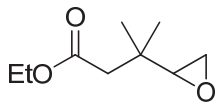

2.85

400 MHz, $CDCl_3$

100 MHz, $CDCl_3$

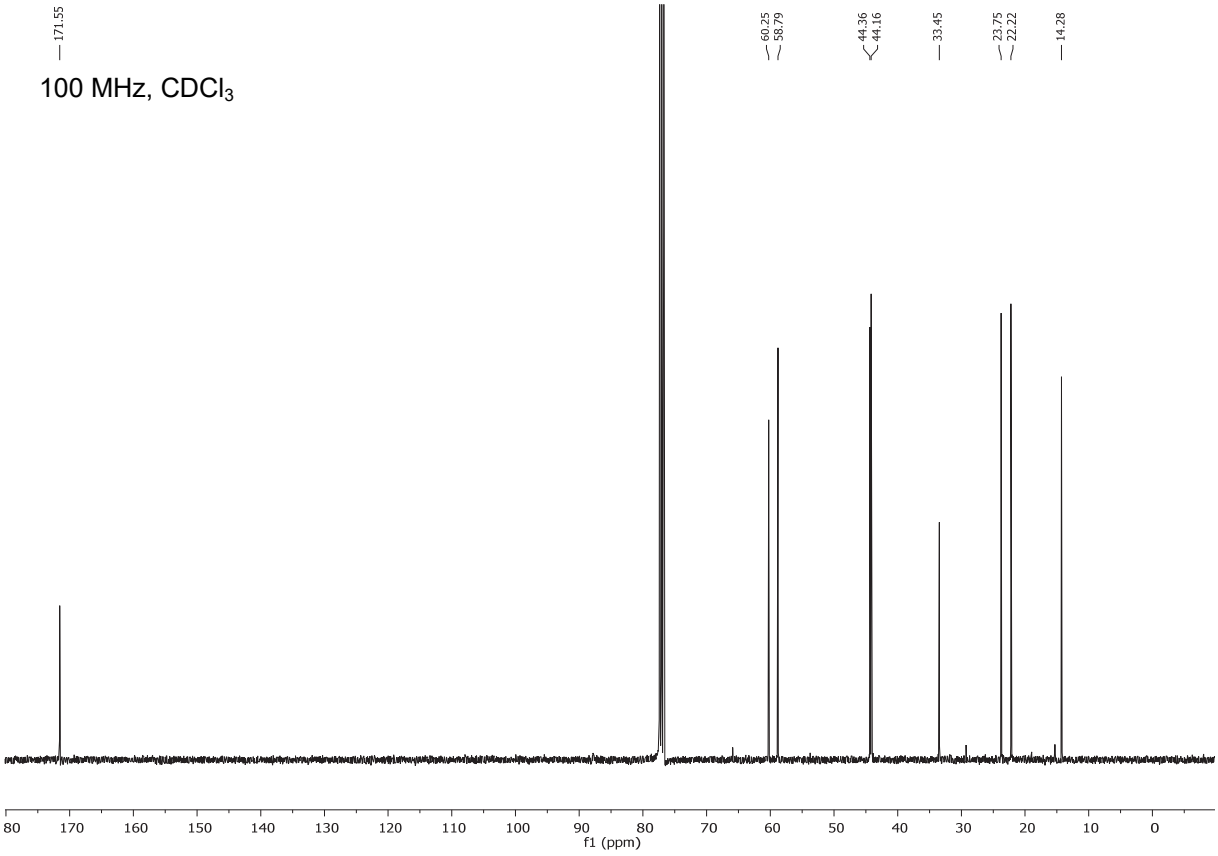

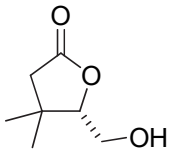

2.84

400 MHz, $CDCl_3$

100 MHz, $CDCl_3$

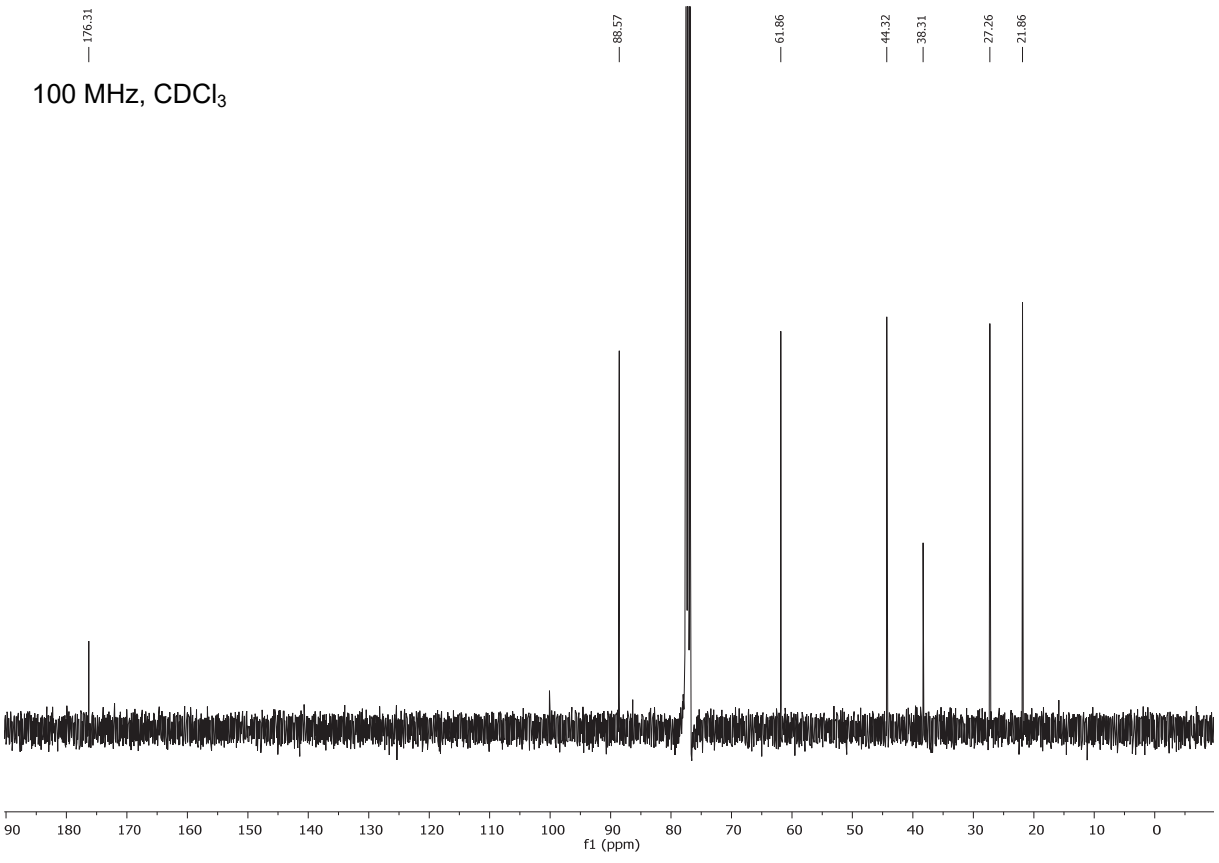

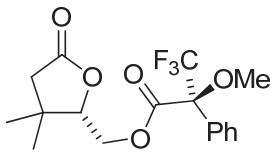

S5

400 MHz, $CDCl_3$

100 MHz, $CDCl_3$

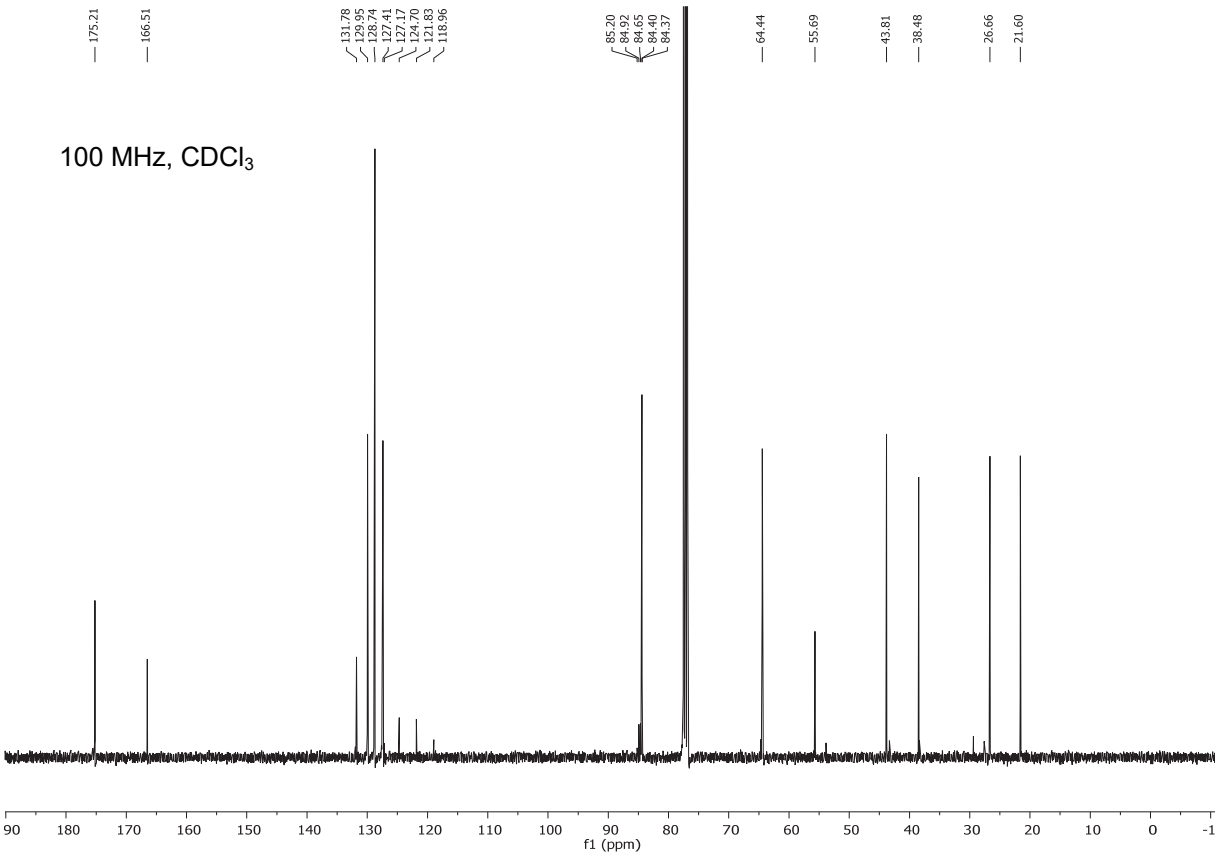

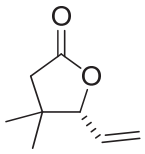

2.73

400 MHz, $CDCl_3$

100 MHz, $CDCl_3$

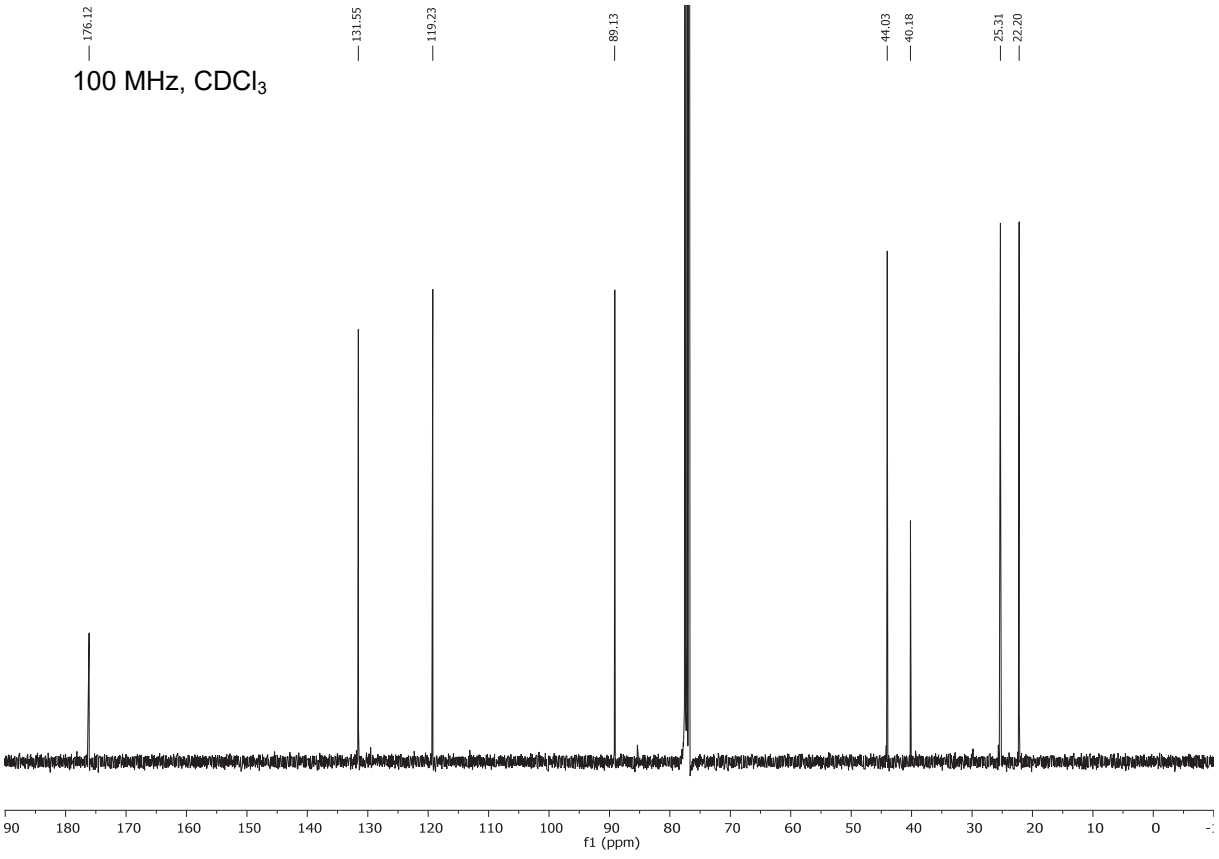

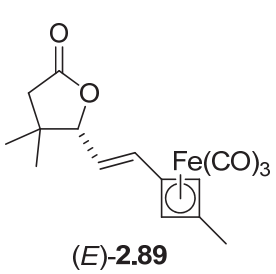

(*E*)-**2.89**

400 MHz, C_6D_6

100 MHz, C_6D_6

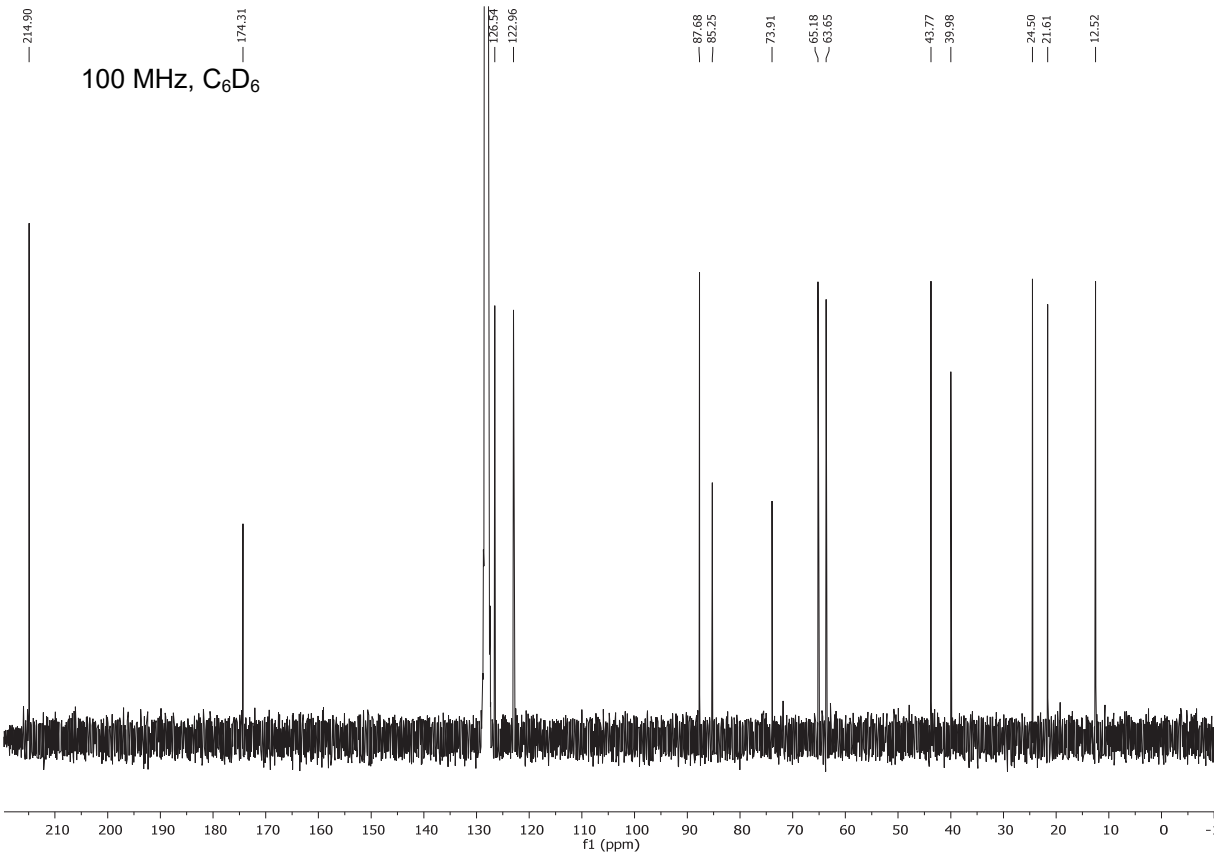

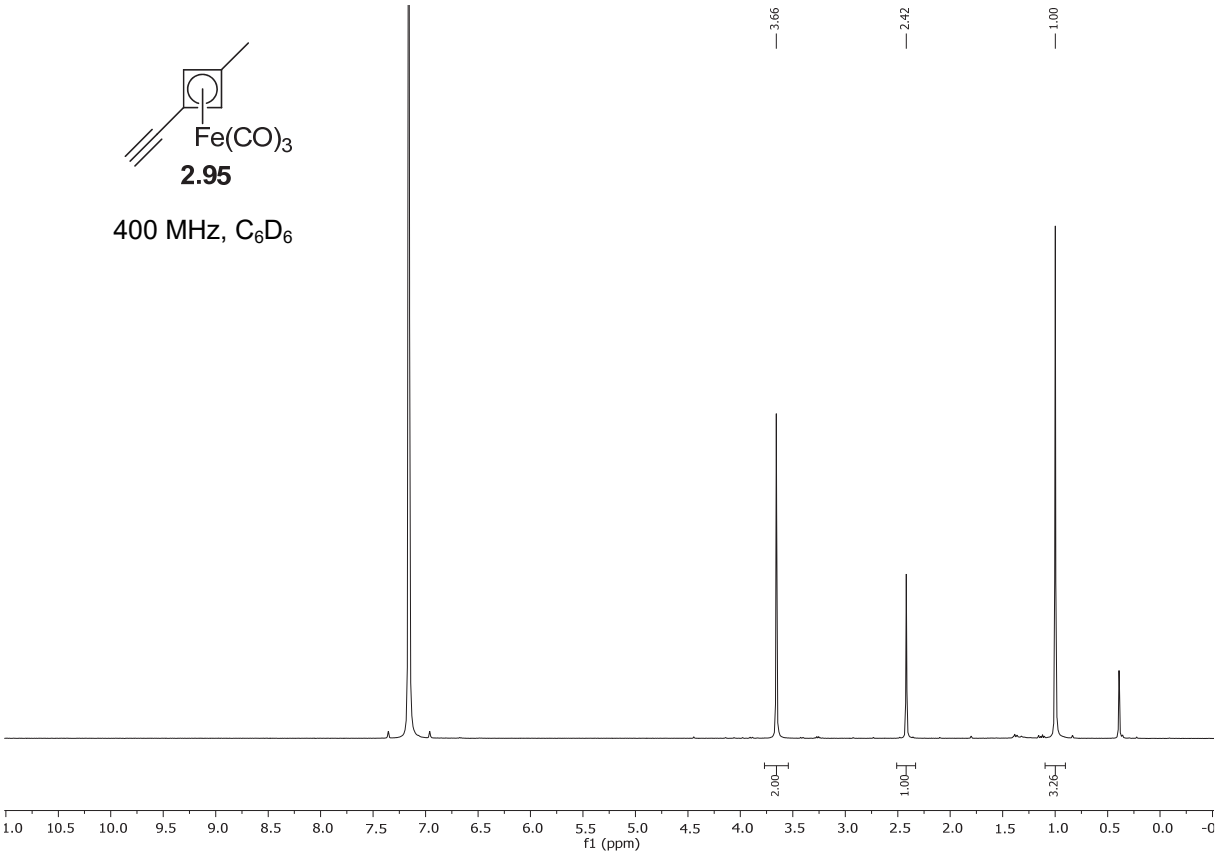
Fe(CO)3
2.95
400 MHz, C6D6
3.66
2.42
1.00
2.00
1.00
3.26
f1 (ppm)

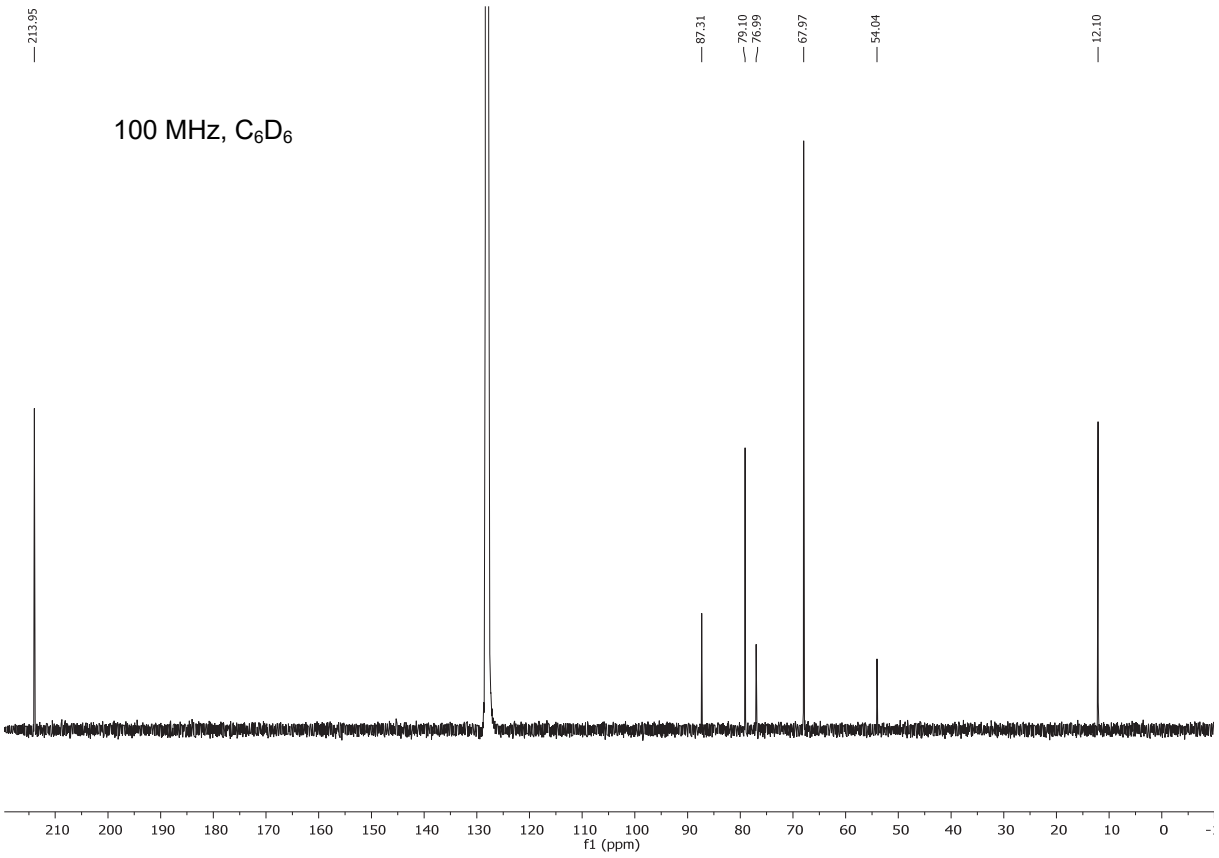
100 MHz, C6D6
213.95
87.31
79.10
76.99
67.97
54.04
12.10
f1 (ppm)

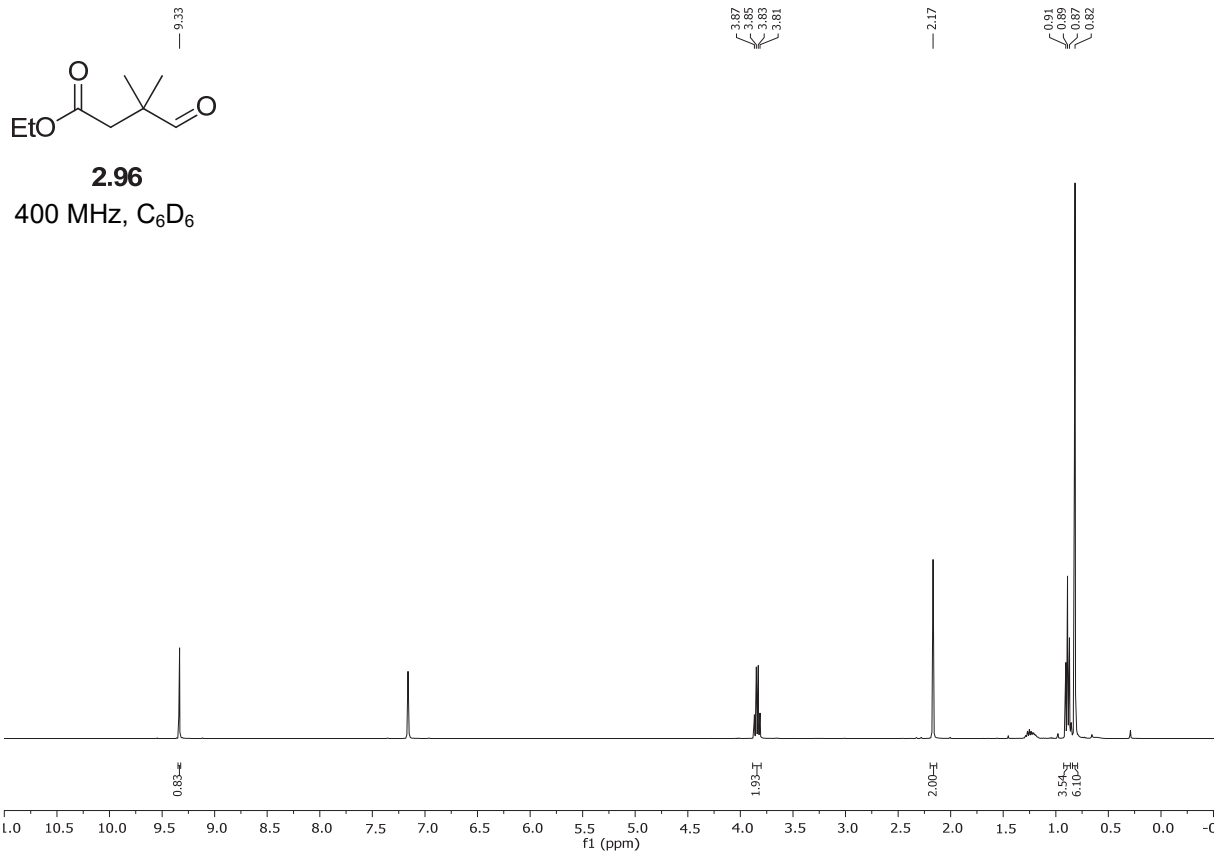

2.96

400 MHz, C_6D_6

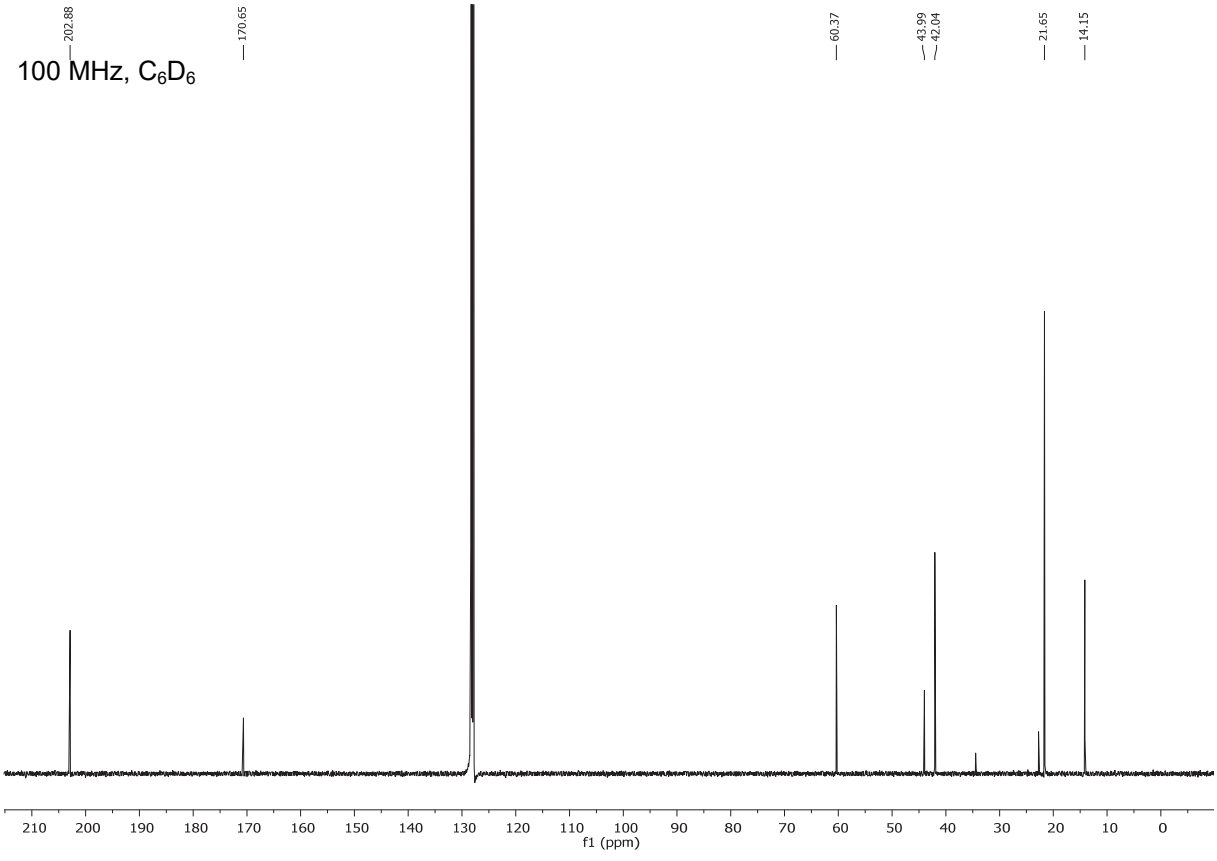

100 MHz, C_6D_6

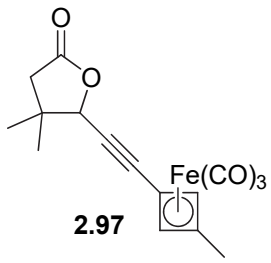

2.97

400 MHz, C_6D_6

100 MHz, C_6D_6

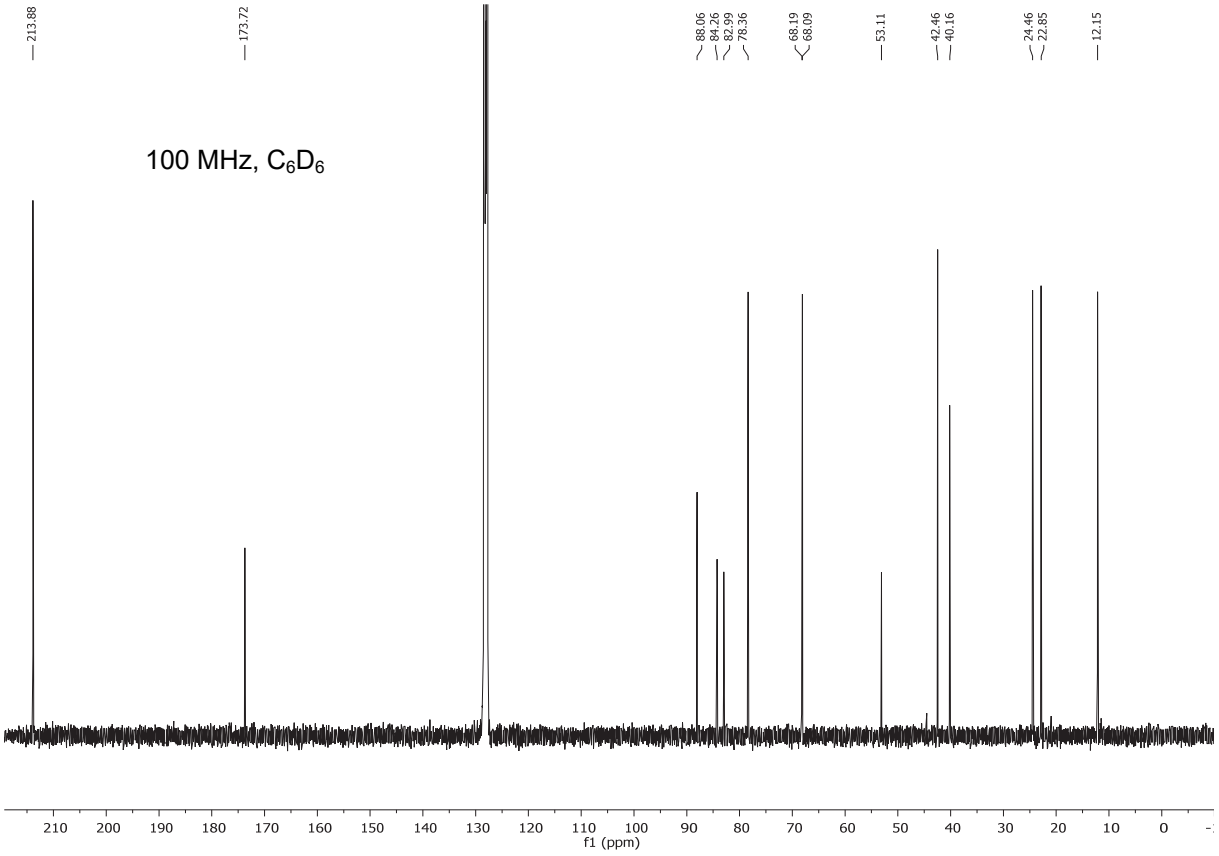

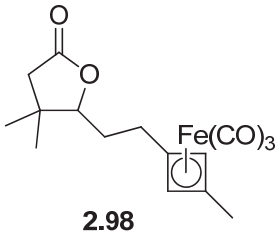

2.98

400 MHz, C_6D_6

100 MHz, C_6D_6

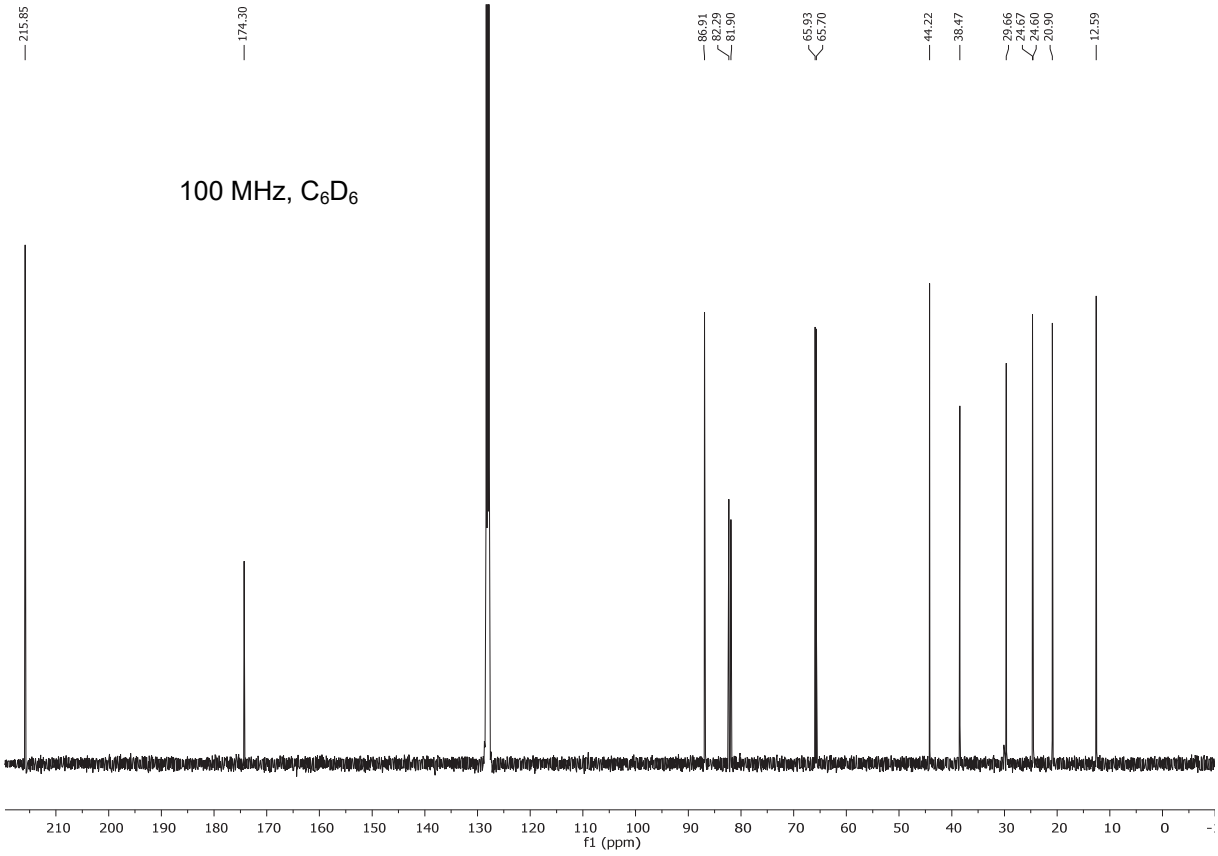

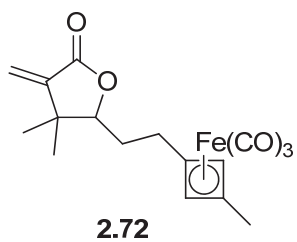

2.72

400 MHz, C_6D_6

100 MHz, C_6D_6

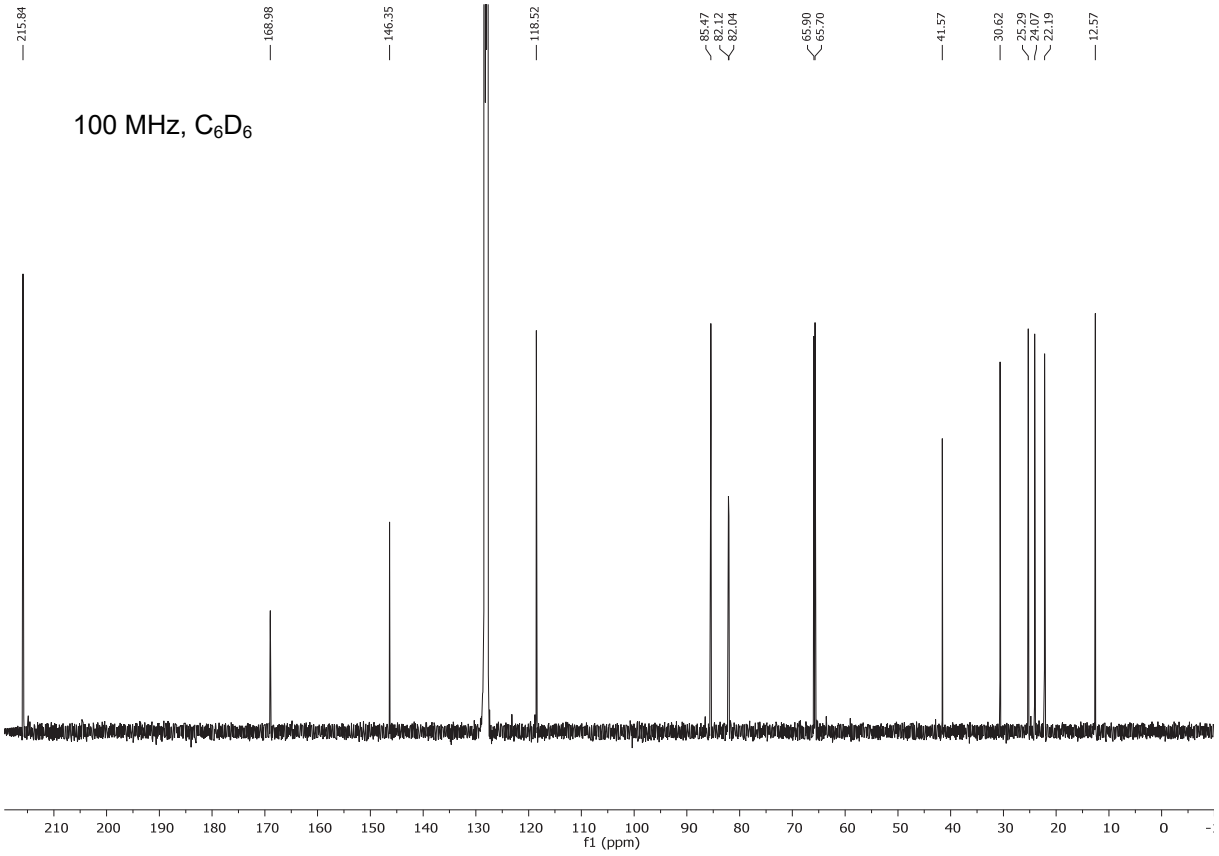

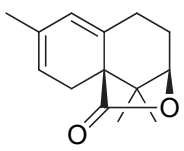

2.100

400 MHz, C_6D_6

100 MHz, C_6D_6

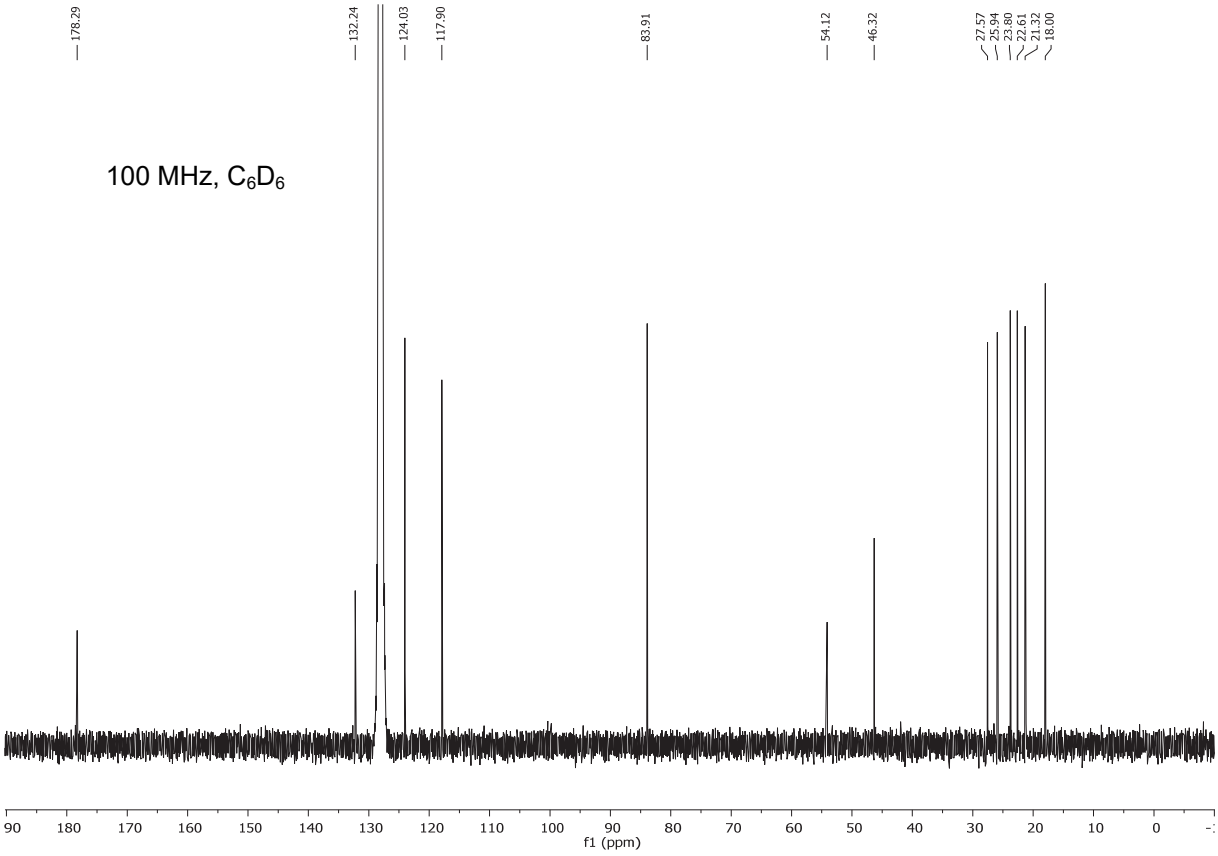

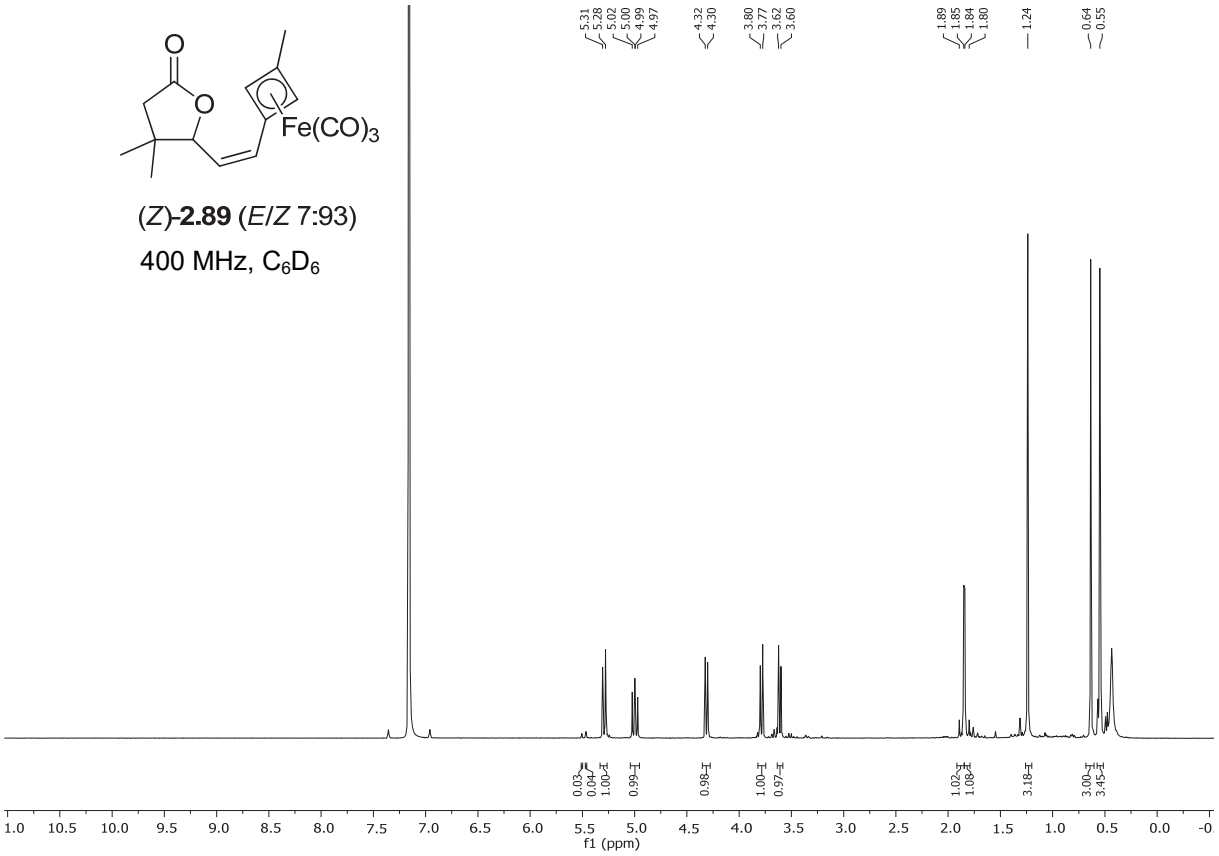

(*Z*)-**2.89** (*E*/*Z* 7:93)

400 MHz, C_6D_6

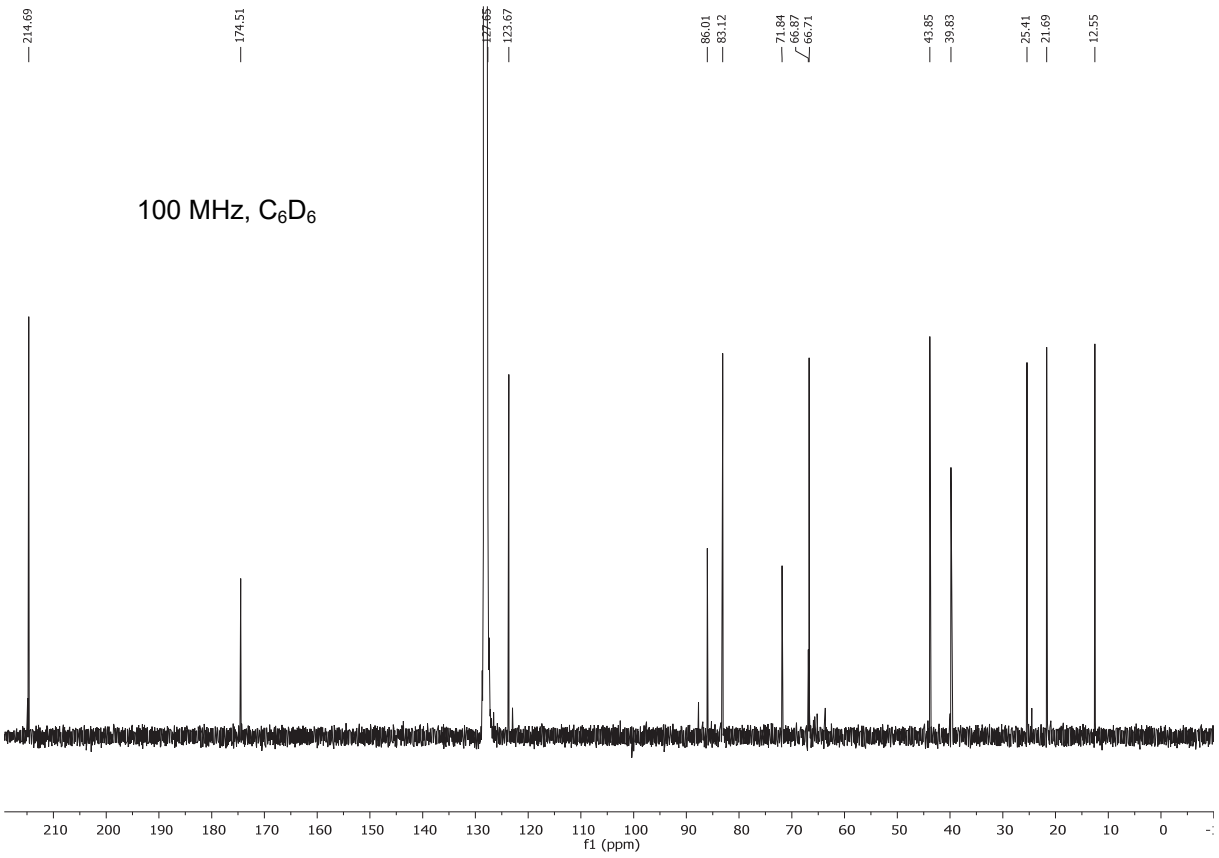

100 MHz, C_6D_6

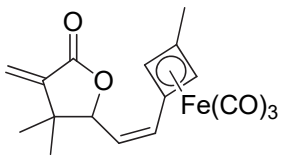

2.106 (*E*/*Z* 15:85)

400 MHz, C_6D_6

100 MHz, C_6D_6

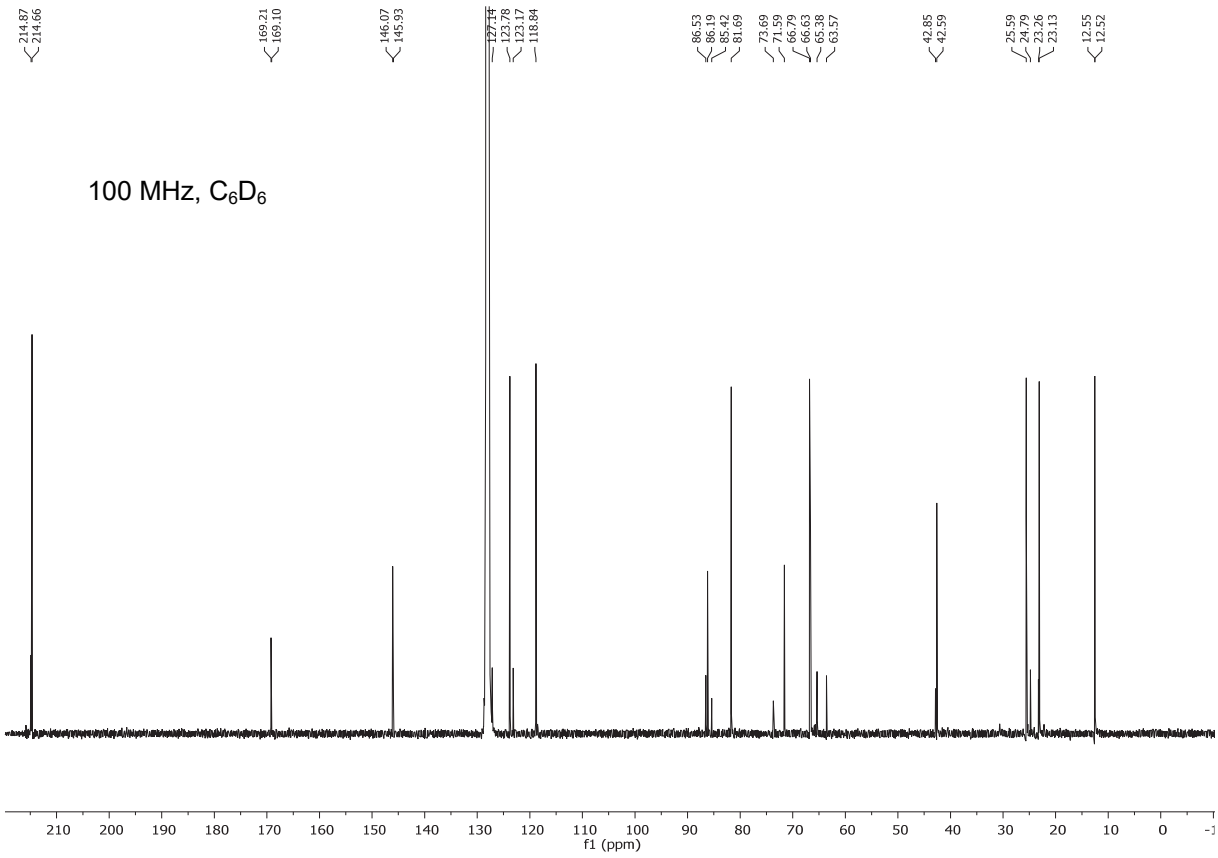

400 MHz, C_6D_6

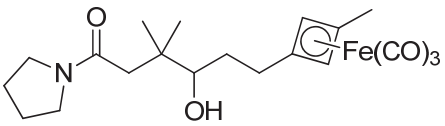

2.114

100 MHz, C_6D_6

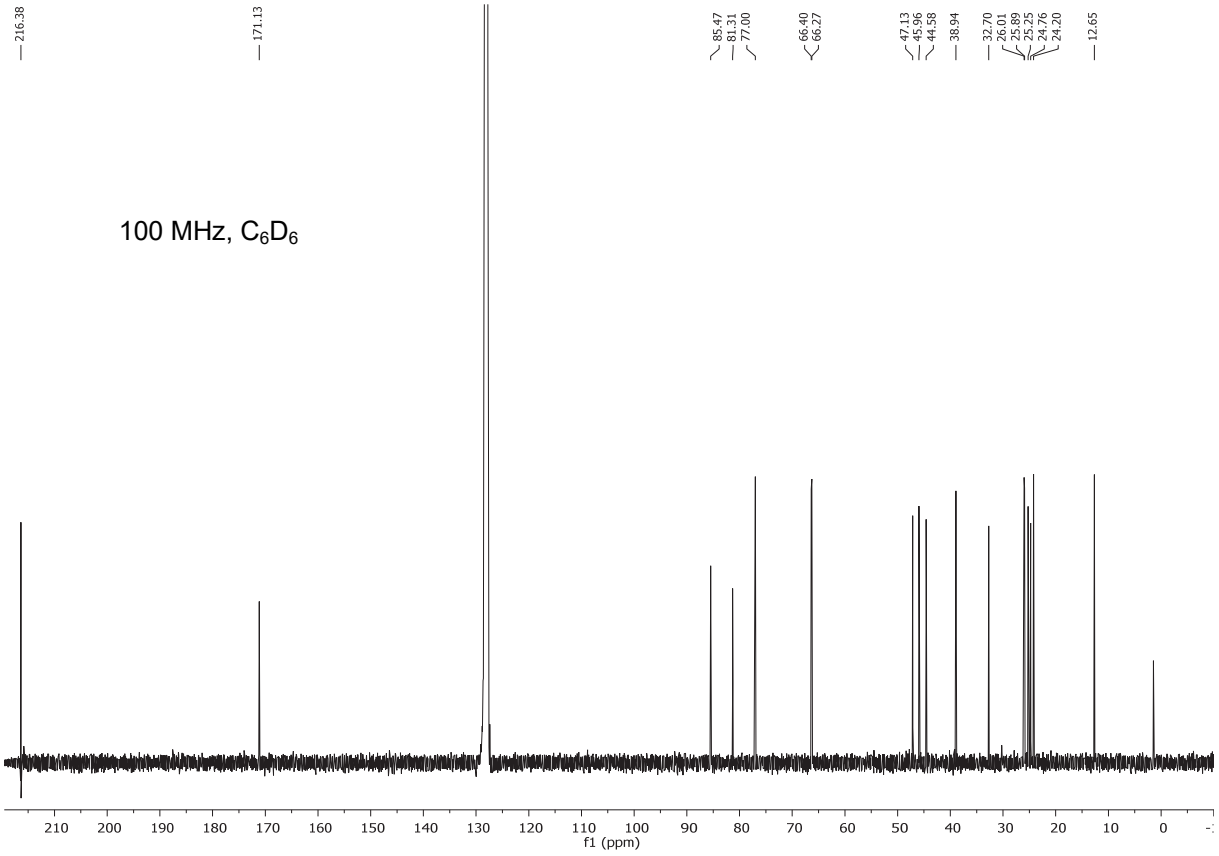

400 MHz, C_6D_6

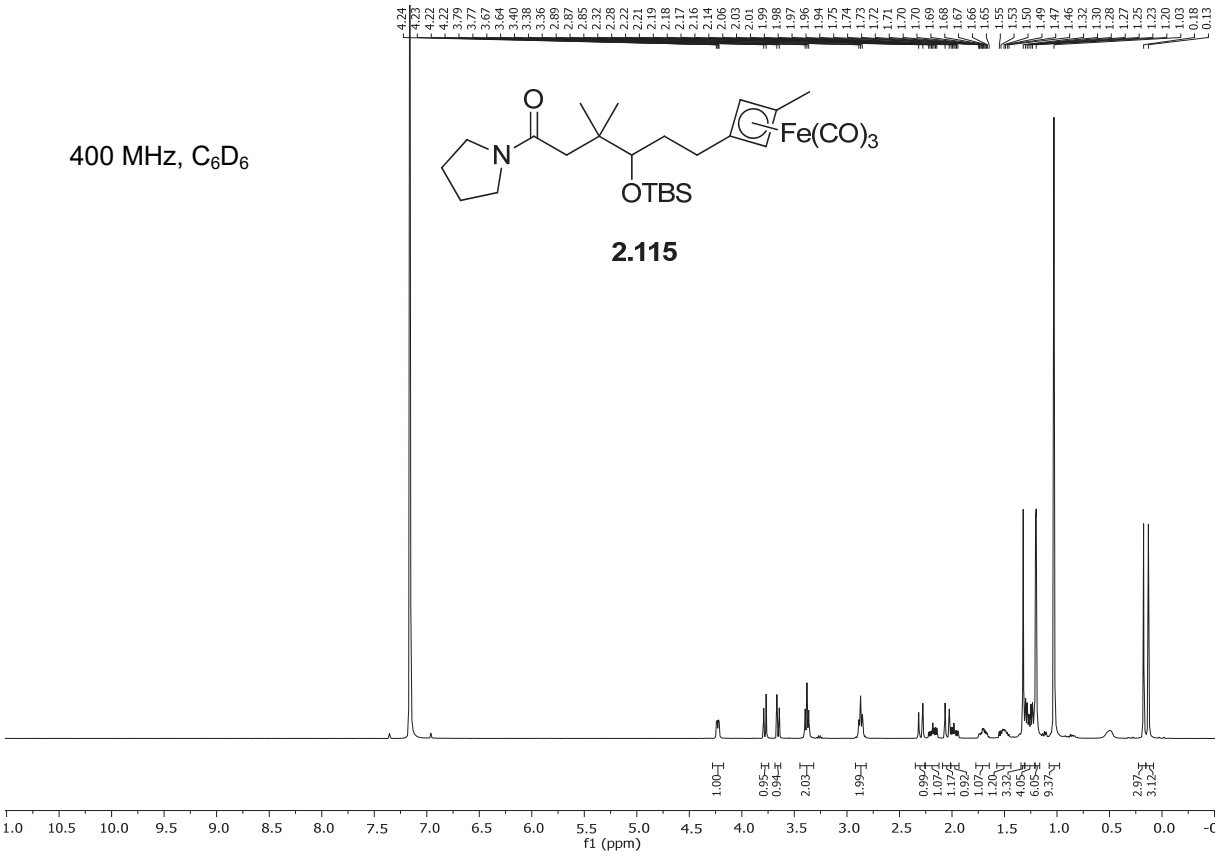

2.115

100 MHz, C_6D_6

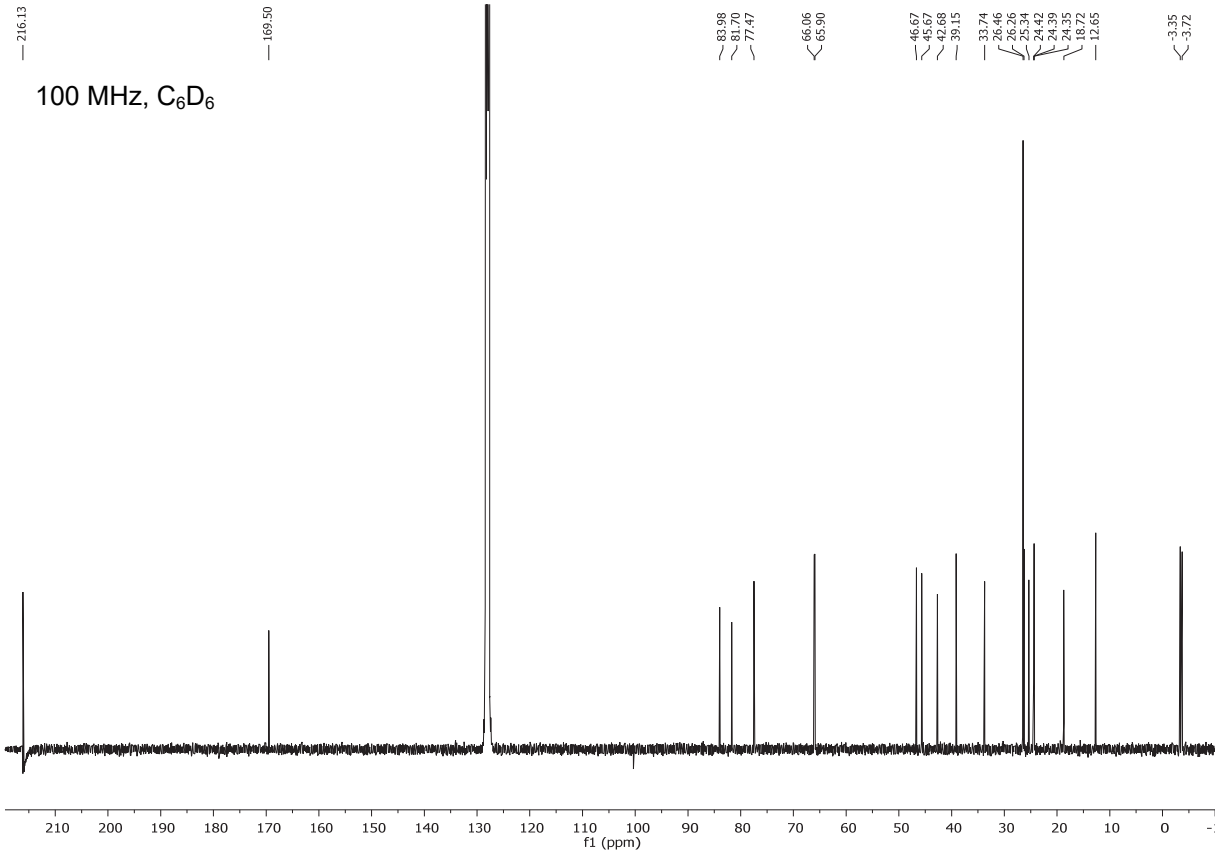

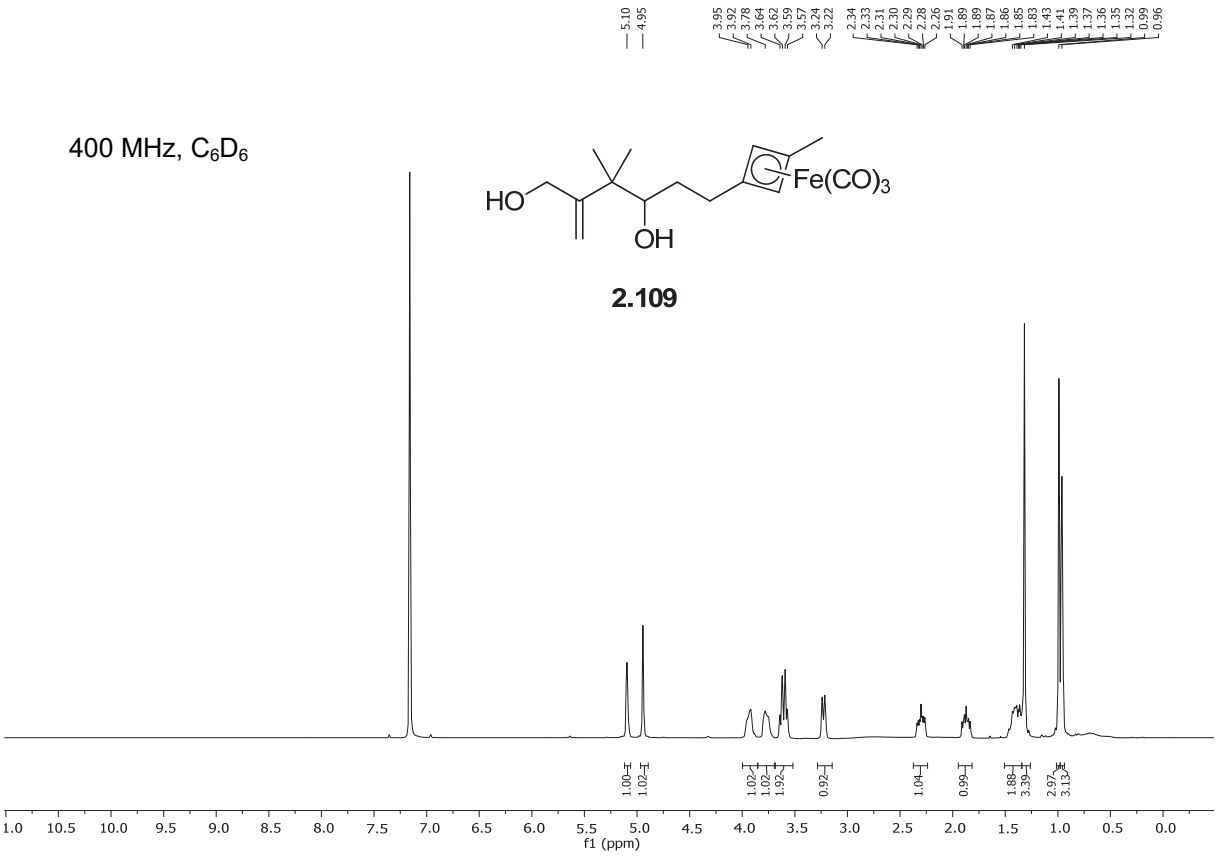
5.10
4.95
3.95
3.92
3.78
3.64
3.62
3.59
3.57
3.24
3.22
2.34
2.33
2.31
2.30
2.29
2.28
2.26
1.91
1.89
1.89
1.87
1.86
1.85
1.83
1.43
1.41
1.39
1.37
1.36
1.35
1.32
0.99
0.96
400 MHz, C6D6
HO
OH
Fe(CO)3
2.109
1.00
1.02
1.02
1.02
1.92
0.92
1.04
0.99
1.88
3.39
2.97
3.13
f1 (ppm)

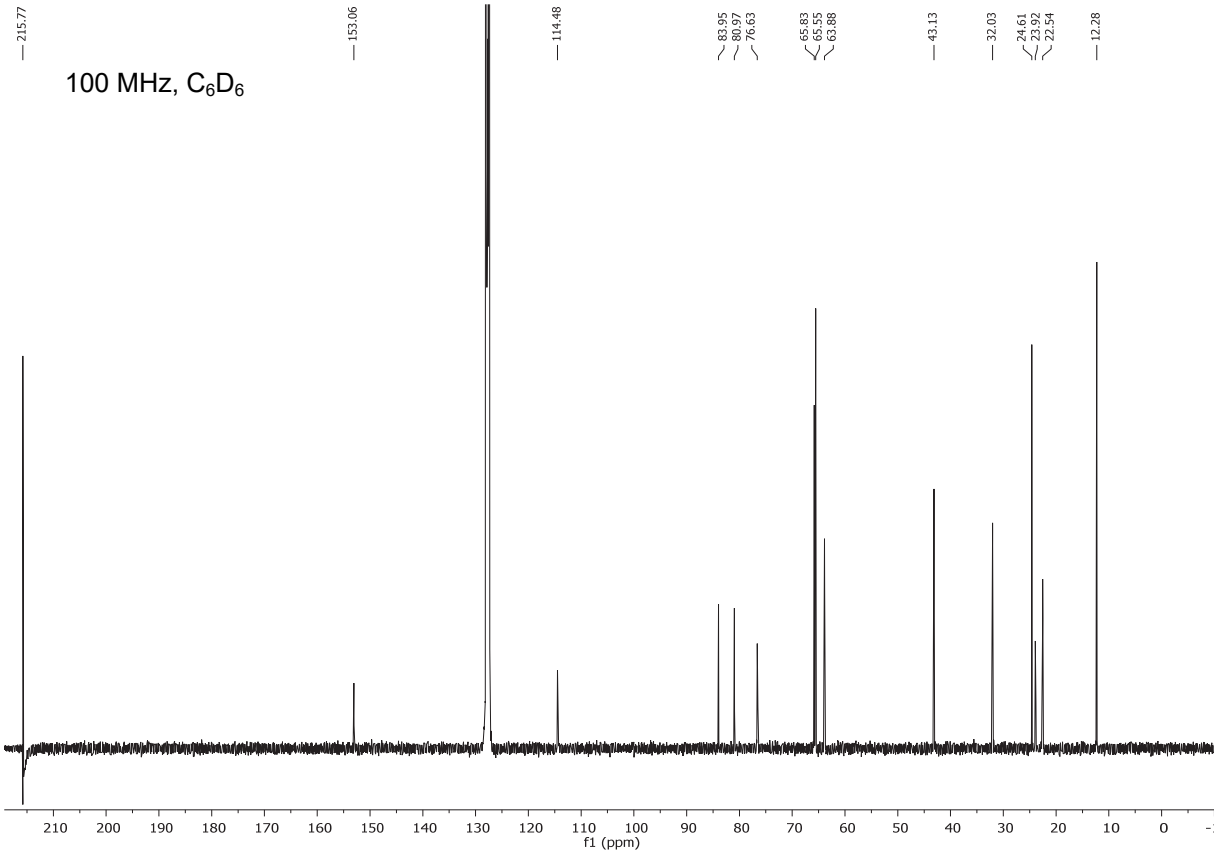
215.77
153.06
114.48
83.95
80.97
76.63
65.83
65.55
63.88
43.13
32.03
24.61
23.92
22.54
12.28
100 MHz, C6D6
f1 (ppm)

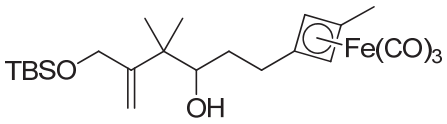

2.110

400 MHz, C_6D_6

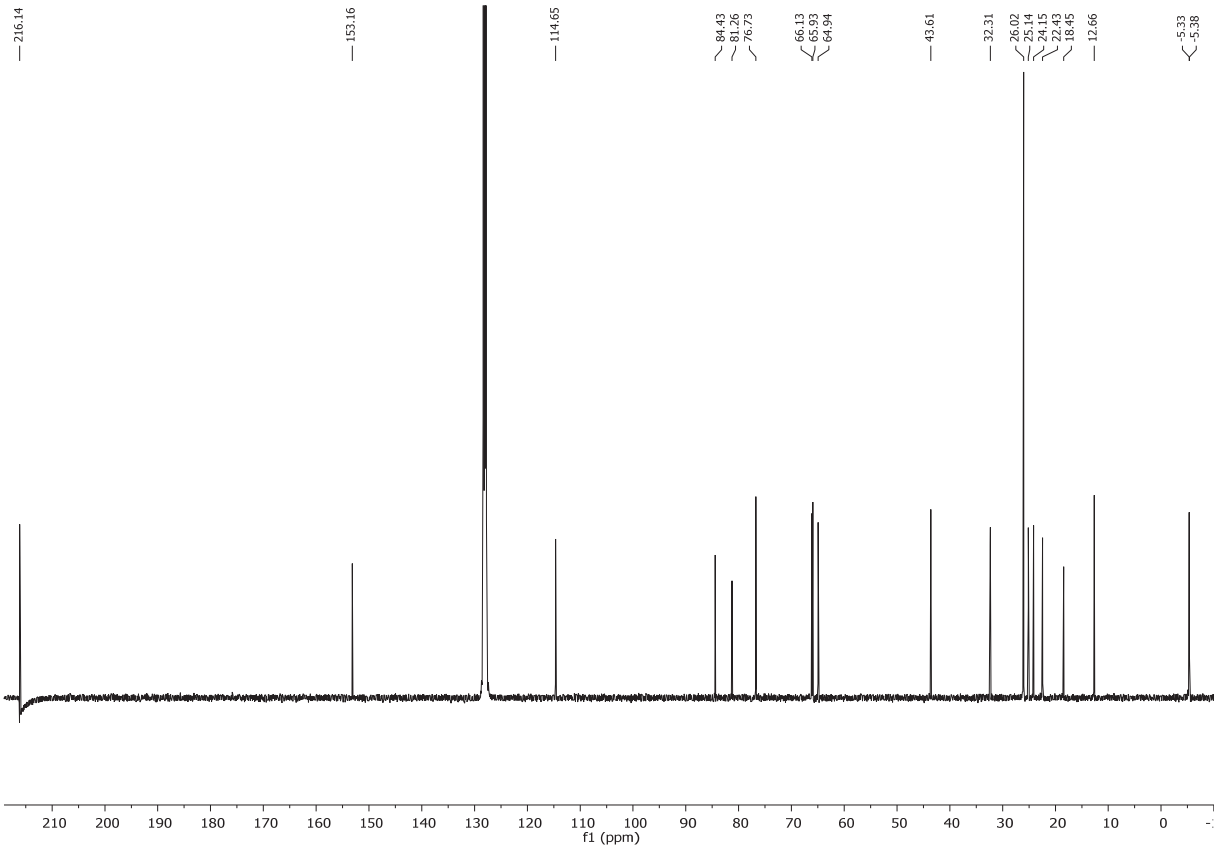

6.1.3 X-ray crystallographic data

Ketal 2.68

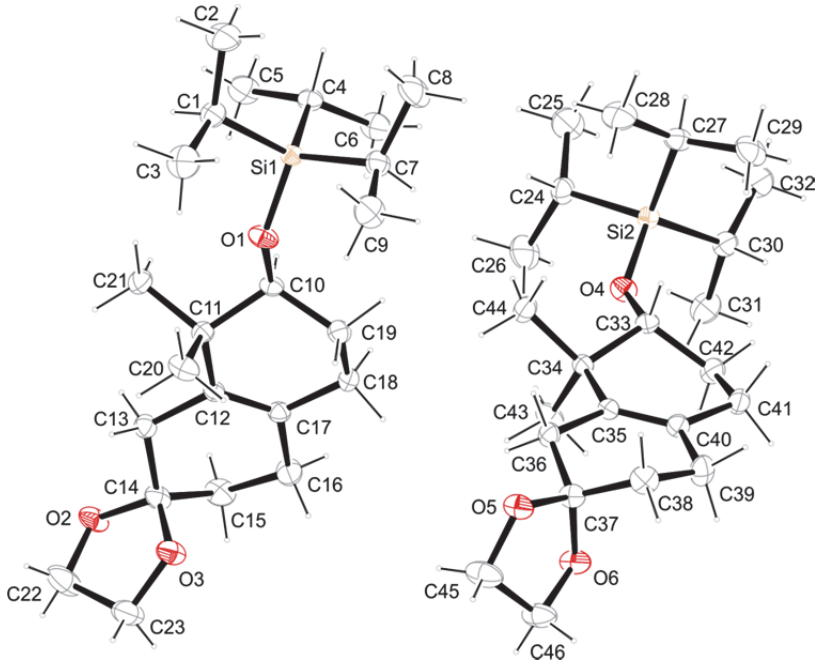

Figure 6.1 ORTEP of the molecular structure of ketal **2.68**.

Table 6.1 Crystallographic data for ketal 2.68.

net formula	$C_{23}H_{42}O_3Si$
M_r/g mol^{-1}	394.663
crystal size/mm	0.510 × 0.382 × 0.152
T/K	173(2)
radiation	MoKα
diffractometer	'Oxford XCalibur'
crystal system	triclinic
space group	'P -1'
a/Å	8.1169(3)
b/Å	13.7341(7)
c/Å	21.3233(9)
α/°	92.039(4)
β/°	95.567(3)
γ/°	90.004(4)
V/Å^3	2364.36(18)
Z	4
calc. density/g cm^{-3}	1.10874(8)
μ/mm^{-1}	0.118
absorption correction	'multi-scan'
transmission factor range	0.57289–1.00000

refls. measured	13675
R_{int}	?
mean σ(I)/I	0.0515
θ range	4.192–28.305
observed refls.	9506
x, y (weighting scheme)	0.1225,
hydrogen refinement	constr
refls in refinement	13675
parameters	504
restraints	0
$R(F_{obs})$	0.0636
$R_w(F^2)$	0.1853
S	0.987
shift/error$_{max}$	0.001
max electron density/e Å^{-3}	0.544
min electron density/e Å^{-3}	−0.376

BASF 0.42.

Iron tricarbonyl complex 2.81

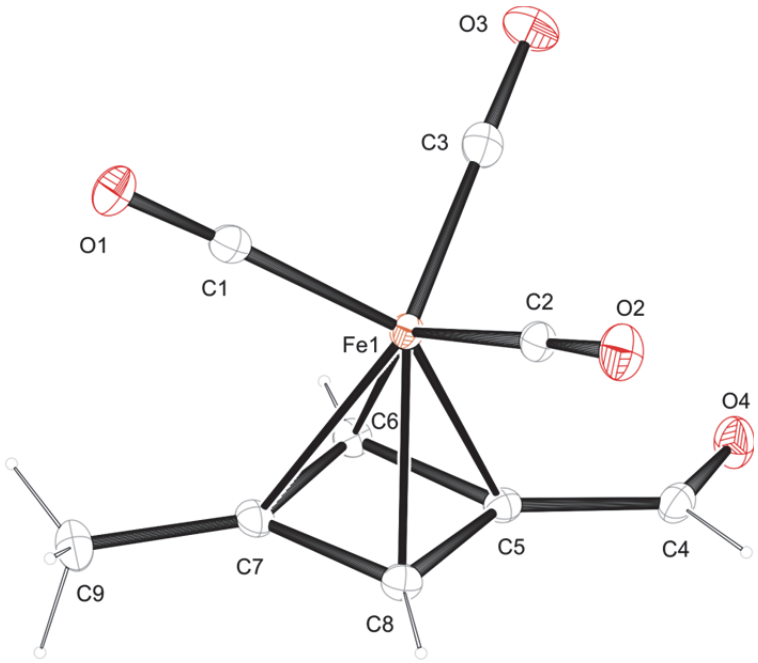

Figure 6.2 ORTEP of the molecular structure of iron tricarbonyl complex **2.81**.

Table 6.2 Crystallographic data for iron tricarbonyl complex 2.81.

net formula	$C_9H_6FeO_4$
Mr/g mol^{-1}	233.99
crystal size/mm	0.120 × 0.060 × 0.010
T/K	100(2)
radiation	MoKα
diffractometer	'Bruker D8Venture'
crystal system	monoclinic
space group	'C 2/c'
a/Å	14.4029(7)
b/Å	6.2050(3)
c/Å	20.8861(10)
α/°	90
β/°	92.2073(16)
γ/°	90
V/Å^3	1865.21(16)
Z	8
calc. density/g cm^{-3}	1.667
μ/mm^{-1}	1.599
absorption correction	multi-scan
transmission factor range	0.6933–0.7454
refls. measured	16100
R_{int}	0.0389
mean σ(I)/I	0.0234
θ range	3.376–26.45
observed refls.	1643
x, y (weighting scheme)	0.0252, 1.5046
hydrogen refinement	refall
refls in refinement	1917
parameters	151
restraints	0
R(F_{obs})	0.0236
Rw(F^2)	0.0532
S	1.063
shift/errormax	0.001
max electron density/e Å^{-3}	0.348
min electron density/e Å^{-3}	−0.191

Lactone 2.84

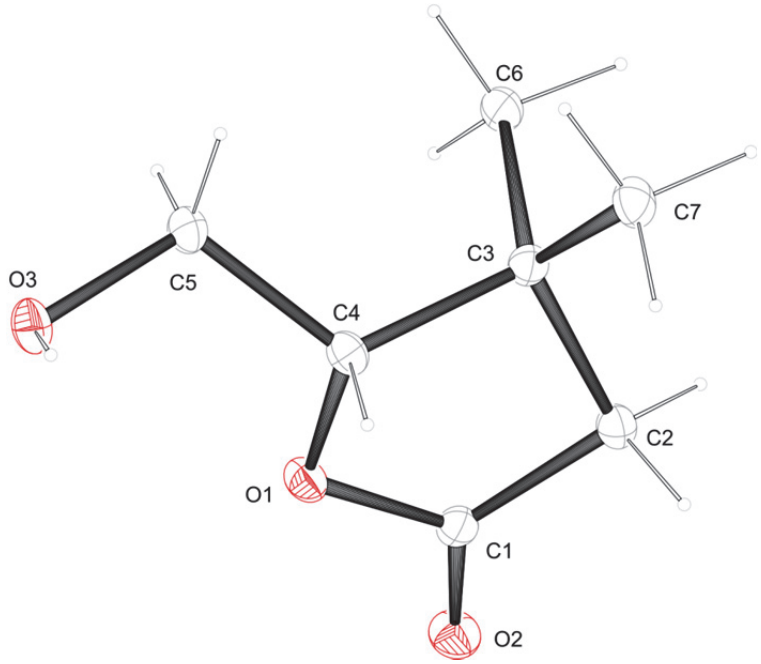

Figure 6.3 ORTEP of the molecular structure of lactone **2.84**.

Table 6.3 Crystallographic data for lactone 2.84.

net formula	$C_7H_{12}O_3$
M_r/g mol^{-1}	144.17
crystal size/mm	0.100 × 0.030 × 0.020
T/K	100(2)
radiation	MoKα
diffractometer	'Bruker D8Venture'
crystal system	monoclinic
space group	'P 21'
a/Å	6.6788(3)
b/Å	6.2350(3)
c/Å	9.0525(4)
α/°	90
β/°	96.602(3)
γ/°	90
V/Å^3	374.47(3)
Z	2
calc. density/g cm^{-3}	1.279
μ/mm^{-1}	0.099
absorption correction	multi-scan

transmission factor range	0.7765–0.9582
refls. measured	3507
R_{int}	0.0245
mean σ(I)/I	0.1000
θ range	3.070–26.39
observed refls.	1068
x, y (weighting scheme)	0.00, 0.00
hydrogen refinement	mixed
Flack parameter	−0.4(10)
refls in refinement	1176
parameters	97
restraints	1
$R(F_{obs})$	0.0382
$R_w(F^2)$	0.1069
S	0.943
shift/error$_{max}$	0.001
max electron density/e Å^{-3}	0.189
min electron density/e Å^{-3}	−0.186

C-H: constr, O-H: refall.

Iron tricarbonyl complex 2.72

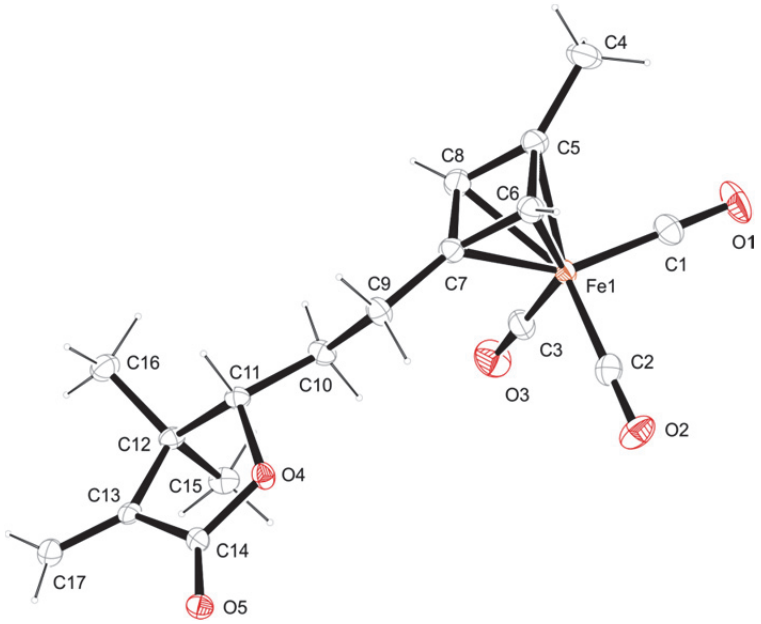

Figure 6.4 ORTEP of the molecular structure of iron tricarbonyl complex **2.72**.

Table 6.4 Crystallographic data for iron tricarbonyl complex 2.72.

net formula	$C_{17}H_{18}FeO_5$
M_r/g mol^{-1}	358.16
crystal size/mm	0.090 × 0.030 × 0.010
T/K	100(2)
radiation	MoKα
diffractometer	'Bruker D8Venture'
crystal system	monoclinic
space group	'P 21/c'
a/Å	11.8594(9)
b/Å	18.1861(14)
c/Å	7.7976(7)
α/°	90
β/°	94.188(2)
γ/°	90
V/Å^3	1677.3(2)
Z	4
calc. density/g cm^{-3}	1.418
μ/mm^{-1}	0.920
absorption correction	multi-scan
transmission factor range	0.6646–0.7452
refls. measured	28158
R_{int}	0.0660
mean σ(*I*)/*I*	0.0373
θ range	3.229–25.12
observed refls.	2342
x, y (weighting scheme)	0.0314, 1.9213
hydrogen refinement	constr
refls in refinement	2981
parameters	211
restraints	0
$R(F_{obs})$	0.0357
$R_w(F^2)$	0.0878
S	1.033
shift/error$_{max}$	0.001
max electron density/e Å^{-3}	0.611
min electron density/e Å^{-3}	−0.405

6.2 Supporting information for Chapter 2.2.1.6

6.2.1 Experimental procedures

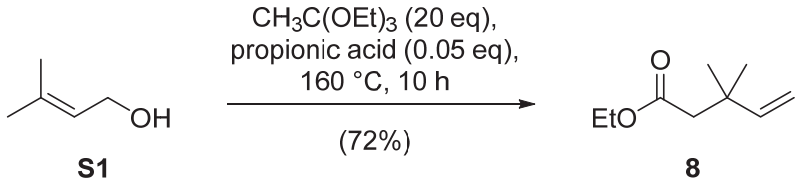

S1 **8**

Ethyl 3,3-dimethylpent-4-enoate (8) A stirred solution of prenol (**S1**, 19.5 mL, 191 mmol, 1.0 eq) and propionic acid (715 µL, 9.55 mmol, 0.05 eq) in triethylorthoacetate (700 mL, 3.82 mol, 20 eq) was refluxed for 10 h. The reaction mixture was poured into a solution of conc. H_2SO_4 (50 mL) in ice-water (800 mL) and the resulting mixture was stirred for 24 h at r.t. The layers were separated and the aqueous layer was extracted with Et_2O (3 × 500 mL). The combined organic layers were washed with sat. aq. Na_2CO_3 solution (5 × 400 mL), brine (500 mL) and dried over Na_2SO_4. After filtration and concentration *in vacuo*, the crude product was purified by distillation under reduced pressure (80 – 90 °C, 75 – 89 mbar) to afford ethyl ester **8** (21.5 g, 138 mmol, 72%) as a colorless liquid. Compound **8** has been reported in the literature.[130]

Data for 8: R_f: 0.71 (hexanes:EtOAc 7:1); **^{1}H NMR (400 MHz, $CDCl_3$):** δ = 5.89 (dd, J = 17.4, 10.7 Hz, 1H), 5.01 – 4.90 (m, 2H), 4.10 (q, J = 7.1 Hz, 2H), 2.28 (s, 2H), 1.24 (t, J = 7.1 Hz, 3H), 1.13 (s, 6H) ppm; **^{13}C NMR (100 MHz, $CDCl_3$):** δ = 171.9, 147.0, 110.9, 60.2, 47.0, 36.3, 27.1, 14.5 ppm; **IR (ATR):** ν_{max} = 3086 (w), 2966 (w), 2932 (w), 2873 (w), 1731 (s), 1641 (w), 1465 (w), 1447 (w), 1416 (w), 1367 (m), 1325 (w), 1236 (m), 1207 (m), 1126 (m), 1096 (w), 1033 (w), 999 (w), 913 (m), 845 (w), 792 (w), 715 (w), 678 (w) cm^{-1}; **HRMS (EI):** calc. for $C_9H_{16}O_2$ $[M]^+$: 156.1145, found: 156.1150.

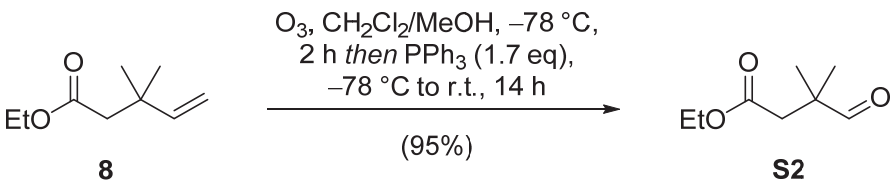

8 **S2**

Ethyl 3,3-dimethyl-4-oxobutanoate (S2) Ozone was bubbled through a stirred solution of ester **8** (21.5 g, 138 mmol, 1.0 eq) in CH_2Cl_2/MeOH (500 mL, 4:1) at –78 °C. After a slightly blue color persisted (2 h), N_2 was bubbled through the reaction mixture for 15 min followed by addition of PPh_3 (61.3 g, 234 mmol, 1.7 eq). The resulting mixture was stirred at r.t. for 14 h. After concentration *in vacuo*, the crude product was purified by flash column

chromatography (pentane:Et_2O 9:1) on silica to afford aldehyde **S2** (20.7 g, 131 mmol, 95%) as a colorless liquid. **S2** was stored as solution in THF (72 mL) at –20 °C. Compound **S2** has been reported in the literature.[130,160]

Data for S2: R_f: 0.77 (hexanes:EtOAc 4:1); **^{1}H NMR (400 MHz, C_6D_6):** δ = 9.33 (s, 1H), 3.84 (q, J = 7.1 Hz, 2H), 2.17 (s, 2H), 0.89 (t, J = 7.1 Hz, 3H), 0.82 (s, 6H) ppm; **^{13}C NMR (100 MHz, C_6D_6):** δ = 202.9, 170.7, 60.4, 44.0, 42.0, 21.7, 14.2 ppm; **IR (ATR):** ν_{max} = 2980 (w), 2938 (w), 2877 (w), 2815 (w), 2713 (w), 1727 (s), 1472 (w), 1448 (w), 1397 (w), 1370 (m), 1342 (m), 1207 (m), 1135 (m), 1097 (m), 1032 (m), 948 (w), 922 (w), 888 (m), 860 (w), 808 (w), 733 (w) cm^{-1}; **HRMS (EI):** calc. for $C_8H_{14}O_3$ $[M]^+$: 158.0937, found: 158.0940.

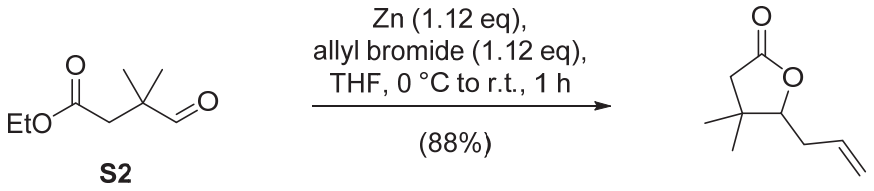

S2 **S3**

Lactone S3 Zn powder (16.0 g) was activated by stirring with aq. 2% HCl (200 mL) for 5 min at r.t. After filtration, the grey powder was washed with EtOH (100 mL), acetone (100 mL) and Et_2O (100 mL) and then dried under high vacuum at 80 °C for 15 min. To a stirred suspension of activated Zn powder (9.58 g, 147 mmol, 1.12 eq) in THF (50 mL) at 0 °C was added allyl bromide (12.6 mL, 147 mmol, 1.12 eq) in THF (50 mL) *via* canula. After 45 min at r.t., **S2** (20.7 g, 131 mmol, 1.00 eq) in THF (50 mL) was added *via* canula at 0 °C and the resulting reaction mixture was stirred for 1 h at r.t. The reaction was quenched by addition of H_2O (200 mL) and then filtered over Celite (Et_2O), followed by extraction with Et_2O (2 × 200 mL). The combined organic layers were dried over Na_2SO_4. After filtration and concentration *in vacuo*, the crude product was purified by flash column chromatography (pentane:Et_2O 9:1→3:1) on silica to afford lactone **S3** (17.8 g, 115 mmol, 88%) as a colorless liquid.

Data for S3: R_f: 0.48 (hexanes:EtOAc 4:1); **^{1}H NMR (400 MHz, C_6D_6):** δ = 5.77 – 5.63 (m, 1H), 5.03 – 4.95 (m, 2H), 3.50 (dd, J = 9.5, 3.9 Hz, 1H), 2.07 – 1.92 (m, 1H), 1.84 – 1.69 (m, 3H), 0.47 (s, 3H), 0.46 (s, 3H) ppm; **^{13}C NMR (100 MHz, C_6D_6):** δ = 174.4, 134.5, 117.5, 86.9, 44.4, 38.6, 33.9, 24.8, 20.9 ppm; **IR (ATR):** ν_{max} = 3079 (w), 2964 (w), 2936 (w), 2876 (w), 1772 (s), 1643 (w), 1467 (w), 1421 (w), 1373 (w), 1345 (w), 1287 (m), 1229 (m), 1197 (m), 1160 (m), 1116 (m), 1078 (w), 1026 (m), 992 (s), 974 (s), 949 (w), 923 (s), 913(s),

866 (w), 826 (w), 800 (w), 672 (w) cm^{-1}; **HRMS (EI):** calc. for $C_9H_{14}O_2$ $[M]^+$: 154.0988, found: 154.0941.

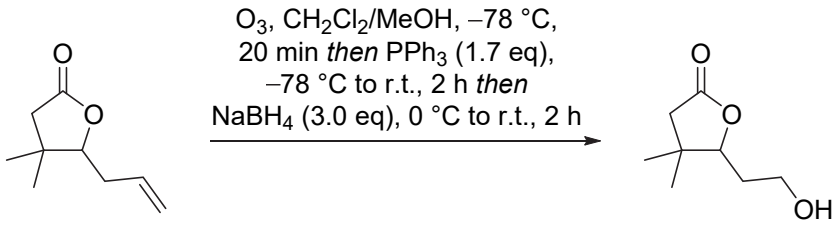

S3 **S4**

Alcohol S4 Ozone was bubbled through a stirred solution of lactone **S3** (2.98 g, 19.3 mmol, 1.0 eq) in CH_2Cl_2/MeOH (64 mL, 4:1) at –78 °C. After a slightly blue color persisted (20 min), N_2 was bubbled through the reaction mixture for 15 min followed by addition of PPh_3 (8.60 g, 32.8 mmol, 1.7 eq). The resulting mixture was stirred at r.t. for 2 h. $NaBH_4$ (2.19 g, 57.9 mmol, 3.0 eq) was added portionwise at 0 °C and the resulting reaction mixture was stirred at r.t. for 2 h. The reaction was quenched by addition of sat. aq. NH_4Cl solution (75 mL) and H_2O (25 mL) at 0 °C and the resulting mixture was stirred for 20 min. The layers were separated and the aqueous layer was extracted with CH_2Cl_2 (100 mL) and EtOAc (6 × 30 mL). The combined organic layers were dried over Na_2SO_4. After filtration and concentration *in vacuo*, the crude product was purified by flash column chromatography (Et_2O) on silica to afford alcohol **S4**, inseparable from PPh_3O impurities. Crude **S4** was used without further purification in the next step.

Data for S4: R_f: 0.20 (hexanes:EtOAc 1:1); **^{1}H NMR (400 MHz, C_6D_6):** δ = 3.71 (dd, J = 10.4, 2.7 Hz, 1H), 3.47 – 3.35 (m, 2H), 1.78 (d, J = 16.6 Hz, 1H), 1.72 (d, J = 16.7 Hz, 1H), 1.29 – 1.11 (m, 2H), 0.82 (s, 1H), 0.46 (s, 3H), 0.43 (s, 3H) ppm; **^{13}C NMR (100 MHz, C_6D_6):** δ = 174.9, 84.7, 59.6, 44.3, 38.4, 31.9, 24.4, 21.0 ppm; **HRMS (ESI):** calc. for $C_8H_{18}NO_3$ $[M+NH_4]^+$: 176.1281, found: 176.1281.

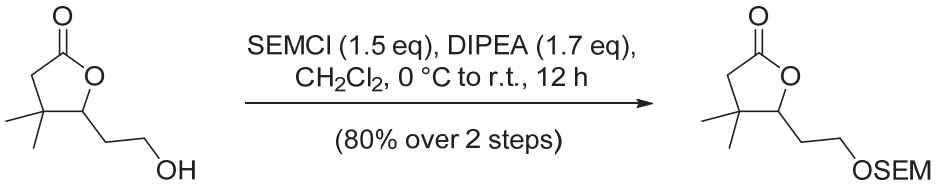

S4 **9**

Protected lactone 9 To a stirred solution of crude alcohol **S4** in CH_2Cl_2 (120 mL) at 0 °C was added DIPEA (5.58 mL, 32.8 mmol, 1.7 eq) and SEMCl (5.13 mL, 29.0 mmol, 1.5 eq).

The resulting reaction mixture was allowed to warm up to r.t. overnight and was quenched by addition of H_2O (200 mL). The layers were separated and the aqueous layer was extracted with CH_2Cl_2 (50 mL) and EtOAc (5 × 50 mL). The combined organic layers were dried over Na_2SO_4. After filtration and concentration *in vacuo*, the crude product was purified by flash column chromatography (pentane:Et_2O 3:1) on silica to afford SEM protected lactone **9** (4.44 g, 15.4 mmol, 80% over 2 steps) as a colorless oil.

Data for 9: R_f: 0.44 (hexanes:EtOAc 4:1); **^{1}H NMR (400 MHz, C_6D_6):** δ = 4.61 (s, 2H), 3.92 (dd, J = 10.6, 2.6 Hz, 1H), 3.70 – 3.56 (m, 4H), 1.85 – 1.71 (m, 2H), 1.53 – 1.33 (m, 2H), 1.04 – 0.93 (m, 2H), 0.52 (s, 3H), 0.46 (s, 3H), 0.02 (s, 9H) ppm; **^{13}C NMR (100 MHz, C_6D_6):** δ = 174.5, 95.3, 84.2, 65.3, 64.6, 44.4, 38.3, 29.8, 24.6, 21.0, 18.3, –1.3 ppm; **IR (ATR):** ν_{max} = 2955 (w), 2932 (w), 2877 (w), 1778 (s), 1467 (w), 1422 (w), 1395 (w), 1374 (w), 1350 (w), 1287 (w), 1247 (m), 1231 (m), 1197 (m), 1163 (m), 1143 (w), 1111 (m), 1057 (s), 1033 (s), 968 (m), 955 (m), 927 (m), 959 (s), 764 (w), 694 (w) cm^{-1}; **HRMS (ESI):** calc. for $C_{14}H_{32}NO_4Si$ [M+NH_4]$^+$: 306.2095, found: 306.2099.

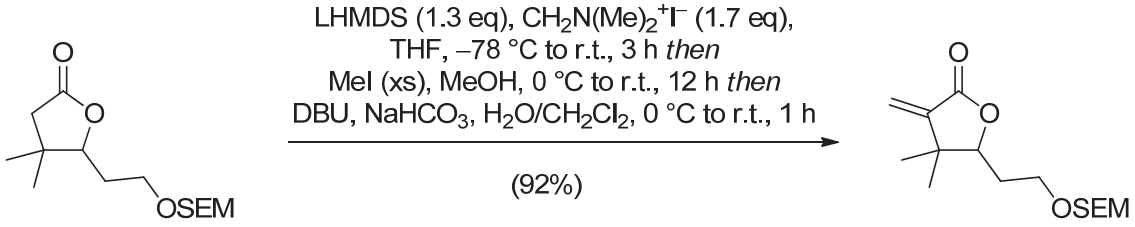

9 **S5**

Enone S5 The following procedure was performed in two separate flasks with identical amounts of substrate and reagents and the reactions were combined for work up and purification. To a stirred solution of lactone **9** (3.00 g, 10.4 mmol, 1.0 eq) in THF (130 mL) at –78 °C was added LHMDS (1.0 M in THF, 13.5 mL, 13.5 mmol, 1.3 eq) and the resulting mixture was allowed to warm up to –50 °C within 2.5 h. Eschenmoser's salt (3.27 g, 17.7 mmol, 1.7 eq) was added to the reaction mixture in one portion at –78 °C and the resulting reaction mixture was allowed to warm up to r.t. over 3 h. The solvent was evaporated and the crude material was dissolved in MeOH (30 mL). Methyliodide (13 mL) was added dropwise at 0 °C and the reaction was allowed to warm up to r.t. overnight. The solvent was evaporated and the crude material was dissolved in CH_2Cl_2 (150 mL). Aq. 5% $NaHCO_3$ solution (115 mL) and DBU (15.5 mL, 104 mmol, 10 eq) were added at 0 °C and the resulting reaction mixture was stirred at r.t. for 1 h followed by addition of H_2O (100 mL). The separate reactions were combined and the layers were separated. The aqueous layer was extracted with CH_2Cl_2 (100 mL) and Et_2O (3 × 100 mL). The combined organic layers were dried over Na_2SO_4. After filtration and concentration *in vacuo*, the crude product was purified

by flash column chromatography (pentane:Et_2O 4:1) on silica to afford enone **S5** (5.76 g, 19.2 mmol, 92%) as a colorless oil.

Data for S5: R_f: 0.39 (hexanes:EtOAc 4:1); **^{1}H NMR (400 MHz, C_6D_6):** δ = 6.03 (s, 1H), 4.84 (s, 1H), 4.59 (s, 2H), 4.00 (dd, *J* = 11.0, 2.5 Hz, 1H), 3.72 – 3.62 (m, 3H), 3.62 – 3.54 (m, 1H), 1.58 – 1.46 (m, 1H), 1.42 – 1.32 (m, 1H), 1.03 – 0.94 (m, 2H), 0.69 (s, 3H), 0.58 (s, 3H), 0.02 (s, 9H) ppm; **^{13}C NMR (100 MHz, C_6D_6):** δ = 169.1, 146.7, 118.2, 95.3, 83.0, 65.3, 64.2, 41.4, 30.7, 25.0, 22.4, 18.3, –1.3 ppm; **IR (ATR):** ν_{max} = 2955 (w), 2923 (w), 2876 (w), 1765 (s), 1661 (w), 1465 (w), 1410 (w), 1370 (w), 1345 (w), 1295 (m), 1248 (m), 1192 (m), 1109 (m), 1055 (s), 1030 (s), 967 (m), 937 (m), 858 (s), 833 (s), 758 (w), 692 (m) cm^{-1}; **HRMS (ESI):** calc. for $C_{15}H_{32}NO_4Si$ $[M+NH_4]^+$: 318.2095, found: 318.2099.

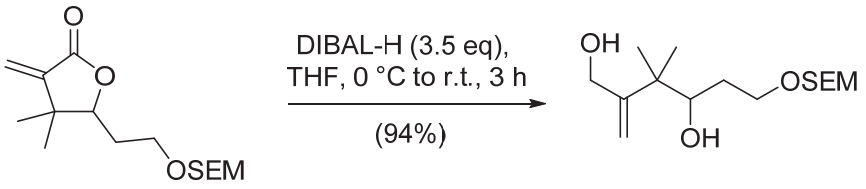

S5 **S6**

Diol S6 The following procedure was performed in two separate flasks with identical amounts of substrate and reagents and the reactions were combined for work up and purification. To a stirred solution of enone **S5** (2.88 g, 9.58 mmol, 1.0 eq) in THF (120 mL) at 0 °C was slowly added DIBAL-H (1.0 M in THF, 33.5 mL, 33.5 mmol, 3.5 eq). The resulting reaction mixture was allowed to warm up to r.t. over 3 h. The reaction mixture was poured in a mixture of ice-water (200 mL), Et_2O (200 mL) and aq. sat. K^+-Na^+-tartrate solution (600 mL) and stirred at r.t. for 2 h. The separate reactions were combined and the layers were separated. The aqueous layer was extracted with EtOAc (3 × 200 mL). The combined organic layers were dried over Na_2SO_4. After filtration and concentration *in vacuo*, the crude product was purified by flash column chromatography (hexanes:EtOAc 2:1) on silica to afford diol **S6** (5.50 g, 18.1 mmol, 94%) as a colorless oil.

Data for S6: R_f: 0.33 (hexanes:EtOAc 2:1); **^{1}H NMR (400 MHz, C_6D_6):** δ = 5.17 (d, *J* = 1.2 Hz, 1H), 4.95 (d, *J* = 1.4 Hz, 1H), 4.48 (s, 2H), 4.13 (dd, *J* = 12.8, 1.0 Hz, 1H), 3.97 (dd, *J* = 12.8, 1.0 Hz, 1H), 3.73 – 3.55 (m, 5H), 1.63 – 1.55 (m, 2H), 1.06 (s, 3H), 1.04 (s, 3H), 0.97 – 0.90 (m, 2H), 0.01 (s, 9H) ppm; **^{13}C NMR (100 MHz, C_6D_6):** δ = 154.3, 113.6, 95.2, 76.7, 67.2, 65.4, 64.4, 43.1, 31.9, 23.9, 23.7, 18.3, –1.3 ppm; **IR (ATR):** ν_{max} = 3361 (br w) 2954 (w), 2877 (w), 1635 (w), 1469 (w), 1409 (w), 1380 (w), 1248 (m), 1191 (w), 1152 (w),

1109 (m), 1054 (s), 1023 (s), 971 (w), 936 (m), 919 (m), 905 (m), 857 (s), 833 (s), 757 (m), 692 (w), 664 (w) cm^{-1}; **HRMS (ESI):** calc. for $C_{15}H_{33}O_4Si$ $[M+H]^+$: 305.2143, found: 305.2145.

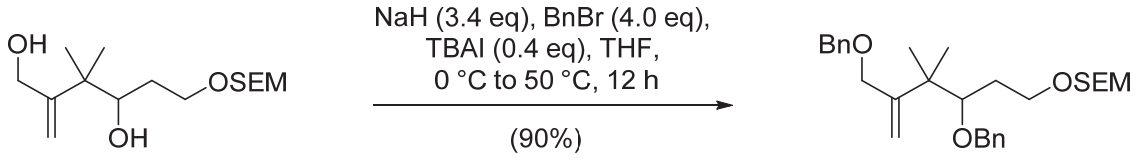

S6 **S7**

Protected triol S7 The following procedure was performed in two separate flasks with identical amounts of substrate and reagents and the reactions were combined for work up and purification. To a stirred solution of diol **S6** (2.00 g, 6.57 mmol, 1.0 eq) in THF (15 mL) at 0 °C was slowly added NaH (60% dispersion in mineral oil, 892 mg, 22.3 mmol, 3.4 eq). The resulting reaction mixture was allowed to warm up to r.t. for 40 min followed by the addition of benzyl bromide (3.13 mL, 26.3 mmol, 4.0 eq) and TBAI (971 mg, 2.63 mmol, 0.4 eq). The resulting reaction mixture was heated to 50 °C overnight and was poured afterwards in ice-water (200 mL). The separate reactions were combined and the layers were separated. The aqueous layer was extracted with EtOAc (3 × 200 mL). The combined organic layers were dried over Na_2SO_4. After filtration and concentration *in vacuo*, the crude product was purified by flash column chromatography (hexanes:EtOAc 30:1) on silica to afford protected triol **S7** (5.70 g, 11.8 mmol, 90%) as colorless oil.

Data for S7: R_f: 0.56 (hexanes:EtOAc 9:1); **^{1}H NMR (400 MHz, $CDCl_3$):** δ = 7.40 – 7.27 (m, 10H), 5.30 (d, J = 1.3 Hz, 1H), 5.11 (s, 1H), 4.68 – 4.55 (m, 4H), 4.52 (s, 2H), 4.16 – 4.07 (m, 2H), 3.66 – 3.55 (m, 4H), 3.52 (dd, J = 9.8, 2.1 Hz, 1H), 1.87 – 1.75 (m, 1H), 1.67 – 1.58 (m, 1H), 1.18 (s, 3H), 1.14 (s, 3H), 0.96 – 0.88 (m, 2H), 0.00 (s, 9H) ppm; **^{13}C NMR (100 MHz, $CDCl_3$):** δ = 150.8, 139.1, 138.7, 128.5, 128.4, 127.7, 127.6, 127.6, 127.5, 112.2, 95.0, 82.7, 75.3, 72.5, 71.2, 65.5, 65.3, 43.7, 32.1, 25.3, 22.5, 18.3, –1.3 ppm; **IR (ATR):** ν_{max} = 3089 (w), 3064 (w), 3031 (w), 2953 (w), 2925 (w), 2871 (w), 1635 (w), 1496 (w), 1453 (w), 1378 (w), 1361 (w), 1306 (w), 1248 (m), 1204 (w), 1155 (w), 1093 (s), 1058 (s), 1027 (s), 935 (m), 918 (m), 857 (s), 833 (s), 732 (s), 695 (s), 605 (m) cm^{-1}; **HRMS (ESI):** calc. for $C_{29}H_{48}NO_4Si$ $[M+NH_4]^+$: 502.3347, found: 502.3355.

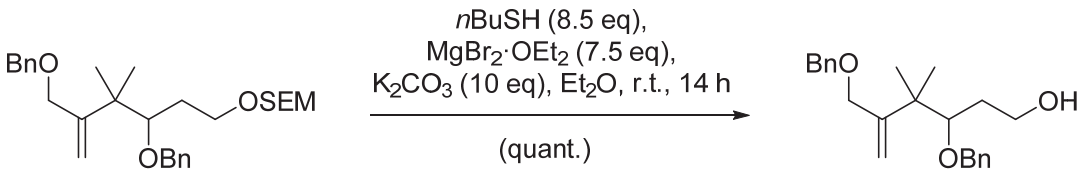

S7 **S8**

Primary alcohol S8 To a stirred solution of alkene **S7** (3.90 g, 8.05 mmol, 1.0 eq) in Et_2O (150 mL) at r.t. was added *n*BuSH (7.35 mL, 68.4 mmol, 8.5 eq), magnesium bromide diethyl etherate (15.6 g, 60.4 mmol, 7.5 eq) and potassium carbonate (11.1 g, 80.5 mmol, 10 eq). The resulting reaction mixture was stirred for 14 h followed by addition of H_2O (500 mL). The layers were separated and the aqueous layer was extracted with EtOAc (3 × 100 mL). The combined organic layers were dried over Na_2SO_4. After filtration and concentration *in vacuo*, the crude product was purified by flash column chromatography (hexanes:EtOAc 7:2) on silica to afford alcohol **S8** (2.84 g, 8.01 mmol, quant.) as a colorless oil.

Data for S8: R_f: 0.45 (hexanes:EtOAc 2:1); **^{1}H NMR (400 MHz, $CDCl_3$):** δ = 7.39 – 7.26 (m, 10H), 5.29 (s, 1H), 5.13 (s, 1H), 4.65 (d, *J* = 11.1 Hz, 1H), 4.58 (d, *J* = 11.0 Hz, 1H), 4.56 (d, *J* = 11.0 Hz, 1H), 4.52 (d, *J* = 11.9 Hz, 1H), 4.13 (d, *J* = 12.9 Hz, 1H), 4.08 (d, *J* = 12.8 Hz, 1H), 3.76 – 3.59 (m, 3H), 1.73 (dddd, *J* = 13.8, 8.1, 5.4, 2.6 Hz, 1H), 1.66 – 1.58 (m, 2H), 1.19 (s, 3H), 1.14 (s, 3H) ppm; **^{13}C NMR (100 MHz, $CDCl_3$):** δ = 150.7, 138.9, 138.4, 128.5, 128.5, 127.9, 127.8, 127.8, 127.7, 113.2, 83.2, 75.4, 72.6, 71.3, 60.9, 44.0, 34.4, 25.4, 22.1 ppm; **IR (ATR):** ν_{max} = 3413 (br w), 3088 (w), 3063 (w), 3030 (w), 2964 (w), 2928 (w), 2873 (w), 1635 (w), 1496 (w), 1453 (m), 1399 (w), 1380 (w), 1360 (m), 1307 (w), 1250 (w), 1206 (w), 1138 (w), 1086 (s), 1071 (s), 1054 (s), 1027 (s), 967 (w), 906 (m), 964 (w), 841 (w), 733 (s), 695 (s) cm^{-1}; **HRMS (ESI):** calc. for $C_{23}H_{31}O_3$ $[M+H]^+$: 355.2268, found: 355.2271.

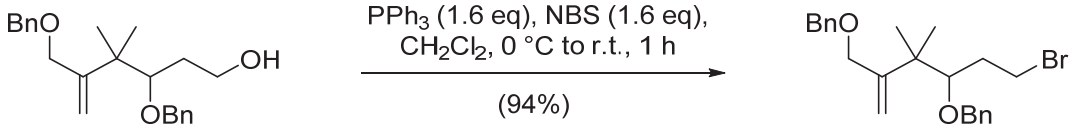

S8 **10**

Primary bromide 10 The following procedure was performed in two separate flasks with identical amounts of substrate and reagents and the reactions were combined for work up and purification. To a stirred solution of alcohol **S8** (2.08 g, 5.87 mmol, 1.0 eq) in CH_2Cl_2 (35 mL) at 0 °C was added PPh_3 (2.46 g, 9.39 mmol, 1.6 eq) and *N*-bromosuccinimide (1.67 g, 9.39 mmol, 1.6 eq). The resulting reaction mixture was stirred for 1 h at r.t. followed by addition of H_2O (100 mL). The separate reactions were combined and the layers were

separated. The aqueous layer was extracted with CH_2Cl_2 (100 mL) and EtOAc (3 × 150 mL) and the combined organic layers were dried over Na_2SO_4. After filtration and concentration *in vacuo*, the crude product was purified by flash column chromatography (pentane:Et_2O 30:1) on silica to afford bromide **10** (4.60 g, 11.0 mmol, 94%) as a colorless oil.

Data for 10: R_f: 0.60 (hexanes:EtOAc 9:1); **^{1}H NMR (400 MHz, $CDCl_3$):** δ = 7.43 – 7.27 (m, 10H), 5.31 (d, *J* = 1.3 Hz, 1H), 5.12 (s, 1H), 4.71 (d, *J* = 11.2 Hz, 1H), 4.61 (d, *J* = 11.2 Hz, 1H), 4.55 (s, 2H), 4.16 – 4.08 (m, 2H), 3.63 (dd, *J* = 7.5, 4.5 Hz, 1H), 3.51 (dt, *J* = 10.5, 5.2 Hz, 1H), 3.47 – 3.38 (m, 1H), 2.01 – 1.88 (m, 2H), 1.20 (s, 3H), 1.15 (s, 3H) ppm; **^{13}C NMR (100 MHz, $CDCl_3$):** δ = 150.5, 138.8, 138.5, 128.5 (2C), 127.8, 127.7, 127.7, 127.6, 112.6, 83.4, 75.9, 72.6, 71.1, 43.7, 35.1, 32.2, 25.6, 22.2 ppm; **IR (ATR):** ν_{max} = 3088 (w), 3064 (w), 3030 (w), 2970 (w), 2859 (w), 1635 (w), 1605 (w), 1496 (w), 1453 (m), 1398 (w), 1381 (w), 1360 (m), 1306 (w), 1264 (w), 1208 (w), 1092 (s), 1068 (s), 1028 (s), 969 (w), 909 (m), 733 (s), 696 (s) cm^{-1}; **HRMS (ESI):** calc. for $C_{23}H_{33}Br^{79}NO_2$ $[M+NH_4]^+$: 434.1690, found: 434.1693.

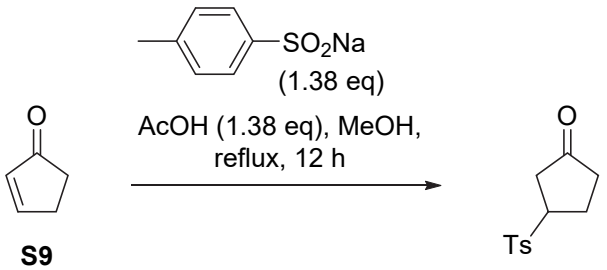

S9 **S10**

3-Tosylcyclopentan-1-one (S10) To a stirred solution of cyclopentenone (**S9**, 4.43 mL, 52.9 mmol, 1.00 eq) in MeOH (60 mL) at r.t. was added sodium *p*-toluenesulfinate (13.0 g, 73.0 mmol, 1.38 eq) and acetic acid (4.17 mL, 73.0 mmol, 1.38 eq). The resulting reaction mixture was refluxed for 12 h. The reaction was quenched by addition of H_2O (300 mL) and the layers were separated. The aqueous layer was extracted with EtOAc (3 × 100 mL) and the combined organic layers were dried over Na_2SO_4. After filtration and concentration *in vacuo*, the crude ketone **S10** (10.8 g) was obtained as a colorless oil and was used in the next step without further purification. Compound **S10** has been reported in the literature.[161]

Data for S10: R_f: 0.40 (hexanes:EtOAc 1:1); **^{1}H NMR (400 MHz, $CDCl_3$):** δ = 7.78 (d, *J* = 8.3 Hz, 2H), 7.38 (d, *J* = 7.9 Hz, 2H), 3.74 (quint, *J* = 7.3 Hz, 1H), 2.66 (dd, *J* = 18.9, 8.1 Hz, 1H), 2.58 – 2.37 (m, 6H), 2.32 – 2.17 (m, 2H) ppm; **^{13}C NMR (100 MHz, $CDCl_3$):** δ = 213.1, 145.5, 134.5, 130.3, 128.7, 60.9, 38.8, 37.1, 23.3, 21.8 ppm; **HRMS (EI):** calc. for $C_{12}H_{14}O_3S$ $[M]^+$: 238.0658, found: 238.0656.

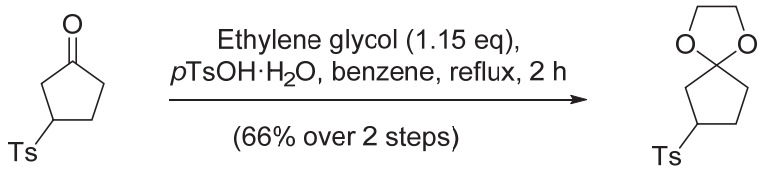

S10 **11**

Sulfone 11 To a stirred solution of crude ketone **S10** in benzene (50 mL) at r.t. was added glycol (3.40 mL, 60.8 mmol, 1.15 eq) and *p*-toluenesulfonic acid monohydrate (91.1 mg, 529 µmol, 0.01 eq). The resulting reaction mixture was refluxed for 2 h in a Dean-Stark apparatus. The reaction was poured in aq. half-sat. $NaHCO_3$ solution (300 mL) at 0 °C and the layers were separated. The aqueous layer was extracted with EtOAc (3 × 100 mL) and the combined organic layers were dried over Na_2SO_4. After filtration and concentration *in vacuo*, the crude product was purified by flash column chromatography (hexanes:EtOAc 2:3) on silica to afford sulfone **11** (9.80 g, 34.7 mmol, 66% over 2 steps) as a white solid. Compound **11** has been reported in the literature.[161]

Data for 11: R_f: 0.52 (hexanes:EtOAc 1:1); **^{1}H NMR (400 MHz, C_6D_6):** δ = 7.69 (d, J = 8.2 Hz, 2H), 6.77 – 6.70 (m, 2H), 3.43 (quint, J = 8.4 Hz, 1H), 3.37 – 3.19 (m, 4H), 2.47 (dd, J = 13.4, 10.1 Hz, 1H), 2.31 – 2.17 (m, 1H), 2.04 – 1.90 (m, 2H), 1.86 (s, 3H), 1.79 – 1.68 (m, 1H), 1.64 – 1.53 (m, 1H) ppm; **^{13}C NMR (100 MHz, C_6D_6):** δ = 144.0, 136.8, 129.8, 128.9, 116.6, 64.8, 64.1, 61.8, 37.1, 35.3, 24.3, 21.2 ppm; **IR (ATR):** ν_{max} = 3093 (w), 3056 (w), 2986 (w), 2961 (w), 2948 (w), 2900 (w), 1597 (w), 1504 (w), 1475 (w), 1432 (w), 1352 (w), 1338 (w), 1309 (m), 1281 (s), 1208 (w), 1177 (w), 1150 (s), 1110 (s), 1087 (s), 1065 (m), 1008 (m), 966 (w), 946 (m), 915 (w), 887 (m), 833 (m), 803 (w), 752 (w), 714 (w), 660 (m), 604 (w) cm^{-1}; **melting point:** 72.6 – 76.0 °C (lit.: 61.5 – 62 °C)[161]; **HRMS (ESI):** calc. for $C_{14}H_{22}O_4NS$ $[M+NH_4]^+$: 300.1264, found: 300.1266.

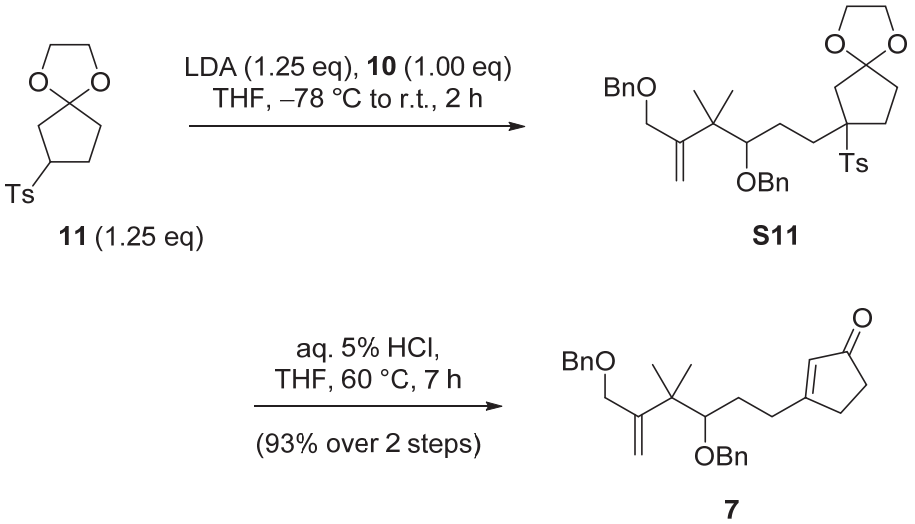

Enone 7 The following procedure was performed in two separate flasks with identical amounts of substrate and reagents and the reactions were combined for work up and purification after the hydrolysis step. To a stirred solution of sulfone **11** (2.54 g, 8.98 mmol, 1.25 eq) in THF (60 mL) at –78 °C was added LDA (0.45 M in THF, 20.0 mL, 8.98 mmol, 1.25 eq) and the resulting reaction mixture was stirred for 1.5 h. Bromide **10** (3.00 g, 7.18 mmol, 1.0 eq) dissolved in THF (20 mL) was added dropwise. The resulting reaction mixture was stirred at –78 °C for 15 min and r.t. for 2 h. The reaction was quenched by addition of H_2O (200 mL) and the layers were separated. The aqueous layer was extracted with EtOAc (3 × 100 mL) and the combined organic layers were dried over Na_2SO_4. After filtration and concentration *in vacuo*, the crude alkylated sulfone **S11** was obtained as a colorless oil and was used in the next step without further purification.

To a stirred solution of crude sulfone **S11** in THF (60 mL) was added aq. 5% HCl solution (60 mL) and the resulting reaction mixture was heated to 60 °C for 7 h followed by addition of H_2O (300 mL). The two separate reactions were combined and the layers were separated. The aqueous layer was extracted with EtOAc (3 × 200 mL) and the combined organic layers were dried over Na_2SO_4. After filtration and concentration *in vacuo*, the crude product was purified by flash column chromatography (hexanes:EtOAc 5:1→4:1) on silica to afford enone **7** (5.58 g, 13.3 mmol, 93% over 2 steps) as a colorless oil.

Data for 7: R_f: 0.45 (hexanes:EtOAc 2:1); **^{1}H NMR (400 MHz, $CDCl_3$):** δ = 7.38 – 7.27 (m, 10H), 5.86 (s, 1H), 5.29 (s, 1H), 5.12 (s, 1H), 4.67 (d, J = 11.3 Hz, 1H), 4.52 (s, 2H), 4.49 (d, J = 11.3 Hz, 1H), 4.13 (d, J = 12.8 Hz, 1H), 4.07 (d, J = 12.7 Hz, 1H), 3.40 (dd, J = 9.5, 2.4 Hz, 1H), 2.55 – 2.39 (m, 3H), 2.38 – 2.23 (m, 3H), 1.79 – 1.59 (m, 2H), 1.20 (s, 3H), 1.15 (s, 3H) ppm; **^{13}C NMR (100 MHz, $CDCl_3$):** δ = 210.2, 183.2, 150.7, 138.9, 138.5, 129.5, 128.5 (2C), 127.8, 127.8, 127.7, 127.5, 113.4, 85.7, 75.7, 72.6, 71.6, 44.2, 35.4, 31.6, 31.2, 29.3, 25.6, 22.1 ppm; **IR (ATR):** ν_{max} = 3091 (w), 3063 (w), 3030 (w), 2956 (w), 2926 (w), 2871 (w), 1703 (s), 1675 (m), 1614 (m), 1496 (w), 1453 (m), 1437 (w), 1407 (w), 1358 (w),

1306 (w), 1282 (w), 1234 (w), 1184 (m), 1089 (s), 1067 (s), 1028 (m), 907 (w), 840 (m), 734 (s), 696 (w) cm^{-1}; **HRMS (ESI):** calc. for $C_{28}H_{35}O_3$ $[M+H]^+$: 419.2581, found: 419.2589.

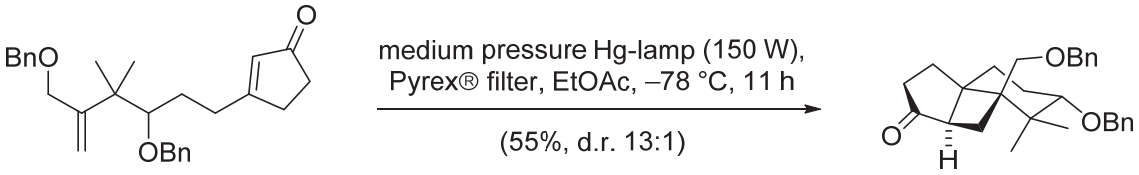

7 **6**

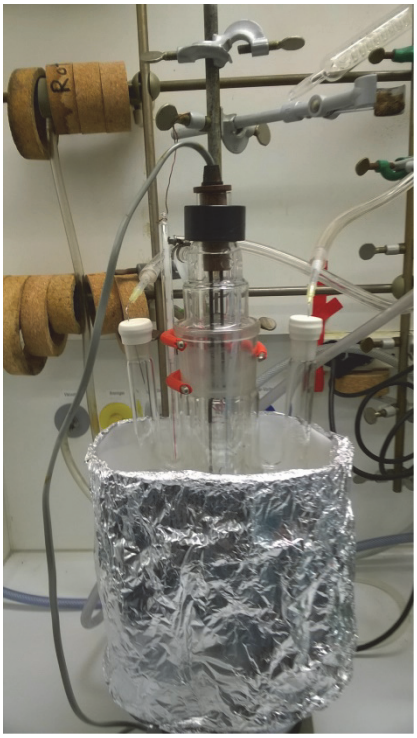

Cyclobutane 6 A stirred solution of enone **7** (3.00 g, 7.17 mmol, 1.0 eq) in EtOAc (300 mL, degassed by sparging with argon for 30 min) at –78 °C was irradiated for 11 h using a medium pressure mercury lamp (150W) in an immersion well photoreactor containing a Pyrex® filter. After evaporation of the solvent, the crude product was purified by flash column chromatography (pentane:Et_2O 10:1→6:1) on silica to afford cyclobutane **6** (1.65 g, 3.94 mmol, 55%, d.r. 13:1) as a colorless oil.

Data for 6 (major diastereomer): R_f: 0.56 (hexanes:EtOAc 3:1); **^{1}H NMR (800 MHz, $CDCl_3$):** δ = 7.40 – 7.26 (m, 10H), 4.65 (d, J = 11.8 Hz, 1H), 4.48 (d, J = 12.0 Hz, 1H), 4.46 (d, J = 12.0 Hz, 1H), 4.35 (d, J = 11.8 Hz, 1H), 3.51 (d, J = 10.0 Hz, 1H), 3.43 (d, J = 10.1 Hz, 1H), 3.27 (dd, J = 7.2, 4.2 Hz, 1H), 2.73 (dd, J = 12.2, 11.2 Hz, 1H), 2.64 – 2.56 (m, 2H), 2.37 (ddd, J = 14.4, 10.0, 5.1 Hz, 1H), 2.26 (dddd, J = 18.1, 10.9, 5.1, 1.7 Hz, 1H), 2.08 (dtd, J = 14.6, 7.2, 3.4 Hz, 1H), 1.90 (dddd, J = 14.9, 11.4, 7.4, 4.2 Hz, 1H), 1.86 (dd, J = 12.4, 5.3 Hz, 1H), 1.81 (ddd, J = 14.5, 10.9, 7.3 Hz, 1H), 1.63 –1.59 (m, 1H), 1.51 (ddd, J = 14.0, 10.9, 8.0 Hz, 1H), 1.01 (s, 3H), 0.94 (s, 3H) ppm; **^{13}C NMR (200 MHz, $CDCl_3$):** δ = 223.4, 139.3, 138.3, 128.5, 128.4, 127.7, 127.7, 127.4, 127.4, 84.1, 73.4, 72.9, 72.0, 46.5, 46.3, 46.2, 39.5, 39.0, 31.7, 31.4, 27.2, 25.7, 24.5, 22.3 ppm; **IR (ATR):** ν_{max} = 3071 (w), 3030 (w), 2928 (w), 2856 (w), 1730 (s), 1604 (w), 1496 (w), 1454 (m), 1403 (w), 1383 (w), 1363 (m), 1306 (w), 1252 (w), 1205 (w), 1174 (w), 1088 (s), 1066 (s), 1027 (m), 987 (w), 941 (w), 884 (w), 836 (m), 775 (w), 733 (s), 696 (s) cm^{-1}; **HRMS (ESI):** calc. for $C_{28}H_{38}NO_3$ $[M+NH_4]^+$: 436.2846, found: 436.2851.

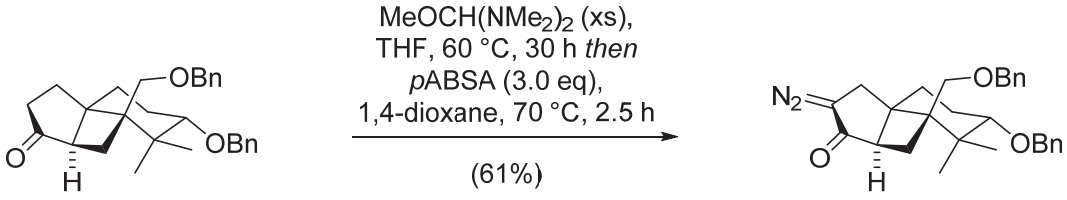

6 **13**

Diazo ketone 13 In a two-neck 100 mL flask equipped with an open Vigreux column (20 cm) a stirred solution of ketone **6** (800 mg, 1.91 mmol, 1.0 eq) and $MeOCH(NMe_2)_2$ (7.5 mL) in THF (19 mL) was heated to 60 °C for 30 h with a weak stream of N_2 bubbling through the reaction mixture. After evaporation of the solvent, the crude product was dissolved in 1,4-dioxane (45 mL) followed by addition of *p*ABSA (1.38 g, 5.73 mmol, 3.0 eq) in one portion. The resulting reaction mixture was heated to 70 °C for 2.5 h. After evaporation of the solvent the crude product was purified by flash column chromatography (hexanes:EtOAc 9:1) on silica to afford diazo ketone **13** (515 mg, 1.16 mmol, 61%) as a yellow oil.

Data for 13: R_f: 0.44 (hexanes:EtOAc 3:1); **^{1}H NMR (600 MHz, CD_2Cl_2):** δ = 7.38 – 7.24 (m, 10H), 4.64 (d, *J* = 11.7 Hz, 1H), 4.48 (d, *J* = 11.9 Hz, 1H), 4.44 (d, *J* = 11.9 Hz, 1H), 4.35 (d, *J* = 11.7 Hz, 1H), 3.63 (d, *J* = 10.5 Hz, 1H), 3.59 (d, *J* = 10.5 Hz, 1H), 3.54 (d, *J* = 14.2 Hz, 1H), 3.31 (dd, *J* = 8.0, 4.2 Hz, 1H), 2.88 (dd, *J* = 12.5, 10.8 Hz, 1H), 2.69 (dd, *J* = 10.8, 4.3 Hz, 1H), 2.60 (d, *J* = 14.2 Hz, 1H), 2.27 – 2.19 (m, 1H), 1.99 – 1.87 (m, 2H), 1.77 – 1.66 (m, 2H), 1.06 (s, 3H), 0.99 (s, 3H) ppm; **^{13}C NMR (150 MHz, CD_2Cl_2):** δ = 203.5, 139.9, 139.0, 128.8, 128.7, 128.1 (2C), 127.9, 127.8, 84.4, 73.8, 73.8, 72.4, 60.2, 47.7, 47.6, 44.2, 40.2, 34.1, 31.6, 29.1, 26.9, 25.7, 22.6 ppm; **IR (ATR):** ν_{max} = 3063 (w), 3029 (w), 2929 (w), 2863 (w), 2075 (s), 1744 (w), 1661 (w), 1496 (w), 1453 (m), 1383 (w), 1361 (m), 1325 (s), 1294 (m), 1269 (m), 1245 (m), 1224 (m), 1190 (m), 1156 (w), 1090 (s), 1059 (s), 1027 (s), 982 (m), 912 (m), 888 (m), 806 (m), 733 (s), 696 (s) cm^{-1}; **HRMS (ESI):** calc. for $C_{28}H_{33}N_2O_3$ $[M+H]^+$: 445.2486, found: 445.2487.

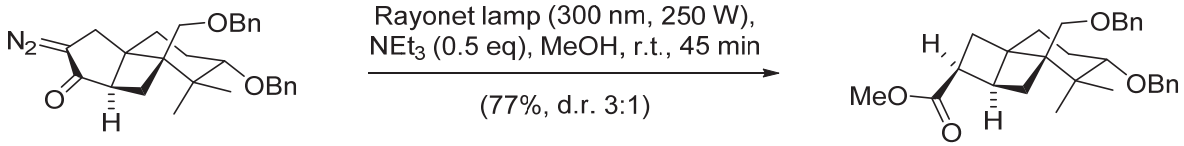

13 **14** major diastereomer

[2]-Ladderane 14 A stirred solution of diazo ketone **13** (480 mg, 1.08 mmol, 1.0 eq) in MeOH (130 mL, degassed by sparging with argon for 25 min) and triethylamine (74.9 µL, 540 µmol, 0.5 eq) in a Duran® cylinder at r.t was irradiated for 45 min using a Rayonet lamp (300 nm, 250 W). After evaporation of the solvent, the crude product was purified by flash column chromatography (pentane:Et_2O 9:1→8:1) on silica to afford [2]-ladderane **14** (375 mg, 836 µmol, 77%, d.r. 3:1) as a colorless oil.

For clarity just the ^{1}H-NMR shifts of the major diastereomer are reported. In the ^{13}C-data shifts of the minor isomer are marked by an asterisk *.

Data for 14: R_f: 0.79 (hexanes:EtOAc 3:1); **^{1}H NMR (600 MHz, CD_2Cl_2):** δ = 7.36 – 7.22 (m, 10H), 4.56 (d, *J* = 11.6 Hz, 1H), 4.44 – 4.39 (m, 2H), 4.37 (d, *J* = 11.7 Hz, 1H), 3.78 (d, *J* = 10.0 Hz, 1H), 3.66 – 3.62 (m, 1H), 3.61 (s, 3H), 3.54 (d, *J* = 10.4 Hz, 1H), 3.32 – 3.24 (m, 1H), 2.99 (dd, *J* = 13.0, 8.7 Hz, 1H), 2.77 – 2.70 (m, 1H), 2.14 (dd, *J* = 13.2, 7.7 Hz, 1H), 1.93 – 1.83 (m, 2H), 1.83 – 1.75 (m, 1H), 1.75 – 1.58 (m, 2H), 1.52 (dd, *J* = 20.5, 13.6 Hz, 1H), 1.10 (s, 3H), 1.02 (s, 3H) ppm; **^{13}C NMR (150 MHz, CD_2Cl_2):** δ = 176.8*, 174.8, 140.5, 139.7, 139.6*, 128.7, 128.6, 128.1, 127.9, 127.8, 127.6, 83.6*, 83.0, 74.1*, 73.7, 73.5, 72.3, 72.3*, 52.0*, 51.7, 49.5, 47.9*, 47.0*, 45.3, 42.9*, 40.1, 39.9*, 39.6, 38.2, 33.3*, 32.9, 32.1*, 31.8, 31.5*, 26.8, 24.7, 24.3*, 24.2, 20.9*, 20.6 ppm; **IR (ATR):** ν_{max} = 3091 (w), 3063 (w), 3027 (w), 2946 (m), 2900 (w), 2865 (w), 1730 (s), 1496 (w), 1476 (w), 1453 (m), 1434 (w), 1377 (w), 1358 (w), 1224 (m), 1196 (m), 1175 (m), 1091 (s), 1072 (s), 1028 (m), 975 (m), 907 (w), 792 (w), 735 (m), 697 (m) cm^{-1}; **HRMS (ESI):** calc. for $C_{29}H_{40}NO_4$ $[M+NH_4]^+$: 466.2952, found: 466.2959.

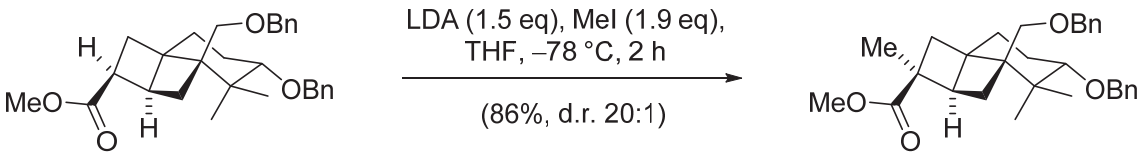

14 **5**

Methyl ester 5 [2]-Ladderane **14** (375 mg, 836 µmol, 1.0 eq, d.r. 3:1) dissolved in THF (18 mL) was added to a solution of LDA (0.45M in THF, 2.78 mL, 1.25 mmol, 1.5 eq) in THF (2.0 mL) at –78 °C and the resulting reaction mixture was stirred for 45 min. Methyl iodide (99.0 µL, 1.59 mmol, 1.9 eq) in THF (0.5 mL) was added dropwise and the reaction mixture

was allowed to warm up to –50 °C within 1 h. The reaction was quenched by addition of H_2O (50 mL) and the layers were separated. The aqueous layer was extracted with Et_2O (3 × 30 mL) and the combined organic layers were dried over Na_2SO_4. After filtration and concentration *in vacuo*, the crude product was purified by flash column chromatography (pentane:Et_2O 9:1) on silica to afford methyl ester **5** (333 mg, 720 µmol, 86%, d.r. 20:1) as a colorless oil.

Data for 5 (major diastereomer): R_f: 0.78 (hexanes:EtOAc 4:1); **^{1}H NMR (400 MHz, CD_2Cl_2):** δ = 7.39 – 7.20 (m, 10H), 4.55 (d, *J* = 11.7 Hz, 1H), 4.40 (s, 2H), 4.36 (d, *J* = 11.7 Hz, 1H), 3.69 (d, *J* = 10.0 Hz, 1H), 3.66 (dd, *J* = 9.2, 4.1 Hz, 1H), 3.60 (s, 3H), 3.50 (d, *J* = 10.0 Hz, 1H), 3.16 (d, *J* = 13.2 Hz, 1H), 2.41 (ddd, *J* = 7.6, 4.8, 2.7 Hz, 1H), 2.18 (dd, *J* = 13.3, 7.8 Hz, 1H), 1.95 – 1.85 (m, 1H), 1.82 – 1.59 (m, 3H), 1.54 (dd, *J* = 13.2, 2.7 Hz, 1H), 1.38 (s, 3H), 1.30 (dd, *J* = 13.4, 4.8 Hz, 1H), 1.09 (s, 3H), 1.00 (s, 3H) ppm; **^{13}C NMR (100 MHz, CD_2Cl_2):** δ = 177.5, 140.5, 139.6, 128.7, 128.6, 128.0, 127.9, 127.8, 127.6, 82.8, 73.9, 73.4, 72.3, 51.8, 48.3, 45.9, 44.6, 42.8, 40.1, 40.0, 33.7, 27.9, 25.6, 24.9, 24.1, 20.4 ppm; **IR (ATR):** ν_{max} = 3091 (w), 3063 (w), 3031 (w), 2935 (m), 2904 (m), 2869 (m), 1728 (s), 1496 (w), 1480 (w), 1453 (m), 1434 (m), 1359 (m), 1299 (m), 1216 (m), 1196 (m), 1179 (m), 1144 (s), 1131 (s), 1092 (s), 1028 (m), 989 (m), 907 (w), 734 (s), 697 (s) cm^{-1}; **HRMS (ESI):** calc. for $C_{30}H_{42}NO_4$ $[M+NH_4]^+$: 480.3108, found: 480.3109.

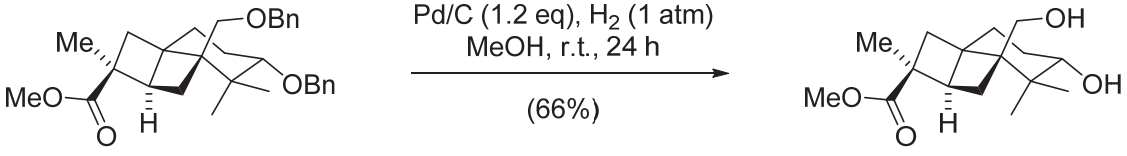

5 **15**

Diol 15 To a stirred solution of **5** (55.0 mg, 119 µmol, 1.0 eq) in MeOH (6 mL) at r.t. was added Pd/C (10% Pd on activated charcoal, 25.0 mg, 23.5 µmol, 0.2 eq) and the reaction vessel was backfilled three times with H_2 followed by sparging with H_2 for 2 min. After 8 h Pd/C (10% Pd on activated charcoal, 25.0 mg, 23.5 µmol, 0.2 eq) and after 20 h additional Pd/C (10% Pd on activated charcoal, 100.0 mg, 94.0 µmol, 0.8 eq) was added. The reaction was filtered over Celite (EtOAc) after 24 h. After concentration *in vacuo*, the crude product was purified by flash column chromatography (pentane:EtOAc 1:1) on silica to afford diol **15** (22.3 mg, 79.0 µmol, 66%) as a white solid. A crystal, suitable for single crystal X-ray diffraction analysis, was obtained by crystallization from Et_2O/pentane.

Data for 15: R_f: 0.20 (hexanes:EtOAc 1:1); **^{1}H NMR (400 MHz, CD_2Cl_2):** δ = 3.91 (dd, *J* = 11.6, 3.8 Hz, 1H), 3.85 – 3.78 (m, 1H), 3.69 (dd, *J* = 11.7, 5.3 Hz, 1H), 3.62 (s, 3H), 3.21

(d, *J* = 13.1 Hz, 1H), 2.41 (ddd, *J* = 7.7, 4.9, 2.7 Hz, 1H), 2.12 (dd, *J* = 13.4, 7.8 Hz, 1H), 1.92 (dd, *J* = 12.5, 5.0 Hz, 1H), 1.73 – 1.53 (m, 4H), 1.42 (d, *J* = 4.3 Hz, 1H), 1.39 (s, 3H), 1.30 (dd, *J* = 13.5, 4.9 Hz, 1H), 1.23 – 1.18 (m, 1H), 1.03 (s, 3H), 1.01 (s, 3H) ppm; **^{13}C NMR (100 MHz, CD_2Cl_2):** δ = 177.4, 74.6, 65.7, 51.9, 49.1, 45.7, 44.7, 42.6, 40.0, 39.9, 34.1, 28.8, 27.5, 25.5, 23.7, 19.2 ppm; **IR (ATR):** ν_{max} = 3514 (br w), 3439 (br w), 2932 (m), 2900 (m), 2873 (w), 1727 (m), 1701(s), 1481 (w), 1457 (m), 1435 (m), 1408 (w), 1383 (w), 1371 (w), 1360 (w), 1333 (w), 1295 (m), 1265 (m), 1227 (m), 1194 (s), 1180 (m), 1171 (m), 1144 (s), 1103 (m), 1057 (m), 1036 (m), 1023 (m), 999 (s), 989 (s), 967 (m), 947 (w), 936 (w), 861 (w), 768 (w), 722 (s), 683 (w) cm^{-1}; **melting point:** 149.5 – 152.8 °C; **HRMS (ESI):** calc. for $C_{16}H_{27}O_4$ $[M+H]^+$: 283.1904, found: 283.1904.

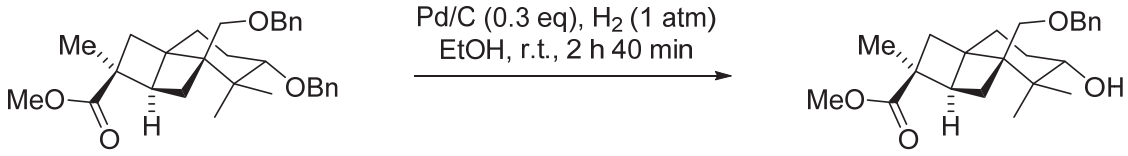

5 **S12**

Secondary alcohol S12 To a stirred solution of **5** (315 mg, 681 µmol, 1.0 eq) in EtOH (25 mL) at r.t. was added Pd/C (10% Pd on activated charcoal, 250 mg, 23.5 µmol, 0.3 eq) and the reaction vessel was backfilled three times with H_2 followed by sparging with H_2 for 2 min. To prevent overreduction the reaction was controlled by TLC every 20 min. The reaction was filtered over Celite (EtOAc) after 2 h 40 min. After concentration *in vacuo* crude alcohol **S12** (250 mg) was used in the next step without further purification.

Data for S12: R_f: 0.33 (hexanes:EtOAc 4:1); **^{1}H NMR (400 MHz, CD_2Cl_2):** δ = 7.38 – 7.21 (m, 5H), 4.45 – 4.35 (m, 2H), 3.88 (d, *J* = 9.7 Hz, 1H), 3.68 (d, *J* = 10.0 Hz, 1H), 3.60 (s, 3H), 3.49 (d, *J* = 10.0 Hz, 1H), 3.14 (d, *J* = 13.2 Hz, 1H), 2.40 (ddd, *J* = 7.7, 5.0, 2.8 Hz, 1H), 2.13 (dd, *J* = 13.4, 7.8 Hz, 1H), 1.92 – 1.86 (m, 1H), 1.72 – 1.50 (m, 4H), 1.37 (s, 3H), 1.31 (dd, *J* = 13.4, 5.0 Hz, 2H), 1.04 (s, 3H), 0.96 (s, 3H) ppm; **^{13}C NMR (100 MHz, CD_2Cl_2):** δ = 177.5, 139.5, 128.7, 127.9, 127.8, 74.2, 73.8, 73.5, 51.8, 48.4, 46.0, 44.7, 43.1, 40.2, 40.1, 34.0, 28.9, 27.9, 25.4, 23.6, 19.0 ppm; **HRMS (ESI):** calc. for $C_{23}H_{33}O_4$ $[M+H]^+$: 373.2373, found: 373.2374.

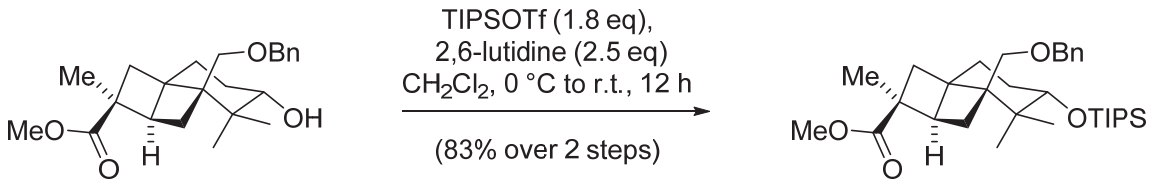

S12 **S13**

Silylated alcohol S13 To a stirred solution of crude alcohol **S12** in CH_2Cl_2 (10 mL) at 0 °C was added 2,6-lutidine (194 µL, 1.68 mmol, 2.5 eq) and TIPSOTf (325 µL, 1.21 mmol, 1.8 eq) and the resulting reaction mixture was allowed to warm up to r.t. overnight. The reaction was quenched by addition of H_2O (50 mL) and the layers were separated. The aqueous layer was extracted with Et_2O (3 × 20 mL) and the combined organic layers were dried over Na_2SO_4. After filtration and concentration *in vacuo*, the crude product was purified by flash column chromatography (pentane:Et_2O 60:1→30:1) on silica to afford silylated alcohol **S13** (297 mg, 562 µmol, 83%) as a colorless oil.

Data for S13: R_f: 0.73 (hexanes:EtOAc 4:1); **^{1}H NMR (400 MHz, CD_2Cl_2):** δ = 7.39 – 7.16 (m, 5H), 4.41 (d, *J* = 11.8 Hz, 1H), 4.36 (d, *J* = 11.8 Hz, 1H), 4.11 (dd, *J* = 10.8, 3.7 Hz, 1H), 3.68 (d, *J* = 9.9 Hz, 1H), 3.60 (s, 3H), 3.50 (d, *J* = 10.0 Hz, 1H), 3.14 (d, *J* = 13.2 Hz, 1H), 2.40 (ddd, *J* = 7.7, 4.9, 2.8 Hz, 1H), 2.12 (dd, *J* = 13.3, 7.7 Hz, 1H), 1.92 – 1.83 (m, 1H), 1.80 – 1.66 (m, 1H), 1.65 – 1.50 (m, 3H), 1.37 (s, 3H), 1.27 (dd, *J* = 13.3, 5.0 Hz, 1H), 1.07 (s, 3H), 1.02 – 0.98 (m, 21H), 0.98 (s, 3H) ppm; **^{13}C NMR (100 MHz, CD_2Cl_2):** δ = 177.5, 139.5, 128.6, 128.1, 127.7, 75.2, 73.9, 73.6, 51.8, 48.6, 46.2, 44.7, 43.1, 41.0, 40.2, 34.4, 29.7, 27.8, 25.4, 24.4, 19.3, 18.6, 13.5 ppm; **IR (ATR):** ν_{max} = 2941 (m), 2863 (m), 1730 (m), 1494 (w), 1454 (m), 1433 (w), 1381 (w), 1357 (w), 1298 (m), 1216 (w), 1195 (w), 1173 (w), 1143 (m), 1130 (m), 1089 (s), 1061 (s), 1023 (m), 1012 (m), 995 (m), 988 (m), 955 (w), 919 (w), 881 (m), 849 (w), 806 (w), 733 (s), 696 (m), 674 (s) cm^{-1}; **HRMS (ESI):** calc. for $C_{32}H_{56}NO_4Si$ $[M+NH_4]^+$: 546.3973, found: 546.3994.

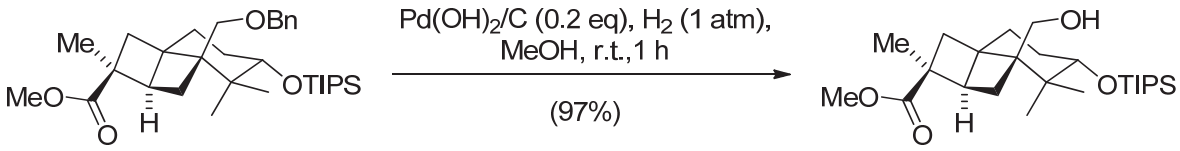

S13 **S14**

Primary alcohol S14 To a stirred solution of **S13** (255 mg, 482 µmol, 1.0 eq) in MeOH (12 mL) at r.t. was added $Pd(OH)_2$/C (10% Pd on activated charcoal, 120 mg, 113 µmol, 0.2 eq) and the reaction vessel was backfilled three times with H_2 followed by sparging with H_2 for 2 min. The reaction was filtered over Celite (EtOAc) after 1 h. After concentration *in*

vacuo, the crude product was purified by flash column chromatography (pentane:Et_2O 5:1) on silica to afford alcohol **S14** (205 mg, 467 µmol, 97%) as a colorless oil.

Data for S14: R_f: 0.48 (hexanes:EtOAc 4:1); **^{1}H NMR (400 MHz, C_6D_6):** δ = 4.23 (dd, J = 10.5, 3.9 Hz, 1H), 3.71 (d, J = 11.0 Hz, 1H), 3.46 – 3.40 (m, 2H), 3.39 (s, 3H), 2.35 (ddd, J = 7.6, 4.9, 2.7 Hz, 1H), 2.05 (dd, J = 13.3, 7.8 Hz, 1H), 1.79 – 1.64 (m, 2H), 1.63 – 1.48 (m, 3H), 1.36 (s, 3H), 1.35 – 1.30 (m, 1H), 1.23 – 1.07 (m, 27H), 0.37 (s, 1H) ppm; **^{13}C NMR (100 MHz, C_6D_6):** δ = 176.6, 75.2, 65.4, 51.1, 49.0, 45.8, 44.6, 42.4, 40.8, 40.0, 34.4, 29.6, 27.4, 25.2, 24.4, 19.4, 18.6, 13.5 ppm; **IR (ATR):** ν_{max} = 3455 (br w), 2914 (m), 2865 (m), 2849 (m), 1730 (s), 1470 (m), 1459 (m), 1435 (w), 1386 (m), 1301 (m), 1272 (m), 1254 (m), 1225 (m), 1199 (m), 1176 (s), 1144 (s), 1129 (m), 1111 (s), 1090 (s), 1061 (m), 1015 (s), 997 (m), 919 (w), 882 (m), 850 (w), 808 (w), 780 (w), 716 (w), 674 (m) cm^{-1}; **HRMS (ESI):** calc. for $C_{25}H_{47}O_4Si$ $[M+H]^+$:439.3238, found: 439.3240.

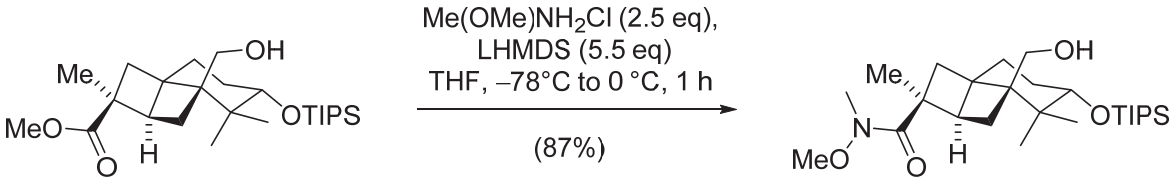

S14 **16**

Weinreb amide 16 To a stirred solution of alcohol **S14** (189 mg, 431 µmol, 1.0 eq) in THF (16 mL) at –78 °C was added Me(OMe)NH_2Cl (105 mg, 1.08 mmol, 2.5 eq) and LHMDS (1.0 M in THF, 2.37 mL, 2.37 mmol, 5.5 eq) and the resulting reaction mixture was stirred at 0 °C for 1 h. The reaction was quenched by addition of H_2O (60 mL) and the layers were separated. The aqueous layer was extracted with EtOAc (3 × 40 mL) and the combined organic layers were dried over Na_2SO_4. After filtration and concentration *in vacuo*, the crude product was purified by flash column chromatography (pentane:EtOAc 1:1) on silica to afford Weinreb amide **16** (175 mg, 374 µmol, 87%) as a white foam.

Data for 16: R_f: 0.40 (hexanes:EtOAc 1:1); **^{1}H NMR (400 MHz, C_6D_6):** δ = 4.28 (dd, J = 10.5, 3.7 Hz, 1H), 3.75 (d, J = 10.8 Hz, 1H), 3.57 (d, J = 13.2 Hz, 1H), 3.45 (dd, J = 10.8, 2.1 Hz, 1H), 3.04 (s, 3H), 2.89 (s, 3H), 2.45 – 2.38 (m, 1H), 2.08 (dd, J = 13.1, 7.7 Hz, 1H), 1.88 – 1.73 (m, 2H), 1.71 – 1.56 (m, 3H), 1.42 (s, 3H), 1.36 (dd, J = 13.1, 5.0 Hz, 1H), 1.25 – 1.17 (m, 21H), 1.17 – 1.08 (m, 6H) ppm; **^{13}C NMR (100 MHz, C_6D_6):** δ = 177.8*, 75.3, 65.4, 60.1, 48.9, 46.1, 45.7, 42.0, 41.7, 40.8, 34.6, 32.9, 29.7, 28.3, 24.7, 24.4, 19.4, 18.7, 13.5 ppm; **IR (ATR):** ν_{max} = 3444 (br w), 2940 (s), 2865 (s), 1633 (br s), 1462 (m), 1381 (m), 1365 (m), 1247 (w), 1226 (w), 1207 (w), 1171 (w), 1158 (w), 1129 (m), 1088 (s), 1068 (s), 1054 (s),

1011 (s), 952 (w), 918 (w), 881 (s), 864 (w), 850 (m), 830 (w), 792 (m), 743 (w), 675 (s) cm^{-1}; **HRMS (EI):** calc. for $C_{26}H_{49}NO_4Si$ $[M]^+$: 467.3425, found: 467.3417.

* The shift of the amide carbonyl was not visible in the ^{13}C spectra, but was extracted from the HMBC data showing corresponding correlations at 177.8 ppm.

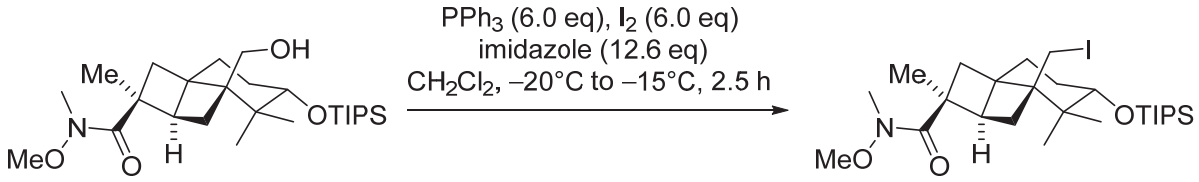

16 **17**

Iodide 17 To a stirred solution of alcohol **16** (25.0 mg, 53.4 µmol, 1.0 eq) in CH_2Cl_2 (1.9 mL) at –20 °C was added PPh_3 (28.1 mg, 107 µmol, 2.0 eq), imidazole (15.2 mg, 224 µmol, 4.2 eq) and iodine (27.2 mg, 107 µmol, 2.0 eq) and the resulting reaction mixture was allowed to warm up to –15 °C within 1 h. The reaction was cooled down to –20 °C and PPh_3 (28.1 mg, 107 µmol, 2.0 eq), imidazole (15.2 mg, 224 µmol, 4.2 eq) and iodine (27.2 mg, 107 µmol, 2.0 eq) was added again. After warming up to –15 °C within 1 h, the reaction was cooled down to –20 °C again and additional PPh_3 (28.1 mg, 107 µmol, 2.0 eq), imidazole (15.2 mg, 224 µmol, 4.2 eq) and iodine (27.2 mg, 107 µmol, 2.0 eq) was added followed by stirring for additional 30 min. The reaction was cooled to –78 °C and diluted with CH_2Cl_2 (5 mL). Reaction quench was performed by cannulation of the reaction mixture into a vigorously stirred, cold (ice bath), aq. 10% $Na_2S_2O_4$ solution. The layers were separated and the aqueous layer was extracted with CH_2Cl_2 (10 mL), Et_2O (2 × 20 mL) and EtOAc (10 mL). The combined organic layers were dried over Na_2SO_4. After filtration and concentration *in vacuo*, the crude product was purified by flash column chromatography (pentane:Et_2O 1:1) on Davisil® to afford iodide **17** (24.9 mg) as a colorless oil. Iodide **17** was immediately used in the next step.

Data for 17: R_f: 0.61 (hexanes:EtOAc 1:1); **^{1}H NMR (400 MHz, C_6D_6):** δ = 4.64 (dd, J = 11.3, 3.9 Hz, 1H), 3.43 (d, J = 13.5 Hz, 1H), 3.37 (d, J = 10.8 Hz, 1H), 3.15 (d, J = 10.8 Hz, 1H), 3.02 (s, 3H), 2.88 (s, 3H), 2.41 (dd, J = 13.3, 7.7 Hz, 1H), 2.28 (ddd, J = 7.5, 4.8, 2.9 Hz, 1H), 1.98 (td, J = 14.1, 5.9 Hz, 1H), 1.88 – 1.74 (m, 2H), 1.70 – 1.55 (m, 2H), 1.55 – 1.48 (m, 1H), 1.36 (s, 3H), 1.23 – 1.08 (m, 27H) ppm.

The iodination reaction was best performed on 20–40 mg scale and it was essential to keep the reaction at low temperature to suppress ring opening. Reverse quenching was more reproducible than direct quenching of the reaction at low temperature. The only side product observed was cyclopentene **18**.

Data for 18: R_f: 0.69 (hexanes:EtOAc 1:1); **^{1}H NMR (400 MHz, C_6D_6):** δ = 5.33 (t, J = 2.0 Hz, 1H), 3.63 (dd, J = 3.2, 1.8 Hz, 1H), 3.12 (d, J = 11.9 Hz, 1H), 3.08 (s, 3H), 2.86 (s, 3H), 2.72 (ddd, J = 17.0, 9.9, 2.0 Hz, 1H), 2.45 (d, J = 10.4 Hz, 1H), 2.38 (ddd, J = 17.1, 4.2, 2.0 Hz, 1H), 2.17 (td, J = 12.9, 3.7 Hz, 1H), 1.92 – 1.83 (m, 2H), 1.82 – 1.74 (m, 1H), 1.58 (dq, J = 10.3, 3.3 Hz, 1H), 1.52 (s, 3H), 1.24 (s, 3H), 1.17 – 1.01 (m, 21H), 0.97 (s, 3H) ppm; **^{13}C NMR (100 MHz, C_6D_6):** δ = 178.5*, 152.6, 122.1, 77.5, 59.7, 53.8, 47.2, 45.2, 44.2, 40.3, 36.1, 33.0, 32.8, 27.3, 27.3, 26.8, 26.0, 18.6, 13.4 ppm; **IR (ATR):** ν_{max} = 2926 (s), 2866 (s), 1660 (br s), 1463 (m), 1381 (m), 1359 (m), 1327 (w), 1289 (w), 1244 (w), 1178 (w), 1159 (w), 1110 (s), 1094 (m), 1079 (m), 1066 (m), 1011 (s), 996 (m), 924 (w), 882 (m), 864 (w), 836 (w), 821 (w), 795 (w), 767 (w), 679 (w) cm^{-1}; **HRMS (EI):** calc. for $C_{26}H_{47}NO_3Si$ [M]$^+$: 449.3320, found: 449.3311.

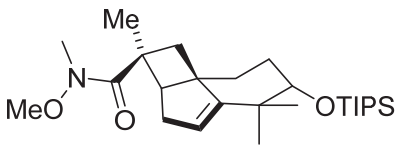

18

* The shift of the amide carbonyl was not visible in the ^{13}C-spectra, but was extracted from the HMBC data showing corresponding correlations at 178.5 ppm.

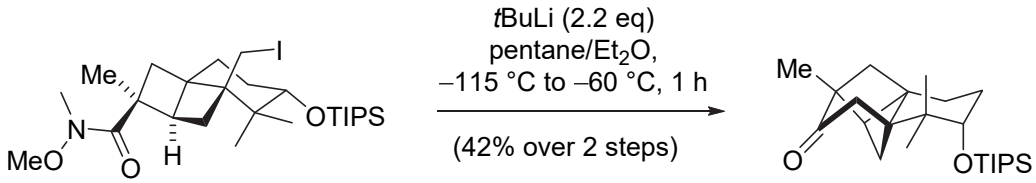

17 **20**

Ketone 20 A solution of iodide **17** (24.9 mg, 43.1 µmol, 1.0 eq) in Et_2O/pentane (2.8 mL, 1:1) at –78 °C was added dropwise to *t*BuLi (1.6M in pentane, 59.3 µL, 94.8 µmol, 2.2 eq) in pentane (2.8 mL) at –115 °C. The resulting reaction mixture was allowed to warm up to –60 °C within 1 h before cooling down to –80 °C. The reaction was quenched by addition of aq. half-sat. NH_4Cl solution (5 mL) and H_2O (5 mL) and the layers were separated. The aqueous layer was extracted with Et_2O (3 × 10 mL) and the combined organic layers were dried over Na_2SO_4. After filtration and concentration *in vacuo*, the crude product was purified by flash column chromatography (pentane:Et_2O 20:1) on silica to afford ketone **20** (8.8 mg, 22.5 µmol, 42% over 2 steps) as a white solid. A crystal, suitable for single crystal X-ray diffraction analysis, was obtained by crystallization from Et_2O/pentane.

Data for 20: R_f: 0.37 (hexanes:EtOAc 20:1); **^{1}H NMR (800 MHz, C_6D_6):** δ = 3.58 – 3.55 (m, 1H), 2.92 (ddd, J = 10.8, 5.5, 2.7 Hz, 1H), 2.57 (dd, J = 16.2, 2.6 Hz, 1H), 2.24 (d, J = 16.2 Hz, 1H), 2.17 (ddd, J = 14.2, 12.5, 6.8 Hz, 1H), 2.02 (d, J = 10.6 Hz, 1H), 1.96 (d, J = 5.4 Hz, 1H), 1.52 (d, J = 10.7 Hz, 1H), 1.43 – 1.40 (m, 2H), 1.36 – 1.31 (m, 2H), 1.22 (s, 3H), 1.09 (d, J = 7.2 Hz, 18H), 1.05 – 0.96 (m, 3H), 0.80 (s, 3H), 0.48 (s, 3H) ppm; **^{13}C NMR**

(200 MHz, C_6D_6): δ = 211.8, 78.4, 49.4, 46.7, 44.0, 42.6, 41.0, 40.3, 37.0, 34.6, 26.5, 26.4, 25.3, 21.3, 19.0, 18.6, 13.3 ppm; **IR (ATR):** ν_{max} = 2922 (s), 2851 (m), 1722 (m), 1462 (w), 1409 (w), 1378 (w), 1363 (w), 1259 (w), 1092 (m), 1057 (s), 1013 (m), 959 (w), 919 (w), 883 (w), 802 (m), 719 (w), 680 (w) cm^{-1}; **melting point:** 58.6 – 60.2 °C; **HRMS (EI):** calc. for $C_{21}H_{35}O_3Si$ [*M*-(CH_3)$_2$*CH*]$^+$: 347.2401, found: 347.2393.

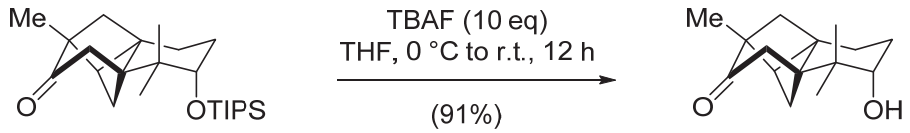

20 **21**

Alcohol 21 To a stirred solution of ketone **20** (17.0 mg, 43.5 µmol, 1.0 eq) in THF (2.5 mL) at 0 °C was added TBAF (1.0 M in THF, 435 µL, 435 µmol, 10 eq) and the resulting reaction mixture was allowed to warm up to r.t. overnight. The reaction was quenched by addition of H_2O (10 mL) and the layers were separated. The aqueous layer was extracted with EtOAc (3 × 10 mL) and the combined organic layers were dried over Na_2SO_4. After filtration and concentration *in vacuo*, the crude product was purified by flash column chromatography (pentane:EtOAc 2:1) on silica to afford alcohol **21** (9.3 mg, 39.7 µmol, 91%) as a white solid.

Data for 21: R_f: 0.60 (hexanes:EtOAc 1:1); **^{1}H NMR (800 MHz, C_6D_6):** δ = 3.07 (s, 1H), 2.88 (ddd, *J* = 10.8, 5.5, 2.7 Hz, 1H), 2.54 (dd, *J* = 16.3, 2.7 Hz, 1H), 2.21 (d, *J* = 16.3 Hz, 1H), 2.15 – 2.07 (m, 1H), 2.00 – 1.95 (m, 2H), 1.50 (d, *J* = 10.7 Hz, 1H), 1.37 – 1.29 (m, 3H), 1.27 – 1.24 (m, 1H), 1.19 (s, 3H), 0.87 (d, *J* = 3.3 Hz, 1H), 0.63 (s, 3H), 0.42 (s, 3H) ppm; **^{13}C NMR (200 MHz, C_6D_6):** δ = 212.0, 76.6, 49.4, 46.7, 43.9, 42.7, 40.8, 40.4, 36.0, 34.8, 26.2, 25.9, 25.0, 20.1, 18.9 ppm; **IR (ATR):** ν_{max} = 3509 (br m), 2936 (m), 2905 (m), 2861 (w), 1706 (s), 1465 (w), 1451 (w), 1410 (w), 1380 (w), 1360 (w), 1340 (w), 1321 (w), 1294 (w), 1278 (w), 1242 (w), 1211 (w), 1196 (w), 1180 (w), 1167 (w), 1132 (w), 1116 (m), 1085 (w), 1048 (w), 1036 (w), 994 (m), 950 (w), 909 (w), 891 (w), 880 (w), 799 (w), 695 (w) cm^{-1}; **melting point:** 115.5 – 116.5 °C; **HRMS (ESI):** calc. for $C_{15}H_{23}O_2$ [*M*+*H*]$^+$: 235.1693, found: 235.1694.

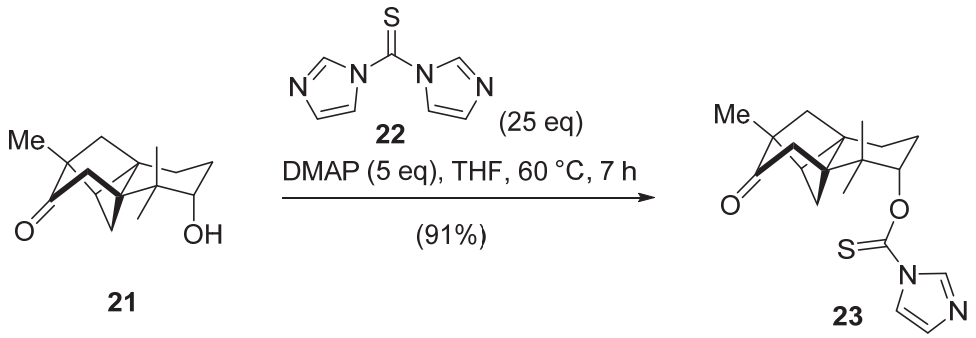

Imidazole 23 To a stirred solution of alcohol **21** (9.3 mg, 39.7 µmol, 1.0 eq) in THF (0.75 mL) was added **22** (177 mg, 993 µmol, 25 eq) and DMAP (24.3 mg, 199 µmol, 5.0 eq). The resulting reaction mixture was heated to 60 °C for 7 h followed by addition of H_2O (10 mL) and EtOAc (2 mL). The layers were separated and the aqueous layer was extracted with EtOAc (4 × 10 mL). The combined organic layers were dried over Na_2SO_4. After filtration and concentration *in vacuo*, the crude product was purified by flash column chromatography (pentane:EtOAc 10:1→8:1) on silica to afford imidazole **23** (12.5 mg, 36.3 µmol, 91%) as a slightly yellow solid.

Data for 23: R_f: 0.40 (hexanes:EtOAc 1:1); **^{1}H NMR (400 MHz, C_6D_6):** δ = 8.38 (s, 1H), 7.50 (s, 1H), 6.98 (s, 1H), 5.37 (dd, *J* = 4.1, 2.9 Hz, 1H), 2.39 (dd, *J* = 16.3, 2.7 Hz, 1H), 2.16 (ddd, *J* = 11.0, 5.6, 2.8 Hz, 1H), 2.05 (d, *J* = 16.3 Hz, 1H), 1.81 (d, *J* = 10.8 Hz, 1H), 1.71 (d, *J* = 5.6 Hz, 1H), 1.49 (dq, *J* = 13.6, 4.6 Hz, 1H), 1.44 – 1.34 (m, 2H), 1.32 – 1.22 (m, 1H), 1.20 – 1.12 (m, 5H), 0.43 (s, 3H), 0.36 (s, 3H) ppm; **^{13}C NMR (100 MHz, C_6D_6):** δ = 210.6, 184.3, 136.5, 131.9, 118.6, 88.8, 49.4, 45.7, 43.5, 42.0, 40.5, 40.2, 36.8, 34.7, 26.6, 24.6, 22.6, 19.7, 18.8 ppm; **IR (ATR):** ν_{max} = 3117 (w), 2965 (w), 2921 (w), 2852 (w), 1715 (s), 1528 (w), 1478 (m), 1459 (w), 1383 (s), 1331 (s), 1282 (s), 1250 (s), 1234 (s), 1200 (m), 1186 (m), 1194 (w), 1131 (w), 1115 (w), 1099 (m), 1093 (m), 1035 (w), 973 (s), 964 (s), 951 (m), 927 (m), 888 (w), 880 (w), 853 (m), 839 (w), 731 (m) cm^{-1}; **melting point:** 115.2 – 117.4 °C; **HRMS (EI):** calc. for $C_{19}H_{24}N_2O_2S$ $[M]^+$: 344.1553, found: 344.1540.

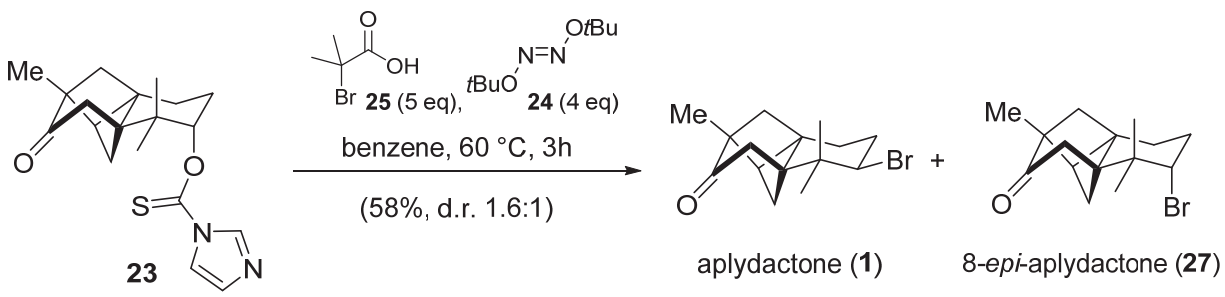

Aplydactone (1) and 8-*epi*-aplydactone (27) To a stirred solution of imidazole **23** (4.2 mg, 12.2 µmol, 1.0 eq) and α-bromo acid **25** (10.2 mg, 61.0 µmol, 5.0 eq) in benzene (0.5 mL,

degassed by sparging with argon for 15 min) at 60 °C was added hyponitrite **24**[162] (8.5 mg, 48.8 µmol, 4.0 eq) in benzene (0.5 mL, degassed by sparging with argon for 15 min) over 2 h by syringe pump followed by stirring for 30 min. The reaction was cooled to r.t. and filtered over a plug of silica (pentane:EtOAc 8:1). After concentration *in vacuo*, the crude product was purified by flash column chromatography (pentane:EtOAc 30:1→18:1) on silica to afford aplydactone (**1**, 1.3 mg, 4.37 µmol, 36%) and 8-*epi*-aplydactone (**27**, 0.8 mg, 2.69 µmol, 22%).

Data for 8-*epi*-aplydactone (27): R_f: 0.35 (hexanes:EtOAc 9:1); **IR (ATR):** ν_{max} = 2921 (m), 2852 (w), 1718 (s), 1464 (w), 1444 (w), 1407 (s), 1385 (w), 1367 (w), 1339 (w), 1274 (w), 1264 (w), 1236 (w), 1228 (w), 1209 (w), 1149 (w), 1127 (w), 1105 (w), 1092 (w), 1070 (w), 1024 (w), 977 (w), 963 (w), 949 (w), 899 (w), 866 (w), 804 (w), 704 (w), 691 (w) cm^{-1}; **HRMS (EI):** calc. for $C_{15}H_{21}Br^{79}O$ $[M]^+$: 296.0770 found: 296.0776.

NMR-data:

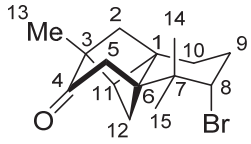

8-*epi*-aplydactone (**27**)

^{1}H NMR (800 MHz, C_6D_6): δ = 3.86 (t, J = 3.4 Hz, 1H, H-8), 3.08 (ddd, J = 11.2, 5.6, 2.9 Hz, 1H, H-12), 2.38 (dd, J = 16.2, 2.8 Hz, 1H, H'-5), 2.24 (td, J = 14.3, 4.7 Hz, 1H, H-10), 2.11 (d, J = 16.2 Hz, 1H, H-5), 1.90 (d, J = 5.6 Hz, 1H, H-11), 1.85 (d, J = 10.8 Hz, 1H, H'-2), 1.59 – 1.55 (m, 1H, H-9), 1.41 (d, J = 10.8 Hz, 1H, H-2), 1.40 – 1.35 (m, 1H, H'-9), 1.33 – 1.30 (m, 2H, H'-10, H'-12), 1.15 (s, 3H, H-13), 0.80 (s, 3H, H-15), 0.41 (s, 3H, H-14) ppm; **^{13}C NMR (200 MHz, C_6D_6):** δ = 210.9 (C-4), 66.3 (C-8), 49.1 (C-3), 45.6 (C-11), 44.1 (C-6), 43.0 (C-5), 40.6 (C-1), 40.6 (C-2), 36.5 (C-7), 34.4 (C-12), 28.2 (C-9 or C-10), 28.1 (C-9 or C-10), 25.8 (C-14), 25.0 (C-15), 18.7 (C-13) ppm;

Data for aplydactone (1): R_f: 0.41 (hexanes:EtOAc 1:9); **IR (ATR):** ν_{max} = 2956 (m), 2918 (m), 2845 (w), 1709 (s), 1470 (w), 1455 (w), 1437 (w), 1411 (s), 1389 (w), 1365 (w), 1341 (w), 1302 (w), 1278 (w), 1250 (w), 1236 (w), 1189 (w), 1147 (w), 1131 (w), 1113 (w), 1092 (w), 1062 (w), 1026 (w), 981 (w), 957 (w), 947 (w), 846 (w), 711 (w), 691 (w) cm^{-1}; **HRMS (EI):** calc. for $C_{15}H_{21}Br^{79}O$ $[M]^+$: 296.0770 found: 296.0768.

NMR-data:[95]

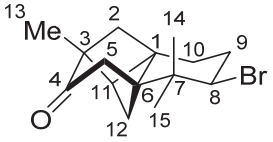

aplydactone (**1**)

No.	^{1}H NMR Isolation 300 MHz, C_6D_6 [ppm]	^{1}H NMR Synthetic 800 MHz, C_6D_6 [ppm]	^{13}C NMR Isolation 75 MHz, C_6D_6 [ppm]	^{13}C NMR Synthetic 200 MHz, C_6D_6 [ppm]
1			40.2	40.2
2	1.29 (d, *J* = 11.0 Hz, 1H) 1.81 (d, *J* = 11.0 Hz, 1H)	1.29 (d, *J* = 10.9 Hz, 1H) 1.80 (d, *J* = 10.9 Hz, 1H)	40.6	40.6
3			48.9	48.9
4			210.4	210.5
5	2.12 (d, *J* = 16.5 Hz, 1H) 2.51 (dd, *J* = 16.5, 2.7 Hz, 1H)	2.13 (d, *J* = 16.4 Hz, 1H) 2.51 (dd, *J* = 16.4, 2.8 Hz, 1H)	42.9	42.9
6			47.1	47.1
7			38.2	38.2
8	3.90 (m, 1H)	3.89 (dd, *J* = 11.9, 3.9 Hz, 1H)	65.7	65.8
9	1.69 (m, 2H)	1.70 – 1.65 (m, 2H)	31.0	31.0
10	1.30 (m, 2H)	1.35 – 1.25 (m, 2H)	33.8	33.9
11	1.58 (d, *J* = 5.6 Hz, 1H)	1.58 (d, *J* = 5.6 Hz, 1H)	45.5	45.5
12	1.05 (d, *J* = 11.3 Hz, 1H) 1.72 (ddd, *J* = 11.3, 5.6, 2.7 Hz, 1H)	1.04 (d, *J* = 11.3 Hz, 1H) 1.73 – 1.70 (m, 1H)	31.7	31.7
13	1.09 (s, 3H)	1.10 (s, 3H)	18.6	18.7
14	0.75 (s, 3H)	0.75 (s, 3H)	18.3	18.3
15	0.70 (s, 3H)	0.70 (s, 3H)	22.9	22.9

6.2.2 ^{1}H and ^{13}C NMR spectra

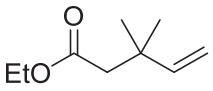

8

400 MHz, $CDCl_3$

100 MHz, $CDCl_3$

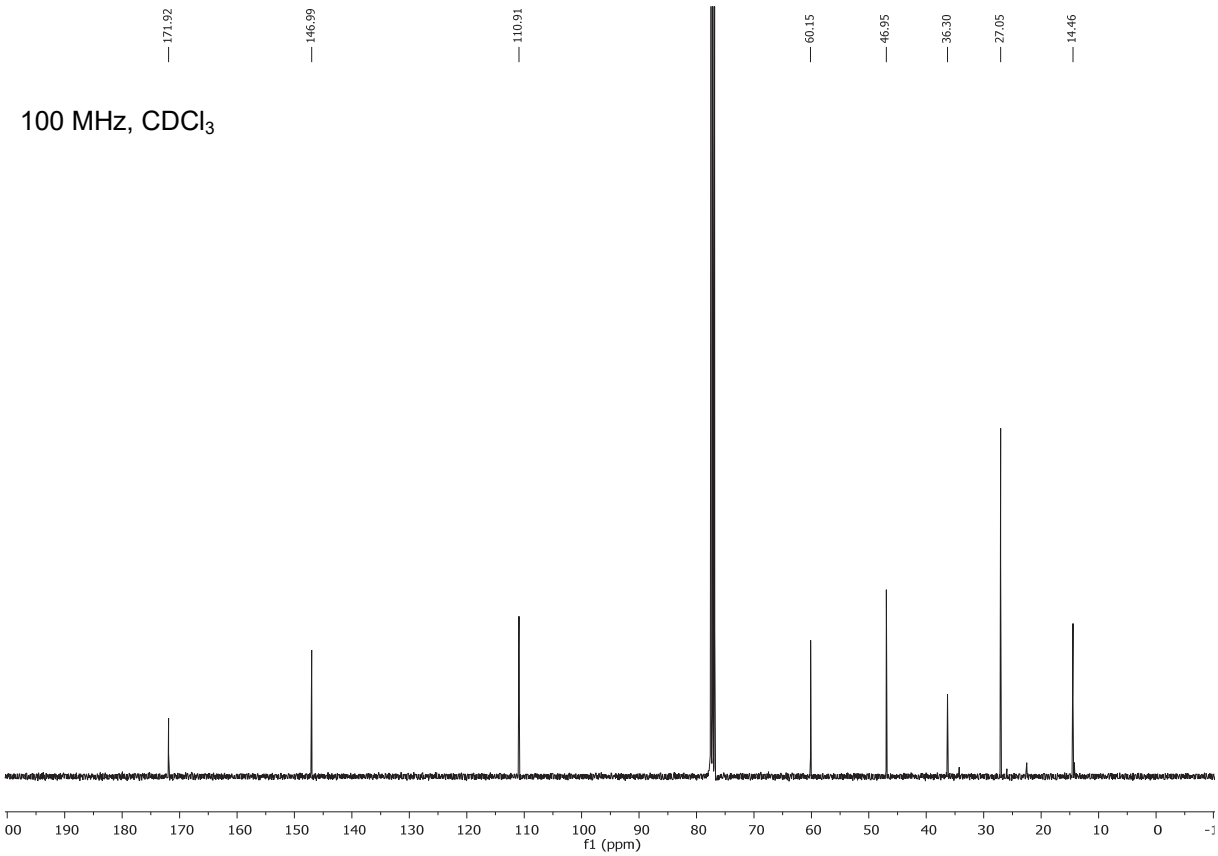

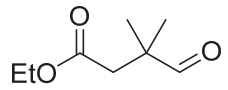

S2

400 MHz, C_6D_6

100 MHz, C_6D_6

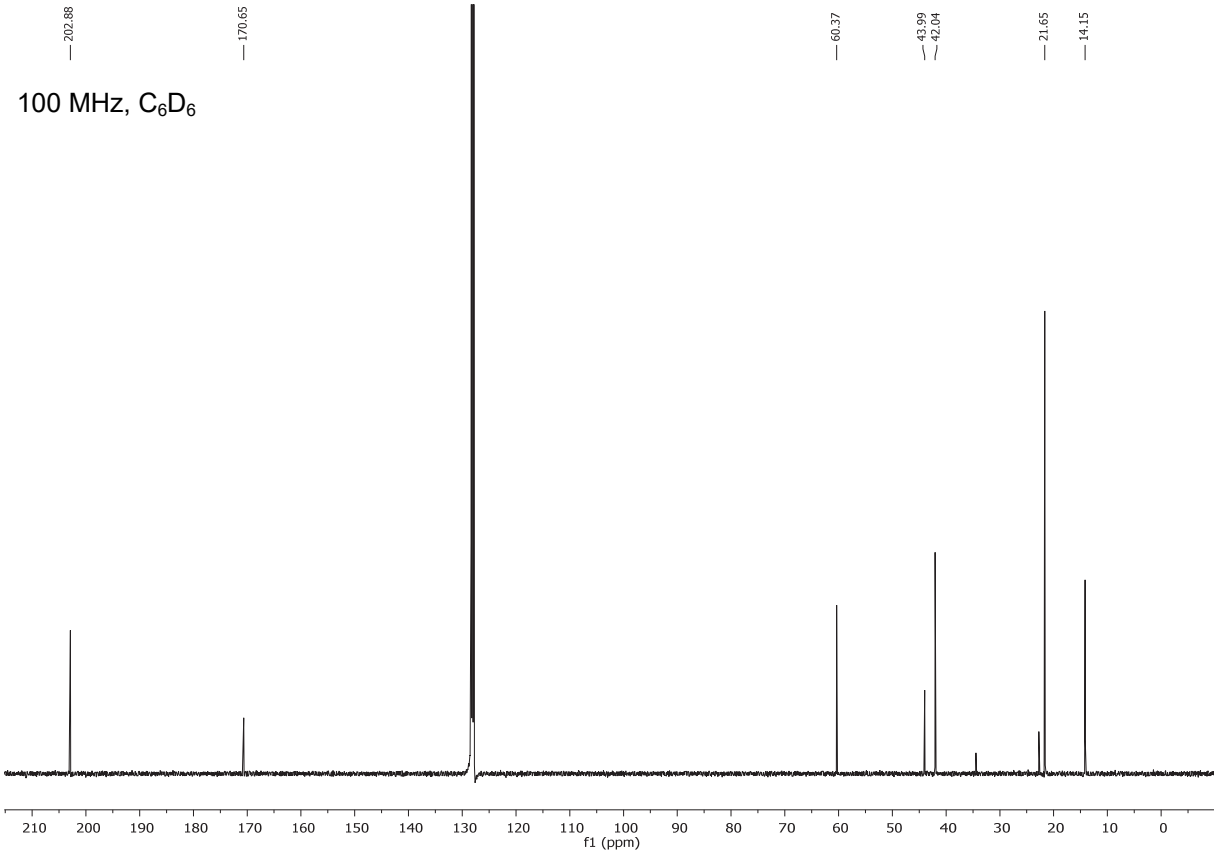

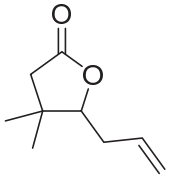

S3

400 MHz, C_6D_6

100 MHz, C_6D_6

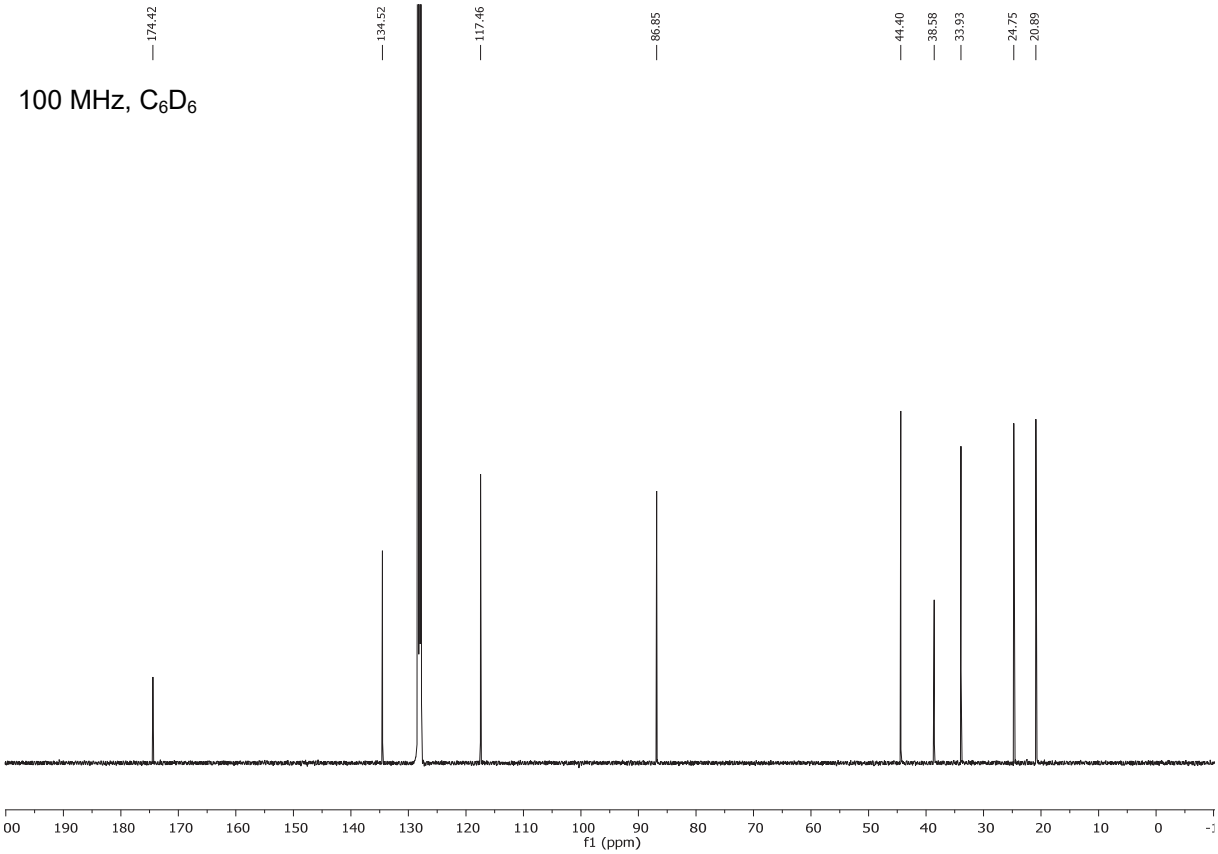

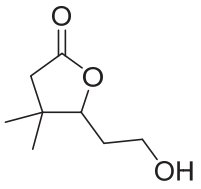

S4

400 MHz, C_6D_6

100 MHz, C_6D_6

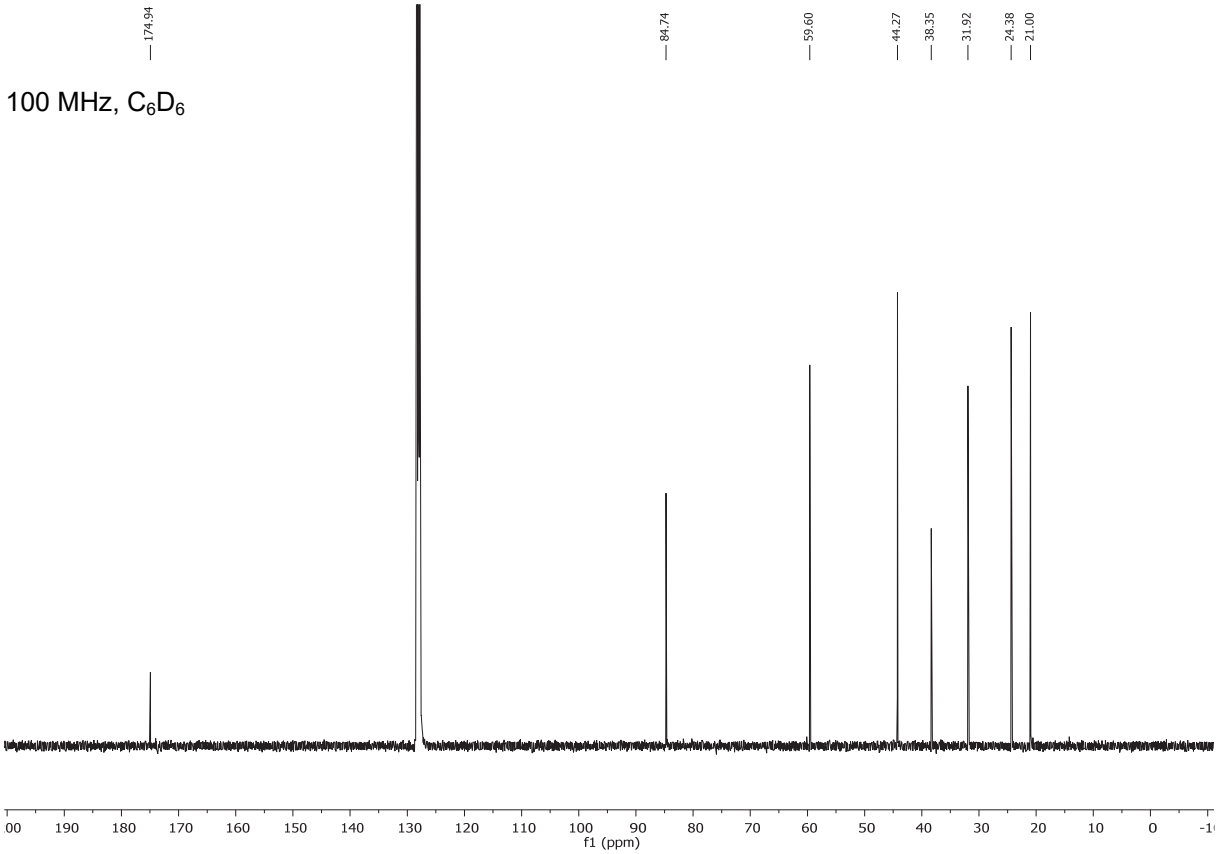

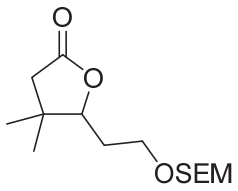

9

400 MHz, C_6D_6

100 MHz, C_6D_6

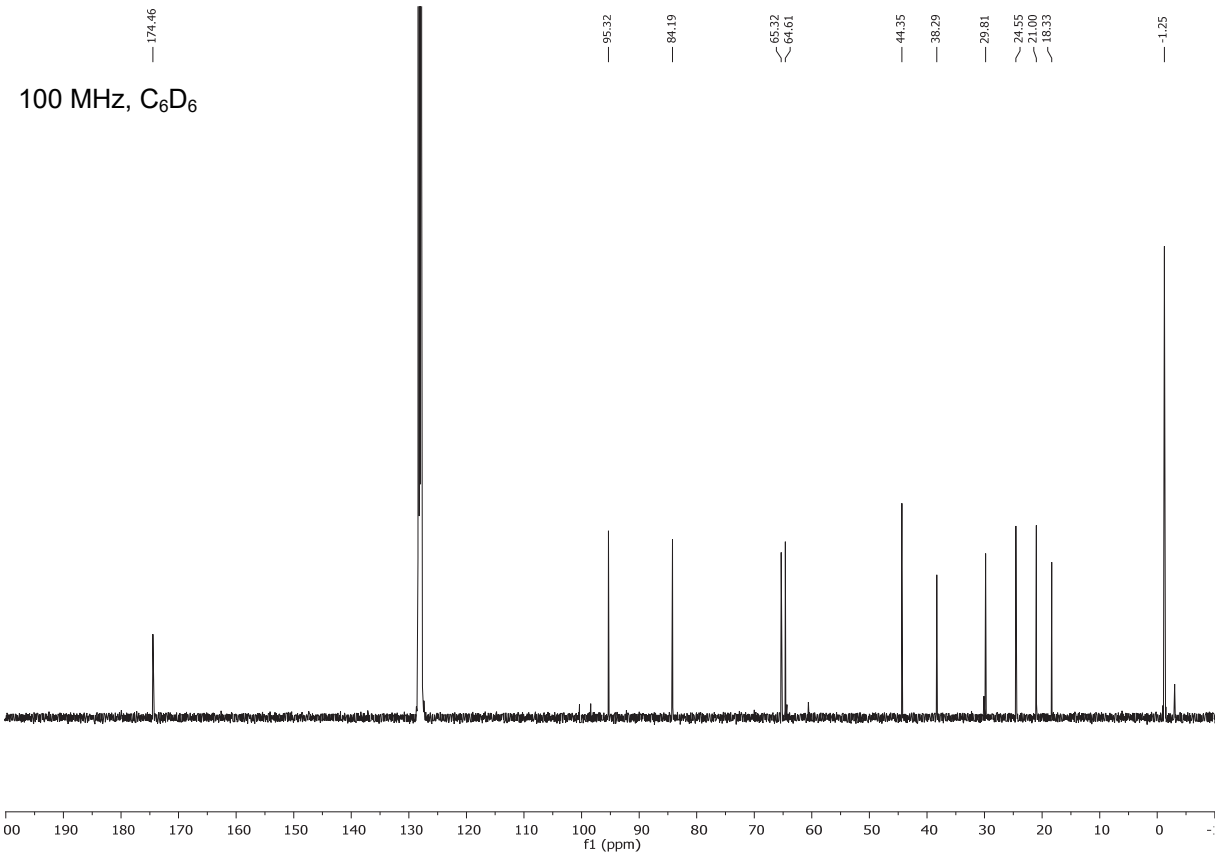

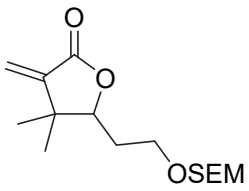

S5

400 MHz, C_6D_6

100 MHz, C_6D_6

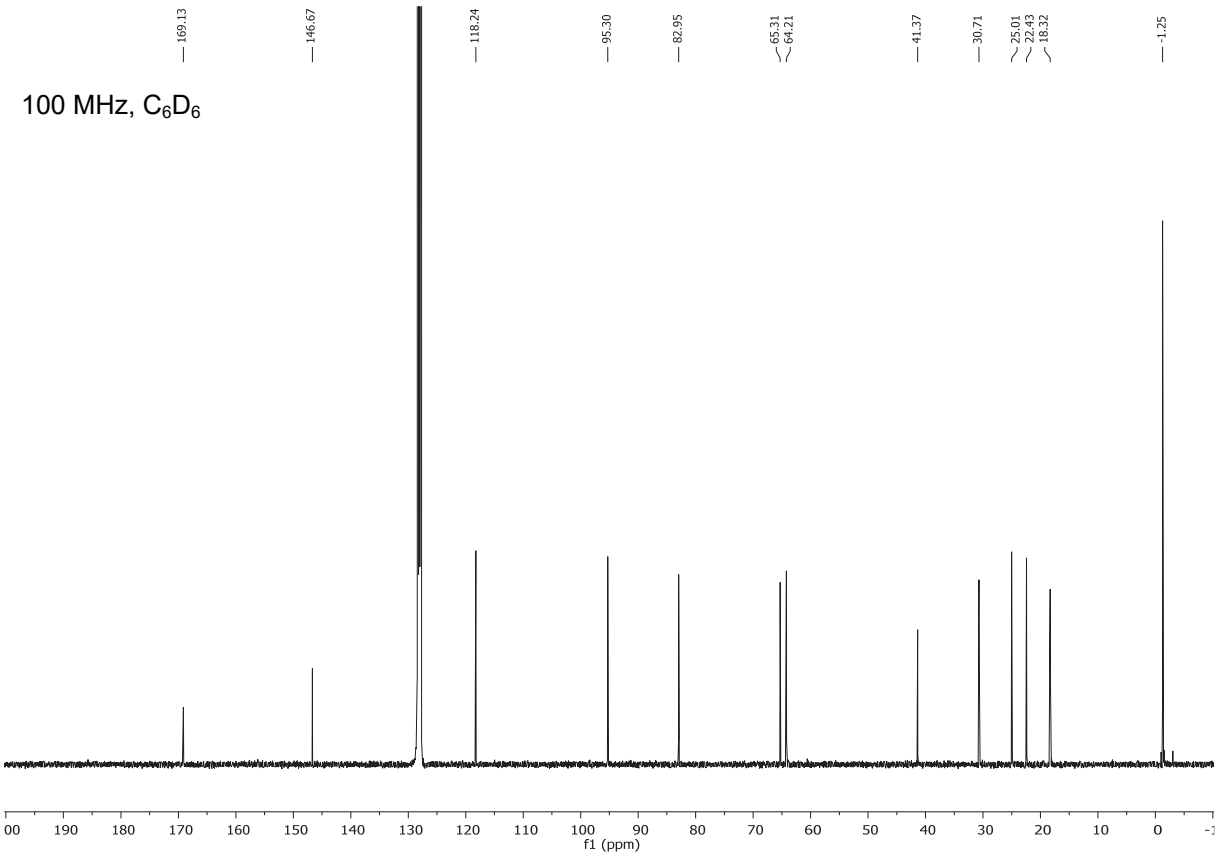

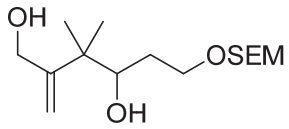

S6

400 MHz, C_6D_6

100 MHz, C_6D_6

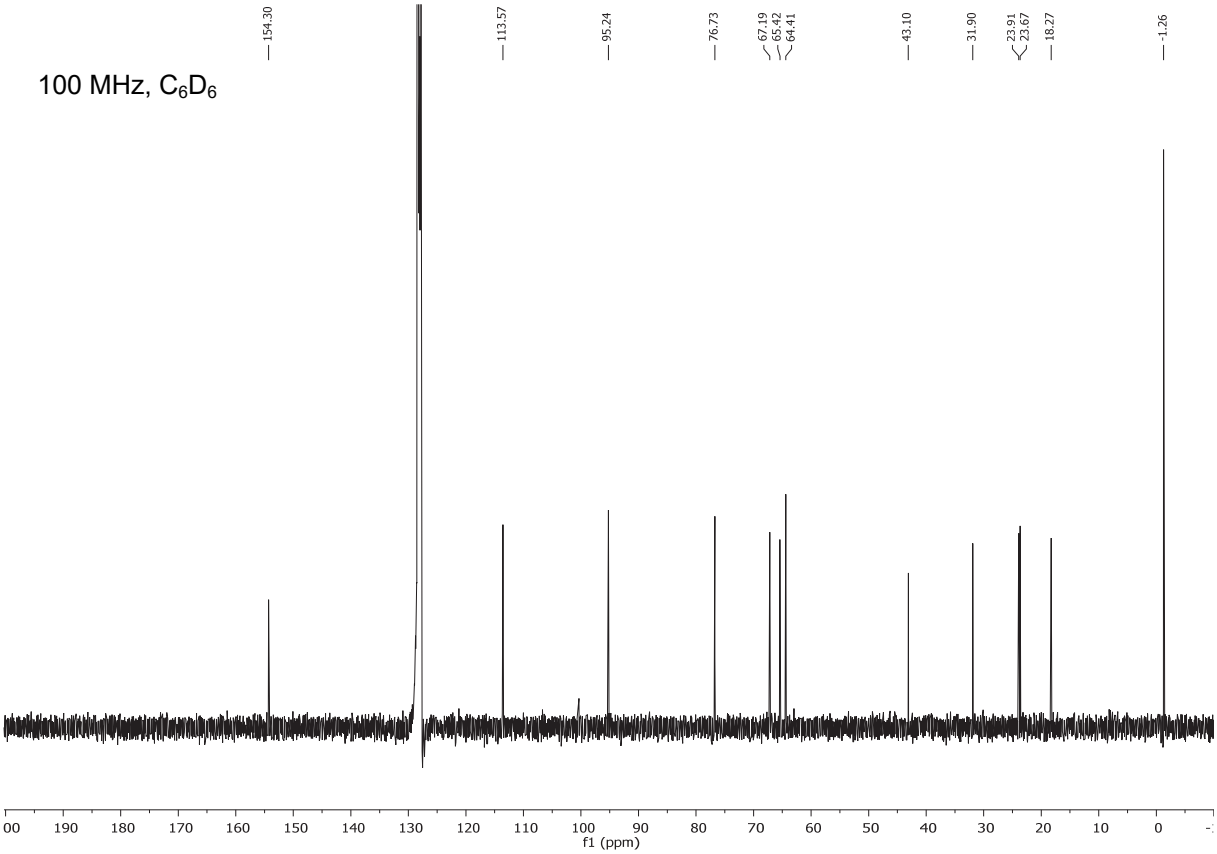

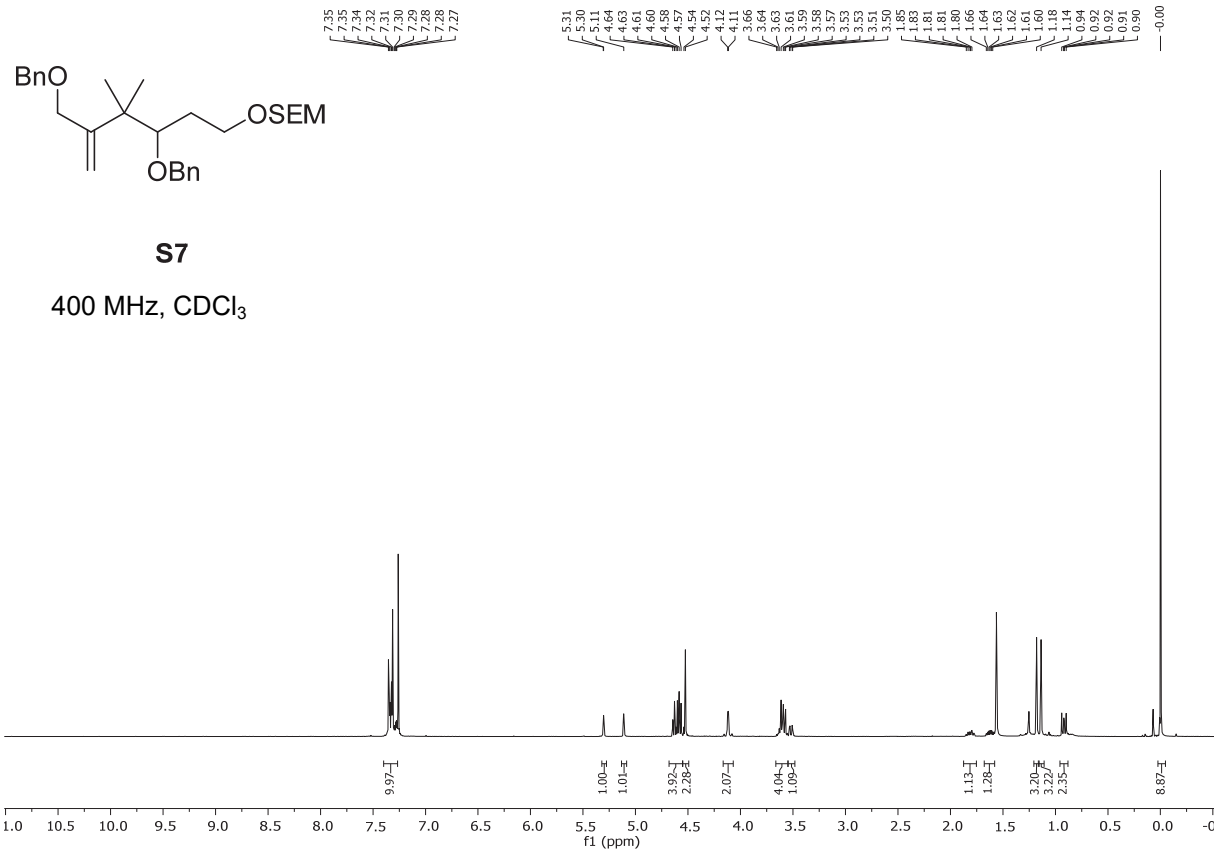

S7

400 MHz, $CDCl_3$

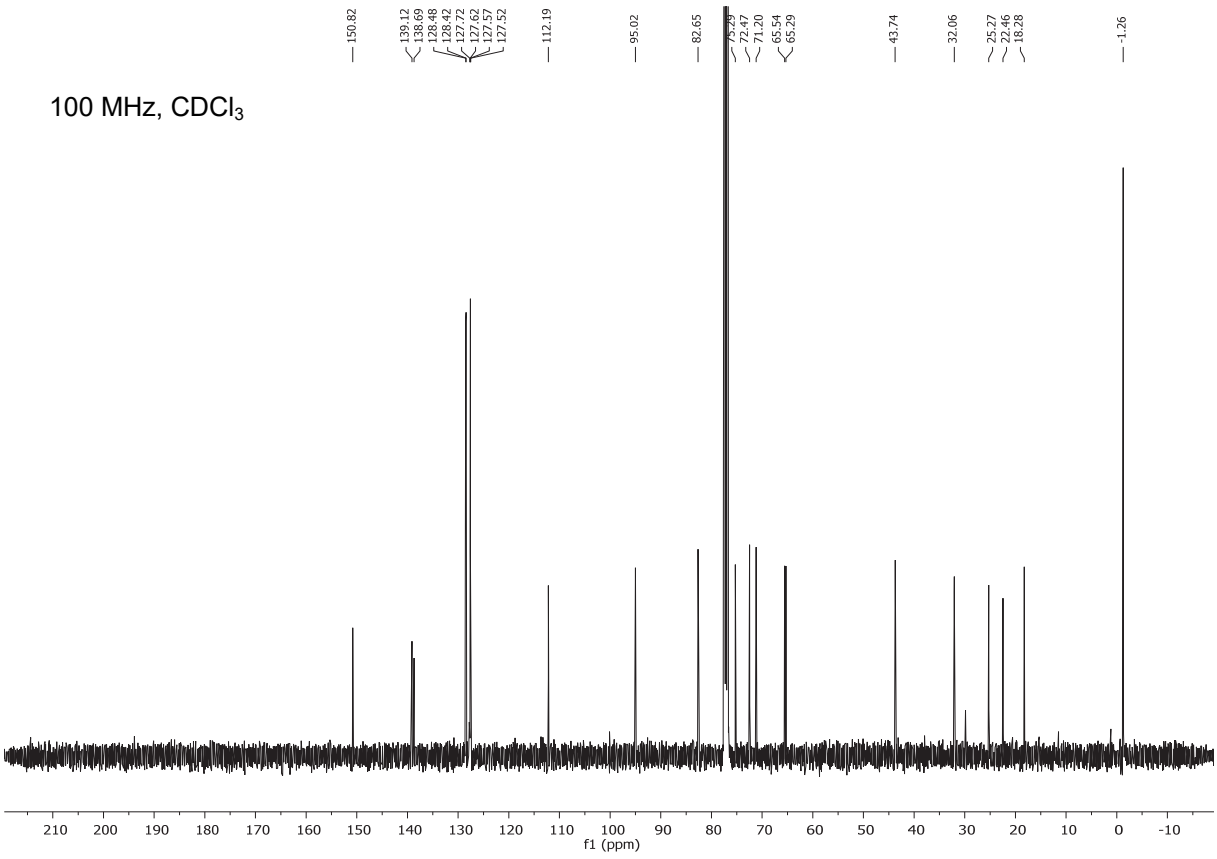

100 MHz, $CDCl_3$

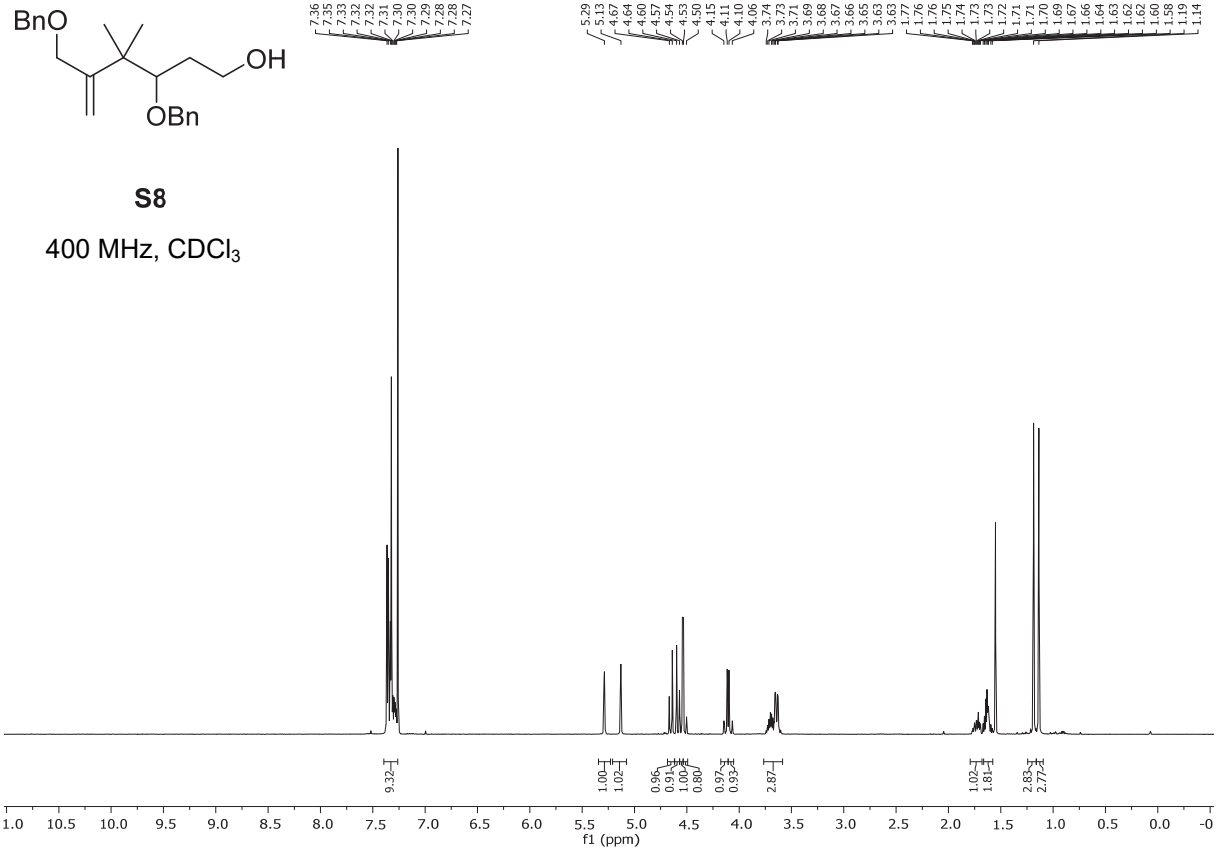

S8

400 MHz, $CDCl_3$

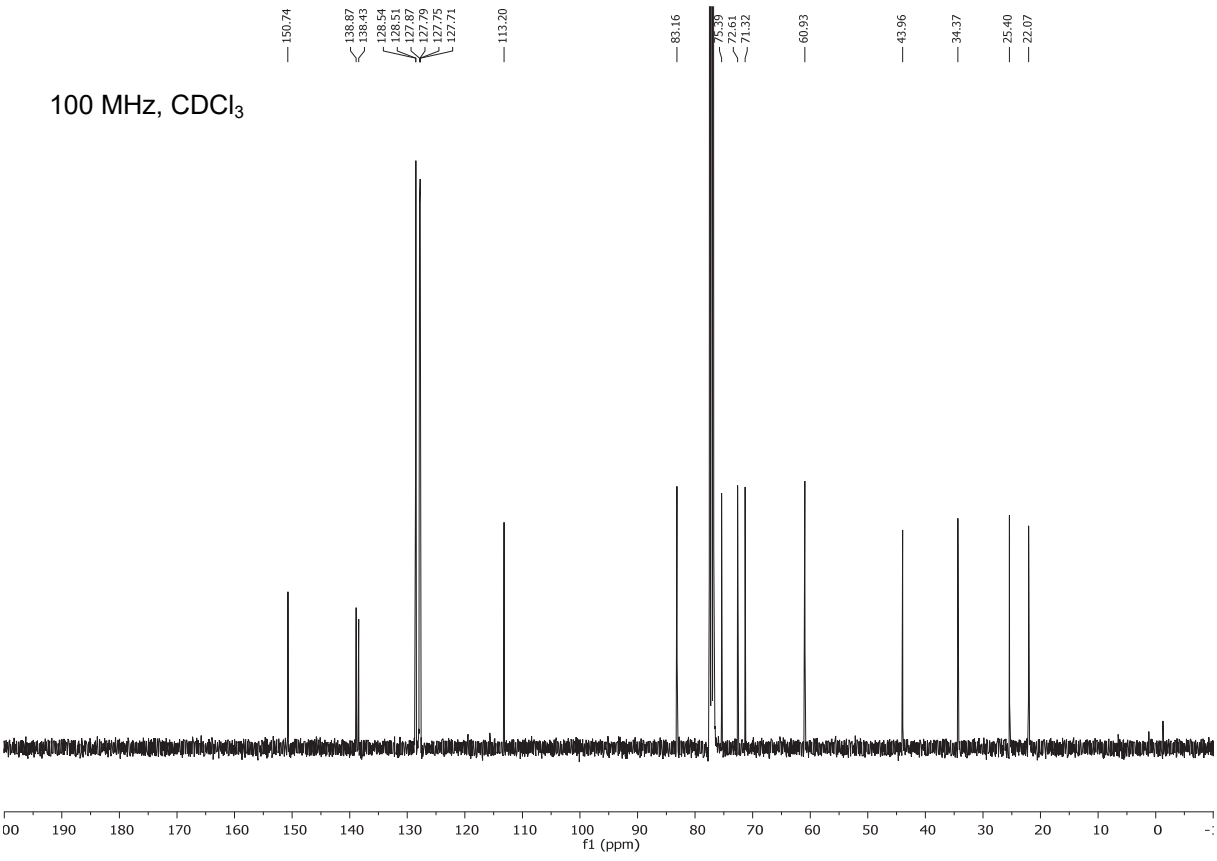

100 MHz, $CDCl_3$

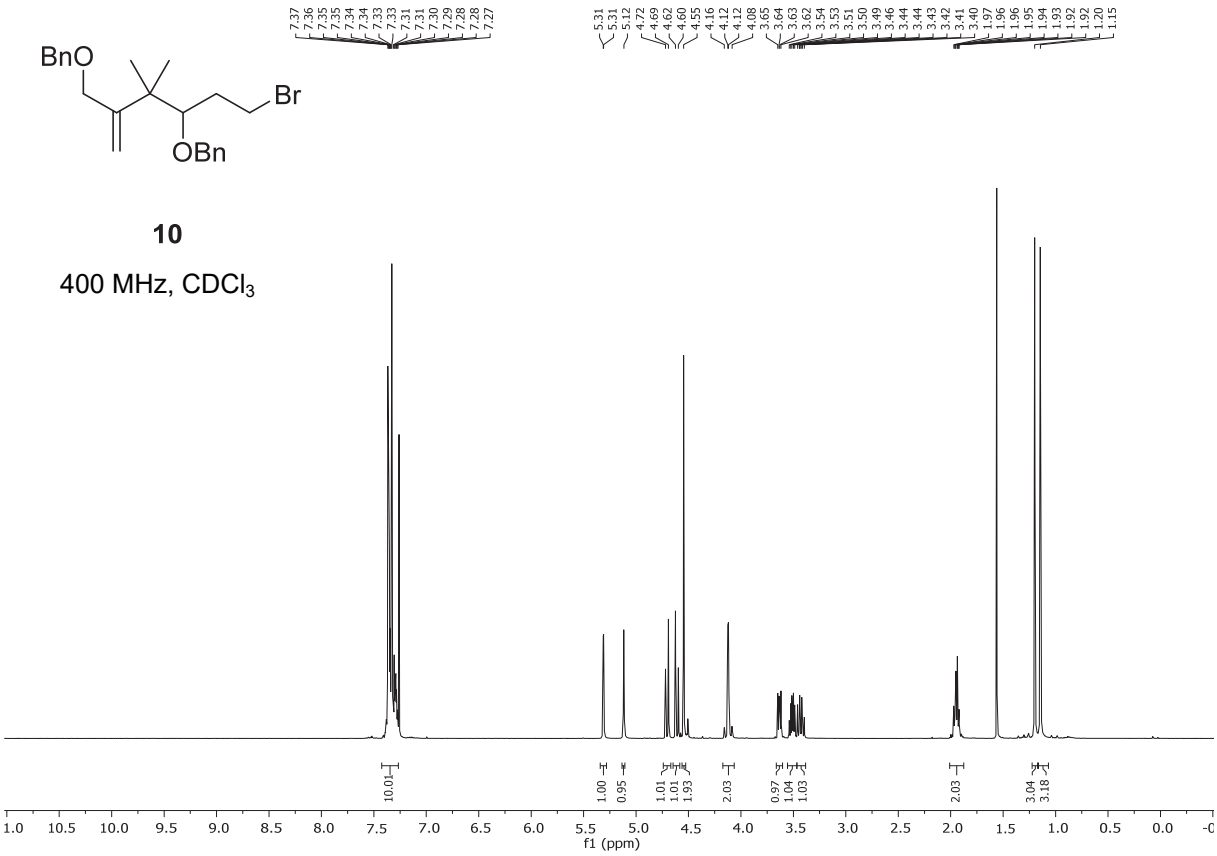
BnO
Br
OBn
10
400 MHz, CDCl3
f1 (ppm)

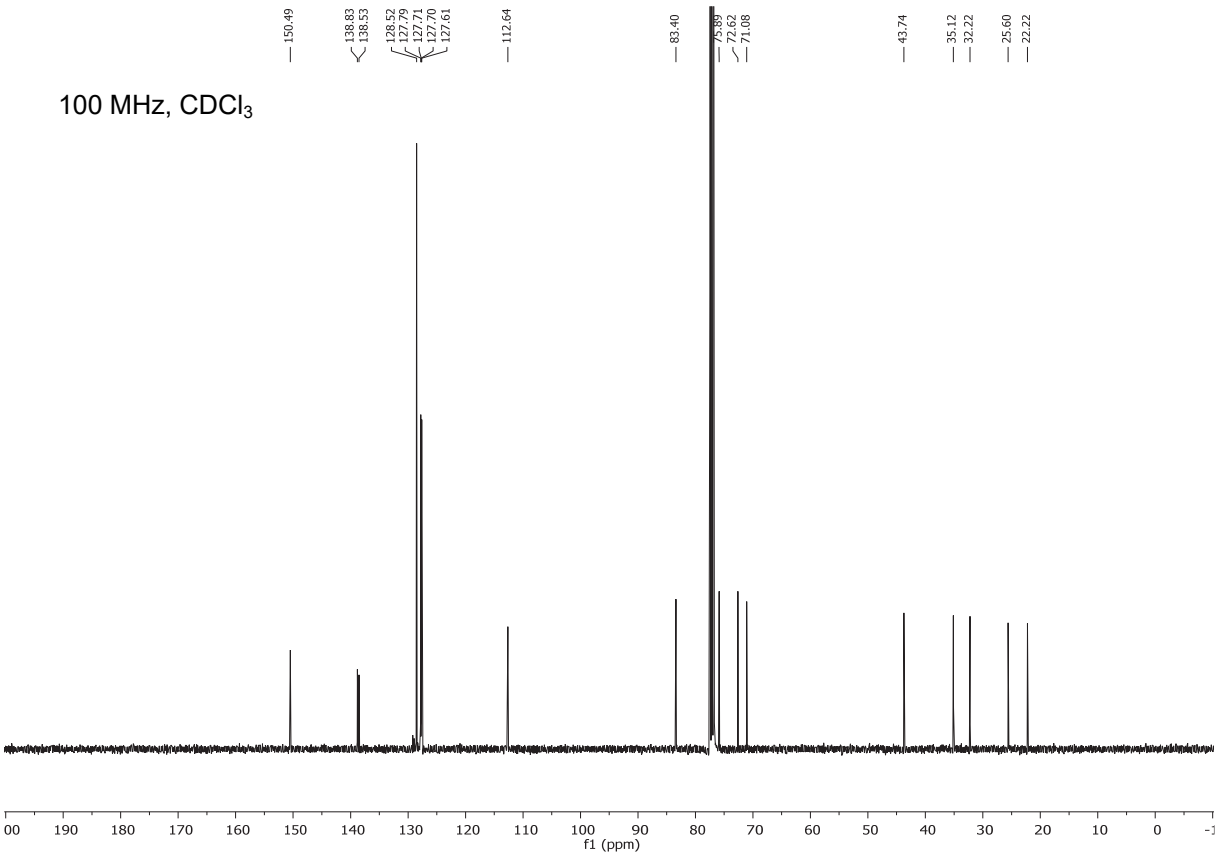
100 MHz, CDCl3
f1 (ppm)

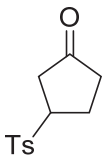

S10

400 MHz, $CDCl_3$

100 MHz, $CDCl_3$

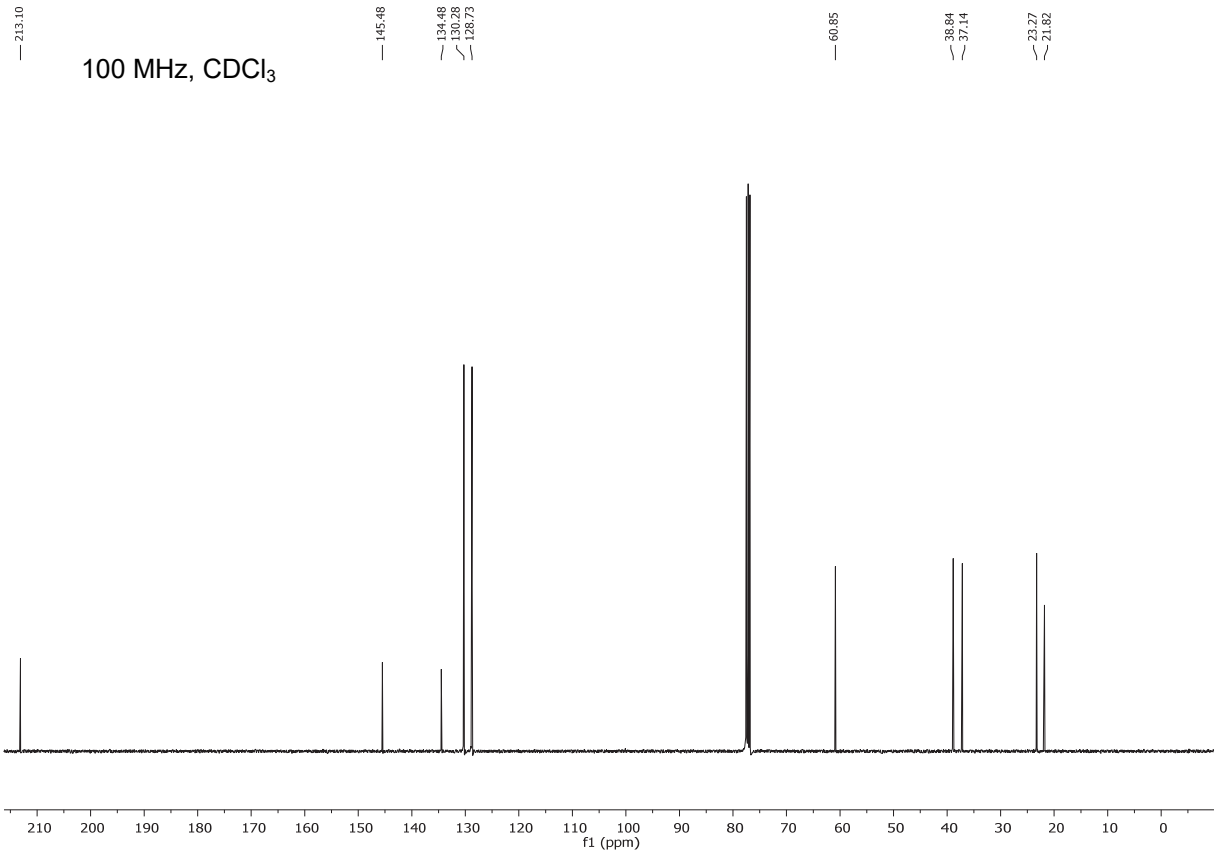

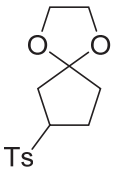

11

400 MHz, C_6D_6

100 MHz, C_6D_6

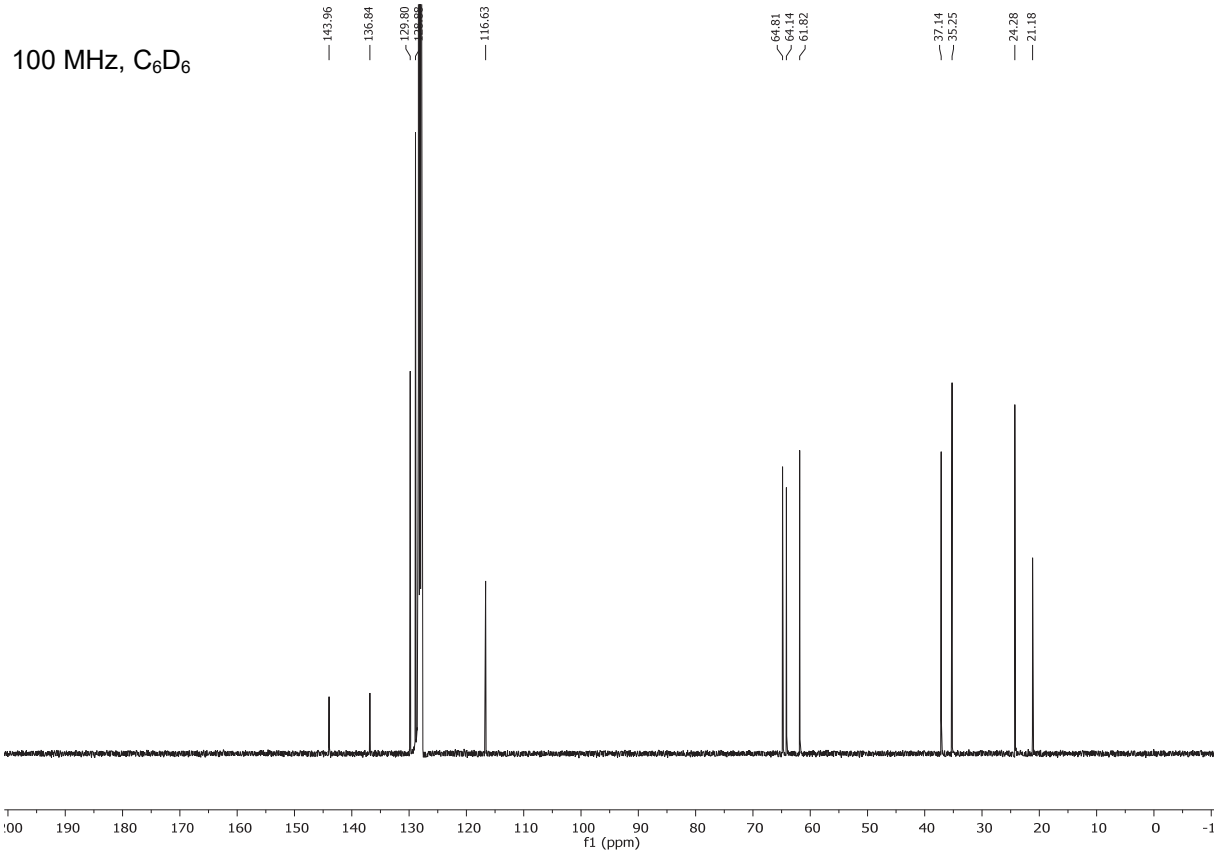

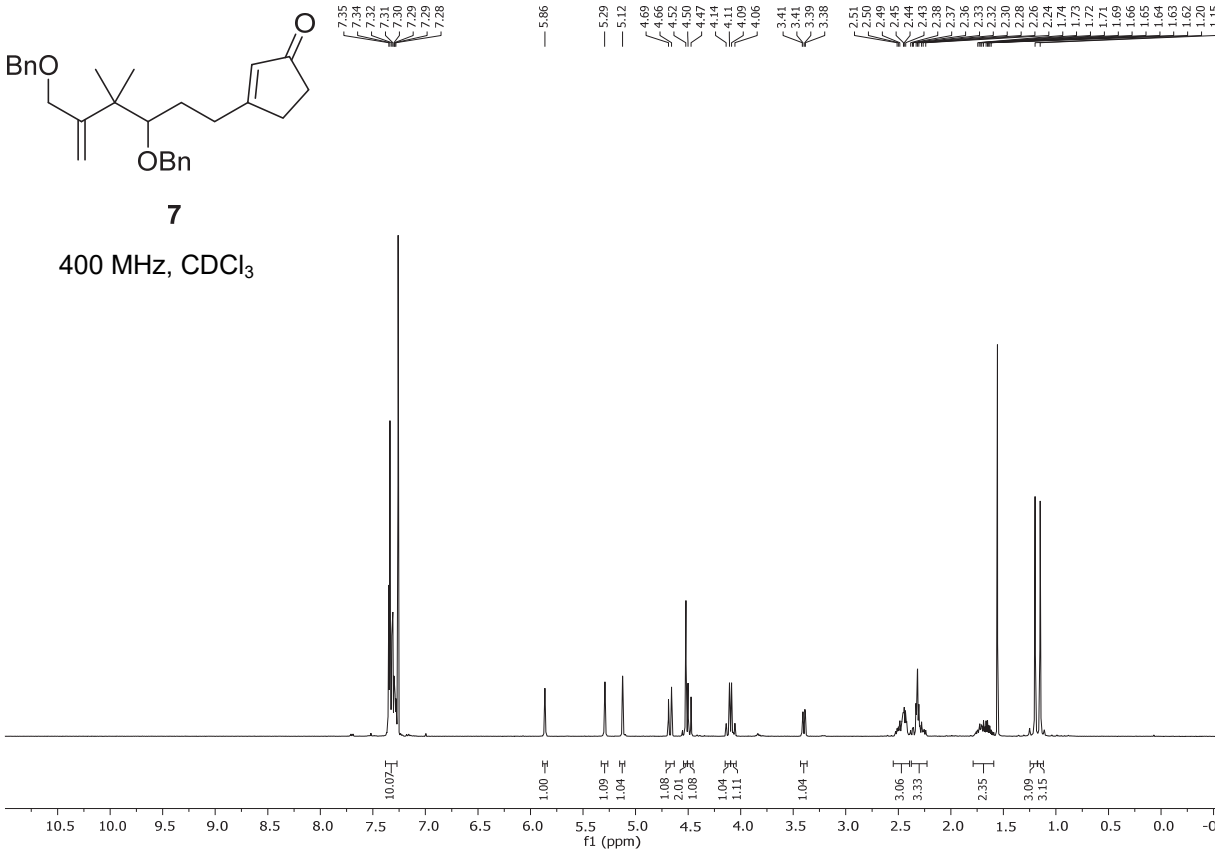

7

400 MHz, $CDCl_3$

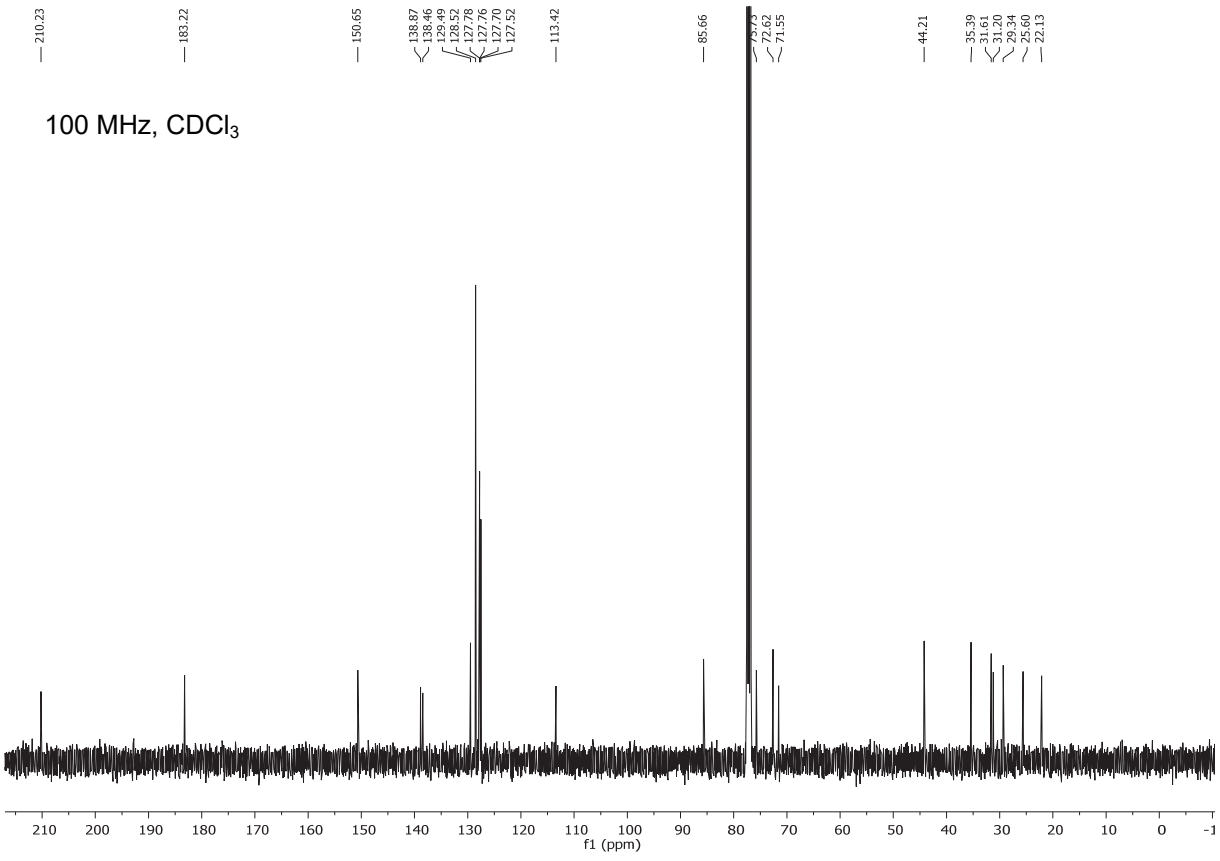

100 MHz, $CDCl_3$

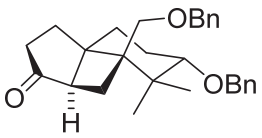

(d.r. 13:1)

6

^{1}H-NMR, 800 MHz, $CDCl_3$

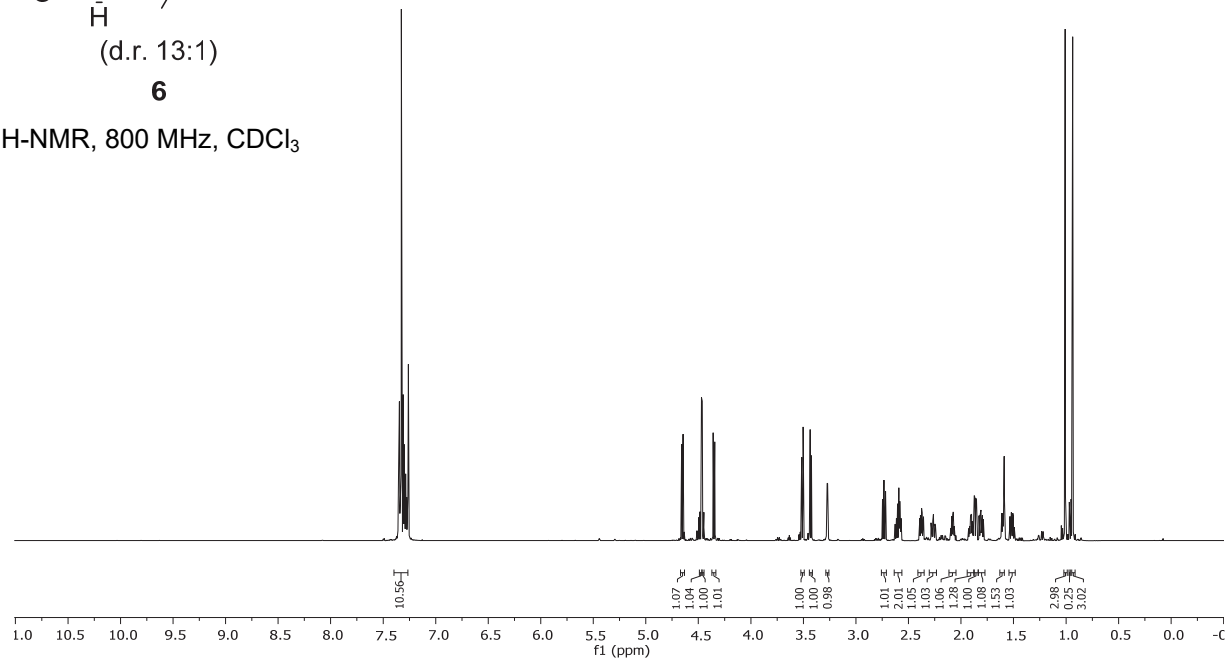

^{1}H-NMR, 800 MHz, $CDCl_3$

range: 4.7 – 0.7 ppm

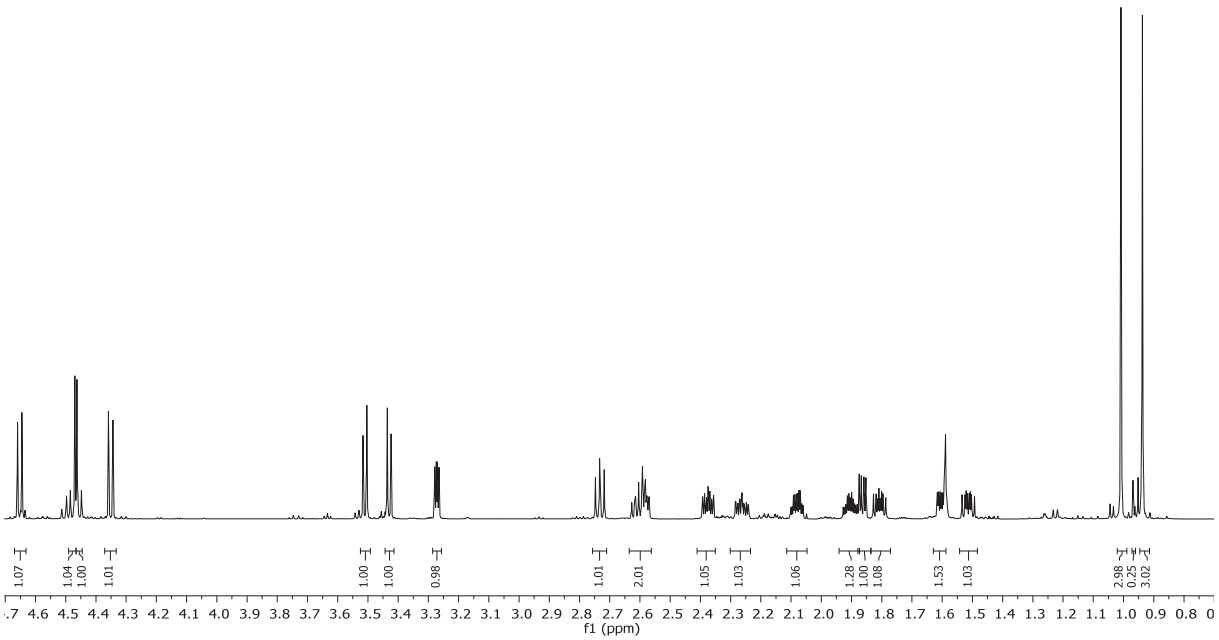

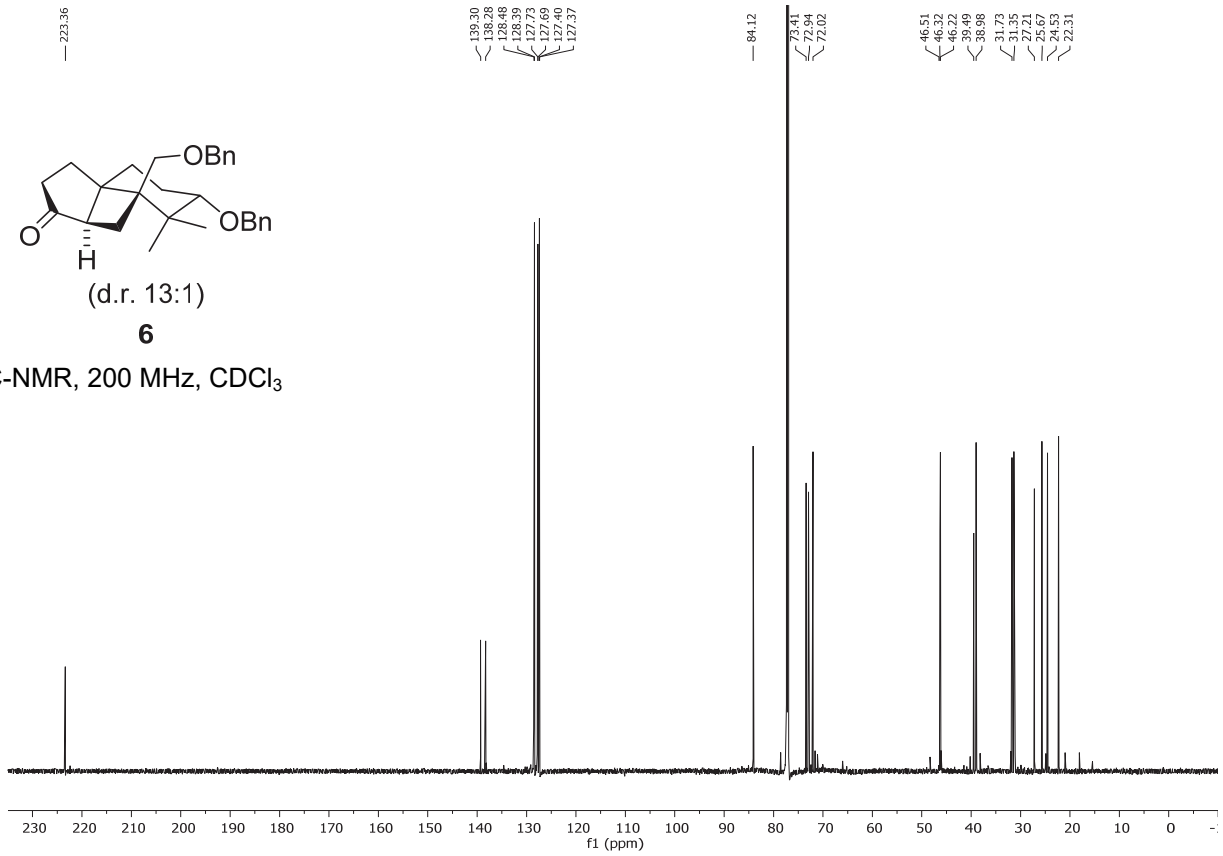

(d.r. 13:1)

6

^{13}C-NMR, 200 MHz, $CDCl_3$

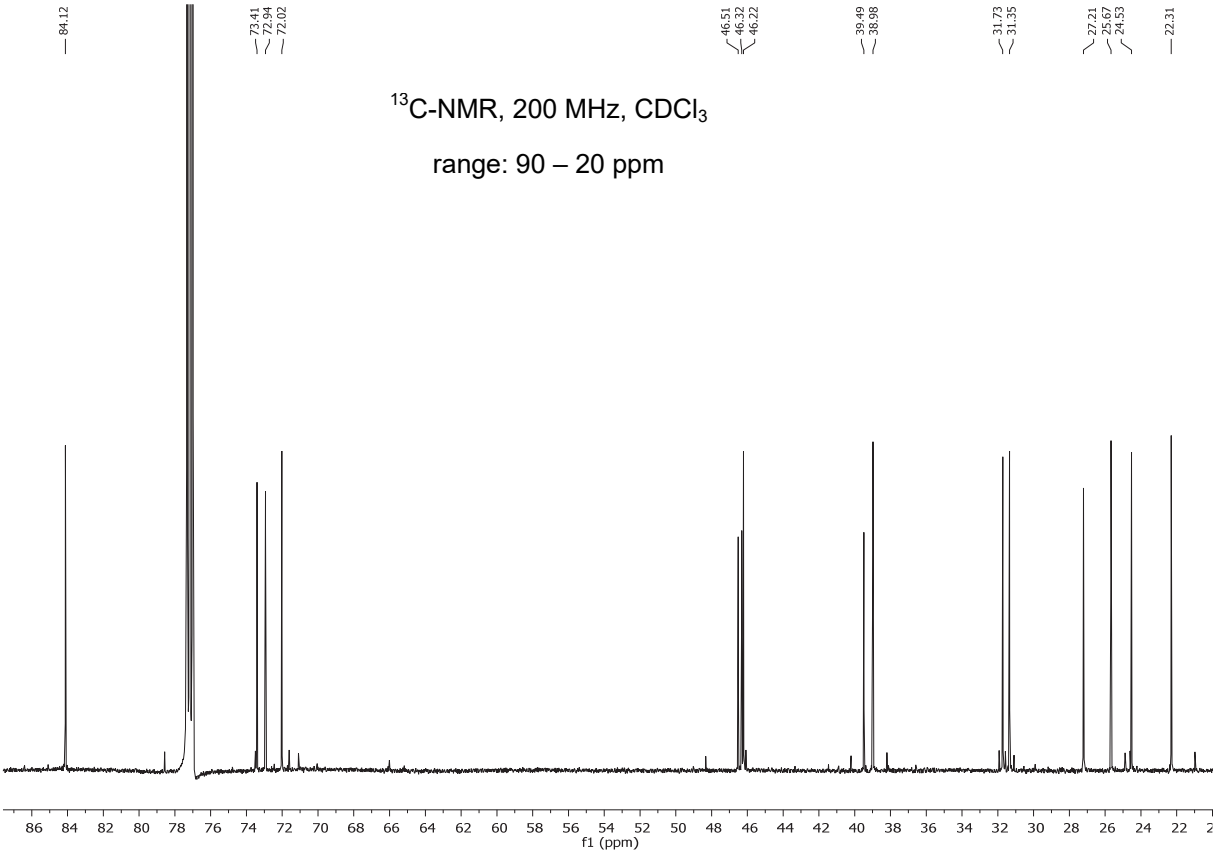

^{13}C-NMR, 200 MHz, $CDCl_3$

range: 90 – 20 ppm

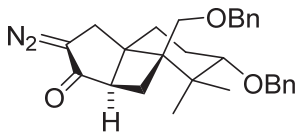

13

^{1}H-NMR, 600 MHz, CD_2Cl_2

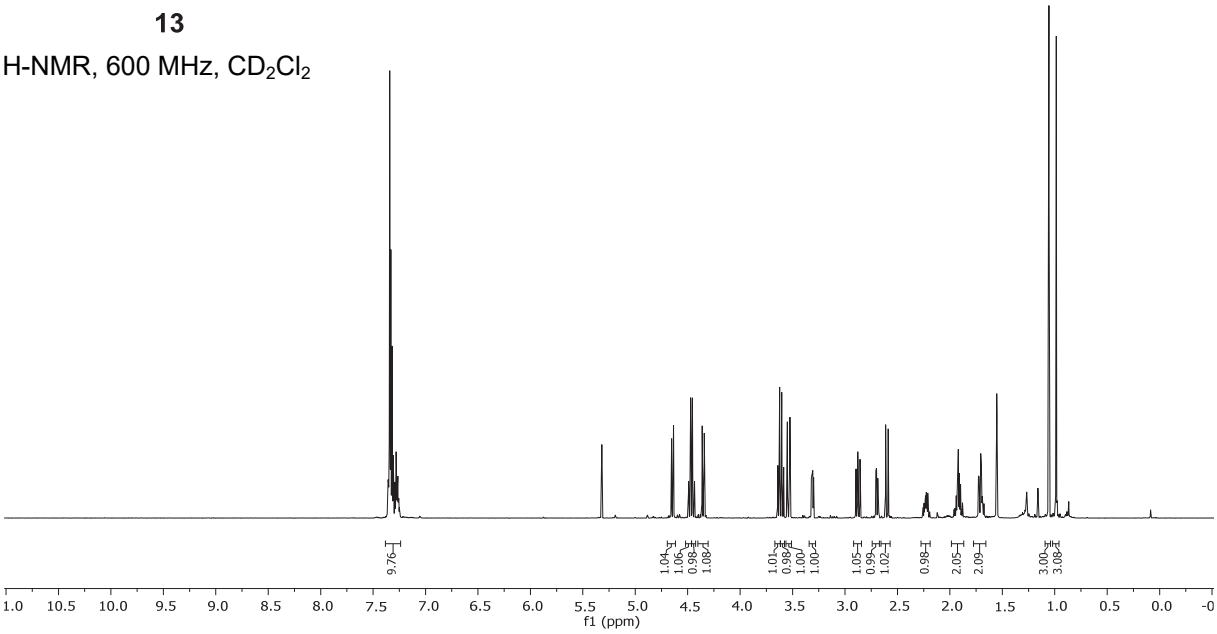

^{1}H-NMR, 600 MHz, CD_2Cl_2

range: 4.7 – 0.7 ppm

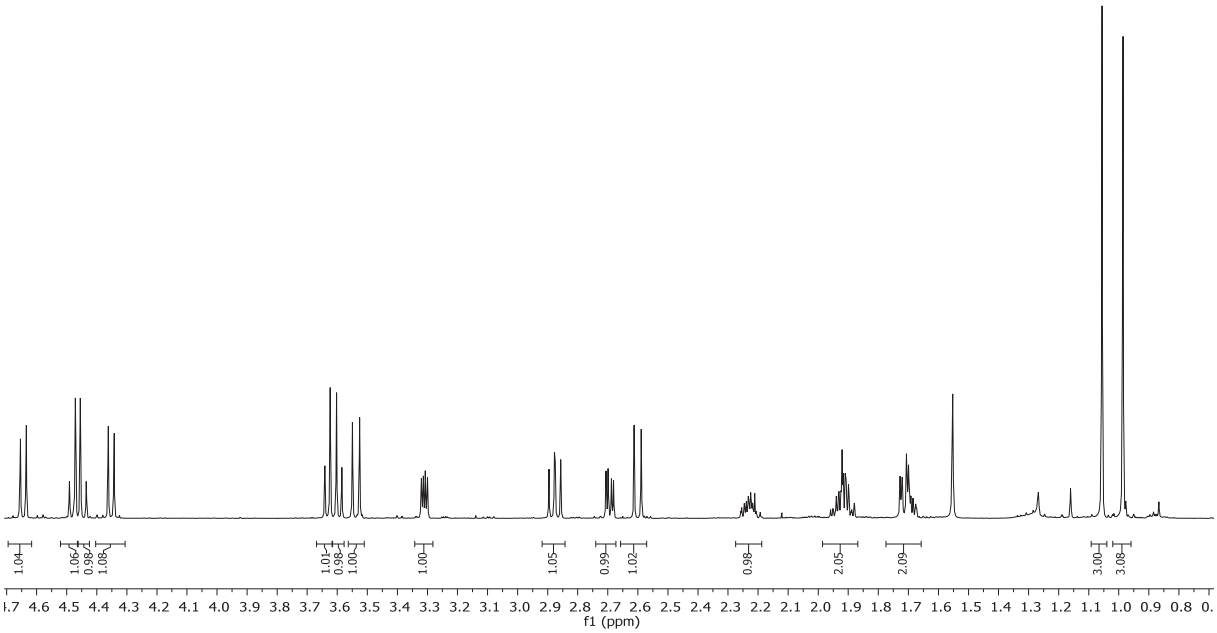

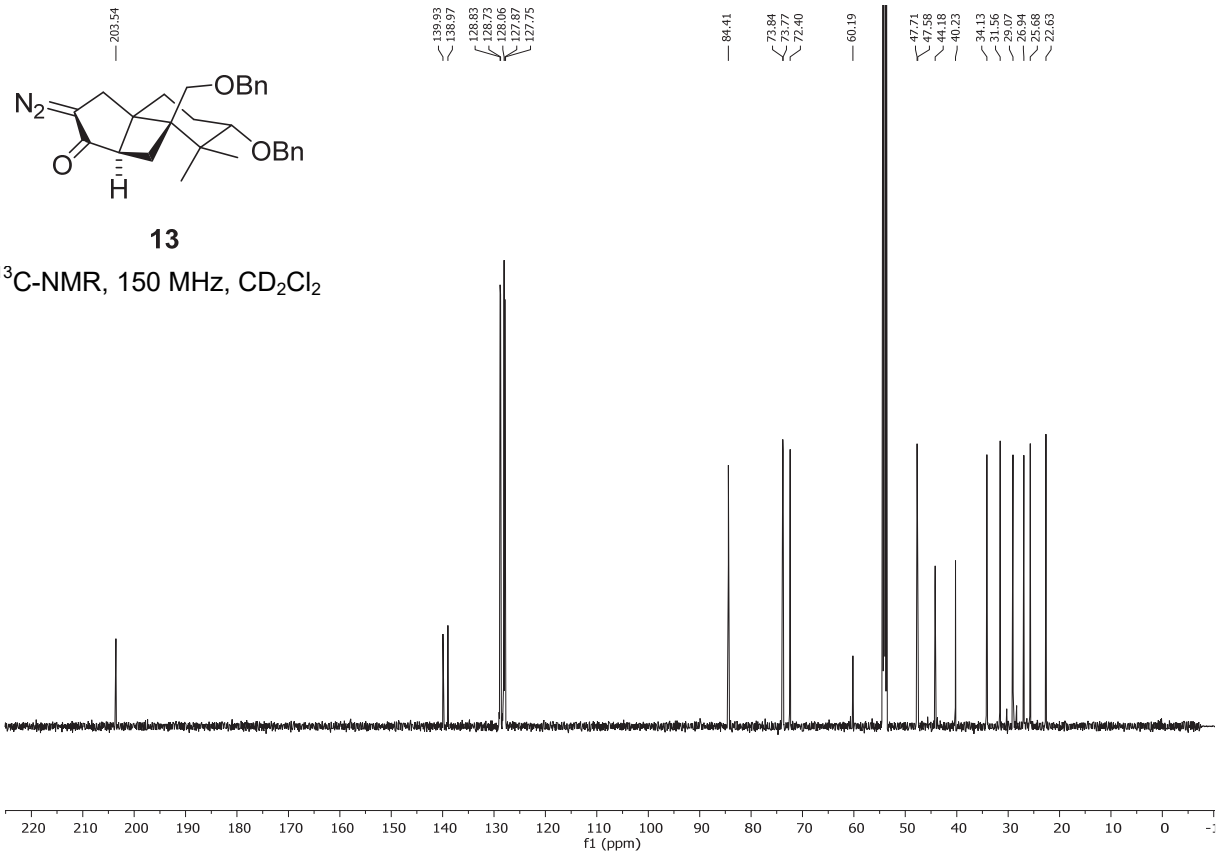

13

^{13}C-NMR, 150 MHz, CD_2Cl_2

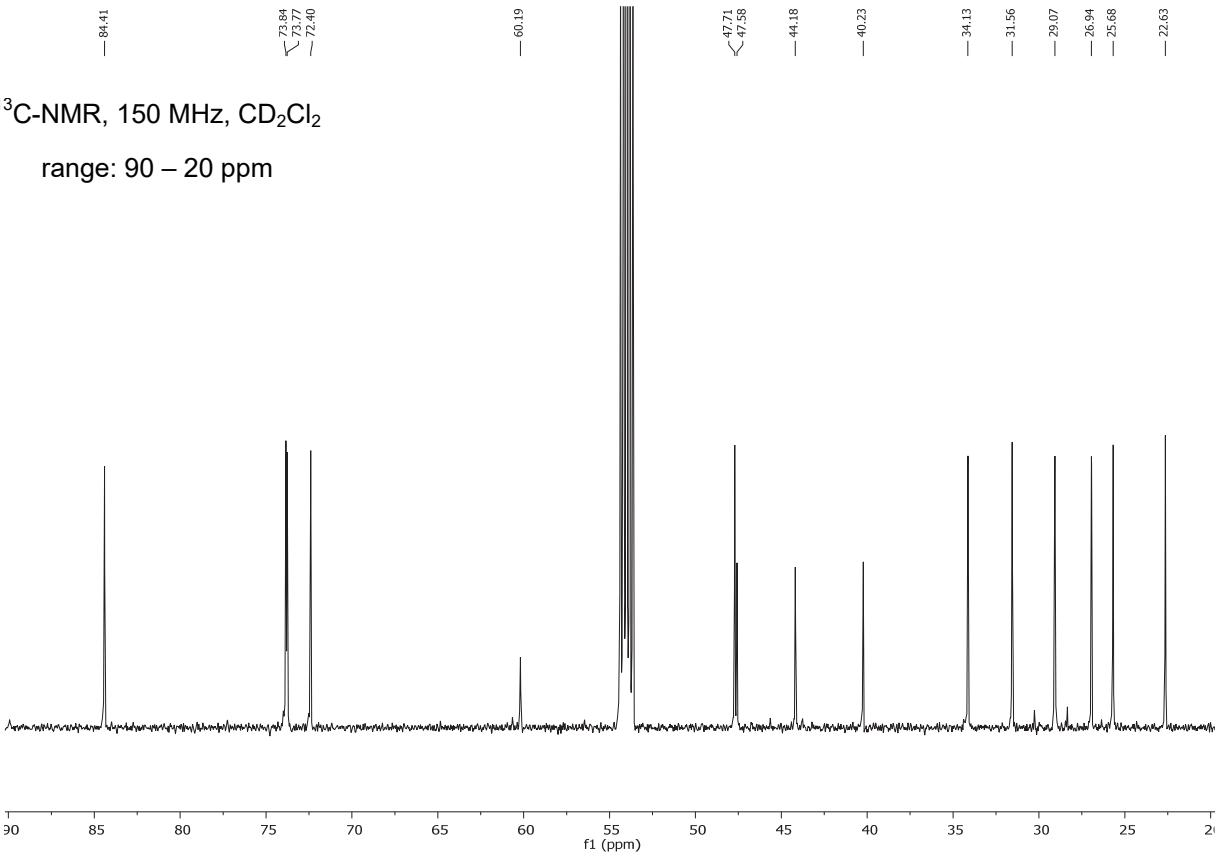

^{13}C-NMR, 150 MHz, CD_2Cl_2

range: 90 – 20 ppm

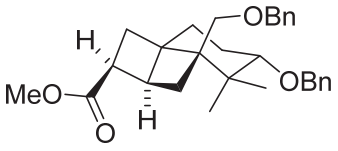

14

major diastereomer (d.r. 3:1)

^{1}H-NMR, 600 MHz, CD_2Cl_2

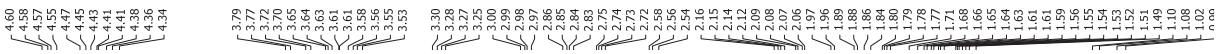

^{1}H-NMR, 600 MHz, CD_2Cl_2

range: 4.7 – 0.7 ppm

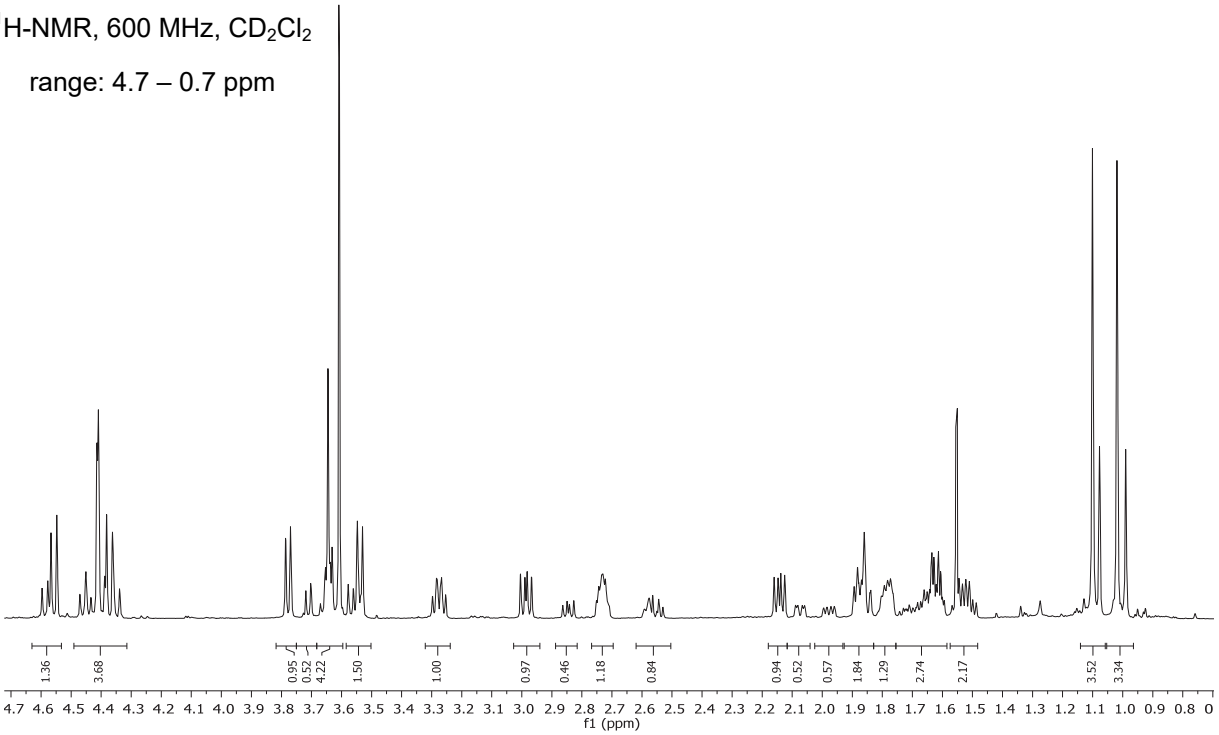

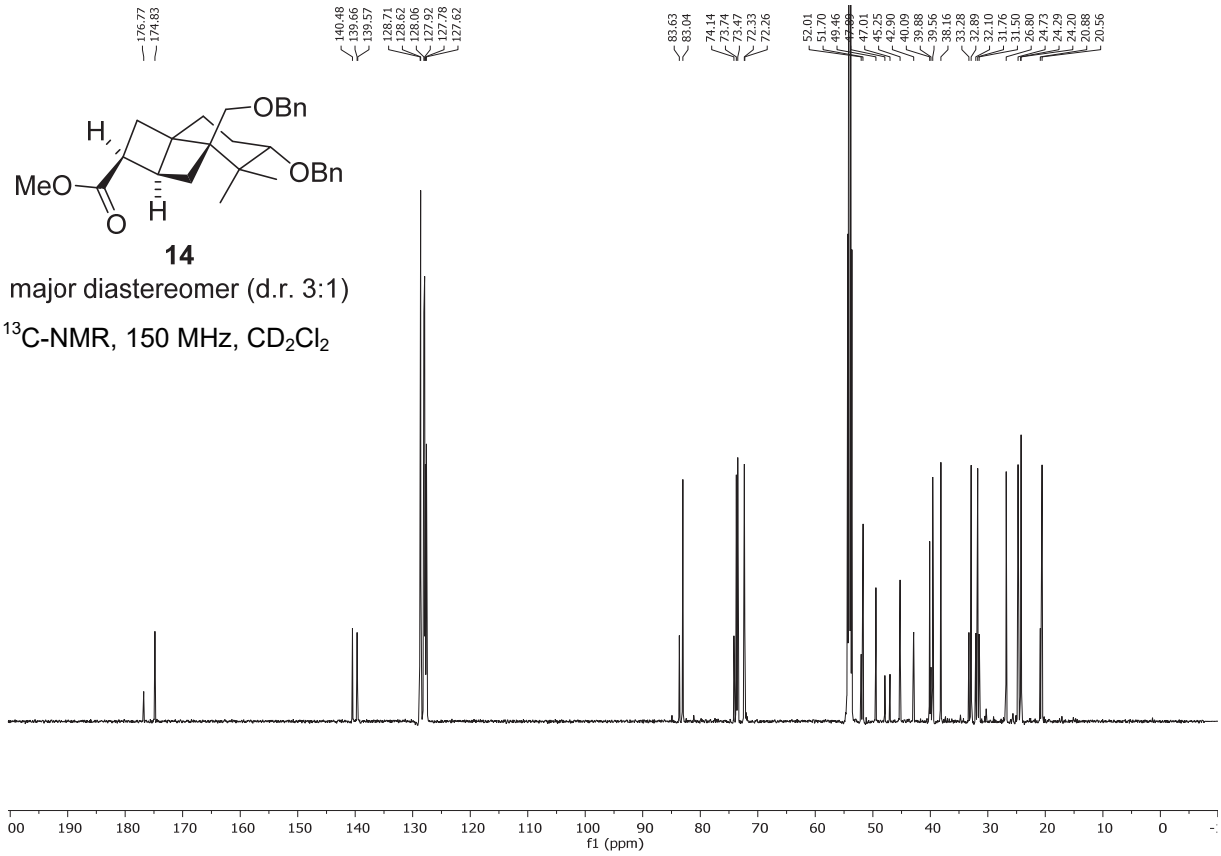

14

major diastereomer (d.r. 3:1)

^{13}C-NMR, 150 MHz, CD_2Cl_2

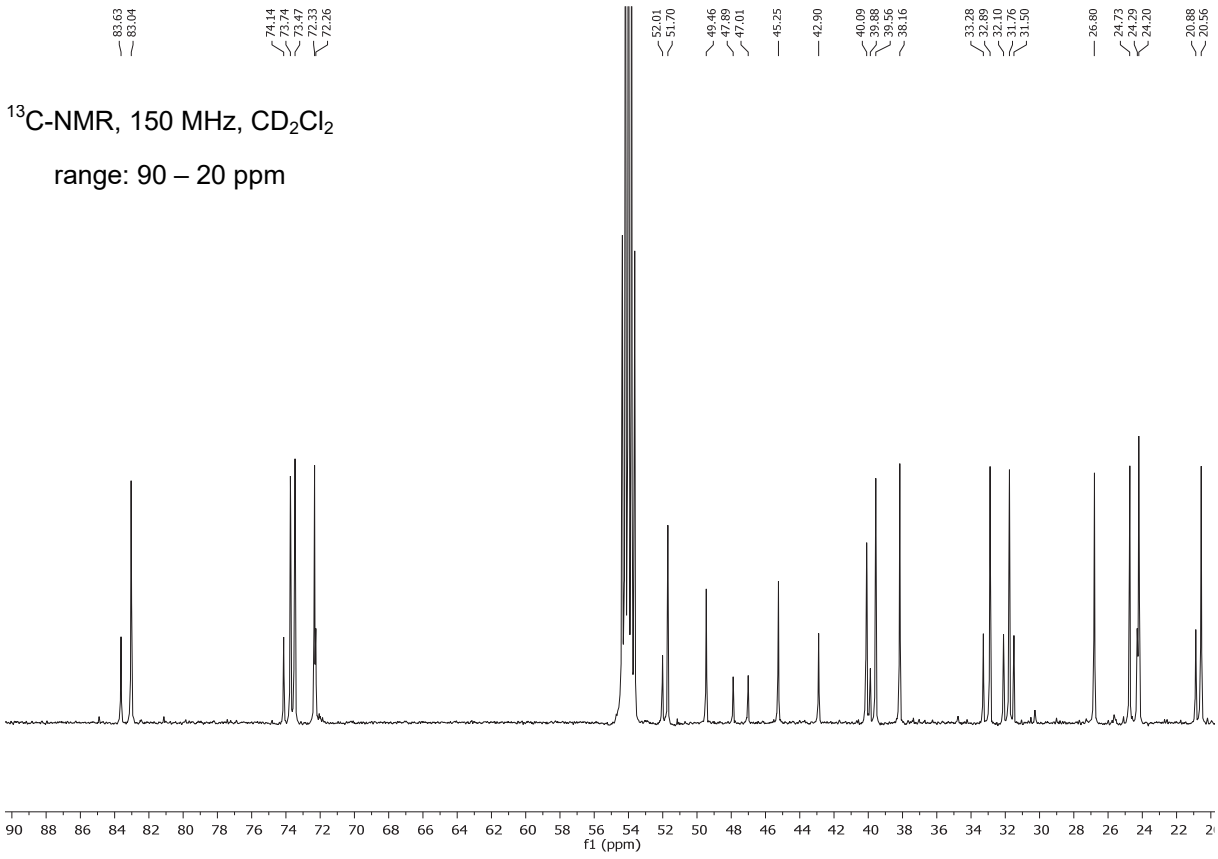

^{13}C-NMR, 150 MHz, CD_2Cl_2

range: 90 – 20 ppm

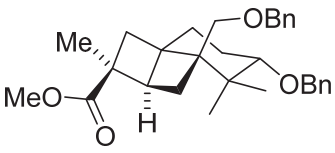

5

(d.r. 20:1)

^{1}H-NMR, 400 MHz, CD_2Cl_2

^{1}H-NMR, 400 MHz, CD_2Cl_2

range: 4.7 – 0.7 ppm

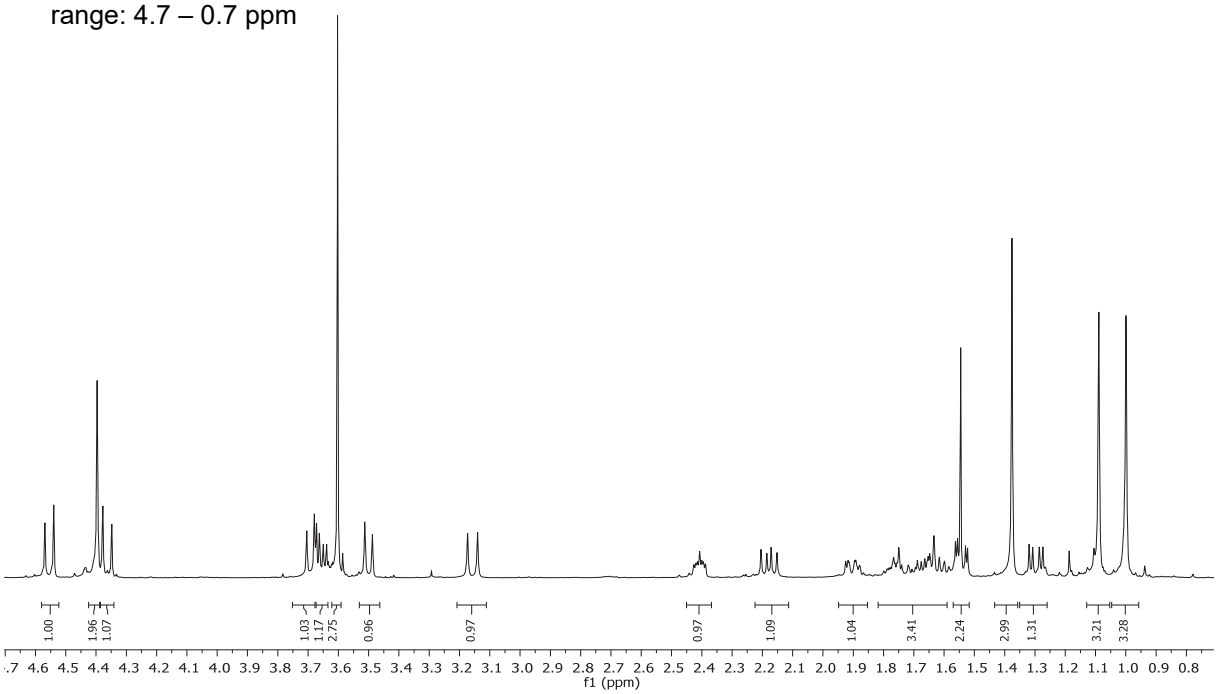

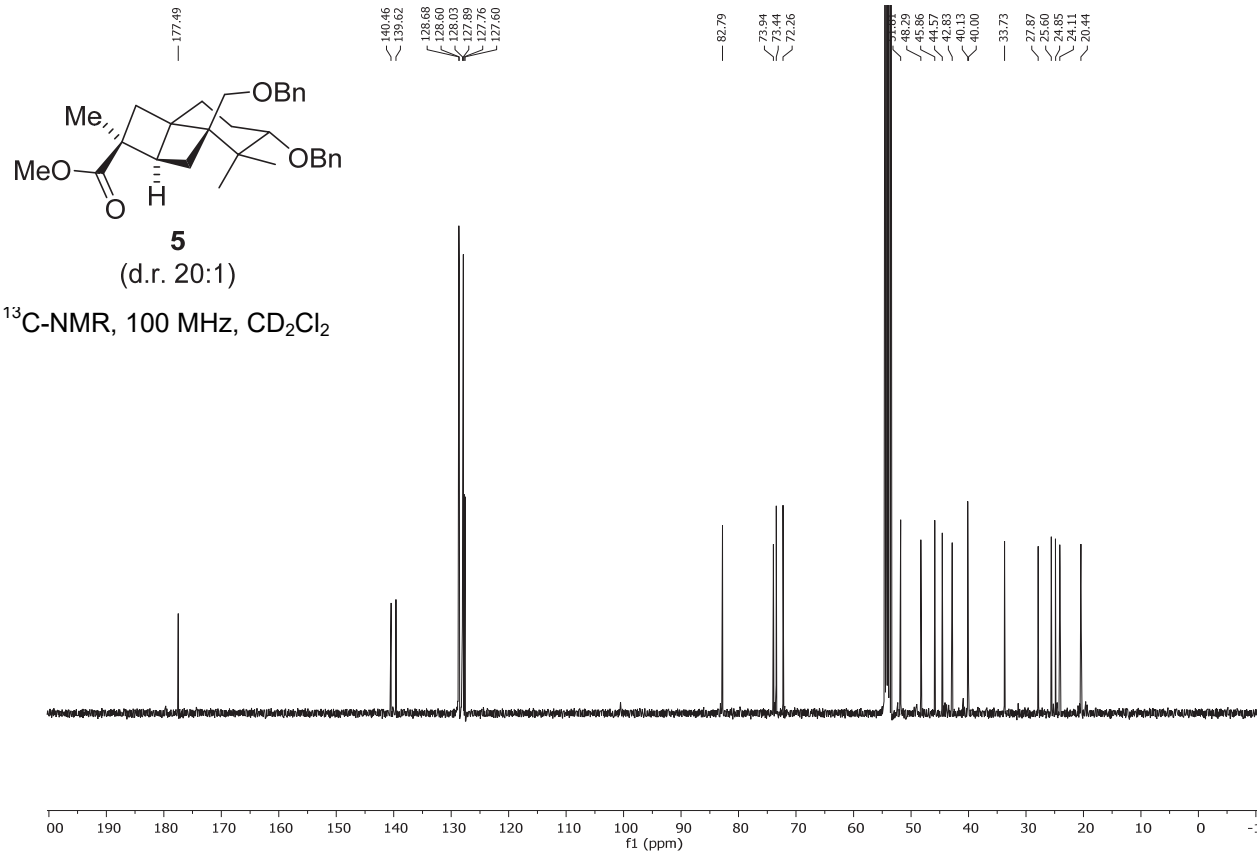

5

(d.r. 20:1)

^{13}C-NMR, 100 MHz, CD_2Cl_2

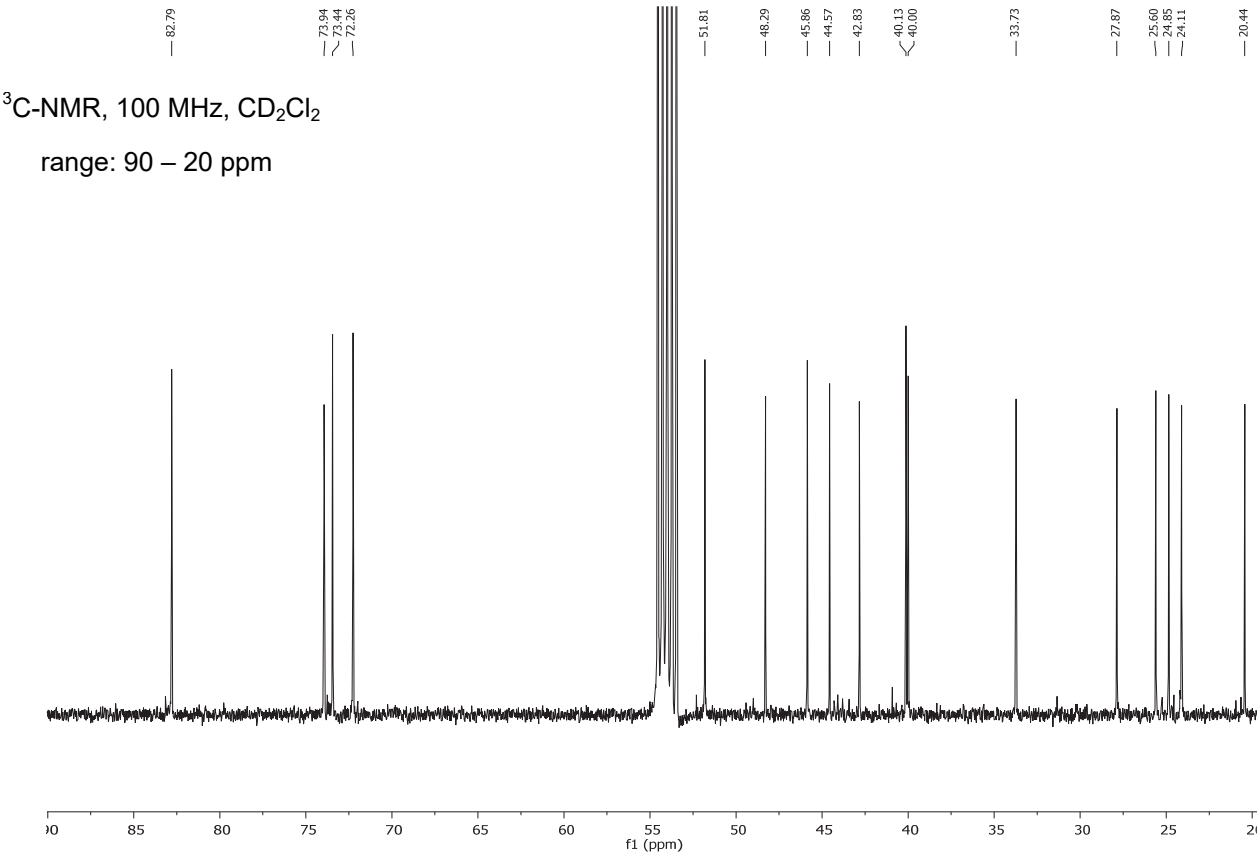

^{13}C-NMR, 100 MHz, CD_2Cl_2

range: 90 – 20 ppm

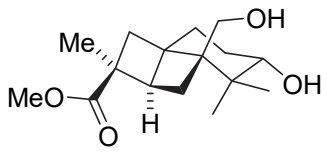

15

^{1}H-NMR, 400 MHz, CD_2Cl_2

^{1}H-NMR, 400 MHz, CD_2Cl_2

range: 4.7 – 0.7 ppm

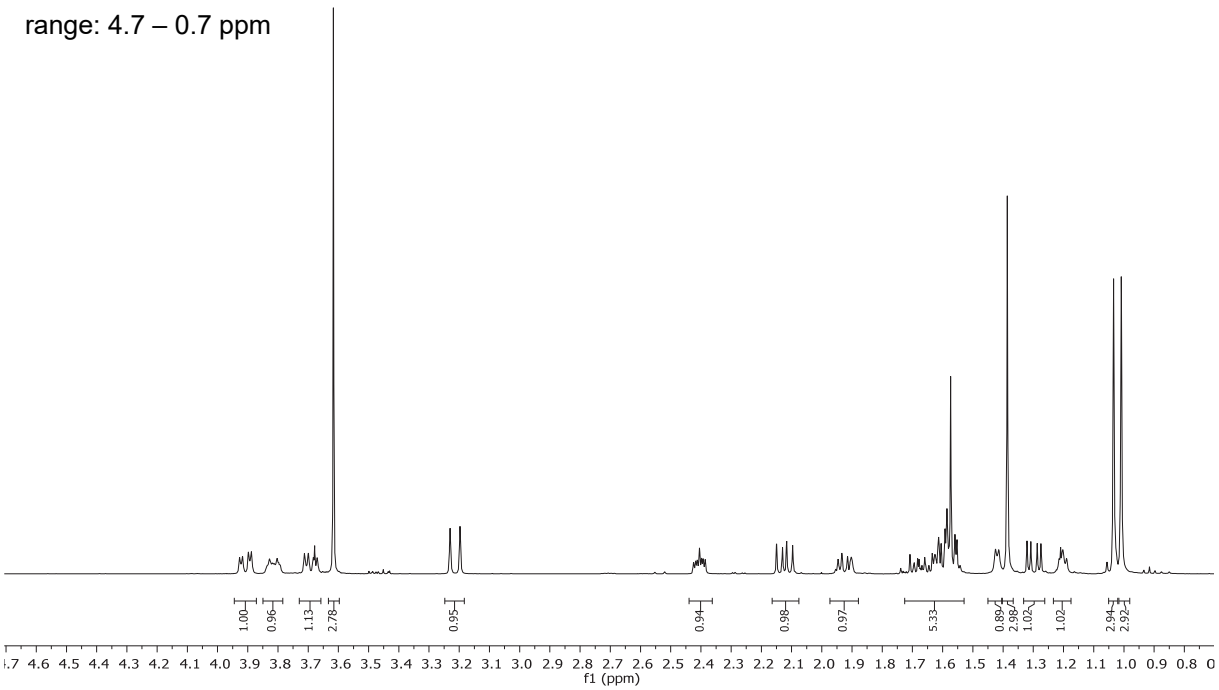

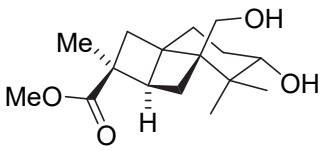

15

^{13}C-NMR, 100 MHz, CD_2Cl_2

^{13}C-NMR, 100 MHz, CD_2Cl_2

range: 90 – 15 ppm

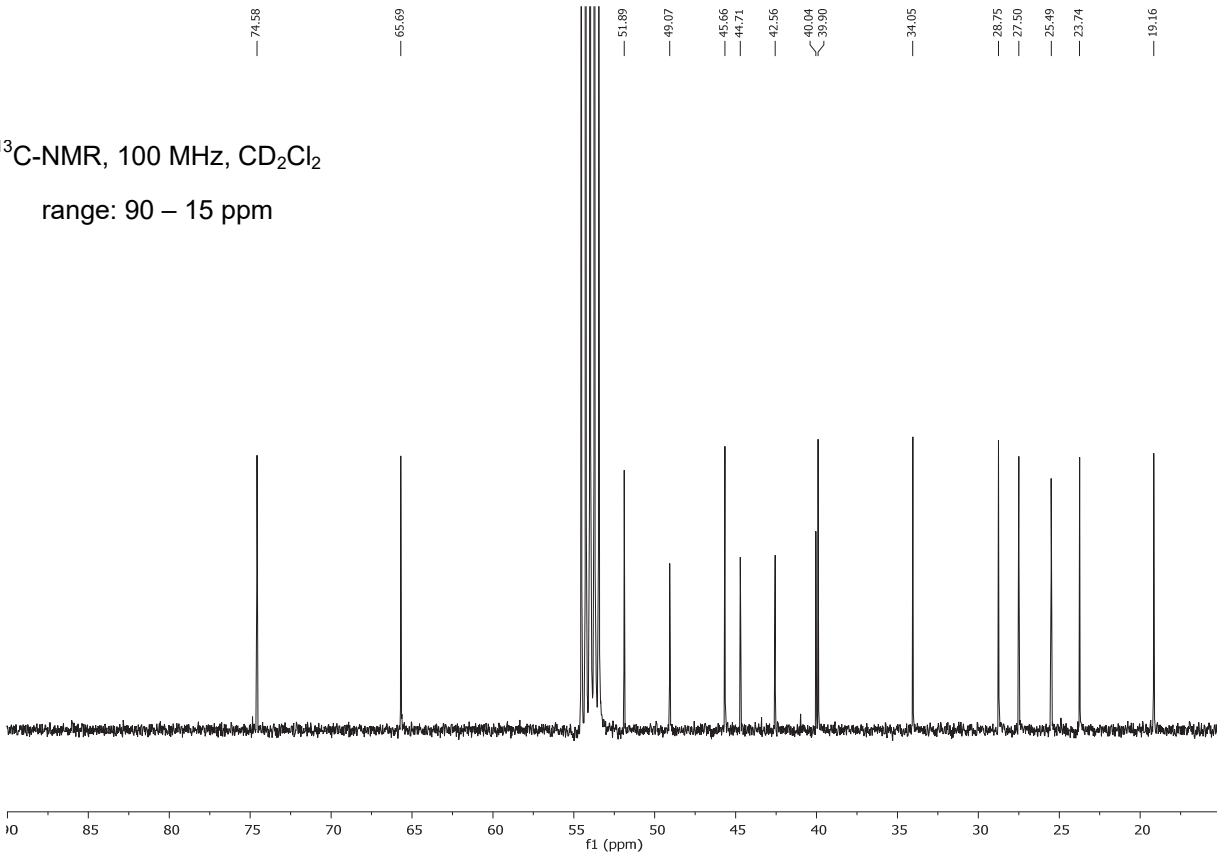

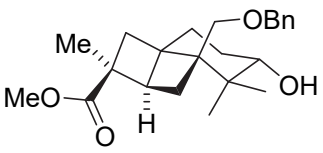

S12

^{1}H-NMR, 400 MHz, CD_2Cl_2

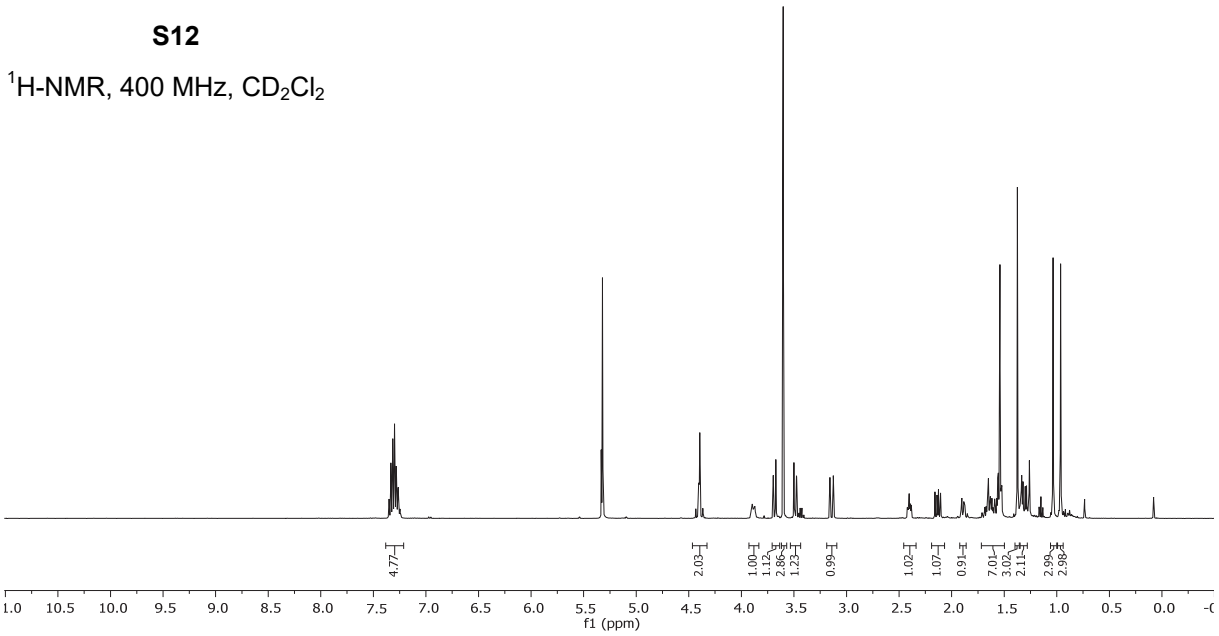

^{1}H-NMR, 400 MHz, CD_2Cl_2

range: 4.7 – 0.7 ppm

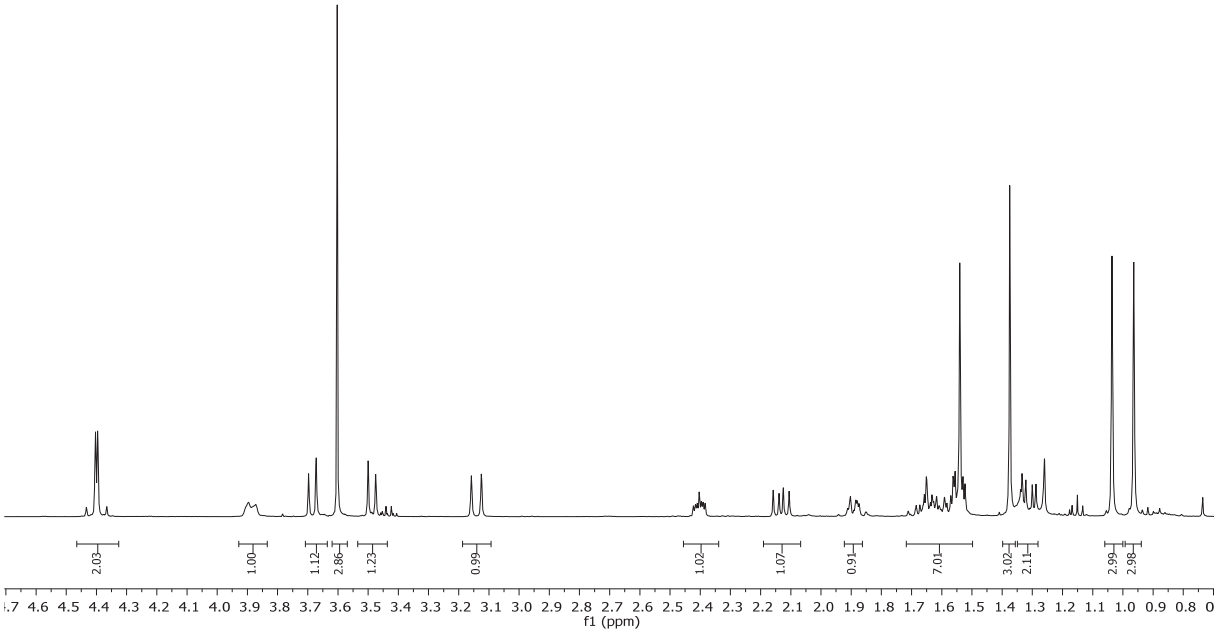

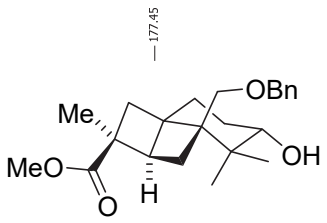

S12

^{13}C-NMR, 100 MHz, CD_2Cl_2

^{13}C-NMR, 100 MHz, CD_2Cl_2

range: 90 – 15 ppm

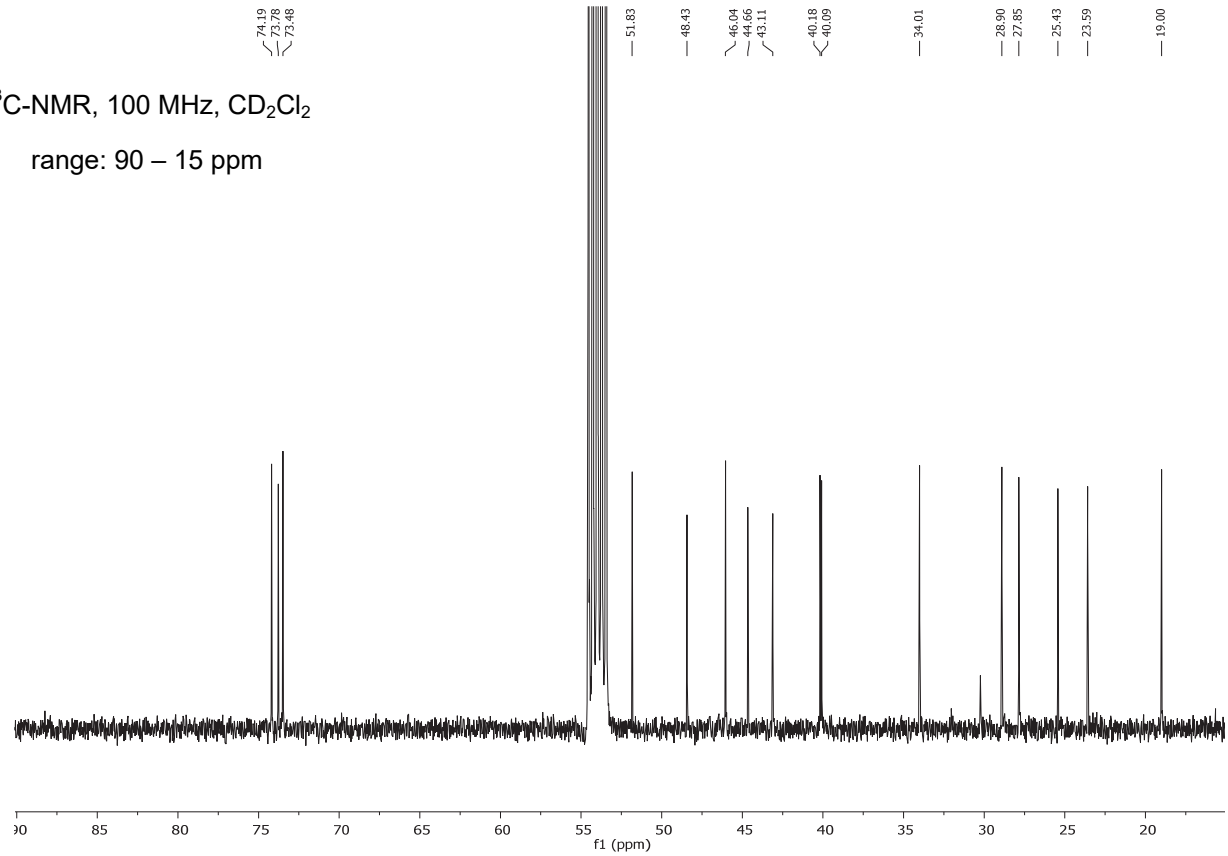

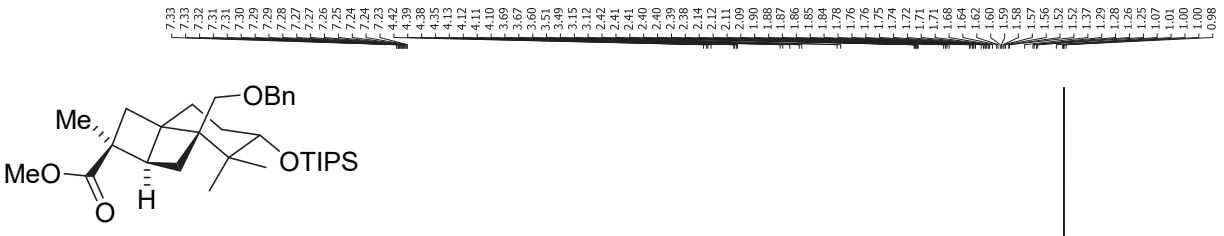

S13

^{1}H-NMR, 400 MHz, CD_2Cl_2

^{1}H-NMR, 400 MHz, CD_2Cl_2

range: 4.7 – 0.7 ppm

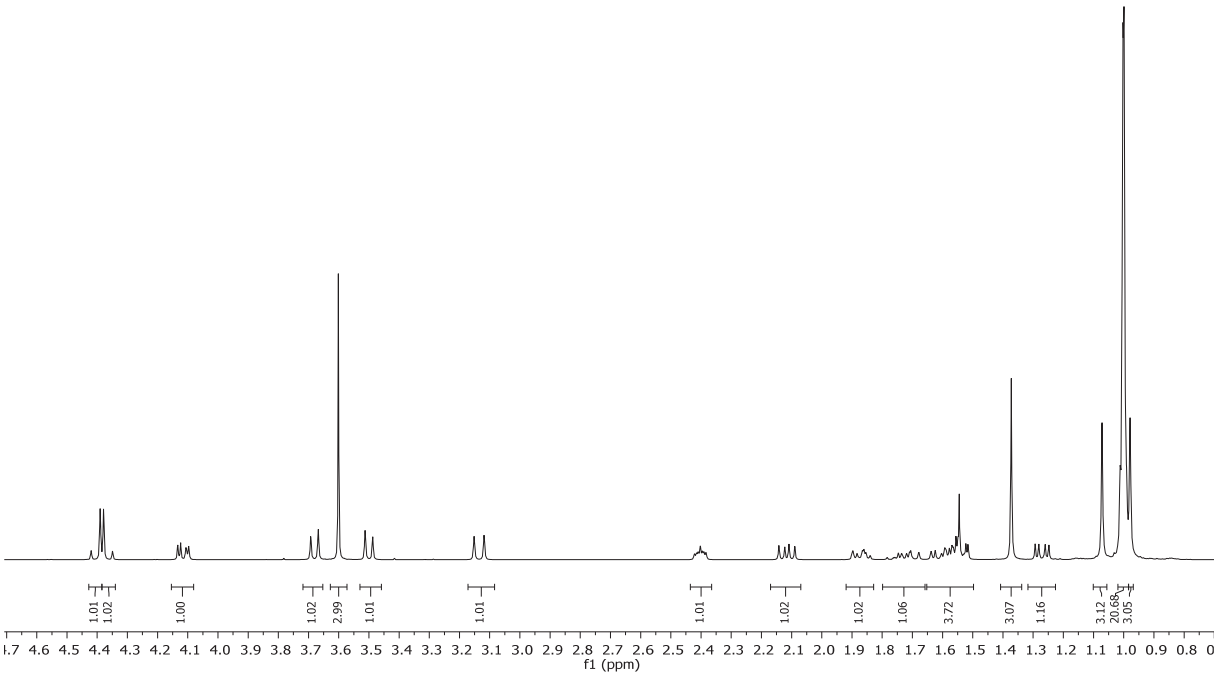

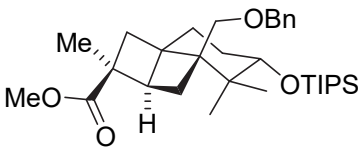

S13

^{13}C-NMR, 100 MHz, CD_2Cl_2

^{13}C-NMR, 100 MHz, CD_2Cl_2

range: 90 – 10 ppm

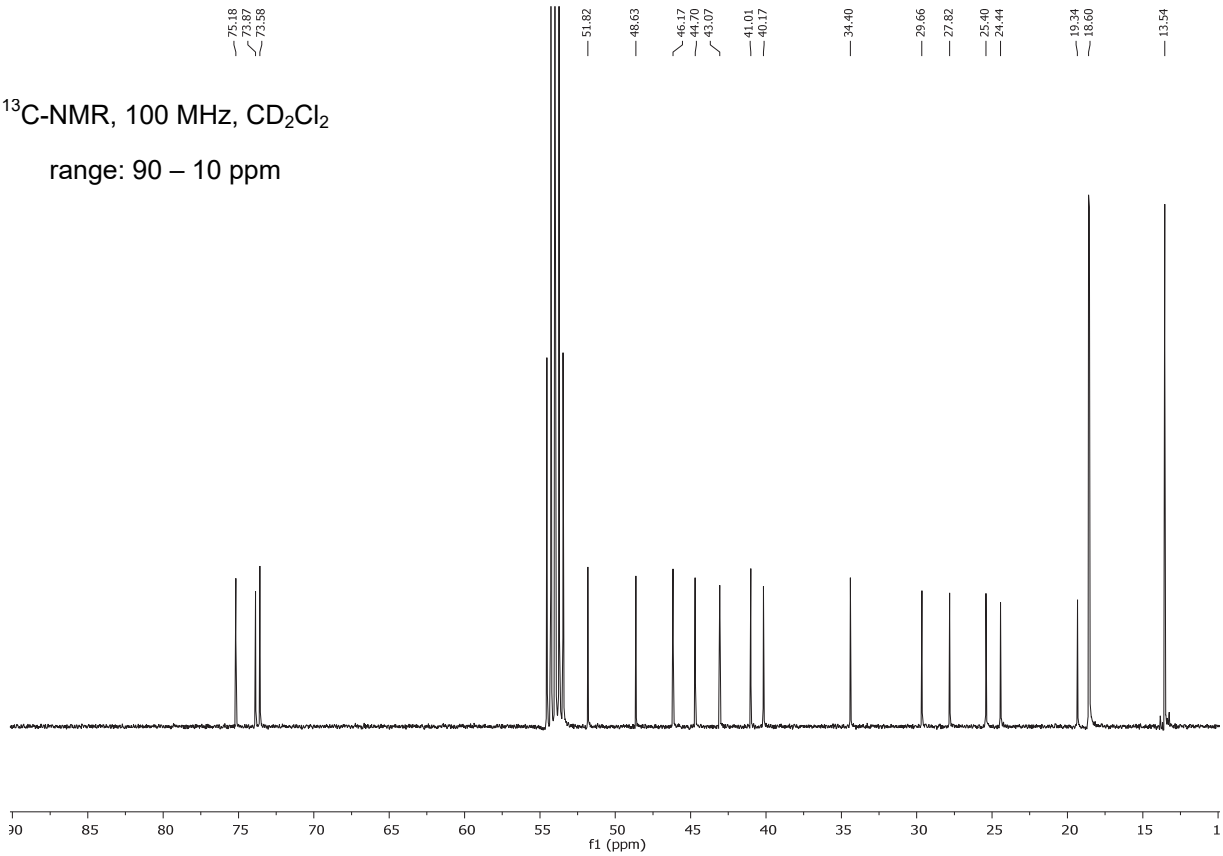

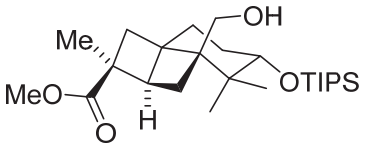

S14

^{1}H-NMR, 400 MHz, C_6D_6

^{1}H-NMR, 400 MHz, C_6D_6

range: 4.7 – 0.7 ppm

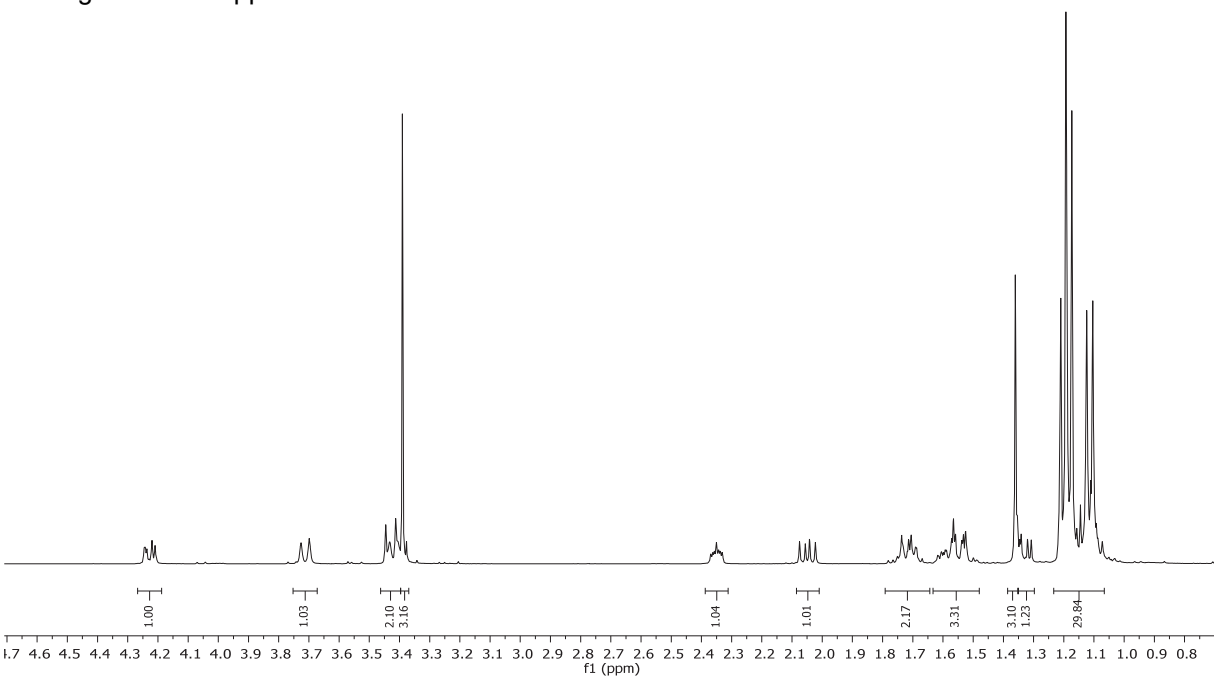

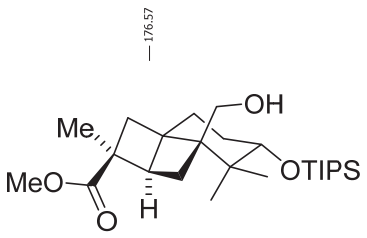

S14

^{13}C-NMR, 100 MHz, C_6D_6

^{13}C-NMR, 100 MHz, C_6D_6

range: 90 – 10 ppm

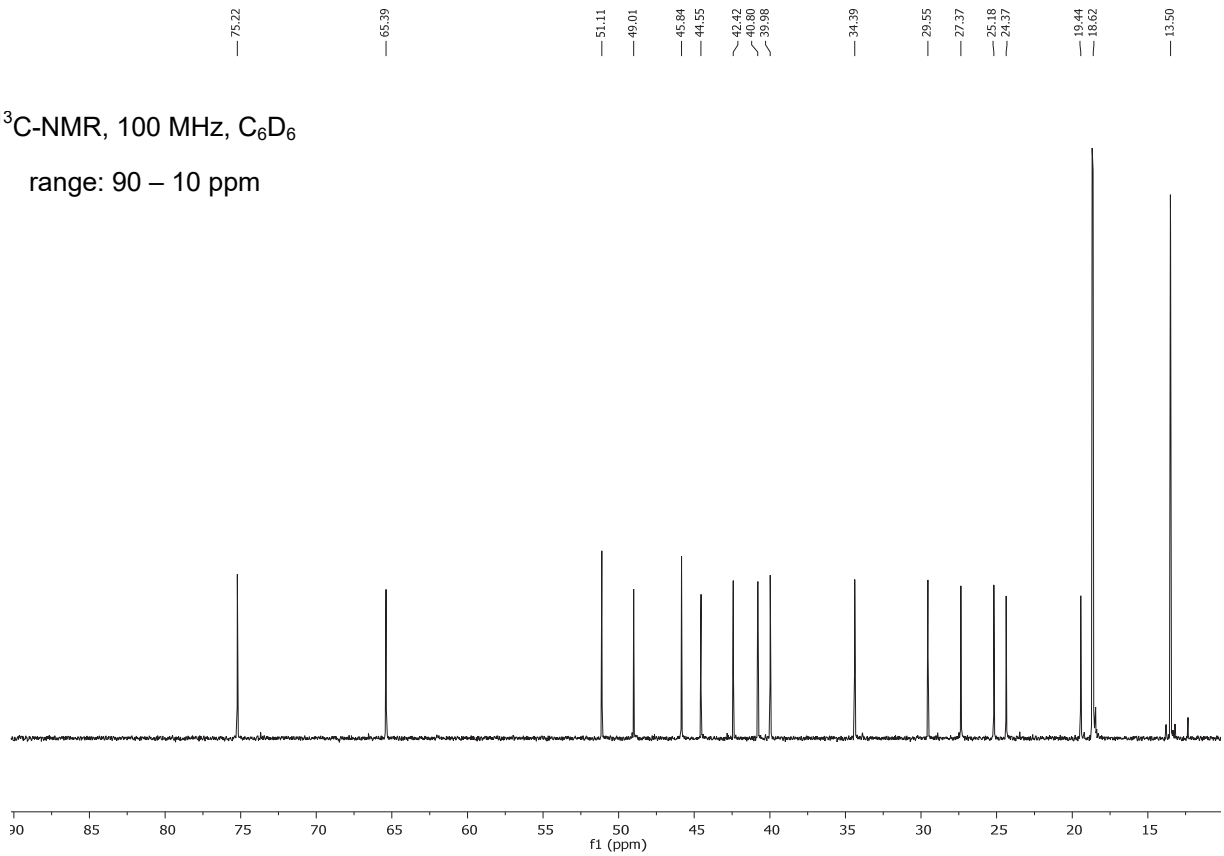

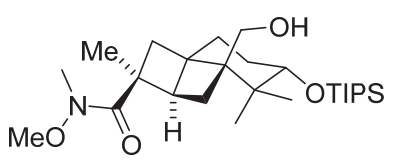

16

^{1}H-NMR, 400 MHz, C_6D_6

^{1}H-NMR, 400 MHz, C_6D_6

range: 4.7 – 0.7 ppm

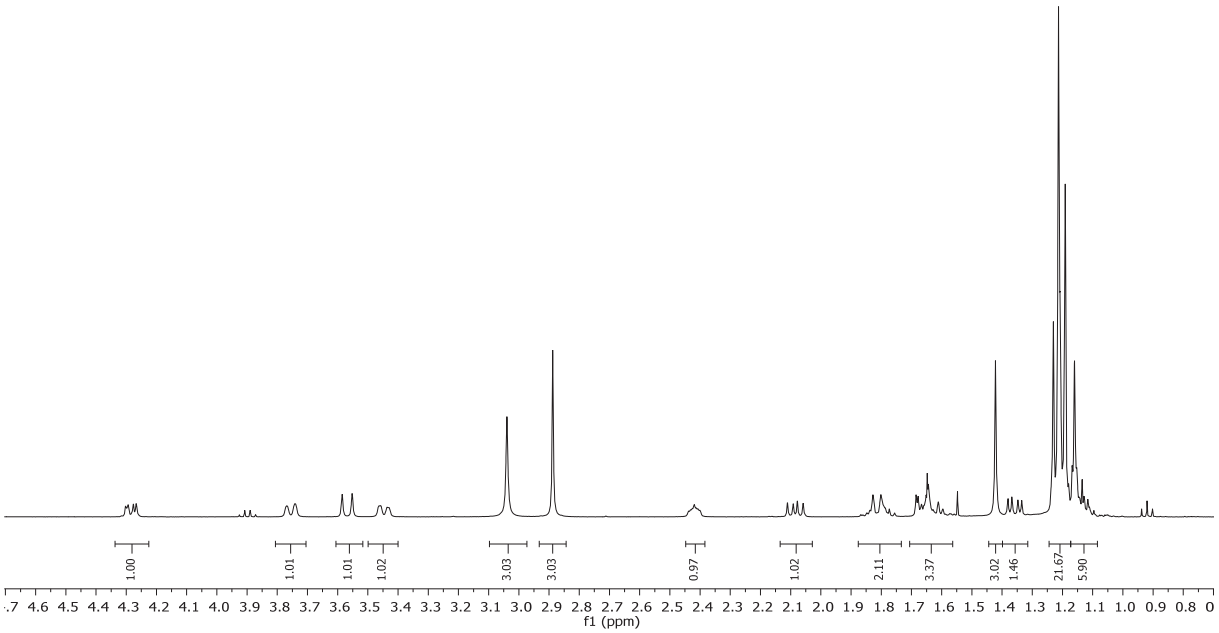

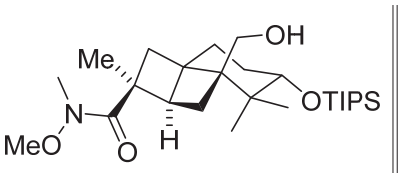

16

^{13}C-NMR, 100 MHz, C_6D_6

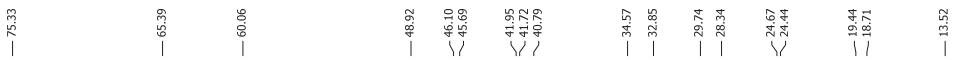

^{13}C-NMR, 100 MHz, C_6D_6

range: 90 – 10 ppm

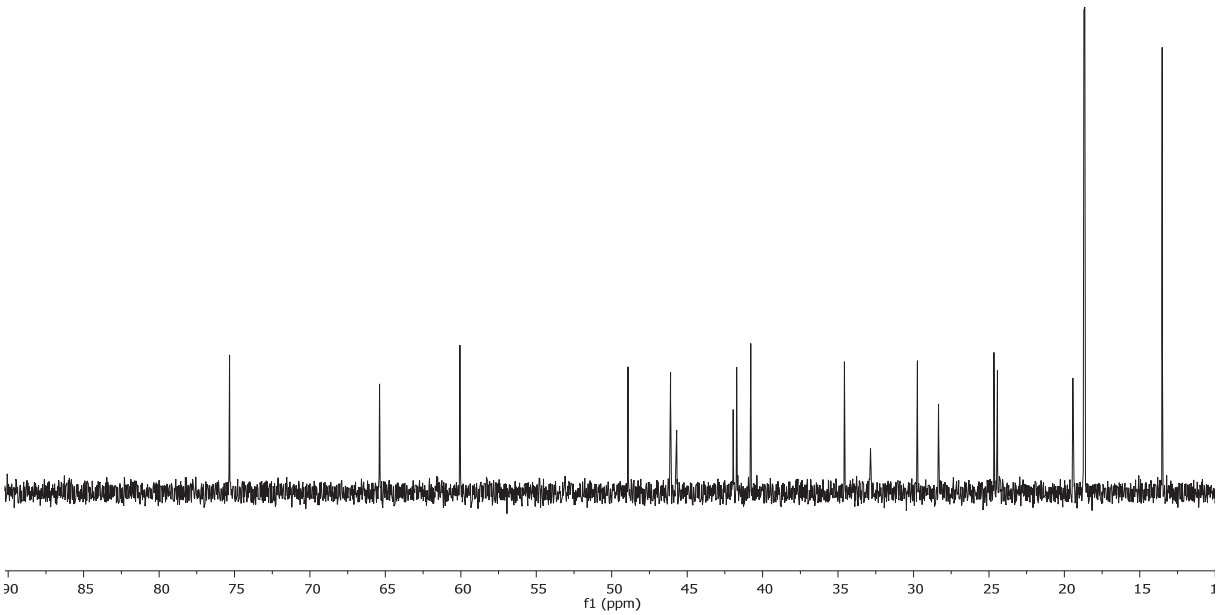

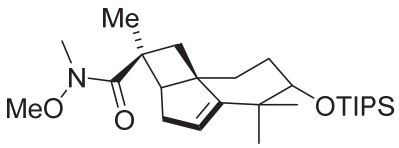

18

^{1}H-NMR, 400 MHz, C_6D_6

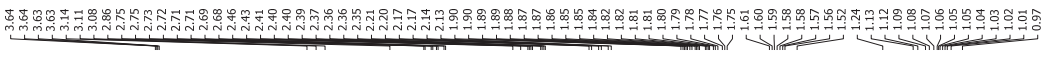

^{1}H-NMR, 400 MHz, C_6D_6

range: 4.7 – 0.7 ppm

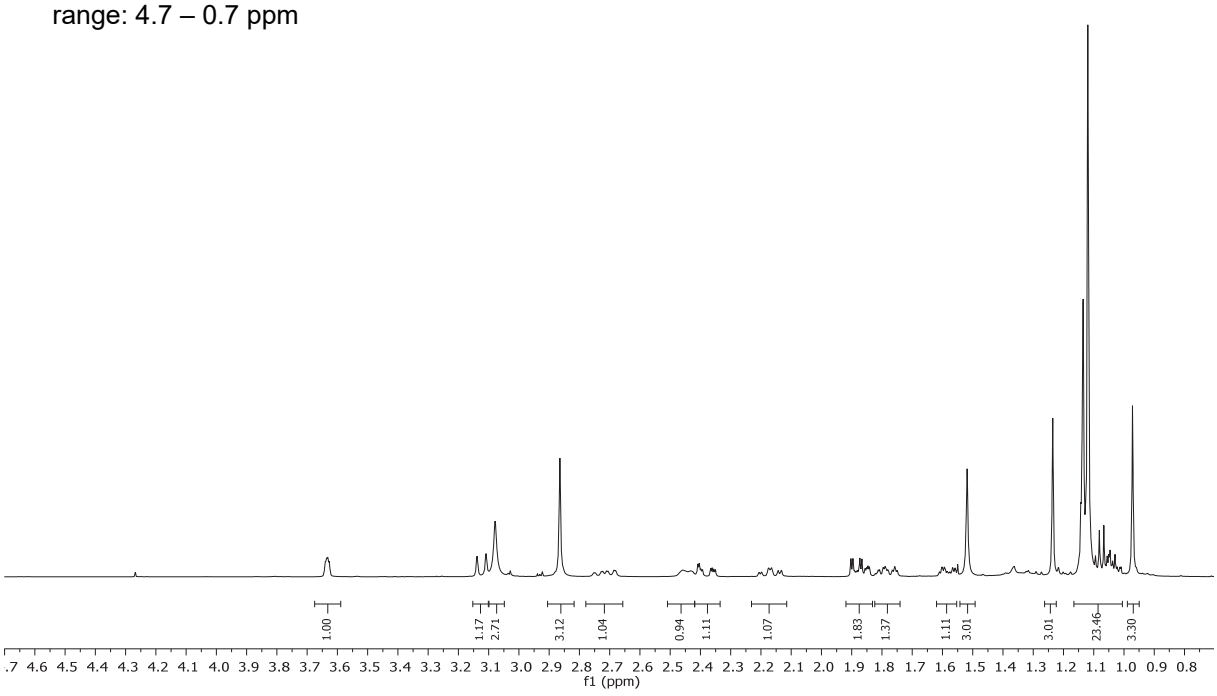

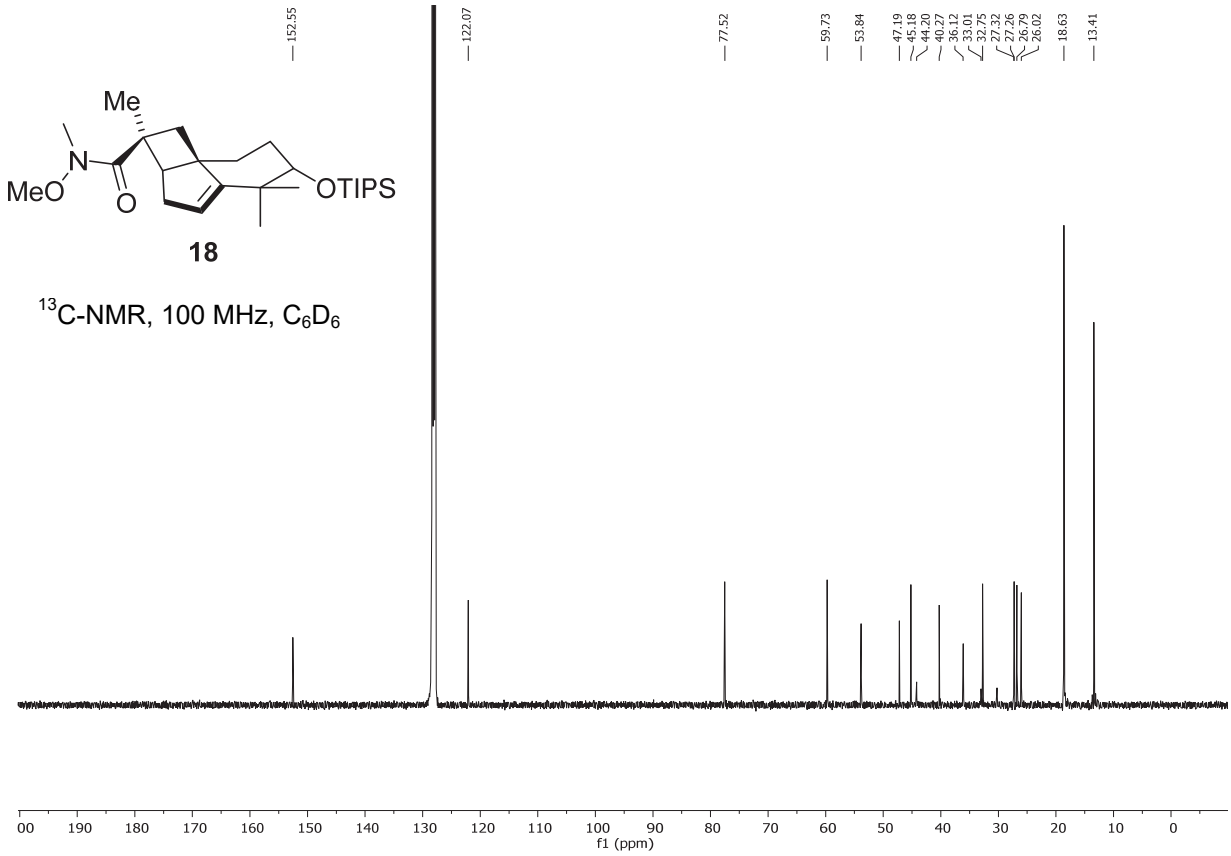

18

^{13}C-NMR, 100 MHz, C_6D_6

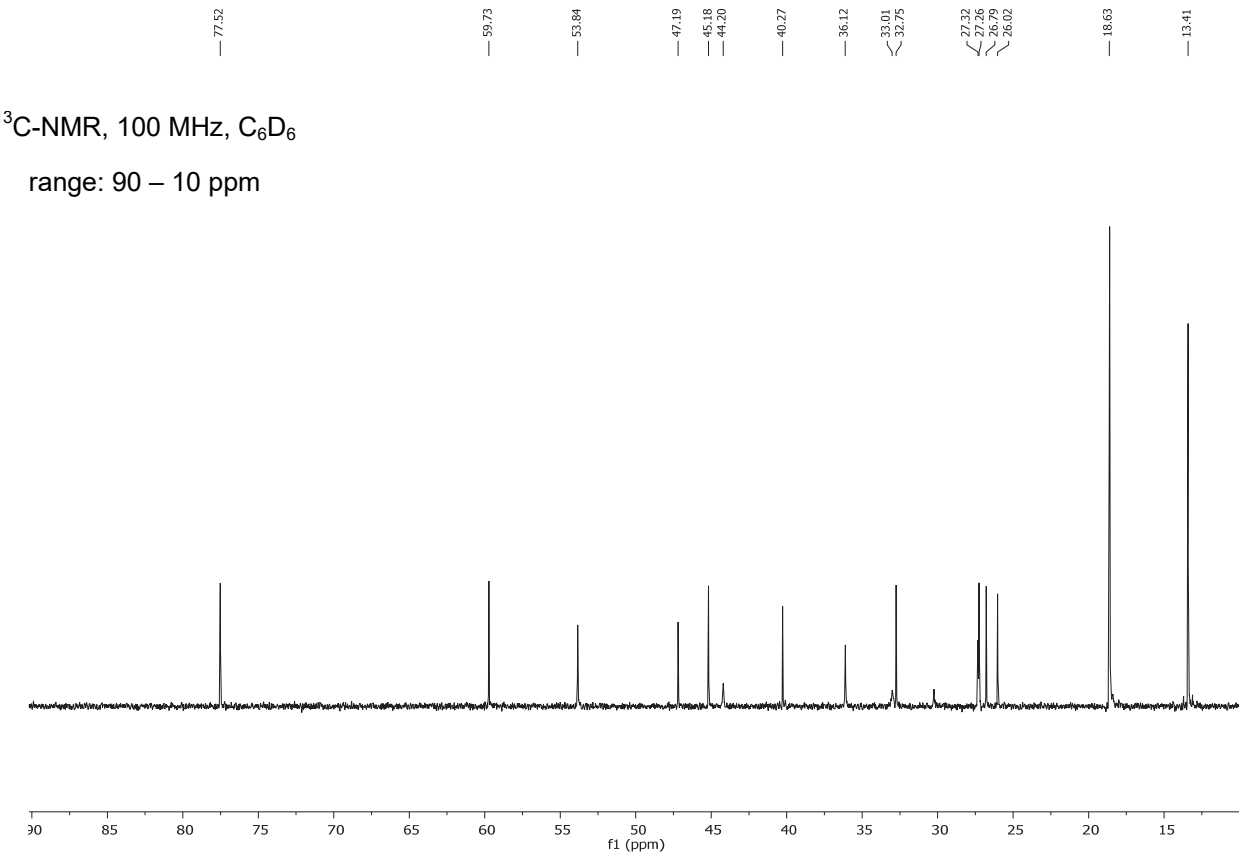

^{13}C-NMR, 100 MHz, C_6D_6

range: 90 – 10 ppm

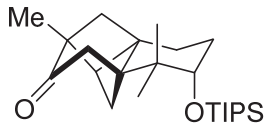

20

^{1}H-NMR, 800 MHz, C_6D_6

^{1}H-NMR, 800 MHz, C_6D_6

range: 4.5 – 0.3 ppm

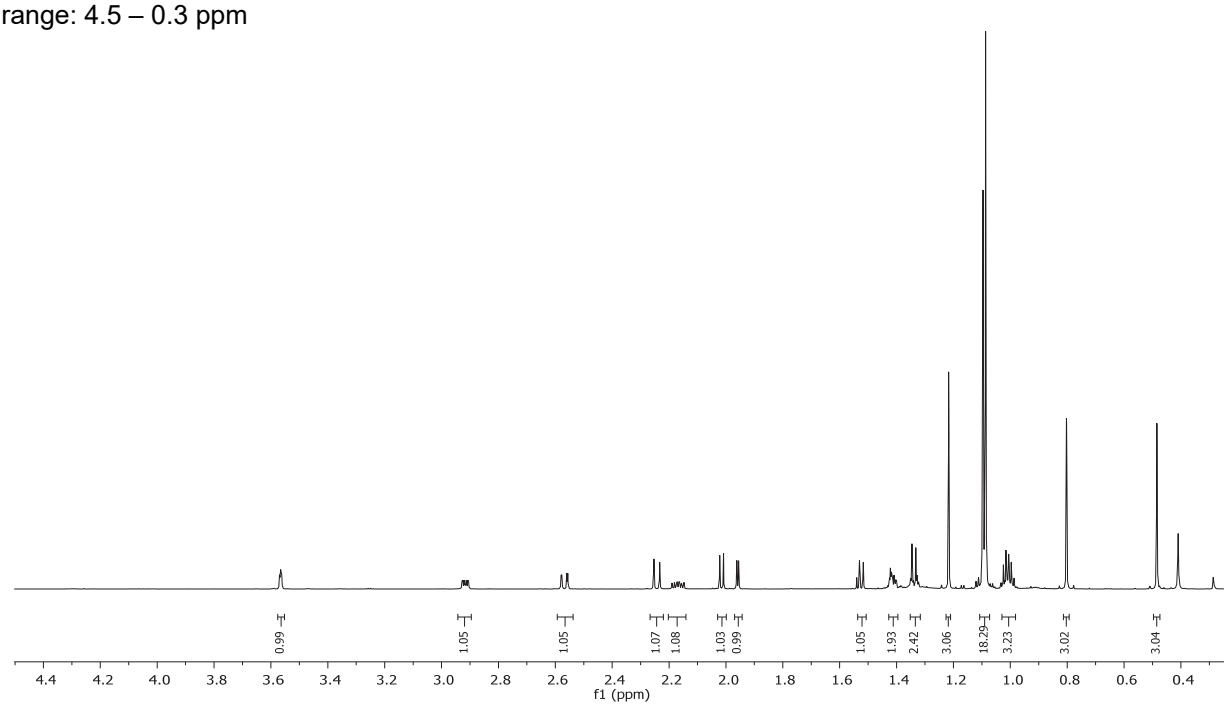

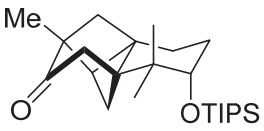

20

^{13}C-NMR, 200 MHz, C_6D_6

^{13}C-NMR, 200 MHz, C_6D_6

range: 90 – 10 ppm

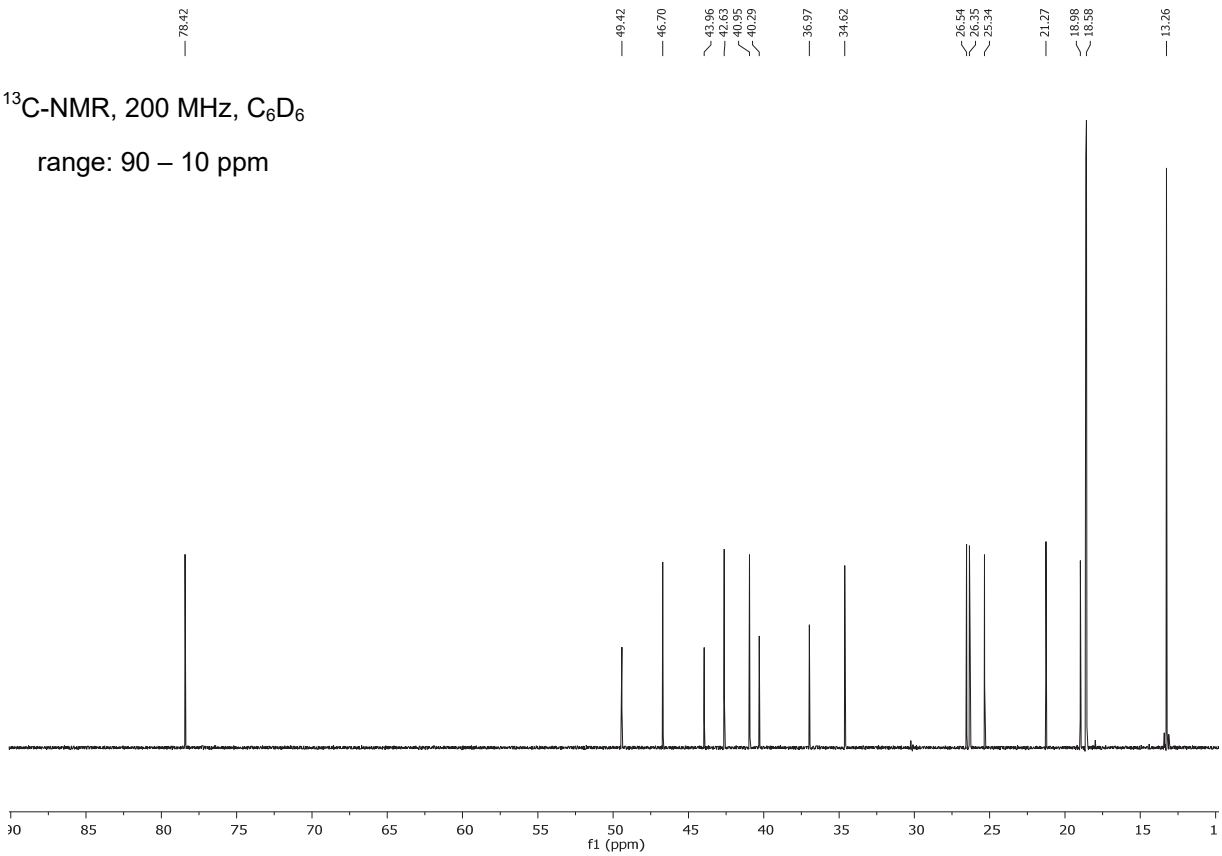

21

^{1}H-NMR, 800 MHz, C_6D_6

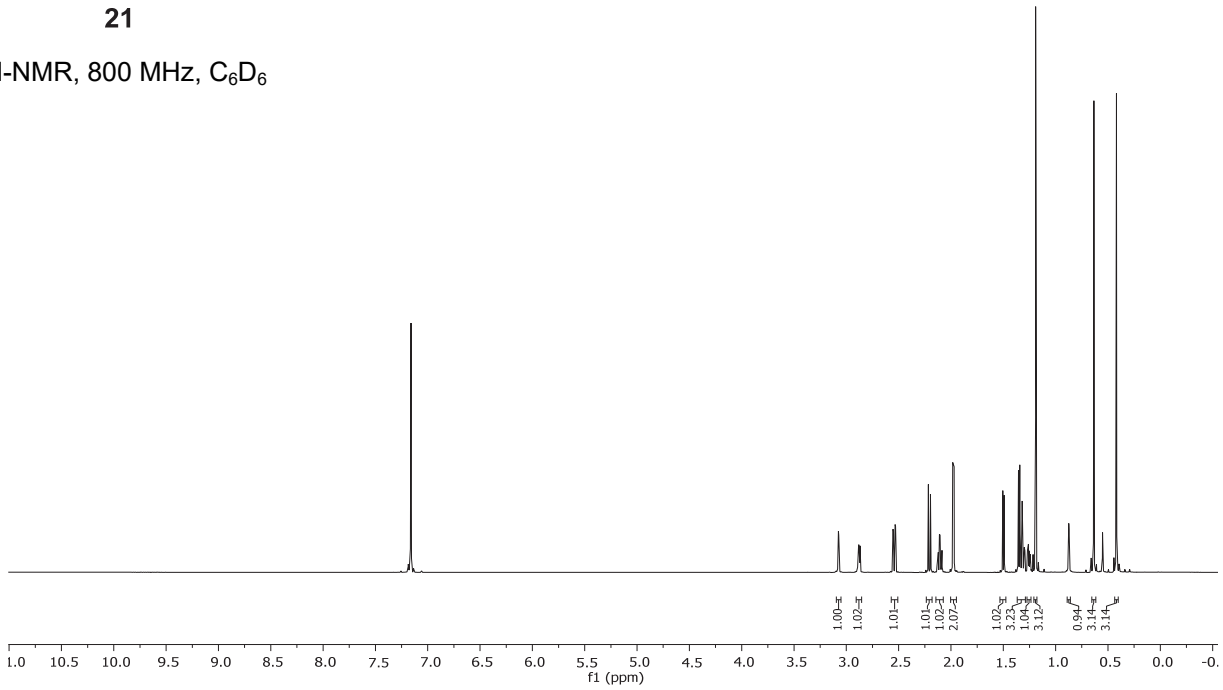

^{1}H-NMR, 800 MHz, C_6D_6

range: 3.5 – 0.3 ppm

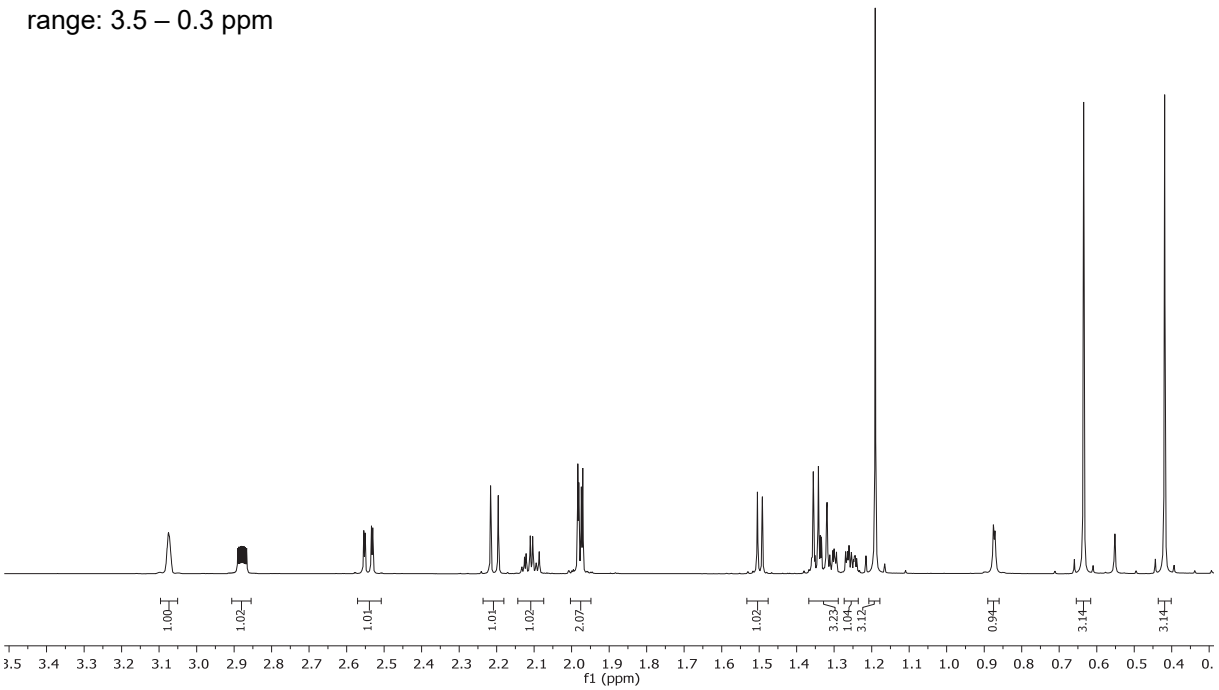

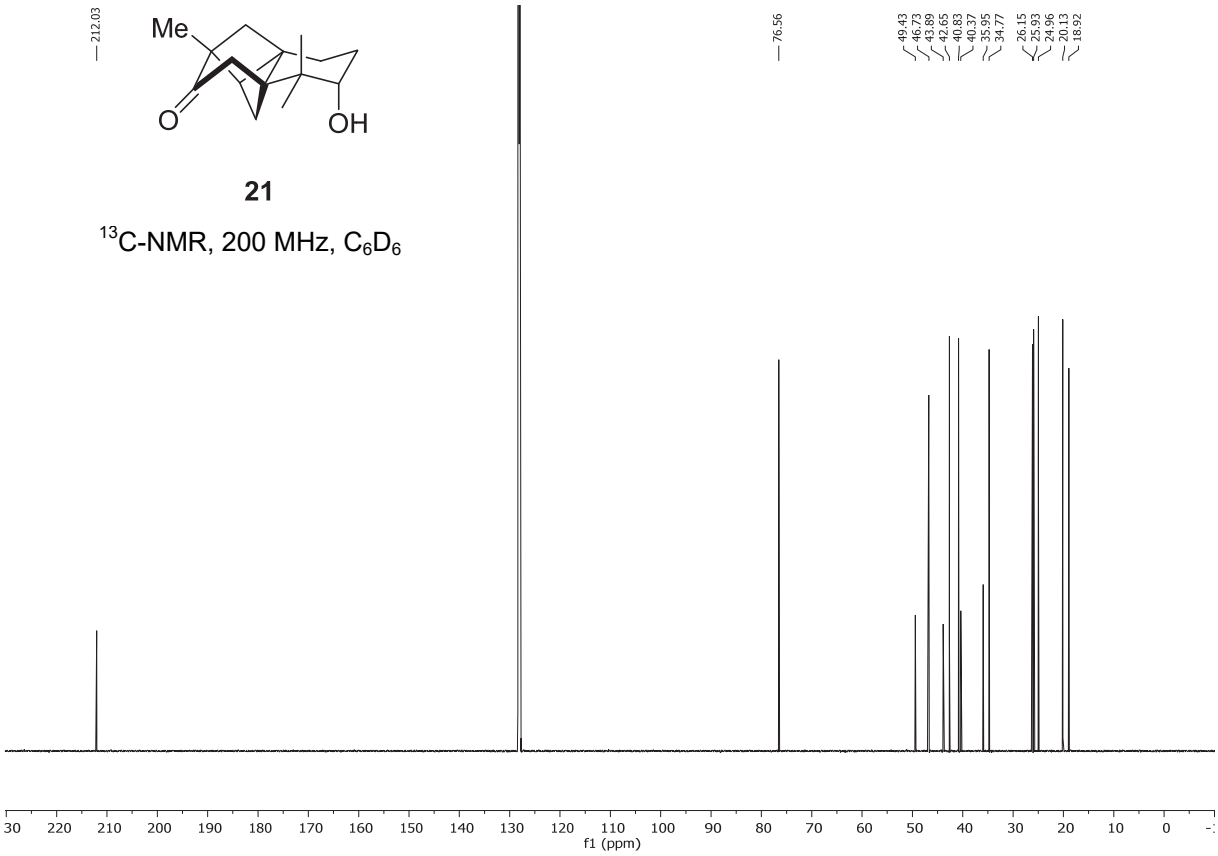

21

^{13}C-NMR, 200 MHz, C_6D_6

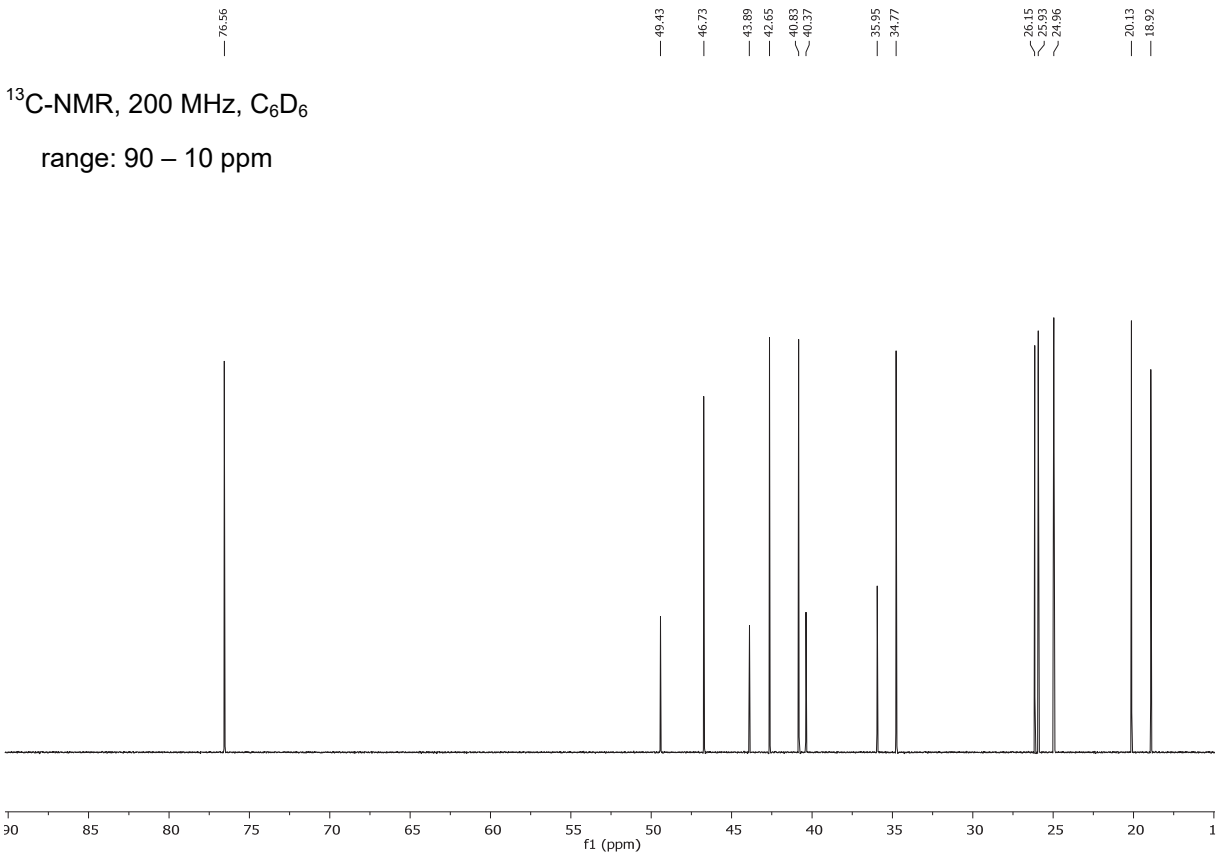

^{13}C-NMR, 200 MHz, C_6D_6

range: 90 – 10 ppm

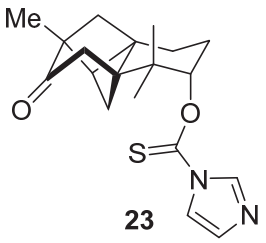

23

^{1}H-NMR, 400 MHz, C_6D_6

^{1}H-NMR, 400 MHz, C_6D_6

range: 3.5 – 0.3 ppm

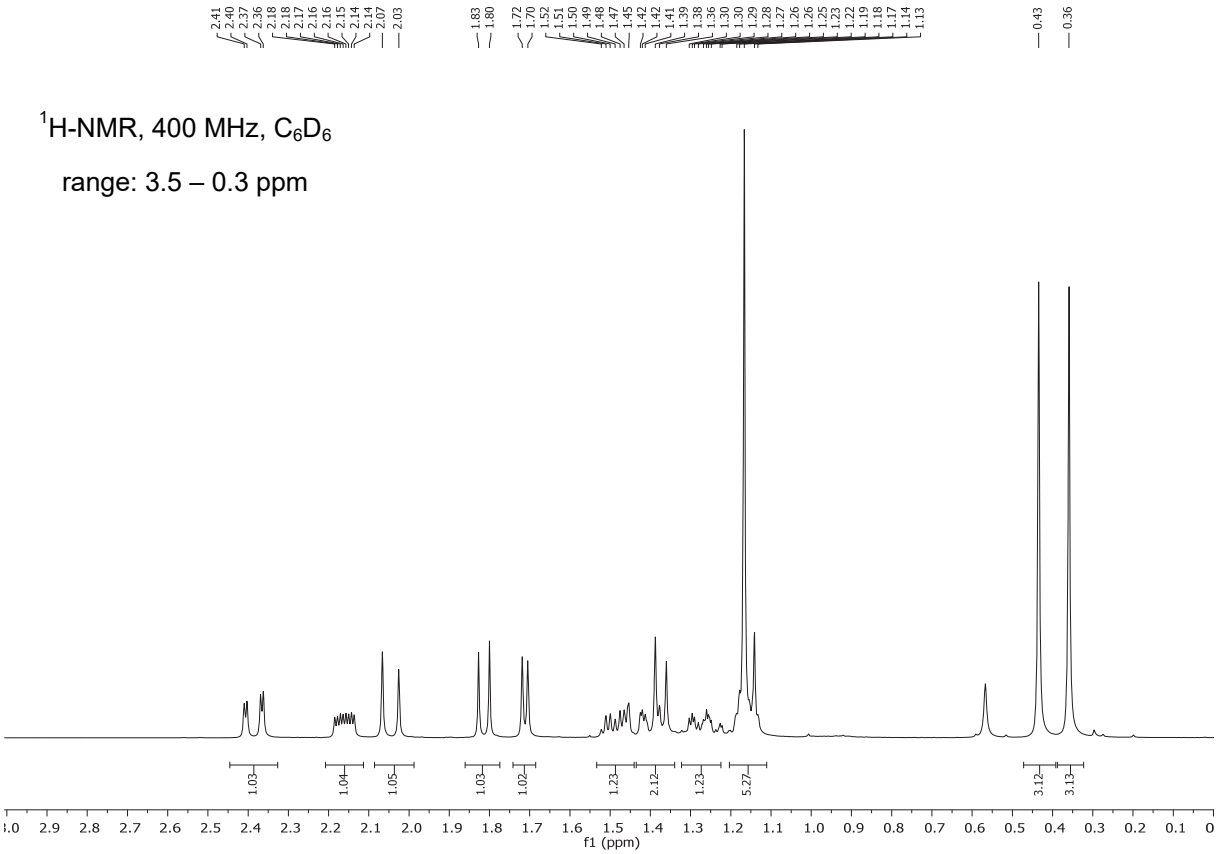

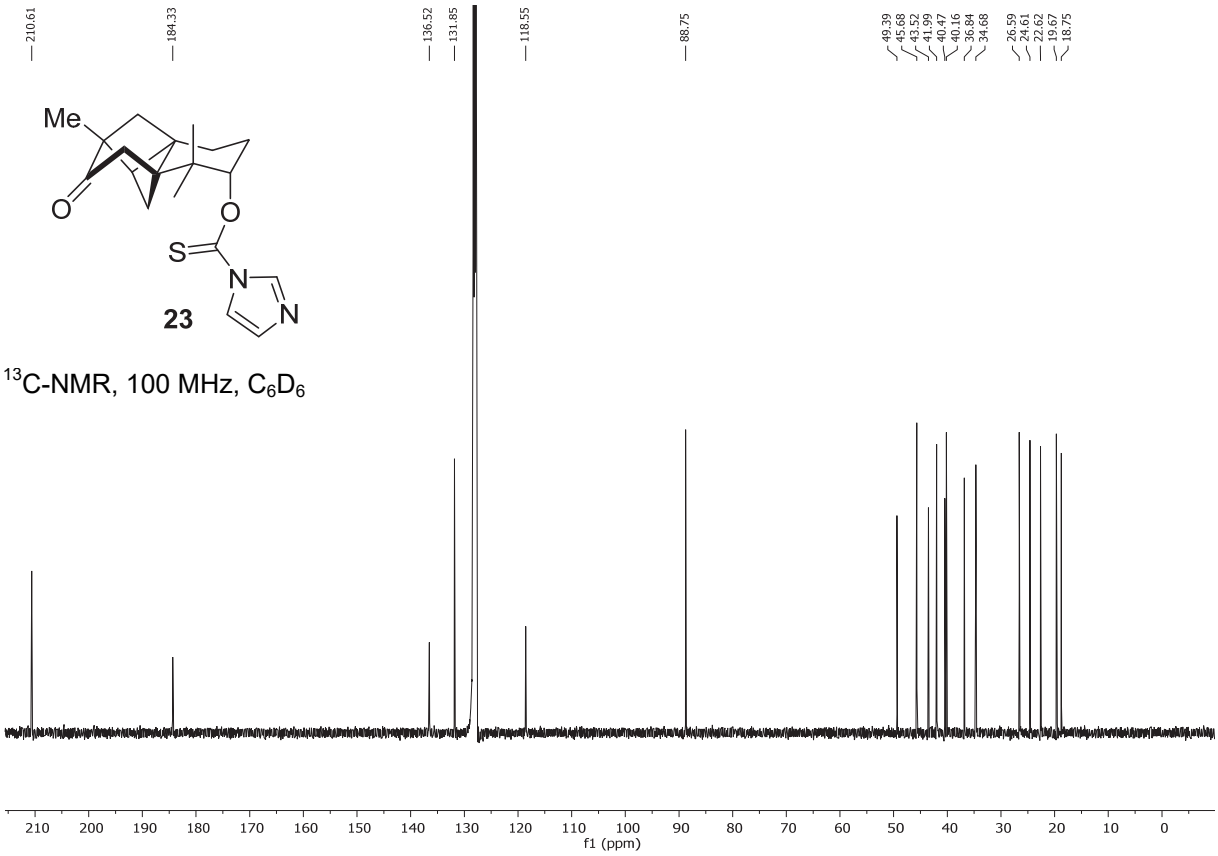

23

^{13}C-NMR, 100 MHz, C_6D_6

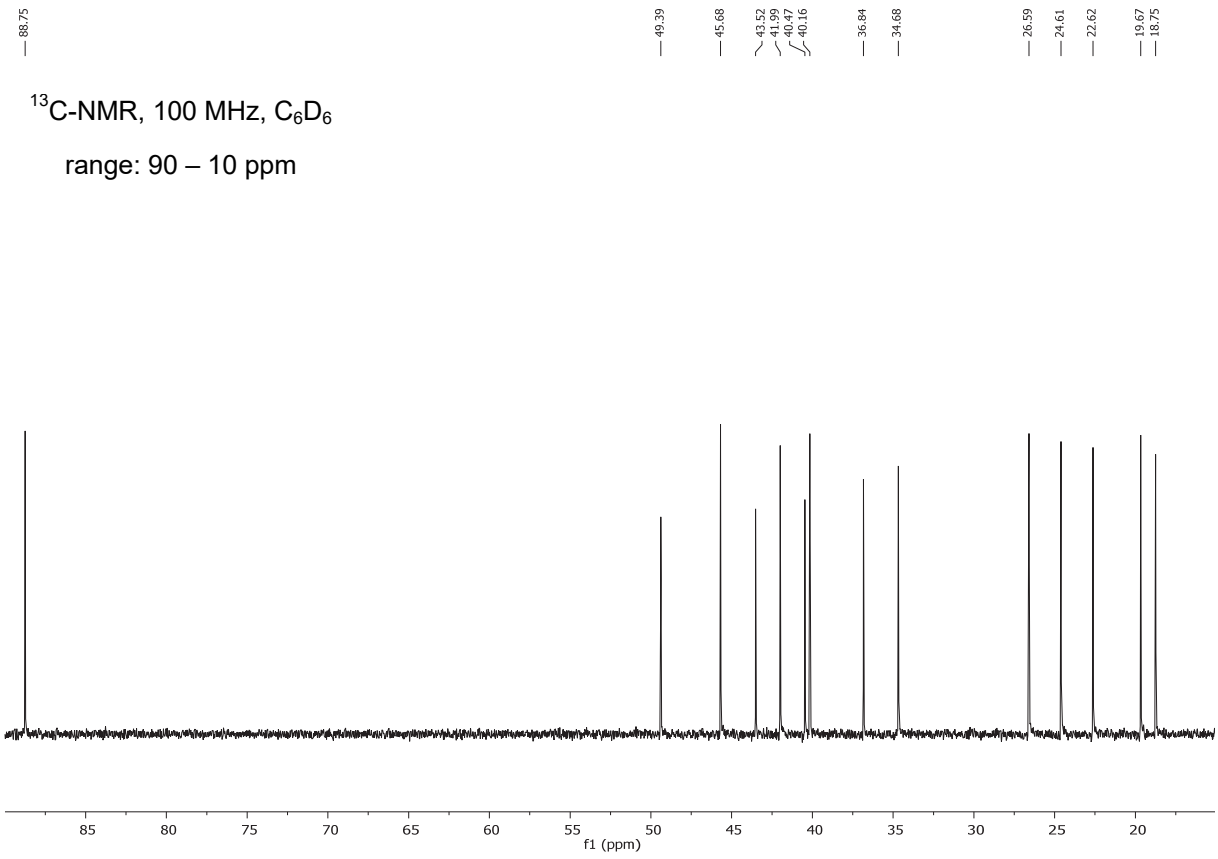

^{13}C-NMR, 100 MHz, C_6D_6

range: 90 – 10 ppm

8-*epi*-aplydactone (**27**)

^{1}H-NMR, 800 MHz, C_6D_6

^{1}H-NMR, 800 MHz, C_6D_6

range: 3.5 – 0.3 ppm

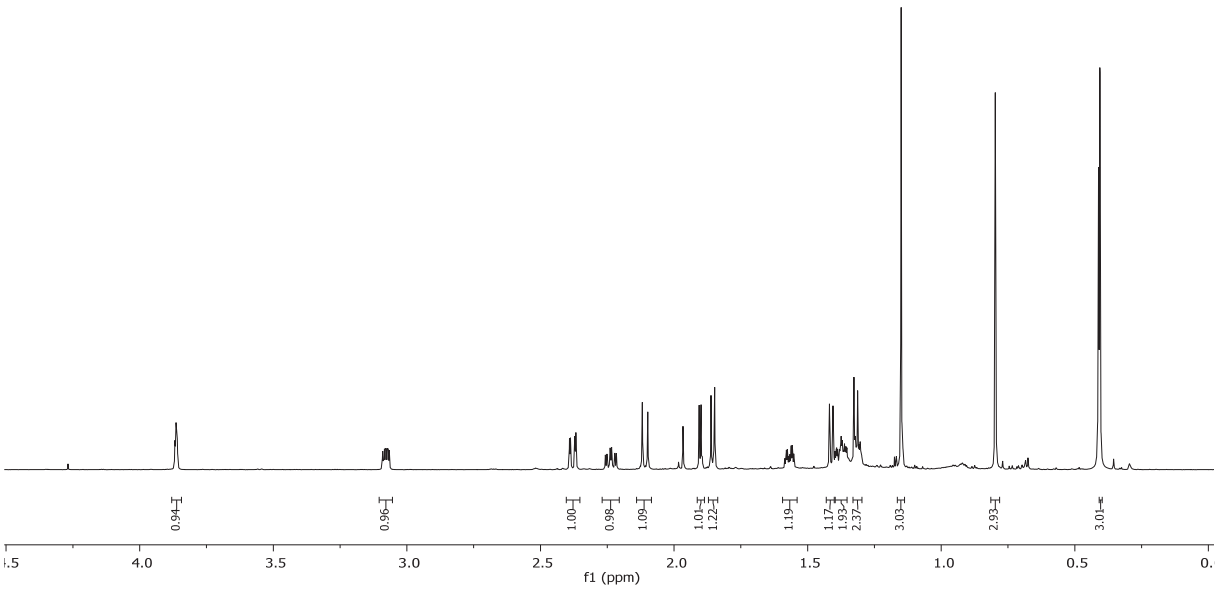

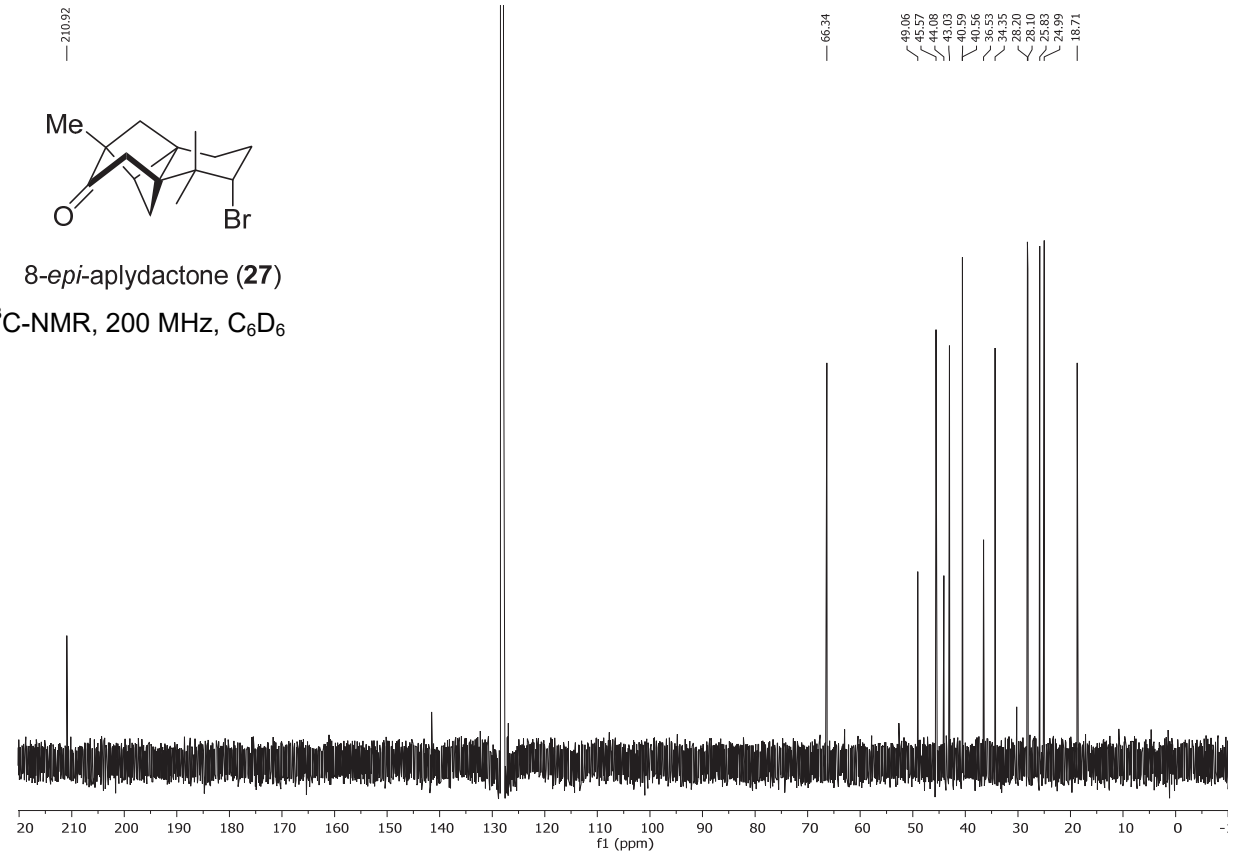

8-*epi*-aplydactone (**27**)

^{13}C-NMR, 200 MHz, C_6D_6

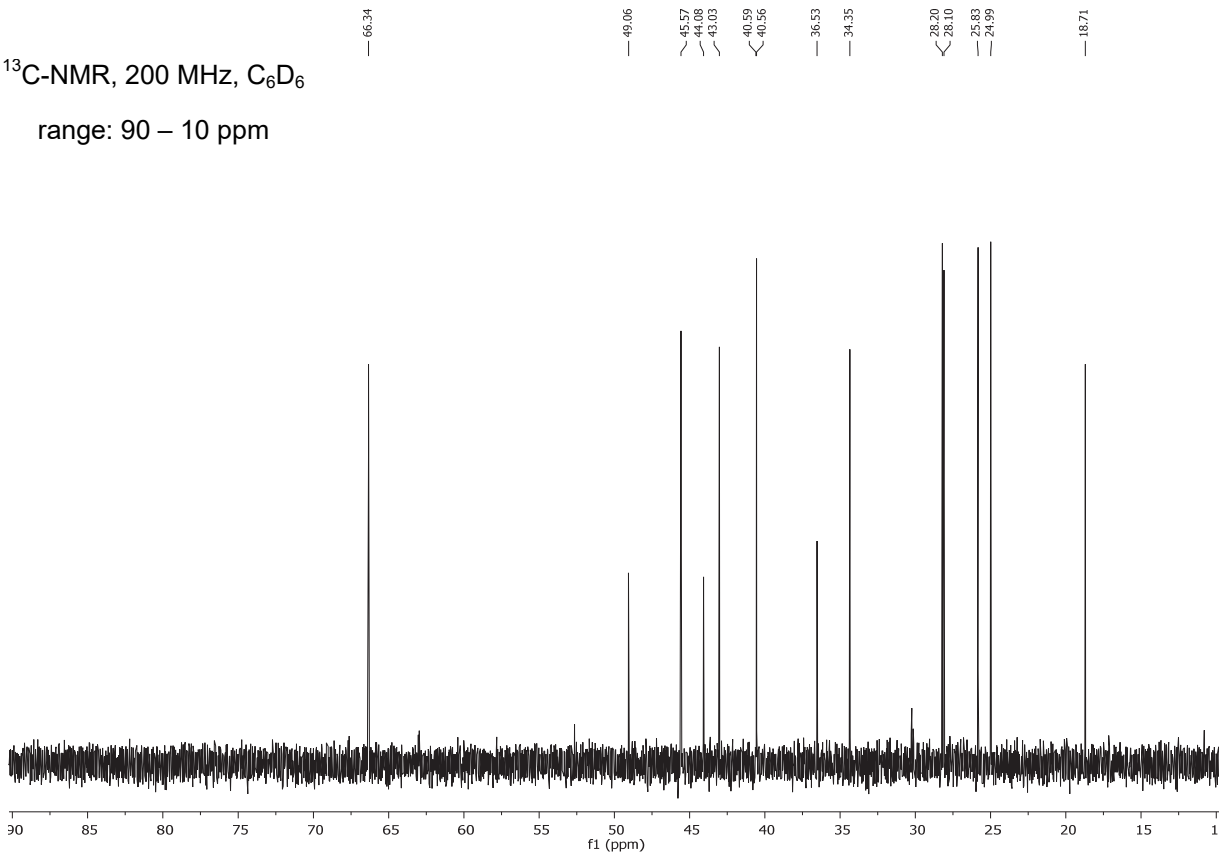

^{13}C-NMR, 200 MHz, C_6D_6

range: 90 – 10 ppm

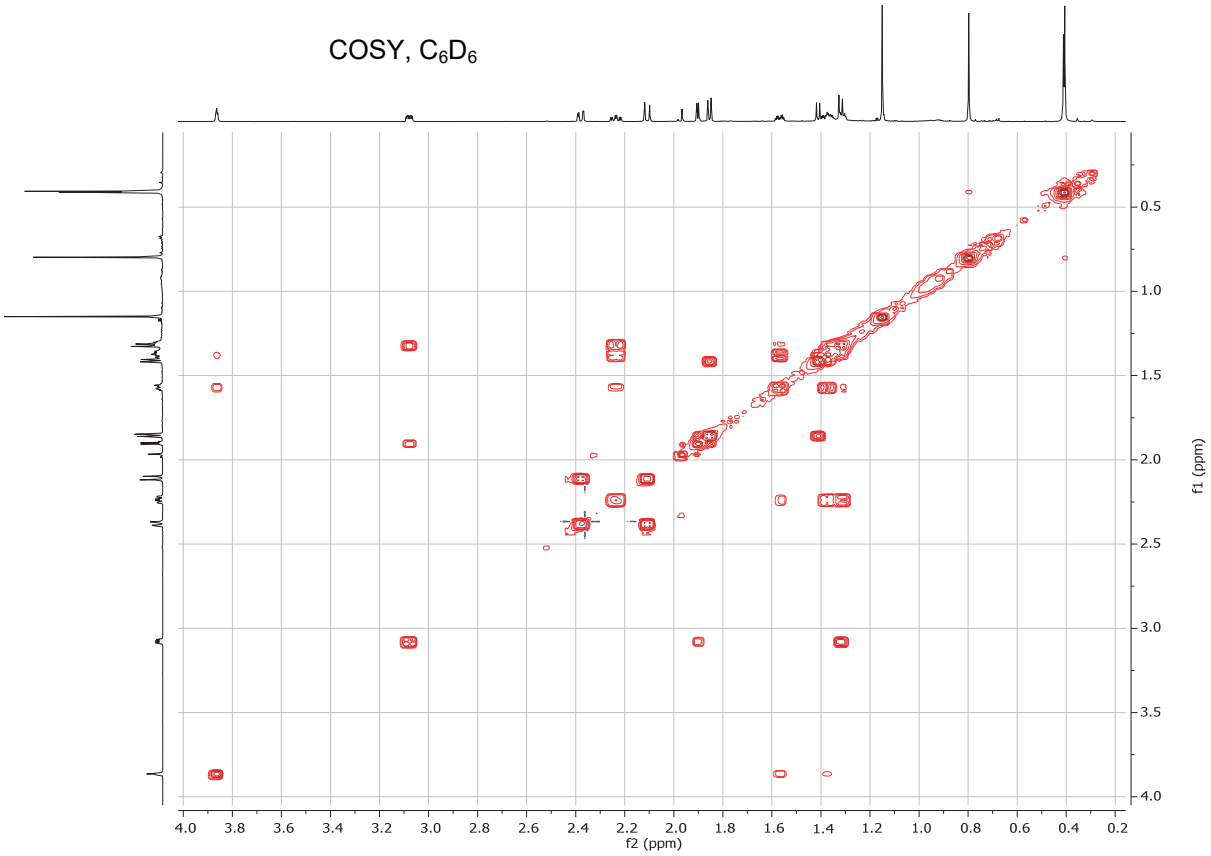
COSY, C6D6
f2 (ppm)
f1 (ppm)

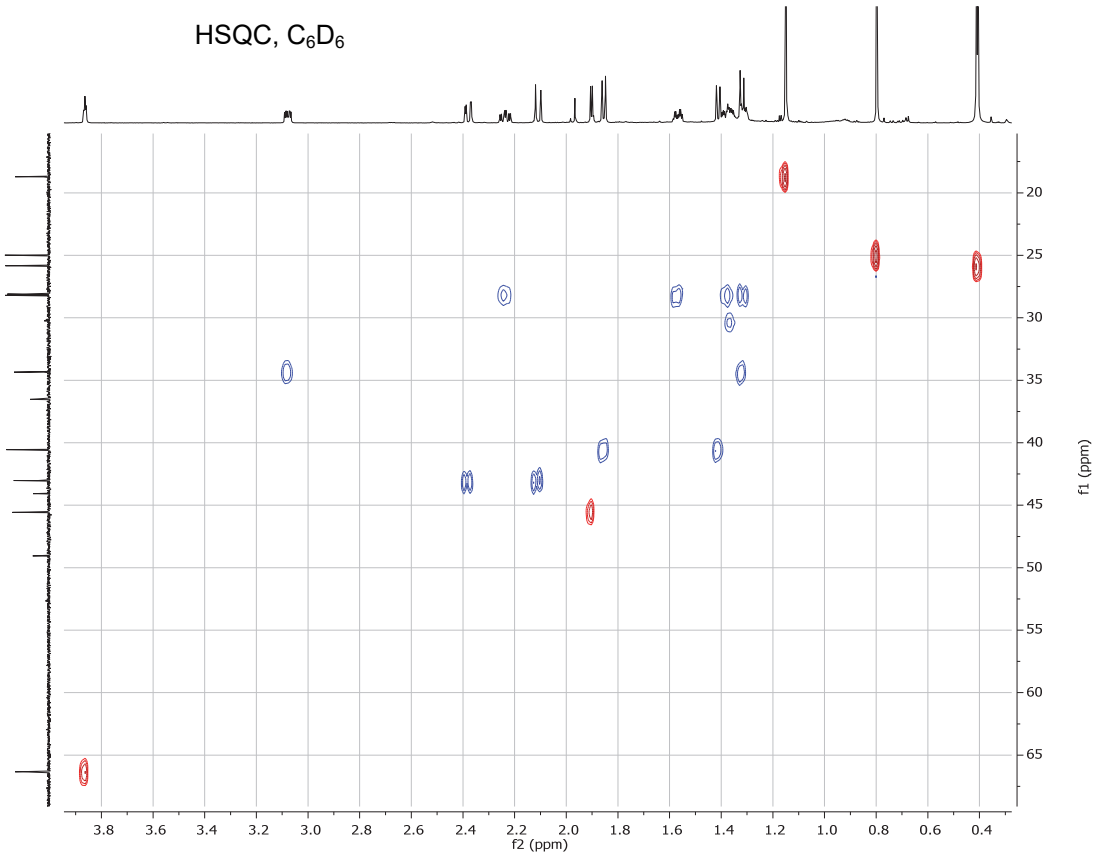
HSQC, C6D6
f2 (ppm)
f1 (ppm)

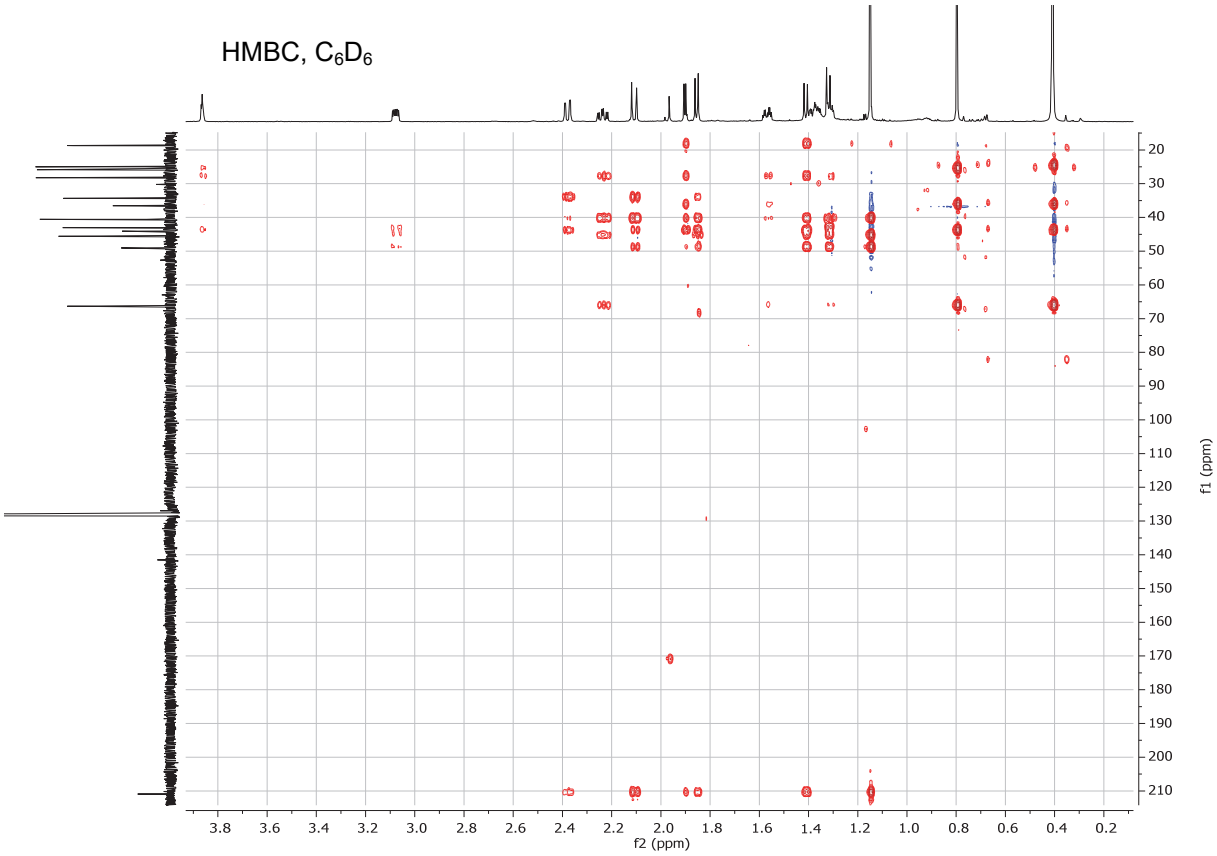
HMBC, C_6D_6
f2 (ppm)
f1 (ppm)

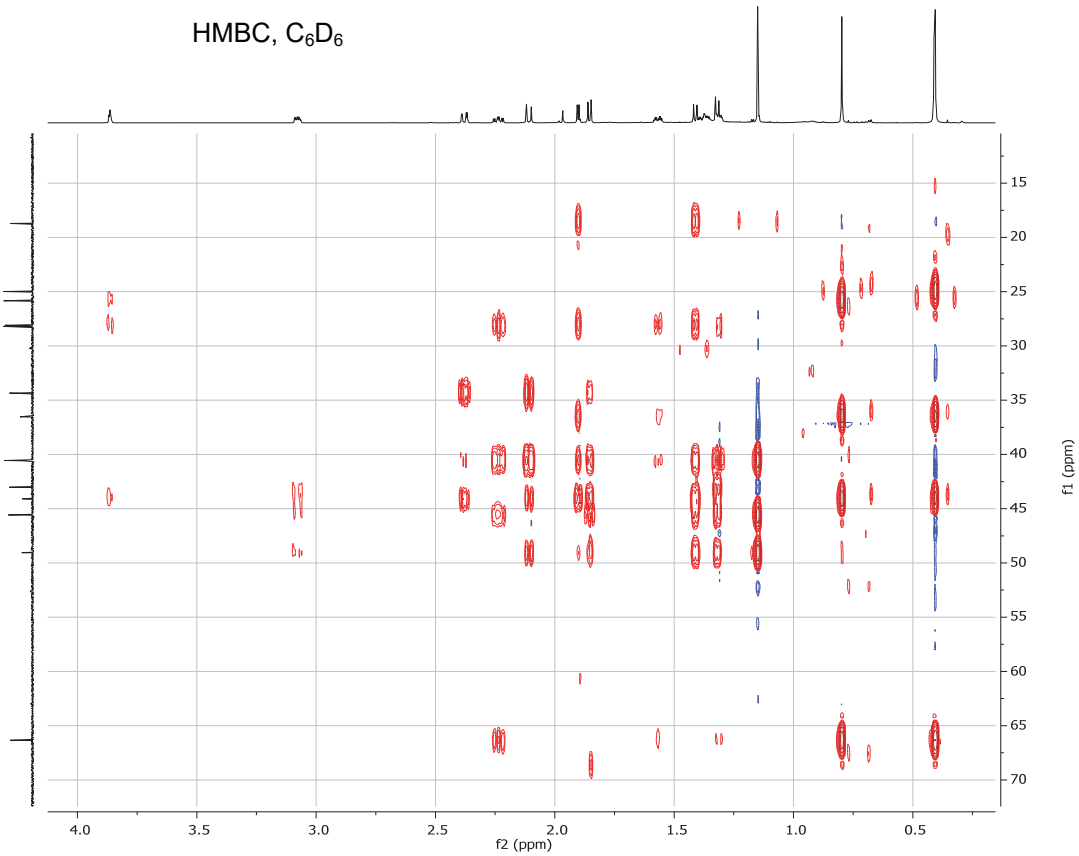
HMBC, C_6D_6
f2 (ppm)
f1 (ppm)

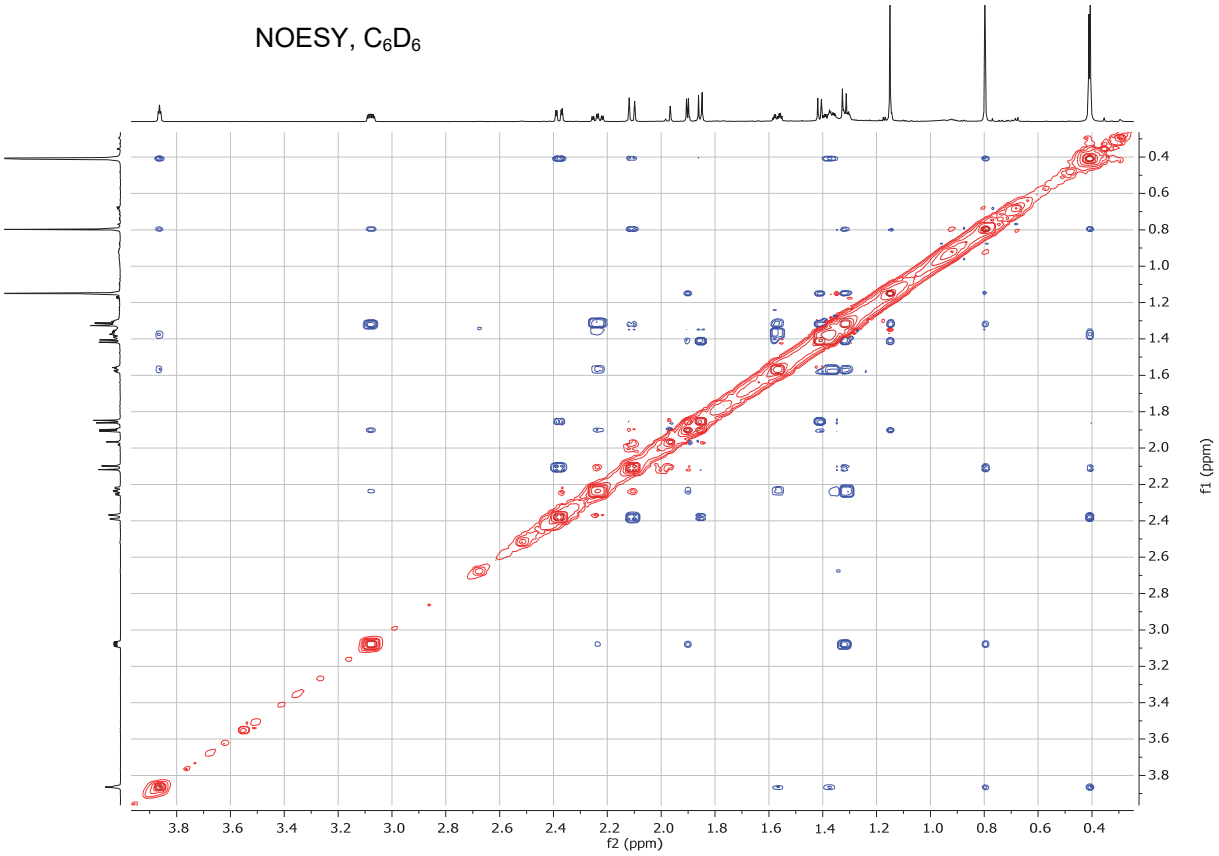
NOESY, C6D6
f2 (ppm)
f1 (ppm)

aplydactone (**1**)

^{1}H-NMR, 800 MHz, C_6D_6

^{1}H-NMR, 800 MHz, C_6D_6

range: 4.3 – 0.5 ppm

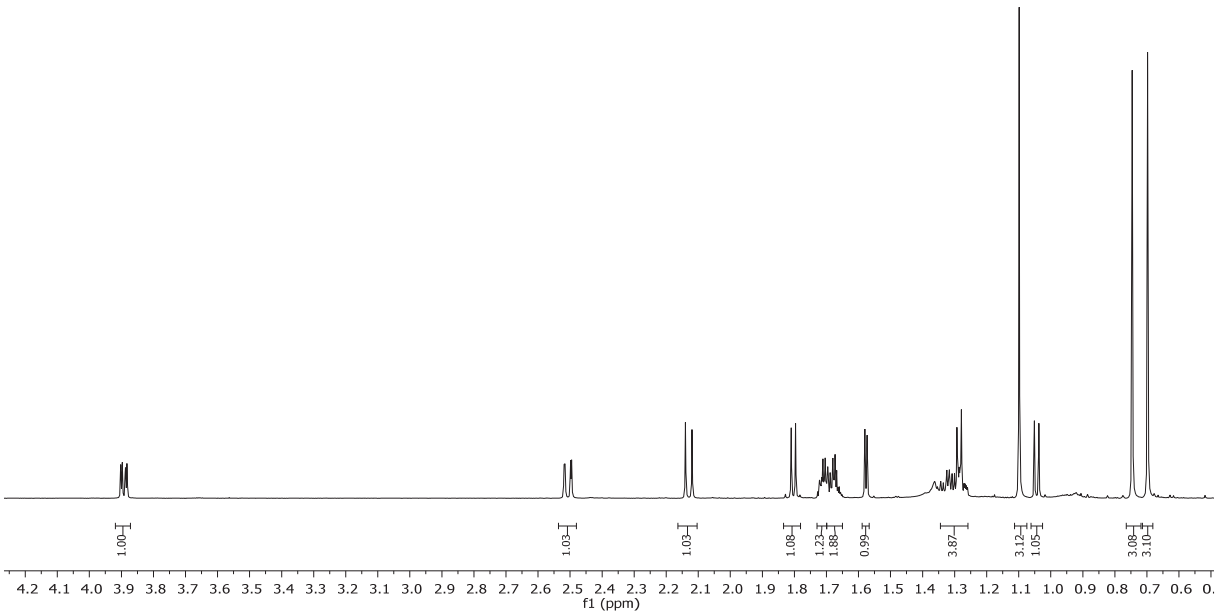

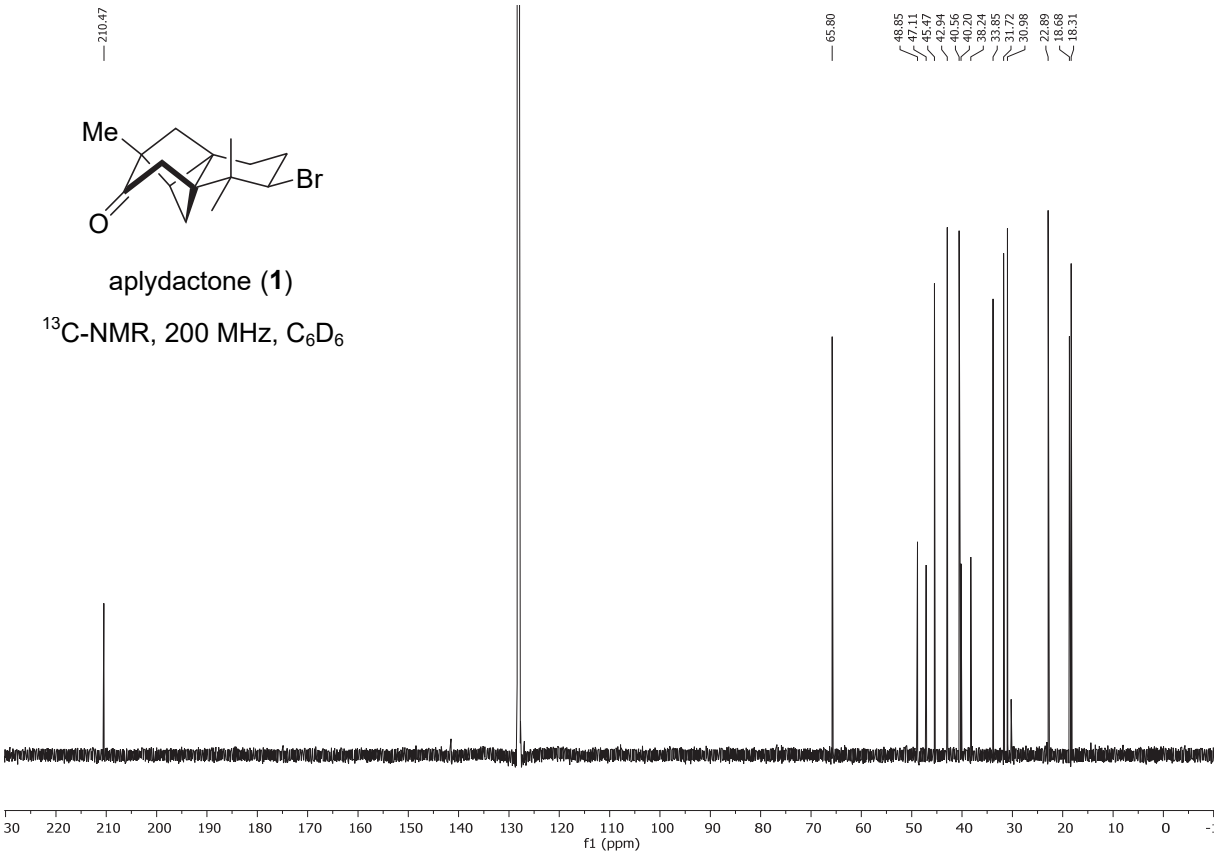

aplydactone (**1**)

^{13}C-NMR, 200 MHz, C_6D_6

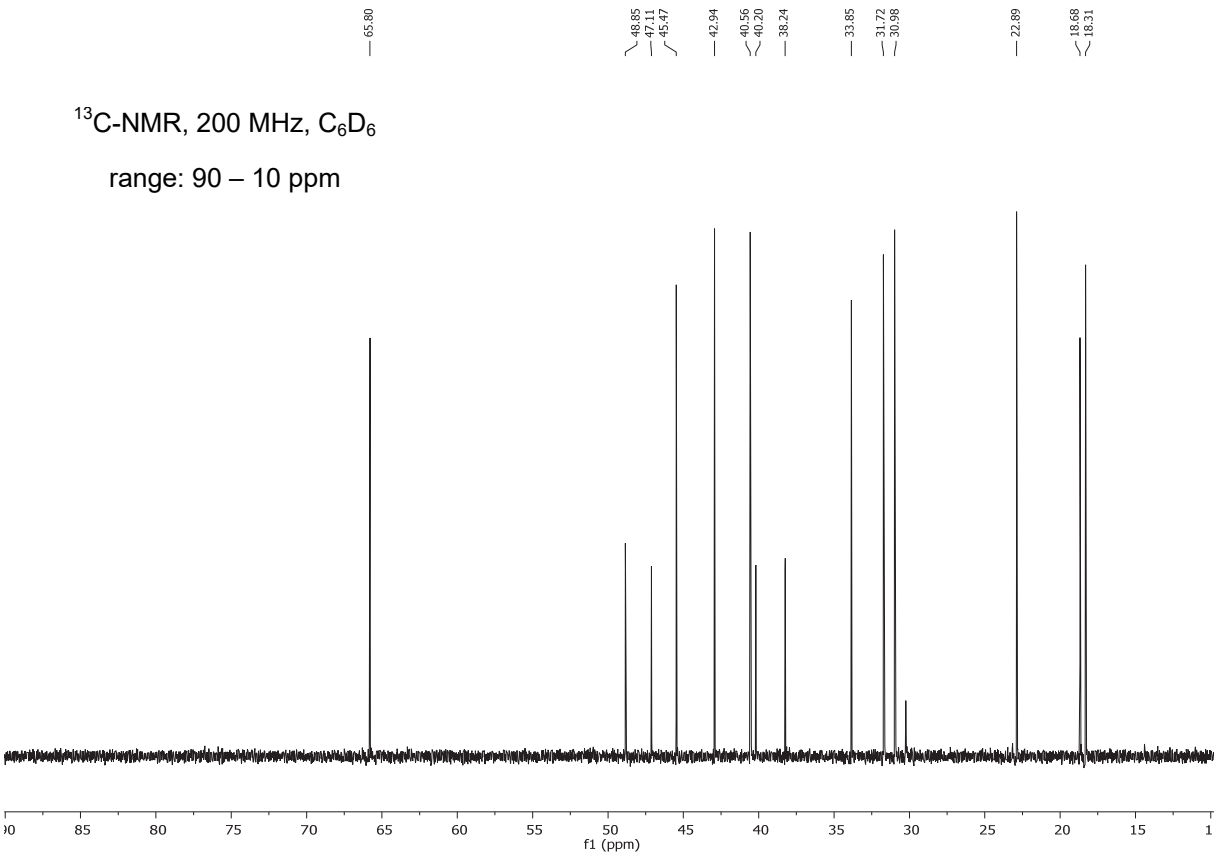

^{13}C-NMR, 200 MHz, C_6D_6

range: 90 – 10 ppm

COSY, C_6D_6

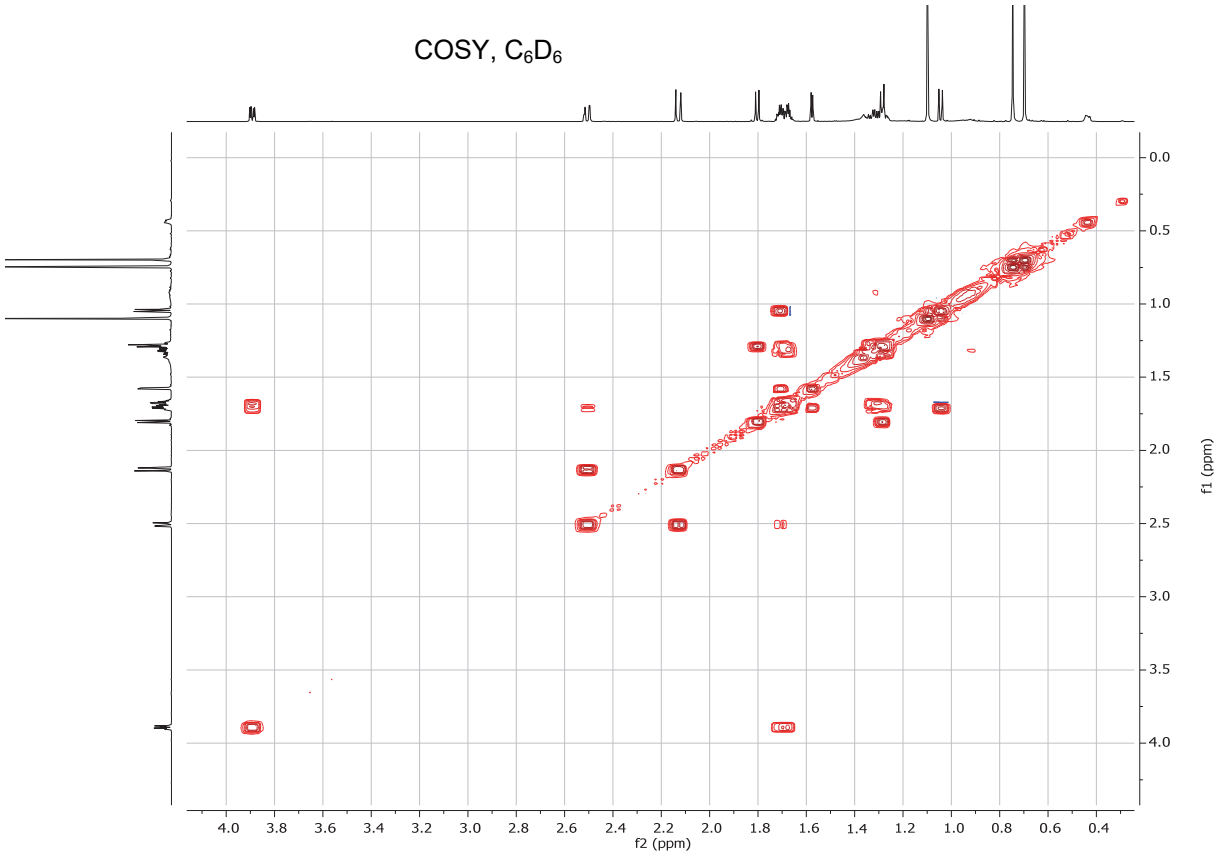

HSQC, C_6D_6

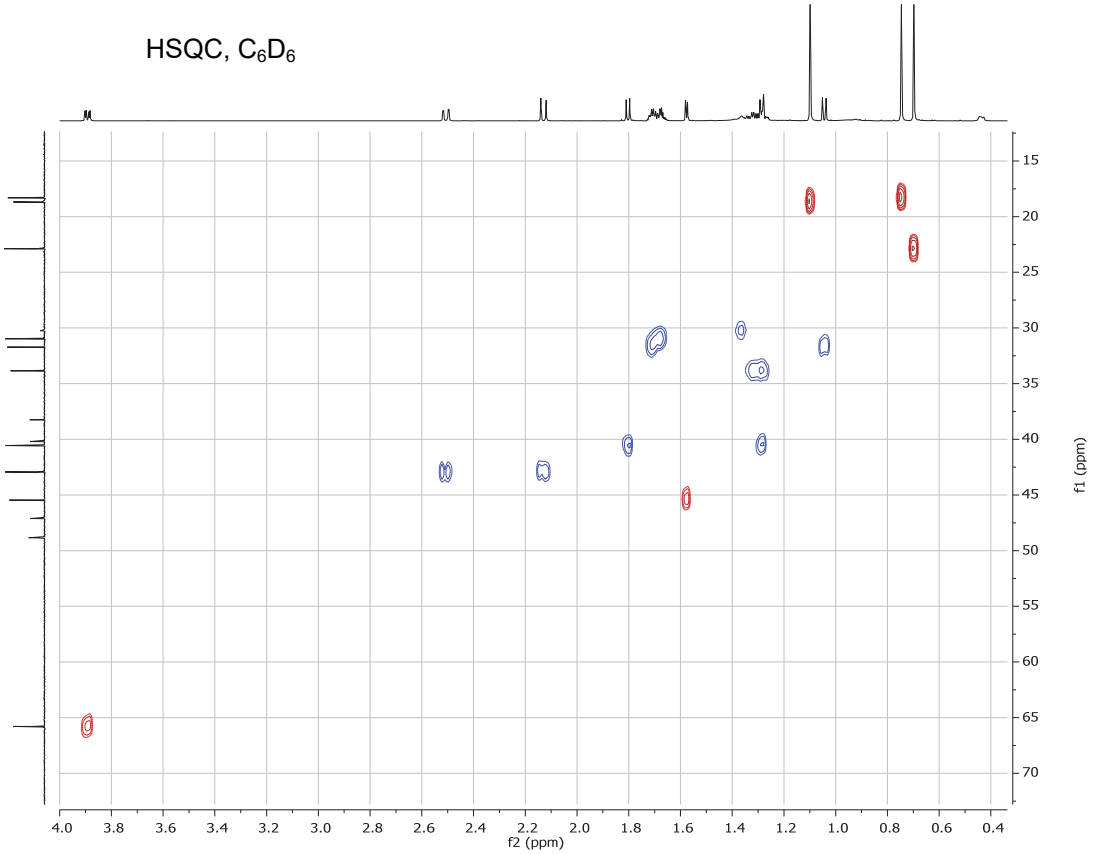

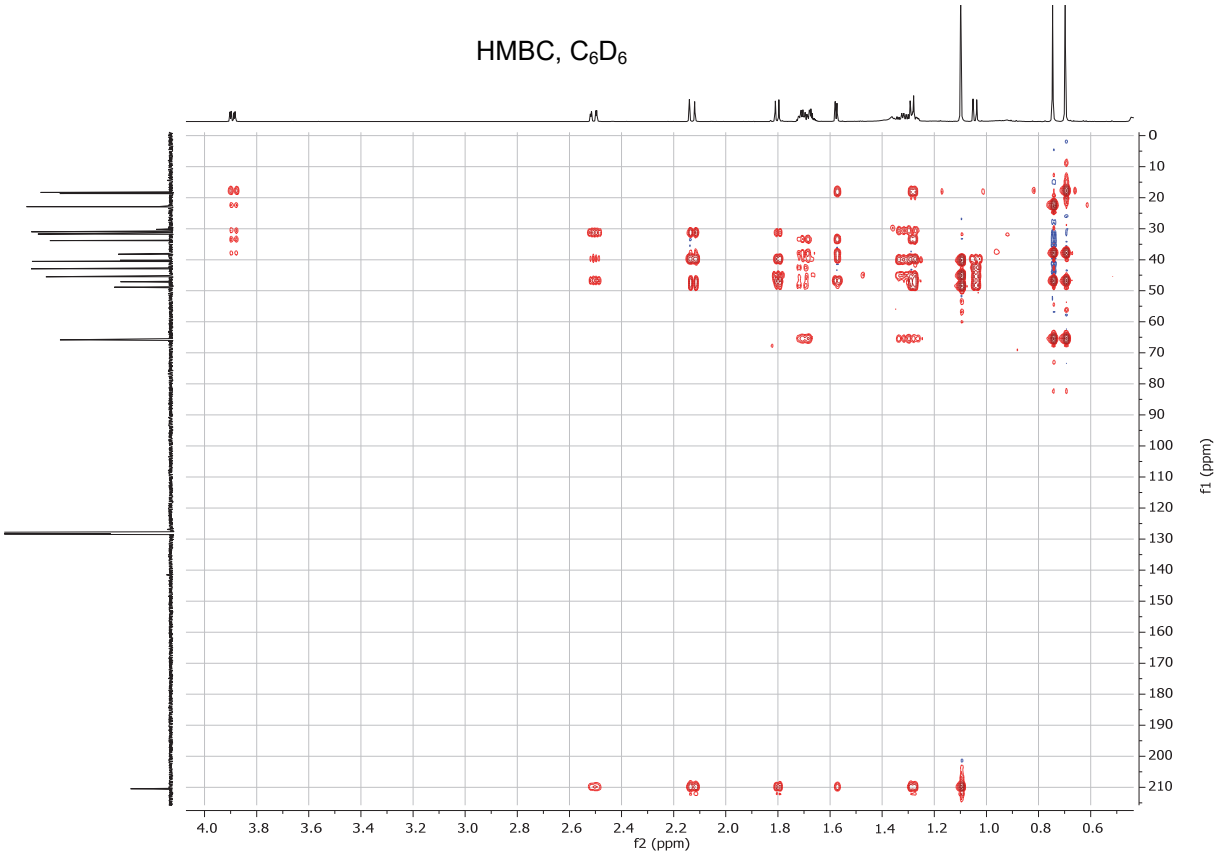
HMBC, C6D6
f2 (ppm)
f1 (ppm)

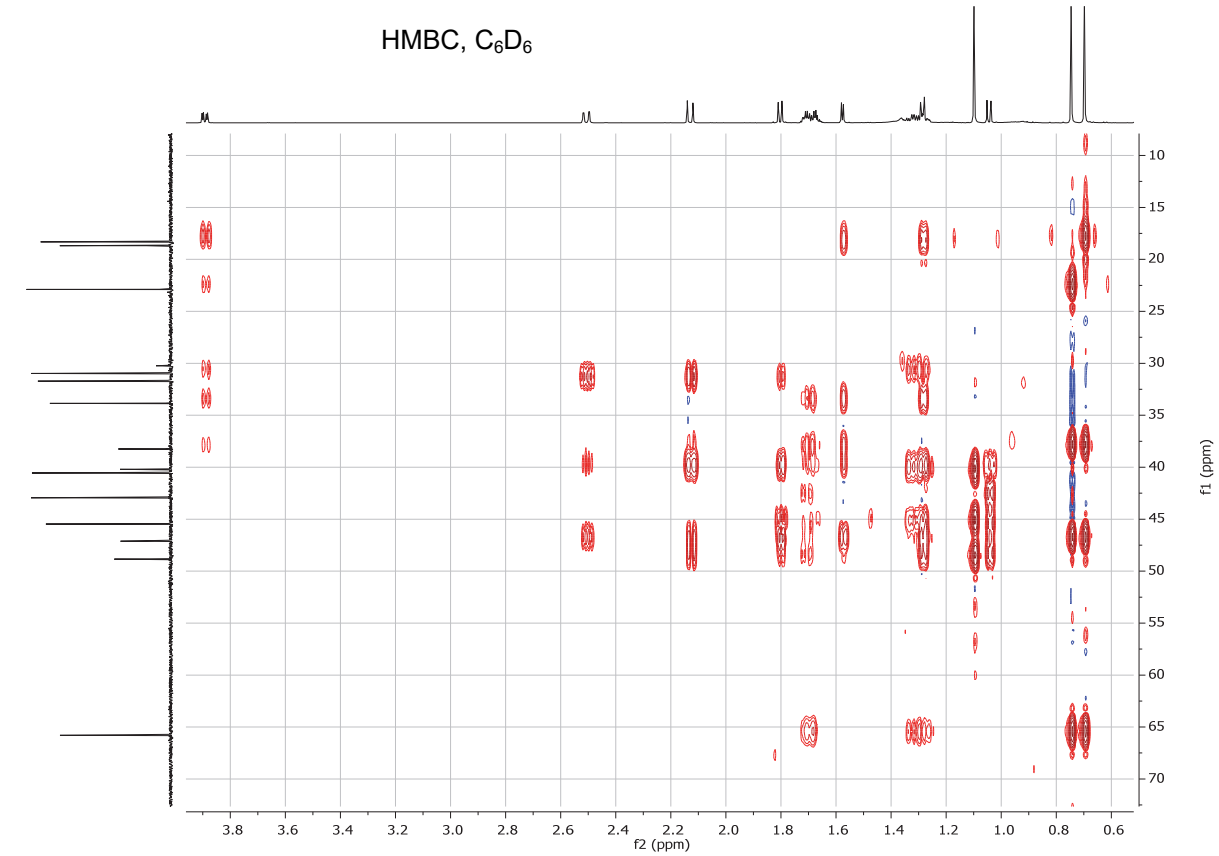
HMBC, C6D6
f2 (ppm)
f1 (ppm)

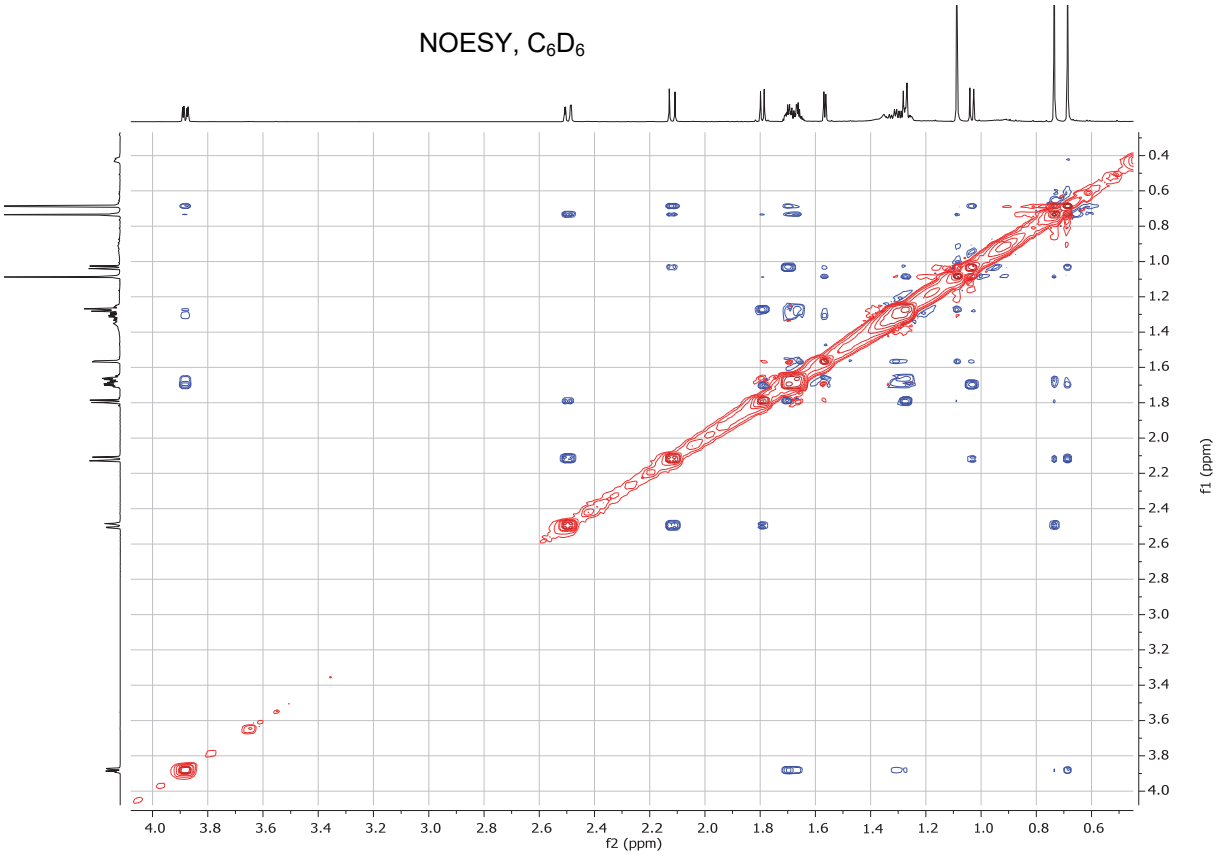
NOESY, C_6D_6
f2 (ppm)
f1 (ppm)

6.2.3 X-ray crystallographic data

1. Ladderane 15

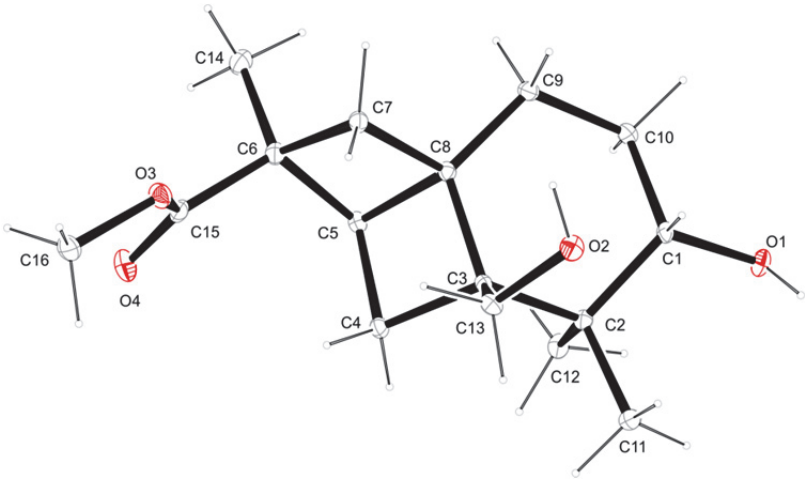

Figure 6.5 ORTEP of the molecular structure of ladderane **15**.

CCDC 1475334 contains the supplementary crystallographic data for ladderane **15**. These data can be obtained free of charge from The Cambridge Crystallographic Data Centre via www.ccdc.cam.ac.uk/data_request/cif.

Table 6.5 Crystallographic data for ladderane 15.

net formula	$C_{16}H_{26}O_4$
M_r/g mol^{-1}	282.37
crystal size/mm	0.100 × 0.080 × 0.060
T/K	100(2)
radiation	MoKα
diffractometer	'Bruker D8Venture'
crystal system	monoclinic
space group	'P 21'
a/Å	7.4267(2)
b/Å	10.8919(3)
c/Å	9.6608(3)
α/°	90
β/°	111.1920(11)
γ/°	90
V/Å^3	728.62(4)
Z	2
calc. density/g cm^{-3}	1.287
μ/mm^{-1}	0.091
absorption correction	multi-scan
transmission factor range	0.9233–0.9585
refls. measured	8756

R_{int}	0.0264
mean σ(I)/I	0.0269
θ range	2.942–26.40
observed refls.	2854
x, y (weighting scheme)	0.0405, 0.1831
hydrogen refinement	mixed
Flack parameter	1.7(11)
refls in refinement	2973
parameters	194
restraints	1
$R(F_{obs})$	0.0304
$R_w(F^2)$	0.0788
S	1.056
shift/error$_{max}$	0.001
max electron density/e Å^{-3}	0.285
min electron density/e Å^{-3}	−0.170

C-H: constr, O-H: refall. Refined as inversion twin.

2. Ketone 20

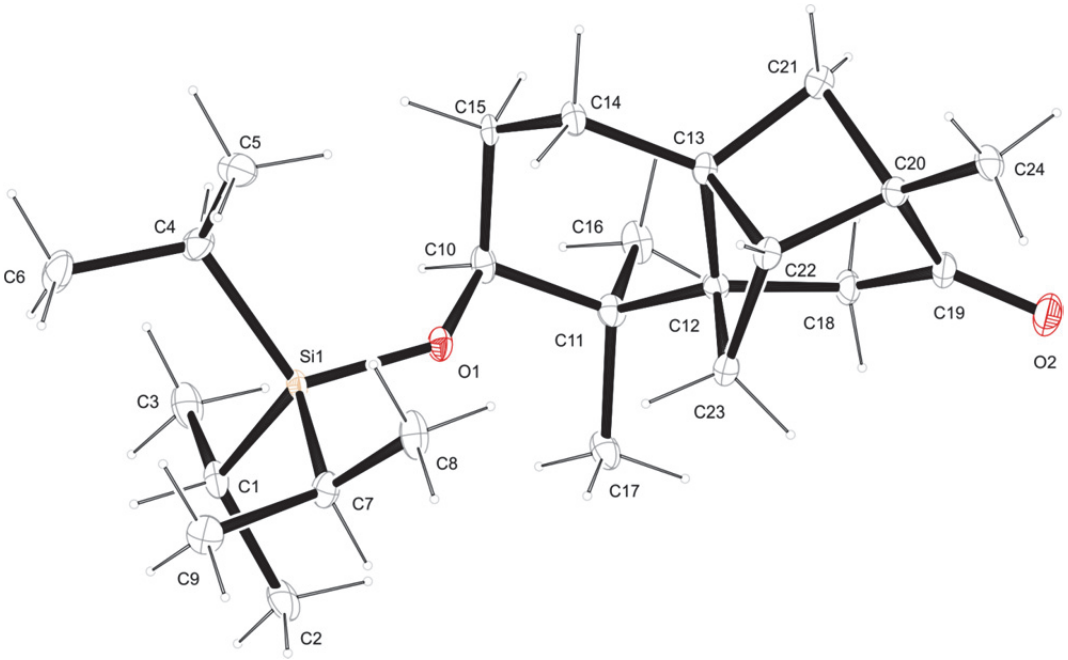

Figure 6.6 ORTEP of the molecular structure of ketone **20**.

CCDC 1475333 contains the supplementary crystallographic data for ketone **20**. These data can be obtained free of charge from The Cambridge Crystallographic Data Centre via www.ccdc.cam.ac.uk/data_request/cif.

Table 6.6 Crystallographic data for ketone 20.

net formula	$C_{24}H_{42}O_2Si$
M_r/g mol^{-1}	390.66
crystal size/mm	0.100 × 0.070 × 0.040
T/K	100(2)
radiation	MoKα
diffractometer	'Bruker D8 Venture TXS'
crystal system	triclinic
space group	'P -1'
a/Å	8.2947(12)
b/Å	9.6655(13)
c/Å	15.097(2)
α/°	85.913(5)
β/°	77.552(5)
γ/°	75.220(5)
V/Å^3	1142.6(3)
Z	2
calc. density/g cm^{-3}	1.135
μ/mm^{-1}	0.119
absorption correction	Multi-Scan
transmission factor range	0.8992–0.9705
refls. measured	8198
mean σ(*I*)/*I*	0.0501
θ range	3.180–25.39
observed refls.	3796
x, y (weighting scheme)	0.0000, 2.7536
hydrogen refinement	constr
refls in refinement	4155
parameters	254
restraints	0
$R(F_{obs})$	0.0730
$R_w(F^2)$	0.1484
S	1.215
shift/error$_{max}$	0.001
max electron density/e Å^{-3}	0.466
min electron density/e Å^{-3}	−0.443

2-component twin refinement.

6.3 Supporting information for Chapter 2.2.2

6.3.1 Experimental procedures

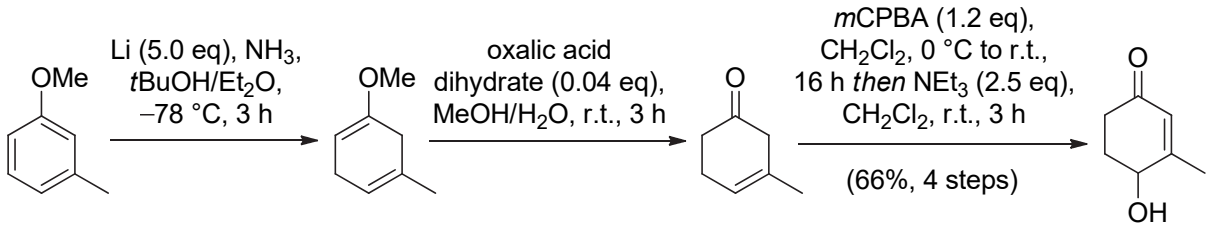

S1 **S2** **S3** **S4**

4-Hydroxy-3-methylcyclohex-2-en-1-one (S4) To a stirred solution of 3-methylanisole (**S1**, 20.0 mL, 159 mmol, 1.0 eq) in a mixture of liquid ammonia (~300 mL, condensed at −78 °C), *t*BuOH (140 mL) and Et_2O (140 mL) in a three-necked 1 L-flask equipped with a dry-ice condenser at −78 °C was added granulated lithium (5.50 g, 793 mmol, 5.0 eq) portionwise and the resulting dark blue reaction mixture was stirred for 3 h. The reaction was quenched by careful addition of NH_4Cl (50 g) and H_2O (300 mL) and the reaction flask was left open while stirring at r.t. for 2 h. The layers were separated and the aqueous layer was extracted with pentane (5 × 130 mL) and the combined organic layers were dried over Na_2SO_4. After filtration, the solvent was removed by distillation with a Vigreux column (25 cm) at atmospheric pressure to obtain crude diene **S2**, which was used in the next step without further purification.

To a stirred solution of crude diene **S2** in a mixture of MeOH/H_2O (360 mL, 3:1) at r.t. was added oxalic acid dihydrate (800 mg, 6.35 mmol, 0.04 eq) and the resulting reaction mixture was stirred for 3 h. The reaction was quenched by addition of H_2O (500 mL). The aqueous layer was extracted with CH_2Cl_2 (5 × 100 mL) and the combined organic layers were dried over Na_2SO_4. After filtration, the solvent was removed by distillation with a Vigreux column (25 cm) at atmospheric pressure to obtain crude ketone **S3**, which was used in the next step without further purification.

To a stirred solution of crude ketone **S3** in CH_2Cl_2 (600 mL) at 0 °C was added *m*CPBA (77% purity, 42.8 g, 191 mmol, 1.2 eq) and the resulting reaction mixture was stirred at r.t. for 16 h. The reaction was quenched by addition of sat. aq. $NaHCO_3$ solution (300 mL). The aqueous layer was extracted with CH_2Cl_2 (3 × 100 mL) and the combined organic layers were dried over Na_2SO_4. After filtration, NEt_3 (55.0 mL, 396 mmol, 2.5 eq) was added to the CH_2Cl_2 solution and the resulting reaction mixture was stirred at r.t. for 3h. The reaction was quenched by addition of brine (300 mL). The aqueous layer was extracted with CH_2Cl_2 (3 × 100 mL) and the combined organic layers were dried over Na_2SO_4. After filtration and concentration *in vacuo*, the crude product was purified by flash column chromatography

(hexanes:EtOAc 1:1) on silica to afford enone **S4** (13.2 g, 105 mmol, 66% over 4 steps) as a white solid. Compound **S4** has been reported in the literature.[163]

Data for S4: R_f: 0.30 (hexanes:EtOAc 1:1); **^{1}H NMR (400 MHz, $CDCl_3$):** δ = 5.87 (s, 1H), 4.39 (dd, *J* = 7.2, 6.7 Hz, 1H), 2.58 (dt, *J* = 15.9, 5.1 Hz, 1H), 2.44 – 2.24 (m, 2H), 2.06 (s, 3H), 2.05 – 1.95 (m, 1H), 1.87 – 1.75 (m, 1H); **^{13}C NMR (100 MHz, $CDCl_3$):** δ = 198.7, 162.8, 127.3, 69.0, 35.0, 32.2, 20.7 ppm; **IR (ATR):** ν_{max} = 3317 (w), 2970 (w), 2950 (w), 2927 (w), 2870 (w), 2849 (w), 1641 (s), 1614 (m), 1442 (m), 1371 (m), 1342 (w), 1324 (m), 1299 (w), 1253 (m), 1191 (m), 1178 (m), 1139 (w), 1079 (m), 1065 (m), 1046 (m), 1024 (m), 1007 (m), 965 (m), 884 (m), 809 (m), 751 (m), 679 (m), 662 (m) cm^{-1}; **melting point:** 43.6 – 46.4 °C; **HRMS (EI):** calc. for $C_7H_{10}O_2$ $[M]^+$: 126.0675, found: 126.0672.

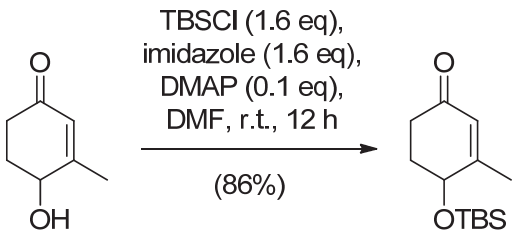

S4 **12**

4-((*tert*-Butyldimethylsilyl)oxy)-3-methylcyclohex-2-enone (12) To a stirred solution of alcohol **S4** (13.4 g, 106 mmol, 1.0 eq) in DMF (400 mL) at r.t. was added imidazole (11.6 g, 170 mmol, 1.6 eq), DMAP (1.29 g, 10.6 mmol, 0.1 eq) and TBSCl (25.6 g, 170 mmol, 1.6 eq) and the resulting reaction mixture was stirred at r.t. for 12 h. The reaction was quenched by addition of H_2O (400 mL) and brine (400 mL). The aqueous layer was extracted with Et_2O (3 × 250 mL) and the combined organic layers were washed with H_2O (4 × 250 mL) and dried over Na_2SO_4. After filtration and concentration *in vacuo*, the crude product was purified by flash column chromatography (hexanes:EtOAc 10:1) on silica to afford protected enone **12** (22.0 g, 91.5 mmol, 86%) as a colorless oil. Compound **12** has been reported in the literature.[164]

Data for 12: R_f: 0.85 (hexanes:EtOAc 1:1); **^{1}H NMR (400 MHz, $CDCl_3$):** δ = 5.82 (s, 1H), 4.35 (dd, *J* = 8.2, 4.5 Hz, 1H), 2.55 (dt, *J* = 16.8, 5.0 Hz, 1H), 2.32 (ddd, *J* = 16.7, 11.7, 4.7 Hz, 1H), 2.17 (dq, *J* = 14.5, 4.9 Hz, 1H), 2.04 – 1.93 (m, 4H), 0.92 (s, 9H), 0.14 (s, 3H), 0.13 (s, 3H) ppm; **^{13}C NMR (100 MHz, $CDCl_3$):** δ = 199.0, 164.5, 126.7, 69.8, 35.3, 32.7, 25.9, 21.3, 18.2, −4.2, −4.8 ppm; **IR (ATR):** ν_{max} = 2954 (w), 2929 (w), 2887 (w), 2857 (w), 1673 (s), 1628 (w), 1472 (w), 1440 (w), 1374 (w), 1360 (m), 1324 (m), 1252 (m), 1195 (w),

1098 (s), 1004 (m), 989 (w), 972 (m), 938 (w), 895 (m), 879 (m), 855 (m), 835 (s), 803 (m), 774 (s), 671 (m) cm^{-1}; **HRMS (EI):** calc. for $C_{13}H_{24}O_2Si$ $[M]^+$: 240.1540, found: 240.1541.

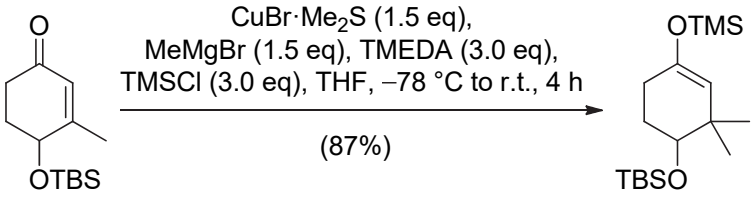

12 **S5**

Enol ether S5 To a stirred suspension of $CuBr·Me_2S$ (2.30 g, 11.3 mmol, 1.5 eq) in THF (50 mL) at −78 °C was added MeMgBr (1.0 M in dibutyl ether, 11.3 mL, 11.3 mmol, 1.5 eq) dropwise and the resulting reaction mixture was stirred at −78 °C for 1 h. A solution of enone **12** (1.80 g, 7.49 mmol, 1.0 eq), TMEDA (3.37 mL, 22.5 mmol, 3.0 eq) and freshly distilled TMSCl (2.85 mL, 22.5 mmol, 3.0 eq) in THF (30 mL) was added dropwise and the resulting reaction mixture was warmed to r.t. over 4h. The reaction was quenched by addition of Et_2O (50 mL), sat. aq. $NaHCO_3$ solution (300 mL) and H_2O (150 mL). The layers were separated and the aqueous layer was extracted with Et_2O (4 × 30 mL) and the combined organic layers were washed with H_2O (5 × 30 mL) and dried over Na_2SO_4. After filtration and concentration *in vacuo*, enol ether **S5** (2.15 g, 6.54 mmol, 87%) was obtained as a colorless oil which was used in the next step without further purification.

Data for S5: R_f: 0.40 (hexanes); **^{1}H NMR (400 MHz, C_6D_6):** δ = 4.74 (s, 1H), 3.50 (dd, J = 9.8, 3.2 Hz, 1H), 2.17 – 2.06 (m, 2H), 1.82 – 1.70 (m, 1H), 1.70 – 1.58 (m, 1H), 1.12 (s, 3H), 1.05 (s, 3H), 0.99 (s, 9H), 0.20 (s, 9H), 0.04 (s, 3H), 0.03 (s, 3H) ppm; **^{13}C NMR (100 MHz, C_6D_6):** δ = 148.6, 114.0, 75.7, 37.0, 29.7, 28.9, 28.3, 26.1, 24.5, 18.4, 0.4, −4.0, −4.8 ppm; **IR (ATR):** ν_{max} = 2955 (w), 2929 (w), 2857 (w), 1665 (w), 1471 (w), 1383 (w), 1366 (w), 1251 (m), 1205 (w), 1158 (m), 1142 (w), 1099 (m), 1084 (m), 1010 (w), 943 (m), 882 (m), 831 (s), 771 (m), 756 (m), 669 (m) cm^{-1}; **HRMS (EI):** calc. for $C_{17}H_{36}O_2Si_2$ $[M]^+$: 328.2248, found: 328.2240.

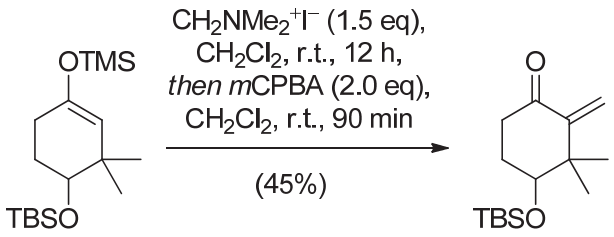

S5 **S6**

Enone S6 To a stirred solution of enol ether **S5** (400 mg, 1.22 mmol, 1.0 eq) in CH_2Cl_2 (12 mL) at r.t. was added $CH_2NMe_2^+I^-$ (338 mg, 1.82 mmol, 1.5 eq) and the resulting reaction mixture was stirred at r.t. for 12 h. The reaction was quenched by addition of aq. HCl solution (0.5 M, 8 mL), followed by addition of sat. aq. Na_2CO_3 solution (160 mL) until pH 12. The layers were separated and the aqueous layer was extracted with EtOAc (3 × 20 mL) and the combined organic layers were dried over Na_2SO_4. After filtration and concentration *in vacuo*, the crude amine was obtained as a colorless oil which was used in the next step without further purification. To a stirred solution of the crude amine in CH_2Cl_2 (8 mL) at r.t. was added *m*CPBA (77% pure, 547 mg, 2.44 mmol, 2.0 eq) and the resulting reaction mixture was stirred at r.t. for 90 min. The reaction was quenched by addition of H_2O (80 mL). The layers were separated and the aqueous layer was extracted with CH_2Cl_2 (3 × 20 mL) and the combined organic layers were dried over Na_2SO_4. After filtration and concentration *in vacuo*, the crude product was purified by flash column chromatography (pentane:Et_2O 50:1) on silica to afford enone **S6** (154 mg, 547 µmol, 45%) as a colorless oil.

Data for S6: R_f: 0.34 (pentane:Et_2O 20:1); **^{1}H NMR (400 MHz, C_6D_6):** δ = 5.96 (d, J = 1.5 Hz, 1H), 4.97 (d, J = 1.5 Hz, 1H), 3.31 (dd, J = 6.6, 3.0 Hz, 1H), 2.54 (ddd, J = 16.8, 8.5, 7.0 Hz, 1H), 2.15 (dt, J = 16.9, 6.5 Hz, 1H), 1.64 (dddd, J = 14.0, 8.6, 6.5, 3.1 Hz, 1H), 1.54 (dq, J = 13.6, 6.7 Hz, 1H), 0.97 (s, 3H), 0.91 (s, 9H), 0.84 (s, 3H), −0.03 (s, 3H), −0.07 (s, 3H) ppm; **^{13}C NMR (100 MHz, C_6D_6):** δ = 200.2, 154.0, 117.7, 75.4, 43.1, 36.0, 27.7, 26.7, 26.0, 23.7, 18.3, −4.3, −4.9 ppm; **IR (ATR):** ν_{max} = 2955 (m), 2930 (m), 2857 (m), 1698 (m), 1614 (w), 1472 (w), 1462 (w), 1389 (w), 1361 (w), 1285 (w), 1254 (m), 1178 (w), 1158 (w), 1084 (s), 1006 (w), 993 (w), 961 (w), 935 (m), 884 (w), 835 (s), 803 (w), 774 (s), 735 (w), 676 (w), 606 (w), 587 (w), 568 (w), 558 (w) cm^{-1}; **HRMS (EI):** calc. for $C_{14}H_{25}O_2Si$ [M-CH_3]$^+$: 253.1618, found: 253.1609.

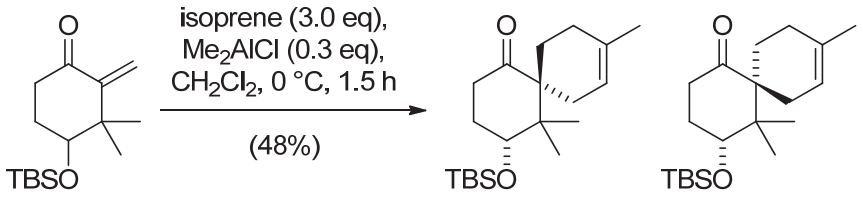

S6 **S7** d.r. 1:1.2 **S7'**

Spirocycle S7/S7' To a stirred solution of enone **S6** (12.2 mg, 45.4 µmol, 1.0 eq.) in CH_2Cl_2 (0.8 mL) at 0 °C was added isoprene (1.0 M in CH_2Cl_2, 0.136 mL, 136 µmol, 3.0 eq) and Me_2AlCl (0.2 M, 86.0 µL, 13.6 µmol, 0.3 eq) and the resulting reaction mixture was stirred for 1.5 h. The reaction was quenched by addition of half sat. aq. Na_2CO_3 solution (10 mL) and the aqueous layer was extracted with Et_2O (3 × 10 mL). The combined organic layers were dried over Na_2SO_4. After filtration and concentration *in vacuo*, the crude product was purified by flash column chromatography (hexanes:EtOAc 80:1) on silica to afford enone **S7/S7'** (7.3 mg, 21.7 µmol, 48%) in an inseparable 1:1.2 diastereomeric mixture as a colorless oil.

NMR shifts which could be clearly assigned to the major diastereomer are marked with an asterisk * and shifts which could be clearly assigned to the minor diastereomer are marked with a hash #. Due to the ratio of the two diastereomer the integrals in the ^{1}H-NMR differ from the expected values.

Data for S7/S7': R_f: 0.34 (hexanes:EtOAc 1:19); **^{1}H NMR (800 MHz, C_6D_6):** δ = 5.48 (s, 1H)#, 5.42 (s, 1H)*, 3.88 (dd, *J* = 11.0, 5.0 Hz, 1H)#, 3.44 (dd, *J* = 5.5, 3.6 Hz, 1H)*, 2.71 (td, *J* = 12.1, 6.0 Hz, 1H)*, 2.65 (dd, *J* = 13.3, 5.4 Hz, 1H)*, 2.52 (d, *J* = 15.5 Hz, 1H)#, 2.34 (d, *J* = 18.6 Hz, 1H)*, 2.26 (td, *J* = 13.6, 6.6 Hz, 1H)#, 2.17 (dt, *J* = 12.3, 5.9 Hz, 1H)*, 2.08 (ddd, *J* = 13.3, 5.1, 2.9 Hz, 1H)#, 2.02 (t, *J* = 14.3 Hz, 1H)#, 1.86 (d, *J* = 16.9 Hz, 1H)*, 1.79 – 1.71 (m, 5H), 1.69 – 1.54 (m, 13H), 1.51 – 1.45 (m, 2H), 0.96 (s, 22H), 0.89 (s, 4H)*, 0.88 (s, 3H)#, 0.78 (s, 3H)# , 0.66 (s, 4H)*, 0.05 (s, 3H)#, 0.02 (s, 3H)#, 0.01 (s, 4H)*, −0.04 (s, 4H)* ppm; **^{13}C NMR (200 MHz, C_6D_6):** δ = 212.1*, 210.4#, 132.9*, 130.7#, 121.7#, 120.0*, 76.1*, 73.1#, 54.7*, 54.4#, 45.5*, 44.9#, 35.0#, 33.5*, 31.8, 31.6, 28.5, 28.3, 27.8, 27.2, 27.1, 27.0, 26.1 (2C), 23.5 (2C), 23.3, 21.9#, 19.5*, 18.3 (2C), 16.2#, −3.8#, −4.3*, −4.7#, −4.9* ppm; **IR (ATR):** ν_{max} = 2954 (w), 2929 (w), 2899 (w), 2857 (w), 1709 (m), 1472 (w), 1462 (w), 1446 (w), 1390 (w), 1366 (w), 1328 (w), 1296 (w), 1255 (m), 1230 (w), 1160 (w), 1133 (w), 1115 (w), 1085 (m), 1056 (m), 1042 (w), 1026 (w), 1004 (w), 991 (w), 971 (w), 938 (w), 924 (w), 907 (w), 880 (m), 834 (s), 804 (w), 773 (s), 714 (w), 669 (w), 640 (w) cm^{-1}; **HRMS (ESI):** calc. for $C_{20}H_{37}O_2Si$ $[M+H]^+$: 337.2557, found: 337.2559.

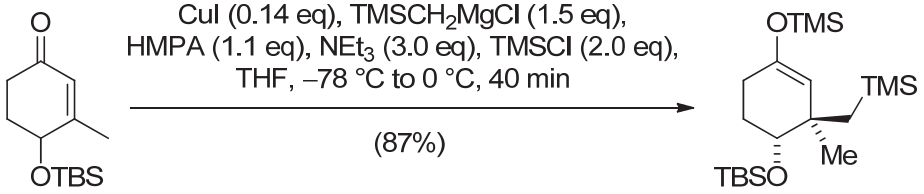

12 **13**

Enol ether 13

Preparation of the Grignard reagent:

Magnesium turnings (2.60 g, 107 mmol, 1.0 eq) and a catalytic amount of iodine were suspended in Et_2O (75 mL). $TMSCH_2Cl$ (14.7 mL, 105 mmol, 1.0 eq) was added in small portions over 20 min. The resulting mixture was heated under reflux for 30 min. The obtained Grignard solution was titrated with iodine solution, transferred to a flame dried flask and stored under Argon atmosphere.

*1,4-Addition to enone **12**:*

The Grignard-reagent (1.25 M, 20.0 mL, 25.0 mmol, 1.5 eq) was added to a stirred suspension of CuI (442 mg, 2.32 mmol, 0.14 eq) in THF (32 mL). The mixture was cooled to −30 °C and protected enone **12** (4.00 g, 16.6 mmol, 1.0 eq) in THF (15 mL) was added. The resulting reaction mixture was stirred for 1 h and then cooled to –60 °C. HMPA (3.18 mL, 18.3 mmol, 1.1 eq), NEt_3 (6.92 mL, 50.0 mmol, 3.0 eq) and freshly distilled TMSCl (4.28 mL, 33.3 mmol, 2.0 eq) were added. The reaction was immediately cooled to –78 °C and stirred for 30 min. The reaction mixture was warmed to 0 °C over 10 min and was stirred at this temperature for 30 min. The reaction was quenched by addition of half-sat. aq. $NaHCO_3$ solution (140 mL) and the aqueous layer was extracted with Et_2O (3 × 100 mL). The combined organic layers were washed with H_2O (5 × 150 mL) and dried over Na_2SO_4. After filtration and concentration *in vacuo*, enol ether **13** (5.81 g, 14.5 mmol, 87%) was obtained as a colorless oil which was used in the next step without further purification.

Data for 13: R_f: 0.53 (hexanes); **^{1}H NMR (400 MHz, C_6D_6):** δ = 4.89 (s, 1H), 3.59 (dd, J = 7.2, 4.8 Hz, 1H), 2.20 – 2.06 (m, 2H), 1.79 – 1.67 (m, 2H), 1.19 (s, 3H), 1.01 (s, 9H), 0.91 (d, J = 14.5 Hz, 1H), 0.86 (d, J = 14.5 Hz, 1H), 0.23 (s, 9H), 0.15 (s, 9H), 0.10 (s, 3H), 0.07 (s, 3H) ppm; **^{13}C NMR (100 MHz, C_6D_6):** δ = 148.2, 113.8, 76.3, 40.0, 31.4, 28.3, 27.8, 26.2, 25.9, 18.4, 1.2, 0.6, −3.8, −4.5 ppm; **IR (ATR):** ν_{max} = 2954 (w), 2857 (w), 1664 (w), 1375 (w), 1250 (m), 1201 (w), 1175 (w), 1102 (m), 1005 (w), 946 (w), 893 (m), 834 (s), 772 (m), 687 (w) cm^{-1}; **HRMS (ESI):** calc. for $C_{20}H_{45}O_2Si_3$ $[M+H]^+$: 401.2722, found: 401.2727.

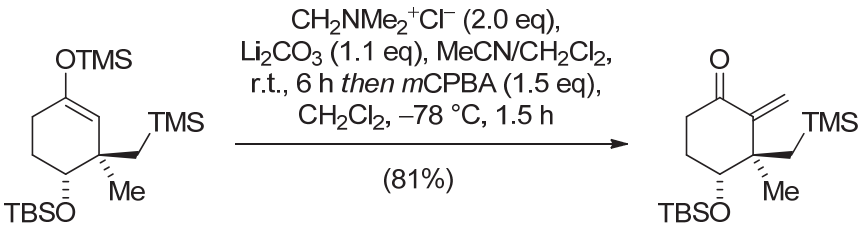

13 **14**

Enone 14 A solution of enol ether **13** (6.60 g, 16.5 mmol, 1.0 eq) in CH_2Cl_2 (110 mL) was added to a stirred suspension of $CH_2NMe_2^+Cl^-$ (3.08 g, 32.9 mmol, 2.0 eq) and Li_2CO_3 (1.34 g, 18.1 mmol, 1.1 eq) in MeCN (110 mL) at 0 °C and the resulting reaction mixture was stirred at r.t. for 6 h. The reaction was quenched by addition of H_2O (350 mL). The layers were separated and the aqueous layer was extracted with EtOAc (6 × 150 mL) and the combined organic layers were dried over Na_2SO_4. After filtration and concentration *in vacuo*, the crude amine was obtained as a colorless oil which was used in the next step without further purification. To a stirred solution of the crude amine in CH_2Cl_2 (220 mL) at −78 °C was added freshly purified *m*CPBA[165] (4.26 g, 24.7 mmol, 1.5 eq) dissolved in CH_2Cl_2 (110 mL) and the resulting reaction mixture was stirred for 1.5 h. The reaction was quenched by addition of ice-cold sat. aq. $NaHCO_3$ solution (containing 1% $Na_2S_2O_3$, 300 mL). The layers were separated and the aqueous layer was extracted with CH_2Cl_2 (3 × 250 mL) and the combined organic layers were dried over Na_2SO_4. After filtration and concentration *in vacuo*, the crude product was purified by flash column chromatography (pentane:Et_2O 20:1) on silica to afford enone **14** (4.53 g, 13.3 mmol, 81%) as a white solid. The compound was stored in benzene matrix at −20 °C. Evaporation from benzene afforded crystals suitable for single crystal X-ray diffraction analysis.

Data for 14: R_f: 0.43 (hexanes:EtOAc 9:1); **^{1}H NMR (400 MHz, C_6D_6):** δ = 5.86 (s, 1H), 4.90 (s, 1H), 3.46 (s, 1H), 2.66 (ddd, *J* = 16.4, 12.7, 7.5 Hz, 1H), 2.31 (ddd, *J* = 16.4, 5.8, 1.7 Hz, 1H), 1.92 (dddd, *J* = 14.7, 12.8, 5.8, 2.1 Hz, 1H), 1.57 – 1.46 (m, 1H), 1.12 (s, 3H), 0.91 (s, 9H), 0.60 (d, *J* = 14.8 Hz, 1H), 0.50 (d, *J* = 14.8 Hz, 1H), 0.02 (s, 3H), 0.01 (s, 9H), −0.03 (s, 3H) ppm; **^{13}C NMR (100 MHz, C_6D_6):** δ = 201.5, 154.8, 116.9, 76.3, 46.3, 35.4, 29.6, 27.2, 26.0, 24.2, 18.4, 1.0, −4.3, −4.8 ppm; **IR (ATR):** ν_{max} = 2954 (w), 2894 (w), 2858 (w), 1698 (m), 1612 (w), 1472 (w), 1411 (w), 1362 (w), 1286 (w), 1250 (m), 1190 (w), 1083 (m), 1046 (w), 993 (w), 966 (w), 937 (w), 863 (w), 835 (s), 774 (m), 738 (w), 687 (w) cm^{-1}; **melting point:** 45.0 – 46.0 °C; **HRMS (ESI):** calc. for $C_{18}H_{40}NO_2Si_2$ $[M+NH_4]^+$: 358.2592, found: 358.2598.

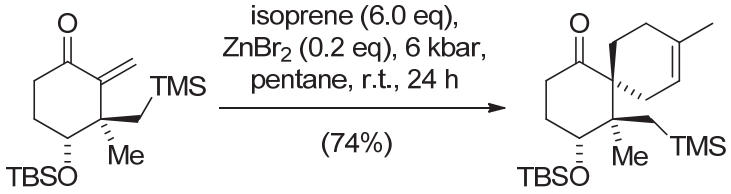

14 **15**

Spirocycle 15 To a solution of enone **14** (1.00 g, 2.94 mmol, 1.0 eq) in pentane (14 mL) in a high pressure Teflon vial (left picture) was added isoprene (1.76 mL, 17.6 mmol, 6.0 eq) and anhydrous $ZnBr_2$ (132 mg, 587 µmol, 0.2 eq) and the resulting reaction mixture was placed in a Hofer high pressure apparatus (right picture) at 6 kbar for 24 h. The reaction was quenched by addition of sat. aq. $NaHCO_3$ solution (120 mL) and H_2O (60 mL). The layers were separated and the aqueous layer was extracted with CH_2Cl_2 (3 × 50 mL) and the combined organic layers were dried over Na_2SO_4. After filtration and concentration *in vacuo*, the crude product was purified by flash column chromatography (pentane:CH_2Cl_2 5:1→1:1) on silica to afford spirocycle **15** (897 mg, 2.19 mmol, 74%) as a white solid.

Data for 14: R_f: 0.38 (hexanes:EtOAc 19:1); **^{1}H NMR (400 MHz, C_6D_6):** δ = 5.48 – 5.40 (m, 1H), 3.80 (dd, *J* = 6.9, 3.8 Hz, 1H), 2.92 (d, *J* = 17.4 Hz, 1H), 2.61 (dt, *J* = 13.0, 8.1 Hz, 1H), 2.32 – 2.11 (m, 3H), 2.02 (dd, *J* = 13.8, 4.8 Hz, 1H), 1.90 – 1.73 (m, 2H), 1.69 – 1.59 (m, 4H), 1.46 (td, *J* = 12.2, 6.2 Hz, 1H), 0.98 (s, 9H), 0.96 (s, 3H), 0.86 (d, *J* = 15.2 Hz, 1H), 0.77 (d, *J* = 15.2 Hz, 1H), 0.08 (s, 3H), 0.04 (s, 9H), 0.02 (s, 3H) ppm; **^{13}C NMR (100 MHz, C_6D_6):** δ = 212.2, 133.1, 120.2, 75.9, 55.8, 49.8, 34.1, 31.9, 30.5, 28.4, 26.1, 25.8, 25.7, 23.5, 18.5, 18.3, 1.5, −4.2, −4.4 ppm; **IR (ATR):** ν_{max} = 2952 (w), 2929 (w), 2896 (w), 2857 (w), 1706 (m), 1471 (w), 1463 (w), 1445 (w), 1432 (w), 1377 (w), 1304 (w), 1249 (m), 1204 (w), 1193 (w), 1147 (w), 1085 (m), 1066 (m), 1023 (w), 944 (m), 959 (w), 937 (w), 914 (w), 880 (m), 857 (m), 832 (s), 804 (m), 772 (s), 685 (m), 666 (m), 629 (w), 611 (w), 589 (w), 557 (w) cm^{-1}; **melting point:** 95.0 – 97.0 °C; **HRMS (ESI):** calc. for $C_{23}H_{44}O_2Si_2$ $[M+H]^+$: 409.2953, found: 409.2958.

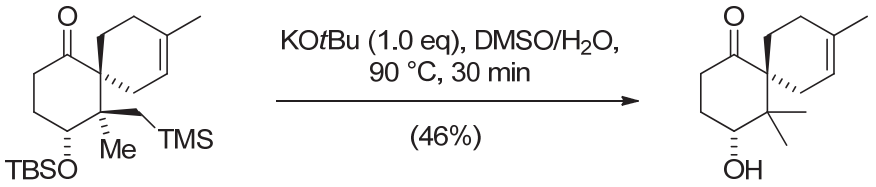

15 **16**

Spirocycle 16 To a stirred solution of cyclohexene **15** (36.5 mg, 89.3 µmol, 1.0 eq) in DMSO (1 mL) was added H_2O (54 µL) and KO*t*Bu (10.0 mg, 89.3 µmol, 1.0 eq) and the resulting reaction mixture was heated to 90 °C for 30 min. The reaction was quenched by addition of sat. aq. NH_4Cl solution (15 mL). The layers were separated and the aqueous layer was extracted with EtOAc (4 × 10 mL) and the combined organic layers were dried over Na_2SO_4. After filtration and concentration *in vacuo*, the crude product was purified by flash column chromatography (hexanes:EtOAc 2:1) on silica to afford spirocycle **16** (9.2 mg, 41.4 mmol, 46%) as a white solid. Crystallization from hexanes/CH_2Cl_2 afforded crystals suitable for single crystal X-ray diffraction analysis.

Data for 16: R_f: 0.34 (hexanes:EtOAc 1:1); **^{1}H NMR (800 MHz, CD_2Cl_2):** δ = 5.34 (dd, J = 4.5, 1.7 Hz, 1H), 4.18 (dd, J = 11.4, 3.5 Hz, 1H), 2.76 (td, J = 13.9, 6.7 Hz, 1H), 2.26 – 2.21 (m, 1H), 2.18 – 2.12 (m, 2H), 2.08 (dddd, J = 13.0, 7.0, 4.9, 2.4 Hz, 1H), 1.88 – 1.82 (m, 2H), 1.75 – 1.67 (m, 2H), 1.60 – 1.56 (m, 4H), 1.50 (s, 1H), 1.03 (s, 3H), 0.69 (s, 3H) ppm; **^{13}C NMR (200 MHz, CD_2Cl_2):** δ = 213.0, 131.8, 121.1, 72.2, 54.8, 44.5, 35.7, 31.5, 27.8, 27.5, 26.9, 23.4, 21.3, 15.7 ppm; **IR (ATR):** ν_{max} = 3448 (br w), 2965 (m), 1702 (s), 1451 (w), 1432 (m), 1367 (w), 1328 (w), 1288 (w), 1225 (w), 1150 (w), 1106 (w), 1065 (m), 1040 (m), 1019 (m), 966 (m), 826 (w), 801 (w), 761 (w), 726 (w) cm^{-1}; **melting point:** 95.8 – 98.6 °C; **HRMS (EI):** calc. for $C_{14}H_{20}O$ [M-H_2O]$^+$: 204.1509, found: 204.1508.

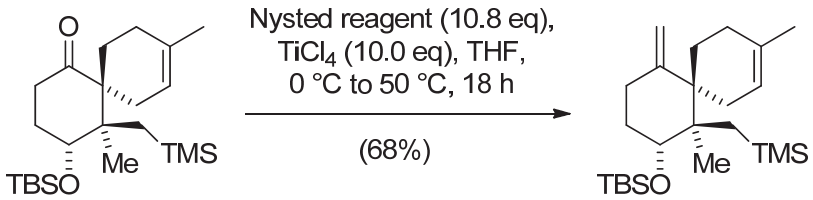

15 **17**

Alkene 17 To a stirred suspension of Nysted reagent (20% in THF, 46.8 mL, 21.1 mmol, 10.8 eq) was added $TiCl_4$ (1.0 M in toluene, 19.6 mL, 19.6 mmol, 10.0 eq) at 0 °C followed by ketone **15** (800 mg, 1.96 mmol, 1.0 eq) in THF (20 mL) and the resulting reaction mixture was stirred at 50 °C for 18 h. The reaction was quenched by addition of sat. aq. NH_4Cl

solution (200 mL), brine (150 mL) and aq. HCl solution (1.0 M, 100 mL). The layers were separated and the aqueous layer was extracted with pentane/Et_2O (1:1, 3 × 150 mL) and Et_2O (100 mL) and the combined organic layers were washed with brine (150 mL) and dried over Na_2SO_4. After filtration and concentration *in vacuo*, the crude product was purified by flash column chromatography (pentane) on silica to afford enone **17** (540 mg, 1.33 mmol, 68%) as a white solid.

Data for 17: R_f: 0.88 (hexanes); **^{1}H NMR (400 MHz, C_6D_6):** δ = 5.34 (s, 1H), 4.98 (s, 1H), 4.74 (s, 1H), 3.75 (dd, *J* = 11.1, 4.8 Hz, 1H), 2.28 – 1.98 (m, 4H), 1.77 – 1.49 (m, 9H), 1.22 (d, *J* = 15.3 Hz, 1H), 1.02 (s, 9H), 1.01 (s, 3H), 0.76 (d, *J* = 15.3 Hz, 1H), 0.20 (s, 9H), 0.13 (s, 3H), 0.10 (s, 3H) ppm; **^{13}C NMR (100 MHz, C_6D_6):** δ = 148.0, 133.0, 120.3, 111.9, 76.9, 47.7, 46.5, 33.2, 31.4, 30.3, 28.0, 26.3, 26.2, 25.0, 23.7, 18.5, 15.9, 1.9, −3.8, −4.0 ppm; **IR (ATR):** ν_{max} = 2954 (m), 2932 (m), 2896 (m), 2871 (w), 2857 (m), 1632 (w), 1462 (w), 1446 (w), 1408 (w), 1379 (w), 1364 (w), 1249 (m), 1234 (w), 1151 (w), 1093 (m), 1084 (m), 1064 (s), 988 (w), 956 (w), 894 (s), 835 (s), 802 (m), 773 (s), 692 (w), 680 (w), 668 (w) cm^{-1}; **melting point:** 83.0 – 84.0 °C; **HRMS (EI):** calc. for $C_{24}H_{46}OSi_2$ [*M*]$^+$: .406.3082, found: 406.3073.

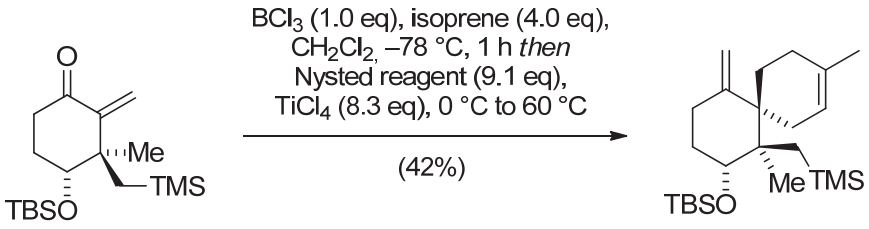

14 **17**

One step protocol for 17 A solution of exocyclic alkene **14** (227 mg, 666 µmol, 1.0 eq) in CH_2Cl_2 (2.0 mL) was cooled to –78 °C. Isoprene (265 µL, 2.64 mmol, 4.0 eq) and BCl_3 (1.0 M in heptane, 865 µL, 865 µmol, 1.3 eq) were added and the reaction was stirred for 1 h. To a separate flask charged with a suspension of Nysted reagent (20% in THF, 13.5 mL, 6.09 mmol, 9.1 eq) was added $TiCl_4$ (1 M in CH_2Cl_2, 5.54 ml, 5.54 mmol, 8.3 eq) at 0 °C turning the suspension brown. As soon as the addition of $TiCl_4$ was complete, the reaction was heated to 60 °C. When the Diels–Alder reaction was deemed complete by TLC the yellow solution was cannulated into the suspension of Nysted reagent and allowed to react overnight. After completion, it was cooled to 0 °C, quenched with methanol. The solution was filtered through a pad of silica (EtOAc). The crude organic solution was concentrated and diluted with methanol. This methanol layer was extracted with hexanes and dried over

Na_2SO_4. After filtration and concentration *in vacuo*, the crude product was purified by flash chromatography (pentane) on silica to afford alkene **17** (115 mg, 283 µmol, 42% yield) as a white solid.

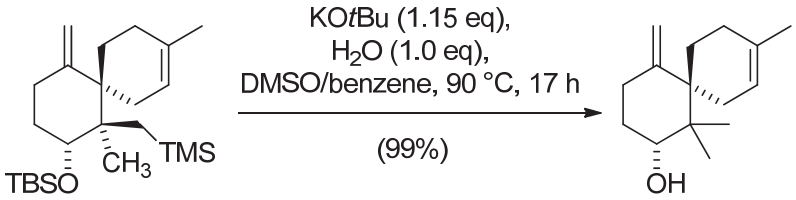

17 **18**

Alcohol X To a stirred solution of silane **X** (530 mg, 1.30 mmol, 1.0 eq) in DMSO/benzene (20 mL, 3:2) was added H_2O (23.5 µL, 1.30 mmol, 1.0 eq) and KO*t*Bu (168 mg, 1.50 mmol, 1.15 eq) at r.t. and the resulting reaction mixture was stirred at 90 °C for 17 h. The reaction was quenched by addition of sat. aq. NH_4Cl solution (30 mL). The layers were separated and the aqueous layer was extracted with EtOAc (3 × 40 mL) and the combined organic layers were washed with brine (2 × 40 mL) and dried over Na_2SO_4. After filtration and concentration *in vacuo*, the crude product was purified by flash column chromatography (hexanes:EtOAc 9:1) on silica to afford alcohol **X** (285 mg, 1.29 mmol, 99%) as a white solid.

Data for X: R_f: 0.23 (hexanes:EtOAc 9:1); **^{1}H NMR (400 MHz, C_6D_6):** δ = 5.31 (s, 1H), 4.93 (t, *J* = 1.8 Hz, 1H), 4.69 (s, 1H), 3.50 (dt, *J* = 11.6, 4.9 Hz, 1H), 2.08 (dddd, *J* = 15.1, 7.3, 3.7, 1.7 Hz, 2H), 2.00 – 1.87 (m, 2H), 1.66 – 1.49 (m, 7H), 1.43 – 1.30 (m, 2H), 0.94 (s, 3H), 0.79 (s, 3H), 0.68 (d, *J* = 5.1 Hz, 1H) ppm; **^{13}C NMR (100 MHz, C_6D_6):** δ = 147.5, 132.6, 120.5, 111.9, 73.0, 45.6, 42.2, 32.7, 30.5, 29.6, 27.9, 26.0, 23.6, 20.6, 15.3 ppm; **IR (ATR):** ν_{max} = 3376 (br w), 2934 (m), 2905 (m), 2830 (w), 1638 (w), 1472 (w), 1449 (m), 1428 (m), 1386 (m), 1364 (m), 1258 (w), 1226 (w), 1160 (w), 1079 (m), 1066 (m), 1040 (s), 1023 (s), 983 (s), 957 (m), 890 (s), 822 (w), 802 (m), 762 (w), 694 (m), 666 (w) cm^{-1}; **melting point:** 69.0 – 71.0 °C; **HRMS (EI):** calc. for $C_{15}H_{24}O_1$ $[M]^+$: 220.1822, found: 220.1826.

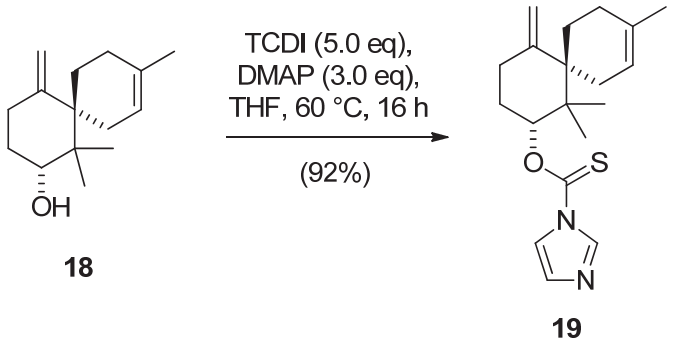

18 **19**

Imidazole 19 To a stirred solution of alcohol **18** (287 mg, 1.30 mmol, 1.0 eq) in THF (15 mL) was added TCDI (1.16 g, 6.52 mmol, 5.0 eq) and DMAP (478 mg, 3.91 mmol, 3.0 eq) at r.t. and the resulting reaction mixture was stirred at 60 °C for 16 h. After concentration *in vacuo*, the crude product was purified by flash column chromatography (hexanes:EtOAc 10:1) on silica to afford imidazole **19** (396 mg, 1.20 mmol, 92%) as a colorless oil.

Data for 19: R_f: 0.33 (hexanes:EtOAc 4:1); **^{1}H NMR (400 MHz, C_6D_6):** δ = 8.37 (s, 1H), 7.43 (s, 1H), 6.96 (s, 1H), 5.80 (dd, *J* = 12.1, 4.7 Hz, 1H), 5.24 (s, 1H), 4.87 (t, *J* = 1.6 Hz, 1H), 4.66 (s, 1H), 2.05 (td, *J* = 14.0, 13.5, 4.4 Hz, 1H), 1.97 – 1.75 (m, 4H), 1.65 – 1.50 (m, 6H), 1.40 – 1.25 (m, 2H), 0.72 (s, 3H), 0.70 (s, 3H) ppm; **^{13}C NMR (100 MHz, C_6D_6):** δ = 184.4, 145.7, 136.7, 132.9, 131.6, 119.8, 118.2, 113.1, 87.1, 46.1, 41.8, 29.6, 29.09, 27.7, 27.4, 26.1, 23.5, 20.2, 17.6 ppm; **IR (ATR):** ν_{max} = 2965 (w), 2940 (w), 2907 (w), 2877 (w), 2830 (w), 1640 (w), 1530 (w), 1471 (w), 1458 (m), 1382 (s), 1336 (s), 1280 (s), 1280 (s), 1228 (s), 1195 (m), 1092 (m), 1046 (w), 992 (m), 970 (s), 933 (m), 895 (s), 822 (m), 803 (w), 779 (w), 735 (m), 655 (w) cm^{-1}; **HRMS (EI):** calc. for $C_{19}H_{26}N_2OS$ [*M*]$^+$: 330.1760, found: 330.1768.

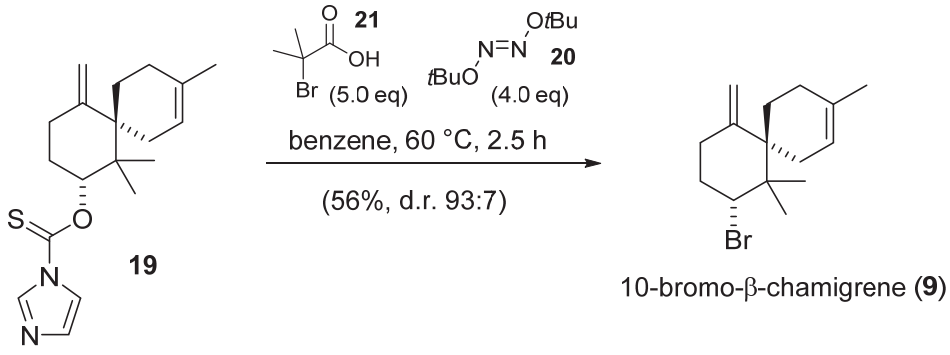

19 10-bromo-β-chamigrene (**9**)

10-Bromo-β-chamigrene (9) To a solution of **19** (253 mg, 766 µmol, 1.0 eq) and α-bromoacid **21** (661 mg, 3.80 mmol, 5.0 eq) at 60 °C in benzene (24 mL, degassed by sparging with N_2 for 15 min) was added hyponitrite **20** (566 mg, 3.04 mmol, 4.0 eq) in benzene (24 mL, degassed by sparging with N_2 for 15 min) over 2 h by syringe pump followed by stirring for an additional 30 min. After concentration *in vacuo*, the crude product

was purified by flash chromatography (pentane:Et_2O 1:0→4:1) to afford the desired product **9** (120 mg, 424 µmol, 56%) as colorless oil in a 93:7 diastereomeric mixture. This compound was found to be volatile over prolonged periods under high vacuum.

Data for 10-bromo-β-chamigrene (9): R_f: 0.46 (pentane); **IR (ATR):** ν_{max} = 2933 (s), 2854 (s), 1638 (m), 1453 (s), 1389 (m), 1369 (m), 1341 (w), 1314 (w), 1288 (w), 1253 (w), 1221 (w), 1157 (m), 1121 (w), 1064 (m), 1020 (w), 981 (w), 943 (w), 894 (s), 870 (s), 820 (w), 802 (w), 778 (w), 724 (w), 677 (w) cm^{-1};**HRMS (EI):** calc. for $C_{15}H_{23}Br^{79}$ $[M]^+$: 282.0978, found: 282.0987.

NMR-data:[94c]

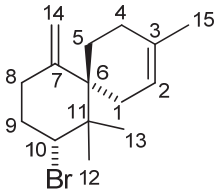

10-bromo-β-chamigrene (9)

No.	^{1}H NMR Isolation 300 MHz, $CDCl_3$ [ppm]	^{1}H NMR Synthetic 600 MHz, $CDCl_3$ [ppm]	^{13}C NMR Isolation 75 MHz, $CDCl_3$ [ppm]	^{13}C NMR Synthetic 150 MHz, $CDCl_3$ [ppm]
1	2.04 (br d, *J* = 15.3 Hz, 1H) 2.23 (br d, *J* = 15.3 Hz, 1H)	2.10 – 2.00 (m, 1H) 2.28 – 2.19 (m, 1H)	30.3	30.3
2	5.28 (br s, 1H)	5.27 (s, 1H)	119.7	119.7
3			132.7	132.7
4	1.62 (m, 1H) 1.76 (m, 1H)	1.68 – 1.58 (m, 1H) 1.78 – 1.73 (m, 1H)	27.5	27.5
5	1.58 (m, 1H) 1.88 (dm, *J* = 10.8 Hz, 1H)	1.68 – 1.58 (m, 1H) 1.90 – 1.85 (m, 1H)	25.6	25.6
6			47.0	47.0
7			145.6	145.6
8	2.14 (ddd, *J* = 13.8, 4.8, 2.2 Hz, 1H) 2.37 (ddd, *J* = 13.8, 13.8, 5.2 Hz, 1H)	2.14 (ddd, *J* = 13.7, 4.9, 2.3 Hz, 1H) 2.36 (tdt, *J* = 13.9, 4.9, 1.4 Hz, 1H)	33.9	33.0
9	2.06 (dddd, *J* = 13.8, 12.8, 12.7, 4.8 Hz, 1H) 2.23 (dddd, *J* = 12.8, 5.2, 4.4, 2.2 Hz, 1H)	2.10 – 2.00 (m, 1H) 2.28 – 2.19 (m, 1H)	35.7	35.7
10	4.65 (dd, *J* = 12.7, 4.4 Hz, 1H)	4.65 (dd, *J* = 12.9, 4.5 Hz, 1H)	66.1	66.1
11			42.7	42.7
12	0.94 (s, 3H)	0.94 (s, 3H)	17.5	17.5
13	1.10 (s, 3H)	1.10 (s, 3H)	23.9	23.8
14	4.61 (br s, 1H) 4.93 (t, *J* = 1.8 Hz, 1H)	4.61 (s, 1H) 4.93 (t, *J* = 1.7 Hz, 1H)	112.6	112.6
15	1.54 (br s, 3H)	1.57 (s, 3H)	23.1	23.1

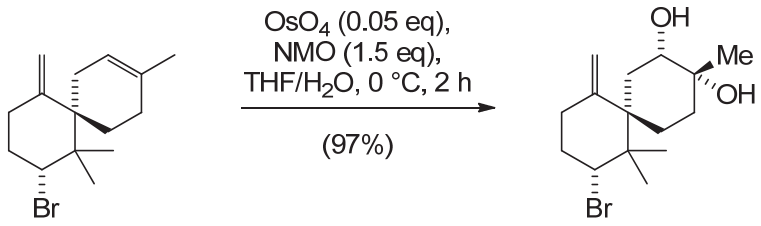

9 **25**

3,4-Dihydroxy-10-bromo-β-chamigrene (25) To a solution of spirocycle **9** (33.0 mg, 117 µmol, 1.0 eq) in THF/Water (5:1, 8.3 mL) was added NMO (20.0 mg, 176 µmol, 1.5 eq) and OsO_4 (2.5% in *t*BuOH, 58.0 µl, 5.85 µmol, 0.05 eq) at 0 °C. The reaction was allowed to stir for 2 h followed by dilution with H_2O/sat. aq. $Na_2S_2O_4$ (1:1). The layers were separated and the aqueous layer was extracted with EtOAc and the combined organic layers were washed with brine and dried over Na_2SO_4. After filtration and concentration *in vacuo*, the crude product was purified by flash column chromatography (pentane:EtOAc 7:3) on silica to afford **25** (36.0 mg, 113 µmol, 97%) as a white solid.

Data for 25: R_f: 0.19 (pentane:EtOAc 7:3); **^{1}H NMR (800 MHz, $CDCl_3$):** δ = 5.13 (s, 1H), 4.85 (s, 1H), 4.58 (dd, *J* = 12.9, 4.7 Hz, 1H), 3.74 (dd, *J* = 11.3, 5.1 Hz, 1H), 2.35 – 2.29 (m, 1H), 2.26 (dtd, *J* = 14.1, 5.0, 2.1 Hz, 1H), 2.10 (ddd, *J* = 13.3, 5.4, 1.9 Hz, 1H), 2.04 (qd, *J* = 12.9, 5.4 Hz, 1H), 1.95 – 1.88 (m, 2H), 1.76 – 1.70 (m, 1H), 1.70 – 1.65 (m, 1H), 1.57 (dt, *J* = 14.2, 3.4 Hz, 1H), 1.21 (s, 3H), 1.21 – 1.17 (m, 1H), 1.16 (s, 3H), 0.97 (s, 3H) ppm; **^{13}C NMR (200 MHz, $CDCl_3$):** δ = 147.0, 113.7, 71.8, 70.6, 65.0, 49.8, 43.8, 36.1, 33.8, 33.4, 33.3, 27.3, 23.7, 22.7, 17.5 ppm; **IR (ATR):** ν_{max} = 3380 (s), 2972 (s), 1638 (w), 1452 (m), 1393 (m), 1373 (m), 1264 (w), 1198 (w), 1139 (w), 1055 (s), 1031 (m), 967 (w), 902 (s), 872 (w), 778 (w), 737 (w), 670 (w) cm^{-1}; **melting point**: 145.6 – 149.5 °C; **HRMS (ESI):** calc. for $C_{17}H_{28}Br^{79}O_4$ [*M+AcO*]$^-$: 375.1171, found: 375.1179.

This diastereomer corresponds to a naturally occurring chamigrane[96c] initially reported by Stonik and coworkers but does not match the reported spectrum. This discrepancy was also noted by Snyder and coworkers in their recent report.[166]

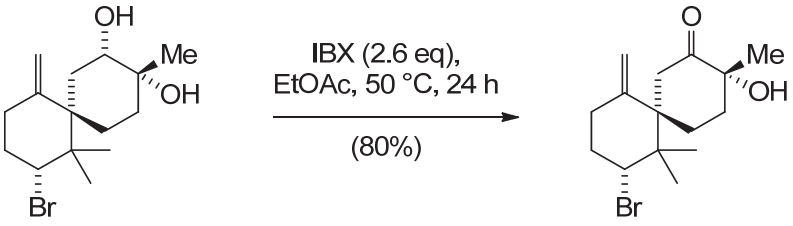

25 **S8**

3-Hydroxy-10-bromo-β-chamigren-4-one (S8) To a solution of diol **25** (24.0 mg, 75.6 µmol, 1.0 eq) in EtOAc (2.8 mL) was added IBX (55.0 mg, 196 µmol, 2.6 eq). The reaction was

vigorously stirred at 50 °C for 24 h. The reaction was filtered over a pad of celite (EtOAc). After concentration *in vacuo*, the crude product was purified by flash column chromatography (pentane/EtOAc 9:1) on silica to afford ketone **S8** (19.0 mg, 60.3 µmol, 80%) as a white solid.

Data for S8: R_f: 0.29 (pentane:EtOAc 9:1); **^{1}H NMR (800 MHz, $CDCl_3$):** δ = 5.00 (s, 1H), 4.71 (s, 1H), 4.61 (dd, *J* = 12.9, 4.4 Hz, 1H), 2.94 (d, *J* = 14.8 Hz, 1H), 2.56 (dd, *J* = 14.8, 3.2 Hz, 1H), 2.31 – 2.19 (m, 3H), 2.16 – 2.11 (m, 1H), 2.06 (qd, *J* = 12.6, 4.9 Hz, 1H), 1.87 (dq, *J* = 13.6, 3.4 Hz, 1H), 1.83 (dt, *J* = 14.4, 3.3 Hz, 1H), 1.64 (s, 1H), 1.48 (td, *J* = 14.1, 3.2 Hz, 1H), 1.25 (s, 3H), 1.22 (s, 3H), 0.96 (s, 3H) ppm; **^{13}C NMR (200 MHz, $CDCl_3$):** δ = 210.7, 147.4, 114.9, 73.4, 63.9, 52.3, 43.2, 42.8, 35.3, 34.4, 33.7, 24.1, 24.0, 22.9, 17.6 ppm; **IR (ATR):** ν_{max} = 3421 (b), 2975 (m), 2940 (s), 1712 (w), 1638 (m), 1452 (m), 1392 (m), 1374 (m),1295 (w), 1202 (w), 1153 (w), 1091 (m), 1038 (w), 933 (w), 966 (w), 908 (m), 871 (m), 780 (w) cm^{-1}; **melting point**: 139.5 °C; **HRMS (ESI)** calc. for $C_{17}H_{26}Br^{79}O_4$ $[M+AcO]^-$: 373.1020, found: 373.1022.

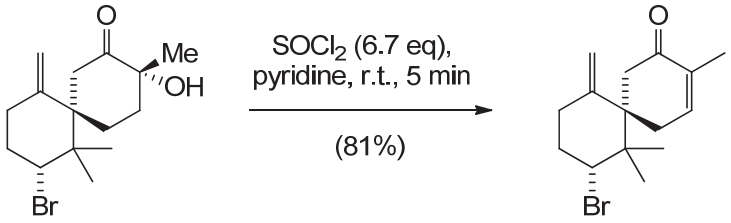

S8 dactylone (**2**)

Dactylone (2) To a solution of **S8** (15.0 mg, 47.6 µmol, 1.0 eq) in pyridine (750 µl) was added thionylchloride (23.2 µl, 319 µmol, 6.7 eq) dropwise at r.t. After 5 min, the reaction was quenched by addition of H_2O. The layers were separated and the aqueous layer was extracted with Et_2O and the combined organic layers were washed with aq. 10% HCl solution, sat. aq. $NaHCO_3$ solution and brine and was dried over Na_2SO_4. After filtration and concentration *in vacuo*, the crude product was purified by flash column chromatography (pentane:EtOAc 19:1) on silica to afford dactylone (**2**, 11.5 mg, 38.7 µmol, 81%) as a white solid. Isomerically pure dactylone (**2**) could be obtained by further purification by reverse-phase semipreparative HPLC (30% MeCN + 0.1% formic acid/70% H_2O + 0.1% formic acid) on a Microsorb 60 C18 column.

Data for dactylone (2): R_f: 0.65 (pentane:Et_2O 9:1); **IR (ATR):** ν_{max} = 2975 (m), 2947 (m), 2922 (m), 2359 (w), 2332 (w), 1670 (s), 1450 (m), 1431 (m), 1390 (m), 1371 (m), 1297 (w), 1260 (w), 1196 (m), 1159 (w), 1113 (m), 904 (m), 872 (m), 782 (m), 716 (w) cm^{-1}; **HRMS (EI)** calc. for $C_{15}H_{21}Br^{79}O$ $[M]^+$: 296.0776 , found: 296.0781.

UV-Vis Spectrum (c = 0.05 mM in CH_2Cl_2)

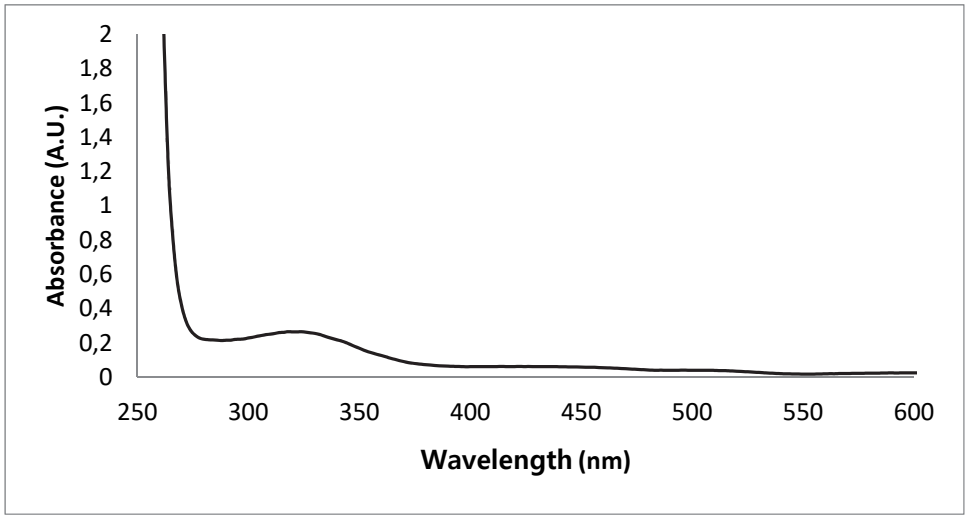

NMR-data:[167]

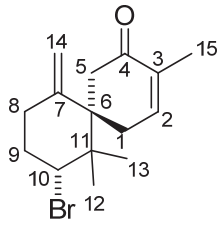

dactylone (**2**)

No.	^{1}H NMR Isolation 300 MHz, $CDCl_3$ [ppm]	^{1}H NMR Synthetic 400 MHz, $CDCl_3$ [ppm]	^{13}C NMR Isolation 75 MHz, $CDCl_3$ [ppm]	^{13}C NMR Synthetic 100 MHz, $CDCl_3$ [ppm]
1	2.65 (m, 2H)	2.68 – 2.61 (m, 2H)	33.7	33.6
2	6.50 (m, 1H)	6.50 (td, *J* = 4.5, 1.4 Hz, 1H)	140.7	141.3
3			135.5	135.4
4			198.8	199.5
5	2.74 (br d, *J* = 16.5 Hz, 1H) 2.57 (d, *J* = 16.5 Hz, 1H)	2.75 (d, *J* = 16.4 Hz, 1H) 2.56 (d, *J* = 16.4 Hz, 1H)	44.2	44.1
6			51.4	51.2
7			146.1	146.0
8	2.37 (m, 1H) 2.17 (m, 1H)	2.41 – 2.31 (m, 1H) 2.20 – 2.11 (m, 1H)	30.0	29.7
9	2.26 (m, 1H) 2.11 (m, 1H)	2.29 – 2.21 (m, 1H) 2.11 – 2.02 (m 1H)	35.5	35.3
10	4.52 (dd, *J* = 12.5, 4.5 Hz, 1H)	4.53 (dd, *J* = 12.5, 4.5 Hz, 1H)	63.0	63.1
11			43.2	43.1
12	1.73 (d, *J* = 1.8 Hz, 3H)	1.73 (s, 3H)	15.3	15.3
13	0.99 (s, 3H)	0.99 (s, 3H)	25.1	25.0
14	4.98 (br d, *J* = 1.5 Hz, 1H) 4.61 (s, 1H)	4.97 (s, 1H) 4.60 (s, 1H)	114.0	114.2
15	1.19 (s, 3H)	1.19 (s, 3H)	17.7	17.5

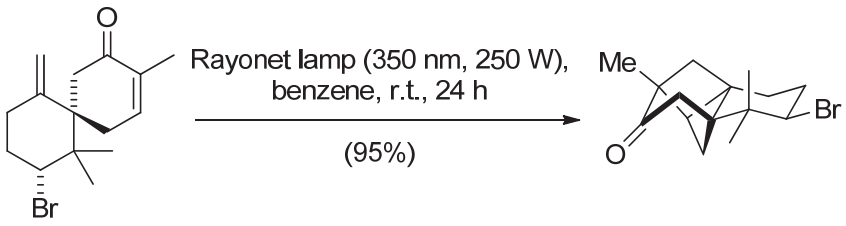

dactylone (**2**) aplydactone (**1**)

Aplydactone (1) A solution of **2** (11.0 mg, 37.0 µmol, 1.0 eq) in benzene (11 mL) was degassed (N_2 sparging, 15 min) and sealed in a screw capped tube. This was irradiated using a Rayonet lamp (350 nm, 250 W) for 24 h. After concentration *in vacuo*, the crude product was purified by flash column chromatography (pentane:CH_2Cl_2 1:1) on silica to afford aplydactone (**1**, 10.5 mg, 35.3 µmol, 95% yield) as a white solid.

Solar irradiation of dactylone (2): Dactylone (**2**) (1.0 mg, 3.36 µmol, 1.0 eq) was dissolved in $CDCl_3$ (0.5 mL) in a NMR tube. This was irradiated in an Erlenmeyer flask filled with water under Munich sunlight for 6 days on top of the LMU Chemistry Building (Munich summer time). The NMR spectrum reveals complete consumption of the starting material during this time period.

Data for aplydactone (1): R_f: 0.64 (pentane:CH_2Cl_2 1:1); **IR (ATR):** ν_{max} = 3423 (w), 2925 (s), 2888 (m), 1733 (m), 1717 (s), 1683 (m), 1669 (m), 1653 (m), 1457 (m), 1446 (m), 1260 (w), 1093 (w), 1025 (w), 803 (w); **HRMS (EI)** calc. for $C_{15}H_{21}Br^{79}O$ $[M]^+$: 296.0770 , found: 296.0787.

Solar Irradiation of dactylone (2)

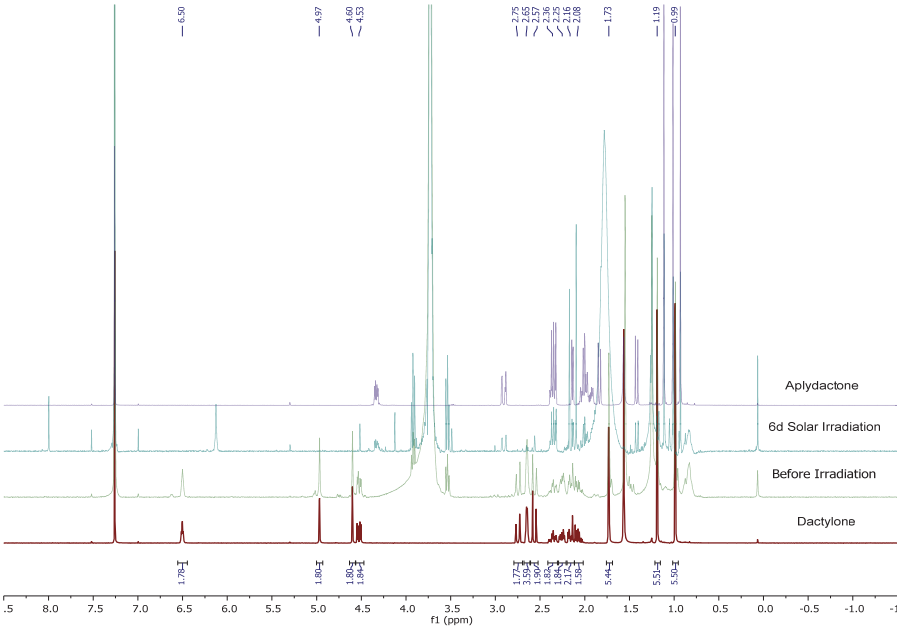

NMR-data:[95]

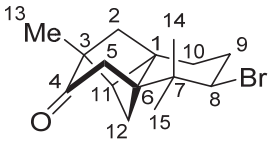

aplydactone (**1**)

No.	^{1}H NMR Isolation 300 MHz, C_6D_6 [ppm]	^{1}H NMR Synthetic 800 MHz, C_6D_6 [ppm]	^{13}C NMR Isolation 75 MHz, C_6D_6 [ppm]	^{13}C NMR Synthetic 200 MHz, C_6D_6 [ppm]
1			40.2	40.2
2	1.29 (d, *J* = 11.0 Hz, 1H) 1.81 (d, *J* = 11.0 Hz, 1H)	1.29 (d, *J* = 10.6 Hz, 1H) 1.80 (d, *J* = 10.9 Hz, 1H)	40.6	40.6
3			48.9	48.9
4			210.4	210.5
5	2.12 (d, *J* = 16.5 Hz, 1H) 2.51 (dd, *J* = 16.5, 2.7 Hz, 1H)	2.13 (d, *J* = 16.4 Hz, 1H) 2.51 (dd, *J* = 16.4, 2.8 Hz, 1H)	42.9	42.9
6			47.1	47.1
7			38.2	38.3
8	3.90 (m, 1H)	3.89 (dd, *J* = 11.9, 3.9 Hz, 1H)	65.7	65.8
9	1.69 (m, 2H)	1.74 – 1.63 (m, 2H)	31.0	31.0
10	1.30 (m, 2H)	1.35 – 1.26 (m, 2H)	33.8	33.9
11	1.58 (d, *J* = 5.6 Hz, 1H)	1.58 (d, *J* = 5.6 Hz, 1H)	45.5	45.5
12	1.05 (d, *J* = 11.3 Hz, 1H) 1.72 (ddd, *J* = 11.3, 5.6, 2.7 Hz, 1H)	1.04 (d, *J* = 11.3 Hz, 1H) 1.74 – 1.63 (m, 1H)	31.7	31.7
13	1.09 (s, 3H)	1.10 (s, 3H)	18.6	18.7
14	0.75 (s, 3H)	0.75 (s, 3H)	18.3	18.3
15	0.70 (s, 3H)	0.70 (s, 3H)	22.9	22.9

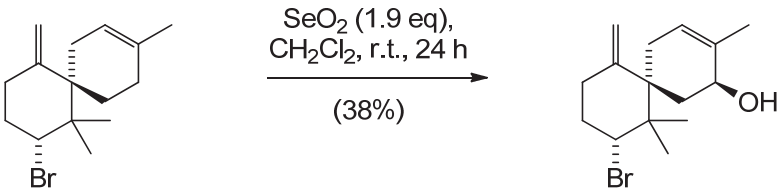

9 **26**

2-Hydroxy-10-bromo-β-chamigrene (26) To a stirred solution of **9** (15.0 mg, 53.0 µmol, 1.0 eq) in CH_2Cl_2 (1 mL) was added SeO_2 (11.0 mg, 99.1 µmol, 1.9 eq) at r.t. The reaction was allowed to stir for 25 h. The reaction was filtered over a pad of celite (EtOAc). After concentration *in vacuo*, the crude product was purified by flash column chromatography (pentane:CH_2Cl_2:EtOAc 9:0.5:0.5) on silica to afford alcohol **26** (6.0 mg, 20.1 µmol, 38%) as a colorless oil. This compound was found to be volatile over prolonged periods under high vacuum.

Data for 26: R_f: 0.19 (pentane:CH_2Cl_2:EtOAc 9:0.5:0.5); **^{1}H NMR (800 MHz, $CDCl_3$):** δ = 5.43 (s, 1H), 4.93 (s, 1H), 4.64 (dd, *J* = 13.0, 4.5 Hz, 1H), 4.59 (s, 1H), 3.74 (s, 1H), 2.46 (td, *J* = 13.9, 5.0 Hz, 1H), 2.33 – 2.24 (m, 3H), 2.22 – 2.17 (m, 1H), 2.11 – 2.03 (m, 2H), 1.71 (s, 3H), 1.58 (m, 1H, overlap), 1.15 (s, 3H), 0.93 (s, 3H) ppm; **^{13}C NMR (200 MHz, $CDCl_3$): δ =** 145.3, 134.8, 122.7, 112.6, 69.1, 65.1, 48.8, 42.8, 35.9, 35.6, 33.1, 30.5, 23.9, 18.4, 16.9 ppm; **IR (ATR):** ν_{max} = 3352 (s), 2973 (s), 2851 (m), 2361 (w), 2340 (w), 1708 (w), 1679 (w), 1639 (w), 1453 (m), 1390 (m), 1369 (m), 1254 (w), 1181 (w), 1159 (w), 1042 (m), 1023 (m), 997 (m), 896 (m), 872 (m) 779 (w); **HRMS (EI)** calc. for $C_{15}H_{21}Br^{79}O$ $[M]^+$: 298.0932, found: 298.0914.

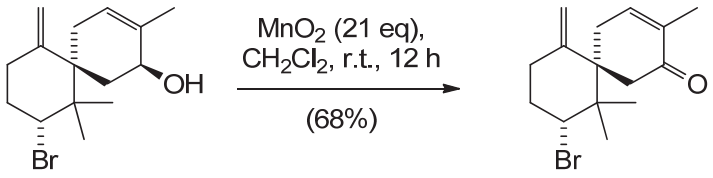

26 10-*epi*-dactylone (**3**)

10-*Epi*-dactylone (3) To a solution of **22** (7.5 mg, 25.1 µmol, 1.0 eq) in CH_2Cl_2 (1.0 mL) was added MnO_2 (45.0 mg, 518 µmol, 21 eq) and the resulting reaction mixture was stirred at r.t. overnight. The reaction was filtered over a pad of celite (EtOAc). After concentration *in vacuo*, the crude product was purified by flash column chromatography (hexanes: CH_2Cl_2 2:3) on silica to afford 10-*epi*-dactylone (**3**, 5.0 mg, 16.7 mmol, 68%) as a colorless oil.

Data for 10-*epi*-dactylone (3): R_f: 0.70 (pentanes:EtOAc 9:1); **IR (ATR):** ν_{max} = 2925 (m), 2872 (m), 1718 (s), 1683 (m), 1675 (w), 1456 (w), 1376 (w), 1367 (w), 1299 (w), 1279 (w),

1237 (w), 1188 (w), 1131 (w), 1112 (w), 984 (w), 847 (w), 779 (w) cm^{-1}; **HRMS (EI)** calc. for $C_{15}H_{21}Br^{79}O$ $[M]^+$: 296.0770 , found: 296.0787.

NMR-data:[96c]

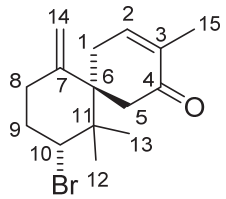

10-*epi*-dactylone (3)

No.	^{1}H NMR Isolation 300 MHz, $CDCl_3$ [ppm]	^{1}H NMR Synthetic 400 MHz, $CDCl_3$ [ppm]	^{13}C NMR Isolation 75 MHz, $CDCl_3$ [ppm]	^{13}C NMR Synthetic 100 MHz, $CDCl_3$ [ppm]
1	2.53 (dm, *J* = 18.9 Hz, 1H) 2.67 (dm, *J* = 18.9 Hz, 1H)	2.52 (dd, *J* = 18.4, 5.5 Hz, 1H) 2.71 – 2.59 (m, 1H)	32.6	32.5
2	6.63 (m, 1H)	6.62 (ddd, *J* = 5.9, 2.5, 1.4 Hz, 1H)	142.9	143.1
3			134.6	134.5
4			198.2	198.4
5	2.81 (dd, *J* = 14.9, 2.3 Hz, 1H) 2.65 (d, *J* = 14.9 Hz, 1H)	2.80 (dd, *J* = 14.8, 2.4 Hz, 1H) 2.71 – 2.59 (m, 1H)	43.2	43.0
6			51.8	51.7
7			144.3	144.1
8	2.42 (m, 1H) 2.15 (m, 1H)	2.47 – 2.37 (m, 1H) 2.18 – 2.10 (m, 1H)	31.7	31.6
9	2.03 (m, 1H) 2.25 (m, 1H)	2.09 – 1.97 (m, 1H) 2.29 – 2.20 (m, 1H)	35.4	35.3
10	4.48 (dd, *J* = 12.4, 4.5 Hz, 1H)	4.48 (dd, *J* = 12.5, 4.5 Hz, 1H)	63.6	63.7
11			43.1	43.0
12	1.00 (s, 3H)	0.99 (s, 3H)	17.3	17.2
13	1.20 (s, 3H)	1.19 (s, 3H)	24.8	24.8
14	5.00 (br s, 1H) 4.54 (s, 1H)	4.98 (s, 1H) 4.54 (s, 1H)	114.6	114.7
15	1.71 (dt, *J* = 2.6, 1.4 Hz, 3H)	1.70 (dt, *J* = 2.6, 1.3 Hz, 3H)	15.2	15.3

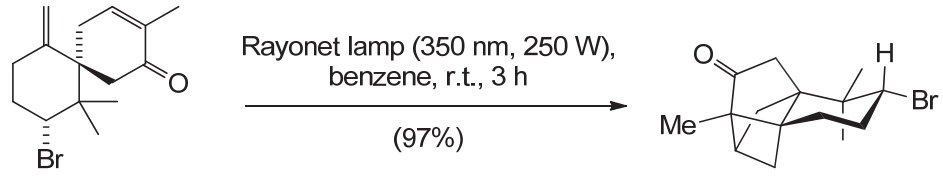

10-*epi*-dactylone (**3**) 8-*epi*-isoaplydactone (**8**)

8-*epi*-isoaplydactone (8) A solution of **3** (3.5 mg, 11.8 µmol, 1.0 eq) in benzene (4.5 mL) was degassed (N_2 sparging, 15 min) and sealed in a screw capped tube. This was irradiated using a Rayonet lamp (350 nm, 250 W) for 3 h. After concentration *in vacuo*, the crude product was purified by flash column chromatography (hexanes: CH_2Cl_2 2:3) to afford 8-*epi*-isoaplydactone (**8**, 3.4 mg, 11,4 µmol, 97%) as a white solid.

Data for 8-*epi*-isoaplydactone (8): R_f: 0.65 (pentanes:Et_2O 9:1); **IR (ATR):** ν_{max} = 2960 (s), 2923 (s), 2850 (m), 1688 (w), 1468 (m), 1447 (m), 1411 (w), 1388 (w), 1367 (w), 1295 (w), 1281 (w), 1259 (w), 1192 (w), 1092 (w), 1052 (w), 970 (w), 861 (w), 780 (w), 711 cm^{-1}; **HRMS (EI)** calc. for $C_{15}H_{21}BrO$ $[M]^+$: 296.0770 , found: 296.0778.

NMR-data:

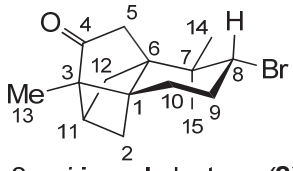

8-*epi*-isoaplydactone (**8**)

^{1}H NMR (400 MHz, $CDCl_3$): δ = 4.33 (dd, *J* = 11.5, 4.9 Hz, 1H, H-8), 2.41 – 2.31 (m, 2H, H-5, H-11), 2.26 – 2.06 (m, 5H, H'-2, H'-5, H-9, H-12), 1.88 (d, *J* = 7.8 Hz, 1H, H-2), 1.66 (dt, *J* = 14.4, 3.4 Hz, 1H, H-10), 1.42 – 1.34 (m, 2H, H'-10, H'-12), 1.27 (s, 3H, H-15), 1.11 (s, 3H, H-13), 1.06 (s, 3H, H-14) ppm; **^{13}C NMR (200 MHz, $CDCl_3$):** δ = 216.5 (C-4), 65.2 (C-3), 63.9 (C-8), 56.1 (C-1), 51.1 (C-6), 48.1 (C-5), 42.3 (C-11), 40.2 (C-2), 39.5 (C-7), 37.7 (C-12), 30.9 (C-9), 27.5 (C-14), 25.8 (C-10), 20.3 (C-15), 7.5 (C-13);

6.3.2 ^{1}H and ^{13}C NMR spectra

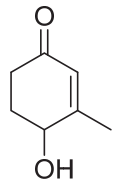

S4

400 MHz, $CDCl_3$

100 MHz, $CDCl_3$

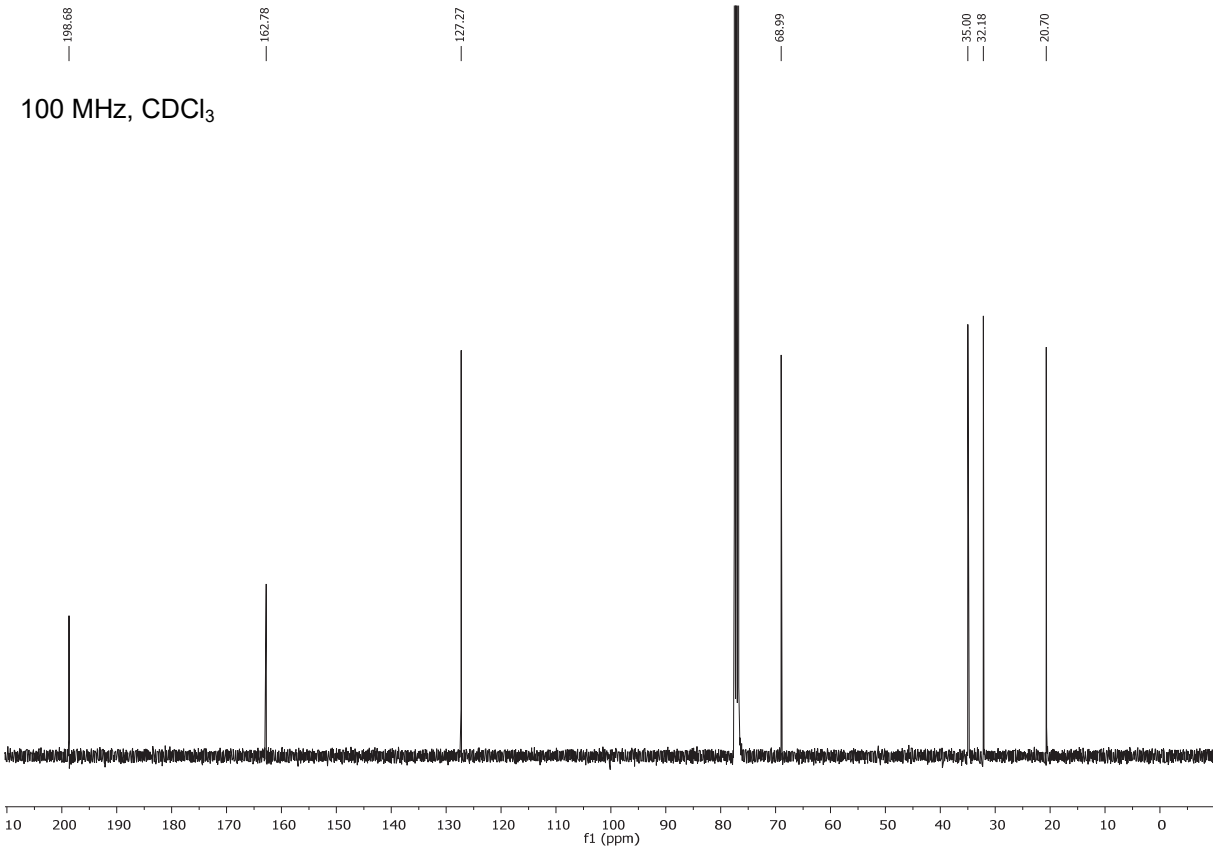

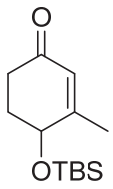

12

400 MHz, $CDCl_3$

100 MHz, $CDCl_3$

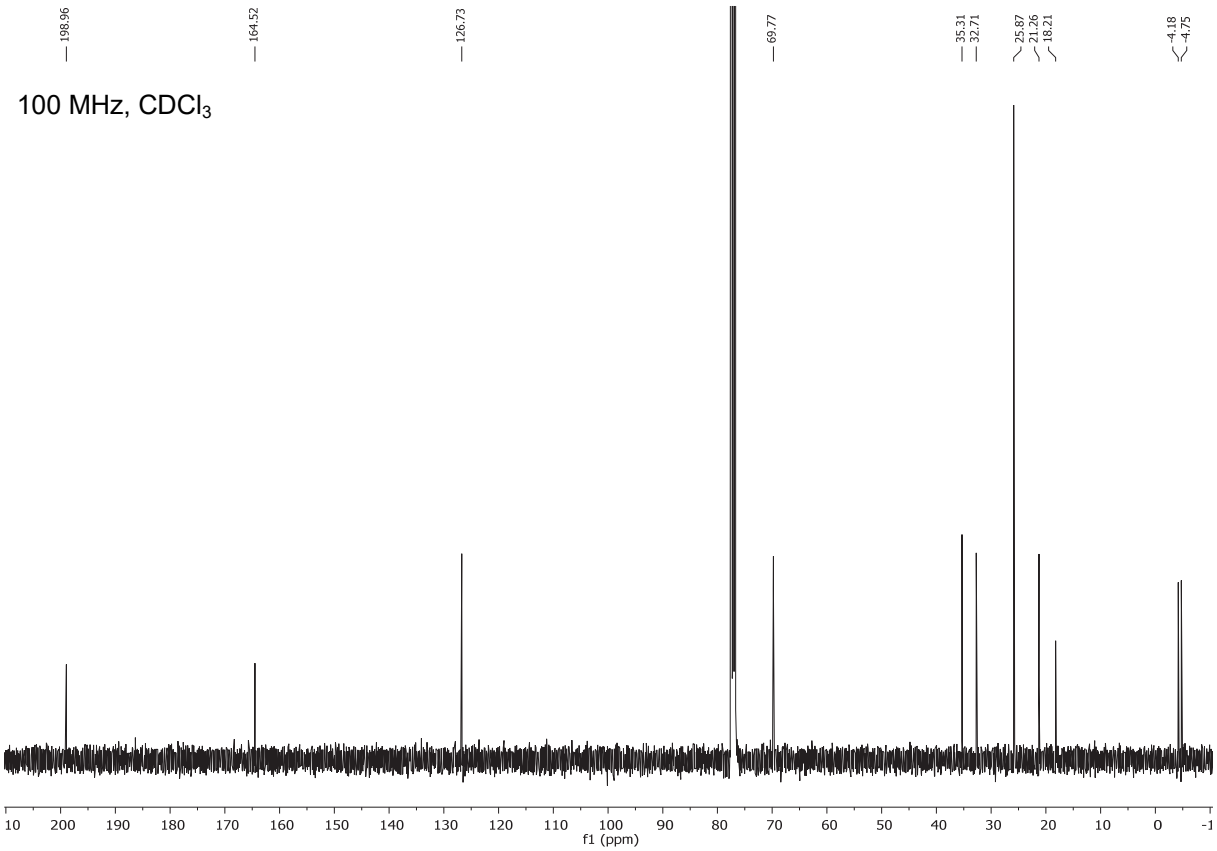

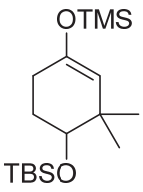

S5

400 MHz, C_6D_6

100 MHz, C_6D_6

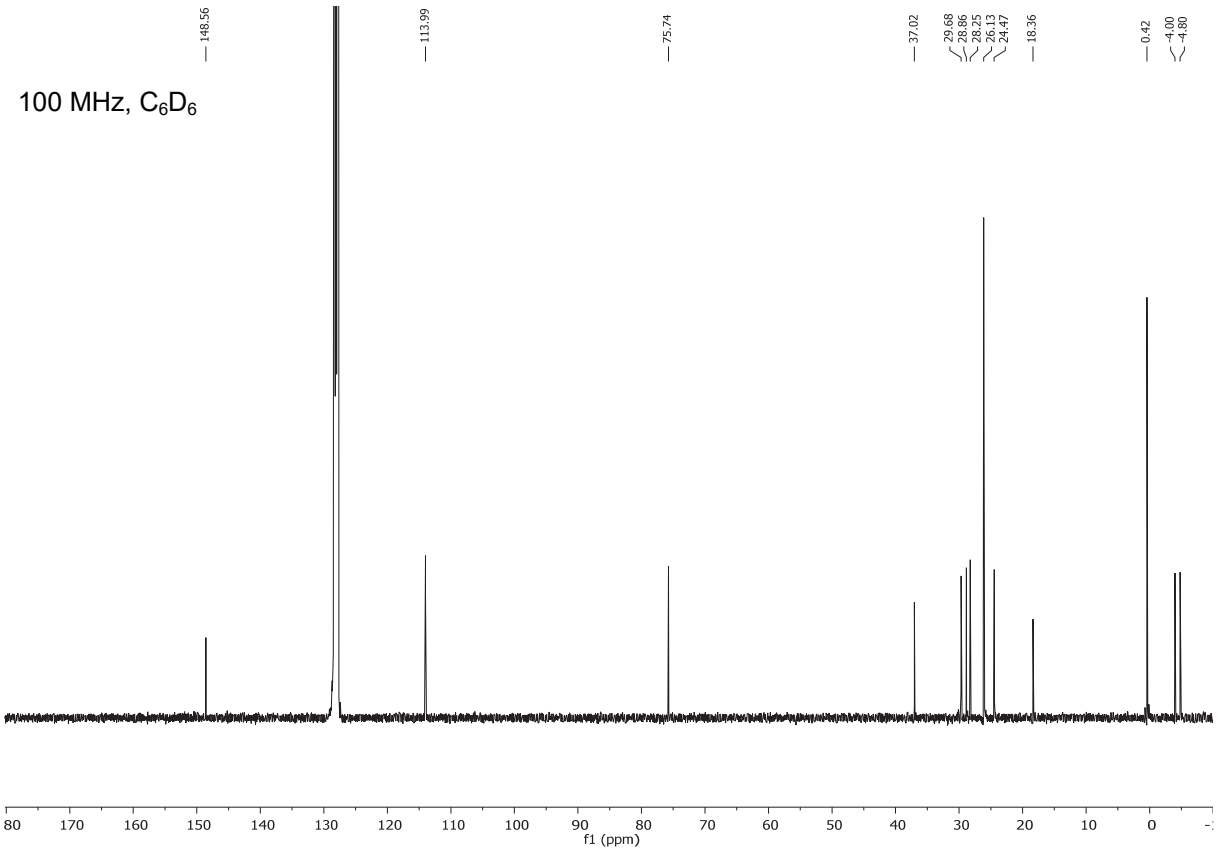

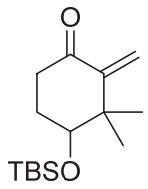

S6

400 MHz, C_6D_6

100 MHz, C_6D_6

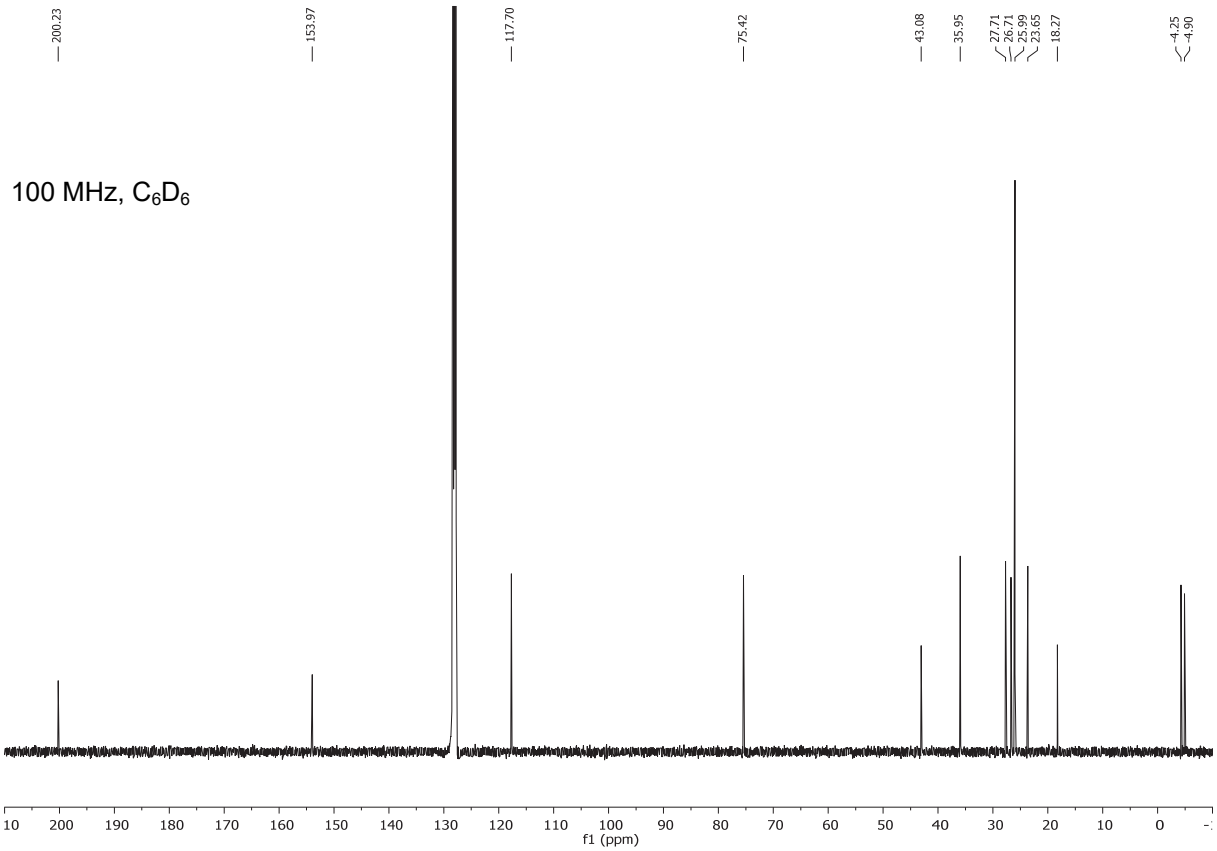

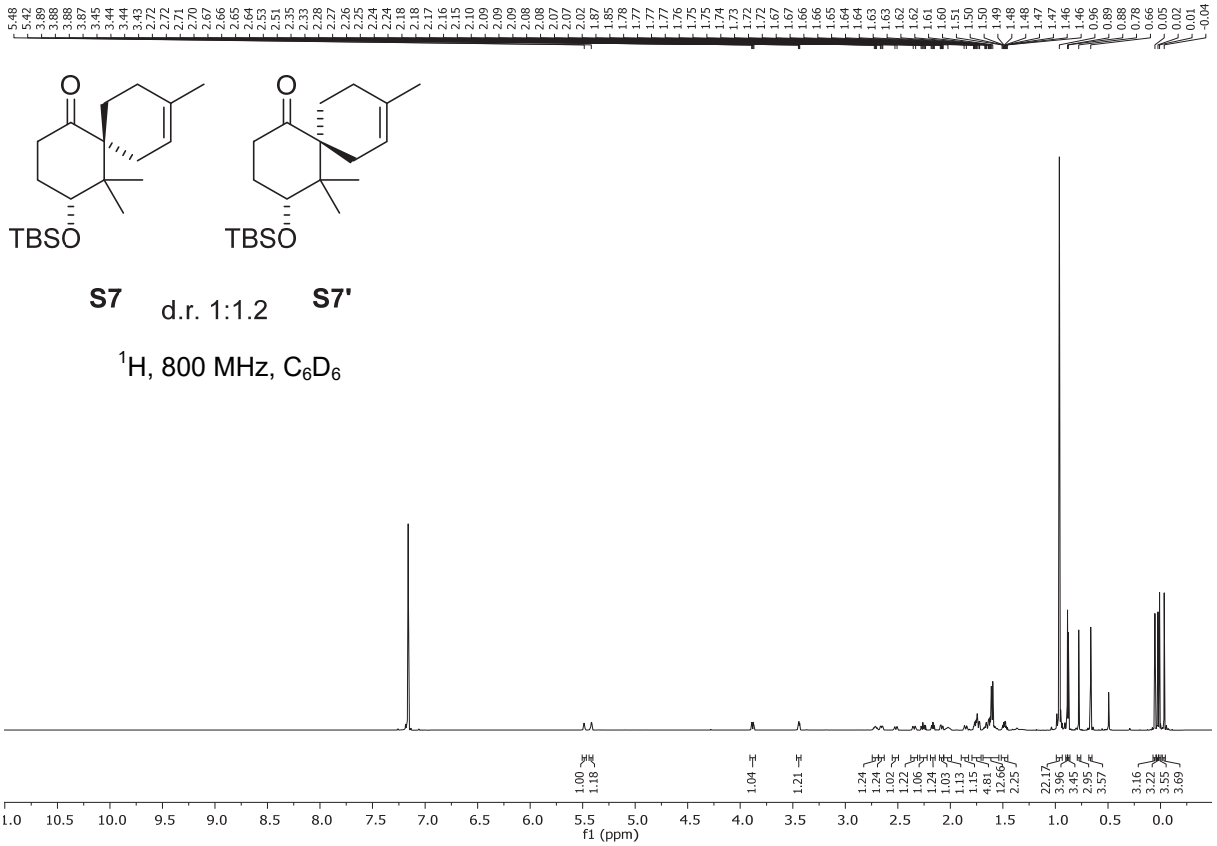

S7 d.r. 1:1.2 **S7'**

^{1}H, 800 MHz, C_6D_6

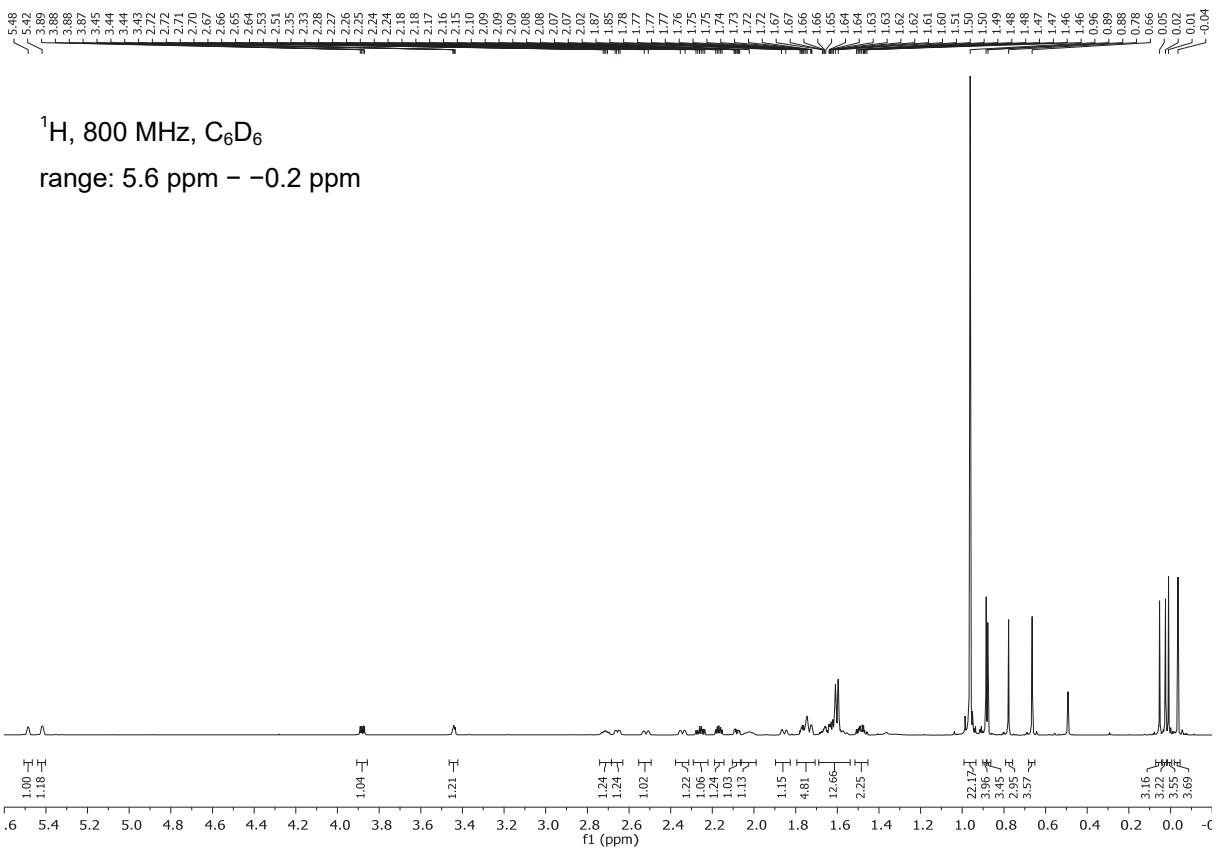

^{1}H, 800 MHz, C_6D_6

range: 5.6 ppm − −0.2 ppm

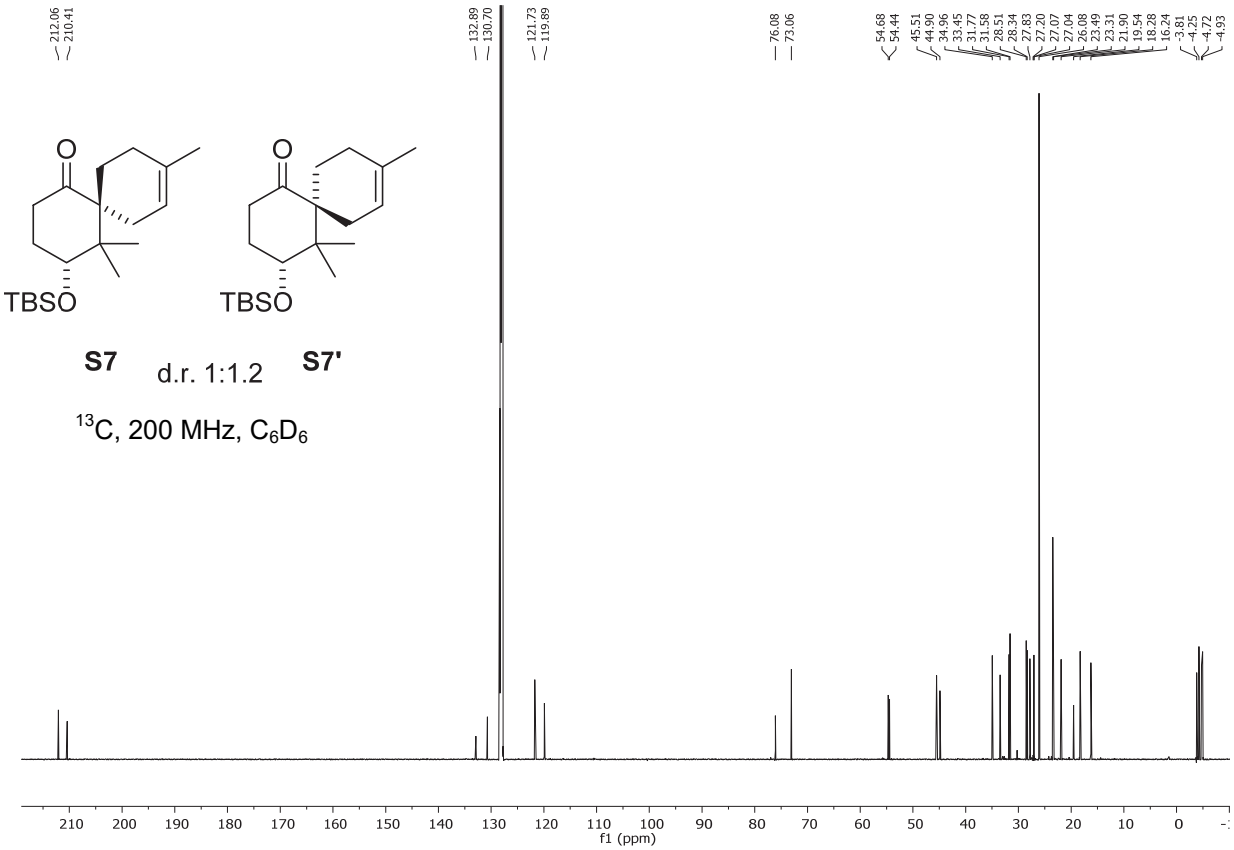

S7 d.r. 1:1.2 **S7'**

^{13}C, 200 MHz, C_6D_6

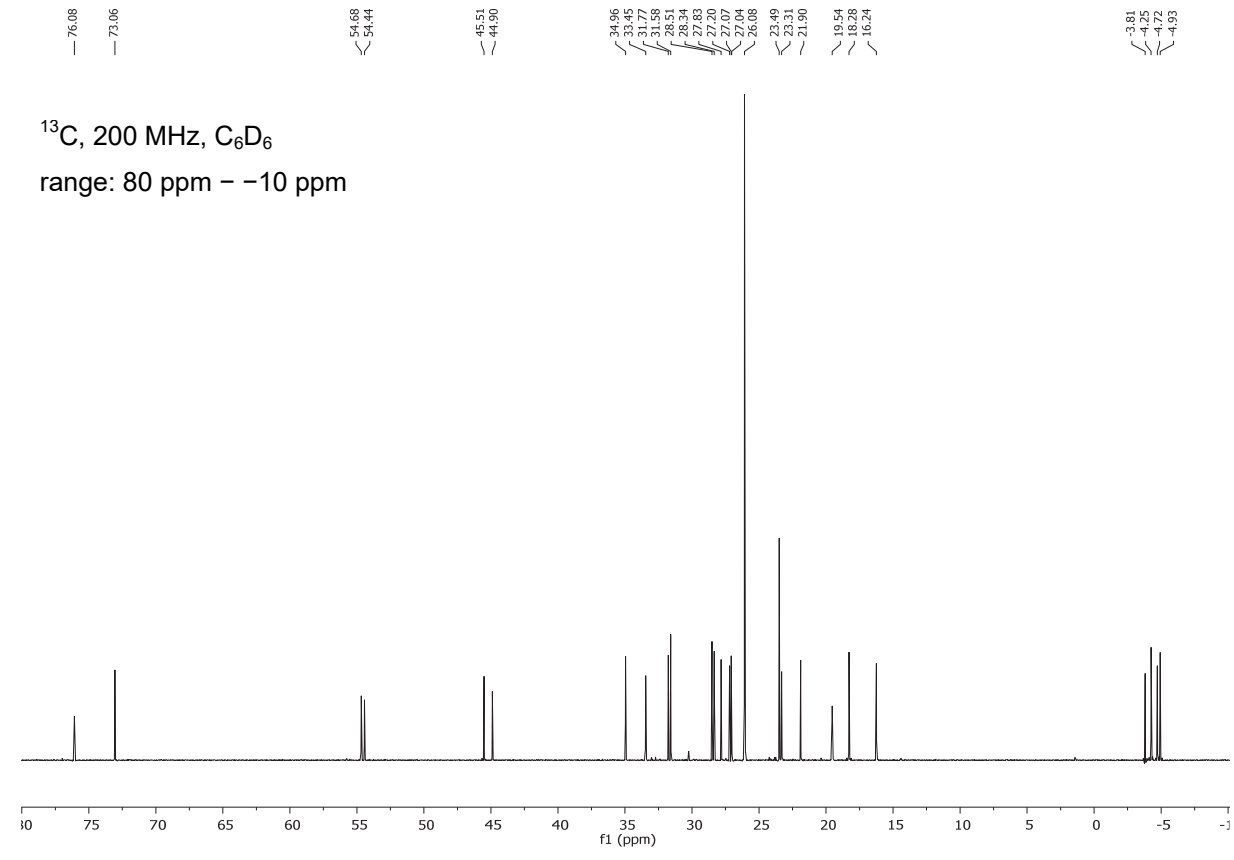

^{13}C, 200 MHz, C_6D_6

range: 80 ppm − −10 ppm

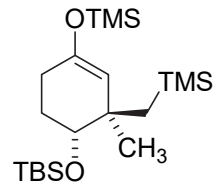

13

400 MHz, C_6D_6

100 MHz, C_6D_6

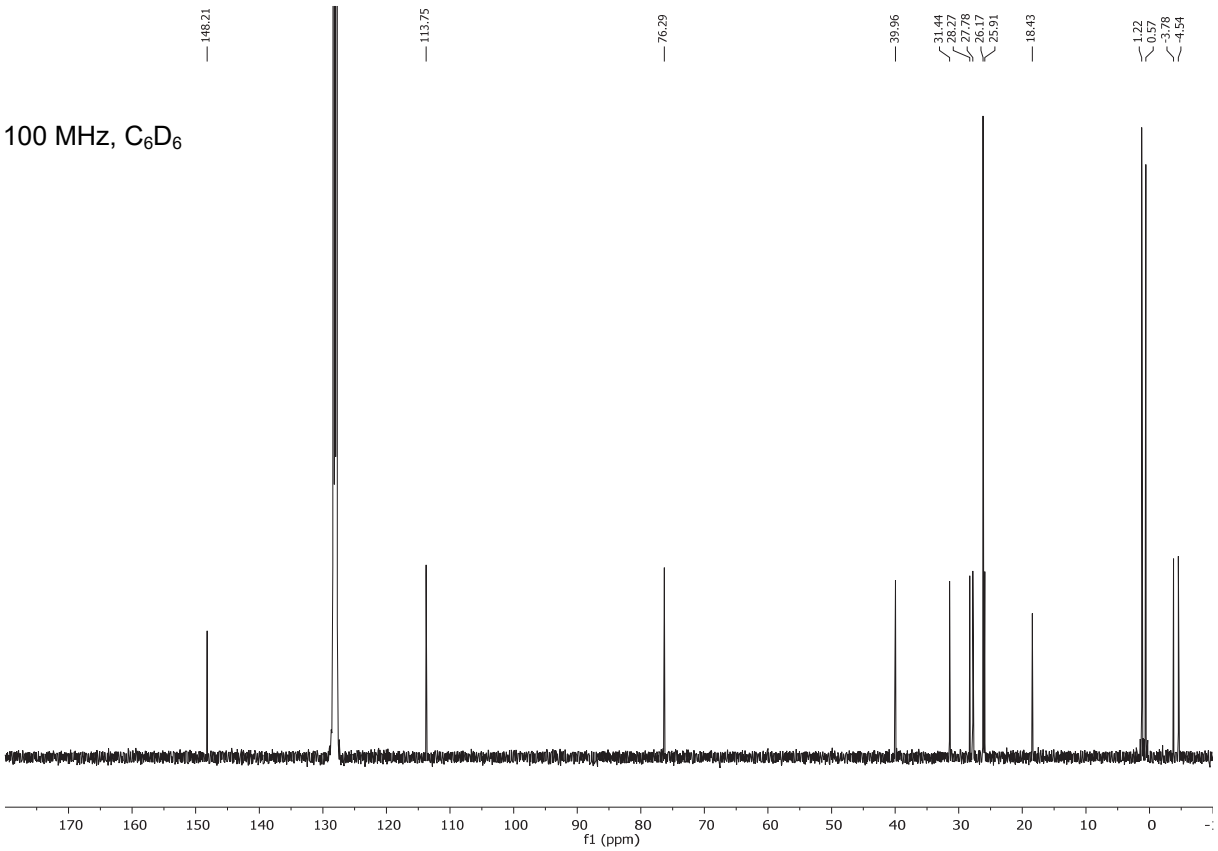

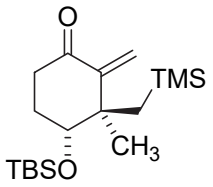

14

400 MHz, C_6D_6

100 MHz, C_6D_6

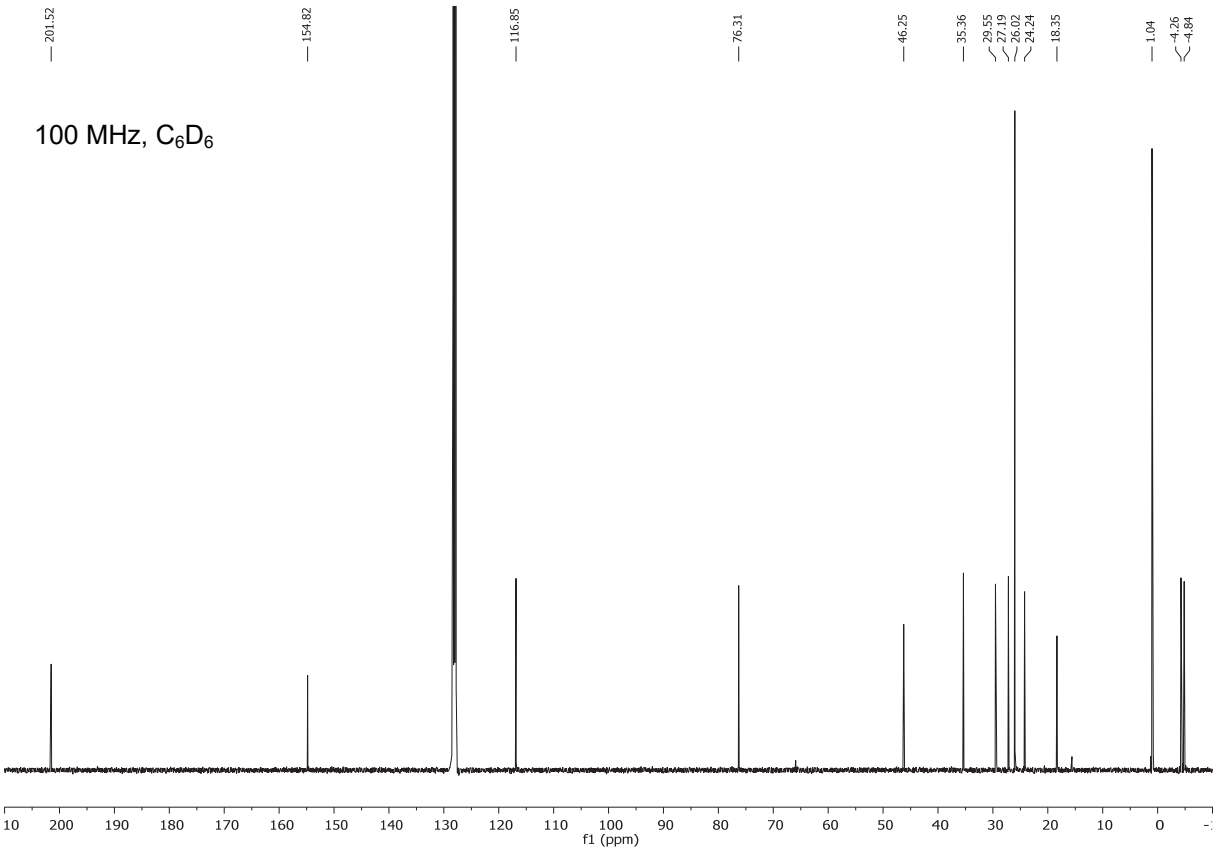

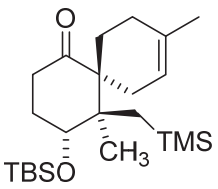

15

^{1}H, 400 MHz, C_6D_6

^{1}H, 400 MHz, C_6D_6

range: 5.5 ppm − −0.1 ppm

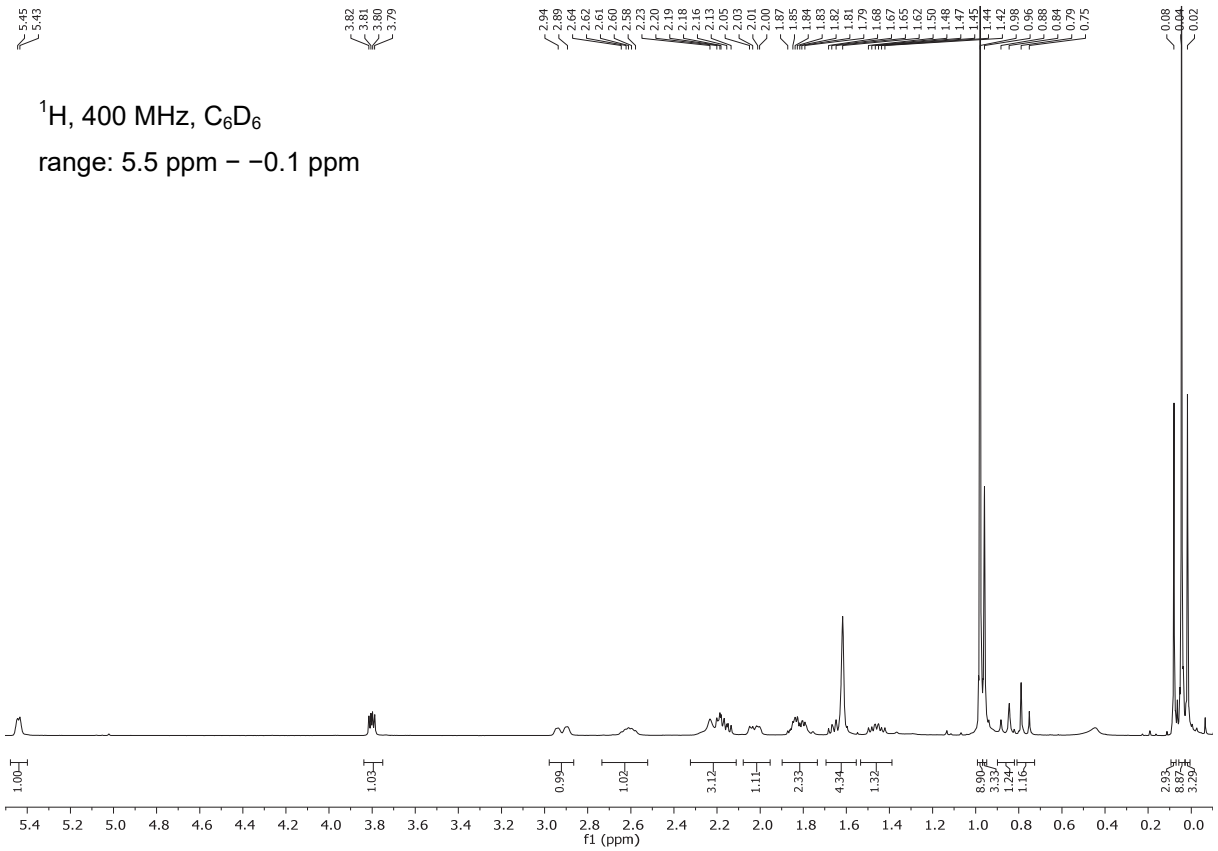

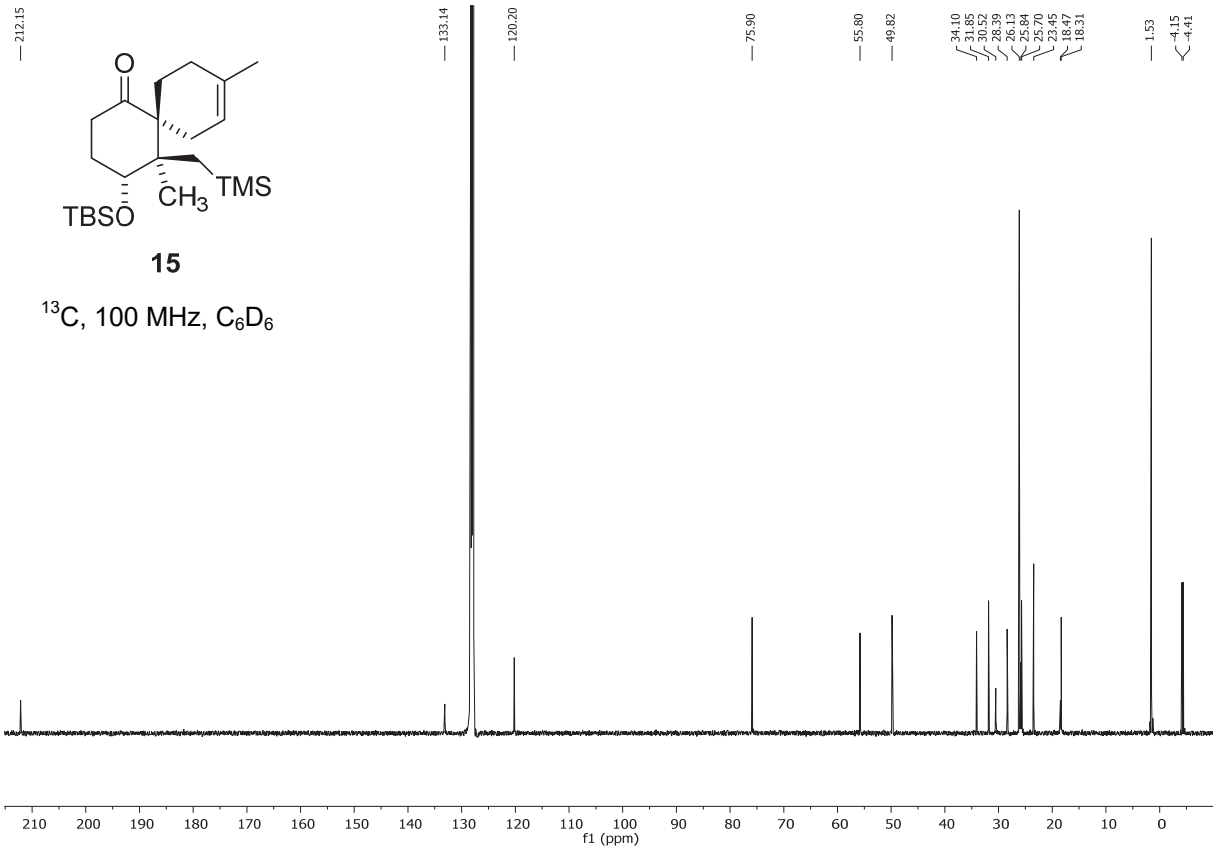

15

^{13}C, 100 MHz, C_6D_6

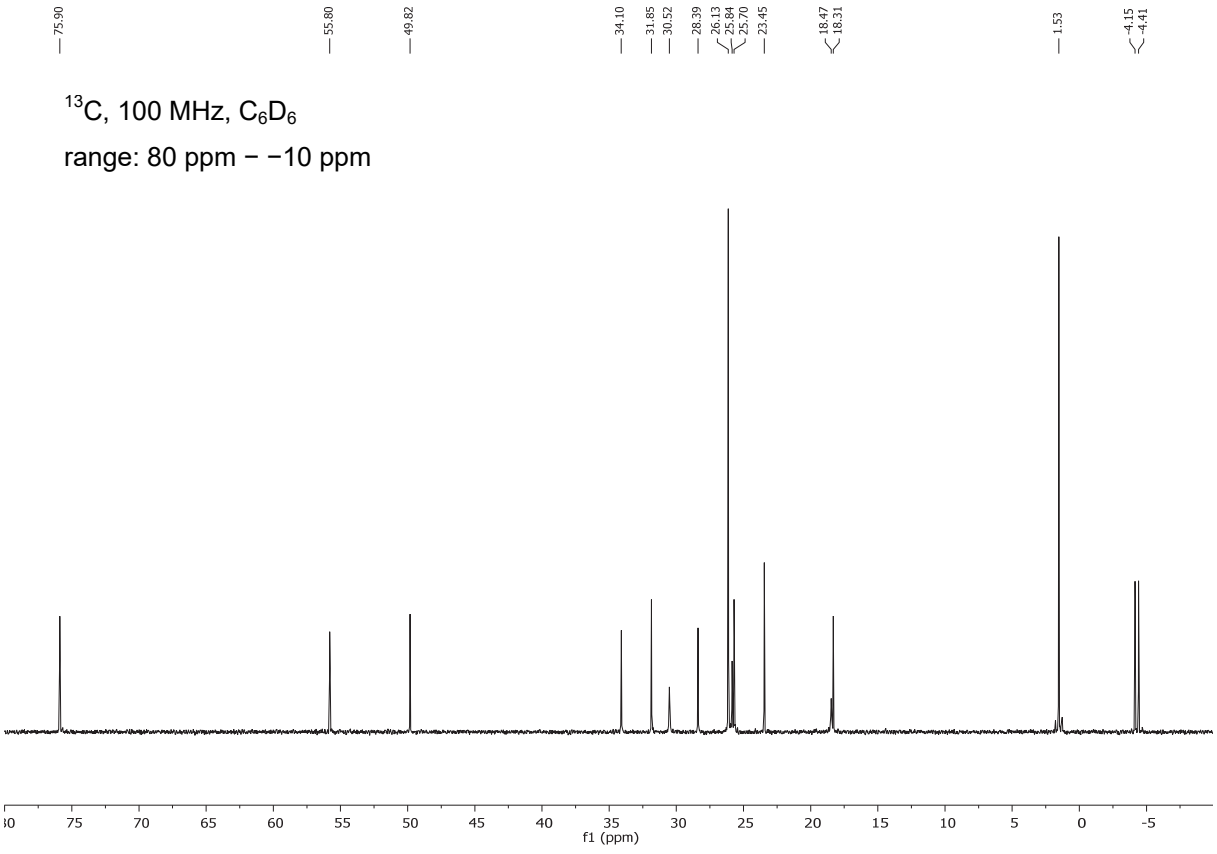

^{13}C, 100 MHz, C_6D_6

range: 80 ppm − −10 ppm

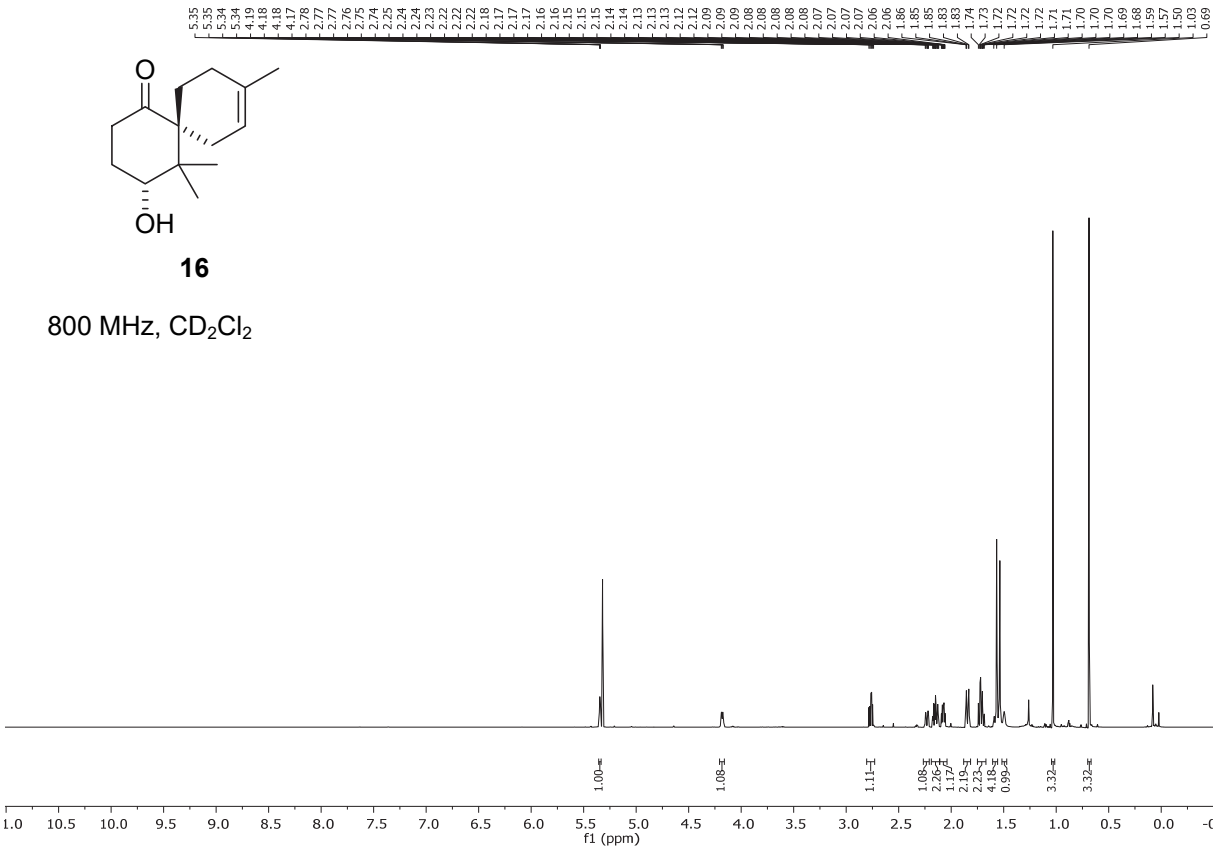

16

800 MHz, CD_2Cl_2

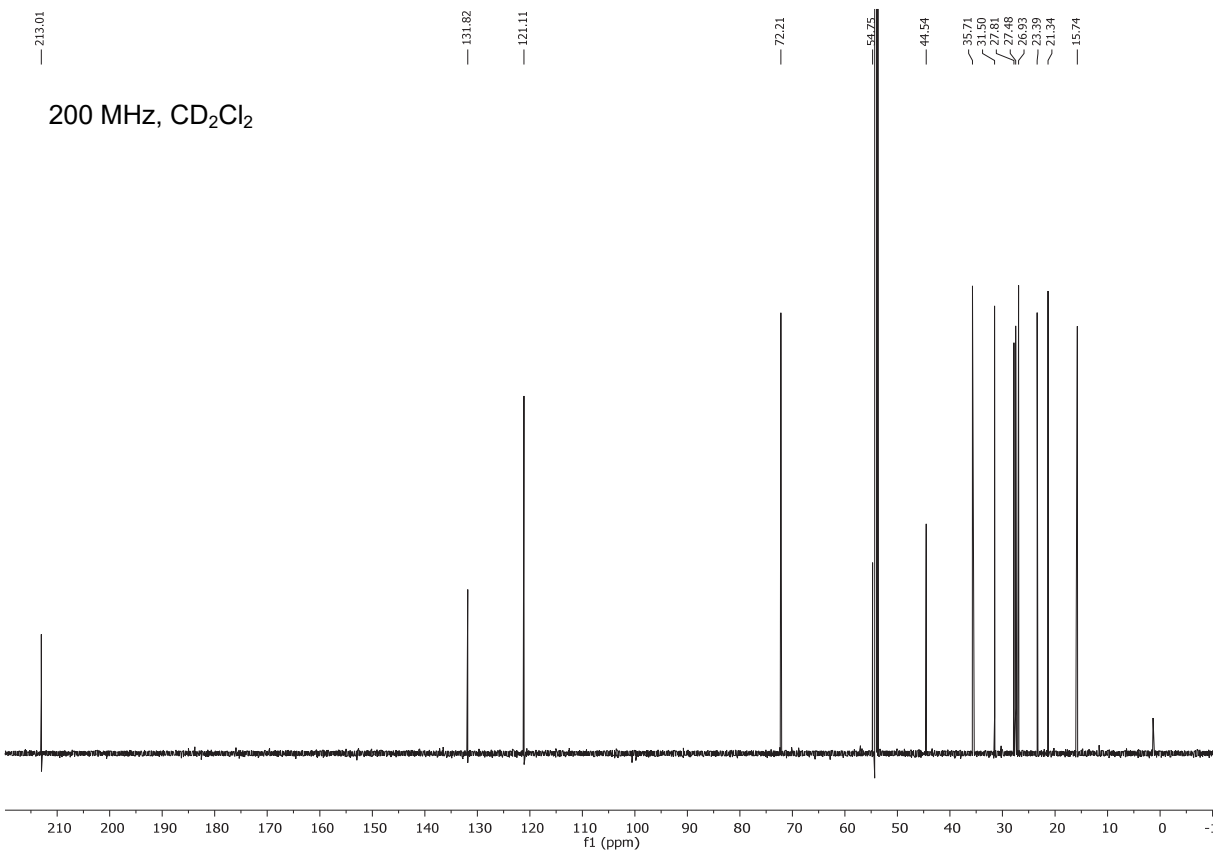

200 MHz, CD_2Cl_2

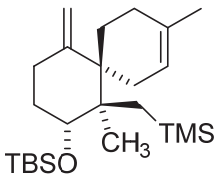

17

400 MHz, C_6D_6

100 MHz, C_6D_6

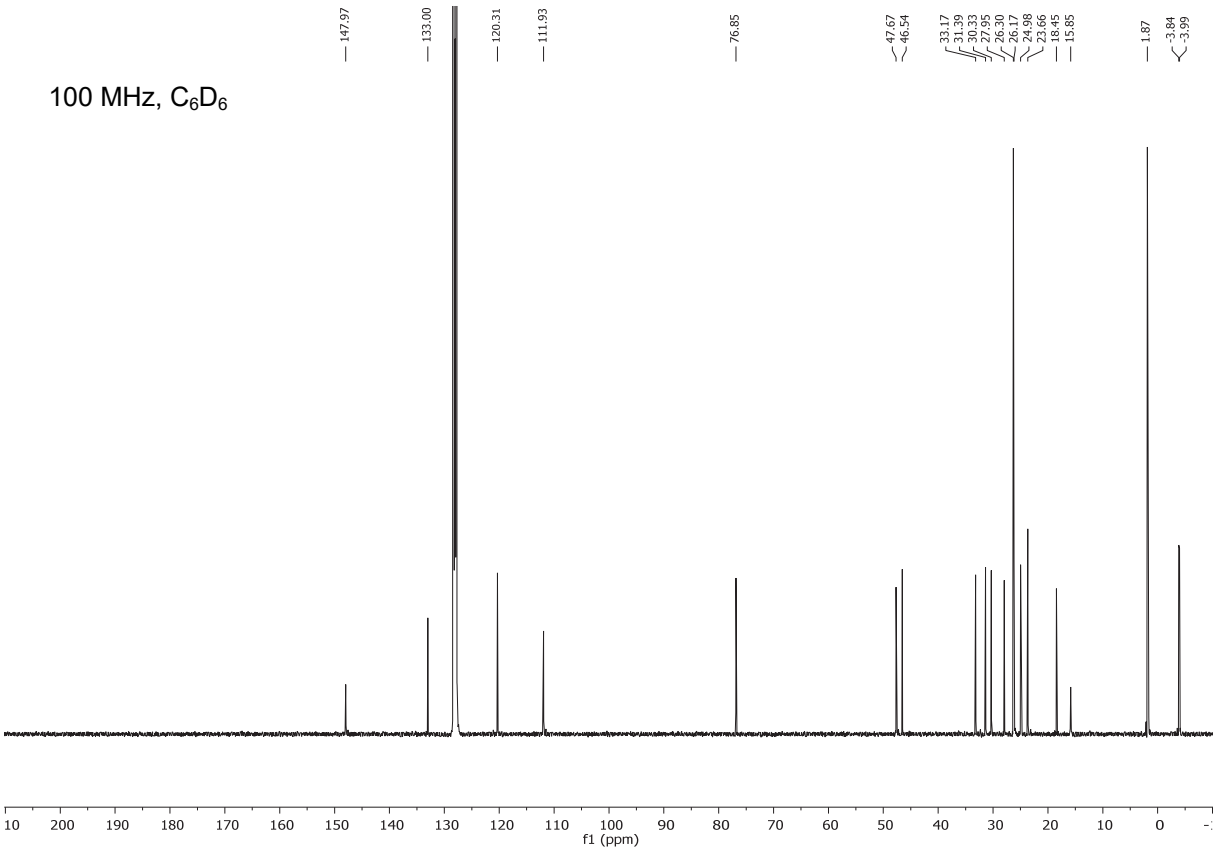

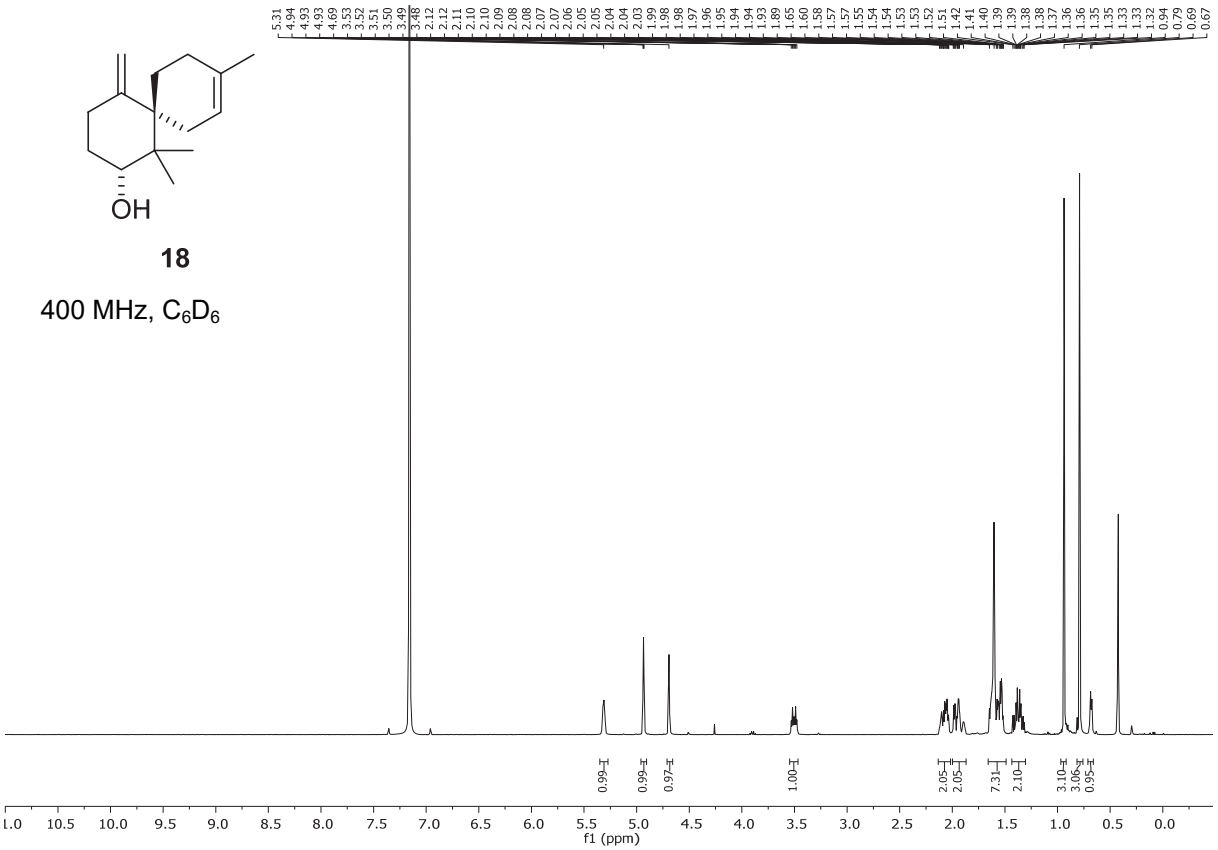
OH
18
400 MHz, C6D6
f1 (ppm)

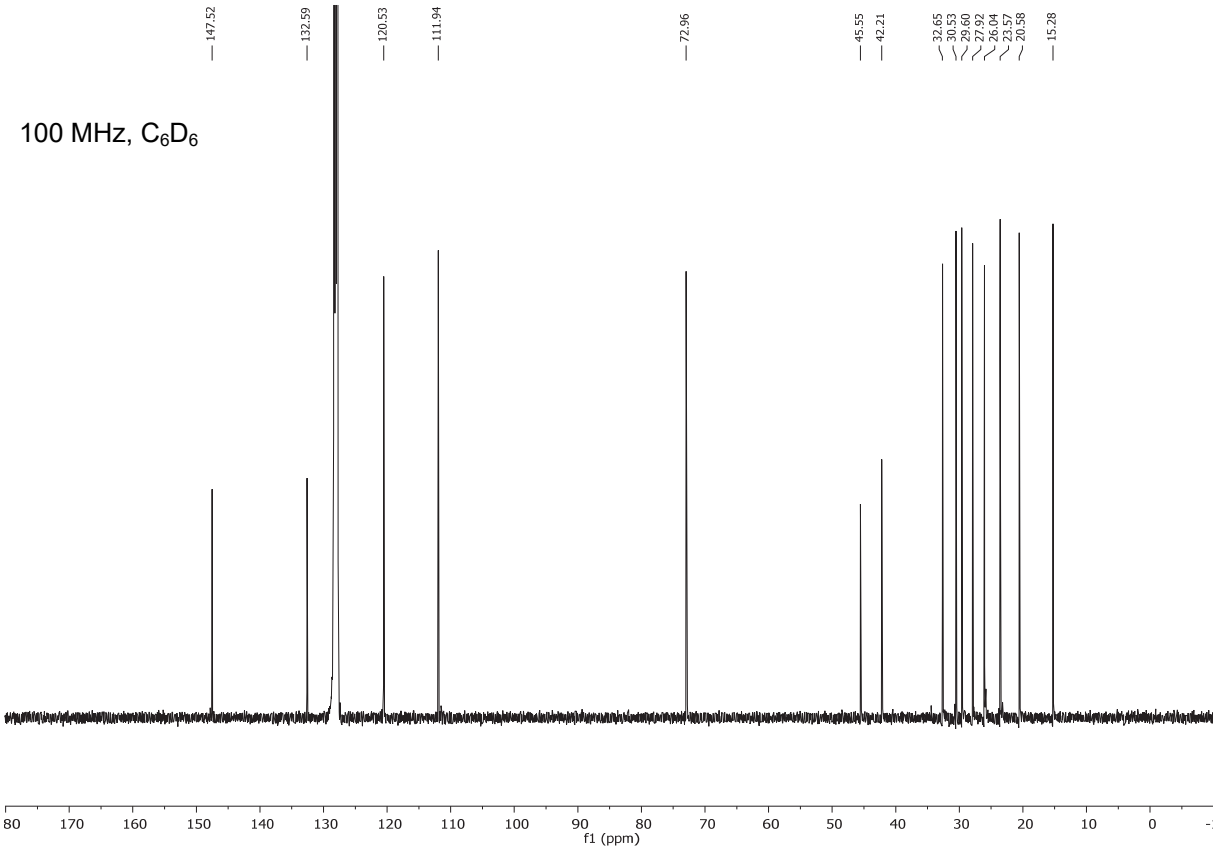
100 MHz, C6D6
f1 (ppm)

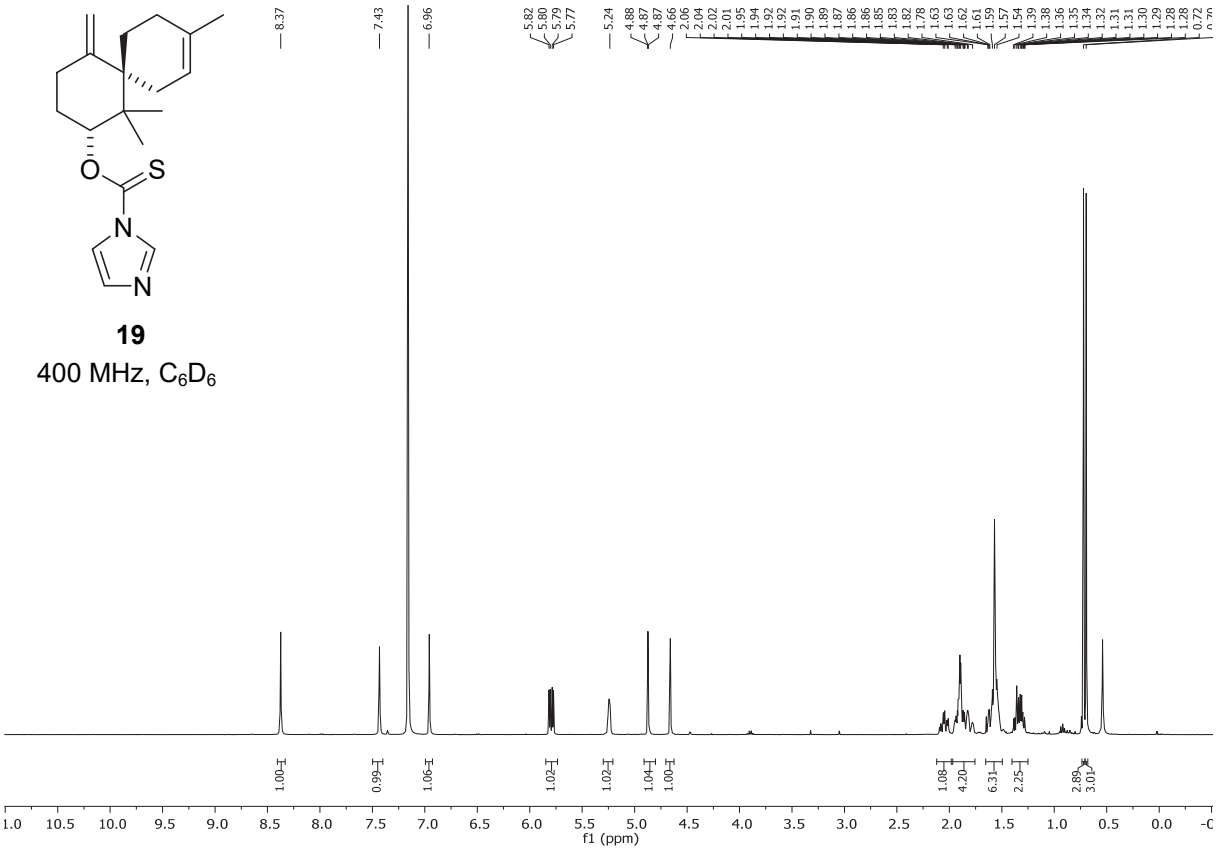

19

400 MHz, C_6D_6

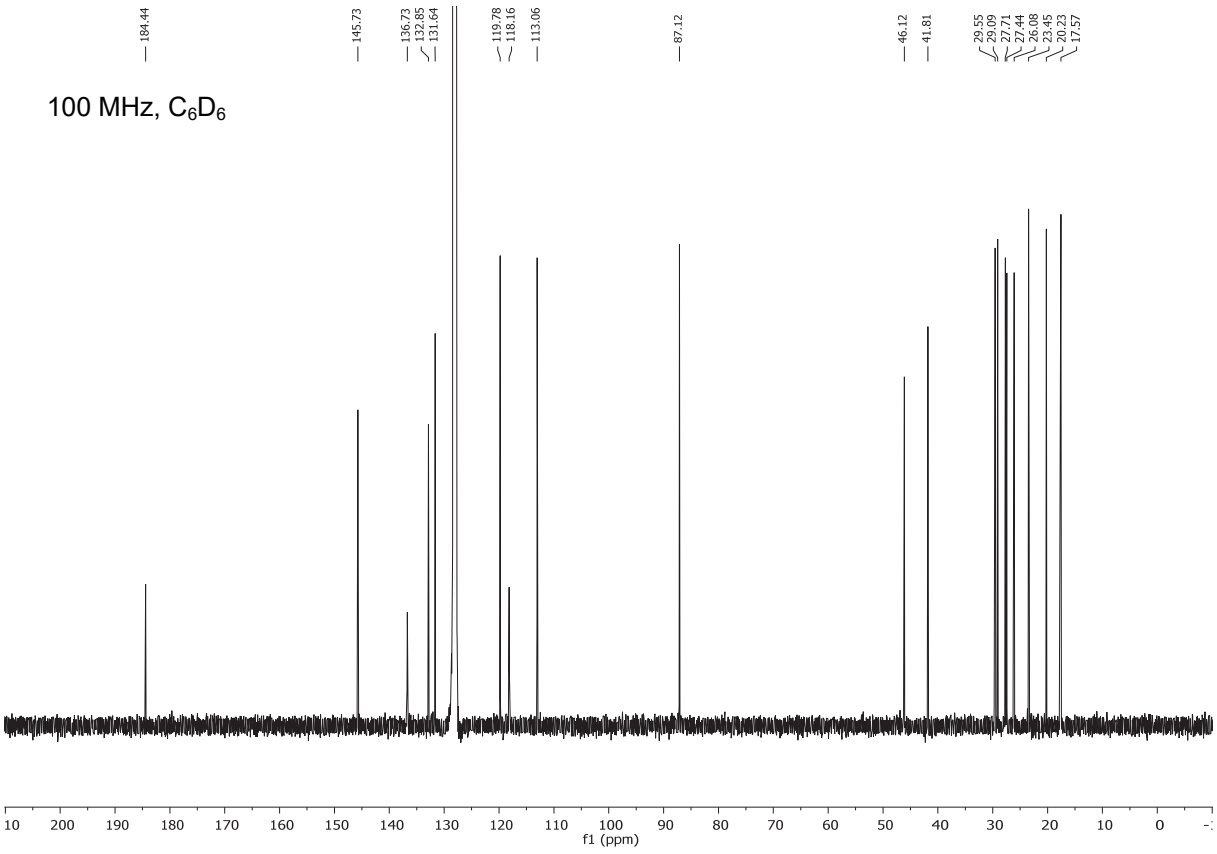

100 MHz, C_6D_6

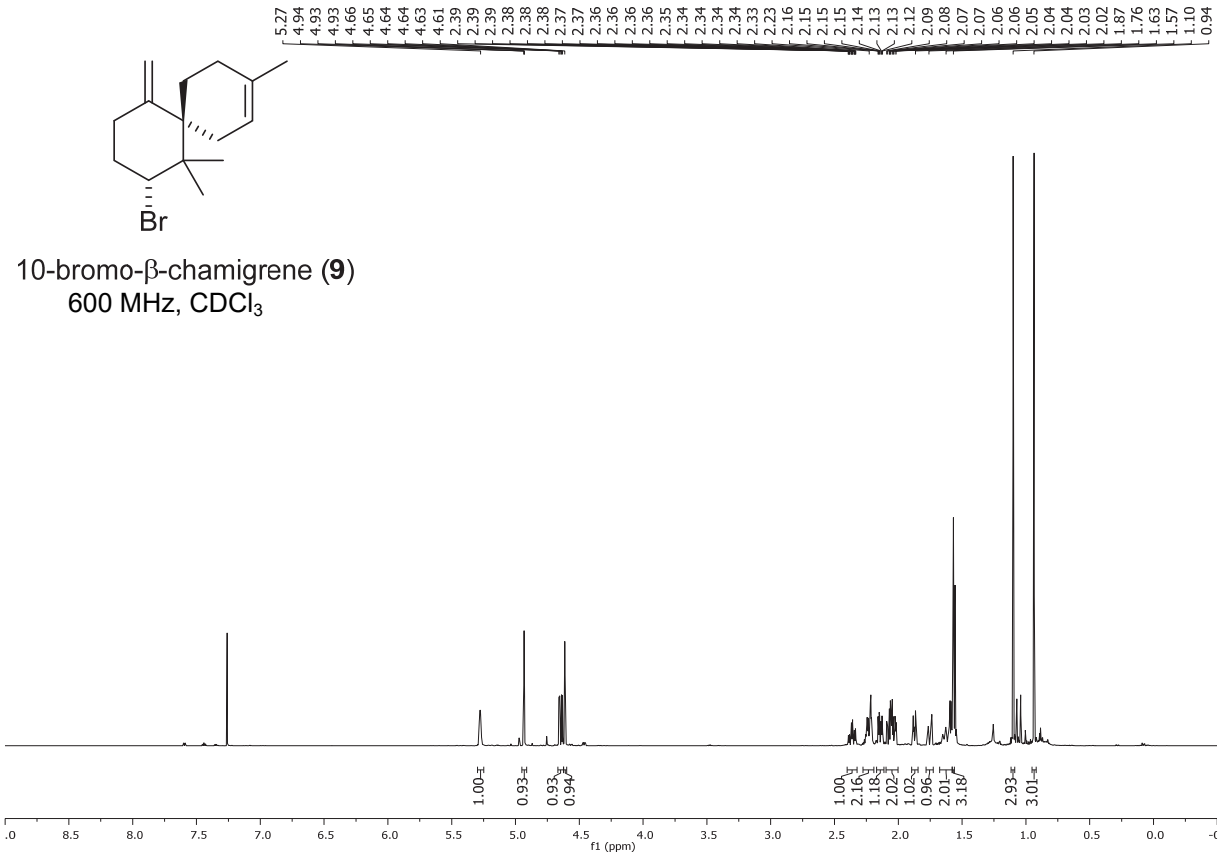
Br
10-bromo-β-chamigrene (9)
600 MHz, CDCl3
f1 (ppm)

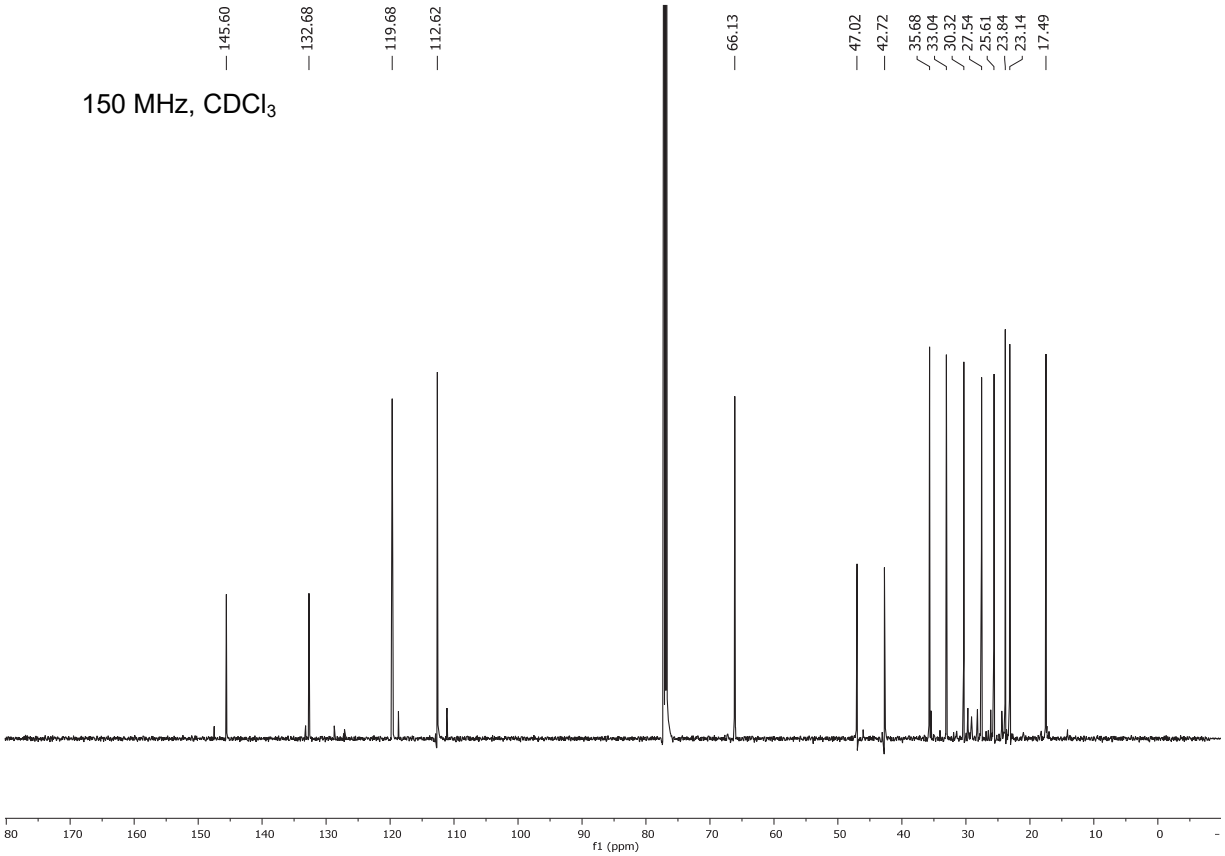
150 MHz, CDCl3
f1 (ppm)

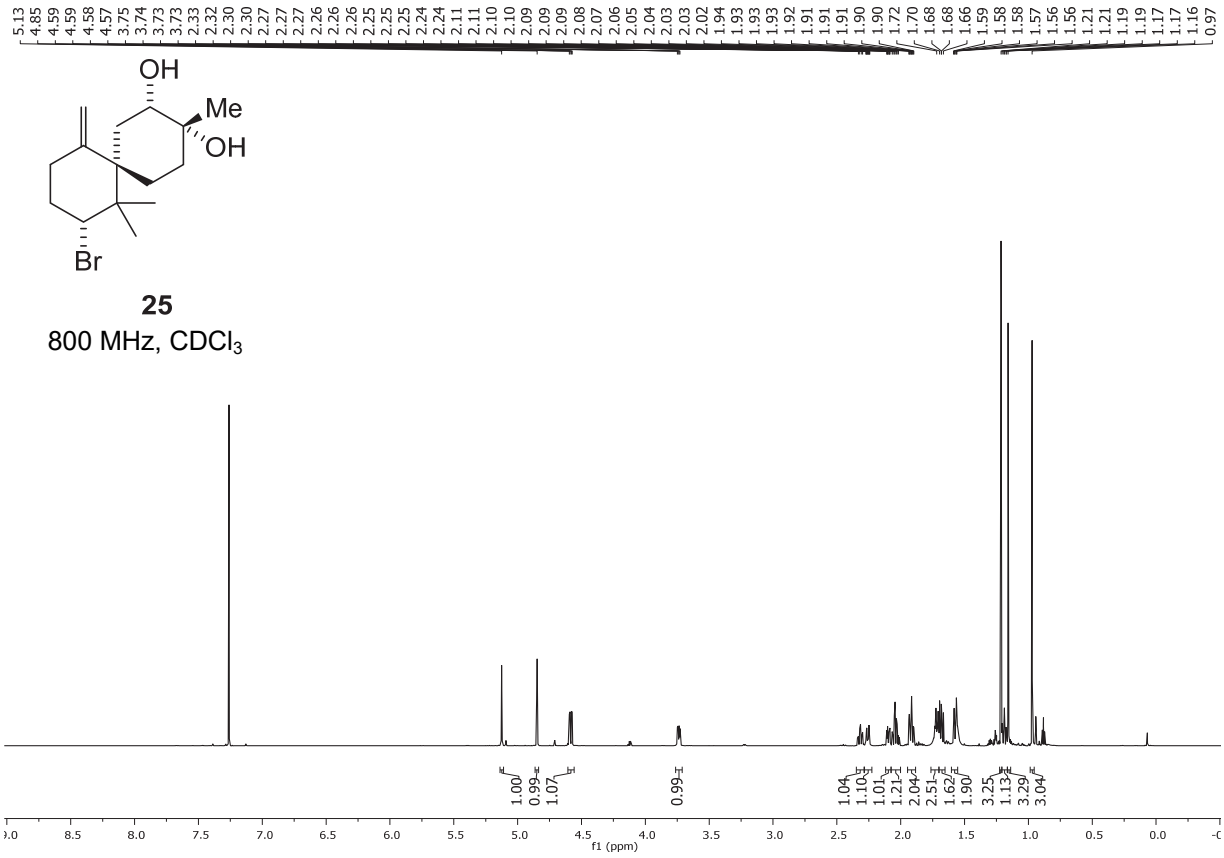

25

800 MHz, $CDCl_3$

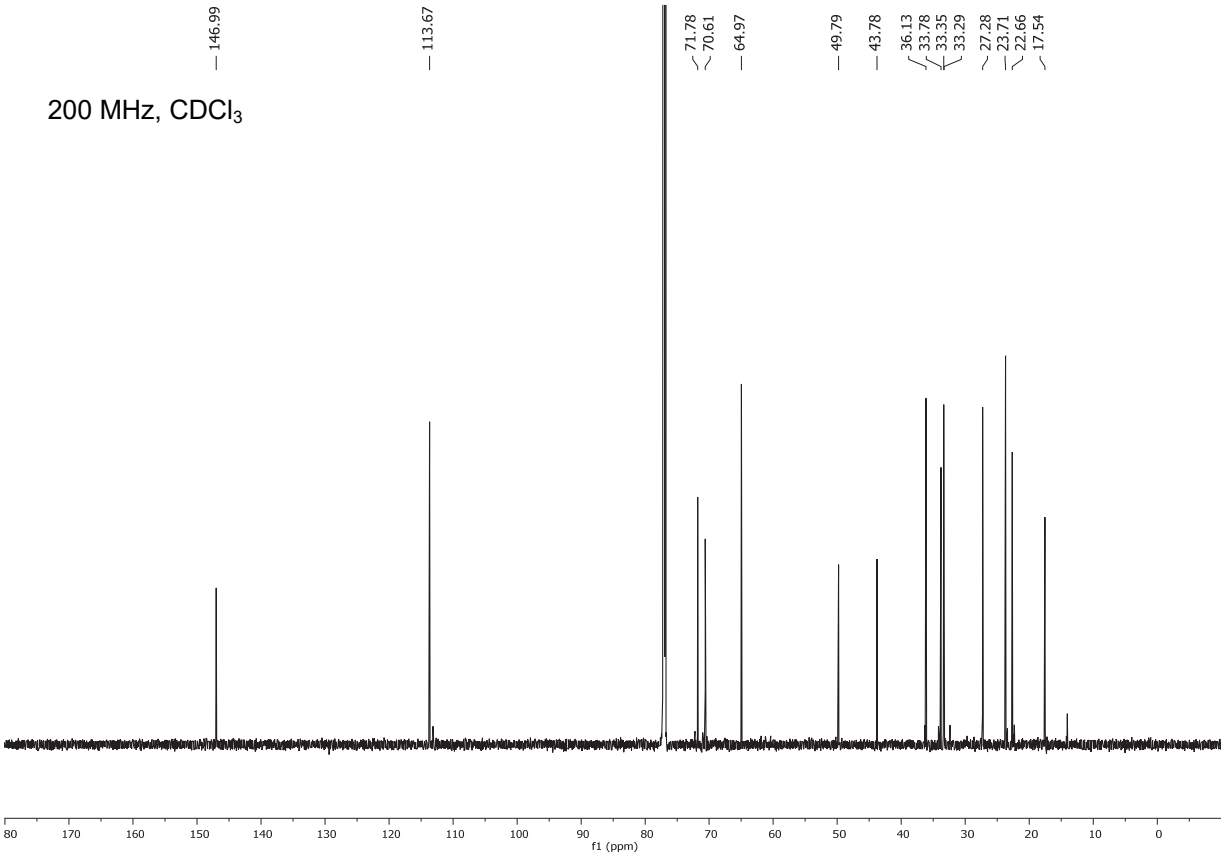

200 MHz, $CDCl_3$

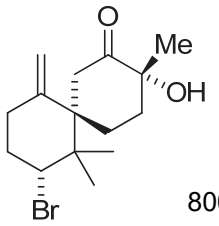

800 MHz, $CDCl_3$

S8

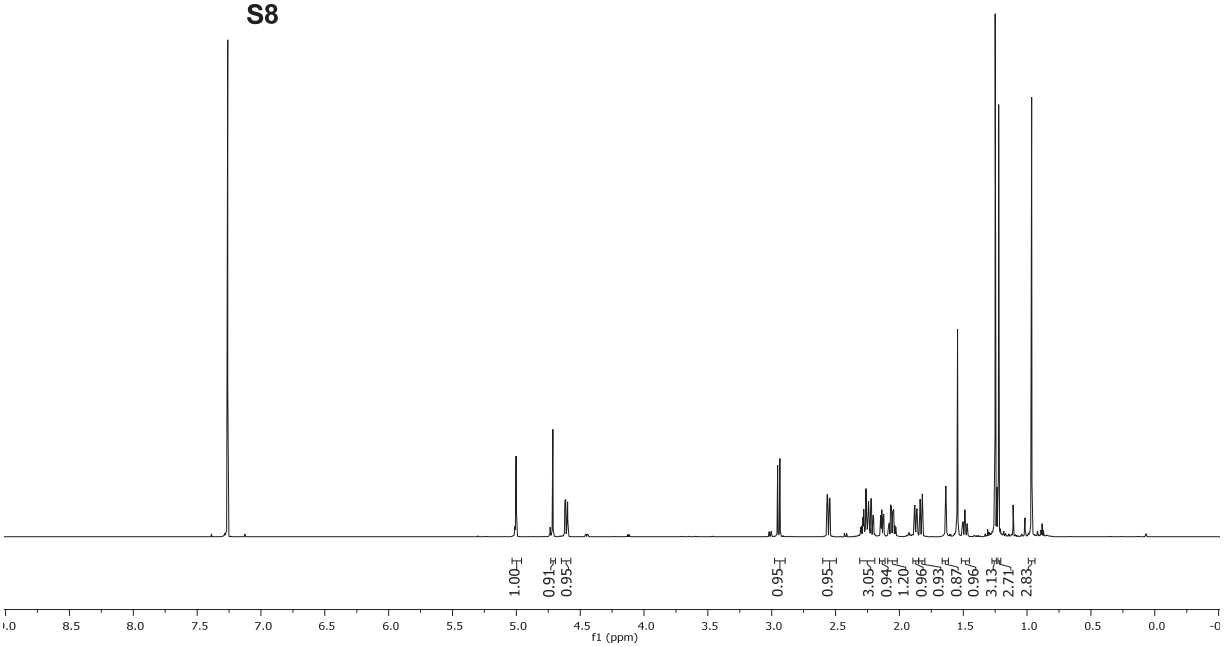

200 MHz, $CDCl_3$

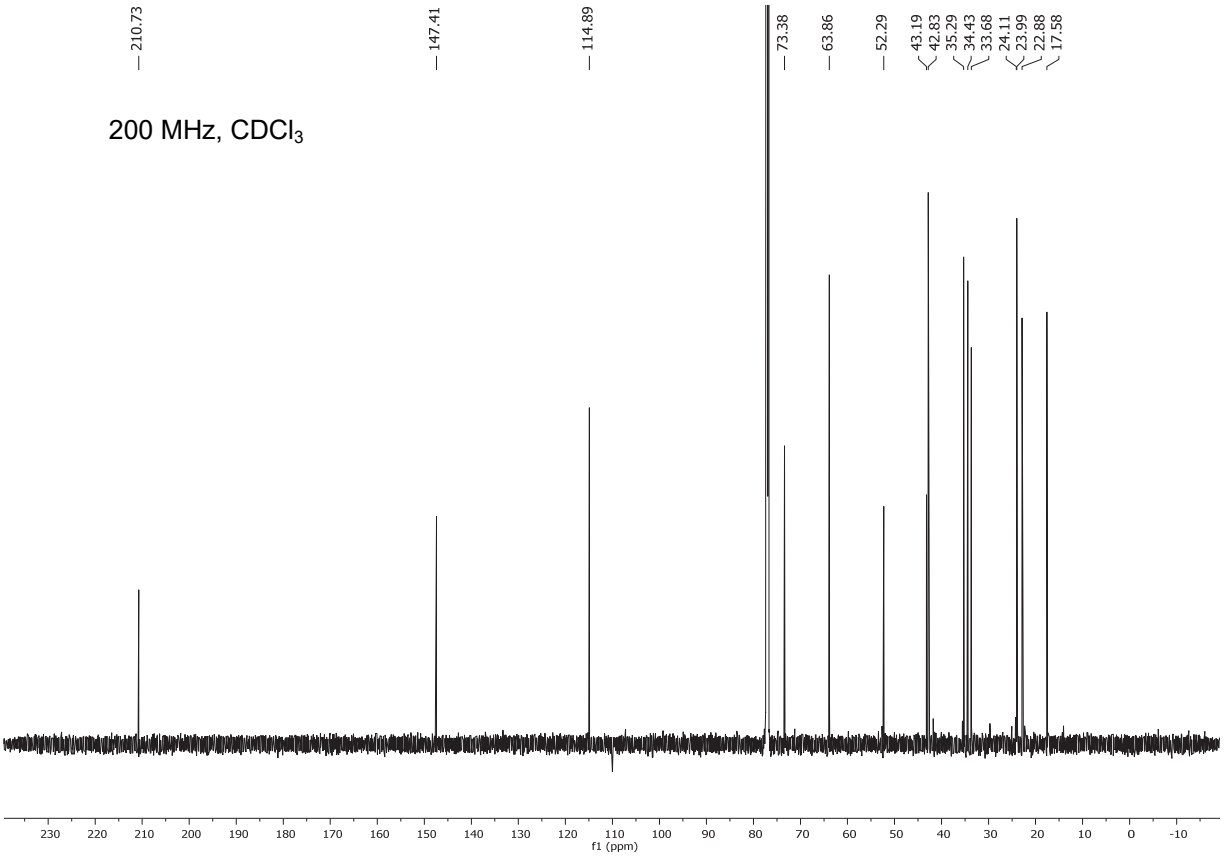

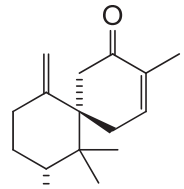

dactylone (**2**)

400 MHz, $CDCl_3$

100 MHz, $CDCl_3$

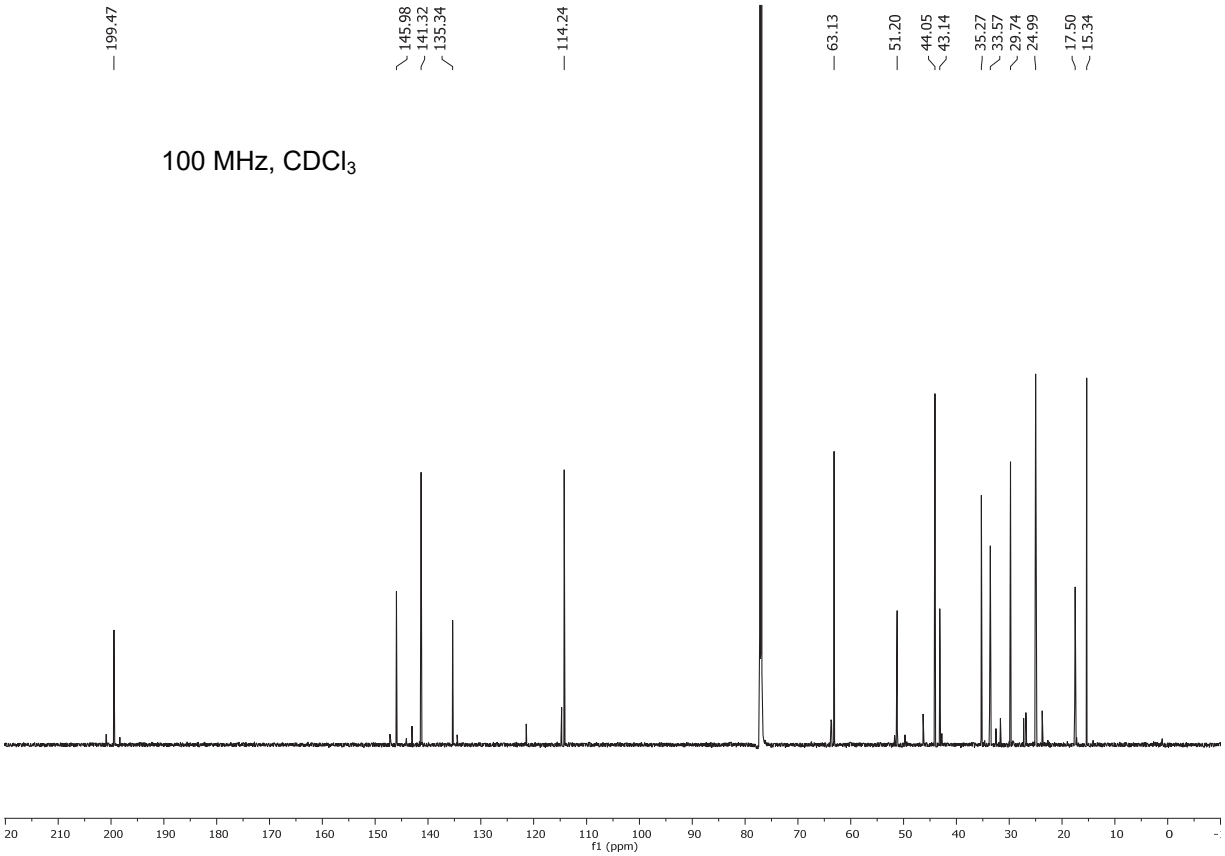

aplydactone (**1**)

800 MHz, C_6D_6

200 MHz, C_6D_6

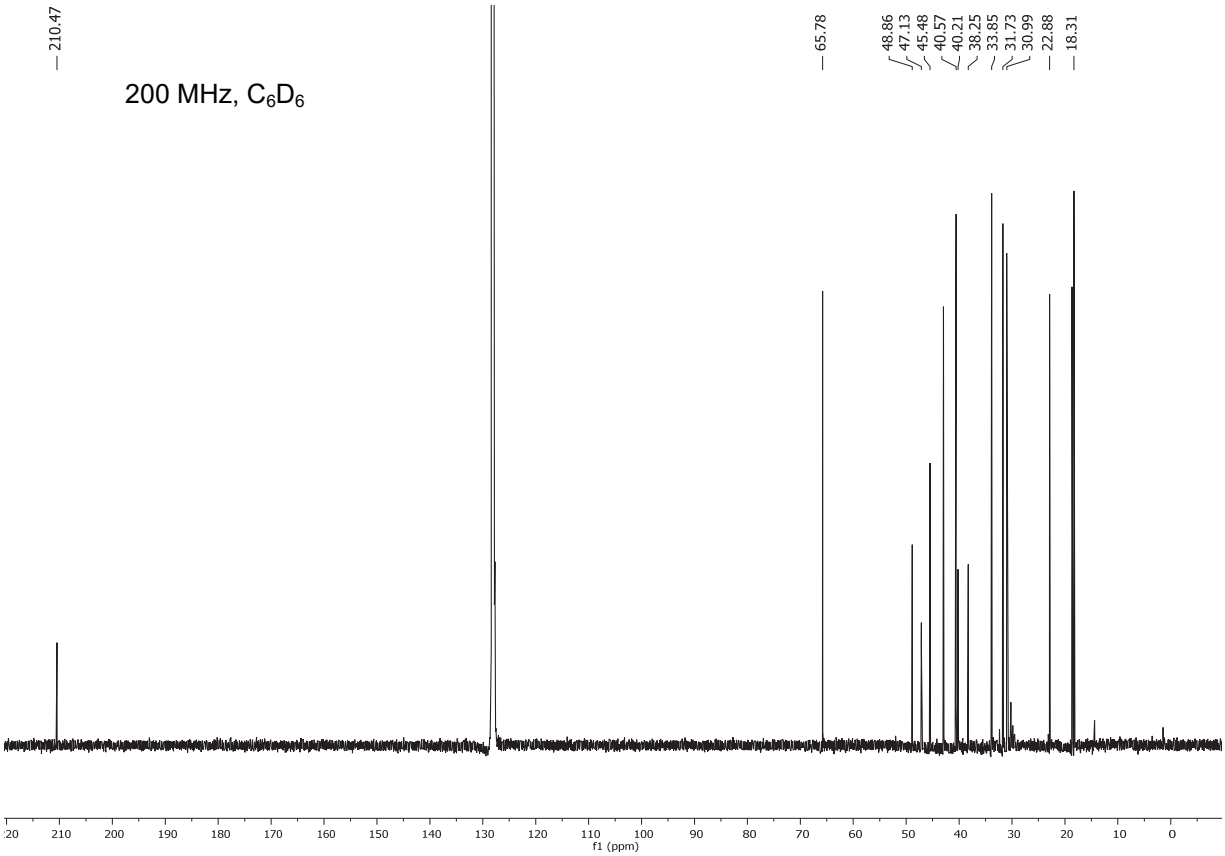

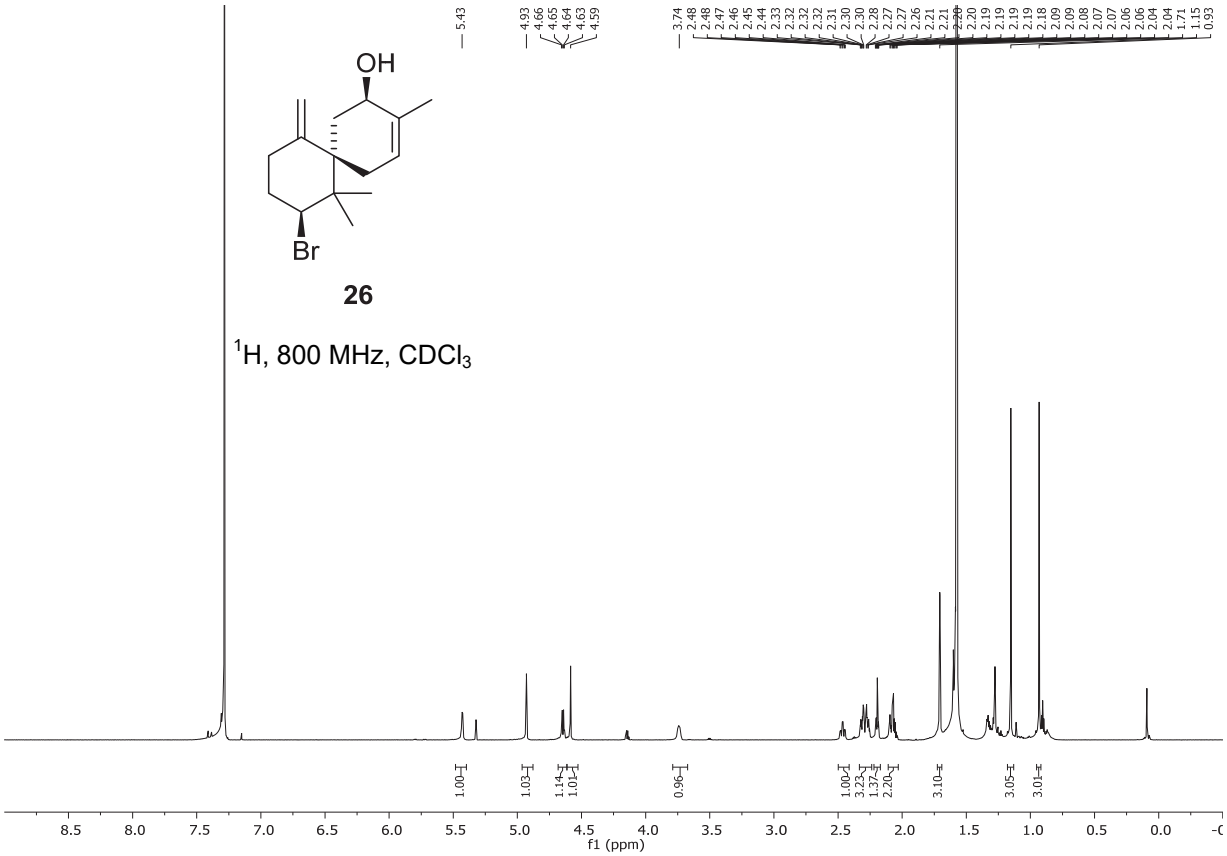
OH
Br
26
^{1}H, 800 MHz, CDCl$_3$
f1 (ppm)

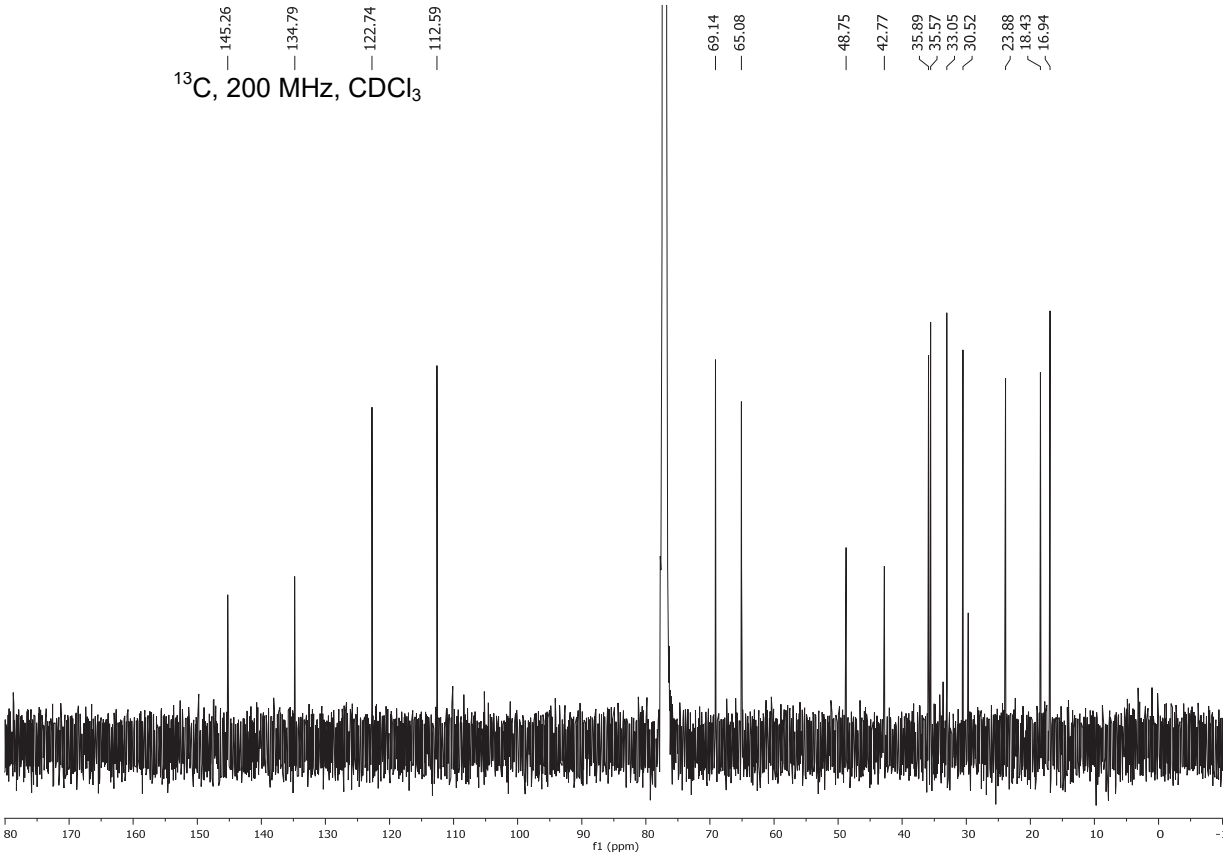
145.26
134.79
122.74
112.59
69.14
65.08
48.75
42.77
35.89
35.57
33.05
30.52
23.88
18.43
16.94
^{13}C, 200 MHz, CDCl$_3$
f1 (ppm)

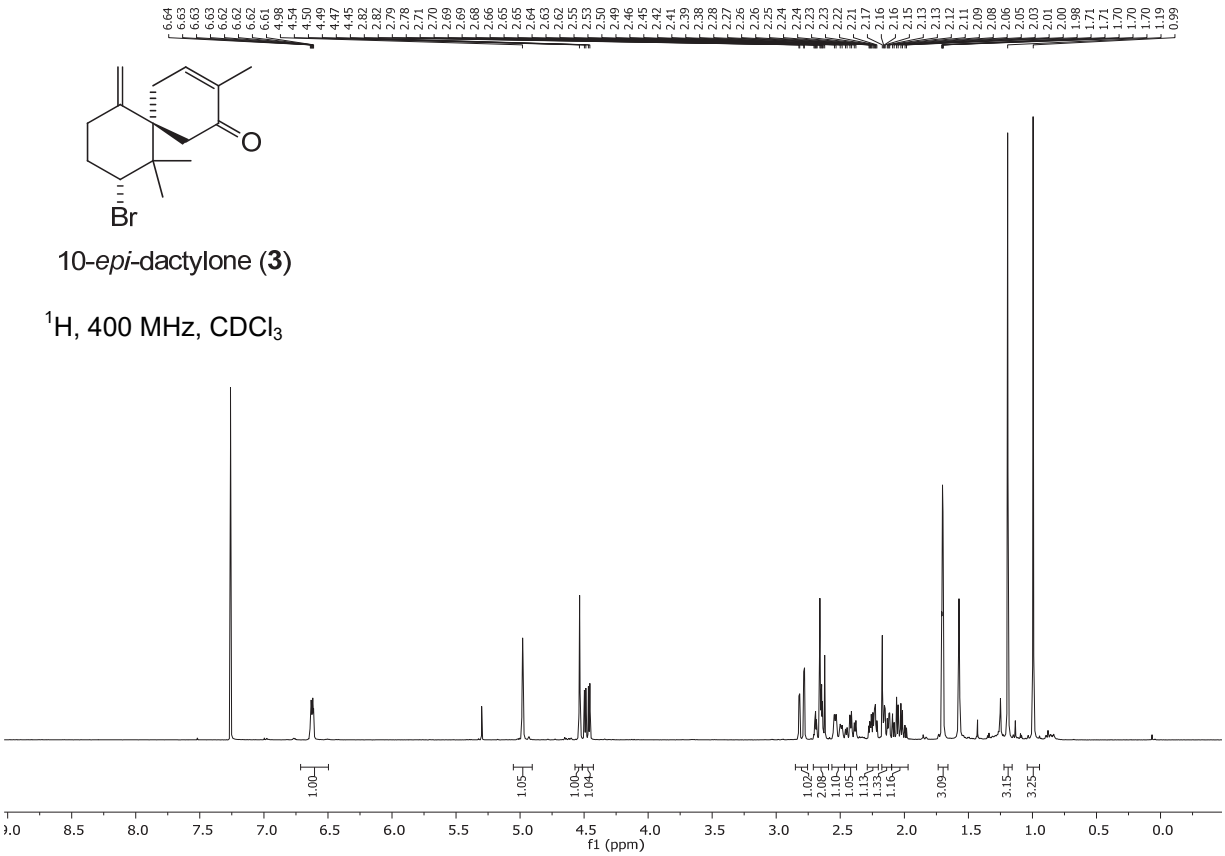

10-*epi*-dactylone (**3**)

^{1}H, 400 MHz, $CDCl_3$

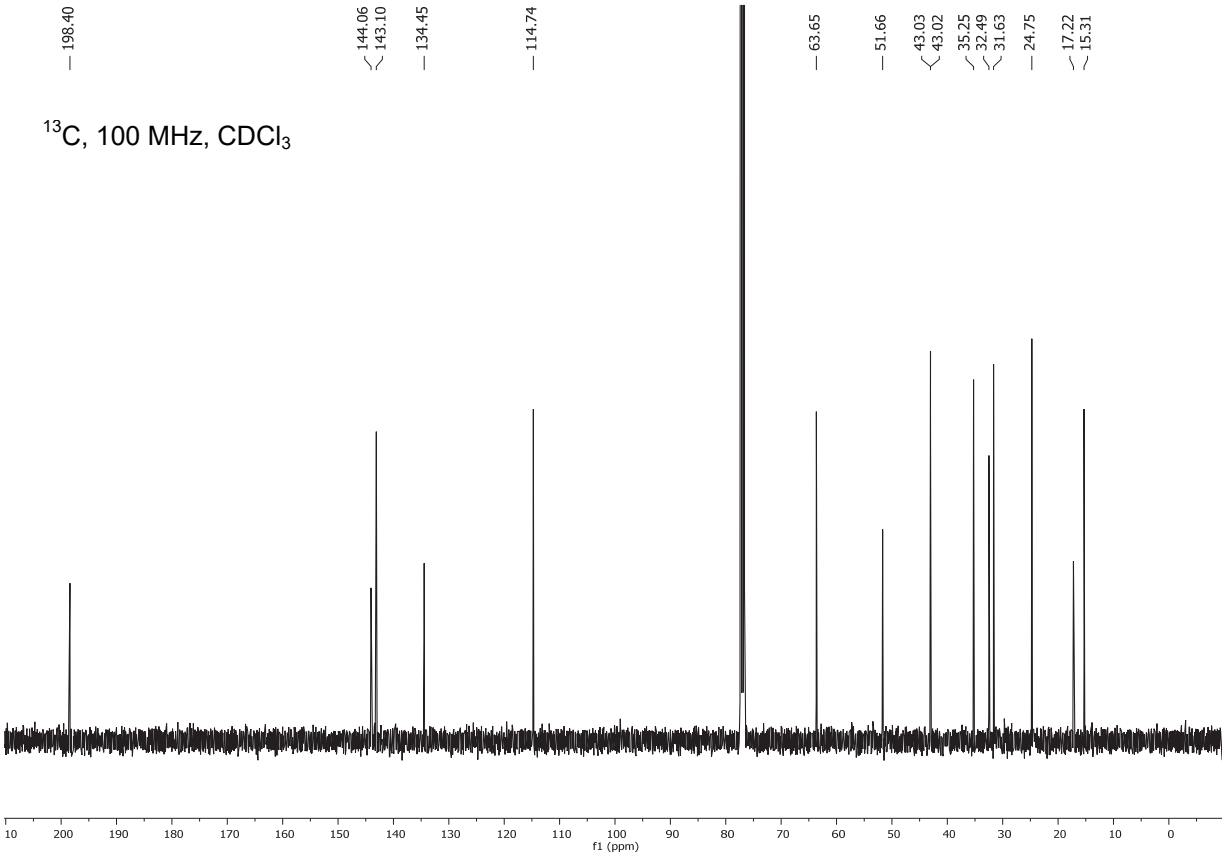

^{13}C, 100 MHz, $CDCl_3$

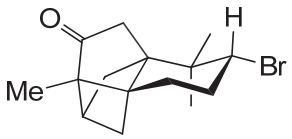

8-*epi*-isoaplydactone (**8**)

800 MHz, $CDCl_3$

200 MHz, $CDCl_3$

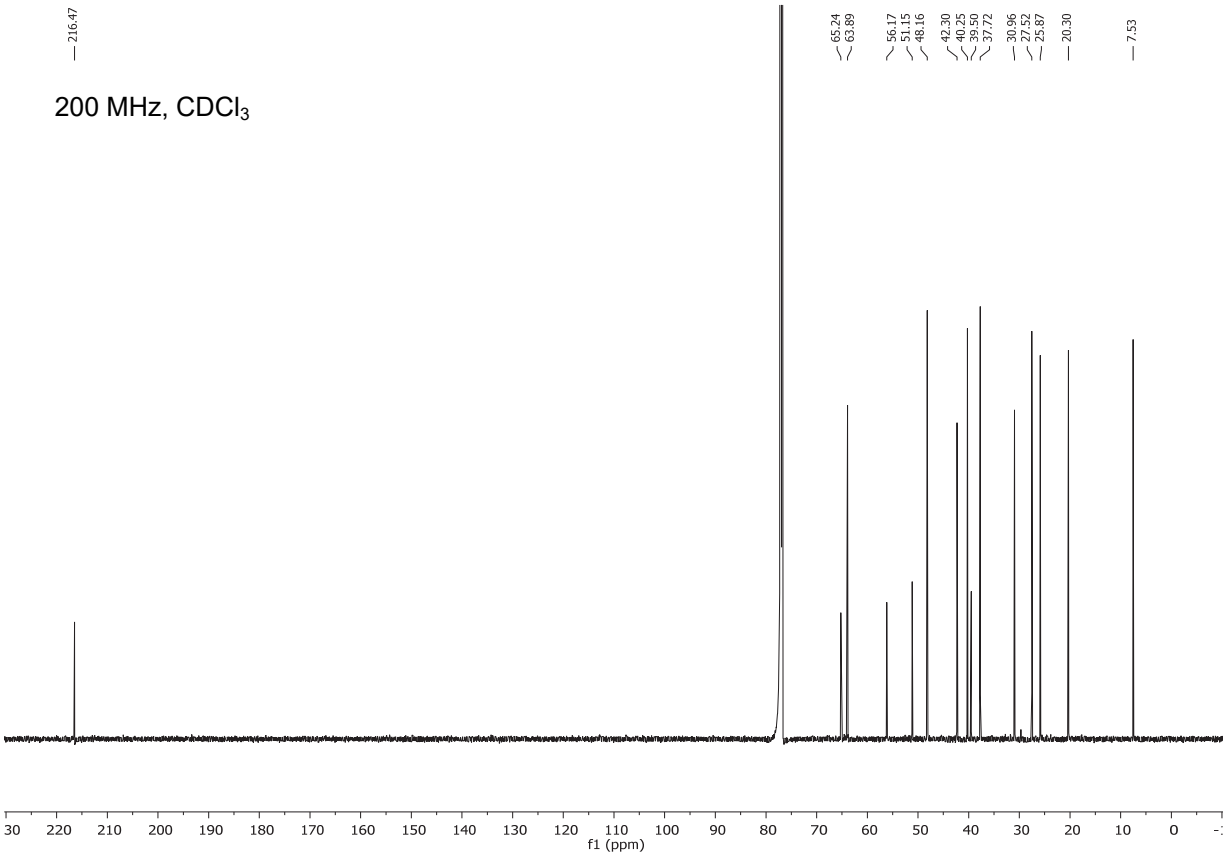

COSY, $CDCl_3$

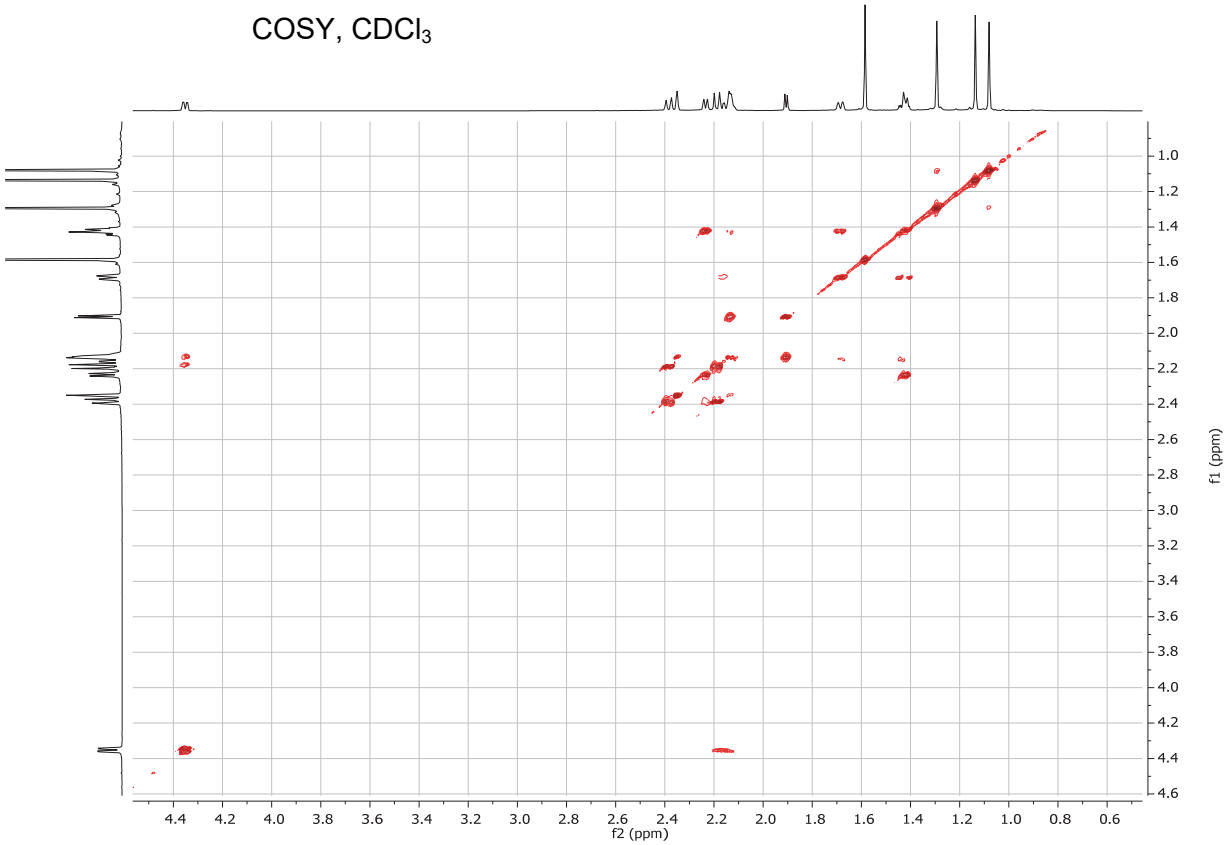

COSY, $CDCl_3$

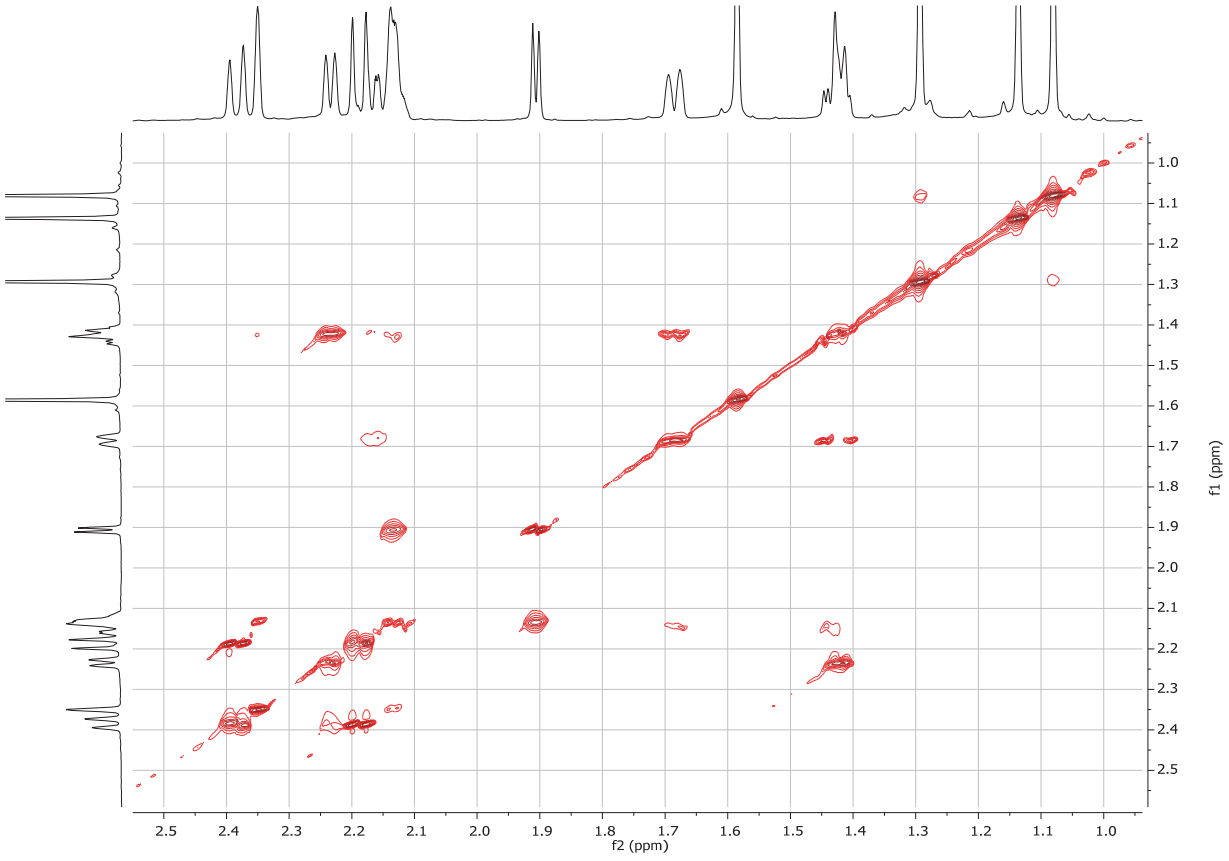

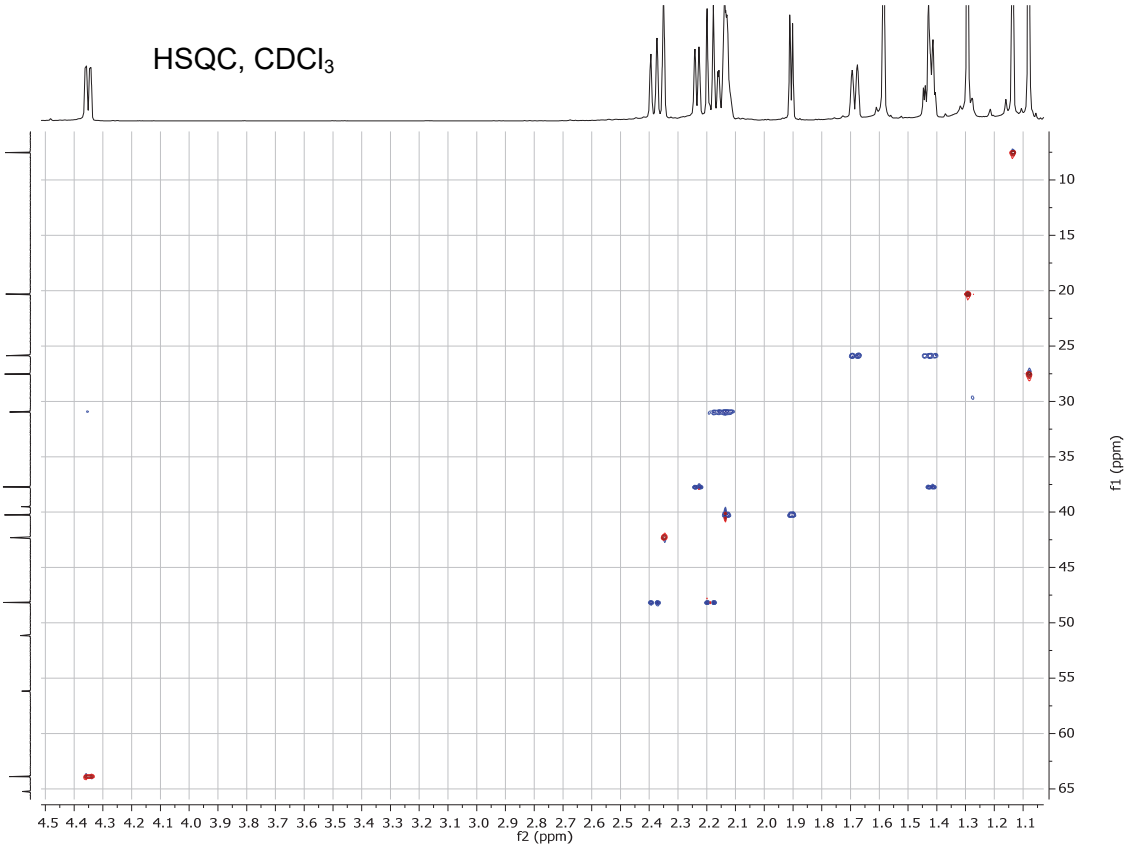
HSQC, CDCl3
f2 (ppm)
f1 (ppm)

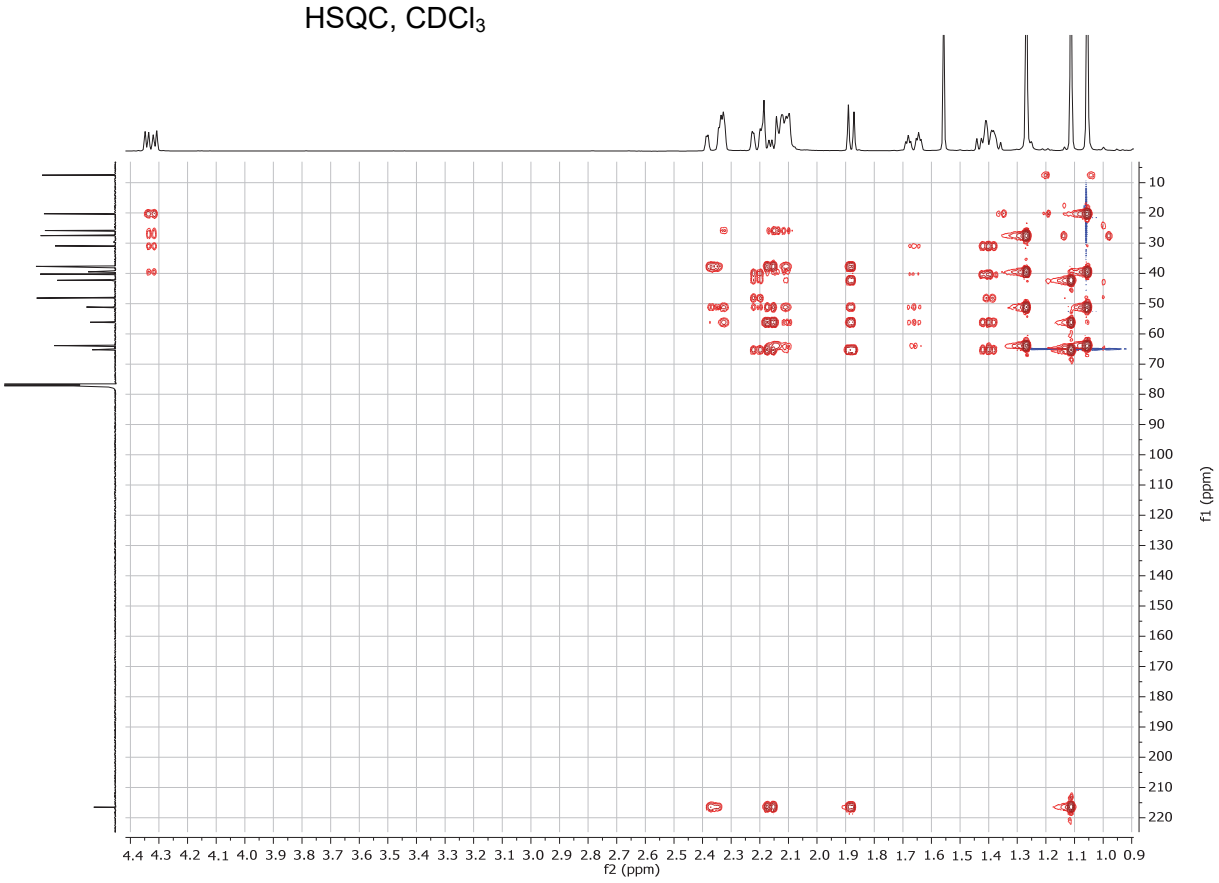
HSQC, CDCl3
f2 (ppm)
f1 (ppm)

HSQC, $CDCl_3$

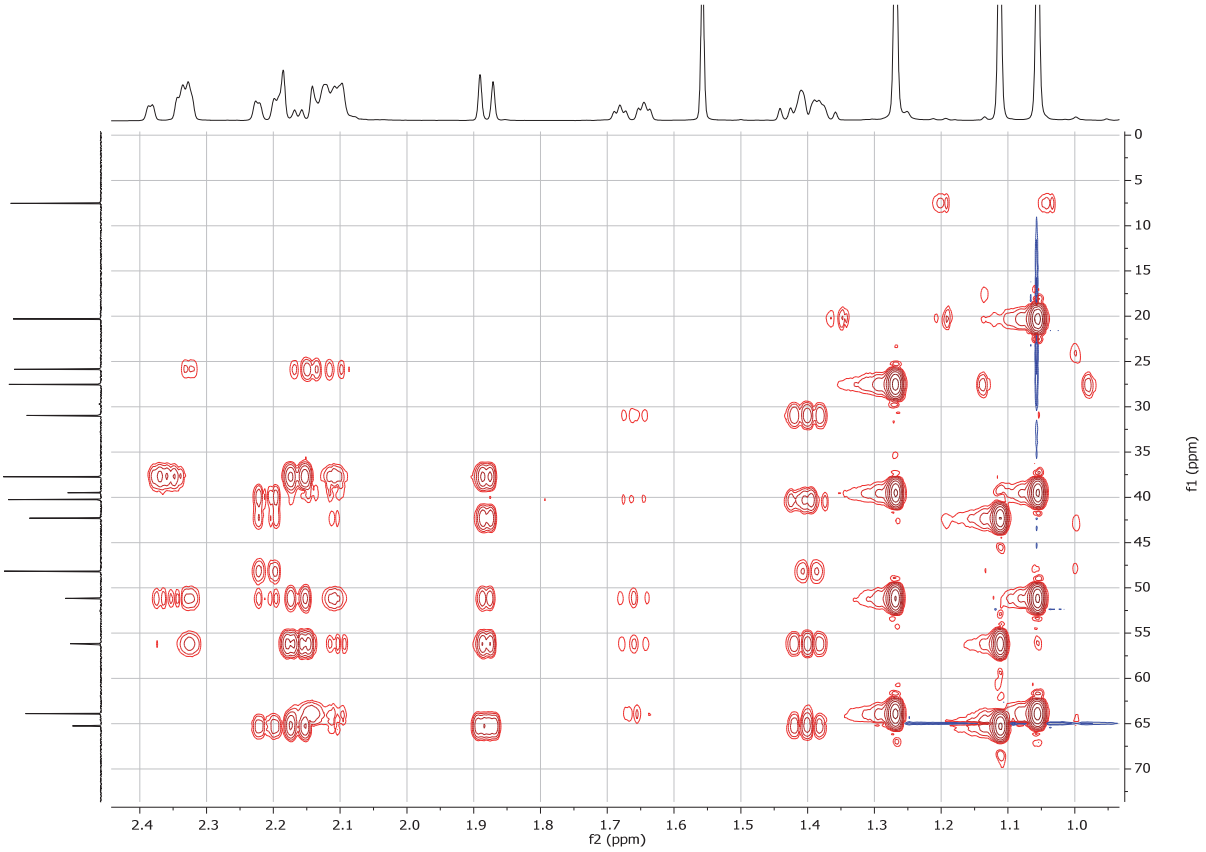

HSQC, $CDCl_3$

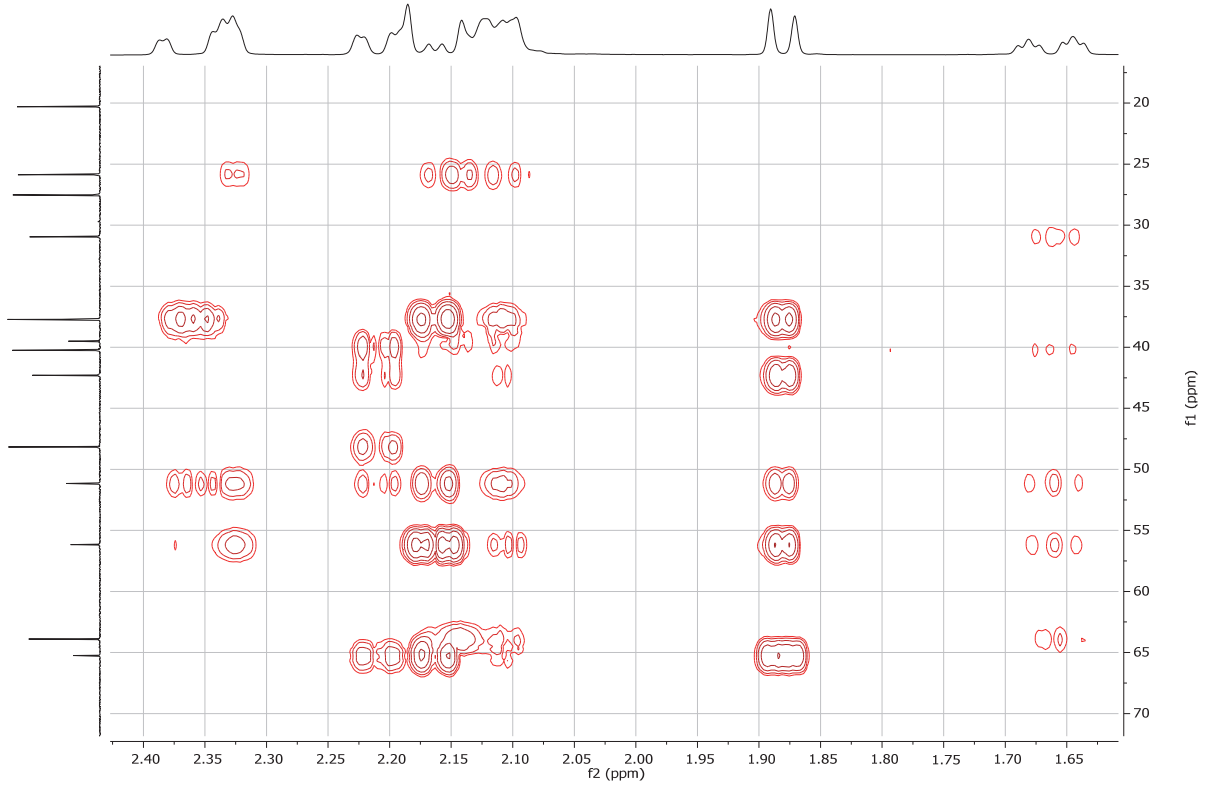

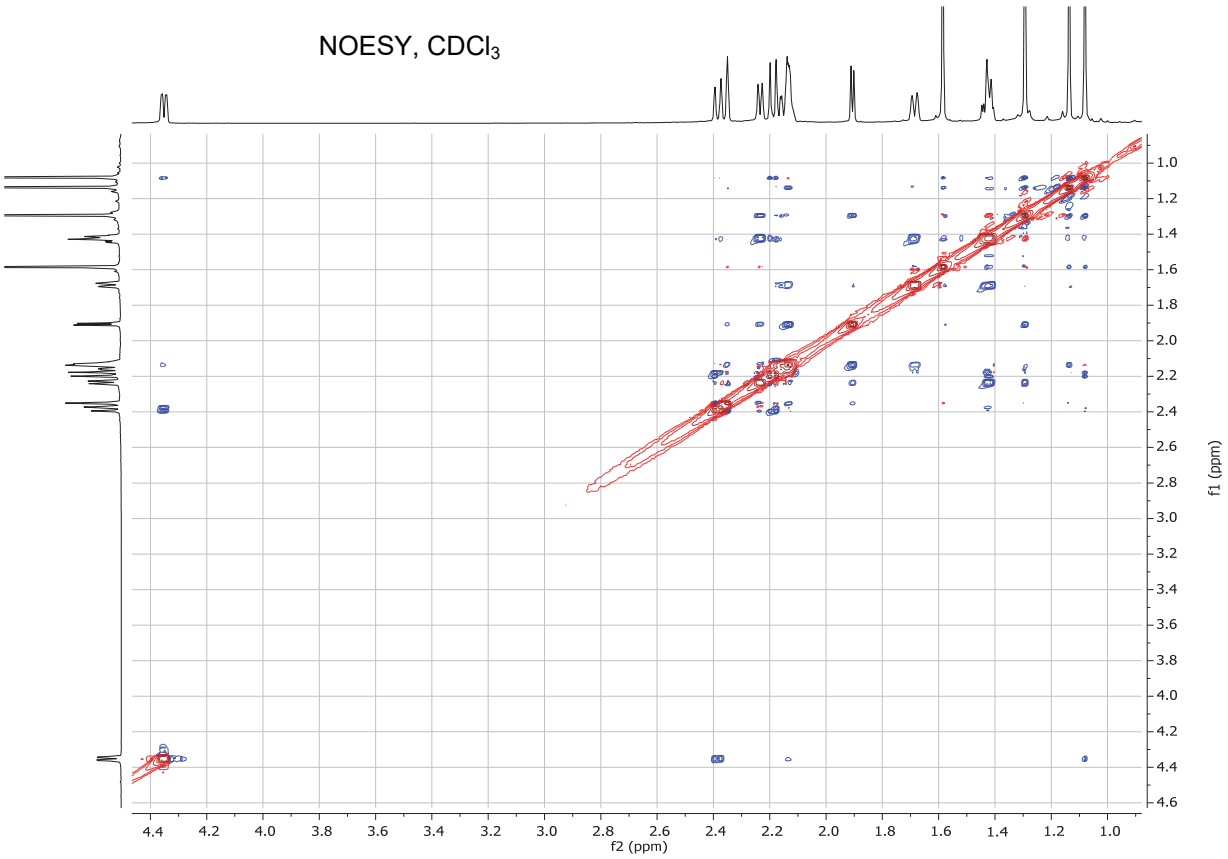
NOESY, CDCl3
f2 (ppm)
f1 (ppm)

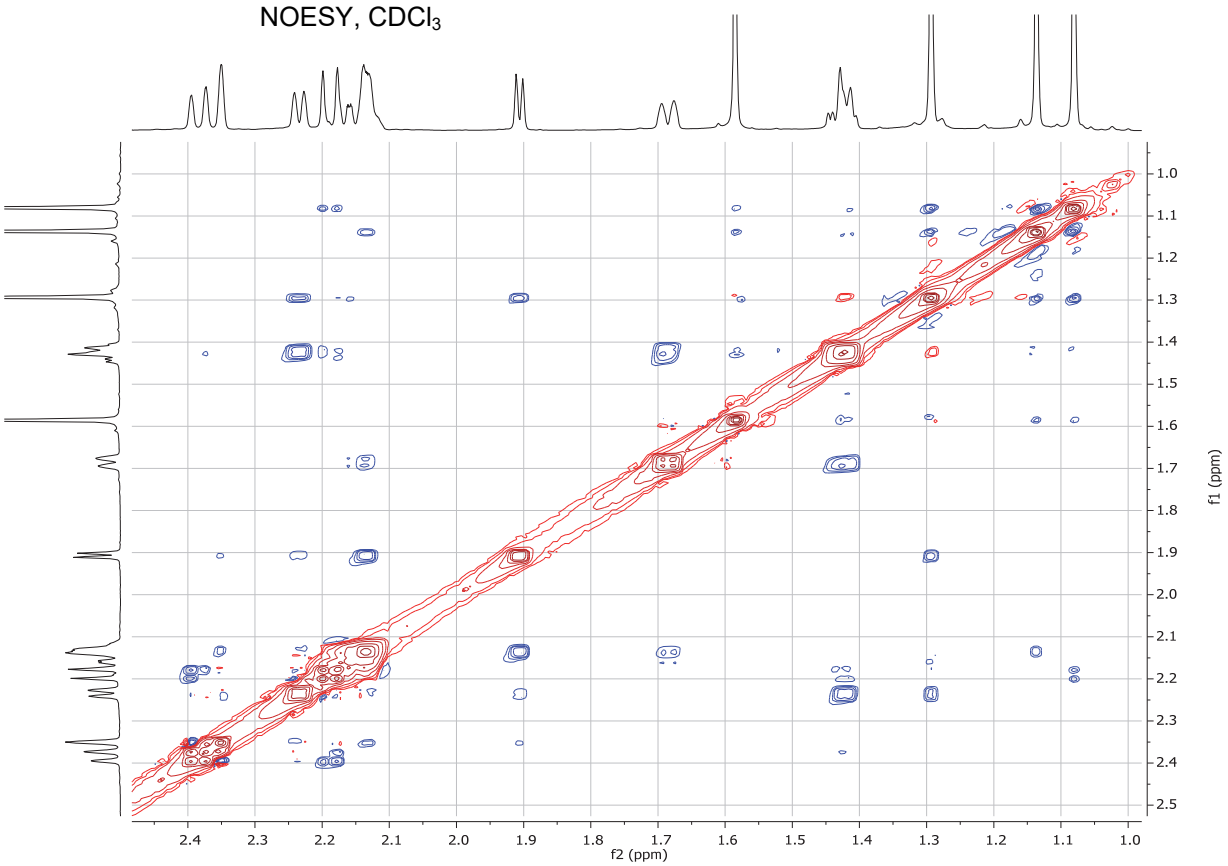
NOESY, CDCl3
f2 (ppm)
f1 (ppm)

6.3.3 X-ray crystallographic data

1. Enone 14

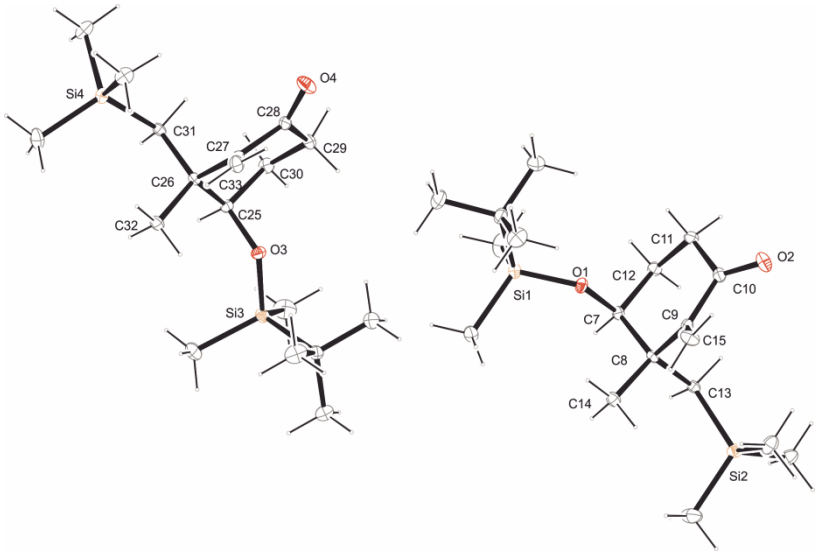

Figure 6.7 ORTEP of the molecular structure of enone **14**.

CCDC 1493586 contains the supplementary crystallographic data for enone **14**. These data can be obtained free of charge from The Cambridge Crystallographic Data Centre via www.ccdc.cam.ac.uk/data_request/cif.

Table 6.7 Crystallographic data for enone 14.

net formula	$C_{18}H_{36}O_2Si_2$
M_r/g mol^{-1}	340.65
crystal size/mm	0.440 × 0.269 × 0.100
T/K	123(2)
radiation	MoKα
diffractometer	'Oxford XCalibur'
crystal system	triclinic
space group	'P -1'
a/Å	6.9583(4)
b/Å	12.3699(9)
c/Å	25.385(2)
α/°	92.024(6)
β/°	91.543(6)
γ/°	101.580(5)
V/Å^3	2137.9(3)
Z	4
calc. density/g cm^{-3}	1.058
μ/mm^{-1}	0.171
absorption correction	'multi-scan'
transmission factor range	0.89289–1.00000
refls. measured	9874
R_{int}	?
mean σ(*I*)/*I*	0.0794
θ range	4.118–28.327
observed refls.	7319
x, y (weighting scheme)	0.0709, 0.0000
hydrogen refinement	constr

refls in refinement	9874
parameters	416
restraints	0
$R(F_{obs})$	0.0537
$R_w(F^2)$	0.1297
S	0.974
shift/error$_{max}$	0.001
max electron density/e Å^{-3}	0.405
min electron density/e Å^{-3}	−0.434
2-component-twin, Rotation by 180° at (001), BASF 0.49	

2. Spirocycle 16

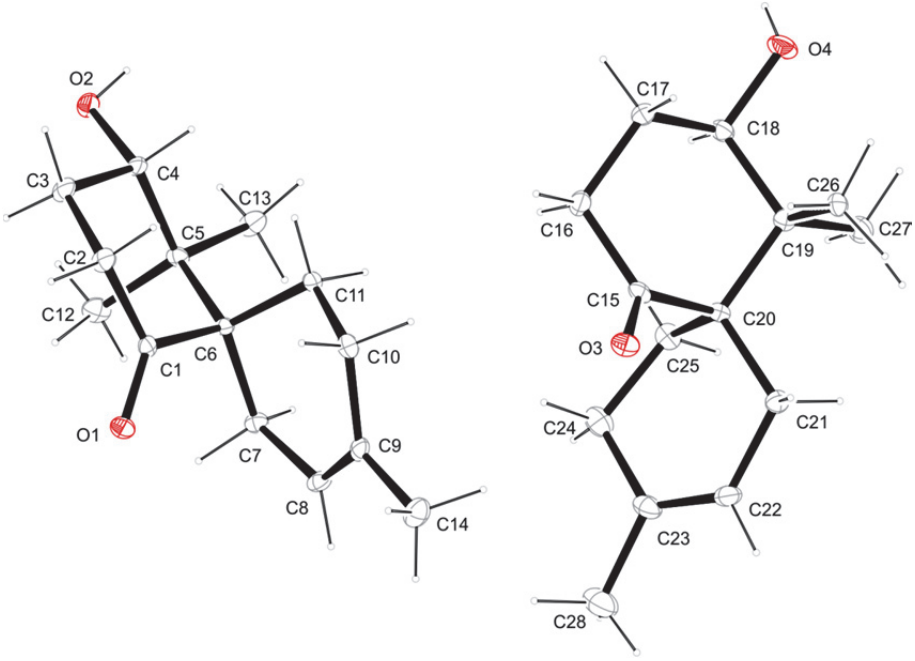

Figure 6.8 ORTEP of the molecular structure of spirocycle **16**

CCDC 1493587 contains the supplementary crystallographic data for spirocycle **16**. These data can be obtained free of charge from The Cambridge Crystallographic Data Centre via www.ccdc.cam.ac.uk/data_request/cif.

Table 6.8 Crystallographic data for spirocycle 16.

net formula	$C_{14}H_{22}O_2$
M_r/g mol^{-1}	222.31
crystal size/mm	0.080 × 0.060 × 0.040
T/K	100(2)
radiation	MoKα
diffractometer	'Bruker D8Venture'
crystal system	triclinic
space group	'P -1'
a/Å	7.5248(9)
b/Å	13.2697(15)
c/Å	13.7491(15)

α/°	107.523(3)
β/°	101.200(3)
γ/°	100.468(3)
V/Å^3	1241.2(2)
Z	4
calc. density/g cm^{-3}	1.190
μ/mm^{-1}	0.077
absorption correction	multi-scan
transmission factor range	0.8824–0.9580
refls. measured	10897
R_{int}	0.0573
mean σ(I)/I	0.0741
θ range	3.069–25.40
observed refls.	3314
x, y (weighting scheme)	0.0369, 0.9403
hydrogen refinement	mixed
refls in refinement	4493
parameters	303
restraints	0
$R(F_{obs})$	0.0586
$R_w(F^2)$	0.1387
S	1.067
shift/error$_{max}$	0.001
max electron density/e Å^{-3}	0.304
min electron density/e Å^{-3}	−0.212

Racemic.

C-H: constr, O-H: refall.

NOTE: The computational calculations were performed by Dr. Patrick Kölle of the research group of Professor Regina de Vivie-Riedle, LMU Munich. Because these investigations were not part of this thesis, they are not reported herein. For further details see: B. S. Matsuura, P. Kölle, D. Trauner, R. de Vivie–Riedle, R. Meier, *ACS Cent. Sci.* **2017**, *3*, 39–46.

6.4 Supporting information for Chapter 4.2

6.4.1 Experimental procedures

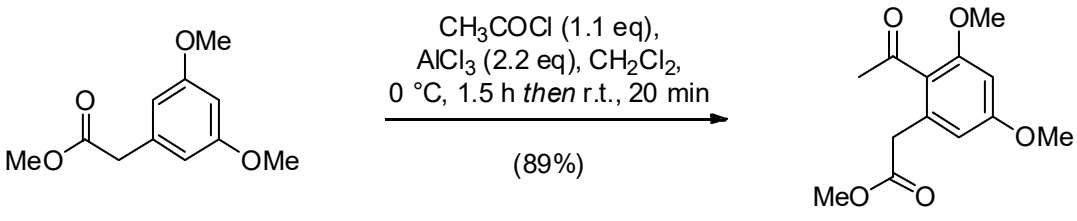

9 **11**

2-Acetyl-3,5-dimethoxyphenylacetic acid methyl ester (11) To a stirred solution of phenylacetic acid methyl ester **9** (5.50 g, 26.2 mmol, 1.0 eq) and acetyl chloride (2.06 mL, 28.8 mmol, 1.1 eq) in CH_2Cl_2 (240 mL) at 0 °C was added $AlCl_3$ (7.68 g, 57.6 mmol, 2.2 eq) and the resulting reaction mixture was stirred at 0 °C for 1.5 h. The reaction mixture was allowed to warm up to r.t. for 20 min before adding aq. 10% HCl solution (450 mL). The layers were separated and the aqueous layer was extracted with CH_2Cl_2 (3 × 150 mL). The combined organic layers were washed with brine (100 mL) and dried over Na_2SO_4. After filtration and concentration *in vacuo*, the crude product was purified by flash column chromatography (hexanes:EtOAc 3:1) on silica to afford methyl ester **11** (5.89 g, 23.3 mmol, 89%) as a white solid. Compound **11** has been reported in the literature.[168]

Data for 11: R_f: 0.32 (hexanes:EtOAc 3:1); **^{1}H NMR (300 MHz, $CDCl_3$):** δ = 6.42 (d, J = 2.3 Hz, 1H), 6.36 (d, J = 2.3 Hz, 1H), 3.84 (s, 3H), 3.82 (s, 3H), 3.70 (s, 2H), 3.68 (s, 3H), 2.51 (s, 3H) ppm; **^{13}C NMR (75 MHz, $CDCl_3$):** δ = 203.9, 171.9, 161.7, 159.6, 135.1, 123.9, 108.4, 97.7, 55.8, 55.6, 52.1, 39.2, 32.4 ppm; **IR (ATR):** ν_{max} = 2951 (m), 2921 (s), 2868 (m), 2851 (m), 1719 (m), 1667 (m), 1594 (m), 1577 (m), 1457 (m), 1425 (m), 1415 (w), 1377 (m), 1354 (m), 1320 (m), 1298 (w), 1276 (s), 1260 (m), 1196 (m), 1175 (m), 1162 (s), 1096 (s), 1073 (s), 1039 (s), 1016 (s), 981 (m), 953 (m), 944 (m), 925 (w), 900 (w), 864 (w), 842 (m), 834 (m), 799 (s), 765 (m), 715 (w), 693 (w), 674 (m) cm^{-1}; **melting point:** 60.9 – 61.4 °C (lit.: 58 – 60 °C)[155]; **HRMS (EI):** calc. for $C_{13}H_{16}O_5$ $[M]^+$: 252.0992, found: 252.0998.

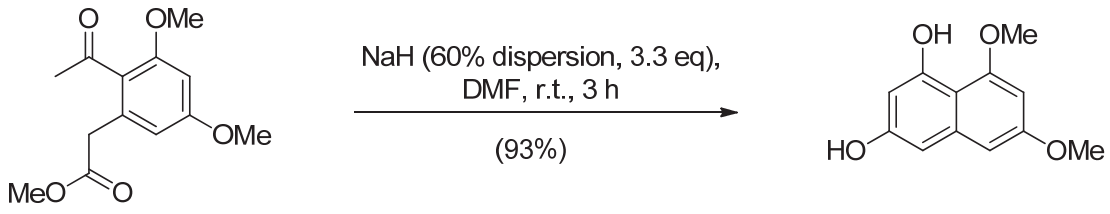

11 **12**

6,8-Dihydroxy-1,3-dimethoxynaphthalene (12) To a stirred solution of ketone **11** (5.89 g, 23.3 mmol, 1.0 eq) in DMF (350 mL) at r.t. was added NaH (60% dispersion in mineral oil, 3.07 g, 76.9 mmol, 3.3 eq) and the resulting reaction mixture was stirred at r.t. for 3 h. The reaction was quenched by addition of sat. aq. NH_4Cl solution (300 mL) and H_2O (300 mL) followed by extraction with EtOAc (3 × 200 mL). The combined organic layers were washed with 10% aq. NaCl solution (4 × 200 mL), brine (200 mL) and dried over Na_2SO_4. After filtration and concentration *in vacuo*, the crude product was purified by flash column chromatography (hexanes:EtOAc 4:1→3:1) on silica to afford naphthalene **12** (4.77 g, 21.7 mmol, 93%) as a slightly yellow solid. Compound **12** has been reported in the literature.[169]

Data for 12: R_f: 0.18 (hexanes:EtOAc 3:1); **^{1}H NMR (300 MHz, $CDCl_3$):** δ = 9.24 (s, 1H), 6.55 (d, J = 2.4 Hz, 1H), 6.51 (d, J = 2.2 Hz, 1H), 6.37 (d, J = 2.4 Hz, 1H), 6.27 (d, J = 2.2 Hz, 1H), 5.60 (s, 1H), 3.97 (s, 3H), 3.84 (s, 3H) ppm; **^{13}C NMR (75 MHz, $CDCl_3$):** δ = 158.5, 157.6, 156.4, 155.8, 138.7, 106.4, 101.3, 99.8, 98.6, 95.7, 56.2, 55.5 ppm; **IR (ATR):** ν_{max} = 3429 (w), 3401 (w), 3246 (w), 2996 (w), 2921 (w), 2841 (w), 1636 (m), 1609 (m), 1544 (w), 1526 (w), 1487 (m), 1452 (m), 1435 (w), 1397 (m), 1385 (s), 1307 (m), 1274 (m), 1243 (m), 1205 (m), 1159 (s), 1148 (s), 1127 (s), 1085 (m), 1054 (m), 1043 (m), 1007 (s), 936 (m), 857 (m), 836 (s), 806 (s), 768 (m), 751 (w), 725 (m) cm^{-1}; **melting point:** 124.1 – 125.5 °C (lit.:119 – 122 °C)[155]; **HRMS (EI):** calc. for $C_{12}H_{12}O_4$ $[M]^+$: 220.0730, found: 220.0731.

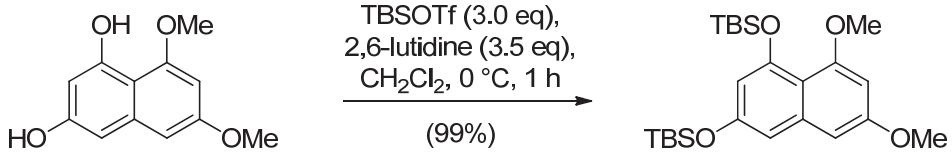

12 **13**

1,3-Dimethoxy-6,8-bis(*tert*-butyldimethylsilyloxy)naphthalene (13) To a stirred solution of naphthalene **12** (200 mg, 908 µmol, 1.0 eq) in CH_2Cl_2 (9 mL) at 0 °C was added 2,6-lutidine (368 µL, 3.18 mmol, 3.5 eq) and TBSOTf (626 µL, 2.72 mmol, 3.0 eq) and the resulting reaction mixture was stirred at 0 °C for 1 h. The reaction was quenched by addition

of H_2O (30 mL) followed by extraction with CH_2Cl_2 (3 × 20 mL). The combined organic layers were washed with brine (30 mL) and dried over Na_2SO_4. After filtration and concentration *in vacuo*, the crude product was purified by flash column chromatography (hexanes:EtOAc 40:1) on silica to afford protected naphthalene **13** (403 mg, 898 µmol, 99%) as a white solid.

Data for 13: R_f: 0.83 (hexanes:EtOAc 4:1); **^{1}H NMR (600 MHz, $CDCl_3$):** δ = 6.69 (d, J = 2.3 Hz, 1H), 6.52 (d, J = 2.3 Hz, 1H), 6.29 − 6.28 (m, 2H), 3.86 (s, 3H), 3.84 (s, 3H), 1.04 (s, 9H), 1.00 (s, 9H), 0.22 (s, 6H), 0.22 (s, 6H) ppm; **^{13}C NMR (150 MHz, $CDCl_3$):** δ = 158.5, 158.4, 154.5, 153.8, 139.1, 111.5, 109.5, 108.8, 97.8, 96.3, 55.3, 55.2, 26.1, 25.9, 18.7, 18.5, −4.1 (2C) ppm; **IR (ATR):** ν_{max} = 3000 (w), 2956 (w), 2929 (w), 2897 (w), 2857 (w), 1619 (m), 1602 (m), 1586 (m), 1504 (w), 1463 (m), 1453 (w), 1425 (w), 1380 (m), 1278 (m), 1255 (m), 1203 (m), 1163 (s), 1157 (s), 1122 (m), 1054 (m), 1019 (m), 1005 (m), 941 (m), 874 (s), 828 (s), 815 (s), 779 (s), 719 (m), 698 (m), 666 (m) cm^{-1}; **melting point:** 57.7 – 58.3 °C; **HRMS (ESI):** calc. for $C_{24}H_{41}O_4Si_2$ $[M+H]^+$: 449.2538, found: 449.2546.

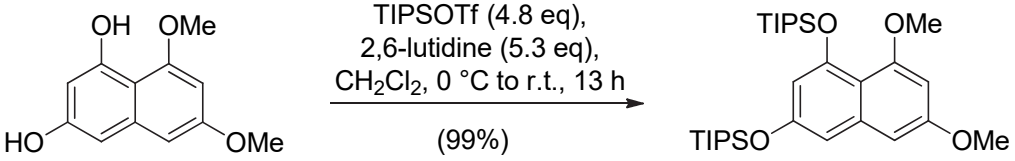

12 **14**

1,3-Dimethoxy-6,8-bis(triisopropylsilyloxy)naphthalene (14) To a stirred solution of naphthalene **12** (4.77 g, 21.7 mmol, 1.0 eq) in CH_2Cl_2 (200 mL) at 0 °C was added 2,6-lutidine (11.3 mL, 97.7 mmol, 4.5 eq) and TIPSOTf (23.3 mL, 86.8 mmol, 4.0 eq). The resulting reaction mixture was allowed to warm up to r.t. over 12 h followed by addition of 2,6-lutidine (2.01 mL, 17.4 mmol, 0.8 eq) and TIPSOTf (4.67 mL, 17.4 mmol, 0.8 eq). The reaction was quenched after additional 45 min of stirring by addition of H_2O (500 mL) followed by extraction with CH_2Cl_2 (3 × 200 mL). The combined organic layers were washed with brine (200 mL) and dried over Na_2SO_4. After filtration and concentration *in vacuo*, the crude product was purified by flash column chromatography (hexanes:Et_2O 40:1) on silica to afford protected naphthalene **14** (11.4 g, 21.4 mmol, 99%) as a colorless oil which turned into a white solid in the freezer (−25 °C).

Data for 14: R_f: 0.87 (hexanes:EtOAc 4:1); **^{1}H NMR (600 MHz, $CDCl_3$):** δ = 6.70 (d, J = 2.3 Hz, 1H), 6.50 (d, J = 2.3 Hz, 1H), 6.33 (d, J = 2.3 Hz, 1H), 6.27 (d, J = 2.3 Hz, 1H), 3.86 (s, 3H), 3.83 (s, 3H), 1.36 – 1.24 (m, 6H), 1.13 – 1.11 (m, 36H) ppm; **^{13}C NMR (150 MHz,**

$CDCl_3$): δ = 158.8, 158.3, 154.9, 154.5, 139.1, 111.2, 108.5, 108.2, 97.7, 96.0, 55.3, 55.2, 18.2, 18.1, 13.5, 12.9 ppm; **IR (ATR):** ν_{max} = 2944 (m), 2892 (m), 2861 (m), 1619 (m), 1604 (m), 1578 (m), 1506 (w), 1463 (m), 1423 (w), 1380 (s), 1348 (m), 1278 (m), 1257 (m), 1205 (m), 1197 (m), 1185 (m), 1171 (s), 1157 (s), 1124 (m), 1056 (s), 1021 (m), 1013 (m), 997 (m), 943 (m), 922 (w), 880 (s), 858 (s), 842 (m), 813 (m), 785 (s), 775 (m), 727 (w), 680 (s) cm^{-1}; **melting point:** 57.1 – 57.7 °C; **HRMS (ESI):** calc. for $C_{30}H_{53}O_4Si_2$ $[M+H]^+$: 533.3477, found: 533.3485.

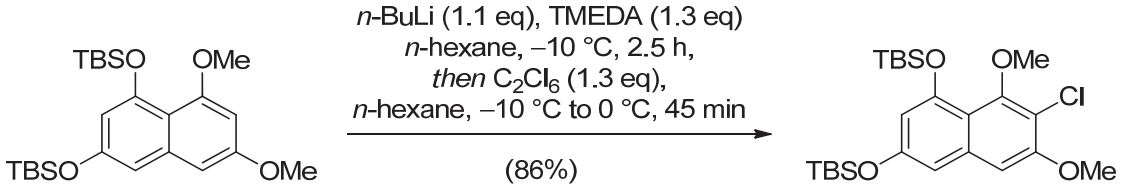

13 **15**

2-Chloro-1,3-dimethoxy-6,8-bis(*tert*-butyldimethylsilyloxy)naphthalene (15) To a stirred solution of protected naphthalene **13** (750 mg, 1.67 mmol, 1.0 eq) in *n*-hexane (15 mL) at −10 °C was added TMEDA (327 µL, 2.17 mmol, 1.3 eq) and *n*-BuLi (2.4 M in *n*-hexane, 770 µL, 1.84 mmol, 1.1 eq). The resulting reaction mixture was stirred at −10 °C for 2.5 h followed by dropwise addition of C_2Cl_6 (514 mg, 2.17 mmol, 1.3 eq) dissolved in *n*-hexane (4 ml). The reaction was allowed to warm up to 0 °C over 45 min before quenching the reaction by addition of H_2O (50 mL) followed by extraction with Et_2O (3 × 100 mL). The combined organic layers were washed with brine (100 mL) and dried over Na_2SO_4. After filtration and concentration *in vacuo*, the crude product was purified by flash column chromatography (hexanes:Et_2O 100:1) on silica to afford chloride **15** (697 mg, 1.44 mmol, 86%) as a colorless oil which turned into a white solid in the freezer (−25 °C).

Data for 15: R_f: 0.73 (hexanes:Et_2O 8:1); **^{1}H NMR (400 MHz, CD_3CN):** δ = 7.02 (s, 1H), 6.85 (d, J = 2.3 Hz, 1H), 6.43 (d, J = 2.3 Hz, 1H), 3.92 (s, 3H), 3.77 (s, 3H), 1.01 (s, 9H), 1.00 (s, 9H), 0.24 (s, 6H), 0.24 (s, 6H) ppm; **^{13}C NMR (100 MHz, CD_3CN):** δ = 155.4, 154.7, 154.5, 153.4, 137.7, 115.6, 114.7, 111.2, 109.6, 103.7, 62.2, 56.8, 26.5, 26.0, 19.5, 18.9, −3.8, −4.1 ppm; **IR (ATR):** ν_{max} = 2956 (m), 2930 (m), 2889 (w), 2859 (m), 1614 (s), 1596 (m), 1571 (m), 1469 (w), 1463 (w), 1380 (s), 1339 (m), 1251 (s), 1197 (m), 1181 (m), 1164 (m), 1101 (m), 1022 (w), 1004 (w), 947 (w), 877 (s), 836 (s), 781 (m) cm^{-1}; **melting point:** 71.6 – 72.7 °C; **HRMS (ESI):** calc. for $C_{24}H_{40}ClO_4Si_2$ $[M+H]^+$: 483.2148, found: 483.2151.

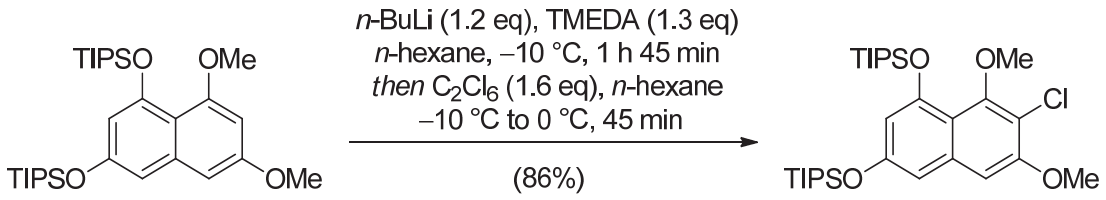

14 **16**

2-Chloro-1,3-dimethoxy-6,8-bis(triisopropylsilyloxy)naphthalene (16) To a stirred solution of protected naphthalene **14** (2.50 g, 4.69 mmol, 1.0 eq) in *n*-hexane (50 mL) at −10 °C was added TMEDA (920 µL, 6.10 mmol, 1.3 eq) and *n*-BuLi (2.85 M in *n*-hexane, 1.98 mL, 5.63 mmol, 1.2 eq). The resulting reaction mixture was stirred at −10 °C for 1 h 45 min followed by dropwise addition of C_2Cl_6 (1.78 g, 7.50 mmol, 1.6 eq) dissolved in *n*-hexane (5 ml). The reaction was allowed to warm up to 0 °C over 45 min before quenching by addition of H_2O (100 mL) followed by extraction with Et_2O (3 × 100 mL). The combined organic layers were washed with brine (100 mL) and dried over Na_2SO_4. After filtration and concentration *in vacuo*, the crude product was purified by flash column chromatography on a Biotage Isolera One automated purification system (normal phase HP Ultra 100 g column, solvent A: hexanes, solvent B: 5% Et_2O/hexanes, starting gradient: 7% B, end gradient: 33% B, over 16 column volumes) to afford chloride **16** (2.29 g, 4.04 mmol, 86%) as a white solid.

Data for 16: R_f: 0.49 (hexanes:Et_2O 20:1); **^{1}H NMR (400 MHz, C_6D_6):** δ = 7.01 (d, *J* = 2.3 Hz, 1H), 6.79 (d, *J* = 2.3 Hz, 1H), 6.63 (s, 1H), 3.78 (s, 3H), 3.31 (s, 3H), 1.49 – 1.28 (m, 6H), 1.20 – 1.14 (m, 36H) ppm; **^{13}C NMR (100 MHz, C_6D_6):** *δ* = 155.2, 154.9, 154.8, 153.9, 137.2, 116.2, 114.6, 109.7, 108.8, 102.7, 61.6, 55.5, 18.3, 18.2, 13.9, 13.2 ppm; **IR (ATR):** ν_{max} = 2944 (m), 2892 (w), 2867 (m), 1612 (s), 1597 (w), 1568 (m), 1491 (w), 1463 (m), 1426 (w), 1412 (w), 1380 (s), 1339 (s), 1271 (w), 1249 (s), 1198 (m), 1185 (m), 1166 (s), 1102 (s), 1072 (w), 1024 (m), 1015 (m), 1002 (m), 948 (w), 920 (w), 881 (s), 862 (s), 819 (s), 786 (w), 757 (m), 685 (s), 659 (m) cm^{-1}; **melting point:** 75.1 – 75.8 °C; **HRMS (ESI):** calc. for $C_{30}H_{52}ClO_4Si_2$ $[M+H]^+$: 567.3087, found: 567.3091.

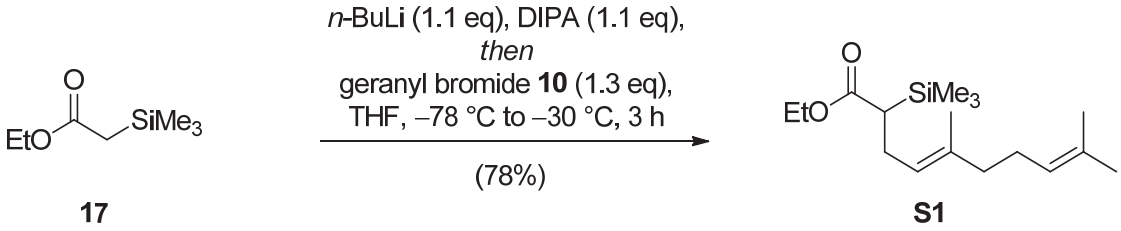

Silylacetate S1 To a stirred solution of DIPA (2.89 mL, 20.6 mmol, 1.1 eq) in THF (40 mL) at –78 °C was added *n*-BuLi (2.4 M in *n*-hexane, 8.57 mL, 20.6 mmol, 1.1 eq) dropwise. The cooling bath was removed for 10 min followed by recooling to –78 °C. Ethyl trimethylsilylacetate (**17**, 3.42 ml, 18.7 mmol, 1.0 eq) was added dropwise over 8 min and the resulting reaction mixture was stirred for 1 h followed by addition of geranyl bromide (**10**, 4.83 mL, 24.3 mmol, 1.3 eq) dissolved in THF (10 mL). The reaction mixture was allowed to warm up to –30 °C over 3 h. The reaction was quenched by addition of sat. aq. NH_4Cl solution (25 mL) and H_2O (25 mL) followed by extraction with Et_2O (3 × 100 mL). The combined organic layers were washed with brine (80 mL) and dried over Na_2SO_4. After filtration and concentration *in vacuo*, the crude product was purified by flash column chromatography (hexanes:Et_2O 80:1) on silica to afford silylacetate **S1** (4.29 g, 14.5 mmol, 78%) as a colorless oil.

Data for S1: R_f: 0.51 (hexanes:EtOAc 20:1); **^{1}H NMR (300 MHz, $CDCl_3$):** δ = 5.16 – 5.02 (m, 2H), 4.09 (q, *J* = 7.2 Hz, 2H), 2.53 – 2.38 (m, 1H), 2.20 – 1.89 (m, 6H), 1.67 (s, 3H), 1.61 (s, 3H), 1.59 (s, 3H), 1.23 (t, *J* = 7.5 Hz, 3H), 0.08 (s, 9H) ppm; **^{13}C NMR (75 MHz, $CDCl_3$):** δ = 176.9, 136.1, 131.5, 124.5, 121.8, 59.9, 41.7, 40.2, 30.2, 26.7, 25.8, 17.8, 16.4, 14.6, −2.1 ppm; **IR (ATR):** ν_{max} = 2962 (w), 2915 (w), 2856 (w), 1716 (s), 1445 (w), 1376 (w), 1365 (w), 1329 (w), 1296 (w), 1250 (m), 1191 (m), 1139 (s), 1047 (w), 1009 (w), 984 (w), 839 (s), 756 (w), 738 (m), 695 (m) cm^{-1}; **HRMS (ESI):** calc. for $C_{17}H_{33}O_2Si$ $[M+H]^+$: 297.2244, found: 297.2248.

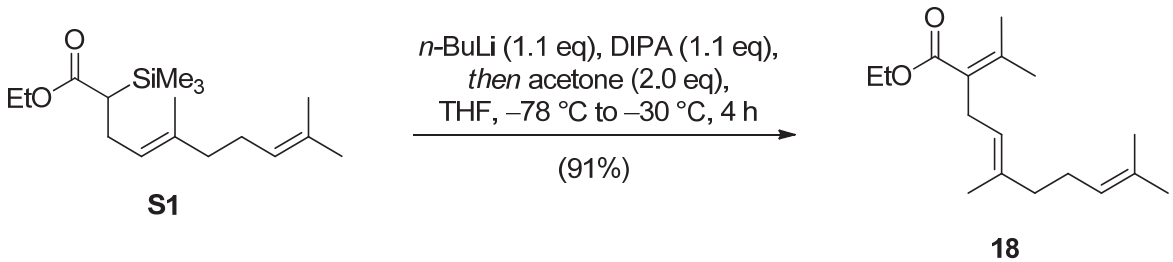

Ethyl ester 18 To a stirred solution of DIPA (2.07 mL, 14.7 mmol, 1.1 eq) in THF (40 mL) at –78 °C was added *n*-BuLi (2.5 M in *n*-hexane, 5.89 mL, 14.7 mmol, 1.1 eq) dropwise. The cooling bath was removed for 10 min followed by recooling to –78 °C. Silylacetate **S1** (3.97 g, 13.4 mmol, 1.0 eq) in THF (10 mL) was added dropwise over 15 min and the resulting

reaction mixture was stirred for 1 h followed by the addition of acetone (1.96 mL, 26.8 mmol, 2.0 eq) dissolved in THF (2 mL). The reaction mixture was allowed to warm up to –30 °C over 4 h. The reaction was quenched by addition of sat. aq. NH_4Cl solution (30 mL) and H_2O (30 mL) followed by extraction with Et_2O (3 × 60 mL). The combined organic layers were washed with brine (50 mL) and dried over Na_2SO_4. After filtration and concentration *in vacuo*, the crude product was purified by flash column chromatography (hexanes:Et_2O 80:1) on silica to afford ethyl ester **18** (3.23 g, 12.2 mmol, 91%) as a colorless oil.

Data for 18: R_f: 0.50 (hexanes:EtOAc 20:1); **^{1}H NMR (300 MHz, $CDCl_3$):** δ = 5.11 – 5.00 (m, 2H), 4.17 (q, J = 7.1 Hz, 2H), 3.00 (d, J = 7.7 Hz, 2H), 2.12 – 1.91 (m, 7H), 1.81 (s, 3H), 1.67 (s, 3H), 1.65 (s, 3H), 1.59 (s, 3H), 1.28 (t, J = 7.1 Hz, 3H) ppm; **^{13}C NMR (75 MHz, $CDCl_3$):** δ = 169.8, 141.8, 135.8, 131.5, 127.4, 124.4, 121.8, 60.1, 39.9, 29.0, 26.8, 25.8, 23.1, 22.0, 17.8, 16.2, 14.5 ppm; **IR (ATR):** ν_{max} = 2978 (w), 2916 (m), 2856 (w), 1711 (s), 1633 (w), 1444 (m), 1375 (m), 1300 (m), 1278 (m), 1251 (w), 1206 (s), 1170 (s), 1066 (s), 1024 (w), 985 (w), 949 (w), 841 (m), 778 (w), 696 (w) cm^{-1}; **HRMS (EI):** calc. for $C_{17}H_{28}O_2$ $[M]^+$: 264.2089, found: 264.2083.

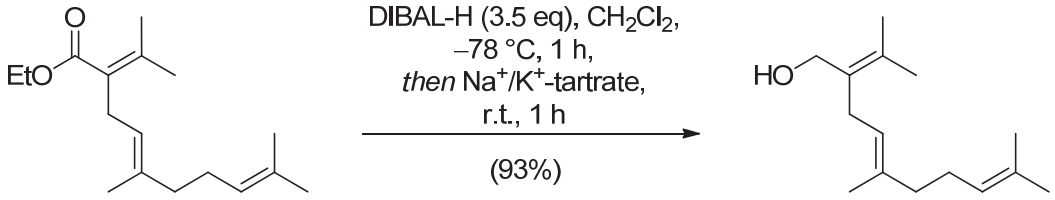

18 **S2**

Alcohol S2 To a stirred solution of ethyl ester **18** (3.20 g, 12.1 mmol, 1.0 eq) in CH_2Cl_2 (80 mL) at –78 °C was added DIBAL-H (1.0 M in CH_2Cl_2, 42.4 mL, 42.4 mmol, 3.5 eq) dropwise over 30 min. The resulting reaction mixture was stirred for 1 h followed by addition of sat. aq. Na^+/K^+-tartrate solution (450 mL) and H_2O (300 mL). The mixture was stirred vigorously for 1 h at r.t. whereupon the layers were separated and the aqueous phase was extracted with CH_2Cl_2 (3 × 300 mL). The combined organic layers were washed with brine (300 mL) and dried over Na_2SO_4. After filtration and concentration *in vacuo*, the crude product was purified by flash column chromatography (hexanes:Et_2O 10:1) on silica to afford alcohol **S2** (2.51 g, 11.3 mmol, 93%) as a colorless oil.

Data for S2: R_f: 0.28 (hexanes:EtOAc 10:1); **^{1}H NMR (300 MHz, $CDCl_3$):** δ = 5.14 – 5.02 (m, 2H), 4.11 (s, 2H), 2.87 (d, J = 7.0 Hz, 2H), 2.17 – 1.92 (m, 4H), 1.77 (s, 3H), 1.72 (s, 3H), 1.68 (s, 6H), 1.60 (s, 3H), 1.17 (br s, 1H) ppm; **^{13}C NMR (75 MHz, $CDCl_3$):** δ = 136.0, 131.7,

131.6, 130.2, 124.4, 122.9, 62.6, 39.9, 29.9, 26.8, 25.8, 20.7, 20.4, 17.8, 16.2 ppm; **IR (ATR):** ν_{max} = 3316 (br m), 2966 (m), 2914 (m), 2853 (m), 2722 (w), 1659 (w), 1442 (m), 1375 (m), 1328 (w), 1263 (w), 1236 (w), 1177 (w), 1141 (w), 1108 (w), 1076 (w), 994 (s), 927 (w), 887 (w), 832 (m), 778 (w), 739 (w), 723 (w) cm^{-1}; **HRMS (EI):** calc. for $C_{15}H_{26}O$ $[M]^+$: 222.1978, found: 222.1985.

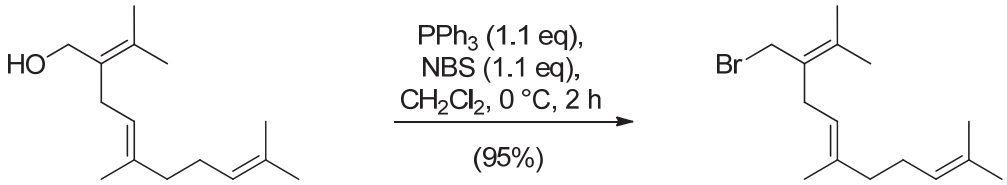

S2 **19**

Bromide 19 To a stirred solution of alcohol **S2** (200 mg, 899 µmol, 1.0 eq) in CH_2Cl_2 (10 mL) at 0 °C was added PPh_3 (259 mg, 987 µmol, 1.1 eq) and NBS (176 mg, 989 µmol, 1.1 eq). The resulting reaction mixture was stirred for 2 h. The reaction was quenched by addition of H_2O (25 mL) followed by extraction with CH_2Cl_2 (3 × 15 mL) and combined organic layers were dried over Na_2SO_4. After filtration and concentration *in vacuo* crude product was purified by filtration over neutral Davisil® (Et_2O) to afford bromide **19** (244 mg, 855 µmol, 95%) as a slightly yellow oil. Due to its instability on silica and neutral aluminium oxide, bromide **19** was used without further purification. Compound **19** was synthesized previously.[156]

Data for 19: R_f: 0.90 (hexanes:Et_2O 10:1, slow degradation on silica plate); **^{1}H NMR (300 MHz, C_6D_6):** δ = 5.22 – 5.08 (m, 2H), 3.93 (s, 2H), 2.92 (d, J = 7.3 Hz, 2H), 2.20 – 2.00 (m, 4H), 1.66 (s, 3H), 1.65 (s, 3H), 1.55 (s, 3H), 1.50 (s, 3H), 1.46 (s, 3H) ppm; **^{13}C NMR (75 MHz, C_6D_6):** δ = 136.5, 133.4, 131.3, 129.4, 124.8, 122.7, 40.2, 34.5, 30.0, 27.1, 25.9, 20.8, 20.4, 17.8, 16.2 ppm; **IR (ATR):** ν_{max} = 2967 (m), 2914 (s), 2855 (m), 2728 (w), 1650 (w), 1597 (w), 1441 (s), 1375 (s), 1330 (w), 1272 (w), 1201 (s), 1167 (w), 1100 (m), 1080 (w), 1044 (w), 983 (w), 951 (w), 895 (m), 829 (m), 777 (w), 743 (w), 715 (w), 665 (m) cm^{-1}; **HRMS (EI):** calc. for $C_{15}H_{24}{}^{79}Br$ $[M\text{-}H]^+$: 283.1056, found: 283.1043.

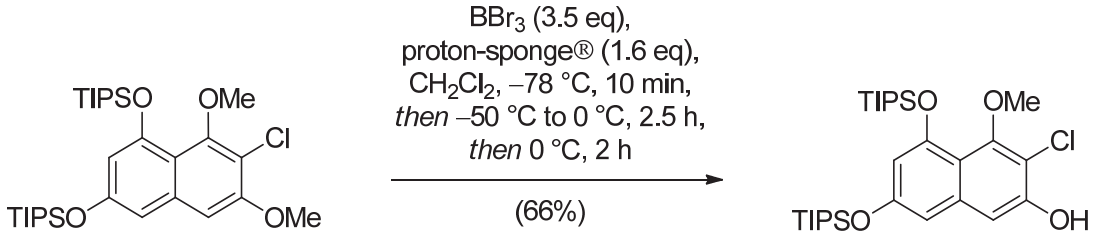

16 **22**

Naphthol 22 To a stirred solution of chloride **16** (600 mg, 1.06 mmol, 1.0 eq) and proton-sponge® (362 mg, 1.69 mmol, 1.6 eq) in CH_2Cl_2 (20 mL) at −78 °C was added BBr_3 (1.0 M in CH_2Cl_2, 3.71 mL, 3.71 mmol, 3.5 eq) dropwise. The resulting reaction mixture was stirred at −78 °C for 10 min and was then allowed to warm up from −50 °C to 0 °C over 2.5 h. After additional stirring for 2 h at 0 °C the reaction was diluted with CH_2Cl_2 (20 mL) and cannulated to a stirred sat. aq. $NaHCO_3$ solution (300 mL) followed by extraction with CH_2Cl_2 (4 × 100 mL). The combined organic layers were dried over Na_2SO_4. After filtration and concentration *in vacuo*, the crude product was evaporated from MeOH (2 × 10 mL) and filtered over a short plug of silica (hexanes:EtOAc 1:1). The resulting crude product was purified by flash column chromatography (hexanes:EtOAc 80:1→20:1) on silica to afford naphthol **22** (388 mg, 701 µmol, 66%) as a slightly rose solid.

Data for 22: R_f: 0.50 (hexanes:EtOAc 9:1); **^{1}H NMR (400 MHz, C_6D_6):** δ = 6.99 (s, 1H), 6.86 (d, J = 2.3 Hz, 1H), 6.72 (d, J = 2.3 Hz, 1H), 5.33 (s, 1H), 3.66 (s, 3H), 1.45 – 1.34 (m, 3H), 1.32 – 1.20 (m, 3H), 1.19 – 1.09 (m, 36H) ppm; **^{13}C NMR (100 MHz, C_6D_6):** δ = 155.3, 154.2, 153.7, 150.7, 137.5, 114.4, 114.1, 109.6, 108.3, 106.6, 61.8, 18.3, 18.2, 13.8, 13.2 ppm; **IR (ATR):** ν_{max} = 3544 (br w), 2946 (s), 2897 (w), 2868 (s), 1625 (m), 1608 (m), 1568 (s), 1493 (w), 1464 (m), 1429 (w), 1382 (s), 1343 (m), 1289 (m), 1255 (w), 1187 (m), 1154 (m), 1118 (w), 1098 (m), 1070 (m), 1014 (m), 997 (w), 965 (w), 918 (w), 882 (m), 864 (m), 826 (m), 787 (w), 759 (w), 688 (w) cm^{-1}; **melting point:** 95.8 – 98.7 °C **HRMS (ESI):** calc. for $C_{29}H_{50}ClO_4Si_2$ $[M+H]^+$: 553.2931, found: 553.2933.

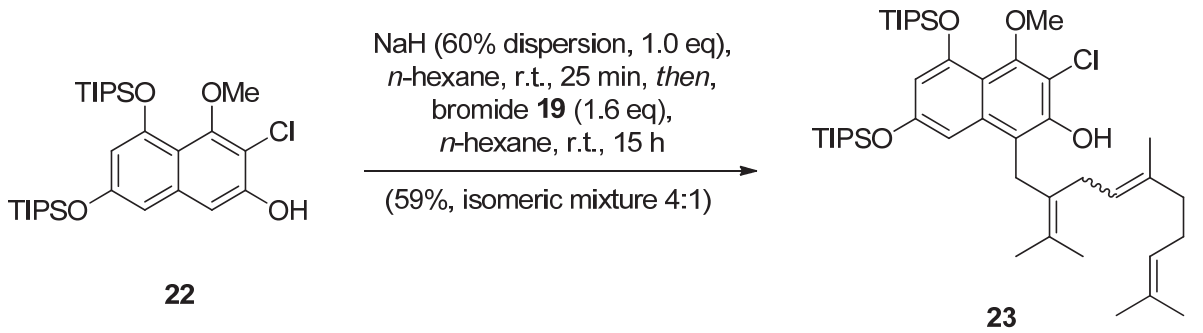

22 **23**

Naphthol 23 To a stirred solution of naphthol **22** (171 mg, 309 µmol, 1.0 eq) in *n*-hexane (3.4 mL) at r.t. was added NaH (60% dispersion in mineral oil, 12.4 mg, 309 µmol, 1.0 eq). The resulting dark purple reaction mixture was stirred for 25 min followed by the addition of bromide **19** (141 mg, 494 µmol, 1.6 eq). After 15 h at r.t. the reaction was quenched by addition of aq. phosphate buffer (pH = 8.0, 15 ml) followed by extraction with Et_2O (3 × 20 mL) and combined organic layers were dried over Na_2SO_4. After filtration and concentration *in vacuo*, the crude product was purified by flash column chromatography (hexanes:EtOAc 100:1) on deactivated silica (by NEt_3 flush) to afford naphthol **23** (139 mg, 183 µmol, 59%) in an inseparable 4:1 isomeric mixture as a colorless oil. Compound **23** was stored at −80 °C under argon atmosphere.

Data for 23 (major isomer): R_f: 0.50 (hexanes:EtOAc 20:1); **^{1}H NMR (400 MHz, C_6D_6):** δ = 7.18 (d, *J* = 2.2 Hz, 1H), 6.76 (d, *J* = 2.2 Hz, 1H), 5.74 (s, 1H), 5.20 (t, *J* = 6.9 Hz, 1H), 5.12 (t, *J* = 7.2 Hz, 1H), 3.99 (s, 2H), 3.73 (s, 3H), 2.73 (d, *J* = 6.7 Hz, 2H), 2.10 – 2.02 (m, 2H), 2.00 – 1.93 (m, 2H), 1.91 (s, 3H), 1.77 (s, 3H), 1.67 (s, 3H), 1.56 (s, 3H), 1.47 – 1.37 (m, 3H), 1.36 – 1.26 (m, 6H), 1.22 – 1.16 (m, 36H) ppm; **^{13}C NMR (100 MHz, C_6D_6):** δ = 155.2, 154.1, 152.5, 148.7, 137.4, 134.1, 131.3, 131.0, 125.7, 125.2, 123.9, 115.1, 114.4, 114.1, 109.5, 106.0, 61.8, 40.3, 30.1, 29.9, 27.2, 25.9, 21.1, 20.9, 18.3, 18.3, 17.8, 15.9, 13.8, 13.2 ppm; **IR (ATR):** ν_{max} = 3537 (br w), 2944 (s), 2926 (s), 2867 (s), 1740 (w), 1610 (s), 1572 (s), 1495 (w), 1462 (m), 1428 (m), 1377 (s), 1348 (s), 1285 (s), 1260 (m), 1195 (m), 1164 (s), 1106 (m), 1072 (m), 1035 (m), 1015 (m), 997 (m), 986 (m), 930 (m), 882 (s), 850 (m), 807 (s), 759 (s), 686 (s) cm^{-1}; **HRMS (ESI):** calc. for $C_{44}H_{72}ClO_4Si_2$ $[M\text{-}H]^-$: 755.4663, found: 755.4658.

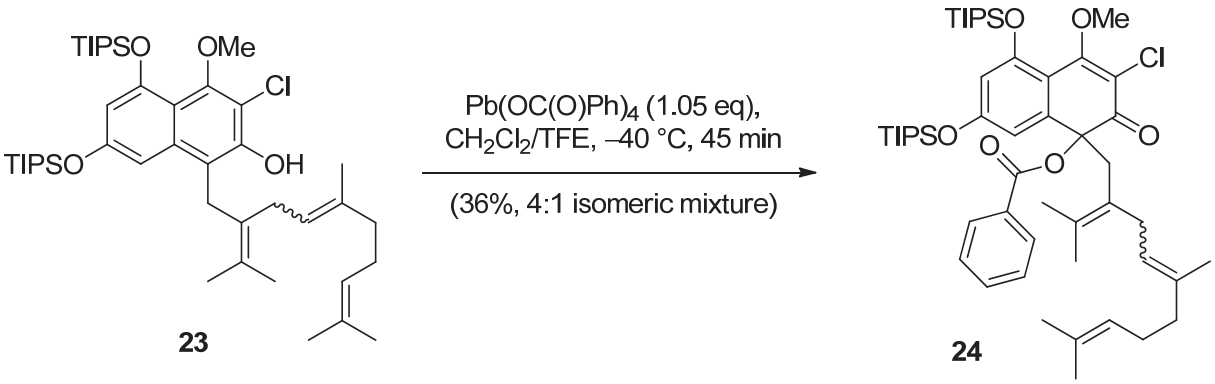

Benzoate 24 Lead(IV) benzoate was prepared from $Pb(OAc)_4$ according to a literature known procedure.[170] To a stirred solution of prenylated naphthol **23** (31.0 mg, 40.9 µmol, 1.0 eq) in CH_2Cl_2/TFE (1:2, 3 mL) at −40 °C was added lead(IV) benzoate (29.8 mg, 43.0 µmol, 1.05 eq) dissolved in CH_2Cl_2/TFE (1:2, 3 mL) by syringe pump over 45 min. The reaction was quenched by addition of sat. aq. NH_4Cl solution (10 mL) followed by extraction with Et_2O (3 × 10 mL) and combined organic layers were dried over Na_2SO_4. After filtration and concentration *in vacuo*, the crude product was purified by flash column chromatography (*n*-pentane:EtOAc 75:1) on silica to afford benzoate **24** (12.9 mg, 14.7 µmol, 36%) in an inseparable 4:1 isomeric mixture as a colorless oil.

Data for 24 (major isomer): R_f: 0.44 (hexanes:EtOAc 10:1); **^{1}H NMR (400 MHz, $CDCl_3$):** δ = 8.05 (d, *J* = 7.1 Hz, 2H), 7.56 (t, *J* = 7.4 Hz, 1H), 7.43 (t, *J* = 7.7 Hz, 2H), 6.53 (d, *J* = 2.4 Hz, 1H), 6.32 (d, *J* = 2.4 Hz, 1H), 5.05 (t, *J* = 6.9 Hz, 1H), 4.92 (t, *J* = 6.8 Hz, 1H), 3.92 (s, 3H), 2.88 (d, *J* = 13.7 Hz, 1H), 2.78 (d, *J* = 13.7 Hz, 1H), 2.59 (d, *J* = 6.6 Hz, 2H), 2.08 – 2.00 (m, 2H), 2.00 – 1.91 (m, 2H), 1.66 (s, 3H), 1.63 (s, 3H), 1.58 (s, 6H), 1.38 (s, 3H), 1.36 – 1.27 (m, 3H), 1.17 – 1.09 (m, 18H), 1.04 – 0.94 (m, 3H), 0.92 – 0.84 (m, 18H) ppm; **^{13}C NMR (100 MHz, $CDCl_3$):** δ = 190.7, 167.3, 164.5, 158.8, 155.5, 144.5, 135.5, 133.3, 133.0, 131.5, 130.0, 129.9, 128.4, 124.8, 124.4, 122.8, 116.3, 112.2, 112.1, 110.8, 84.8, 60.8, 44.0, 39.9, 32.5, 26.8, 25.9, 21.2, 20.9, 18.1, 17.9, 17.7, 16.3, 13.5, 12.6 ppm; **IR (ATR):** ν_{max} = 2943 (s), 2925 (s), 2867 (s), 1730 (m), 1688 (m), 1598 (s), 1582 (s), 1534 (w), 1464 (m), 1447 (m), 1437 (w), 1425 (w), 1385 (w), 1350 (s), 1305 (m), 1273 (s), 1177 (s), 1144 (w), 1089 (m), 1067 (w), 997 (w), 973 (w), 920 (w), 812 (w), 751 (w), 687 (m) cm^{-1}; **HRMS (ESI):** calc. for $C_{51}H_{78}ClO_6Si_2$ $[M+H]^+$: 877.5020, found: 877.5018.

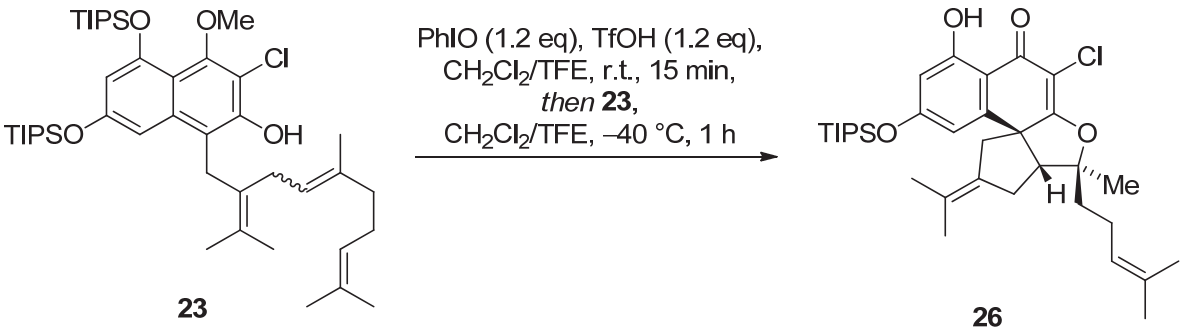

23 **26**

Triisopropylsilyl merochlorin B (26) PhIO was prepared from $PhI(OAc)_2$ by a literature known procedure.[171] To a stirred suspension of PhIO (45.3 mg, 206 µmol, 1.2 eq) in CH_2Cl_2 (10 mL) at room temperature was added TfOH (18.1 µL, 206 µmol, 1.2 eq). After stirring for 15 min a clear solution formed, followed by dilution with TFE (10 mL). The resulting mixture was added to a cloudy solution of prenylated naphthol **23** (130 mg, 172 µmol, 1.0 eq) in CH_2Cl_2/TFE (1:9, 30 mL) at −40 °C by syringe pump over 1 h. The reaction was quenched by addition of sat. aq. NH_4Cl solution (15 mL) and H_2O (15 mL) followed by extraction with Et_2O (3 × 20 mL) and combined organic layers were dried over Na_2SO_4. After filtration and concentration *in vacuo*, the crude product was purified by flash column chromatography (pentane:EtOAc 80:1) on silica to afford crude cyclization product **26** (41.6 mg) inseparable from impurities as pale yellow oil. **26** was used without further purification in the next step.

Data for 26: R_f: 0.41 (hexanes:EtOAc 20:1); **HRMS (ESI):** calc. for $C_{34}H_{50}ClO_4Si$ $[M+H]^+$: 585.3161, found: 585.3158.

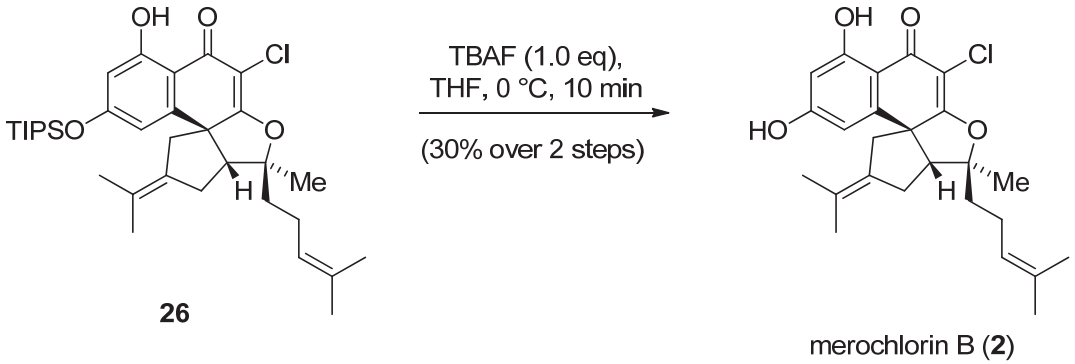

26 merochlorin B (**2**)

Merochlorin B (2) To a stirred solution of ketone **26** (41.6 mg, 71.1 µmol, 1.0 eq) in THF (10 mL) at 0 °C was added TBAF (0.1 M in THF, 0.711 ml, 71.1 µmol, 1.0 eq) and the resulting reaction mixture was stirred for 10 min. The reaction was quenched by addition of H_2O (10 mL) followed by extraction with Et_2O (3 × 10 mL). The combined organic layers were dried over Na_2SO_4. After filtration and concentration *in vacuo*, the crude product was purified by flash column chromatography (pentane:Et_2O 4:1→25:10) on silica to afford merochlorin B (**2**, 21.9 mg, 51.1 µmol, 30% over 2 steps) as pale yellow wax.

Data for merochlorin B (2): R_f: 0.65 (hexanes:EtOAc 3:2); **IR (ATR):** ν_{max} = 3267 (br w), 2974 (w), 2914 (w), 2856 (w), 1643 (m), 1598 (s), 1454 (m), 1383 (w), 1326 (s), 1279 (s), 1238 (m), 1212 (w), 1190 (m), 1160 (m), 1140 (m), 1095 (m), 1063 (s), 1023 (m), 1004 (w), 899 (w), 875 (w), 839 (s), 804 (m), 790 (m), 748 (w), 703 (w), 668 (w) cm^{-1}; **HRMS (ESI):** calc. for $C_{25}H_{30}ClO_4$ $[M+H]^+$: 429.1827, found: 429.1824.

NMR data:[154]

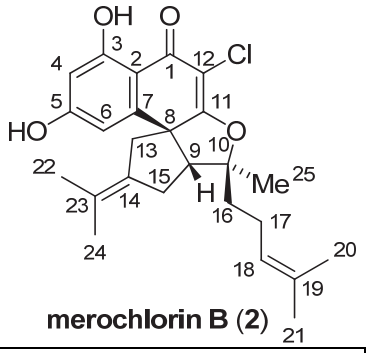

No.	^{1}H NMR Isolation 500 MHz, d_6-DMSO [ppm]	^{1}H NMR Synthetic 400 MHz, d_6-DMSO [ppm]	^{13}C NMR Isolation 125 MHz, d_6-DMSO [ppm]	^{13}C NMR Synthetic 100 MHz, d_6-DMSO [ppm]
1			184.2	184.1
2			105.9	105.9
3			163.8	163.4
4	6.17 (d, *J* = 2.2 Hz, 1H)	6.18 (d, *J* = 2.1 Hz, 1H)	101.3	101.0
5			163.5	163.3
6	6.15 (d, *J* = 2.4 Hz, 1H)	6.16 (d, *J* = 2.2 Hz, 1H)	103.9	103.6
7			147.9	147.7
8			60.2	60.1
9	2.99 (d, *J* = 8.2 Hz, 1H)	3.00 (d, *J* = 7.9 Hz, 1H)	52.2	52.0
10			98.1	97.9
11			176.1	176.0
12			99.9	99.7
13	2.81 (d, *J* = 18.0 Hz, 1H) 2.48 (d, *J* = 18.4 Hz, 1H)	2.82 (d, *J* = 18.6 Hz, 1H) 2.48 (d, *J* = 18.2 Hz, 1H)*	49.3	49.1
14			130.7	130.6
15	2.88 (d, *J* = 18.6 Hz, 1H) 2.72 (d, *J* = 18.0 Hz, 1H)	2.89 (d, *J* = 18.6 Hz, 1H) 2.73 (d, *J* = 18.6 Hz, 1H)	34.6	34.4
16	1.77 – 1.71 (m, 2H)	1.77 – 1.71 (m, 2H)	43.3	43.2
17	2.04 – 1.92 (m, 2H)	2.04 – 1.93 (m, 2H)	22.0	21.9
18	5.05 (t, *J* = 7.5 Hz, 1H)	5.05 (t, *J* = 7.0 Hz, 1H)	123.4	123.3
19			131.5	131.3
20	1.48 (s, 3H)	1.48 (s, 3H)	17.5	17.4
21	1.57 (s, 3H)	1.57 (s, 3H)	25.5	25.4
22	1.48 (s, 3H)	1.48 (s, 3H)	21.4	21.3
23			125.7	125.5
24	1.70 (s, 3H)	1.70 (s, 3H)	21.4	21.3
25	1.41 (s, 3H)	1.41 (s, 3H)	22.3	22.1
5-OH	-	10.55 (br s, 1H)	-	-
3-OH	12.9 (br s, 1H)	12.91 (br s, 1H)	-	-

* This signal partially overlaps with the d_6-DMSO peak. Therefore, the chemical shift and the coupling constant were determined from the COSY and HSQC spectra.

Verification of the relative stereochemistry: NOESY (d_6-DMSO)

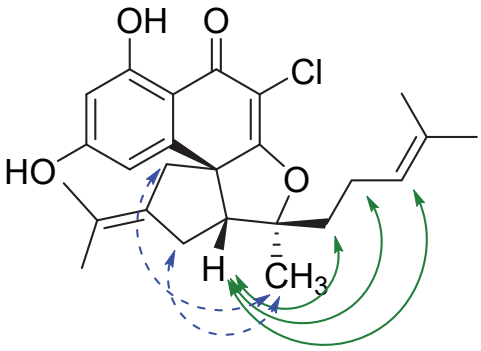

Merochlorin B (**2**)

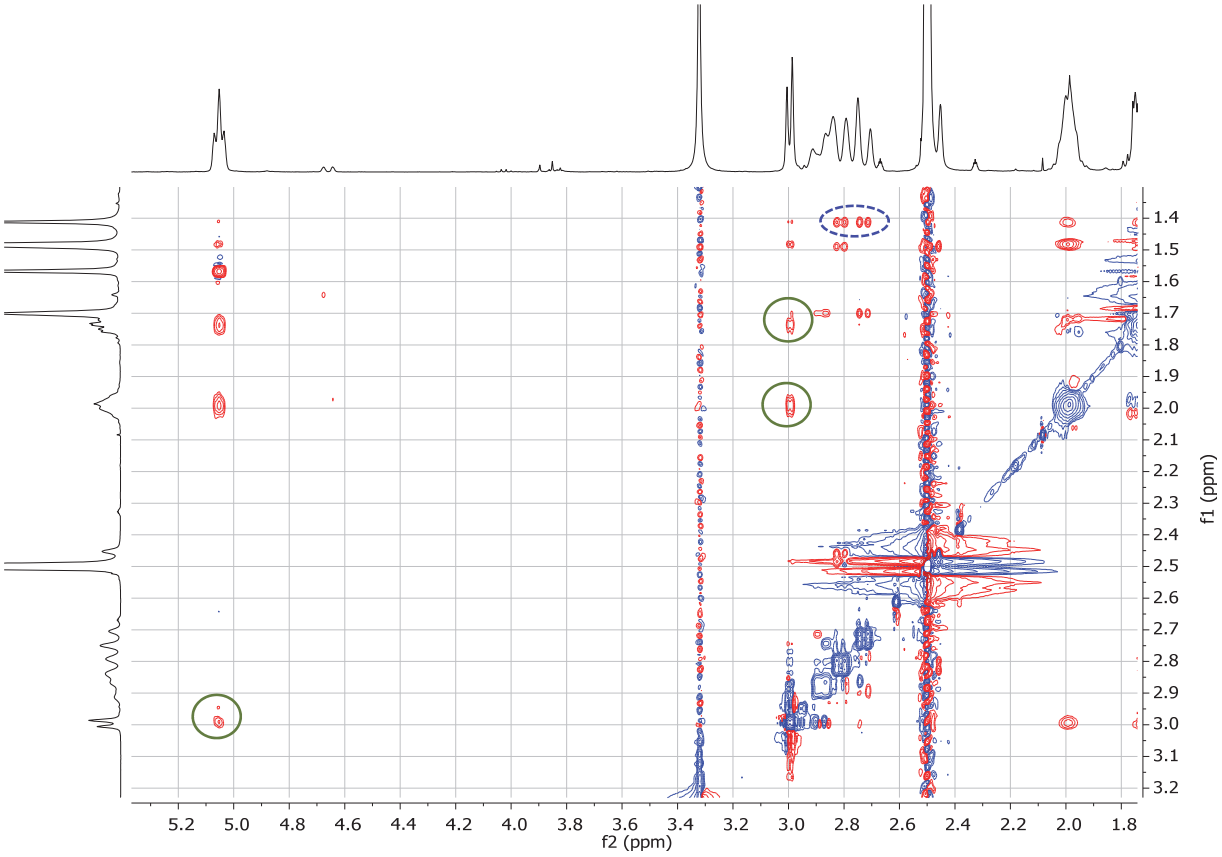

6.4.2 ^{1}H and ^{13}C NMR spectra

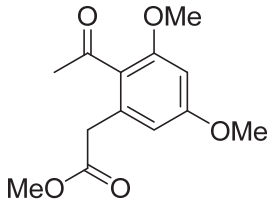

11

300 MHz; $CDCl_3$

75 MHz, $CDCl_3$

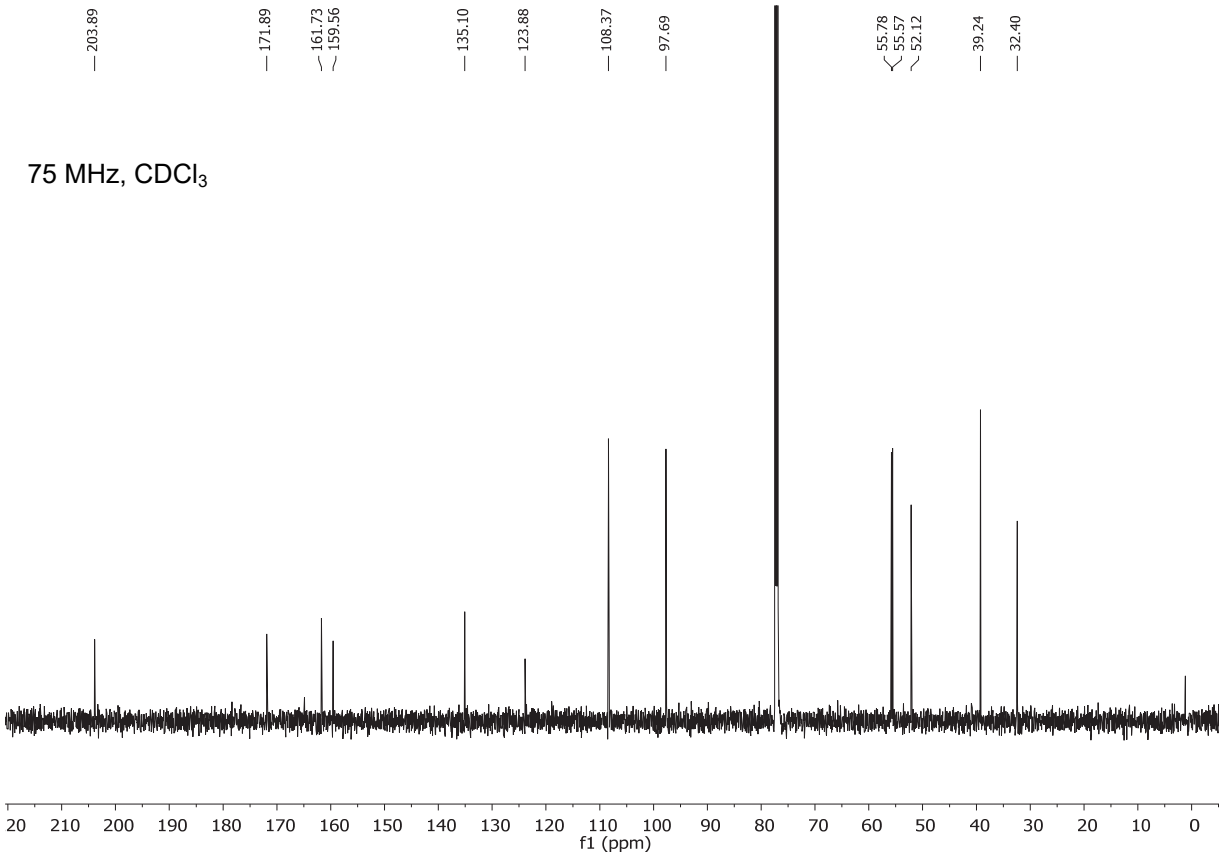

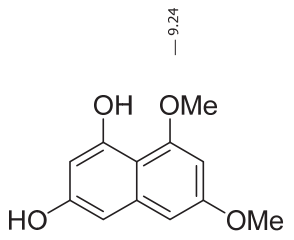

12

300 MHz; $CDCl_3$

75 MHz, $CDCl_3$

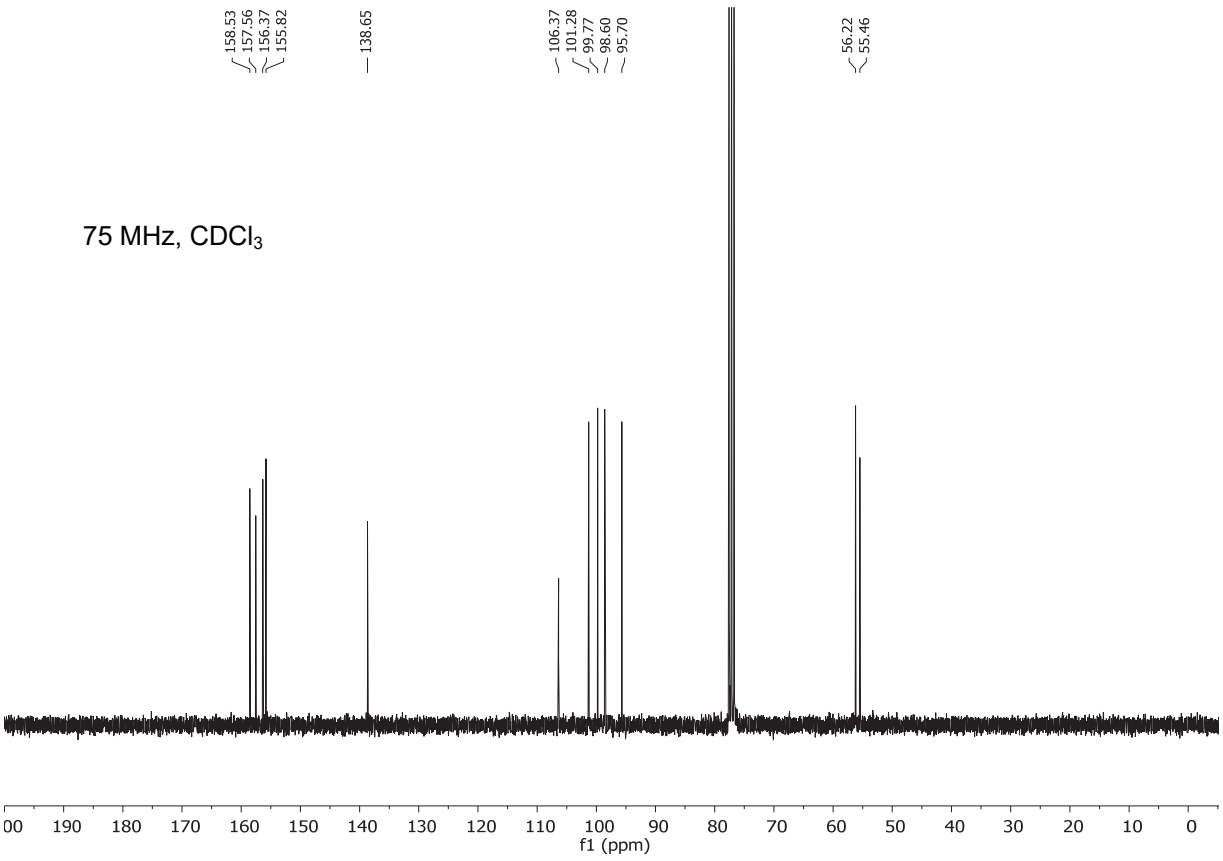

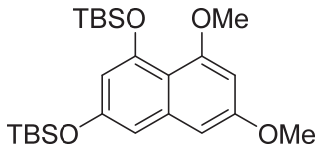

13

600 MHz, $CDCl_3$

150 MHz , $CDCl_3$

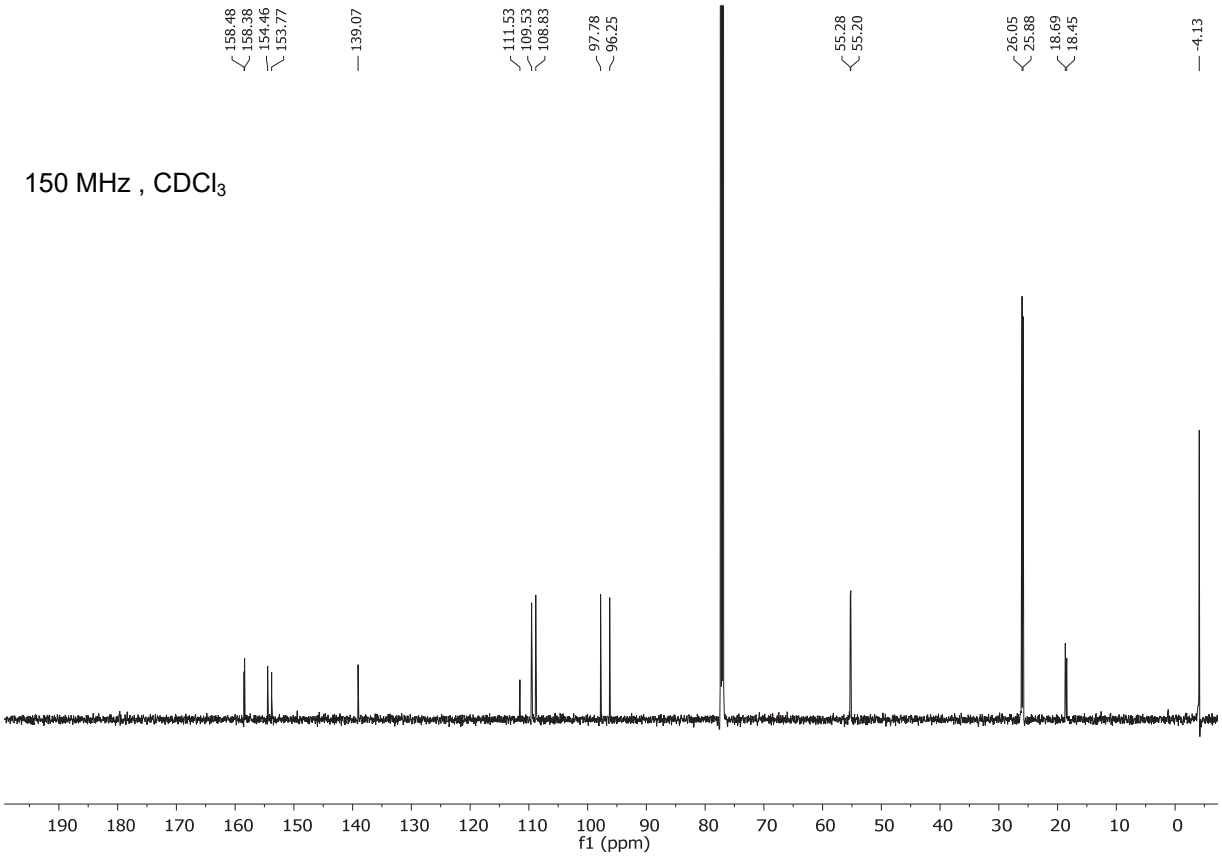

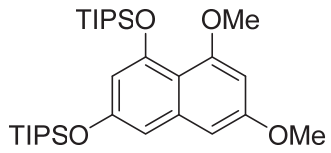

14

600 MHz, $CDCl_3$

150 MHz , $CDCl_3$

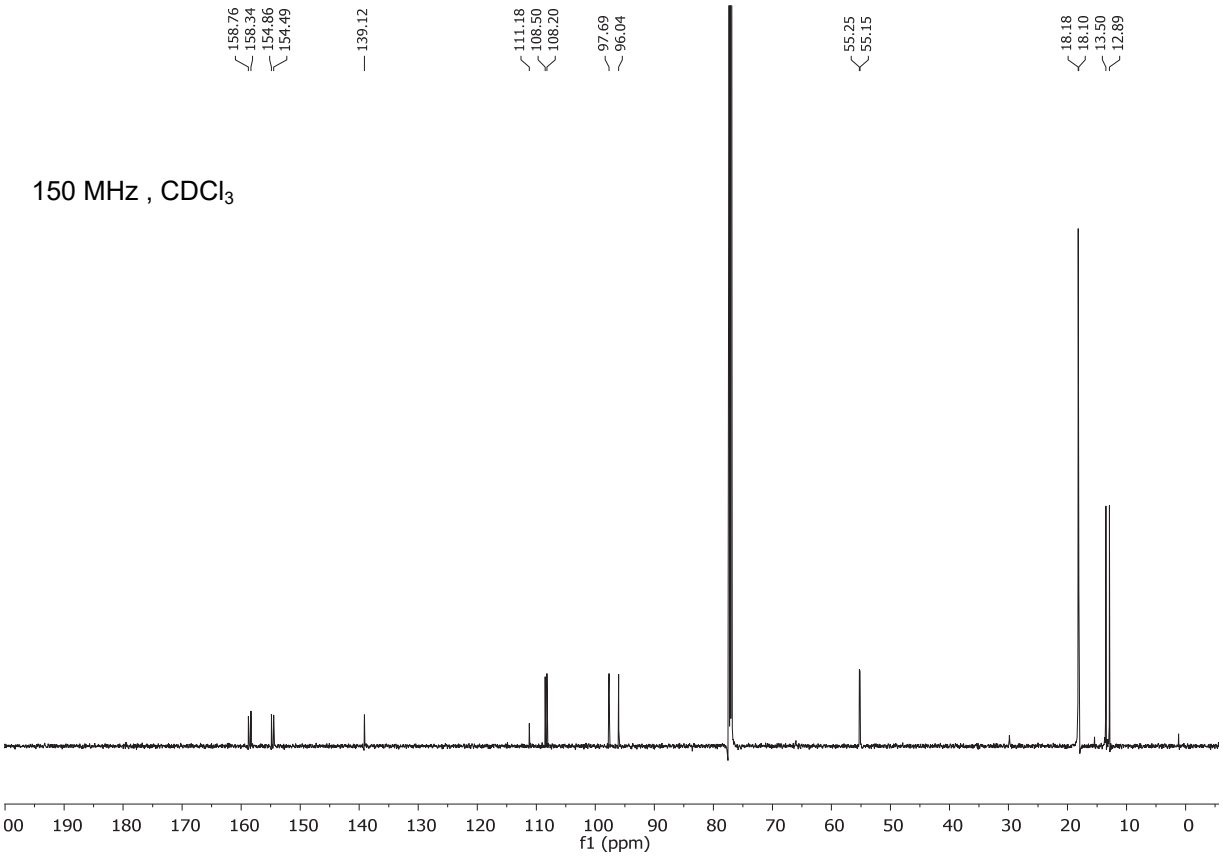

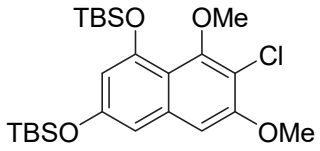

15

400 MHz, CD_3CN

100 MHz, CD_3CN

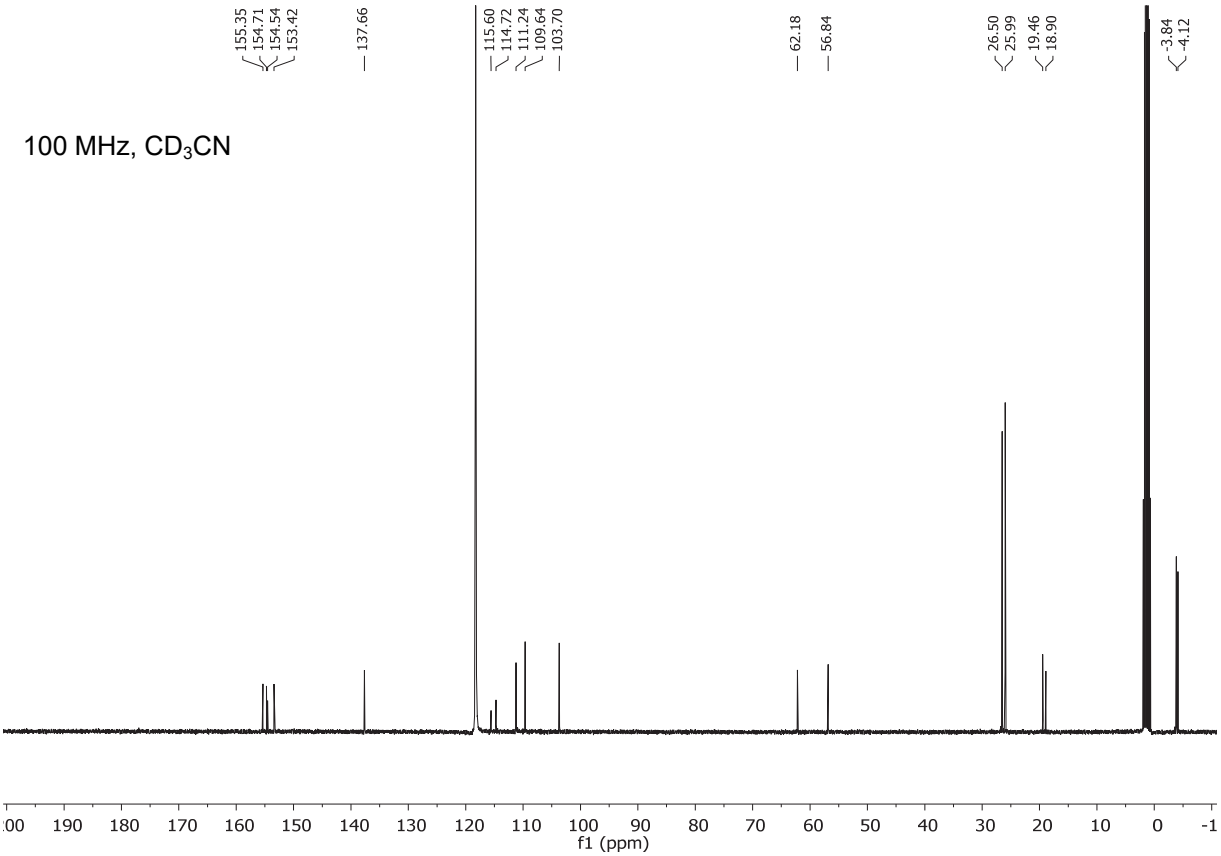

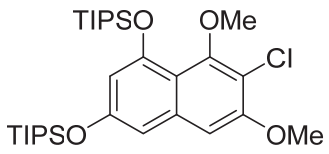

16

400 MHz, C_6D_6

100 MHz, C_6D_6

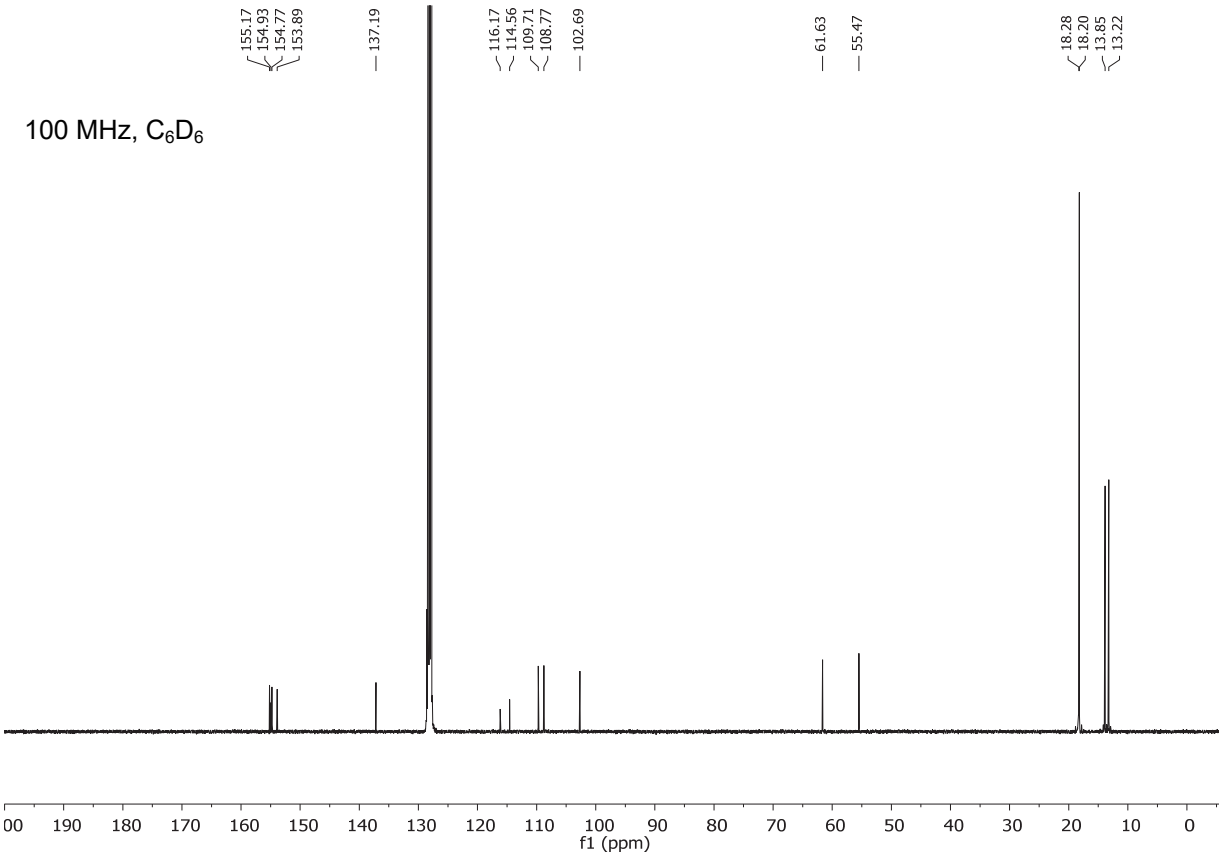

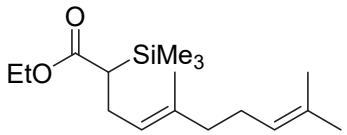

S1

300 MHz, $CDCl_3$

75 MHz, $CDCl_3$

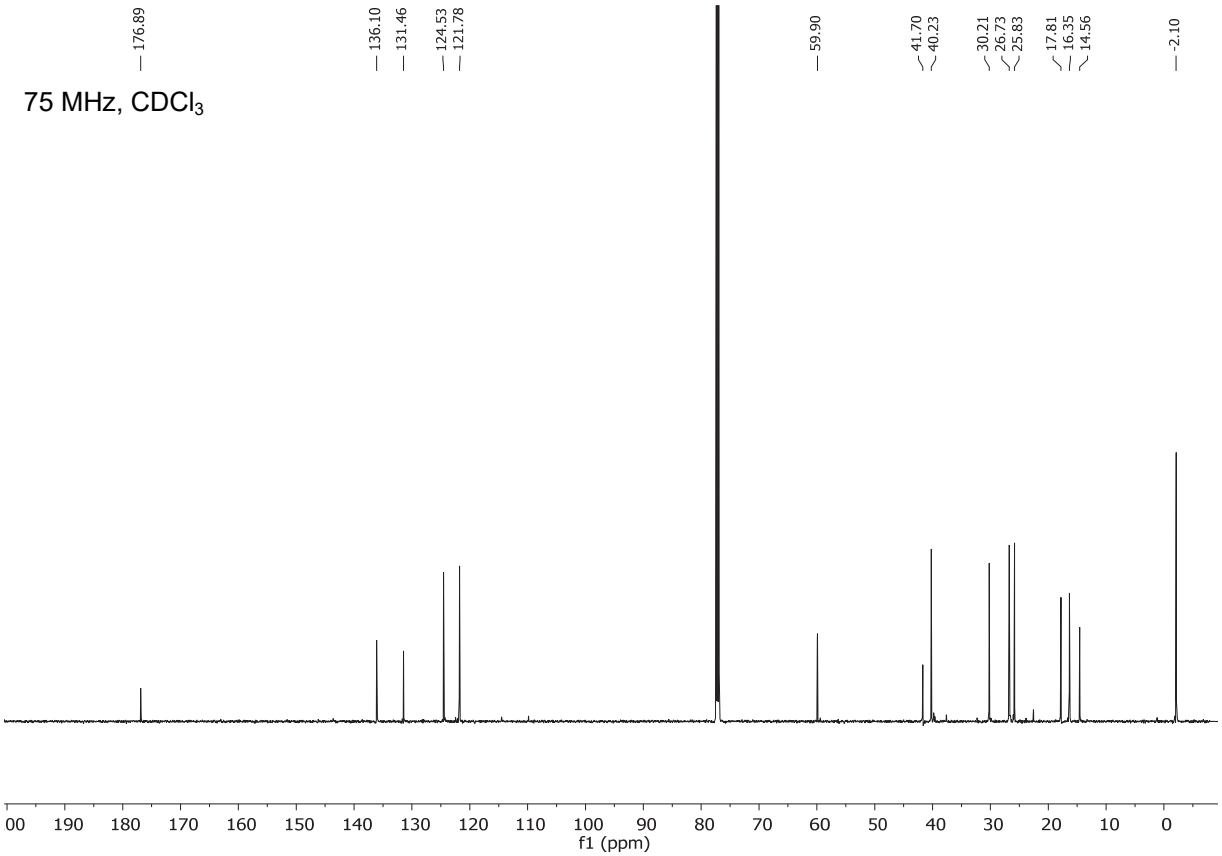

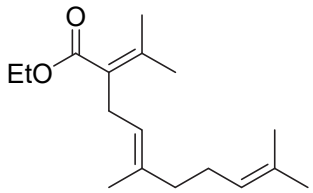

18

300 MHz, $CDCl_3$

75 MHz, $CDCl_3$

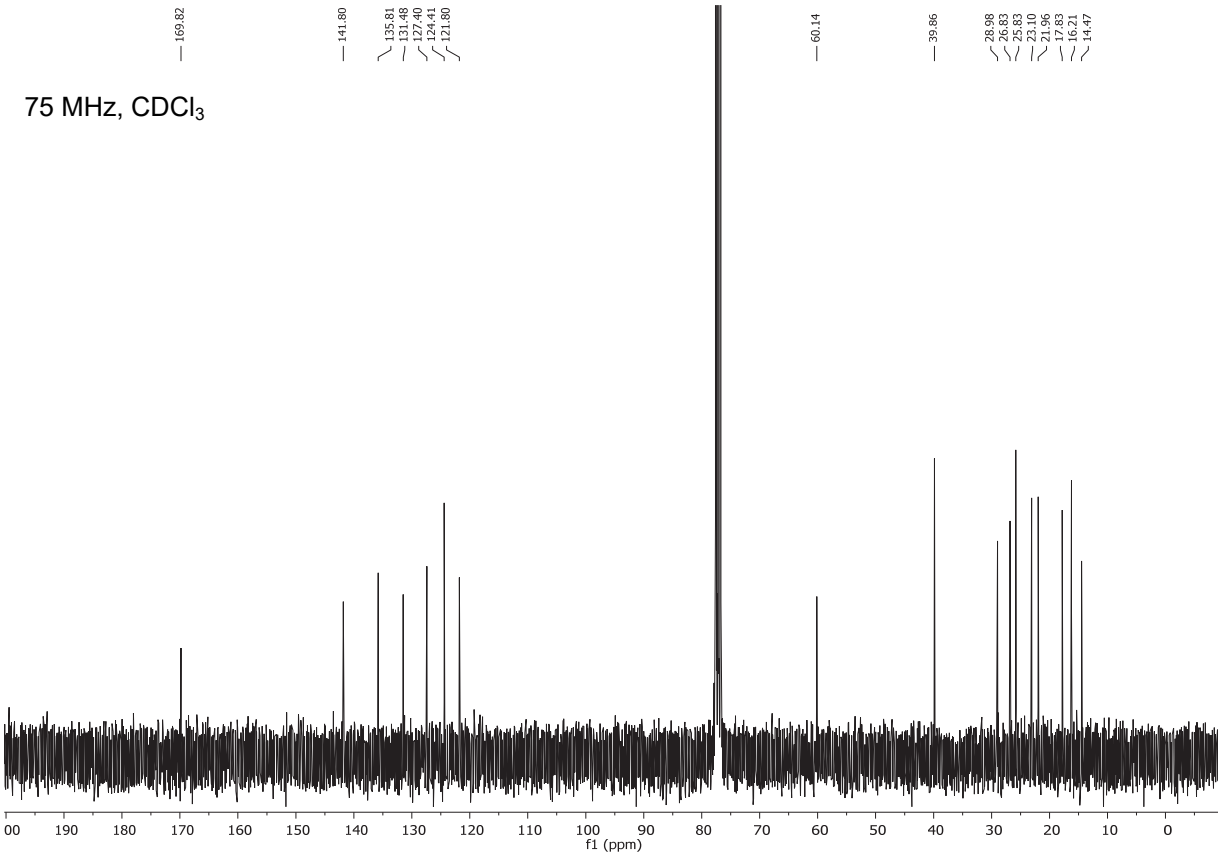

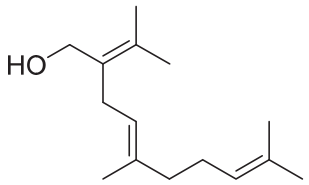

S2

300 MHz, $CDCl_3$

75 MHz, $CDCl_3$

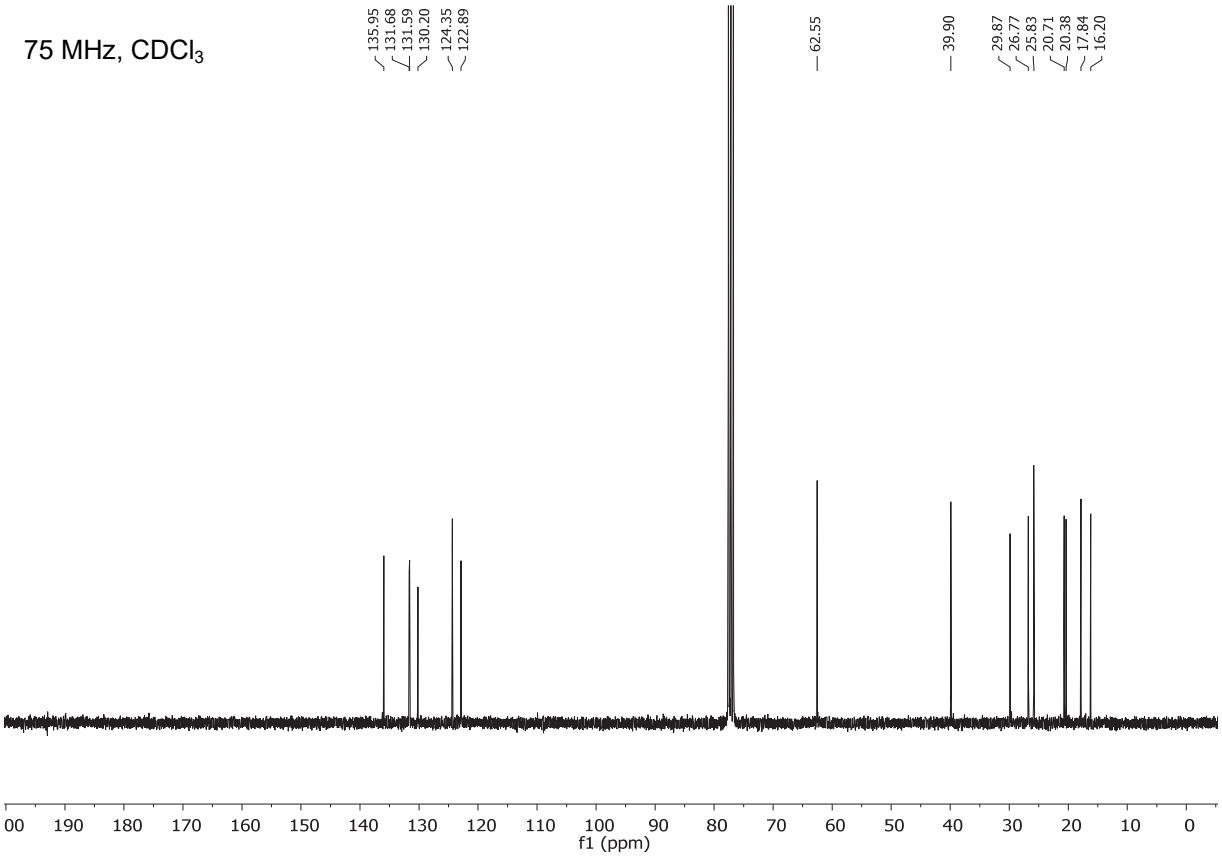

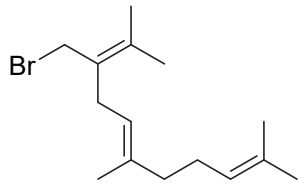

19

300 MHz, C_6D_6

75 MHz, C_6D_6

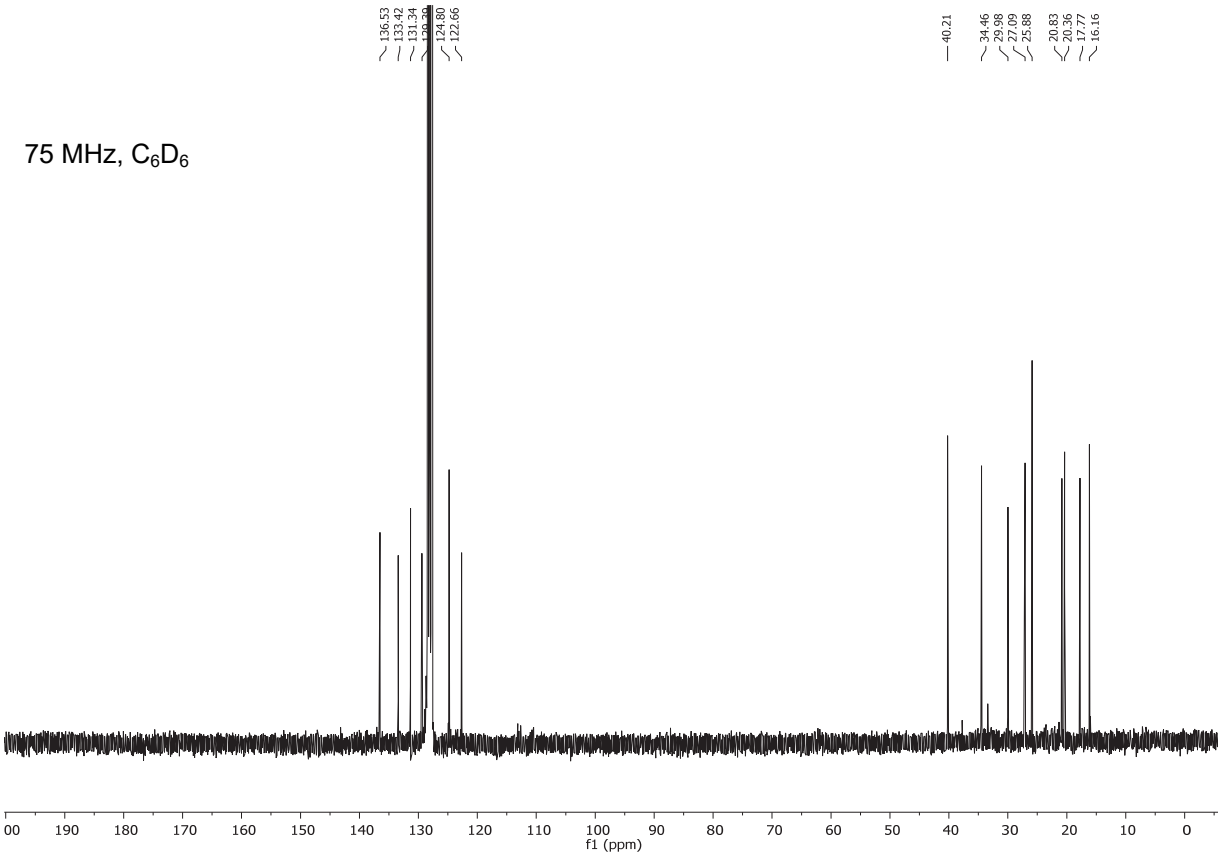

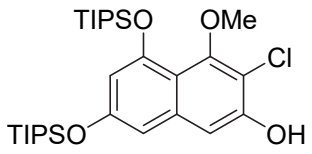

22

400 MHz, C_6D_6

100 MHz, C_6D_6

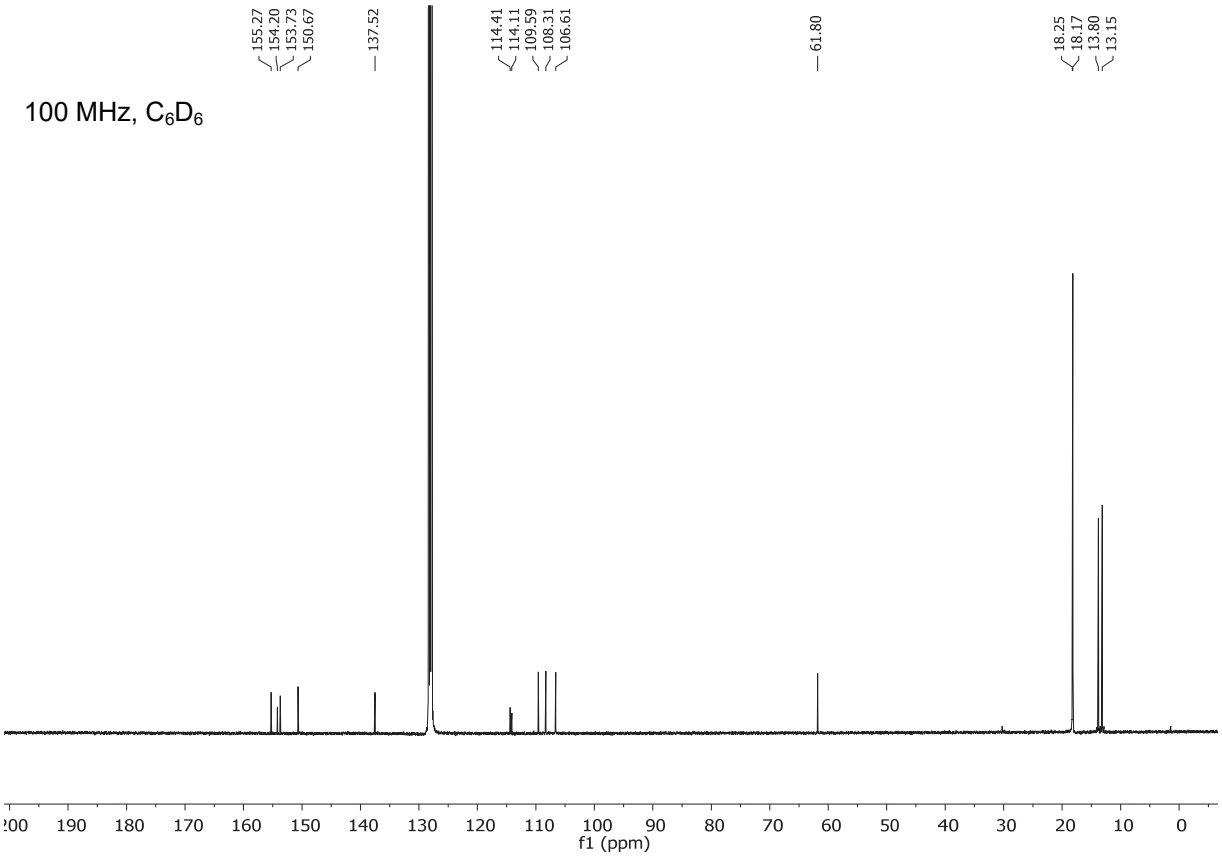

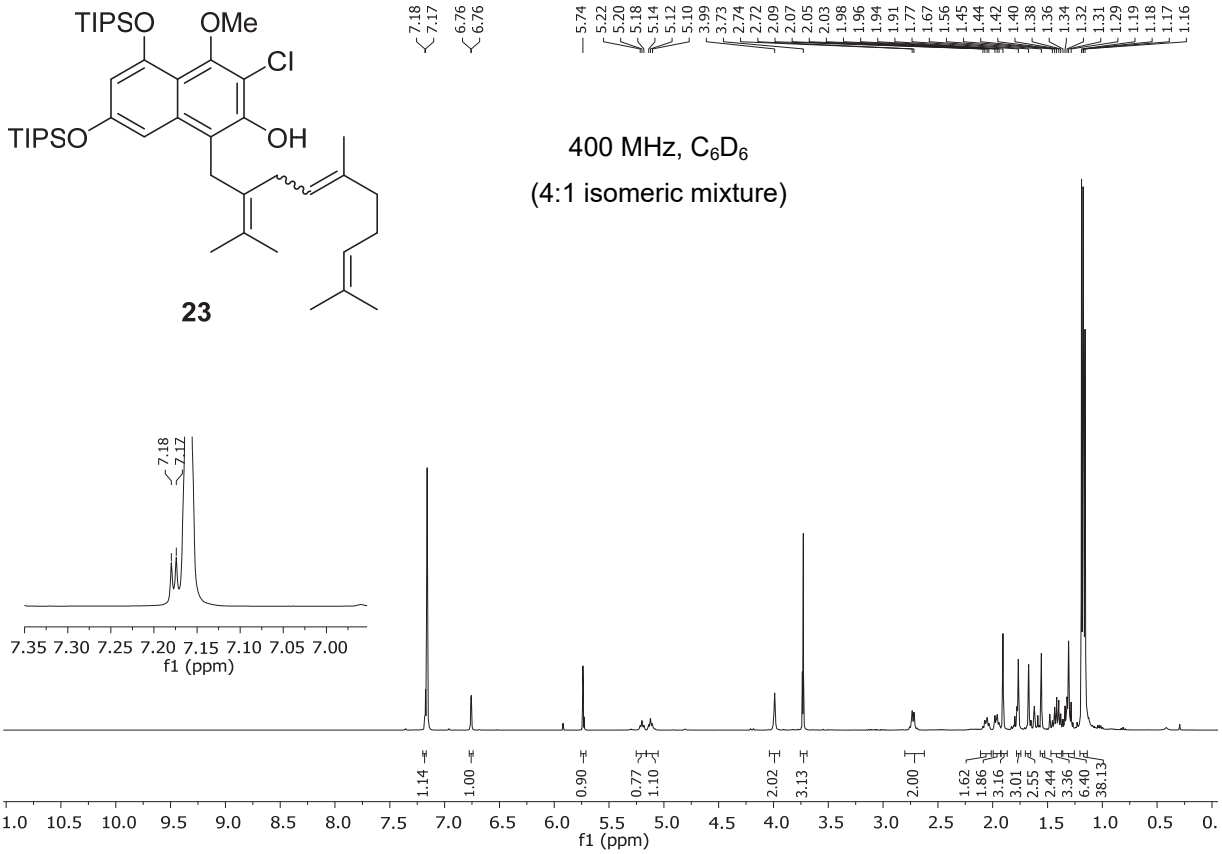
TIPSO
OMe
Cl
TIPSO
OH
23
400 MHz, C6D6
(4:1 isomeric mixture)
f1 (ppm)

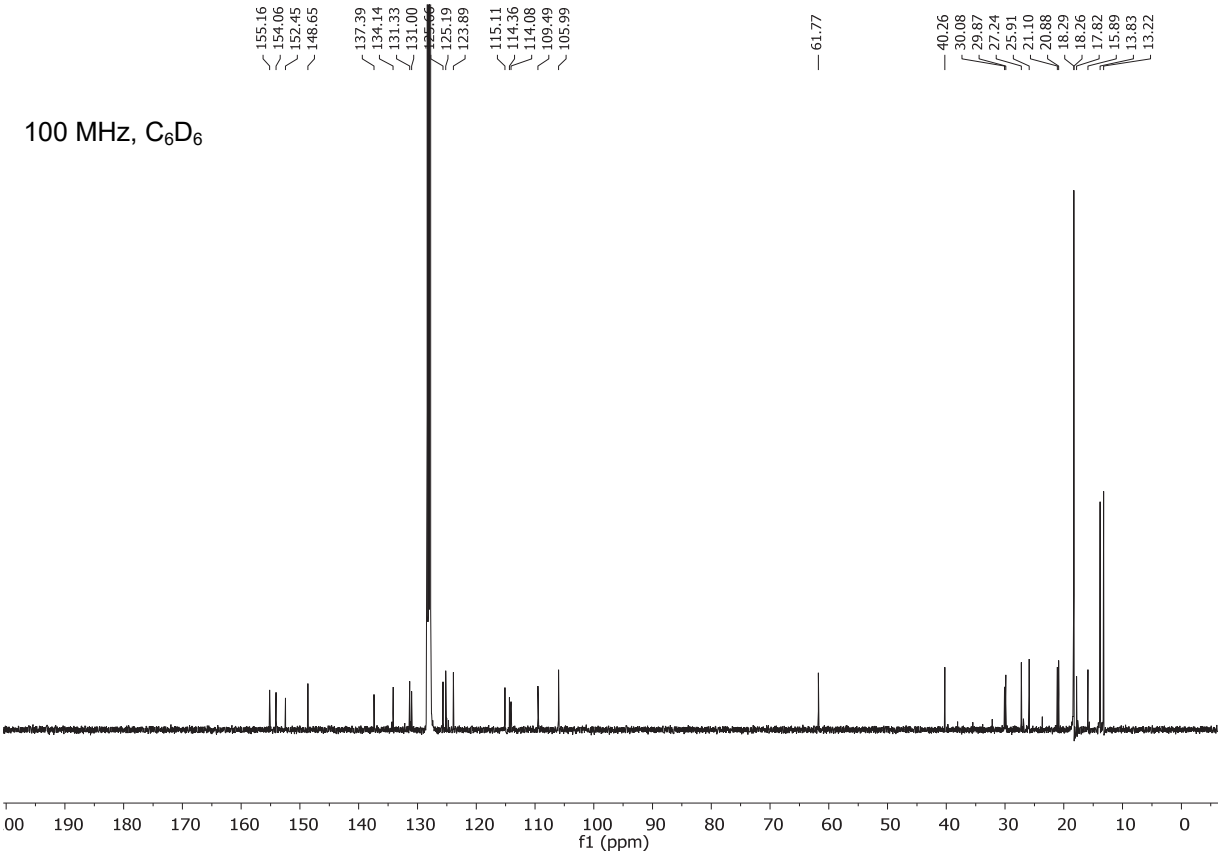
100 MHz, C6D6
f1 (ppm)

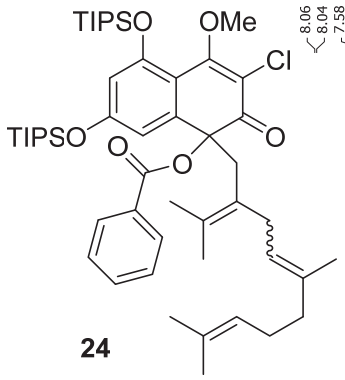

24

400 MHz, $CDCl_3$

(4:1 isomeric mixture)

100 MHz, $CDCl_3$

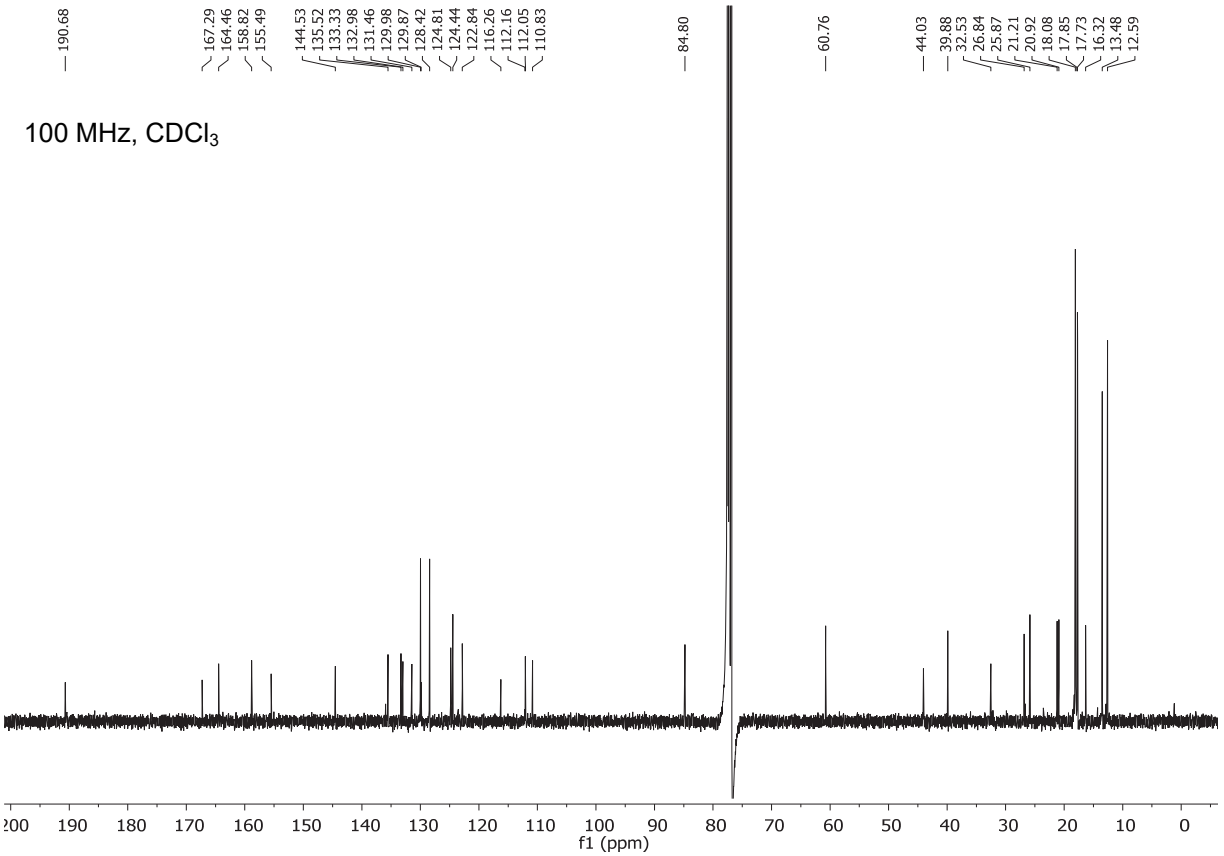

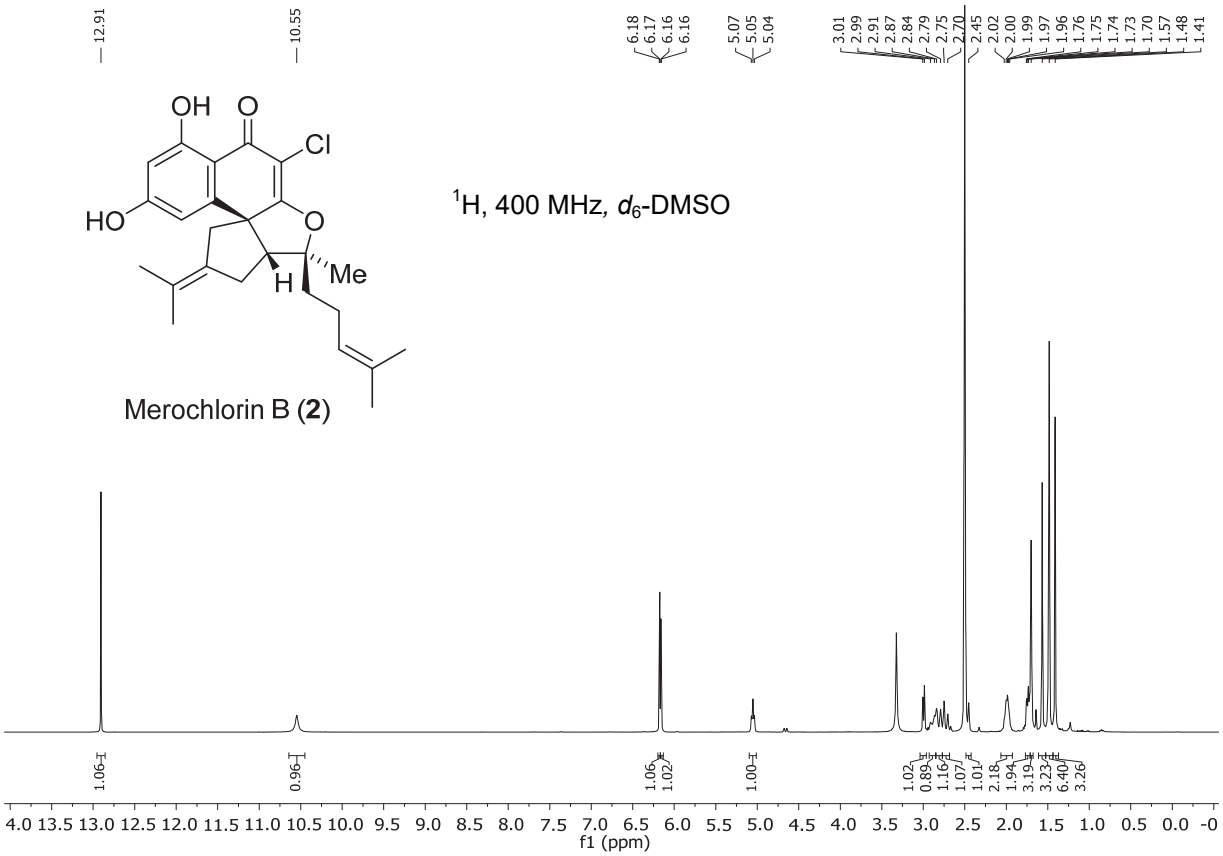
12.91
10.55
6.18
6.17
6.16
6.16
5.07
5.05
5.04
3.01
2.99
2.91
2.87
2.84
2.79
2.75
2.70
2.45
2.02
2.00
1.99
1.97
1.96
1.76
1.75
1.74
1.73
1.70
1.57
1.48
1.41
OH
O
Cl
HO
O
H
Me
1H, 400 MHz, d6-DMSO
Merochlorin B (2)
1.06
0.96
1.06
1.02
1.00
1.02
0.89
1.16
1.07
1.01
2.18
1.94
3.19
3.23
6.40
3.26
4.0 13.5 13.0 12.5 12.0 11.5 11.0 10.5 10.0 9.5 9.0 8.5 8.0 7.5 7.0 6.5 6.0 5.5 5.0 4.5 4.0 3.5 3.0 2.5 2.0 1.5 1.0 0.5 0.0 -0
f1 (ppm)

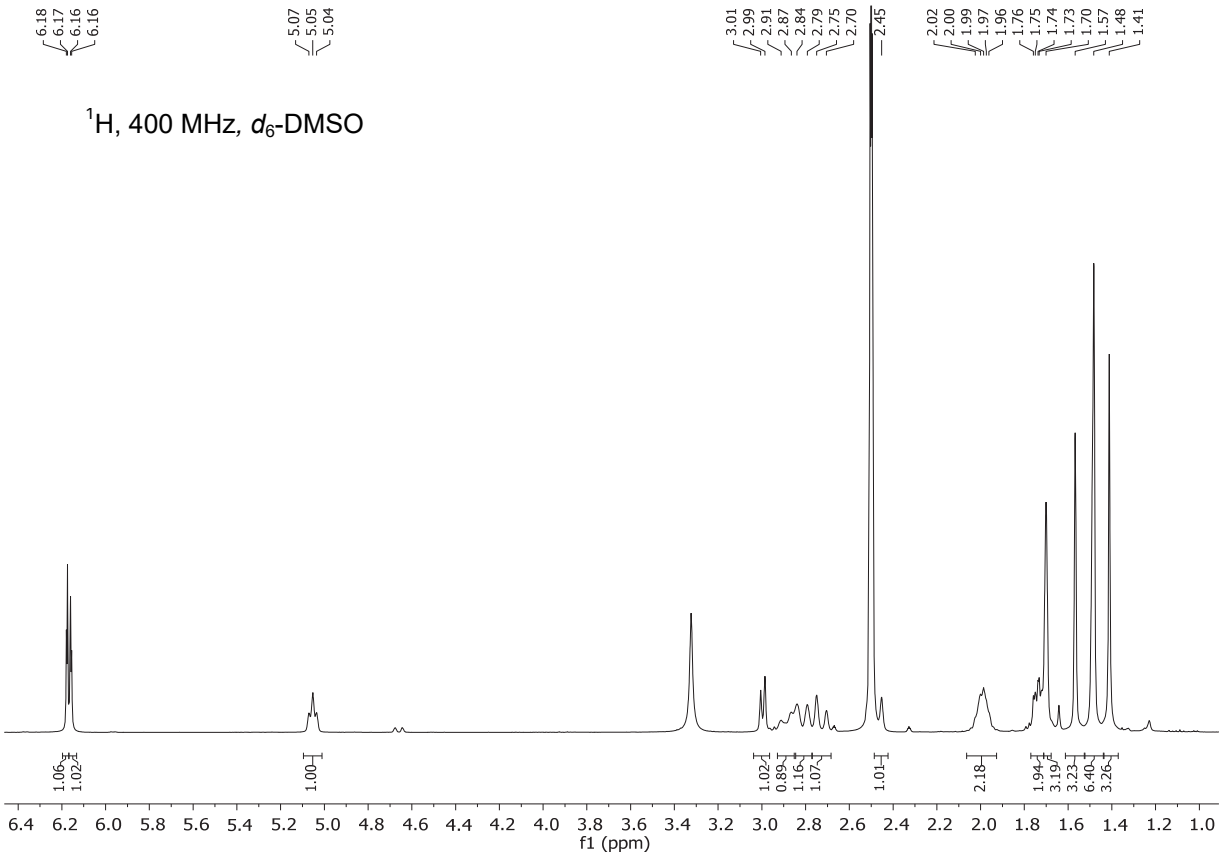
6.18
6.17
6.16
6.16
5.07
5.05
5.04
3.01
2.99
2.91
2.87
2.84
2.79
2.75
2.70
2.45
2.02
2.00
1.99
1.97
1.96
1.76
1.75
1.74
1.73
1.70
1.57
1.48
1.41
1H, 400 MHz, d6-DMSO
1.06
1.02
1.00
1.02
0.89
1.16
1.07
1.01
2.18
1.94
3.19
3.23
6.40
3.26
6.4 6.2 6.0 5.8 5.6 5.4 5.2 5.0 4.8 4.6 4.4 4.2 4.0 3.8 3.6 3.4 3.2 3.0 2.8 2.6 2.4 2.2 2.0 1.8 1.6 1.4 1.2 1.0
f1 (ppm)

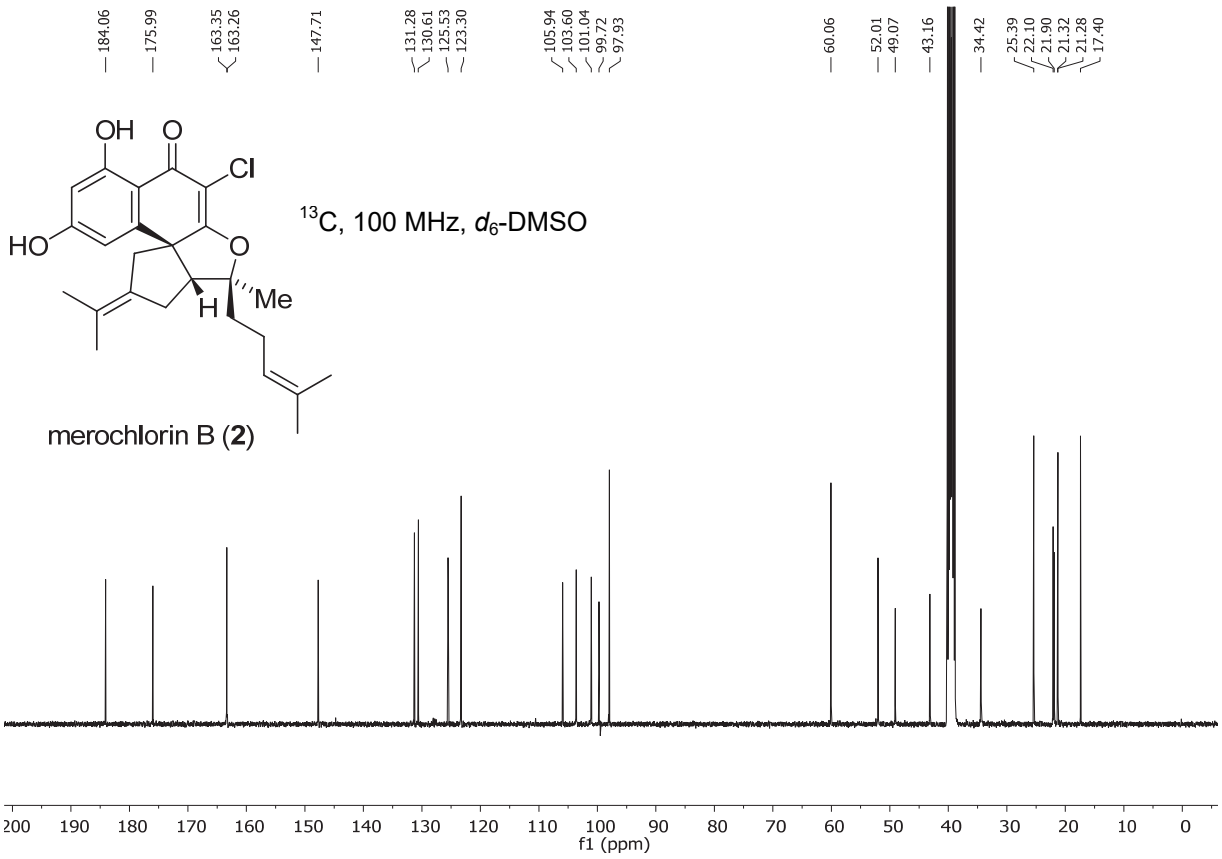

^{13}C, 100 MHz, d_6-DMSO

merochlorin B (**2**)

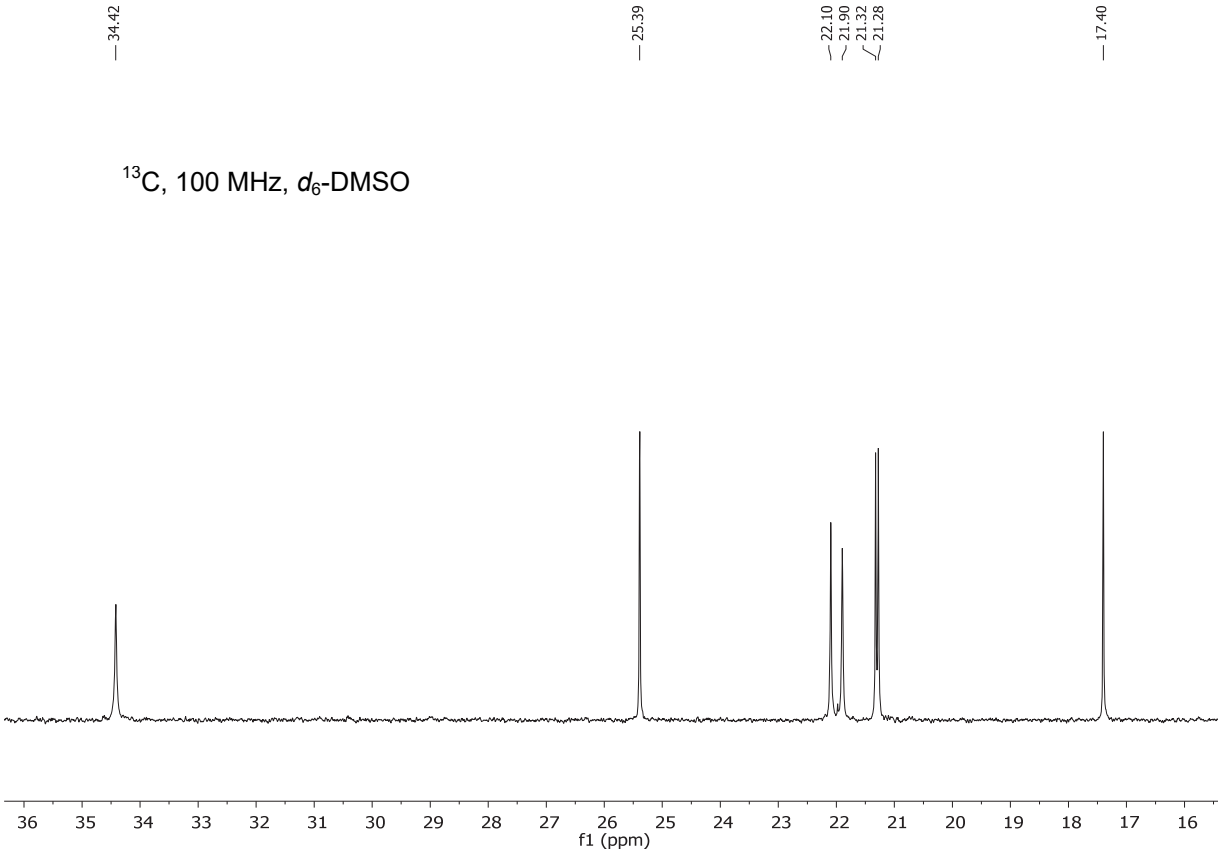

^{13}C, 100 MHz, d_6-DMSO

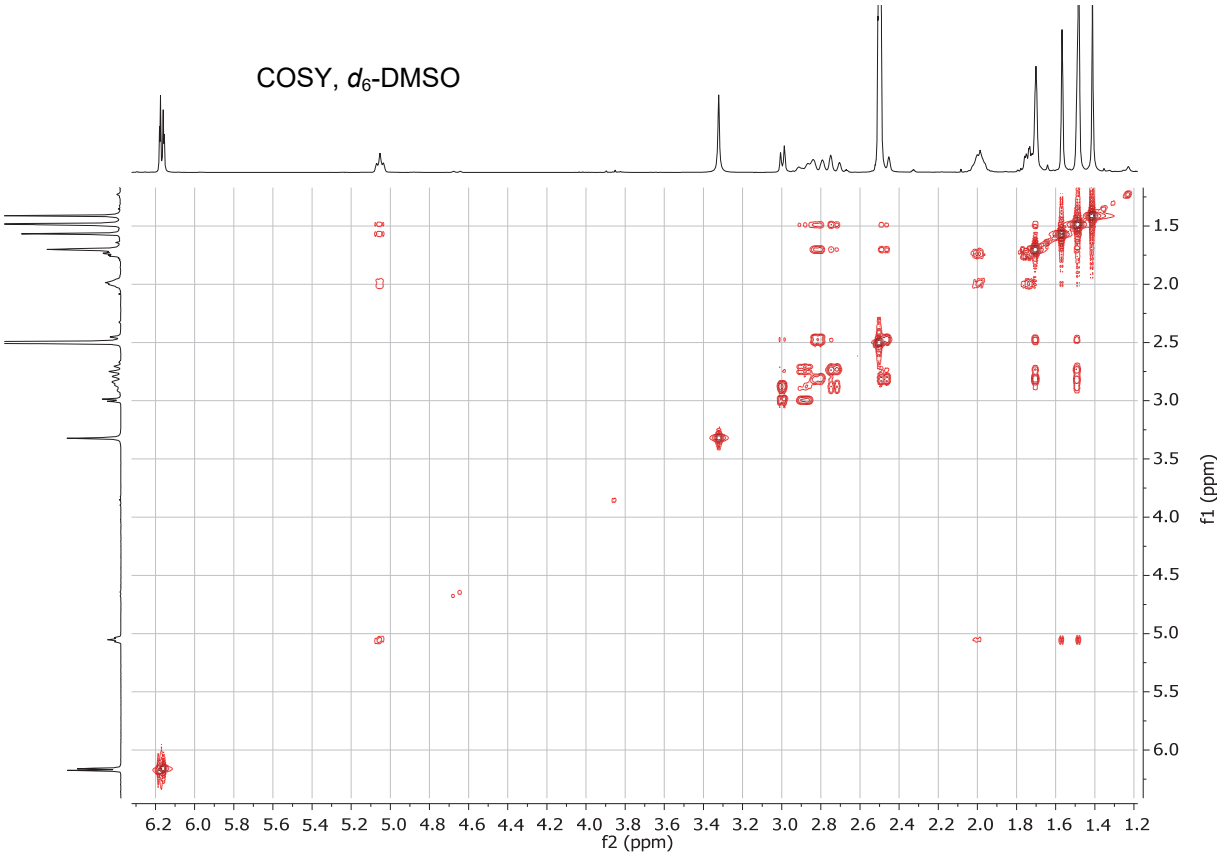
COSY, d_6-DMSO
f2 (ppm)
f1 (ppm)

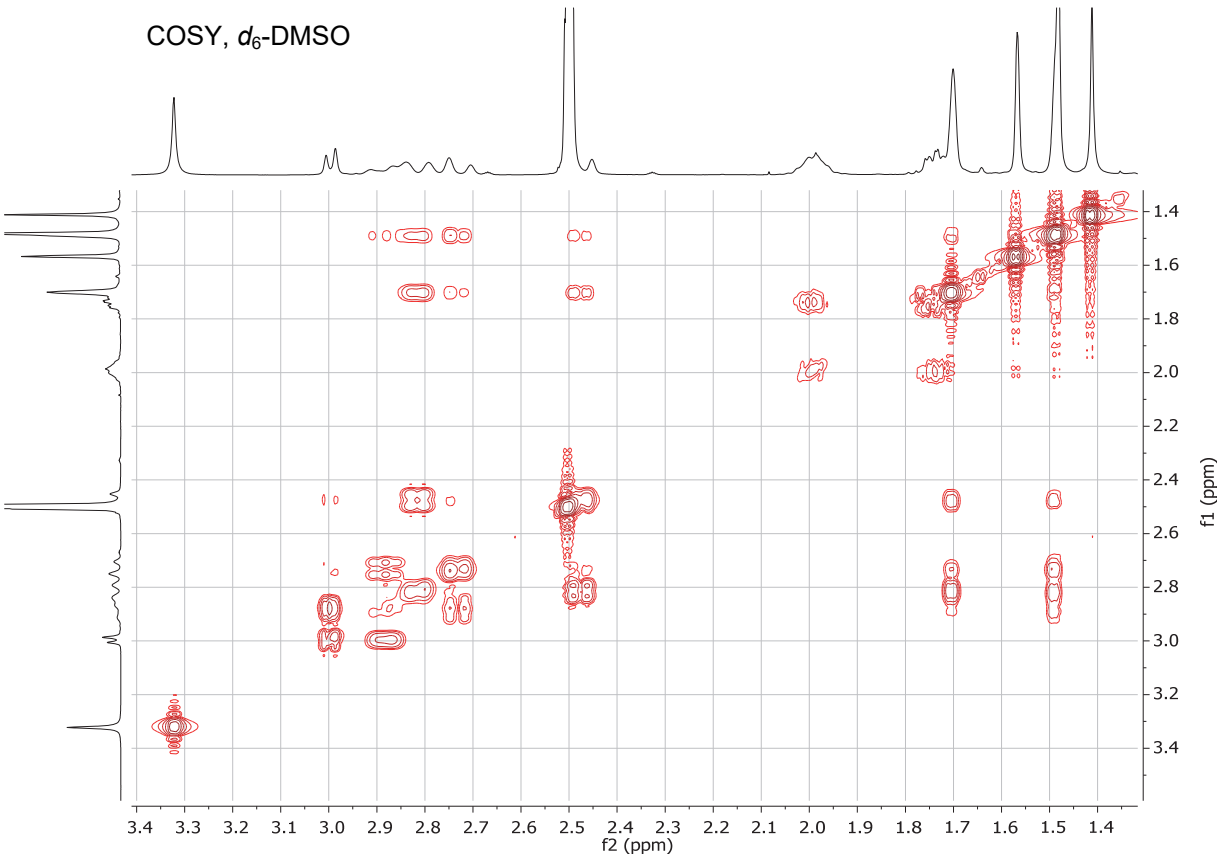
COSY, d_6-DMSO
f2 (ppm)
f1 (ppm)

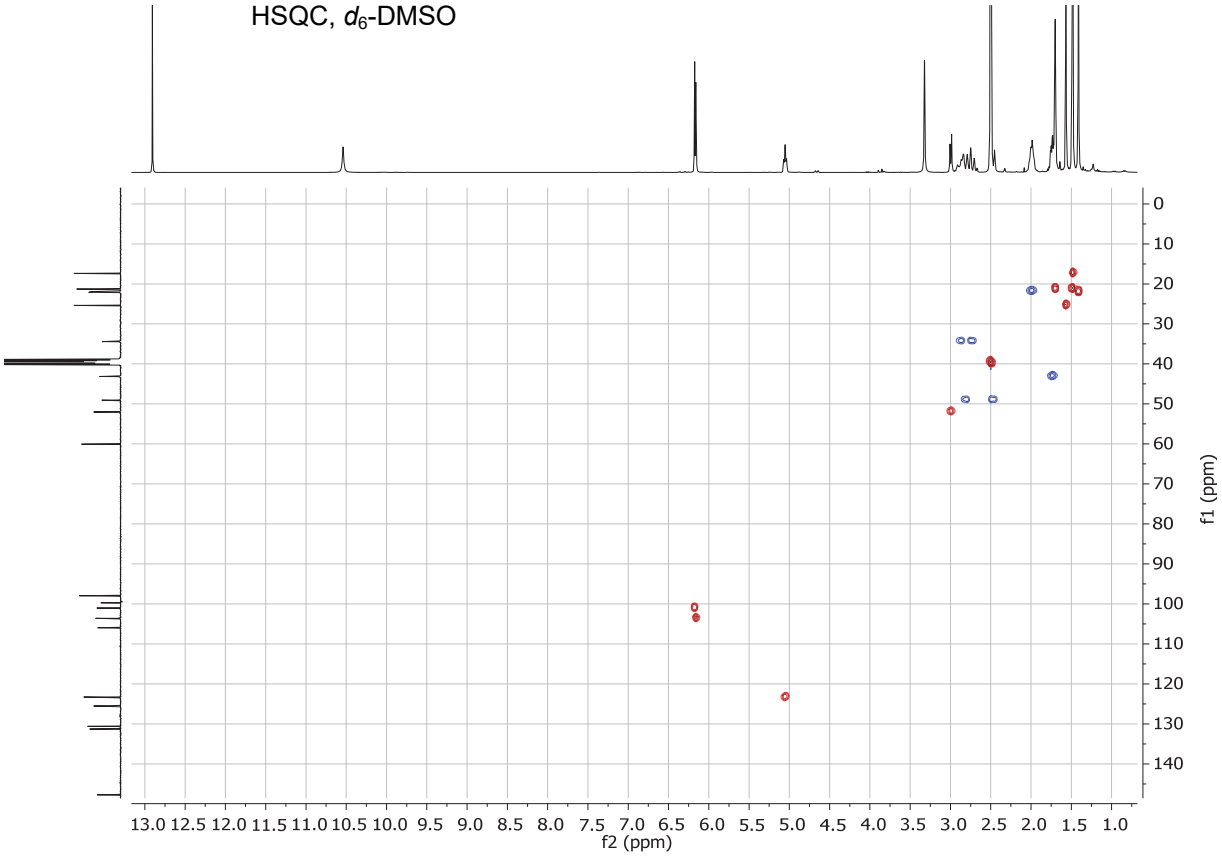
HSQC, d_6-DMSO
f1 (ppm)
f2 (ppm)

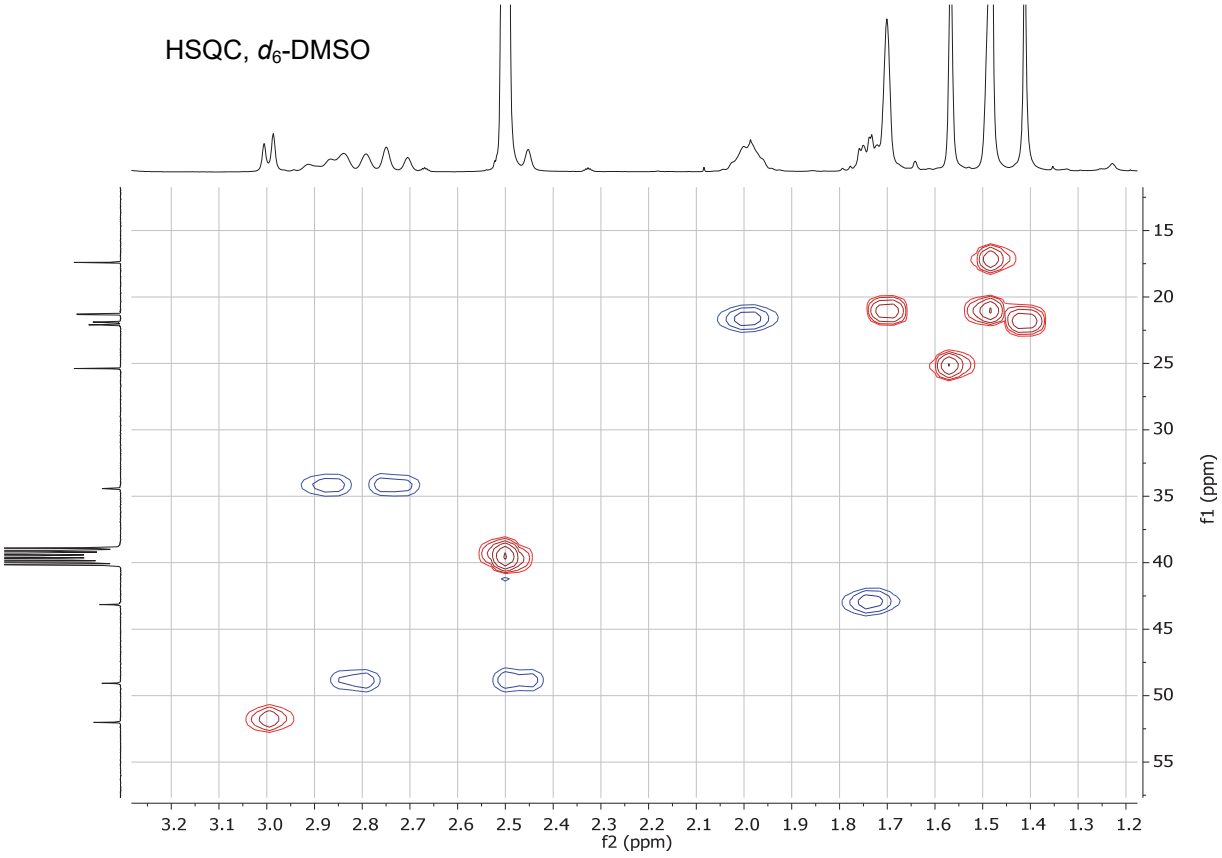
HSQC, d_6-DMSO
f1 (ppm)
f2 (ppm)

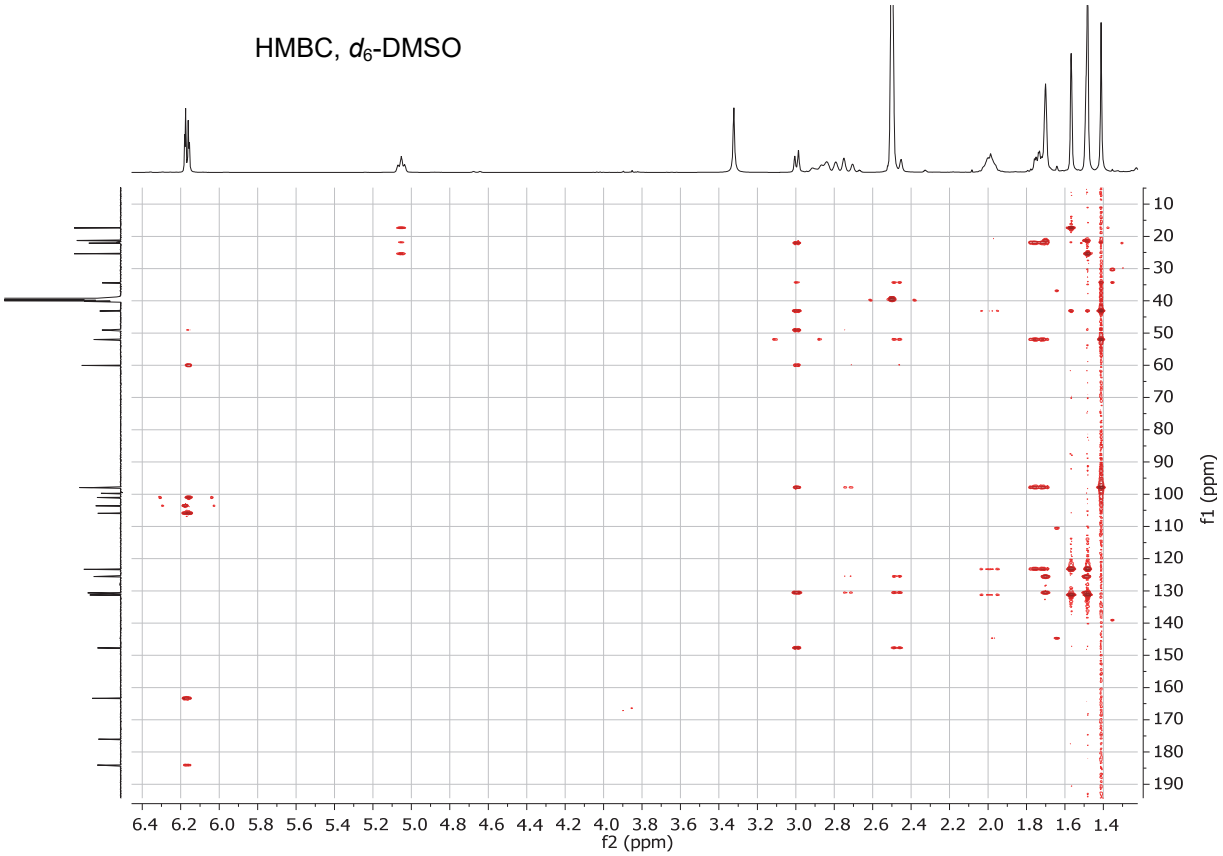
HMBC, d_6-DMSO
f2 (ppm)
f1 (ppm)

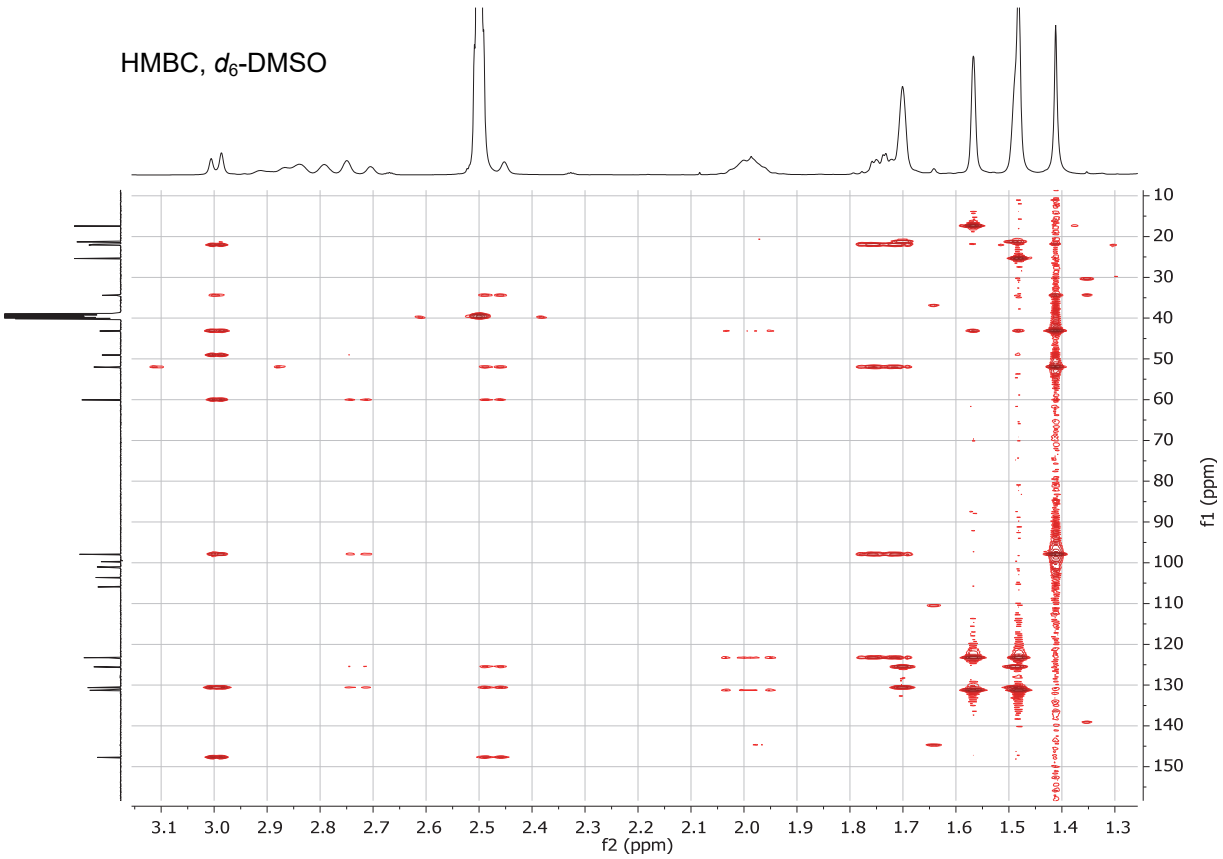
HMBC, d_6-DMSO
f2 (ppm)
f1 (ppm)

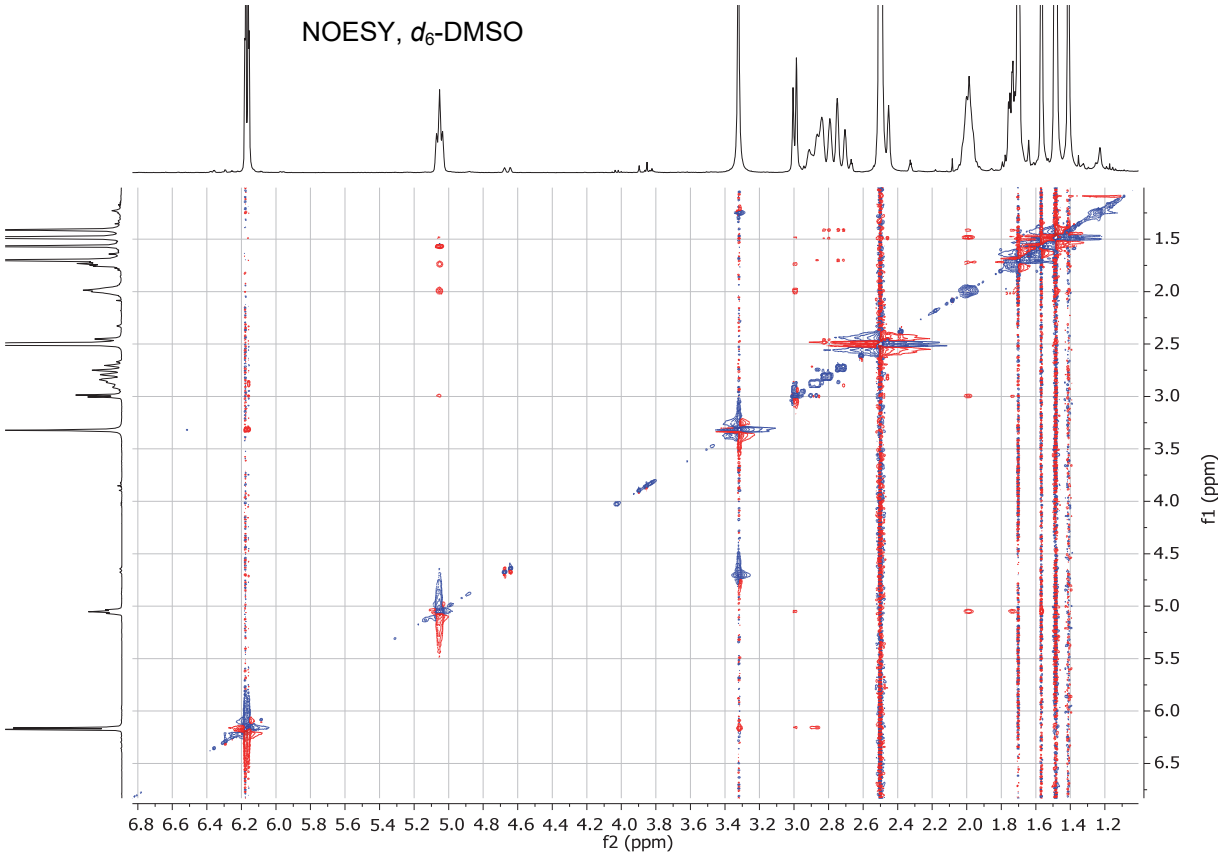
NOESY, d_6-DMSO
f2 (ppm)
f1 (ppm)

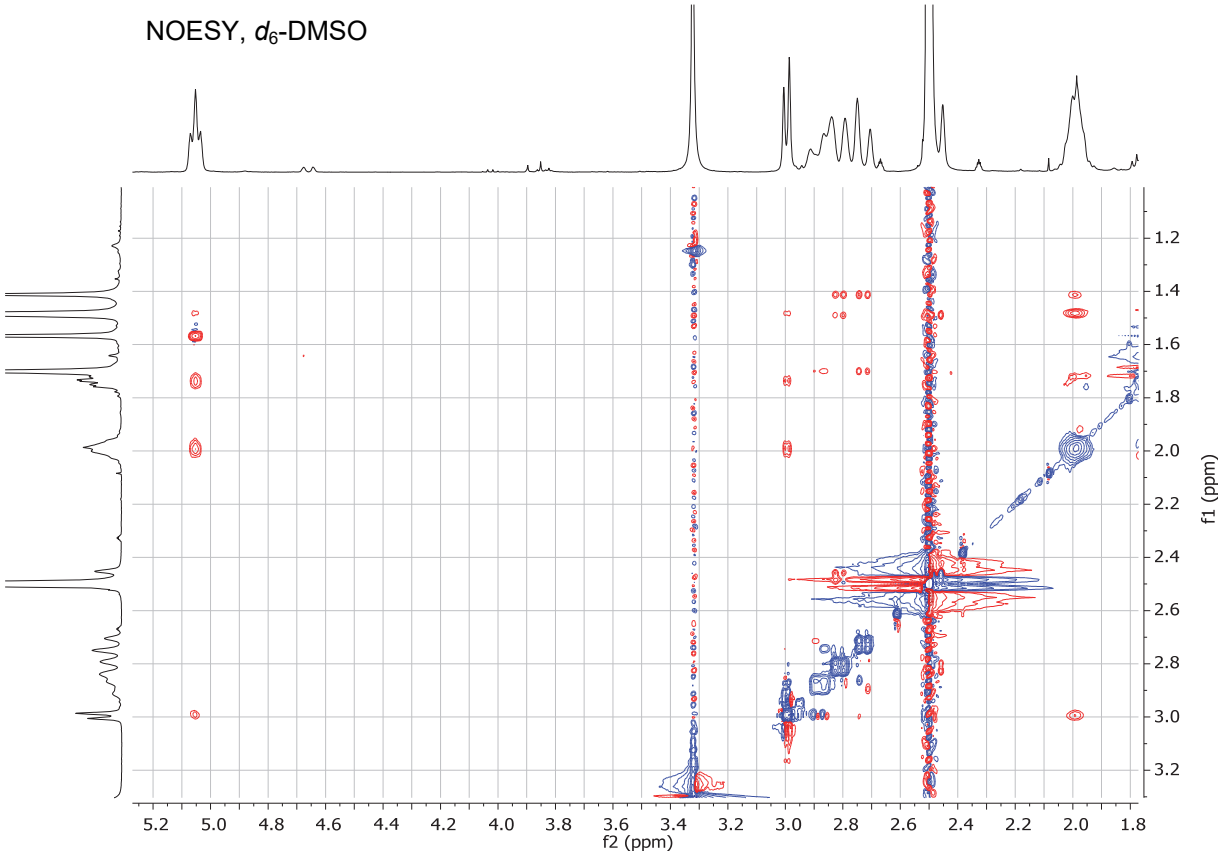
NOESY, d_6-DMSO
f2 (ppm)
f1 (ppm)

7 REFERENCES

[1] A. Albini, M. Fagnoni, *Green Chem.* **2004**, *6*, 1–6.

[2] a) H. D. Roth, *Angew. Chem. Int. Ed.* **1989**, *28*, 1193–1207; b) H. E. Zimmerman, *Pure Appl. Chem.* **2006**, *78*, 2193–2203; (c) S. Poplata, A. Tröster, Y.-Q. Zou, T. Bach, *Chem. Rev.* **2016**, *116*, 9748–9815.

[3] H. Trommsdorff, *Ann. Chem. Pharm.* **1834**, *11*, 190–208.

[4] D. H. R. Barton, P. de Mayo, M. Shafiq, *J. Chem. Soc.* **1958**, 140–145.

[5] H. E. Zimmerman, D. I. Schuster, *J. Am. Chem. Soc.* **1962**, *84*, 4527–4540.

[6] a) C. Liebermann, *Ber.* **1877**, *10*, 2177–2179; b) C. Liebermann, M. Ilinski, *Ber.* **1885**, *18*, 3193–3201.

[7] C. N. Riiber, *Ber.* **1902**, *35*, 2908–2909.

[8] J. Schramm, *Ber.* **1884**, *17*, 2922–2925.

[9] H. Klinger, *Ber.* **1886**, *19*, 1862–1870.

[10] G. Ciamician, P. Silber, *Ber.* **1908**, *41*, 1928–1935.

[11] a) R. Srinivasan, K. H. Carlough, *J. Am. Chem. Soc.* **1967**, *89*, 4932–4936; b) R. S. H. Liu, G. S. Hammond, *J. Am. Chem. Soc.* **1967**, *89*, 4936–4944.

[12] a) E. J. Corey, R. B. Mitra, H. Uda, *J. Am. Chem. Soc.* **1963**, *85*, 362–363; b) E. J. Corey, R. B. Mitra, H. Uda, *J. Am. Chem. Soc.* **1964**, *86*, 485–492.

[13] S. Hatakeyama, M. Kawamura, S. Takano, *J. Am. Chem. Soc.* **1994**, *116*, 4081–4082.

[14] P. A. Wender, S. K. Singh, *Tetrahedron Lett.* **1990**, *31*, 2517–2520.

[15] W. Oppolzer, T. Godel, *J. Am. Chem. Soc.* **1978**, *100*, 2583–2584.

[16] a) M. Inoue, T. Sato, M. Hirama, *J. Am. Chem. Soc.* **2003**, *125*, 10772–10773; b) M. Inoue, T. Sato, M. Hirama, *Angew. Chem. Int. Ed.* **2006**, *45*, 4843–4848.

[17] a) T. P. Yoon, *Acc. Chem. Res.* **2016**, *49*, 2307–2315; b) R. Brimioulle, D. Lenhart, M. M. Maturi, T. Bach, *Angew. Chem. Int. Ed.* **2015**, *54*, 3872–3890.

[18] T. Bach, H. Bergmann, K. Harms, *Angew. Chem. Int. Ed.* **2000**, *39*, 2302–2304.

[19] C. Müller, A. Bauer, T. Bach, *Angew. Chem. Int. Ed.* **2009**, *48*, 6640–6642.

[20] H. Guo, E. Herdtweck, T. Bach, *Angew. Chem. Int. Ed.* **2010**, *49*, 7782–7785.

[21] a) C. K. Prier, D. A. Rankic, D. W. C. MacMillan, *Chem. Rev.* **2013**, *113*, 5322–5363; b) M. H. Shaw, J. Twilton, D. W. C. MacMillan, *J. Org. Chem.* **2016**, *81*, 6898–6926.

[22] a) D. M. Hedstrand, W. H. Kruizinga, R. M. Kellogg, *Tetrahedron Lett.* **1978**, *19*, 1255–1258; b) T. J. Van Bergen, D. M. Hedstrand, W. H. Kruizinga, R. M. Kellogg, *J. Org. Chem.* **1979**, *44*, 4953–4962.

[23] D. A. Nagib, M. E. Scott, D. W. C. MacMillan, *J. Am. Chem. Soc.* **2009**, *131*, 10875–10877.

[24] a) D. N. Primer, I. Karakaya, J. C. Tellis, G. A. Molander, *J. Am. Chem. Soc.* **2015**, *137*, 2195–2198; b) J. C. Tellis, C. B. Kelly, D. N. Primer, M. Jouffroy, N. R. Patel, G. A. Molander, *Acc. Chem. Res.* **2016**, *49*, 1429–1439.

[25] H. F. DeLuca, *FASEB J.* **1988**, *2*, 224–236.

[26] B. Schäfer, *Naturstoffe der chemischen Industrie*, Elsevier, München, **2007**, 435–448 and references therein.

[27] H. F. DeLuca, M. F. Holick, H. K. Schnoes, T. Suda, R. J. Cousins, *Biochemistry* **1971**, *10*, 2799–2804.

[28] Y. J. Hong, D. J. Tantillo, *Chem. Soc. Rev.* **2014**, *43*, 5042–5050.

[29] a) S. Qian, G. Zhao, *Chem. Commun.* **2012**, *48*, 3530–3532; b) B.-X. Zhao, Y. Wang, C. Li, G.-C. Wang, X.-J. Huang, C.-L. Fan, Q.-M. Li, H.-J. Zhu, W.-M. Chen, W.-C. Ye, *Tetrahedron Lett.* **2013**, *54*, 4708–4711; c) T. Fujimori, R. Kasuga, H. Kaneko, S. Sakamura, M. Noguchi, A. Furusaki, N. Hashiba, T. Matsumoto, *J. Chem. Soc., Chem. Commun.* **1978**, 563–564; d) A. Srikrishna, S. S. V. Ramasastry, *Tetrahedron Lett.* **2005**, *46*, 7373–7376; e) A. Skiredj, M. A. Beniddir, D. Joseph, K. Leblanc, G. Bernadat, L. Evanno, E. Poupon, *Angew. Chem. Int. Ed.* **2014**, *53*, 6419–6424; f) S.-J. Piao, Y.-L. Song, W.-H. Jiao, F. Yang, X.-F. Liu, W.-S. Chen, B.-N. Han, H.-W. Lin, *Org. Lett.* **2013**, *15*, 3526–3529.

[30] a) M. T. Crimmins, *Chem. Rev.* **1988**, *88*, 1453–1473; b) D. I. Schuster, G. Lem, N. A. Kaprinidis, *Chem. Rev.* **1993**, *93*, 3–22; c) M. D. Kärkäs, J. A. Porco, C. R. J. Stephenson, *Chem. Rev.* **2016**, *116*, 9683–9747.

[31] a) T. Bach, J. P. Hehn, *Angew. Chem. Int. Ed.* **2011**, *50*, 1000–1045; b) N. Hoffmann, *Chem. Rev.* **2008**, *108*, 1052–1103.

[32] a) I. K. Mangion, D. W. C. MacMillan, *J. Am. Chem. Soc.* **2005**, *127*, 3696–3697; b) Y.-S. Li, K. Matsunaga, M. Ishibashi, Y. Ohizumi, *J. Org. Chem.* **2001**, *66*, 2165–2167.

[33] A. V. Kurdyumov, R. P. Hsung, K. Ihlen, J. Wang, *Org. Lett.* **2003**, *5*, 3935–3938.

[34] N. Tanaka, M. Okasaka, Y. Ishimaru, Y. Takaishi, M. Sato, M. Okamoto, T. Oshikawa, S. U. Ahmed, L. M. Consentino, K.-H. Lee, *Org. Lett.* **2005**, *7*, 2997–2999.

[35] a) K. C. Nicolaou, D. Sarlah, D. M. Shaw, *Angew. Chem. Int. Ed.* **2007**, *46*, 4708–4711; b) K. C. Nicolaou, T. R. Wu, D. Sarlah, D. M. Shaw, E. Rowcliffe, D. R. Burton, *J. Am. Chem. Soc.* **2008**, *130*, 11114–11121; c) C. Du, L. Li, Y. Li, Z. Xie, *Angew. Chem. Int. Ed.* **2009**, *48*, 7853–7856.

[36] a) H. Tan, C. Zheng, Z. Liu, D. Z. Wang, *Org. Lett.* **2011**, *13*, 2192–2195; b) F. Xiao, W. Liu, Y. Wang, Q. Zhang, X. Li, X. Hu, *Asian J. Org. Chem.* **2013**, *2*, 216–219.

[37] Y. M. Syah, N. S. Suastri, J. Latip, B. M. Yamin, *Acta. Crystallogr. Sect. E* **2005**, *61*, o1530–o1531.

[38] G.-Q. Wang, K. Wei, L. Zhang, T. Feng, F. Wang, Q.-A. Wang, J.-K. Liu, *Tetrahedron Lett.* **2011**, *52*, 2719–2721.

[39] J. Marrero, A. D. Rodríguez, C. L. Barnes, *Org. Lett.* **2005**, *7*, 1877–1880.

[40] P. A. Roethle, P. T. Hernandez, D. Trauner, *Org. Lett.* **2006**, *8*, 5901–5904.

[41] a) B. Tang, C. D. Bray, G. Pattenden, *Tetrahedron Lett.* **2006**, *47*, 6401–6404.; b) B. Tang, C. D. Bray, G. Pattenden, *Org. Biomol. Chem.* **2009**, *7*, 4448–4457.

[42] D. Stichnoth, P. Kölle, T. J. Kimbrough, E. Riedle, R. de Vivie-Riedle, D. Trauner, *Nat. Commun.* **2014**, *5*, 5597.

[43] A. D. Rodríguez, J.-G. Shi, Y.-P. Shi, *J. Org. Chem.* **2000**, *65*, 3192–3199.

[44] a) B. Gerard, G. Jones, J. A. Porco, *J. Am. Chem. Soc.* **2004**, *126*, 13620–13621; b) S. P. Roche, R. Cencic, J. Pelletier, J. A. Porco, *Angew. Chem. Int. Ed.* **2010**, *49*, 6533–6538.

[45] a) B. Gerard, S. Sangji, D. J. O'Leary, J. A. Porco, *J. Am. Chem. Soc.* **2006**, *128*, 7754–7755; b) B. Gerard, R. Cencic, J. Pelletier, J. A. Porco, *Angew. Chem. Int. Ed.* **2007**, *46*, 7831–7834.

[46] H. E. Zimmerman, D. Armesto, *Chem. Rev.* **1996**, *96*, 3065–3112.

[47] S. A. Look, W. Fenical, D. Van Engen, J. Clardy, *J. Am. Chem. Soc.* **1984**, *106*, 5026–5027.

[48] G. Majetich, J. Yu, *Org. Lett.* **2008**, *10*, 89–91.

[49] a) G. Majetich, Y. Li, G. Zou, *Heterocycles* **2007**, *73*, 217–225.; b) G. Majetich, J. Yu, Y. Li, *Heterocycles* **2007**, *73*, 227–235.

[50] C. Thommen, M. Neuburger, K. Gademann, *Chem. Eur. J.* **2016**, DOI: 10.1002/chem.201603932.

[51] N. Uchiyama, F. Kiuchi, M. Ito, G. Honda, Y. Takeda, O. K. Khodzhimatov, O. A. Ashurmetov, *J. Nat. Prod.* **2003**, *66*, 128–131.

[52] C. Thommen, C. K. Jana, M. Neuburger, K. Gademann, *Org. Lett.* **2013**, *15*, 1390–1393.

[53] H. Shang, J. Liu, R. Bao, Y. Cao, K. Zhao, C. Xiao, B. Zhou, L. Hu, Y. Tang, *Angew. Chem. Int. Ed.* **2014**, *53*, 14494–14498.

[54] A. A. Mahmoud, *Planta Med.* **1998**, *64*, 724–727.

[55] R. G. S. Berlinck, R. Britton, E. Piers, L. Lim, M. Roberge, R. Moreira da Rocha, R. J. Andersen, *J. Org. Chem.* **1998**, *63*, 9850–9856.

[56] a) S. J. Eade, M. W. Walter, C. Byrne, B. Odell, R. Rodriguez, J. E. Baldwin, R. M. Adlington, J. E. Moses, *J. Org. Chem.* **2008**, *73*, 4830–4839; b) P. Sharma, B. Lygo, W. Lewis, J. E. Moses, *J. Am. Chem. Soc.* **2009**, *131*, 5966–5972; c) P. Sharma, J. E. Moses, *Synlett* **2010**, 525–528.

[57] C. Ireland, J. Faulkner, *Tetrahedron* **1981**, *37*, 233–240.

[58] C. Ireland, P. J. Scheuer, *Science* **1979**, *205*, 922–923.

[59] D. R. Zuidema, A. K. Miller, D. Trauner, P. B. Jones, *Org. Lett.* **2005**, *7*, 4959–4962.

[60] a) J. S. Sinninghe Damsté, M. Strous, W. I. C. Rijpstra, E. C. Hopmans, J. A. J. Geenevasen, A. C. T. van Duin, L. A. van Niftrik, M. S. M. Jetten, *Nature* **2002**, *419*, 708–712; b) D. H. Nouri, D. J. Tantillo, *Curr. Org. Chem.* **2006**, *10*, 2055–2074.

[61] a) V. Mascitti, E. J. Corey, *J. Am. Chem. Soc.* **2006**, *128*, 3118–3119; b) V. Mascitti, E. J. Corey, *J. Am. Chem. Soc.* **2004**, *126*, 15664–15665.

[62] a) P. Javidpour, S. Deutsch, V. K. Mutalik, N. J. Hillson, C. J. Petzold, J. D. Keasling, H. R. Beller, *PLoS One* **2016**, *11*, e0151087; b) J. E. Rattray, J. A. J. Geenevasen, L. Van Niftrik, W. I. C. Rijpstra, E. C. Hopmans, M. Strous, S. Schouten, M. S. M. Jetten, J. S. Sinninghe Damsté, *FEMS Microbiol. Lett.* **2009**, *292*, 115–122.

[63] J. A. M. Mercer, C. M. Cohen, S. R. Shuken, A. M. Wagner, M. W. Smith, F. R. Moss, M. D. Smith, R. Vahala, A. Gonzalez-Martinez, S. G. Boxer, N. Z. Burns, *J. Am. Chem. Soc.* **2016**, *138*, 15845–15848.

[64] R. G. Salomon, J. K. Kochi, *J. Am. Chem. Soc.* **1974**, *96*, 1137–1144.

[65] A. San Feliciano, M. Medarde, J. M. Miguel del Corral, A. Aramburu, M. Gordaliza, A. F. Barrero, *Tetrahedron Lett.* **1989**, *30*, 2851–2854.

[66] M. W. Lodewyk, C. Soldi, P. B. Jones, M. M. Olmstead, J. Rita, J. T. Shaw, D. J. Tantillo, *J. Am. Chem. Soc.* **2012**, *134*, 18550–18553.

[67] A. S. Feliciano, A. F. Barrero, M. Medarde, J. M. M. Del Corral, A. Aramburu, A. Perales, J. Fayos, F. Sanchez-Ferrando, *Tetrahedron* **1985**, *41*, 5711–5717.

[68] J. M. Saya, K. Vos, R. A. Kleinnijenhuis, J. H. van Maarseveen, S. Ingemann, H. Hiemstra, *Org. Lett.* **2015**, *17*, 3892–3894.

[69] B. Wang, Y. Xie, Q. Yang, G. Zhang, Z. Gu, *Org. Lett.* **2016**, *18*, 5388–5391.

[70] a) R. A. Kleinnijenhuis, B. J. J. Timmer, G. Lutteke, J. M. M. Smits, R. de Gelder, J. H. van Maarseveen, H. Hiemstra, *Chem. Eur. J.* **2016**, *22*, 1266–1269, b) K. Tanino, M. Takahashi, Y. Tomata, H. Tokura, T. Uehara, T. Narabu, M. Miyashita, *Nat. Chem.* **2011**, *3*, 484–488.

[71] a) M. T. Crimmins, Z. Wang, L. A. McKerlie, *Tetrahedron Lett.* **1996**, *37*, 8703–8706; b) M. T. Crimmins, Z. Wang, L. A. McKerlie, *J. Am. Chem. Soc.* **1998**, *120*, 1747–1756.

[72] P. Dowd, W. Zhang, *Chem. Rev.* **1993**, *93*, 2091–2115; b) P. Dowd, S. C. Choi, *J. Am. Chem. Soc.* **1987**, *109*, 3493–3494; c) A. L. J. Beckwith, D. M. O'Shea, S. W. Westwood, *J. Am. Chem. Soc.* **1988**, *110*, 2565–2575.

[73] a) W. D. Shipe, E. J. Sorensen, *Org. Lett.* **2002**, *4*, 2063–2066; b) W. D. Shipe, E. J. Sorensen, *J. Am. Chem. Soc.* **2006**, *128*, 7025–7035

[74] D. S. Weiss, *Org. Photochem.* **1981**, *5*, 347–420.

[75] N. Hoffmann in *Handbook of Synthetic Photochemistry* (Eds.: A. Albini, M. Fagnoni), Wiley-VCH Verlag GmbH & Co. KGaA, Weinheim, **2010**, 153–156 and references therein.

[76] N. Itagaki, Y. Iwabuchi, *Chem. Commun.* **2007**, 1175–1176.

[77] a) H. Renata, Q. Zhou, P. S. Baran, *Science* **2013**, *339*, 59–63; b) H. Renata, Q. Zhou, G. Dünstl, J. Felding, R. R. Merchant, C.-H. Yeh, P. S. Baran, *J. Am. Chem. Soc.* **2015**, *137*, 1330–1340.

[78] a) K. E. Stevens, P. Yates, *J. Chem. Soc., Chem. Commun.* **1980**, 990–991; b) P. Yates, K. E. Stevens, *Tetrahedron* **1981**, *37*, 4401–4410.

[79] a) G. Stork, F. H. Clarke, *J. Am. Chem. Soc.* **1955**, *77*, 1072–1073; b) G. Stork, F. H. Clarke, *J. Am. Chem. Soc.* **1961**, *83*, 3114–3125.

[80] P. A. Wender, J. J. Howbert, *J. Am. Chem. Soc.* **1981**, *103*, 688–690.

[81] a) U. Streit, C. G. Bochet, *Beilstein J. Org. Chem.* **2011**, *7*, 525–542; b) R. Remy, C. G. Bochet, *Chem. Rev.* **2016**, *116*, 9816–9849.

[82] a) P. A. Wender, R. Ternansky, M. deLong, S. Singh, A. Olivero, K. Rice, *Pure Appl. Chem.* **1990**, *62*, 1597–1602; b) D. Chappell, A. T. Russell, *Org. Biomol. Chem.* **2006**, *4*, 4409–4430.

[83] S. H. Shim, D. C. Swenson, J. B. Gloer, P. F. Dowd, D. T. Wicklow, *Org. Lett.* **2006**, *8*, 1225–1228.

[84] T. Gaich, J. Mulzer, *J. Am. Chem. Soc.* **2009**, *131*, 452–453.

[85] Q. Zhang, Y.-T. Di, C.-S. Li, X. Fang, C.-J. Tan, Z. Zhang, Y. Zhang, H.-P. He, S.-L. Li, X.-J. Hao, *Org. Lett.* **2009**, *11*, 2357–2359.

[86] Z. Lu, Y. Li, J. Deng, A. Li, *Nat. Chem.* **2013**, *5*, 679–684.

[87] M. J. Schnermann, L. E. Overman, *Angew. Chem. Int. Ed.* **2012**, *51*, 9576–9580.

[88] M. J. Schnermann, L. E. Overman, *J. Am. Chem. Soc.* **2011**, *133*, 16425–16427.

[89] a) G. L. Lackner, K. W. Quasdorf, L. E. Overman, *J. Am. Chem. Soc.* **2013**, *135*, 15342–15345; b) G. L. Lackner, K. W. Quasdorf, G. Pratsch, L. E. Overman, *J. Org. Chem.* **2015**, *80*, 6012–6024; c) C. C. Nawrat, C. R. Jamison, Y. Slutskyy, D. W. C. MacMillan, L. E. Overman, *J. Am. Chem. Soc.* **2015**, *137*, 11270–11273; for a recent total synthesis employing this strategy see: Y. Slutskyy, C. R. Jamison, G. L. Lackner, D. S. Müller, A. P. Dieskau, N. L. Untiedt, L. E. Overman, *J. Org. Chem.* **2016**, *81*, 7029–7035.

[90] L. Furst, J. M. R. Narayanam, C. R. J. Stephenson, *Angew. Chem. Int. Ed.* **2011**, *50*, 9655–9659.

[91] L. Furst, B. S. Matsuura, J. M. R. Narayanam, J. W. Tucker, C. R. J. Stephenson, *Org. Lett.* **2010**, *12*, 3104–3107.

[92] a) M. Kita, H. Kigoshi in *Handbook of Anticancer Drugs from Marine Origin* (Ed.: S. K. Kim), Springer International Publishing, Cham, **2015**, 701–740; b) Y. Kiyoyuki, K. Hideo, *Bull.*

Chem. Soc. Jpn. **1997**, *70*, 1479–1489; c) A. Kawamura, M. Kita, H. Kigoshi, *Angew. Chem. Int. Ed.* **2015**, *54*, 7073–7076; d) T. Kuroda, H. Kigoshi, *Org. Lett.* **2008**, *10*, 489–491; e) B. Vera, A. D. Rodríguez, E. Avilés, Y. Ishikawa, *Eur. J. Org. Chem.* **2009**, 5327–5336.

[93] a) K. Palaniveloo, C. S. Vairappan, *J. Appl. Phycol.* **2014**, *26*, 1199–1205; b) J. Jongaramruong, A. J. Blackman, B. W. Skelton, A. H. White, *Aust. J. Chem.* **2002**, *55*, 275–280; c) M. O. Stallard, D. John Faulkner, *J. Comp. Biochem. Physiol. B* **1974**, *49*, 25–35.

[94] a) M. Harizani, E. Ioannou, V. Roussis in *Progress in the Chemistry of Organic Natural Products 102* (Eds.: A. D. Kinghorn, H. Falk, S. Gibbons, J. Kobayashi), Springer International Publishing, Cham, **2016**, 91–252; b) S. M. Al-Massarani, *Nat. Prod. Chem. Res.* **2014**, *2*, 147; c) G. M. König, A. D. Wright, *Phytochem. Anal.* **1997**, *8*, 167–172; d) B. M. Howard, W. Fenical, *Tetrahedron Lett.* **1976**, *17*, 2519–2520; d) J. J. Sims, G. H. Y. Lin, R. M. Wing, *Tetrahedron Lett.* **1974**, *15*, 3487–3490; e) S. M. Waraszkiewicz, K. L. Erickson, *Tetrahedron Lett.* **1974**, *15*, 2003–2006; f) C. R. Kaiser, L. F. Pitombo, A. C. Pinto, *Spectrosc. Lett.* **1998**, *31*, 573–585; g) J. J. Sims, W. Fenical, R. M. Wing, P. Radlick, *Tetrahedron Lett.* **1972**, *13*, 195–198.

[95] S. N. Fedorov, O. S. Radchenko, L. K. Shubina, A. I. Kalinovsky, A. V. Gerasimenko, D. Y. Popov, V. A. Stonik, *J. Am. Chem. Soc.* **2001**, *123*, 504–505.

[96] a) S. N. Fedorov, M. V. Reshetnyak, A. P. Schedrin, S. G. Ilyin, J. T. Struchkov, V. A. Stonik, G. B. Elyakov, *Dokl. AN SSSR.* **1990**, *307*, 877–879; b) S. N. Fedorov, L. K. Shubina, A. M. Bode, V. A. Stonik, Z. Dong, *Cancer Res.* **2007**, *67*, 5914–5920; c) L. K. Shubina, S. N. Fedorov, A. I. Kalinovskiy, A. S. Dmitrenok, J. O. Jin, M. G. Song, J. Y. Kwak, V. A. Stonik, *Russ. Chem. Bull.* **2007**, *56*, 2109–2114; d) S. N. Fedorov, L. K. Shubina, A. I. Kalinovsky, E. G. Lyakhova, V. A. Stonik, *Tetrahedron Lett.* **2000**, *41*, 1979–1982.

[97] a) L. E. Wolinsky, D. J. Faulkner, *J. Org. Chem.* **1976**, *41*, 597–600; (b) D. J. Faulkner, *Pure Appl. Chem*. **1976**, *48*, 25–28.

[98] J. D. Martin, C. Perez, J. L. Ravelo, *J. Am. Chem. Soc.* **1986**, *108*, 7801–7811.

[99] a) W. Fenical, *J. Phycol.* **1975**, *11*, 245–259; b) J. D. Martin, J. M. Palazon, C. Perez, J. L. Ravelo, *Pure Appl. Chem.* **1986**, *58*, 395–406.

[100] A. Butler, J. N. Carter-Franklin, *Nat. Prod. Rep.* **2004**, *21*, 180–188 and references therein. A more detailed description of haloperoxidases is given in Chapter 3.

[101] a) J. N. Carter-Franklin, A. Butler, *J. Am. Chem. Soc.* **2004**, *126*, 15060–15066; b) J. N. Carter-Franklin, J. D. Parrish, R. A. Tschirret-Guth, R. D. Little, A. Butler, *J. Am. Chem. Soc.* **2003**, *125*, 3688–3689.

[102] For synthetic approaches towards aplydactone, see: J. M. Rohde, PhD thesis, The Scripps Research Institute, La Jolla, California, **2005**.

[103] a) N. J. Demjanow, *Ber.* **1907**, *40*, 4393–4397; b) G. A. Olah, V. P. Reddy, G. K. S. Prakash, *Chem. Rev.* **1992**, *92*, 69–95; c) K. B. Wiberg, D. Shobe, G. L. Nelson, *J. Am. Chem. Soc.* **1993**, *115*, 10645–10652.

[104] a) M. P. Doyle, *Chem. Rev.* **1986**, *86*, 919–939; b) T. Ye, M. A. McKervey, *Chem. Rev.* **1994**, *94*, 1091–1160; c) A. Ford, H. Miel, A. Ring, C. N. Slattery, A. R. Maguire, M. A. McKervey, *Chem. Rev.* **2015**, *115*, 9981–10080 and references therein.

[105] B. B. Snider, *Chem. Rev.* **1988**, *88*, 793–811.

[106] a) H. Zhu, P. Tu, *Synth. Commun.* **2005**, *35*, 71–78; b) S. Copinga, P. G. Tepper, C. J. Grol, A. S. Horn, M. L. Dubocovich, *J. Med. Chem.* **1993**, *36*, 2891–2898; c) D. Song, M. Lee, C. H. Park, S. Ahn, C. S. Yun, C. O. Lee, H. R. Kim, J. Y. Hwang, *Bioorg. Med. Chem. Lett.* **2016**, *26*, 1720–1725.

[107] a) K. Kinoshita, T. Kobayashi, K. Asoh, N. Furuichi, T. Ito, H. Kawada, S. Hara, J. Ohwada, K. Hattori, T. Miyagi, W.-S. Hong, M.-J. Park, K. Takanashi, T. Tsukaguchi, H. Sakamoto, T. Tsukuda, N. Oikawa, *J. Med. Chem.* **2011**, *54*, 6286–6294; b) J. M. Herbert, *Tetrahedron Lett.* **2004**, *45*, 817–819.

[108] R. Soni, J.-M. Collinson, G. C. Clarkson, M. Wills, *Org. Lett.* **2011**, *13*, 4304–4307.

[109] G. S. R. Subba Rao, *Pure Appl. Chem.* **2003**, *75*, 1443–1451.

[110] a) C. J. Blankley, F. J. Sauter, H. O. House *Org. Synth.* **1973**, *5*, 258; b) E. J. Corey, A. G. Myers, *Tetrahedron Lett.* **1984**, *25*, 3559–3562; c) T. Toma, J. Shimokawa, T. Fukuyama, *Org. Lett.* **2007**, *9*, 3195–3197; d) A. Ouihia, L. Rene, J. Guilhem, C. Pascard, B. Badet, *J. Org. Chem.* **1993**, *58*, 1641–1642; e) M. E. Meyer, E. M. Ferreira, B. M. Stoltz, *Chem. Commun.* **2006**, 1316–1318.

[111] a) E. L. Myers, R. T. Raines, *Angew. Chem. Int. Ed.* **2009**, *48*, 2359–2363; b) H.-H. Chou, R. T. Raines, *J. Am. Chem. Soc.* **2013**, *135*, 14936–14939.

[112] a) G. Maas, *Chem. Soc. Rev.* **2004**, *33*, 183–190; b) C. A. Merlic, A. L. Zechman, *Synthesis* **2003**, 1137–1156.

[113] A. Padwa, D. J. Austin, S. F. Hornbuckle, M. A. Semones, M. P. Doyle, M. N. Protopopova, *J. Am. Chem. Soc.* **1992**, *114*, 1874–1876.

[114] a) A. Padwa, D. J. Austin, *Angew. Chem. Int. Ed.* **1994**, *33*, 1797–1815; b) R. G. Salomon, J. K. Kochi, *J. Am. Chem. Soc.* **1973**, *95*, 3300–3310.

[115] R. R. Nani, S. E. Reisman, *J. Am. Chem. Soc.* **2013**, *135*, 7304–7311.

[116] a) S. Levin, R. R. Nani, S. E. Reisman, *Org. Lett.* **2010**, *12*, 780–783; b) S. Levin, R. R. Nani, S. E. Reisman, *J. Am. Chem. Soc.* **2011**, *133*, 774–776; for a review on that topic,

see: S. E. Reisman, R. R. Nani, S. Levin, *Synlett* **2011**, 2437–2442 and references therein.

[117] For similar cyclopropanation using tetralin 2-diazomethyl ketones, see: a) , D. H. Rogers, J. C. Morris, F. S. Roden, B. Frey, G. R. King, F.-W. Russkamp, R. A. Bell, L. N. Mander, *Pure Appl. Chem.* **1996**, *68*, 515–522; b) J. C. Morris, L. N. Mander, D. C. R. Hockless, *Synthesis* **1998**, 455–467.

[118] a) C. Madelaine, V. Valerio, N. Maulide, *Chem. Asian J.* **2011**, *6*, 2224–2239; b) J.-B. Falmagne, J. Escudero, S. Taleb-Sahraoui, L. Ghosez, *Angew. Chem. Int. Ed.* **1981**, *20*, 879–880.

[119] a) J.-M. Adam, L. Ghosez, K. N. Houk *Angew. Chem. Int. Ed.* **1999**, *38*, 2728–2730; b) L.-Y. Chen, L. Ghosez, *Tetrahedron: Asymmetry* **1991**, *2*, 1181–1184; c) O. Irie, K. Shishido, *Chem. Lett.* **1995**, 53–54; d) P.-J. Shim, H.-D. Kim, *Tetrahedron. Lett.* **1995**, *39*, 9517–9520.

[120] a) C. Genicot, B. Gobeaux, L. Ghosez, *Tetrahedron Lett.* **1991**, *32*, 3827–3830; b) C. Genicot, L. Ghosez, *Tetrahedron Lett.* **1992**, *33*, 7357–7360; c) A. V. Chernykh, D. S. Radchenko, A. V. Chernykh, I. S. Kondratov, N. A. Tolmachova, O. P. Datsenko, M. A. Kurkunov, S. X. Zozulya, Y. P. Kheylik, K. Bartels, C. G. Daniliuc, G. Haufe, *Eur. J. Org. Chem.* **2015**, 6466–6471.

[121] H. Hopf, *Angew. Chem. Int. Ed.* **2003**, *42*, 2822–2825.

[122] a) J. Limanto, J. A. Tallarico, J. R. Porter, K. S. Khuong, K. N. Houk, M. L. Snapper, *J. Am. Chem. Soc.* **2002**, *124*, 14748–14758; b) J. Limanto, M. L. Snapper, *J. Am. Chem. Soc.* **2000**, *122*, 8071–8072; c) J. C. Barborak, L. Watts, R. Pettit, *J. Am. Chem. Soc.* **1966**, *88*, 1328–1329.

[123] S. J. Connon, S. Blechert, *Angew. Chem. Int. Ed.* **2003**, *42*, 1900–1923.

[124] J. Agar, F. Kaplan, B. W. Roberts, *J. Org. Chem.* **1974**, *39*, 3451–3452.

[125] B. E. Bursten, R. F. Fenske, *Inorg. Chem.* **1979**, *18*, 1760–1765.

[126] a) A. Efraty, *Chem. Rev.* **1977**, *77*, 691–744; b) D. Seyferth, *Organometallics* **2003**, *22*, 2–20; c) U. Bunz, *Organometallics* **1993**, *12*, 3594–3597; d) J. D. Fitzpatrick, L. Watts, G. F. Emerson, R. Pettit, *J. Am. Chem. Soc.* **1965**, *87*, 3254–3255.

[127] C. M. Adams, E. M. Holt, *Organometallics* **1990**, *9*, 980–986.

[128] a) T. Kauffmann, P. Fiegenbaum, M. Papenberg, R. Wieschollek, D. Wingbermühle, *Ber.* **1993**, *126*, 79–87; b) T. Kauffmann, *Angew. Chem. Int. Ed.* **1997**, *36*, 1258–1275.

[129] T. Okazoe, K. Takai, K. Utimoto, *J. Am. Chem. Soc.* **1987**, *109*, 951–953.

[130] a) L. Carman, L. D. Kwart, T. Hudlicky, *Synth. Commun.* **1986**, *16*, 169–182; b) W. A. Kleschick, *J. Org. Chem.* **1986**, *51*, 5429–5433.

[131] a) K. B. Sharpless, W. Amberg, Y. L. Bennani, G. A. Crispino, J. Hartung, K. S. Jeong, H. L. Kwong, K. Morikawa, Z. M. Wang, *J. Org. Chem.* **1992**, *57*, 2768–2771; b) G. A. Crispino, K. S. Jeong, H. C. Kolb, Z. M. Wang, D. Xu, K. B. Sharpless, *J. Org. Chem.* **1993**, *58*, 3785–3786.

[132] Z.-Y. Liu, J.-X. Ji, B.-G. Li, *J. Chem. Soc., Perkin Trans. 1* **2000**, 3519–3521.

[133] A. De Mico, R. Margarita, L. Parlanti, A. Vescovi, G. Piancatelli, *J. Org. Chem.* **1997**, *62*, 6974–6977.

[134] A. Michrowska, R. Bujok, S. Harutyunyan, V. Sashuk, G. Dolgonos, K. Grela, *J. Am. Chem. Soc.* **2004**, *126*, 9318–9325.

[135] A. K. Chatterjee, T.-L. Choi, D. P. Sanders, R. H. Grubbs, *J. Am. Chem. Soc.* **2003**, *125*, 11360–11370.

[136] a) T. Ohshima in *Comprehensive Chirality* (Eds.; E. M. Carriera, H. Yamamoto), Elsevier, Amsterdam, **2012**, 355–377; b) L. Pu, *Tetrahedron* **2003**, *59*, 9873–9886; c) M. Turlington, L. Pu, *Synlett* **2012**, *23*, 649–684 and references therein.

[137] S. Müller, B. Liepold, G. J. Roth, H. J. Bestmann, *Synlett* **1996**, 521–522.

[138] D. J. Pasto, R. T. Taylor *Org. React.* **1991**, *40*, 91–155.

[139] a) J. L. Roberts, P. S. Borromeo, C. Dale Poulter, *Tetrahedron Lett.* **1977**, *18*, 1621–1623; b) J. Schreiber, H. Maag, N. Hashimoto, A. Eschenmoser, *Angew. Chem. Int. Ed.* **1971**, *10*, 330–331.

[140] a) R. H. Grubbs, R. A. Grey, *J. Am. Chem. Soc.* **1973**, *95*, 5765–5767; b) E. K. G. Schmidt, *Angew. Chem. Int. Ed.* **1973**, *12*, 777–778.

[141] A. G. M. Barrett, D. H. R. Barton, G. Johnson, *J. Chem. Soc., Perkin Trans. 1* **1978**, 1014–1017.

[142] S. Masamune, N. Nakamura, J. Sapadaro, *J. Am. Chem. Soc.* **1975**, *97*, 918–919.

[143] D. J. Thompson, *J. Organomet. Chem.* **1976**, *108*, 381–383.

[144] Y. Shvo, E. Hazum, *J. Chem. Soc., Chem. Commun.* **1974**, 336–337.

[145] J. A. Tallarico, M. L. Randall, M. L. Snapper, *J. Am. Chem. Soc.* **1996**, *118*, 9196–9197.

[146] T. Z. Wang, L. A. Paquette, *J. Org. Chem.* **1986**, *51*, 5232–5234.

[147] a) G. W. Gribble, *Naturally Occurring Organohalogen Compounds – A Comprehensive Update* in *Progress in the Chemistry of Organic Natural Products* (Eds.: A. D. Kinghorn, H. Falk, J. Kobayashi), Springer-Verlag, Wien, **2010**, 1–374; b) G. W. Gribble, *Environ. Chem.* **2015**, *12*, 396–405; c) G. W. Gribble, *J. Chem. Educ.* **2004**, *81*, 1441–1449; d) G. W. Gribble, *Acc. Chem. Res.* **1998**, *31*, 141–152; e) G. W. Gribble, *J. Nat. Prod.* **1992**, *55*, 1353–1395; f) H. M. Senn, *Front. Chem.* **2014**, *2*, 98.

[148] D. O'Hagan, D. B. Harper, *J. Fluorine Chem.* **1999**, *100*, 127–133.

[149] a) J. Wu, W. Vetter, G. W. Gribble, J. S. Jr. Schneekloth, D, H, Blank, *Angew. Chem. Int. Ed.* **2002**, *41*, 1740–1743; b) T. F. Spande, H. M. Garraffo, M. W. Edwards, H. J. C. Yeh, L. Pannell, J. W. Daly, *J. Am. Chem. Soc.* **1992**, *114*, 3475–3478; c) T. Teruya, S. Nakagawa, T. Koyama, K. Suenaga, M. Kita, D. Uemura, *Tetrahedron Lett.* **2003**, *44*, 5171–5173; d) W.-C. Lai, Y.-C. Wu, B. Dankó, Y.-B. Cheng, T.-J. Hsieh, C.-T. Hsieh, Y.-C. Tsai, M. El-Shazly, A. Martins, J. Hohmann, A. Hunyadi, F.-R. Chang, *J. Nat. Prod.* **2014**, *77*, 1624–1631; e) Y.-D. Su, C.-H. Cheng, W.-F. Chen, Y.-C. Chang, Y.-H. Chen, T.-L. Hwang, Z.-H. Wen, W.-H. Wang, L.-S. Fang, J.-J. Chen, Y.-C. Wu, J.-H. Sheu, P.-J. Sung, *Tetrahedron Lett.* **2014**, *55*, 6065–6067; f) P. F. V. Ward, R. J. Hall, R. A. Peters, *Nature* **1964**, *201*, 611–612; g) M. a. L. Souto, C. P. Manríquez, M. Norte, J. J. Fernández, *Tetrahedron* **2002**, *58*, 8119–8125; h) P. A. Cohen, G. H. N. Towers, *J. Nat. Prod.* **1995**, *58*, 520–526; i) T. Kusama, N. Tanaka, K. Sakai, T. Gonoi, J. Fromont, Y. Kashiwada, J. Kobayashi, *Org. Lett.* **2014**, *16*, 5176–5179.

[150] a) I. Yanagisawa, H. Yoshikawa, *Biochim. Biophys. Acta* **1973**, *329*, 283–294; b) S. Torii, K. Mitsumori, S. Inubushi, I. Yanagisawa, *Psychopharmacologia* **1973**, *29*, 65–75.

[151] a) A. Hill, J. Littlechild in *Comprehensive Chirality* (Eds.; E. M. Carriera, H. Yamamoto), Elsevier, Amsterdam, **2012**, 329–349; b) A. Butler, M. Sandy, *Nature* **2009**, *460*, 848–854; c) C. S. Neumann, D. G. Fujimori, C. T. Walsh, *Chem. Biol.* **2008**, *15*, 99–109; d) F. H. Vaillancourt, E. Yeh, D. A. Vosburg, S. Garneau-Tsodikova, C. T. Walsh, *Chem. Rev.* **2006**, *106*, 3364–3378; e) A. Butler, J. V. Walker, *Chem. Rev.* **1993**, *93*, 1937–1944.

[152] G. Sakoulas, S.-J. Nam, S. Loesgen, W. Fenical, P. R. Jensen, V. Nizet, M. Hensler, *PLoS One* **2012**, *7*, e29439.

[153] L. Kaysser, P. Bernhardt, S.-J. Nam, S. Loesgen, J. G. Ruby, P. Skewes-Cox, P. R. Jensen, W. Fenical, B. S. Moore, *J. Am. Chem. Soc.* **2012**, *134*, 11988–11991.

[154] R. Teufel, L. Kaysser, M. T. Villaume, S. Diethelm, M. K. Carbullido, P. S. Baran, B. S. Moore, *Angew. Chem. Int. Ed.* **2014**, *53*, 11019–11022.

[155] H. P. Pepper, J. H. George, *Angew. Chem. Int. Ed.* **2013**, *52*, 12170–12173.

[156] S. Diethelm, R. Teufel, L. Kaysser, B. S. Moore, *Angew. Chem. Int. Ed.* **2014**, *53*, 11023–11026.

[157] G. B. Diamond, M. D. Soffer, *J. Am. Chem. Soc.* **1952**, *74*, 4126–4127.

[158] J. A. Hill, A. W. Johnson, T. J. King, S. Natori, S. W. Tam, *J. Chem. Soc.* **1965**, 361–375.

[159] S. K. Taylor, C. L. Blankespoor, S. M. Harvey, L. J. Richardson, *J. Org. Chem.* **1988**, *53*, 3309–3312.

[160] E. Wenkert, C. A. McPherson, E. L. Sanchez, R. L. Webb, *Synth. Commun.* **1973**, *3*, 255–259.

[161] T. Yoshida, S. Saito, *Bull. Chem. Soc. Jpn.* **1982**, *55*, 3931–3932.

[162] (a) A.-P. Schaffner, P. Renaud, *Angew. Chem. Int. Ed.* **2003**, *42*, 2658–2660; (b) J. T. Banks, J. C. Scaiano, W. Adam, R. S. Oestrich, *J. Am. Chem. Soc.* **1993**, *115*, 2473–2477; (c) G. D. Mendenhall, *Tetrahedron Lett.* **1983**, *24*, 451–452.

[163] R. J. Rafferty, R. M. Williams, *Tetrahedron Lett.* **2011**, *52*, 2037–2040.

[164] J.-P. Uttaro, G. Audran, J.-M. Galano, H. Monti, *Tetrahedron Lett.* **2002**, *43*, 2757–2760.

[165] V. K. Aggarwal, Z. Gultekin, R. S. Grainger, H. Adams, P. L. Spargo, *J. Chem. Soc., Perkin Trans. 1* **1998**, 2771–2782.

[166] M. Shen, M. Kretschmer, Z. G. Brill, S. A. Snyder, *Org. Lett.* **2016**, *18*, 5018–5021.

[167] E. G. Lyakhova, S. N. Fedorov, L. K. Shubina, O. S. Radchenko, A. I. Kalinovsky, P. S. Dvitrenok, V. A. Stonik, *Russ. Chem. Bull.* **2003**, *52*, 1022–1026.

[168] A. M. Beekman, E. Castillo Martinez, R. A. Barrow, *Org. Biomol. Chem.* **2013**, *11*, 1109–1115.

[169] F. Viviani, M. Gaudry, A. Marquet, *J. Chem. Soc., Perkin Trans. 1* **1990**, 1255–1259.

[170] J. E. H. Buston, H. J. Howell, M. G. Moloney, V. C. Manson, R. M. Thompson, *Main Group Met. Chem.* **1998**, *21*, 51–54.

[171] P. Dauban, L. Sanière, A. Tarrade, R. H. Dodd, *J. Am. Chem. Soc.* **2001**, *123*, 7707–7708.